الملتقى العالمى للطاقة « 88 »

energex

'المعرفة حق طبيعى لكل انسان'

مجلدات بحوث الملتقى العالمى للطاقة 88

PROCEEDINGS OF ENERGEX 88
THE GLOBAL ENERGY FORUM

NOVEMBER 25 – 30,1988.

المجلد الثانى
الطاقة الشمسية
الفصول من VII حتى XII

VOLUME 2
SOLAR ENERGY
SECTIONS: VII – XII

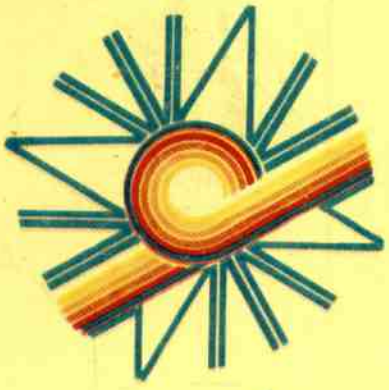

TRIPOLI , LIBYA
(G.S.L.A.J.)

CONTENTS

SECTION VII. PLENARY LECTURES

1. KAZMERSKI, L.L.,
"Overview of the Photovoltaic Technologies: Status and Future Directions"
VII-1

2. GARG, H.P.,
"Solar Energy Technology Development and Applications in India"
VII-17

3. YUL KWON, O.,
"Economic Analysis of Solar Energy for Industrial Usage: Its Methodology"
VII-27

4. STAHL, W.,
"Status of Solar Thermal Energy in the Federal Republic of Germany"
VII-33

5. CORVI, C.,
"The Role of ISES - International Solar Energy Society in the Dissemination of Renewable Energy Technologies"
VII-39

6. MUFTI, A.R.,
"Feasibility & Viability of Silicon Technology Development for Islamic Countries - A Practical Approach"
VII-43

SECTION VIII. THERMAL SYSTEMS

1. EL HISSE, M., FOURNIER, M.,
"Fruits Solar Dryer Modelling"
VIII-1

2. FERWATI, M.A.,
"Analysis of Absorption Cooling Solar System, Study for Benghazi Conditions"
VIII-13

3. DATTA, G., GARG, H.P., PRAKASH, J.,
"Theoretical Studies of a Cabinet Solar Dryer"
VIII-23

4. MISELLATI, M.M., EL-TWATY, A.I.,
"Solar Energy for Space Heating in Libya"
VIII-31

5. EKECHUKWU, O.V., NORTON, B., ODUKWE, O.A.,
"Design and Performance Studies of a Passive Direct-Mode Solar Energy Dryer"
VIII-41

6. YADAV, Y.P.,
"Solar Still with Water Flow in the Basin"
VIII-57

7. MALEK, G.F., BERRO, M.K.,
"Heating of Charged Particles of the Plasma by Wave of Ordinary Modes"
VIII-65

8. KULUNK, H.,
"Mini Scale Solar Pond Activated by Halogenic Lamp"
VIII-71

9. CORVI, C.,
"Italian R & D Activity on Solar Energy Conversion"
VIII-79

10. ALTINISIK, K.,
"Optimum Design of Evaporators for Heat Pumps Working Air/Air, (Air +Liquid)/Air"
VIII-91

SECTION IX . SOLAR COLLECTORS

1. SHARMA, V.K., SHARMA, S., RAY, R.A.,
"Mathematical Modelling and Experimental Evaluation of an Natural Convection Type Solar Cabinet Dryer"
IX-1

2. KASBADJI, N., MERZOUK, M.,
"Comparative Study of Experimental Performance of a Plastsic Flat-Plate Solar Collector Using Water as the Heating Fluid"
IX-11

SECTION X . PHOTOVOLTAIC

1. SALEEM, M.,
"Studies on Electrolyte Semiconductor Junction Solar Cells"
X-1

2. AKKARI, F.R., MOUSA, M.M., AKKI, A.S.,
"Solar Cells Potential in Rural Areas in the Arab World"
X-7

3. KAZMERSKI, L.L.,
"Atomic-Level Analysis of Photovoltaic Devices"
X-21

SECTION XI. RADIATION DATA

1. HUSSAIN, M.,
"Correlation of Beam Irradiation with Sunshine Duration and the Linke Turbidity Factor"
XI-1

2. ZEROUAL, A., AIT OUAHMAN, A., ANKRIM, M.,
"A Prediction Model of Hourly Global Irradiation in Marrakech, Morocco"
XI-11

3. MALIK, A.Q., HISER, H.W., MUFTI, A.R.,
"Development of Insolation Maps for Pakistan Using Satellite Data"
XI-25

4. SIALA, F.M.F., ROSEN, M.A., HOOPER, F.C.,
"On the Modelling of the Directional Distribution of the Diffuse Radiance"
XI-33

5. BUKAMUR, S.M.S.,
"Development and Application of Passive Solar Energy Technology for the Hot Dry Zones"
XI-43

6. SMEDA, M.S.,
"On Tilted Solar Radiation in North Africa"
XI-51

7. JAIN, P.C.,
"Modelling of Hourly Global and Diffuse Irradiation on Horizontal Plane"
XI-61

8. AHMAD, F., HUSAIN, S.A.,
"Comparison of Measured and Estimated Monthly Average Daily Global Solar Radiation on Horizontal Surface at Karachi, Pakistan"
XI-71

9. ABUGHRES, S.M., ELEGELY, Y.M., ELALU, M.B.,
"Optimum Slope of Flat-Plate Solar Collector for Different Applications"
XI-83

10. HELALI, M.M., KHAN, M.H., HUQ, A.M.A.,
"Solar Radiation in Dhaka" XI-95

11. AZIZ, G.M.A., RASHID, A.A., NASSER, A.S.,
"Calculation of Monthly Mean Solar Radiation for Inclined Surfaces"
XI-103

12. SHALTOUT, M.A.M., HASSAN, A.H.,
"Solar Energy Distribution Over Egypt Using Cloudiness From Meteosat Photos"
XI-115

SECTION XII. PASSIVE SYSTEMS

1. AL-MOTAWAKEL, M.K.,
"Passive-Design Features of the Vernacular Buildings in the Yemen Arab Republic"
XII-1

2. RHEAULT, S., BILGEN, E.,
"Experimental Study of the Thermal Performance of Automated Venetian Blind Windows"
XII-13

3. MAGAL, B.S., GAUNEKAR, A.S.,
"Design and Mathematical Modelling of a Roof-Top Wick-Type Solar Still"
XII-19

4. AKSUGUR, E., BAJWA, M., AL-OTAIBI, G.,
"The Potential of the Evaporative Cooling Techniques on the Gulf Region of the Kingdom of Saudi Arabia"
XII-29

5. NABELEK, B., FRANC, F., MALY, M., JIRKA, V.,
"The Use of Linear Fresnel Lenses"
XII-39

SECTION XIII. AGRICULTURAL APPLICATIONS

1. ARSHAD, K., SAID, S.A.M.,
'Pumped Solar Domestic Hot Water (SDHW) System Design Guidelines"
XIII-1

2. ABUGHRES, S.M., MASHENA, M.E., AGHA, K.R.,
"Transient Thermal Behaviour of Solar Ponds with a Constant Energy Extraction Rate"
XIII-7

3. ABUGHRES, S.M., SASSI, M.M., SAMI MUSA,
"Utilization of Solar Pond for a Green House in Jamahiriya"
XIII-17

4. TA'ANI, R.,
"Solar and Wind Energy Activities in Jordan"
XIII-27

AUTHORS INDEX

متاح للتحميل ضمن مجموعة كبيرة من المطبوعات من صفحة
مكتبتي الخاصة
على موقع ارشيف الانترنت
الرابط
https://archive.org/details/@hassan_ibrahem

https://archive.org/details/@hassan_ibrahem

SECTION VII

PLENARY LECTURES

متاح للتحميل ضمن مجموعة كبيرة من المطبوعات من صفحة
مكتبتي الخاصة
على موقع ارشيف الانترنت
الرابط
https://archive.org/details/@hassan_ibrahem

https://archive.org/details/@hassan_ibrahem

OVERVIEW OF THE PHOTOVOLTAIC TECHNOLOGIES: STATUS AND FUTURE DIRECTIONS

Lawrence L. Kazmerski
Solar Energy Research Institute
Golden, CO 80401 USA

تم استعراض الموقف الحالى للتقنيات الفوتوفولتيه مع التركيز على الاغشيه الرقيقه كبديل مخفض التكلفه مناسب لاستعمالات على سطح الارض.نوقشت المشاكل المتعلقهبتقنيات المواد الاحاديه و العديده التبلر و المتزججه و حددت الاتجاهات البحثيه فى هذا المجال رغم ان المناقشه تركزت على الخليه فقد ادرجت مشاكل و تطويرات النماذج

The status of the current photovoltaic technologies is reviewed. Emphasis is placed on the emerging thin-film options for low-cost terrestrial applications. The problems with single-crystal, polycrystalline and amorphous technologies are discussed, and research directions are indicated. The discussions center around the cell, although some important module developments and problems are cited.

1. INTRODUCTION

Photovoltaics (PV) is usually thought to be a *recently-evolved* technology, having been used to produce electricity for a variety of applications primarily since the 1960's. But in fact, photovoltaics has been studied for almost a century and a half, with the pioneering work attributed to Becquerel[1]. Since the 1950's, photovoltaics has developed rapidly. The initial applications were of a small scale, such as power telephone repeaters[1]. The first real impact of solar cells, however, was realized with the advent of space exploration[1]. The terrestrial uses received their major attention in the past 12 years due to concerns about energy resource depletion, energy security, safety, as well as environmental concerns such as the greenhouse effect. The status of photovoltaics, its problems, the status of the technology, the materials and devices under development, research needs, and the future directions are discussed in this paper. It should be emphasized that this work is not intended to be an exhaustive treatment on photovoltaics, but rather a summary of some of the technology's current and future features. The discussions center around the cell, although some module development and problems are cited.

2. ARGUMENTS AND ECONOMICS

The need for affordable and available energy is common to both developing and more developed countries [2]. Although the specific applications vary, photovoltaics--since it is a *modular* energy source--has the potential for matching such requirements, whether several watts of stand-alone or hundreds of megawatts of grid-connected power. The common and interrelated factors in determining the feasibility of such electrical systems are: ***cost, per-***

formance and reliability. A viable photovoltaics option must demonstrate parity with electricity from competing conventional alternatives[3]. Studies by electric utilities provide some insight into what these competitive cost and performance levels might be [53, although the reader should be cautioned that these analyses apply to central station options. Figure 1 presents module costs ($/m^2) as a function of levelized electricity costs ($/kWh) and various module efficiencies for: (a) *fixed flat-plate*, and (b) *concentrator* systems. The cost target for PV-generated electricity is established using estimates of the conventional fuel and capacity that photovoltaic units can displace. This target is the sum of fuel and capacity savings, and is equal to $0.06/kWh in constant 1986 $U.S.[3]. Therefore, this cost is established for photovoltaic plants installed in the year 2000. For a competitive $0.06/kWh 30-year levelized cost, module efficiencies in the range of 15-20% for flat-plate and 25-30% for concentrators are required. These correspond to module-area costs of $45-80/m^2 and $60-100/m^2 , respectively. To put this in perspective, the lower-range area cost of the flat-plate option would be about the same that the consumer now pays for a role of 35mm color slide film. Considering the electronic complexity and reliability demands for photovoltaics, the challenge to make the technology cost-competitive is not trivial.

If one examines the hierarchy of solar cell components, the major barriers to technology feasibility--cost, performance and reliability--remain with the basic building block for the PV system, the solar cell itself. Other system considerations, such as power conditioning, balance of systems, and storage, are much closer to economic and operational realization. Although significant progress has accompanied the development of the single-crystal Si solar cell (still the major commercial product for applications displacing fossil fuels), major cost impediments remain. Therefore, research into photovoltaic alternatives is imperative in order to make the technology competitive. These other options include higher efficiency/lifetime cells utilizing new structures and/or materials, thin films which require less material, and advanced, non-conventional *multiple-cell concepts* providing for enhanced performance. Inherent to any successful option are processing and packaging procedures for large-area production. A number of these various cell options, as well as the status of the current (commercial/laboratory) ones, will be considered and compared in the following sections.

3. TECHNOLOGY STATUS: SINGLE-JUNCTION DEVICES

The traditional concept of a solar cell is that of a solid-state (semiconductor) device which produces useful electricity (direct current and voltage) from the sun's energy via the photovoltaic effect [4]. The *current* is provided through the generation of free negative (electrons) and positive (holes) carriers which can move when experiencing an external force or field. The *voltage* is attributed to the separation of the carriers by some purposely-placed inhomogeneity or **junction**. The most simple are the *single junction devices*--analogous physically and electronically to semiconductor diodes. The variety of materials, junctions and structures utilized for realization of single junction solar cells is examined in this section.

3.1 Single Crystal and Polycrystalline Silicon

Silicon has been the foundation for the photovoltaics industry from its inception. The material is *abundant*, comprising about 20% of earth's crust. Because of its importance to the electronics markets, more is *known* about the electrical, optical, chemical and physical properties of this semiconductor than any other material. Silicon solar cells have *demonstrated-lifetimes* , having performed adequately both in space and terrestrial environments [31-34]. The major limitations have been in the related areas of cost and performance. Much of the activity in this technology has been directed in the past years to either (i) bringing the cost of cell materials and processing down; and/or (ii) improving the operational performance of the device toward theoretically predicted values.

(i) Polycrystalline Approaches : One major cost in the production of a crystalline Si solar cell is that related to making the high-purity, high-crystalline perfection wafer. Therefore, some attention has been directed toward less energy-intensive processes, which sacrifice this

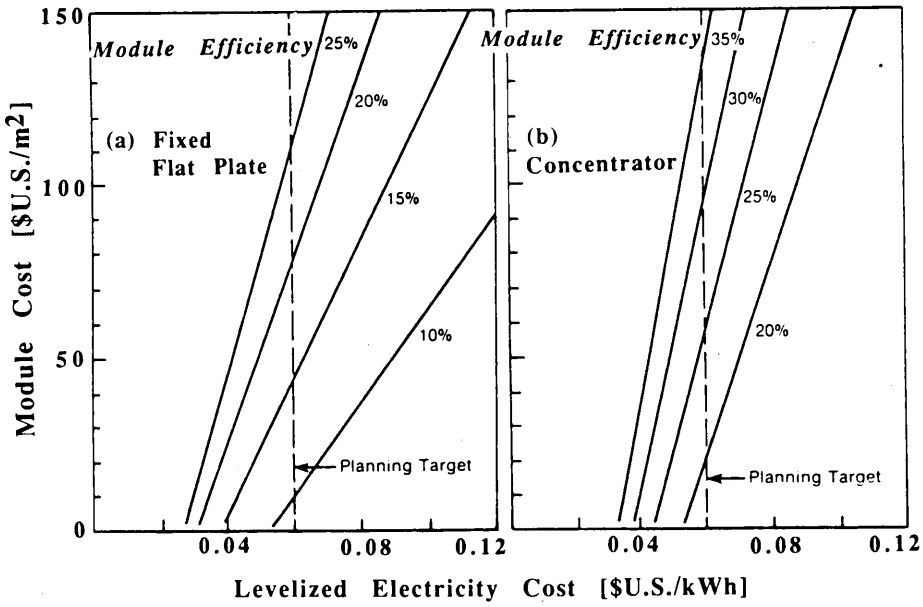

Fig. 1. Module costs as a function of levelized electricity costs (30 year lifetime) and various module efficiencies for (a) fixed flat-plate; and, (b) concentrator system.

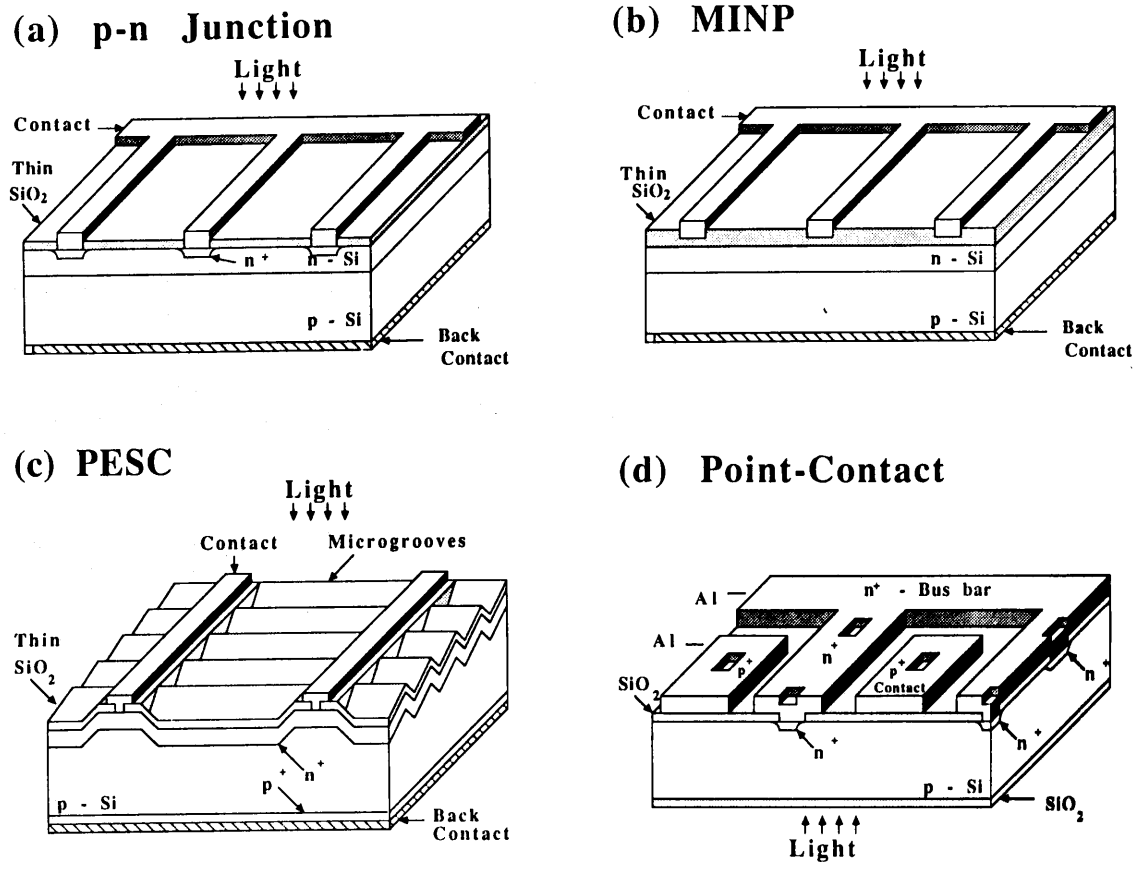

Fig. 2. Device structures for several Si solar cells.

crystalline perfection and perhaps utilized less pure starting material, in order to lower cell cost. The trade-off, of course, is the ultimate performance or efficiency of the device. Bulk and ribbon approaches to providing "sheet" Si material have undergone extensive investigations[4,5]. These have included casting, directional solidification, heat exchanger method (HEM), edge-fed film grown (EFG), edge-supported pulling (ESP), ribbon-to-ribbon (RTR), ribbon against drop (RAD), spinning, dendritic web, and low-angle silicon sheet (LASS)[4,5]. Although some promising performance has been demonstrated in these materials, the techniques have not yet yielded expected significant advantages in cost over single crystal cells. Some methods still require sawing and surface preparation equipment. The ability to produce adequate cross-sections and areas is also a limiting factor. Post treatments, especially chemical ones utilizing hydrogen, lithium, aluminum, arsenic and phosphorous, have been used with mixed success in order to minimize the effects of active defects. The general observation is that these techniques improve the lower efficiency devices, but have far less effect on those having reasonable characteristics.

Early attempts at producing *thin-film* Si have been largely unsuccessful--with efficiencies typically below 5% [6]. Previous vacuum deposition required very high vacuum and rapid deposition (minimizing oxidation and contamination of the films) to fabricate even the minimally-efficient cell[3,7]. Chemical vapor deposition, used extensively in the electronic industry to produce epitaxial Si on Si, indicated some success in fabricating devices on heterotype substrates such as graphite, tungsten and molybdenum[7]. However, chemical interactions between the substrate and the Si during growth impaired the ultimate cell efficiency. Recently however, some promising work utilizing a modified liquid phase growth of Si onto special conducting ceramic substrates has been reported. The researchers have incorporated some innovative, yet low potential-cost, device engineering to minimize both the effects of the substrate impurities and the inherent film defects. Solar cell efficiencies in excess of 12% have been confirmed for small area cells[8]. Recently, a 14.2% [V_{oc}=0.59V, J_{sc}=32.4mA/cm^2, FF=0.74) cell has been reported. These performance levels demonstrate the feasibility of the technique and thin-film Si, and are the highest efficiencies for *thin-film polycrystalline solar cells.* In addition, the technology has entered the near-manufacturing stage, with 1000 cm^2 modules recently reported.

(ii) Single-Crystal Silicon Cells : Until very recently, the gap between the predicted performance of single-crystal Si cells and the reported efficiencies had been wider than in other major cell technologies such as GaAs. In fact, as recently as 1981, many device experts were skeptical that a 17% efficient cell of adequate area could be produced. With the subsequent availability of very high-purity float-zone material, and the increased activities in cell modelling and design, the efficiencies have evolved not only beyond the 17-18% "barrier", but up to 22%. These exceptional efficiencies have caused a reevaluation of the Si solar cell for cost-effective terrestrial use. A parameter summary of the highest efficiency single-crystal and polY- Si cells confirmed in the SERI laboratories is presented in Table 1.

The evolution of the high efficiency Si solar cell is illustrated in the device cross sections provided in Fig. 2. The relatively simple, conventional p-n junction of Fig. 2a has changed considerably in design and structure. The purpose is to better collect the incident light by minimizing the front contact area and improving the antireflection coating, and to improving the junction properties. The PESC design by Green *et al.* (Fig. 2b) has produced cells with efficiencies up to 21%[9]. These cells have especially high open-circuit voltages, and have been fabricated in relatively large areas. Swanson *et al.* [10], making use of previous work on "dot" contact cells, have had cells verified at 22.4% (area of 0.154 cm^2) under one-sun conditions. This cell is being developed primarily for *concentrator applications* and has been reported to have 27.7% conversion efficiency under 100X concentration. The cell, depicted in Fig. 2c, has all contacting provided through the backside, so that no light is obscured by a front contact. The economics of cell processing and materials, the engineering problems in concentrator systems, as well as investigations of the operational reliability of these complex device type have only started to be considered. However, the exceptional performance demonstrations have provided the basis for more research into and further development of high-efficiency cells of these and other innovative structures[10,11].

Table 1. Summary of cell performances for single-crystal and polycrystalline Si technologies. Standard terrestrial (AM1.5 spectrum, 100 mW/cm^2, 25°C, total areas) conditions are used unless otherwise indicated.

Source	Date	Total Area [cm^2]	Voc [mV]	Jsc [mA/cm^2]	FF [%]	Efficiency [%]	Comments
EMC	9/3/85	4.100	592	31.50	79.1	14.8	Ribbon
Spectrolab	6/5/85	15.470	595	36.70	76.9	16.8	Single crystal Si
Spire	10/28/85	4.020	634	36.30	81.6	18.8	Single crystal Si
Stanford	6/3/86	0.152	681	41.00	78.4	21.9	Point-contact cell
Oak Ridge	10/3/86	4.000	657	36.00	81.6	19.3	Single crystal Si Single crystal Si
Astro-Power	11/19/86	0.120	536	26.00	68.5	9.6	Thin film poly on ss
Westinghouse	5/8/85	1.017	602	31.60	80.7	15.4	Web; Direct, 28°C
	11/29/84	24.500	598	30.40	79.5	14.5	Web; Direct, 28°C
	4/11/85	1.004	637	33.70	76.2	16.5	Single crystal Si
Univ. of New South Wales	7/30/86	4.010	666	37.20	83.2	20.6	Single crystal Si
	9/25/85	4.120	608	35.70	73.1	17.3	Poly Si
	4/7/87	0.801	628	41.50	79.6	20.8	Single crystal: Conc.
	7/23/87	11.980	629	37.30	79.1	18.6	Single crystal: Large area

Table 2. Summary of cell performances for thin-film polycrystalline technologies. Standard terrestrial (AM1.5 spectrum, 100 mW/cm^2, 25°C, total areas) conditions are used unless otherwise indicated.

Source	Date	Total Area [cm^2]	Voc [mV]	Jsc [mA/cm^2]	FF [%]	Efficiency [%]	Comments
ARCO	6/17/88	2.400	464	38.50	65.4	11.7	ZnO/CdZnS/$CuInSe_2$
	6/17/88	2.400	430	17.10	66.1	4.9	a-Si on $CuInSe_2$
	6/17/88	—	—	—	—	14.6	Tandem: A-Si on $CuInSe_2$
Boeing	1/14/86	1.076	441	33.80	68.5	10.2	Four-terminal $CdZnS/CuInSe_2$
	12/3/86	97.000	1779	7.98	63.9	9.1	Submodule: $CuInSe_2$
	12/30/86	1.074	509	30.40	66.0	10.2	$CdS/CuInGaSe_2$
IEC	9/2/87	1.028	445	35.00	64.6	10.1	$CdZnS/CuInSe_2$
ISET	5/11/86	1.045	410	26.80	66.6	7.3	Tandem design $CdS/CuInSe_2$
SERI	6/12/85	1.033	446	35.30	65.3	10.3	Electroplated Layer $CdS/CuInSe_2$
SMU	4/14/88	1.022	736	21.90	65.7	10.6	Glass/SnO_2 / CdTe/HgTeAg
AMETEK	4/29/88	1.053	763	20.10	71.8	11.0	Glass/SnO_2 / CdS/CdTe/ZnTe/Ni

3.2 Polycrystalline Thin Films

Improvements in cost and performance may also be realized by utilizing other semiconductors for solar cells. The arguments for *thin-film* devices for terrestrial photovoltaics are primarily based on materials utilization (less needed and more efficient module area coverage), large-scale production potential, and lower energy input production. The first thin-film cells, Cu_2S/CdS were actually developed for *space applications* , with the promise of better power-to-weight ratios--an important parameter for the early satellite missions. The **reliability** problems virtually *eliminated* work on this particular cell type for both space and terrestrial applications -- although 1 cm^2 cells with efficiencies in excess of 10% were reported and several commercial companies were established to market this technology [64,65].

3.2.1 Copper-Indium-Selenide : Interest in Cu-ternary semiconductors for possible solar cell applications began in the early 1970's, precipitated by the problems that existed with both the Si and Cu_2S cells. New or less-studied PV materials were investigated. Among these, I-III-VI_2 and II-IV-V_2 chalcopyrites received serious attention, and the Cu-ternaries evolved as attractive candidate photovoltaic semiconductors after p-$CuInSe_2$/n-CdS had been shown to be a broadband optical detector. The evolution and development of the Cu-ternaries has been remarkable. The first single-crystal cells were demonstrated in 1974-75[12]. Subsequently, thin-film analogues were reported, with efficiencies reaching above 6% by 1978 [13]. Thin-film cells of CdS on $CuInSe_2$ produced by the three-source evaporation techniques were confirmed with greater than 9% efficiencies [14]. The first 10% cells were measured in 1982, with the best devices now confirmed at 11.3-11.7% under AM1.5 global conditions[15]. The best of these cell has been produced by ARCO Solar, with the 11.7% efficiency for a 2.4cm^2 area cell. The current status of the thin-film polycrystalline cells is summarized in Table 2. Large- area cells (100 cm^2) and modules (1000 cm^2) have now been confirmed at 11.1%[30].

Two *positive* and perhaps unique factors can be cited in favor of this thin-film technology. The first is its apparent *stability*. It has been tested unencapsulated for extended periods of time, with and without illumination, and shows no inherent degradation. In this respect, it is probably the most stable of the advanced devices. No degradation trends in any of the parameters are observed for this typical device-even after testing for more than 9000 hours. This feature, along with its reasonable thin-film performance, make this cell a viable candidate for eventual utilization. Recently, some first generation modules have been subjected to the Block V module acceptance tests developed under the U.S. DOE Large-Scale Array Program, with positive results. These reports, although still preliminary, are encouraging. A second positive indication for this thin-film technology is that it is possible to produce larger area modules (~1000 cm^2) with essentially the same conversion efficiencies as the best smaller area (1-4 cm^2) cells--both in excess of 11%. This gives some confidence that the process is scaleable--a definite requirement for any of the PV approaches. This demonstration that the performances are not limited to laboratory or research cells, but can be produced in commercial scale modules, is one of the more significant developments in the evolution of thin-film photovoltaics.

Recent advances in both sputtering and non-vacuum methods (e.g., electroplating) of depositing quality $CuInSe_2$ layers have been encouraging. Commercial products from pilot plants using these methods are expected shortly, and will provide a better basis for evaluating the cost-effectiveness of the processing as well as the performance of the devices/modules. The early criticisms on the supply and costs for In seem to have become less prevalent. Currently, In is produced as a by-produced of the zinc refining process, and resources are only estimated. Proponents of In-based cells minimize any material-constraints, but the issue is one that is not discussed with "competing" technologies such as amorphous and crystalline Si. The cost, abundance and geographical source of materials are always of importance for the development of any technology. Regardless, this material has emerged as one of the more promising of the advanced technologies.

The low V_{OC}, a bothersome problem with this cell type, has prompted the investigation of methods of engineering the material to provide better interface properties. Other window semiconductors, such as ZnO, have shown promise[15]. Gallium has been introduced at the $CuInSe_2$/window-layer interface to unpin the Fermi level, and increase the V_{OC}. (This approach led to the previously-cited highest efficiency $CuInSe_2$ cell to date.) Two approaches provide for the introduction of either Ga to form $(Cu,Ga)InSe_2$ or S to form $CuInSe_xS_{1-x}$. These changes increase the bandgap of the p-absorber somewhat, increasing the built-in potential. Although increases in V_{OC} have been successfully demonstrated, the short-circuit currents have decreased along with cell fill-factors, diminishing the performance significantly. Recently, a $(Cd,Zn)S/CuGaSe_2$ thin-film cell (produced by Boeing Aerospace Co.) was confirmed at 10.2%--an event that is certain to bring some attention since the open-circuit voltages are higher and the In has been replaced, albeit with another less-than-abundant element.

(ii) Cadmium Telluride: Cadmium telluride has been receiving attention as a candidate photovoltaic material since the early-1960's. Although its 1.4eV bandgap is well-matched to the terrestrial spectrum, the problems with this compound semiconductor have been materials-relatee. It is difficult to electrically contact CdTe--especially the p-type material. The electrical properties are very difficult to control. Also, it tends to be semi-insulating. Metallic dopants, such as Cu, that do lower the resistivity, have very high diffusion coefficients. Finally, the cells themselves are many times unstable.

Much of the pioneering and early work with this technology was accomplished on single crystals. Although some thin-film materials/device research was undertaken, the strength of this research was to provide sound technical information on which further device development could be based. Attention was provided for thin films when screen-printed and sintered CdTe cells were reported with greater than 10% efficiencies by Matshusita. This work has further developed, with better than 5%, 0.5 m^2 modules, and a plan to commercialize the thin film product to power calculators. In addition, this company has recently reported adequate stability from outdoor testing. Cadmium telluride cells grown by close-spaced vapor transport were reported to have very high efficiencies by Tyan *et al.* for small areas[16]. The first confirmed high efficiency thin-film CdS/CdTe and $CdS/Hg_xCd_{1-x}Te$ (with $x < 0.15$ to provide a sufficiently wide bandgap, low resistivity and easier contacting) with 9.4% and 10.1%, respectively, for 4 cm^2 devices were reported by Basol *et al. [*18]. Several other devices have been reported in the literature, including a claimed 10.5% SnO_2/CdTe cell with a 4 cm^2 area by ARCO Solar[35]. The best cells (Table 2) include that confirmed from Chu *et al.*, fabricated using closed-space vapor deposition[17]. The efficiency is 10.6%, and has shown no degradation over weeks of testing; and Ametek, an 11% cell made by electrodeposition verified. Recently, a commercial venture, which had its beginnings with the spraying of cuprous sulfide solar cells, announced plans to market 1 ft^2 (0.093 m^2) area panels, fabricated by a proprietary method. This variety of methods for making good, device-quality CdTe thin films (in large areas) is one strength for the technology. Another is that CdTe and its allows have other applications besides photovoltaics, permitting the co-emergence of technologies. The problems of contacting, instability and the low commercial interest and base specifically for solar cells must be offset. Many thin-film photovoltaic experts consider polycrystalline CdTe to be the technology of the future.

3.3 Amorphous Thin Films

In contrast to crystalline materials, amorphous semiconductors have neither short nor long range structural order. Amorphous materials first received attention for the Xerography process in 1938. Switching phenomena in amorphous semiconductors was discovered by S.R. Ovshinsky in 1958, working with chalcogenide glasses[19]. The demonstration of the ability to controllably-dope a-Si:H n- or p-type by Spear and LeComber[20]. was an important discovery for electronic applications. The first solar cells utilizing a-Si:H were fabricated in 1974, and the report of a 5.5% Schottky-barrier cell (with 0.07cm^2 area) by Carlson and

Table 3. Summary of cell performances for amorphous technologies. Standard terrestrial (AM1.5 spectrum, 100 mW/cm^2, 25°C, total areas) conditions are used unless otherwise indicated.

Source	*Date*	*Total Area* [cm^2]	*Voc* [mV]	*Jsc* [mA/cm^2]	*FF* [%]	*Efficiency* [%]	*Comments*
Brookhaven	4/30/86	0.023	832	14.60	66.3	8.1	p-i-n
Chronar	10/15/85	1.045	880	17.20	64/9	9.8	p-i-n
	1/4/88	0.980	2510	7.20	64.8	7.4	a-Si/a-Si/a-Si:Ge
	6/24/88	1.000	1664	7.20	68.3	8.1	a-Si/a-Si:Ge
	3/10/86	0.284	878	14.40	65.9	8.3	Photo CVD
ECD	2/16/88	0.268	940	15.20	69.4	9.9	ITO/a-Si/ss
	2/16/88	0.268	1640	10.10	69.6	11.6	ITO/a-Si/a-Si:Ge/ss
	2/16/88	0.268	739	19.80	59.6	8.7	ITO/a-Si:Ge/ss
	2/16/88	0.268	2541	6.96	70.0	12.4	ITO/a-Si/a-Si/ a-Si/ss
IEC	11/7/87	0.284	862	17.60	65.8	10.0	Photo CVD
3 M	1/22/87	0.140	874	13.80	64.7	7.8	a-Si on Kapton
Solarex	4/16/87	1.077	879	18.80	70.1	11.5	a-Si
	10/1/87	0.758	1685	9.03	68.1	10.3	a-Si/a-Si:Ge
Spire	12/9/86	0.099	878	16.60	72.2	10.5	a-Si
	6/5/85	0.102	1586	6.90	57.4	6.3	a-Si/a-Si:Ge
UPG	1/4/88	1.010	876	13.80	69.6	8.4	a-Si
Vactronics	11/11/86	0.256	822	11.40	60.5	5.7	a-Si
SERI	2/10/88	0.052	852	16.10	64.5	8.9	a-Si

Table 4. Light-induced changes in amorphous Si solar cells.

- Rapid drop in cell efficiency during the first 48 hr, followed by a much less rapid decay (saturation);
- Reversible by thermal annealing at 150-200°C;
- Caused primarily by changes in the properties of the undoped layer;
- Magnitude of the change depends on the thickness of the i-layer. Cells with thin (less than 0.3μm) layers are relatively stable. After some time, degradation is expected as the depletion width shrinks;
- Magnitude of the changes in the cell decreases with increasing temperature. Cells operating above 90°C are essentially stable since the defect creation and annealing rates are similar;
- Most and greatest changes occur when the cell is in the open-circuit condition;
- Cells illuminated through the p-layer of pin cells are more stable than cells illuminated through the n-layer;
- Changes in the cell can be induced by either light or by current injection in dark;
- Addition of ppm concentrations of boron or phosphorus to the undoped layer generally (not al ways) improves cell stability, with loss in efficiency;
- Co-doping the undoped layer with combinations of P and B improves the stability of some de vices, with loss in efficiency;
- The μt product, as well as the hoe diffusion length, decreases with light exposure;
- Light exposure increases the diode quality factor.

Wronski[21] provided the photovoltaic scientific community with a viable new field of R&D. Since then, the amorphous Si:H market has thrived, building experience initially in utilizing the cells to power watches and calculators, and currently expanding with relatively-large (100 kW) field-research evaluations (demonstrations) into the energy generation capabilities.

(i) Amorphous Si:H Cells: The evolution of amorphous cell efficiencies is mirrorred with efficiencies steadily improving from about 2.5% to well above 10% in the past ten years [3]. Some care must be taken in interpreting and comparing efficiency reports, however. Many are *"active-areas"* and not *total area* measurements, and the area definition is not contained in many of the publications. This makes comparisons between reports unfair. Anolther problem with amorphous results relates to cell stability (discussed in a later section). Since many effects can contribute to the change in efficiency, only the highest measured efficiency is usually reported. It is true that many >10% amorphous cells have been fabricated, but relatively few are confirmed at the same efficiency at a later time or at a cooperating measurement facility. Table 3 provides a summary of the confirmed amorphous Si cell parameters. Detailed summaries of cells reported in the literature can be found in several review articles.

The development of various device structures has been an integral part of the evolution of cell performances and reliabilities. The first cells were primarily metal-semiconductor junctions, as shown in Fig. 3a. Severe stability problems were inherent to the Schottky barrier design, although it continues to serve a useful purpose for research diagnostics. The metal-semiconductor-structure was also used in many device studies (Fig. 3c). In 1978, the heteroface p-i-n structure (Fig. 3b) was developed, having the advantages of reproducibility. larger area fabrication, control of cell parameters, and higher efficiency. Most current cells are based upon this structure. Voltages could be increased by using stacks of amorphous cells-called *heterostructure tandem cells*, as shown in Fig. 3c. Many of the improvements in the operating characteristics of these cell types are attributable to the increased understanding of the material and improvements in film quality. Research efforts continue with new cell structures such as the a-SiC/a-Si:H heterojunction, the superlattice window, alloyed structures, and the random reflection interface.

The methods to produce solar-cell-quality amorphous Si alloys have been expanding. Plasma deposition (glow discharge) remains the major film production method. Its rather low deposition rate has initiated work in reactive sputtering, chemical vapor deposition (CVD), sputter-assisted plasma CVD and plasma deposition of higher order silanes, photo-assisted CVD, plasma-confined CVD, and electron cyclotron resonance (ECR) CVD. This variety of useful methods, as well as the introduction of multiple-chamber systems, as made this technology among the leaders in large-area production methodologies. Amorphous Si cells now account for about one-third of the world's photovoltaic market--with more than 10 MW expected to be shipped in 1988.

(ii) Cell Stability Issues: For this or any photovoltaic technology to reach acceptance by a broad market, both cells and modules must have *long-term stability*. Once moderately-efficiency a-Si:H devices wee produced, it was observed that they possessed a quality less than desirable for a solar cell -- they degraded when exposed to light. This is known as the ***Staebler-Wronski effect***, named for those who reported it first in 1977[22]. A number of models accounting for the causes of this *light-induced degradation* have been proposed, but none has yet emerged as the accepted explanation [124,125][. Amorphous cells exhibit changes in performance after exposure to light, independent of their cell configuration--Schottky, MIS or p-i-n. In general, most of the degradation is observed in the first 48 hours of operation, and is accompanied in a drop in efficiency of 15-25%[42]. The major photodegradation is manifest in a change in the device fill-factor[22]. The light-induced degradation problem has become one of the most investigated phenomena in photovoltaics, due obviously to its impact on this expanding and promising technology[22]. Almost every conceivable experimental technique has been used to elucidate the effect. Data have been reported on the kinetics of the annealing process, the reversibility, the incident light wave-

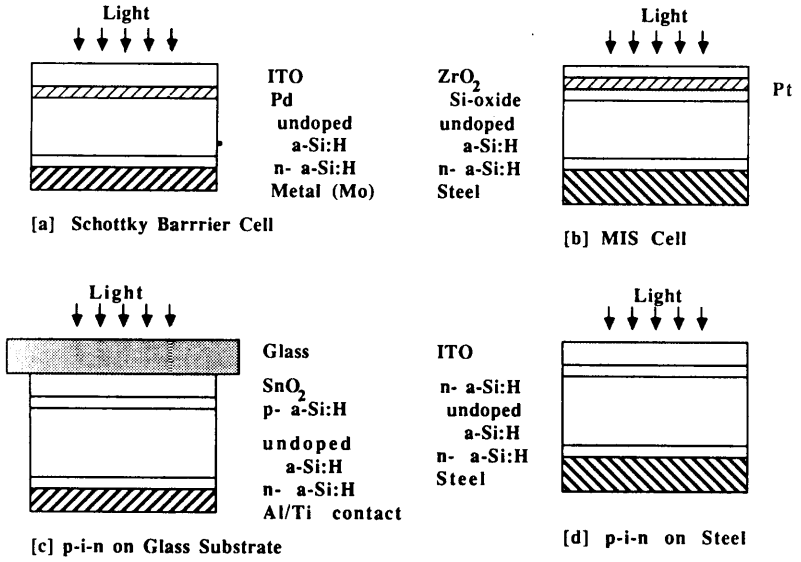

Fig. 3. Amorphous Si:H cell structures.

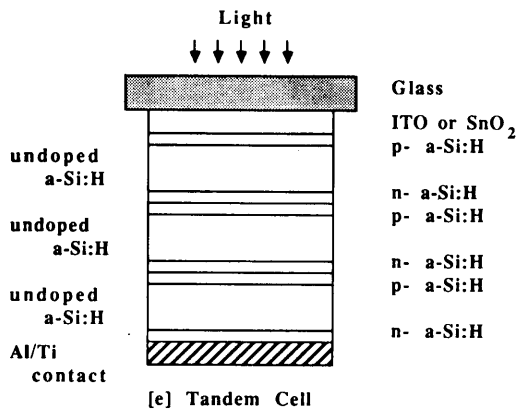

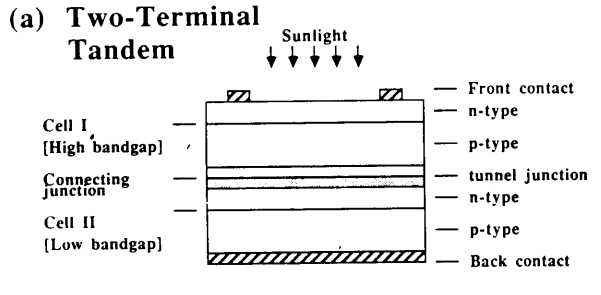

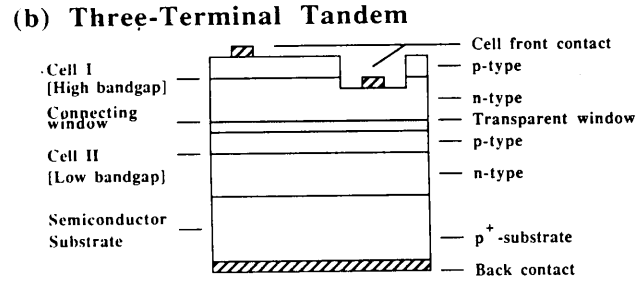

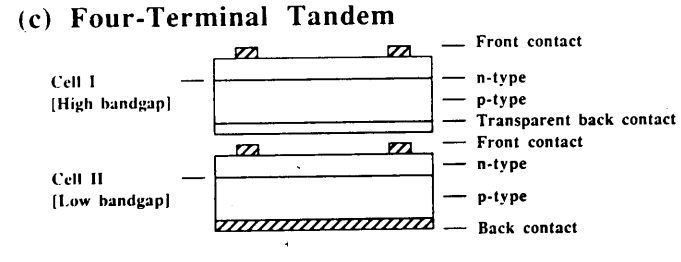

Fig. 4. Structures of very-high efficiency tandem cells.

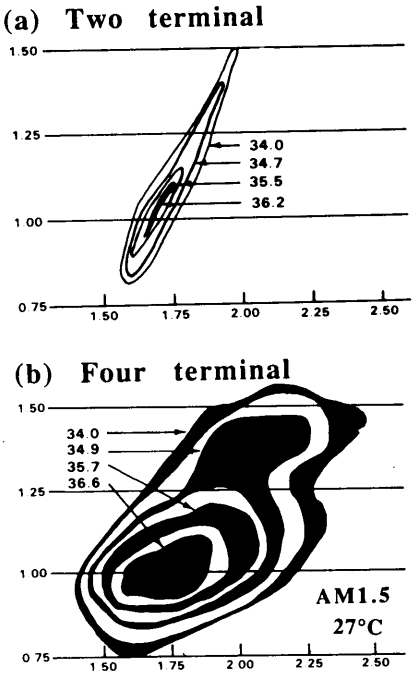

Fig. 5. Calculations of efficiencies for various tandem cell components.

length dependence of the effect, the temperature dependence of defect creation, impurity concentration, electron bombardment, doping, film hydrogen levels, film internal stress, source silane gas composition, etc. The results have been reported by many laboratories, using many techniques, and the experiments have been performed on many different amorphous Si:H films. Common to most observations is theat optical exposure of the semiconductor increases the density of neutral silicon dangling bonds. The optical exposure causes metastable states in the gap to increase in density, and the Fermi level moves toward midgap. These meta-stable defects in undoped a-Si:H are produced by recombination of excess carriers, after these excess carriers are created--either by illumination or by carrier injection. The generally-observed properties associated with a-Si:H solar cells are summarized in Table 4.

The problem remains an important and tenacious one for this technology. The reasons are scientific (amorphous physics is still embryonic and developing), experimental (the *"amorphous silicon"* investigated varies from laboratory to laboratory) and political (research groups and the industry are reluctant to publish data because of the sensitivity of the issue). However, this area is beginning to open, and technological advances are providing a basis for understanding the problem. The general major features of the light-induced degradation effect have been identified and progress is being made. Control of material quality and doping-impurity concentrations helps to minimize the degradation. Stability data on multijunction cells suggest that they are currently more stable than single-junction devices, primarily because the layers are (especially the i-layers) thinner, the current is lower, and the electric field covers more of the material. Controlled doping of the intrinsic amorphous layer with either boron or phosphorous (or both) improves stability, but at a cost of a decrease in efficiency. Three models are now being considered to explain the kinetics of the light-induced degradation: a bond-breaking model, a negative effective correlation energy model, and a void-defect model. Each of these theories has its strengths and limitations, but progress toward explanation of the light-instabilities is being made. These results are required for ultimate solution of the problem and acceptable module stability.

Before closing this brief discussion of cell stability--primarily the Staebler-Wronski effect -- it should be pointed out that reliability issues do not terminate with the cell. Certainly the experience with the deployment of single-crystal Si modules has shown that problems with encapsulants, corrosion, polymer degradation, glass or polymer fracture, delamination, electrochemical effects, environmentally-induced layer interdiffusions all exist. In fact, initial, but extensive, outdoor exposures testing and laboratory measurements indicate that the amorphous and other thin-film technologies -- although they do benefit from previous module work on single crystal Si -- have some special problems due to the device structures, configurations, current densities, cell size and separation, laser scribe lines, metallizations used, etc. Of equal importance to the cell stability issues will be module reliability issues, and researchers and the photovoltaic industry are aware of them. Currently, several joint industry-research laboratory-university-utility programs are underway to establish standardized thin-film module test and acceptance procedures.

3.4 III-V Semiconductors

Semiconductors such as GaAs, GaAlAs, GaInAsP, InAsP and InP have been receiving considerable attention for high-speed and optical electronics applications. These materials also have exceptional characteristics for photovoltaic applications. Because of their cost, solar cells utilizing these III-V semiconductors are usually considered for terrestrial concentrator or for space applications, in which the cost of the cell is less significant due either to the increased irradiation or requirements for extremely high performance. In this section, however, single-junction III-V cells will be discussed for both flat-plate and for concentrator modes of operation, since there are arguments that these materials will eventually be cost-effective for both applications. Concentrator systems are more competitive with their flat-plate counterparts in high-irradiance, very sunny locations, and pehaps have promise in the shorter term for economic deployment.

Table 5. Summary of cell performances for III-V technologies. Standard terrestrial (AM1.5 spectrum, 100 mW/cm^2, 25°C, total areas) conditions are used unless otherwise indicated.

Source	*Date*	*Total Area* [cm^2]	*Voc* [mV]	*Jsc* [mA/cm^2]	*FF* [%]	*Efficiency* [%]	*Comments*
ASEC	12/14/85	4.044	1006	24.80	82.7	20.7	Direct; 28°C,GaAs
				24.30			(Global)
Kopin	5/12/88	4.000	979	26.70	79/7	20.9	CLEFT, Separated
	10/13/87	1.003	976	27.50	83.4	22.4	CLEFT, Unseparated
	6/3/88	1.000	1208	18.20	85.5	18.8	AlGaAs/GaAs
	10/13/88	1/003	1019	27.40	84.9	23.7	GaAs
SMU	7/23/85	1.009	822	19.70	62.2	10.1	Direct; 28°C, Thin Film, GaAs:Ge:Graphite
Spire	12/15/86	0.249	1021	27.80	83.7	23.7	GaAs
	4/30/86	0.250	1200	16.20	82.6	16.0	GaAlAs
	4/9/87	0.250	860	27.80	84.4	20.4	InP
	4/24/87	0.249	1213	17.60	83.0	17.7	GaAsP
	11/19/87	0.250	869	22.70	76.9	15.1	GaAs on Si
	11/19/87	0.249	1199	26.50	73.9	23.4	GaAs on Ge tandem (Eff. may be higher)
Varian	8/6/87	0.496	2382	11.30	81.8	22.1	Two terminal tandem
			1393	11.60	75.9	12.2	1.93eV GaAlAs top cell
			993	13.70	80.4	10.9	GaAs bottom cell
						23.1	3-terminal tandem
	8/6/87	4.000	1244	16.00	84.6	16.8	1.75eV GaAsAs
	7/9/87	4.008	1037	26.70	88.2	22.7	GaAs
	7/9/87	2.932	730	17.40	78.7	10.0	1.15eV GaInAs bottom cell under 1 75eV GaAlAs
	8/15/88	4.000	1046	27.12	84.5	24.0	p-n GaAs
SERI	10/29/84	0.099	973	22.80	85.2	18.9	Direct; 28°C, GaAs
SERI	4/11/85	0.100	1254	13.10	85.8	14.1	GaAsP
SERI	5/2/88	0.108	810	27.50	82.6	18.4	ITO/InP
	2/25/88	0.108	878	27.80	83.1	20.3	InP

Table 6. Summary of thin-film tandem cell approaches.

Bottom cell	*Top cell*	*Comments*
a-Si:Ge:H	a-Si:H	12.7% achieved by EDC
$CuInSe_2$	a-Si:H	14.6 % achieved by ARCO
$CuInSe_2$	CdTe-alloy	Alloys with Mn, Mg or Zn
[Hg,Cd]Te	CdTe-alloy	Research cells studied
[Hg,Cd]Te	[Hg,Zn]Te	Structure proposed
$CuInSe_2$	$CuGaSe_2$	In development
[Hg,Cd]Te	a-Si:H	In development
$CuInSe_2$	GaAs	Space applications
[Hg,Cd]Te	GaAs	In development
Si	GaAs	In development

The best efficiencies for single-junction cells are summarized in Table 5. It should be noted that a number of laboratories (Varian, MIT Lincoln Laboratory, Spire Corporation, Kopin, for example) have been able to produce GaAs-based cells with efficiencies in excess of 21%, with large areas. These efficiencies are higher under concentration. For example, the Varian cell was tested with 26% conversion efficiency at 800 suns. An interesting development for III-V semiconductor cell technologies is the cleavage of lateral epitaxial film technology of CLEFT process, developed by Fan et al., which allows reuse of expensive substrates[23]. In the CLEFT process, a *single-crystal GaAs film* is formed on the reusable GaAs substrate by organo-metallic CVD. Cells in excess of 20% have been produced from thin CLEFT material. The cost of the high-quality, single-crystal III-V substrate is a major one in these technologies, and this process has the potential to lower this component cost considerable. Much of the work on InP cells has been directed recently toward space applications. Cell efficiencies in excess of 21% have been reported for homojunctions, with several confirmed results at or near 20.4% AM1.5 (17.7% AM0). Alternative approaches, using thin conductive oxides to produce either heterostructures or shallow homojunctions, have also shown promising performance characteristics, with the best cells having AM1.5 efficiencies of 18.5%.

4. MULTIPLE-JUNCTION APPROACHES

In order to approach the extreme performance limits (e.g., concentrators with greater than 35% efficiency, thin-film modules exceeding 20% efficiency), some non-conventional approaches to photovoltaics must be employed. Single-junction cells are constrained by the second law of thermodynamics to efficiencies below ~30% for usual device configurations [24]. The motivation to adopt multiple junction or tandem arrangements is simple. If one stacks two or more solar cells in such a way that a portion of the light passes through the top cell and can be utilized by the bottom device, one can more effectively use the solar spectrum, and have increased efficiencies since the two (or more) cells occupy the same area. This concept has already been utilized in the case of amorphous tandem cells, discussed in the previous sections, in which the primary objective is to increase the output voltage. The cascade system can also utilize different semiconductors which utilize or respond to different portions of the solar spectrum. Two such methods have been used. The first (Fig. 5a) is the spectrum-splitting approach, which utilizes special optics to provide two (or more) separated cells with different energy portions of the solar spectrum. This system has been demonstrated for Si GaAs cells by Varian, with a reported efficiency of about 28% (with optical losses subtracted)[24]. However, not much further work has continued with this concept. More attention is devoted to the second case, the tandem configuration.

This tandem configuration really has several options, and these are illustrated in the cell structures of Fig. 4. The *first* is a completely integrated structure or **two-terminal tandem**, presented for a two-cell configuration in Fig. 4a. A major problem is the identification and fabrication of a conducting region which has adequate electrical properties as well as sufficient optical transparency for the bottom cell. A usual technique is to use a *tunnel junction*, which sometimes has stability problems[46]. The *second approach is a* **three-terminal tandem**, shown in Fig. 4b. Problems with voltage matching have initially impeded work on this structure, although some recent design suggestions have revived some interest in it[47]. The *third approach*, the **four-terminal connection**, has the cells completely separated. The top cell is sufficiently transparent (both top and bottom contacts) to allow the required light to be incident on the bottom device. This approach has several advantages, including a larger number of semiconductors available for optimal utilization. Figure 5a shows the calculated bandgap of the bottom cell as a function of the top cell bandgap, illustrating efficiency contours for the *two-terminal tandem*. The "target" for the best devices is quite small, as is the range of available semiconductors. Comparing this to the same calculation for a three-terminal system (Fig. 5b), it can be seen that the possibility of available semiconductors is significantly larger--indicated by the sizeable "target" area. Thus, the top cell can have a bandgap in the range of about 0.9 to 1.1 eV and the bottom cell in the range of 1.6 to 1.85 eV for optimum efficiency. This argument holds not only for tandems utilized for concentrators, but for flat-plate applications as well.

The combinations of four-terminal tandems are more likely for flat-plate, ***thin-film cascades***. Table 6 presents a summary of semiconductors that are being considered for such configurations, along with some reported performance results. The conditions under which many of these preliminary results were taken are unknown. Problems exist in measuring the efficiencies of stacked cells since it is extremely difficult to measure the spectral response of the system. However, the important feature in each case is that the total stacked efficiency is higher than the efficiency of either cell--indicating that the tandem is operating. Many groups believe that the eventual economic deployment of thin-film photovoltaic technologies will be in the form of these tandem, thin-film structures [137,138], with operating efficiencies in the 17-22% range. Some recent and important impetus to the development of commercial thin-film tandem modules was provided by the ARCO Solar approach which utilizes higher-bandgap amorphous Si:H over a thin-film CdS/ZnO/$CuInSe_2$ structure in a four-terminal configuration. The confirmed efficiency of this tandem was 14.6%, with the top amorphous cell having a 9.7% efficiency, and the bottom lower-bandgap cell, 4.9%.

5. SUMMARY

This has been a rather brief discussion of a large number of solar cell approaches. This paper is not meant to be an *exhaustive* treatment. The major and state-of-the-art approaches have been discussed. The choice of technologies has not been made by any of the photovoltaic programs worldwide. The promise exists both for thin films and single crystals, for flat-plate and concentrator approaches. These alternatives will receive their closest scrutiny in the next five years, and some will be abandoned. It is probable that other devices and other materials will be introduced. The process needs a large amount of *quality* technical input. Performance includes not only energy output and efficiency, but reliability and long lifetime under real operating conditions. The emphasis is sometimes on cell performance due to the requirements for alternative approaches, but module research and reliability will grow in importance as the technologies come on line. Photovoltaics has developed significantly during the past 30 years. Arguments for its deployment can be made on social, philosophical, political and technical grounds. However, realistically, *much* research and development remains before the technology can have a large impact on the world's energy generation. This is a challenge, and currently one primarily for the scientific community which must take the lead in providing the understanding and demonstrations that photovoltaics requires.

Acknowledgements: This work was performed, in part, under U.S. Department of Energy contract DE-AC02-83H10093 with the Solar Energy Research Institute. However, some of the research opinions and conclusions are those of the author, and do not necessarily conform to those of SERI or the federal government. The author would like to express his appreciation to Dr. Fouad Abou-Elfotouh, Dr. Timothy Coutts, Keith Emery, Kenneth Zweibel, Dr. Ed Sabisky, Dr. John Benner, and Dr. Robert McConnell of SERI, Dr. M.A. Almass'ari of King Saud University and Dr. Ashraf Yahia of Ain Shams University for their information, help and criticisms in preparing this review.

[1] - See, for example, Wolf, M., "Historical development of Solar Cells", Proc. 25th Power Sources Symp., IEEE, New York, 1972, pp. 120-124.
[2] - Coutts, T.J., Ed., Solar Cells 6, 207, 1982.
[3] - R. Annan, Ed., U.S. Department of Energy Five Year Research Plan 1987-1991, Photo voltaics: Electricity from Sunlight, U.S. Dept. of Energy, Washington, DC, 1987.
[4] - Fahrenbruch, A.L., and Bube, R.H. Fundamentals of Solar Cells, Academic Press, New York, Chapter 1, 1-25, 1983.
[5] - Fisher, H. and Pschunder, W., Proc. 12th IEEE Photovoltaic Spec. Conf., IEEE, New York, pp. 528-533, 1977; Also, Ciszek, T.F., J. Crystal Growth 66, 655, 1984.
[6] - Ghosh, A.K., Fisherman, C., and Fang, T., J., Appl. Phys. 50, 1976, 1979.
[7] - Chu, T.L., van der Leedem. G.A., and Yoo, H.I., J. Electrochem. Soc. 125, 661, 1978.
[8] - Barnett, A.H., Proc. 8th European Photovoltaic Solar Energy Conf., Italy, Reidel, The Netherlands, 1988.

[9] - Green, M.A., Blakers, A.W., Wenham, S.R., Narayanan, S., Willison, M.R., Taouk, M., and Szpitalak, T., Proc. 18th IEEE Photovoltaic Spec. Conf., IEEE, New York, pp. 39-42, 1986.
[10] - Swanson, Proc. 19th IEEE Photovoltaic Spec. Conf., IEEE, New York, pp., 1987.
[11] - Rohatgi, A., Ed., Solar Cells, Special Issue on High Conversion Efficiency in Single-Crystal Silicon Solar Cells 17, 1-166, 1986.
[12] - Wagner, S., Shay, J.L., Migliorato, P. and Kasper, H.M., Appl. Phys. Lett. 25, 434, 1974.
[13] - Kazmerski, L.L., Ayyagari, M.S., Sanborn, G.A. and White, F.R., J. Vac. Sci. Technol. 13, 139, 1976.
[14] - Mickelsen, R.A., and Chen, W.S., Appl. Phys. Lett. 36, 371, 1980.
[15] - Mitchell, K.W., Ref. 8.
[16] - Tyan, Y.S., U.S. Patent, Polycrystalline Thin Film CdS/CdTe PhotovoltaicCell, 4,207,119, June 10, 1980.
[17] - Chu, T.L., Ref. 10.
[18] - Basol, B.M., Tseng, E.S. and Stafsudd, O.M., Ref. 9, pp. 1745-1746.
[19] - Ovshinsky, S.R., Phys. Rev. Lett. 21, 1450, 1968.
[20] - Spear, W.E., and LeComber, P.G., J. Non-Cryst. Solids 8-10, 727, 1972.
[21] - Carlson, D.E., and Wronski, C.R., Appl. Phys. Lett. 28, 671, 1976.
[22] - Staebler, D., and Wronski, C., Appl. Phys. Lett. 31, 292 (1977).
[23] - Fan, J.C.C., McClelland, R.W., and King, B.D., Proc. 17th IEEE Photovoltaic Spec. Conf., IEEE, New York, 1984, pp. 31-35.
[24] - See, for example, Proc. IEEE Photovoltaic Spec. Conferences, 1976-1988.

SOLAR ENERGY TECHNOLOGY DEVELOPMENT AND APPLICATIONS IN INDIA

Prof. H.P. Garg
Coordinator, Solar Energy Programme
Centre of Energy Studies
Indian Institute of Technology
Hauz Khas, New Delhi - 110016
India

ABSTRACT

India has been the pioneer in the field of Solar Energy Research and the first practical solar cooker was made in India in early fifties. Presently more than 20 research institutions, universities, IITs' are engaged in basic and applied type of research in solar energy. More than 110 private and public undertaking industries are involved in the fabrication and installation of solar energy devices. The Government of India has established a full-fledged Department of Non-Conventional Energy Sources (DNES), whose primary aim has been to coordinate, funding, and demonstration of systems in the field of Non-Conventional Energy Sources. The estimated budget of DNES alone for the year 1987-88, was 77 million U.S. Dollars. Apart from this there are several International collaborative programmes and also of major research organizations like of Council of Scientific and Industrial Research (CSIR), and Indian Council of Agricultural Research (ICAR), whose budget may also be of the order of 30-35 million US dollars. Short term (2-6 weeks) and long term courses (6-18 months) are also offered to students in the field of Non-Conventional Energy in several Indian universities and IITs'.

The Government of India has established nodel agencies, one in each state (more than 20 agencies), whose primary functions have been to demonstrate, install and monitor the various Non-Conventional Energy Devices in their states.

Research and Demonstration programme is in progress in almost all the areas of Solar Energy Research. There is a plan to have 30 MW central power tower system to be installed soon in India. There are three public undertaking firms who are manufacturing silicon single crystal solar cells on commercial scale. A pilot plant for the manufacturing of amorphous silicon cells is also being established.

INTRODUCTION

India has a population of little more than 750 million people living in an area of about 3.28 million sq.km. Around 70 percent of this

population lives in rural areas and the rest in urban centres. The country can be divided into a large number of climatic zones as well as soil, water and geographical conditions. It has 24 states and 7 union territories, which are administered by democratically elected government. The state and Central Governments are all responsible for the production, distribution and consumption of energy in different parts of the country.

India has a good potential for economic growth and much depends on appropriate development strategy and proper direction in the energy sector. The country can become economically viable and self-reliant to a considerable extent if its large manpower and abundant land resources alongwith known technology of development are successfully utilized. The problem is to harness them in a collective national effort so that the latent productivity is realized. Although there is no direct relation between GNP/capita and energy consumption/capita but for India their values are US $ 100 and 366 Kg. coal equivalent respectively while for USA their values are US $ 4990 and 10331 Kg. coal equivalent.

Out of 5.8 lakhs villages having more than 70 percent of Indian population only about 30 percent villages are being supplied with electricity. Nearly forty percent of the total energy consumed in India comes from non-commercial fuels with major portions of these supplies consumed in rural areas. The energy-GDP elasticity coefficient-the ratio of the percentage increase per year of the total energy consumption to the percentage increase per year in the GDP- is high (about 1.8) compared to developed countries. This may be partly due to progressive substitution of non-commercial fuels by commercial fuels and also due to improved equipment, technology, processes employed in industry, transportation and other sectors. Since the consumption of non-commercial fuels is quite high (little more than 40 percent) and that is mostly in rural areas, there is a large scope for the use of renewable sources such as solar energy, biomass, wind, and bio-gas to meet the decentralised requirements such as for lighting, heating, cooking, pumping, and low grade heat.

SOLAR RADIATION AVAILABILITY

India is blessed with high level of solar insolation over wide areas. In the clearest month of the year i.e. in May the global solar insolation varies from about 6.0 kwh/m^2 day in the south and east to about 7.5 kwh/m^2 day in the north and west parts of the country as shown in fig. 1 (Ref.1). During winter months there is more solar insolation (5-6 kwh/m^2 day) in the south and low (4-5 kwh/m^2 day) in the north. During April the radiation received is high and fairly uniform over the whole subcontinent, Gujarat and adjoing areas receiving over 6.5 kwh/m^2 day. On an average the diffuse solar radiation varies from 25-30 percent of global radiation in the dusty cloud free pre monsoon summer months to 50 percent in the monsoon months (Fig. 2). A study of the distribution of sunshine duration for the whole year over the Indian subcontinent shows that 3300-3700 hrs of bright sunshine are received in a year in the northwest and west central zones of the subcontinent and 2900 hrs over the central Peninsula. From these observations, it appears that the whole country is suitable for the utilization of solar energy for various applications throughout the year.

SOLAR THERMAL APPLICATIONS

India was the pioneer in utilising solar energy and the first attempt in this direction was made in early fiftees by a group of scientists at

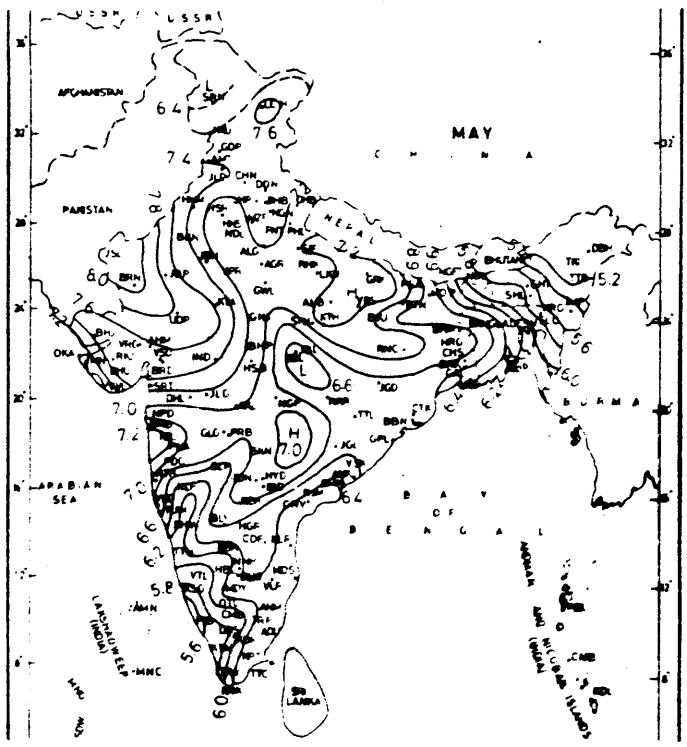

FIG. 1. DISTRIBUTION OF MEAN DAILY GLOBAL SOLAR RADIATION IN MAY (UNIT : kwh/m^2 day)

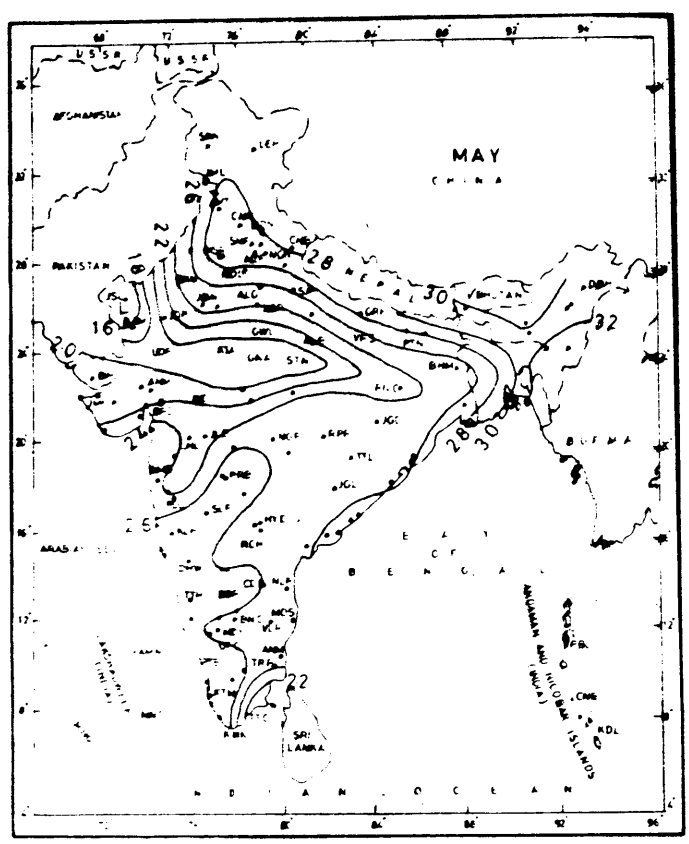

FIG. 2. DISTRIBUTION OF MEAN DAILY DIFFUSE SOLAR RADIATION IN MAY (UNIT : kwh/m^2 day)

the National Physical Laboratory, New Delhi. Presently with the coordinated and sustained efforts of the Department of Non-Conventional Energy Sources (DNES) and many other organisations like Council of Scientific and Industrial Research (CSIR), etc., more than 25 National Laboratories, Universities and IITs' are engaged in R & D activities in the field of Solar Thermal Applications. The studies today include basic materials development, fabrication of solar collectors, concentrators and systems such as water heaters, driers, pumps, passive houses, solar cold storages, greenhouses, cookers etc. Priority is being accorded to applications in agriculture and industrial sectors with a view to reduce the pressure on fossil fuels in these sectors. Increasing emphasis is being laid on system designs for community use. Several public sector undertakings such as Bharat Heavy Electricals Limited, Central Electronics Limited, Tungabhadra Steel Products Limited, National Instrument Limited, Bharat Electronics Limited etc. and more than 110 private firms are actively engaged in the fabrication and demonstration of various solar thermal utilisation devices. An integrated solar energy R & D Programme is shown in Figure 3. From the figure, it is clearly seen that India has a very ambitious programme in the field of Solar Energy Utilisation.

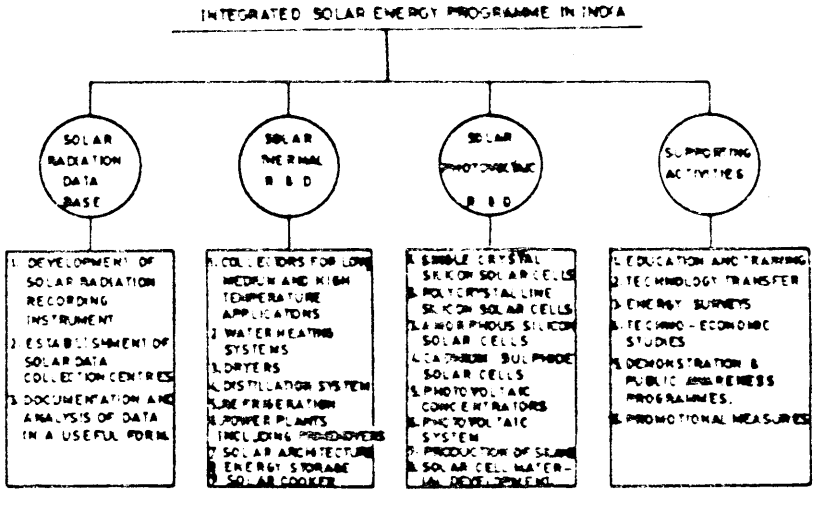

FIG. 3. INTEGRATED SOLAR ENERGY PROGRAMME IN INDIA

The coordinate effort in the development of solar energy collectors and related materials is conducted at several institutions both for low temperature and high temperature applications. The solar collector development programme conducted in India is shown in Figure 4. Presently all flat plate collectors are made of copper tube and copper plate material (Ref.2) coated with black paint or selective coating. Other type of collector systems such as vacuum tube collectors, plastic collectors, etc. are under development. Efforts are also made for the development of linear parabolic and paraboloid concentrating systems and tracking systems for use with the concentrators. The idea of developing these concentrators is to provide low to medium pressure steam for various industrial applications.

Solar water heaters both for domestic and industrial applications are becoming popular in India (Ref. 3). More than 1322 commercial and industrial solar hot water systems of total capacity 3414995 litres/day with 66307 m^2 collector area have been installed by January 1988. In addition to these, 1800 domestic hot water systems with a total capacity 212250 litres/per day and 4333 m^2 collector area have also been isntalled (Ref.4).

Significant advances have also been made in the development and and commissioning of solar drying systems. Several (32 nos.) solar crop driers ranging with a drying capacity from 1 tonne/day to 50 tonne/day have been installed for drying various perishable and cash crops. Solar timber seasoning kilns (35 nos.) have been installed in a few places and have shown promising results. Solar stills (6840 nos.) for providing distilled water for battery charging and also for supplying drinking water in remote areas have been installed and commissioned (Ref. 5).

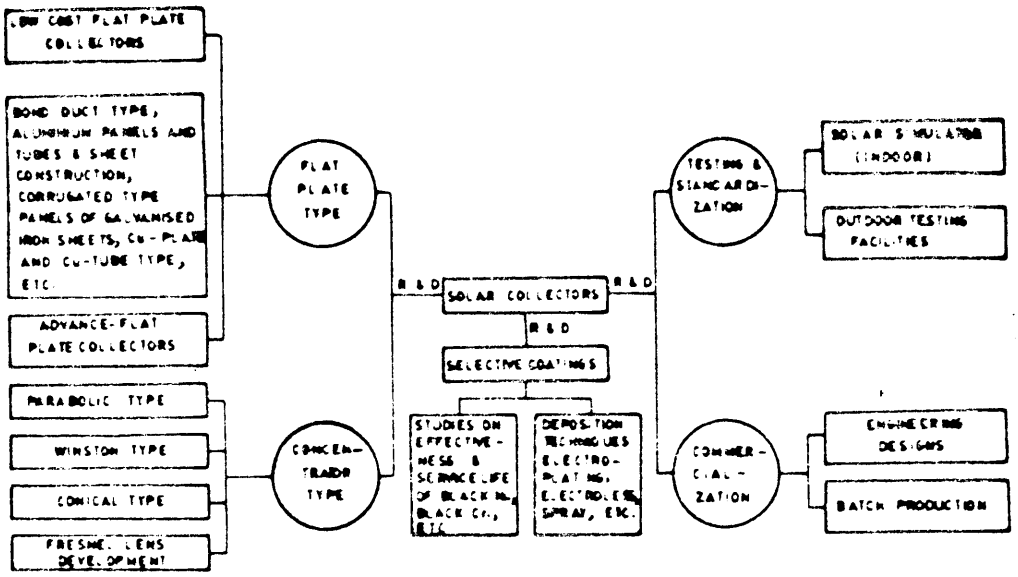

FIG. 4. SOLAR COLLECTOR DEVELOPMENT PROGRAMME

Solar cookers have becomes one of the most popular thermal devices among the users in India. The Department of Non-Conventional Energy Sources provide a subsidy of Rs.150/- for each cooker and under this scheme more than 72000 solar cookers have been sold so far. Efforts are also being made to develop and demonstrate the community type solar cookers. Development work on other solar thermal applications such as pumping of water, refrigeration and air-conditioning, motive power, small scale power generation, solar architecture, green houses, etc. has also been undertaken. Some of the areas identified by DNES for further R & D are systems for generation of power through the solar thermal route, advanced collectors for medium and high temperature applications, refrigeration and airconditioning, solar energy greenhouses in high altitude areas.

The solar energy centre of the Department of Non-Conventional Energy Sources is trying to put up a 50 KW solar thermal power plant using line focus collectors and steam turbine (Ref. 4) at a place near Delhi. A feasibility report for setting up of 30 MW solar thermal power plant has been prepared and various aspects for setting up such a power plant in Rajasthan are being studied. A 30 tonne solar cold storage has been installed at Gorakhpur and the same is functioning well. More than 100 solar huts and TAP collectors for over 140 houses have been supplied to ITBP and army at Leh in the North of India. Three greenhouses for ITBP, Leh have already been installed for growing vegetables.

A 30 tonne solar absorption refrigeration plant is operating in Deoria in Uttar Pradesh and another plant of 10 tonne capacity in Baroda are working satisfactorily. Three solar milk chilling plants of capacity 5000

litres per day, 400 litres per day and 200 litres per day respectively are being installed in Haryana, Maharashtra and Rajasthan. Ten numbers of solar ice-pack freezers are also being installed at ten health centres to study their suitability for preserving life saving drugs and other medicines.

Nearly 50 research and development projects are currently under progress in various research and academic institutions in India in the field of solar thermal energy. Solar thermal energy has successfully been used in the process of extracting Alcohol from sugar cane. A pilot plant based on this technology is now in operation in Maharashtra.

PHOTOVOLTAICS

Electricity is in short supply in India and particularly in rural India. More than 5,00,000 villages are still unelectrified. Looking to the acute shortage of electricity, the Government of India has accorded a high priority to the development of photovoltaic (PV) technology and industrial activity. The government policy provides for scientific and technical cooperation with other countries, and building up a broad range of R & D capabilities and utilizing these from laboratory scale to the pilot plants and industrial activities. The main emphasis is to indigenous production of solar photovoltaic panels supported by indigenous R & D.

The photovoltaic programme in India was initiated about twelve years before by the Department of Science and Technology. By 1980, this development had reached to the stage of bench scale fabrication of solar cells and few solar photovoltaic array were actually fabricated and demonstrated. During the period of sixth five year (1980-1985), a five year National Solar Photovoltaic Energy Demonstration Programme (NASPED) was started in 1980. During the period, the technology for manufacturing of solar cells was unscaled to a level of one mega watt per year at the Central Electronics Limited, Sahibabad, a public enterprise. In 1982, the solar photovoltaic programme was took over by Department of Non-Conventional Energy Sources (DNES) and several R & D projects were sponsored during the year with a view to explore low-cost technologies for silicon suitable for PV applications.

The notable work in the field of silicon is the indigenous production of polysilicon at Metkam Silicon Limited, a company in private sector, and the technology is based on cracking of a mixture of silicon tetrachloride and trichlorosilane in a Siemens type reactor. This company has started regularly production of material at a rate of 25 tonnes per year only about two years ago (Ref. 6). Another breakthrough in India is in the area of crystal growing and wafering. A supply capacity of 5,00,000 wafers per year is available in three companies, viz., Metkam Silicon Ltd., Metur, Tamilnadu; Siltronics, Hosur, Tamilnadu; and Super Semi Conductors Limited, Calcutta. Crystal pulling capacity in public sector is available in CEL, BEL, and BHEL.

A National coordinated R & D project in the area of amorphous silicon solar cells was initiated 1984 involving seven research institutions. The integrated programme is shown in fig. 5. Under this programme small area amorphous silicon solar cells were fabricated which resulted in 8.5 percent efficiency. The scope of the project was further enlarged with a view to establish a pilot plant producing cells at the level of 1 MW per year capacity. Some R & D areas identified are: improving efficiency and stability of cells, increasing film deposition rates, development of multi-

junction cells, new alloying materials and compatible structure. The pilot plant is scheduled to be commissioned in mid 1989.

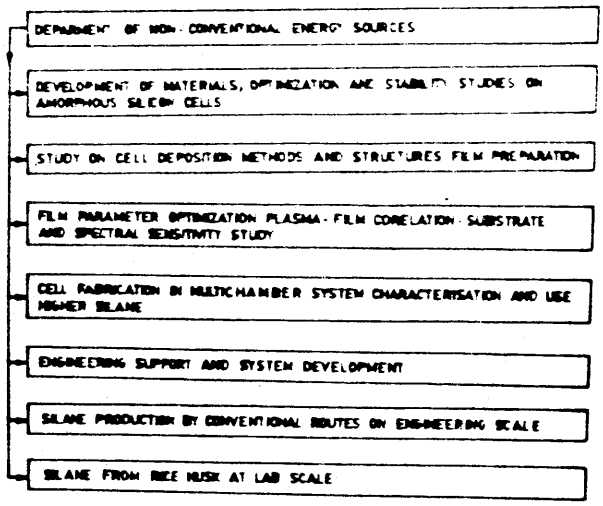

FIG. 5. INTEGRATED PROGRAMME FOR THE DEVELOPMENT OF AMORPHOUS SILICON SOLAR CELL IN INDIA

While basic research in this field is continuing in several National laboratories and IIT's, the technology development efforts are conducted in industries like CEL and BHEL. The Central Electronics Limited (CEL) has a PV production capacity of 2 MW per year and BHEL with a production capacity of 500 kw per year. The Rajasthan Electronics and Instruments Limited and CEL in the year 1985 started producing PV modules at the rate of 1 MW per year. The entire prouction is based on single crystal silicon wafers. The actual production rate is much lower and depends on the funds available from DNES and demand from market. The technological efforts are to reduce the cell/module cost and increase its efficiency.

To create awareness and confidence among users and also to obtain feed back on performance in the field, the DNES has launched a PV demonstration programme which includes; water pumping unit for the supply of drinking water and micro-irrigation, street lights and community lights, PV powered TV, battery chargers, PV operated refrigerators, etc. The demonstration programme is implemented with the assistance of state nodle agencies, acedemic and research Institutions and State electricity boards. So far 9200 street lights, 852 water pumps, 350 television and community lighting units and 631 battery charging units have been supplied upto Feb. 29, 1988 (Ref. 4).

For conducting the above activities like Research & Development, providing subsidy, demonstration programmes, educational and training programmes etc. large amount of funding is required. The Government of India is very keen to sustain the above activity and has allocated around 77 million US dollars for the financial year 1987-88. Although this budget allocation is very small compared to the total plan outlay for this year, however, it is hoped that in future the Department of Non-Conventional Energy Sources would be getting considerably higher budget for the above activities. The approved budget allocation for 1987-88 is shown in Table 1.

Table 1 Approved budget of DNES, India for 1987-88*

Item/head	Allocation (in millions of US $)
I SOLAR THERMAL ENERGY	
(a) Research, Development and Demonstration	1.33
(b) Solar Energy Centre	0.52
(c) Solar Cooker Subsidy	0.23
(d) Subsidy on other Solar Thermal Systems	3.17
Total (I)	5.25
II SOLAR PHOTOVOLTAIC PROGRAMME	
(a) NASPED/Subsidy Programme/others	3.15
(b) Research & Development/Amorphous Silicon Pilot Plant	3.46
Total (II)	6.61
III BIOGAS PROGRAMME	
(a) National Project on Biogas Development	32.85
(b) Community & Institutional Biogas Plants	3.42
(c) Research & Development	0.77
Total (III)	37.04
IV WIND ENERGY PROGRAMME	
(a) Strengthening of Wind Data Base	0.07
(b) Research & Development	1.84
(c) Demonstration & Field Testing	3.46
Total (IV)	5.37
V BIOMASS & DRAUGHT ANIMAL POWER	
(a) Energy Plantation/Demonstration Programme	3.07
(b) Research & Development	1.92
(c) Draught Animal Power	1.15
Total (V)	**6.14**
VI NATIONAL PROJECT ON IMPROVED CHULHAS	6.72
Total (VI)	6.72
VII OTHER RENEWABLE SOURCES OF ENERGY	
(a) Micro Hydel Power	0.77
(b) Ocean Energy	0.07
(c) Chemical Sources of Energy	0.42

(d) Geo-Thermal Energy		0.04
(e) Hydrogen Energy		0.38
(f) Battery Powered Vehicles		0.47
(g) Other Charges		0.04
	Total (VII)	2.19
VIII INFORMATION AND PUBLIC EDUCATION		0.65
	Total (VIII)	0.65
IX M.N.E.S.		
(a) Grants-in-aid, Research & Development		1.46
(b) Other Charges		0.07
	Total (IX)	1.53
X REFUSE INCINERATION PLANT FOR DELHI		1.85
	Total (X)	1.85
XI RURAL RENEWABLE ENERGY SYSTEMS PROGRAMME		0.57
	Total (XI)	0.57
XII REGIONAL OFFICER		0.23
	Total (XII)	0.23
XIII RENEWABLE ENERGY DEVELOPMENT AGENCY		1.73
	Total (XIII)	1.73
XIV SECRETARIAT		0.95
	Total (XIV)	0.95
XV INTERNATIONAL COOPERATION		0.04
	Total (XV)	0.04
	Grand Total	76.87

REFERENCES

1. Mani, A., 'Handbook of solar radiation for India' Allied Publishers, New Delhi, 1981.

2. Garg, H.P., 'Treatise on Solar Energy' John Wiley and Sons, England, 1982.

3. Garg, H.P., 'Solar Water Heating Systems' D. Reidel Publication Co. Ltd., The Netherlands, 1986.

4. Annual Report, 'Department of Non-Conventional Energy Sources (Ministry of Energy), India, 1987-88.

5. Garg, H.P., 'Advances in Solar Energy Tehnology, Vol. I, II & III' D. Reidel Publication Co. Ltd., The Netherlands, 1987.

6. Garg, H.P., M. Dayal, G. Furlan, A.A.M. Sayigh and V.K. Sharma, 'Physics and Technology of Solar Energy, Vol. I & II' D. Reidel Publication Co. Ltd., The Netherlands.

ECONOMIC ANALYSIS OF SOLAR ENERGY FOR INDUSTRIAL USAGE: ITS METHODOLOGY

O. Yul Kwon, Ph.D.
Faculty of Administration
University of Regina
Regina, Saskatchewan, S4S 0A2
CANADA

ABSTRACT

A systematic model of economic evaluation of solar energy for industrial usage has been developed from the perspectives of private firms and government policy makers. This model takes into account institutional aspects of energy as it is utilized in industry. The importance of the sunk cost (or fixed cost) is pointed out in evaluating solar energy. The sunk cost associated with an energy system is continuously incurred regardless of whether the system is in operation or not. Hence, if a solar system replaces an existing conventional system, the sunk cost of the latter should not be part of the benefit of solar energy.

Several important differences between private financial analysis and (social) cost-benefit analysis are pointed out. Interest payments, depreciation charges, and taxes are all treated differently under the two analyses. Also, external effects associated with energy should be included in cost-benefit analysis, while they may not be so in financial analysis.

1. INTRODUCTION

Energy is a vital input for industrialization and economic development. It has been recognized that fossil fuels are finite in extent and that diversification of energy sources other than hydrocarbon is a must for future development. As an alternative energy source, solar energy has been brought into focus because of its pollution-free nature as well as its immense amount of energy, and it has been technically explored to a substantial extent. If, however, solar energy is to make a meaningful contribution to the quest for energy, it should be properly accepted and used widely by the public. This requires proper economic analysis, upon which government policy will be formulated.

Economic analysis of solar energy appears to be still at a preliminary stage. Available studies are typically based on a comparison of the private cost of conventional energy with that of solar energy in terms

of present value. These studies appear to have a few shortcomings. First, they have not properly taken into account special institutional aspects of energy. Second, differences between the social and private costs of energy are not properly taken into account. Thus, existing studies do not provide suitable guidelines for policy formulation. The purpose of this paper is therefore to provide a general model of economic evaluation of solar energy, that can be employed by private users and policy makers alike. Since the cost and benefit of a solar energy system arise over the life of the system, its evaluation should incorporate the benefits and costs over its life time. In essence, therefore, economic evaluation of a solar system consists in comparing the present value of benefits with that of costs.

The extent of solar energy varies with climatic conditions, and government policy is national in nature and in scope. Hence, the nature and results of economic analysis of solar energy will differ from country to country. Even within a country, financial and institutional aspects differ by the usage of solar energy particularly between domestic and industrial usages. Therefore, the approach of this study is to develop a general model of economic evaluation of solar energy for industrial usage from the perspectives of both private companies and the society as a whole. The industry sector is the largest energy user where solar energy can provide direct thermal energy. The main areas of solar thermal applications in industry are process hot water, drying/dehydration, and process steam. Of these different types of industrial usage, solar energy for grain drying in Western Canada will be used as an illustration.

2. PRIVATE BENEFITS OF SOLAR ENERGY

The benefit of solar energy is the cost of conventional energy which will be saved or replaced. Assuming that a conventional energy system is set up for the first time, the following types of costs should be assessed over the life of the system: (1) the original capital costs including costs of acquisition, delivery, and installation of the system, (2) system repair, replacement, maintenance, and insurance costs; (3) operating costs, comprising labor and energy costs; (4) taxes (and tax savings), and (5) the salvage value net of removal and disposal costs. Operating costs may be further broken down into (a) labor costs of operating the system, (b) oil or natural gas costs, and (c) electric power costs. Once these obvious cost elements are assessed, the effects of various institutional arrangements which alter the effective cost of the energy system must be taken into account. Assuming that there is no specific incentive for the energy system at present, taxation would be the most important institutional aspect. Many countries provide investment tax credit for the original capital cost of energy systems, and tax-depreciation on the original capital cost less the amount of investment tax credit. Operating costs are in general deductible for tax purposes. The capital cost of the energy system may be financed either by equity or debt capital, and interest on debt capital is deductible for tax purposes. Then, the basic formula for computing the present value of the costs of a conventional energy system may be written as

$$PVC = K(1-c) + \left[\sum_{t=1}^{N} \frac{M(1+m)^t}{(1+r)^t} + \sum_{t=1}^{N} \frac{W(1+w)^t}{(1+r)^t} + \sum_{t=1}^{N} \frac{G(1+g)^t}{(1+r)^t} + \sum_{t=1}^{N} \frac{E(1+e)^t}{(1+r)^t}\right](1-u) - \sum_{t=1}^{N} \frac{CCA_t.u}{(1+r)^t} + \sum_{t=1}^{N} \frac{L_t.r.(1-u)}{(1+r)^t} - \frac{S_n(1-u)}{(1+r)^n} \qquad (1)$$

where PVC = the present value of the costs of the energy system over period N,

K = the initial capital cost, including costs of acquisition, delivery, and installation,

c = the investment tax credit, as a percentage of the original capital cost,

N = the life of the energy system,

M = annual repair, maintenance and insurance costs in year 1,

W = annual labor costs of operating the system in year 1,

G = annual oil or natural gas costs of operating the system in year 1,

E = annual electric power costs of operating the system in year 1,

m,w,g and e = annual rates of increases in M,W,G, and E respectively (assumed to be constant over time)

L_t = the remaining balance in year t of the initial loan principle,

r = the interest rate for the term loan which is assumed to be the discount rate,

u = the marginal tax rate,

CCA_t = tax-depreciation in year t, and

S_n = the salvage value net of removal and disposal costs in year N.

The first term on the right-hand side shows the initial capital cost less investment tax credits. The four terms inside the square brackets comprise operating and maintenance costs, and they are deductible for tax purposes. The third term shows tax savings through tax depreciation, and the fourth term shows net of tax interest payments. Finally, the last term shows the salvage net of removal and disposal costs and taxes. Tax treatment of the salvage value varies with countries. It may be regarded as taxable income, or the undepreciated capital cost at the time of capital disposal will be reduced by the amount of salvage value, whereby tax savings from depreciation deductions may decrease. For the sake of simplicity, equation (1) is based on the idea that the salvage value is fully taxable.

The original capital cost less (a) investment tax credit, less (b) the present value of tax savings from tax-depreciations, plus (c) the present value of net of tax interest payments, and less (d) the present value of salvage values (i.e., the first term plus the last three terms) are the so-called sunk cost. Once the energy system is installed, the sunk cost will be incurred regardless of whether it is used or not. Therefore, it should be noted that the sunk cost is not saved even if the conventional energy system is replaced by a solar system. In other words, if a solar system replaces an existing conventional energy system, the sunk cost is irrelevant for financial evaluation of the solar system. Under a set of reasonable assumptions, the present value of grain drying costs by propane gas was estimated to be $3727 in 1978 dollars for average farmers in Saskatchewan, Canada (1). Of the total present value, $2402 were for the sunk cost, clearly indicating its importance.

3. PRIVATE COSTS OF SOLAR ENERGY

The cost model developed for a conventional energy system as shown by equation (1) can be applied for a solar energy system for industry with a few modifications. In case the solar system replaces completely the conventional energy system (oil or natural gas), then the term for oil or natural gas costs will be eliminated. Each term will then be estimated for the solar system, and the present value of the costs of the solar system will then be compared with that of the conventional energy system. If the former is lesser than the latter, it may be concluded that the solar system is economically viable. It should be noted that this conclusion is valid only if the two energy systems are considered before neither of them is installed. If, however, a solar system replaces an existing conventional system, the conclusion is simply wrong. There are numerous studies on solar energy which have committed this type of error. This might well be the reason why solar energy was not accepted widely during the late 1970s even though most studies on solar energy argued for its economic viability.

In case a solar system replaces an existing conventional energy system, a correct conclusion should be based on a comparison of the present value of private costs of the solar system with that of the conventional system without the sunk cost. Based on an experiment undertaken in Saskatchewan (2) and on a set of reasonable assumptions, the present value of solar grain drying costs was estimated to be $2786 in 1978 dollars for average farmers in Saskatchewan, Canada (1). If this estimate is compared with the present value of grain drying costs by propane gas of $3727, a conclusion may be drawn that solar energy is economically viable and cheaper than conventional grain drying. However, the present value of solar grain drying costs of $2786 is well over that of conventional energy without the sunk cost ($1325), indicating solar energy is not viable.

4. SOCIAL BENEFITS AND COSTS OF SOLAR ENERGY

Although (social) cost-benefit analysis is similar to private investment evaluation, it takes a much wider perspective by assessing all the gains and losses of a project regardless of to whom they accrue. A benefit is then any gain in real goods and services from a project, and a cost is the foregone goods and services from a project, and a cost is the foregone goods and services by allocating economic resources to the project from other usages. As it is concerned with the society as a

whole, cost-benefit analysis is in effect different from private financial analysis in several important aspects. Frist, interest, while relevant for financial evaluation, has no relation to the value of real resources required. It should therefore be ignored in estimating costs. Second, depreciation charges are purely a bookkeeping device and therefore should not be included as a cost. Third, while private firms will net out taxes on their outputs and inputs in calculating their revenues and expenditures, the social benefits should include taxes, because taxes paid by private firms remain within the country, thereby taxes being transfer payments rather than being real gains or losses for the society. Therefore, equation (1), the basic model for the present value of conventional energy costs, should be modified for cost-benefit analysis as follows.

$$PVC = K + \sum_{t=1}^{N} \frac{M(1+m)^t}{(1+r)^t} + \sum_{t=1}^{N} \frac{W(1+w)^t}{(1+r)^t} + \sum_{t=1}^{N} \frac{G(1+g)^t}{(1+r)^t} +$$

$$+ \sum_{t=1}^{N} \frac{E(1+e)^t}{(1+r)^t} - \frac{S_n}{(1+r)^n} \qquad (2)$$

where the notations are as defined for equation (1).

There are a few more differences between cost-benefit analysis and private financial evaluation. The former takes into account externalities. For instance, air pollution from conventional energy may not be taken into account in private financial evaluation, while it must be included in cost-benefit analysis. Thus, in order to measure the benefit of replacing conventional energy with solar energy, equation (2) should be adjusted upward. Risk-taking associated with the installation of a solar system, particularly at this early stage of development, will generate external benefits in the form of new information. This social return in excess of private return on risk-taking should be added as a benefit of solar energy. This may also be done by adjusting upward equation (2). Risk perceived by private firms is usually higher than that perceived by the society as a whole, because risk for society spreads across a large number of citizens and it is pooled by a large number of projects undertaken by the society. This will also adjust upward the benefit of solar energy. These adjustments must be made for cost-benefit analysis if it is to be a proper policy base.

The model for the social cost of conventional energy, as shown by equation (2), can be applied in measuring the social cost of solar energy without the term for natural gas. Once each item of social benefit and cost is estimated, the present value of social benefits of solar energy (the social cost of the conventional energy system) will be compared with the present value of its social costs. Care should be taken in drawing a conclusion with regard to economic viability of solar energy. In case both a conventional energy system and a solar system are considered before neither of them is installed, the present values of overall social benefits and costs, including the sunk cost, will be compared. If, however, a solar system replaces an existing conventional energy system, the benefit which reflects the sunk cost of the conventional system

should not be included as part of benefit of the solar system.

Estimation of externalities is extremely difficult and is beyond the scope of this study. Without taking into account the external effects of conventional energy, the social benefit of solar grain drying in Western Canada appears to be higher than its social cost if the sunk cost of conventional energy is included. If, however, the sunk cost is not included, in all likelihood solar grain drying is far from being economically efficient, even from the social perspective.

5. CONCLUSIONS

A systematic model of economic evaluation of solar energy for industrial usage has been developed from the perspectives of private firms and government policy makers. This model takes into account institutional aspects of energy as it is utilized in industry. The importance of the sunk cost (or fixed cost) is pointed out in evaluating solar energy. Once an energy system is established, its sunk cost is continuously incurred regardless of whether the system is in operation or not. Hence, if a solar system replaces an existing conventional energy system, the sunk cost of the latter should not be part of the benefit of solar energy. In the case of grain drying in Western Canada, solar energy is economically viable for average farmers if the sunk cost is included; otherwise it does not appear to be viable in all likelihood.

Several important differences between private financial analysis and (social) cost-benefit analysis are pointed out. Interest payments and depreciation charges are obviously important variables for financial analysis, while they are irrelevant for cost-benefit analysis. Cost-benefit analysis takes the gross of tax values of outputs, while financial analysis nets out taxes. Finally, cost-benefit analysis takes a much broader perspective and includes externalities associated with energy. Hence, for instance, environmental effects of fossill fuels will be included as part of the benefit of solar energy under cost-benefit analysis. In so far as external effects are assumed away, solar energy for grain drying in Western Canada does not appear to be economically efficient from the societal perspective unless the sunk cost associated with conventional energy is included.

6. REFERENCES

(1) Kwon, O.Y., "An Economic Evaluation of Solar Grain Drying: Its Methodology and Application to Saskatchewan," Proceedings of Canadian Agricultural Economics Society, University of Alberta, Edmonton, Alberta, 1980, pp. 167-174.

(2) Curubleski, E.M. and Catania, P.J., "Experience with a Solar Collector for Grain Drying in Saskatchewan," presented at the 1977 Annual Meeting of Canadian Society of Agricultural Engineering, 1977.

STATUS OF SOLAR THERMAL ENERGY IN THE FEDERAL REPUBLIC OF GERMANY

Dr. Wilhelm Stahl

Fraunhofer-Institut für
Solare Energiesysteme
Oltmannsstr. 22
D-7800 Freiburg
F.R.G.

Abstract

Corresponding to the world energy consumption the Federal Republic of Germany still meets most of the energy requirements by fossil energy sources.

In contrast to many other countries renewable energy sources are of great public interest. This is due to the increasing environmental problems caused by nuclear and fossil energy use.

Up to now the government has spent 1.6 billion DM to support renewable energy research projects. With a yearly budget of 250 million DM the the F.R.G. has large public funds for renewable energy research.

In contrary to the research activities applications of solar energy systems in the F.R.G. are not wide-spread. Low conventional energy prices in connection with neglected environmental and social costs and insufficient economic allowances for the renewable energy sources are the main reasons.

This situation is even more annoying since solar thermal energy systems have a high potential for substituting fossil fuels.

This paper will concentrate on research activities and applications of solar thermal energy systems in the F.R.G.

Present Energy Situation

The primary energy consumption was 11.4 EJ/a in 1987. This is 7 % more than the consumption in 1982 but it is 11 % less than in 1979 when the consumption reached a maximum of 12.0 EJ/a.

The primary energy came from 42 % oil, 27 % coal, 17 % gas, 11 % nuclear power and 3 % water power.

The high contribution of nuclear power shows how political and economic privileges can push forward a special energy source. Beside other institutions only the Ministry for Research and Technology has spent more than 30 billion

DM for nuclear power research. The increase of nuclear power production is a factor of 2 faster than predicted in ther Marchetti diagram.

Secondary energy is used for 31 % process heat, 34 % low temperature heating demand and 35 % mechanical power and light. The high low temperature heating demand is typical for countries in northern latitudes and indicates the important possibilities for solar thermal energy applications.

Beside water power no other renewable energy sources are mentioned in the statistics. The statistics are not complete because solar energy is responsible for significant contributions for space heating. An indication for this is the decreasing space heating demand per living area. Beside the increasing standard of insulation the progress in window technology gives rise to these not neglectable solar energy contributions.

The immense low temperature heat demand is the reason to claim that thermal solar systems have a greater importance for the FRG than PV systems.

Potential of Solar Energy

The FRG has an area of 250 000 km^2. The horizontal global solar radiation is 1 000 kWh/m^2 a, so the solar input is 900 EJ/a. This is theoretically 80 times the primary energy consumption in 1987. Even the solar radiation falling onto the total building area is still 5 times more than the primary energy consumption.

Not only solar radiation but also water power, wind energy and biomass are local energy sources which can decrease the dependance on exhaustable fossil fuels.

On behalf of the Ministry for Economic Affairs the German Institute for Economic Research and the Fraunhofer-Institute for System Teçhnology and Innovation Research have published possible contribution of renewable energies to the primary energy consumption for the year 2000. The total contribution is expected to be between 0.4 and 1.3 EJ/a which is 3.5 to 11.4 % of the primary energy consumption of 1987. The big variation is due to distinctions between favourable, unfavourable, economic and economic usable conditions.

	Infavourable		Favourable	
	Economic	Economic usable	Economic	Economic usable
Solar Low Temperature Heat (Active)	25	27	43	59
Solar Low Temperature Heat (Passive)	11	21	29	29
Photovoltaics	-	-	3	3
Wind Energy	37	362	54	371
Hydro	206	268	217	297
Biomass	147	255	182	311
Geothermal	-	-	-	1
Heat Pumps	16	57	174	242
(PJ/a)	441	990	703	1 313

Unfavourable conditions: low increase of energy cost, high interest rate.

Favourable conditions: high increase of energy cost, low interest rate.

For active solar low temperature systems 25 to 59 PJ/a would correspond to 23 to 55 million m^2 solar collectors if we assume a 30 % yearly efficiency. Today about 350 000 m^2 solar collectors are installed. 25 % of the population lives in one or two family houses corresponding to 11.5 million houses. A 4 m^2 collector system has to be installed on all the houses to meet the predicted upper contribution.

Public Research Activities

New interest in renewable energy technologies was caused by oil price crisis in the 1970 ies. A research programme was started by the Ministry for Research and Technology. Corresponding to political and technological events mainly in connection with nuclear power plants the yearly budget was changing. Up to now the Ministry has spent 1.6 billion DM in the following fields of research /1/:

Photovoltaics	25 %
Cooperation with Third World Countries	16 %
Solar Thermal Electricity Production	18 %
Low Temperature Solar Systems	14 %
Wind Energy	14 %
Geothermal Energy	7 %
Hydrogen Technology	4 %
Biomass	2 %
	100 %

Today photovoltaic projects are even more dominating the research supported by the Ministry. Because of the high technological requirements it is thought to be an appropriate activity for an industrialized country like FRG. From all renewable energy sources PV has the lowest potential for substituting fossil fuels. As already mentioned the potential for solar thermal systems is much more promising. In 1987 the total research support for renewable energy technologies was 230 million DM. PV projects got more than half of this money, low temperature solar thermal research had to live with only 7 million DM.

For the coming years the Ministry plans to increase the research support to 270 million DM per year. This is accompanied by a strongly decreasing support for nuclear power research.

Beside the research allowances renewable energy applications are supported by tax credits and grants:

- Commercial companies: 7.5 % tax-free allowance according to § 4a of a law on investment allowances

- Tax payers: according to § 82 of a tax regulation 10 % of the costs incurred can be claimed against tax for 10 years

- Agricutural concerns: either § 4a or § 82 above; in addition there are other possibilities included in the programme "Improvement to the structure of agriculture and protection of the coastline"

- Favourable loans are available from the Kreditanstalt für Wiederaufbau for the protection of the environment.

- Support can be given within the framework of programmes of the Federal State Governments.

In addition, grants from the European Community are also being made available for German projects.

Main solar thermal research institutions are

- three institutes

  Institut für Solarenergieforschung Hannover, ISFH
  Fraunhofer-Institut für Solare Energiesysteme, ISE
  Stiftung für Sonnenenergie und Wasserstoff Stuttgart

- 10 to 15 groups working in different universities

- 4 to 6 companies

To support solar applications the "Deutsche Gesellschaft für Sonnenenergie (DGS)" was founded in 1976; today this private organisation has 3500 members. Companies producing solar systems have joined together in two commercial orientated organisations, Fachverband Solarenergie and Bundesverband Solarenergie.

Status of Solar Thermal Applications

Solar energy played a neglectable role in the public energy discussion before the oil price crisis. After these events a first push was made in the field of domestic hot water systems. About 30 companies - most of them small and recently promoted - were trying to sell sometimes not fully developed systems. The installed collector area reached about 200 000 m^2 in 1980.

Decreasing oil prices and system failures were followed by a decrease of the collector market. In spite of that scientific activities went on; new and improved thermal applications were tested. Passive solar systems reached public interest, also because of the increased living comfort with greenhouses, integrated part of the house or attached to the building.

6 000 public and more than 270 000 private swimming pools exist in the FRG. With cost of about 0.10 DM/kWh /2/ solar systems are of high economic interest and more than 10 000 m^2 solar absorbers are installed per year.

For domestic hot water systems not very successful years seem to be over. Today a slight increase in market volume can be stated. A very important push came by the successful second collector test carried out by the "Technische Überwachungsverein München". 18 domestic hot water systems were tested from 1985 to 1986 /3/. The typical collector system consisted of 4 m^2 single-glazed collector with selective coating and a 300 l storage. Collectors are mounted on the roof and the storage tank is normally in the cellar of the house. A mean price for such a system is 9 000 DM, the yearly efficiency is 30 % and cost of energy is 0.30 DM/kWh. Gas or electric hot water systems have comparable cost per kWh.

Today the installed collector area reaches 350 000 m^2, the yearly increase is between 10 000 and 20 000 m^2/a.

To simplify collector systems and to decrease installation costs a new "Integrated Storage Collector" /4/ has been developed. The storage tank is the absorber and contains drinking water; no heat exchanger is necessary. Transparent insulation materials (TIM) are used between collector cover and absorber.

Due to high solar transmission and low heat conductivity these materials prevent freezing of the storage tank.

For further developments solar heating systems will play a more important role. A high application potential exists because of the high heating demand. Solar heating systems are more sophisticated because solar input and heat requirement are not parallel.

Seasonal storage systems are expensive or not convincing. An other solution may be to use high efficient systems for utilization of the low winter radiation intensities.

This is also possible with TIM /5/. Like the Trombe-system TIM is mounted on the outer surface of the wall. In this way the wall becomes a heat source for the house. Practical tests and simulation calculations show that the house heating demand can be dramatically decreased. A self-sufficient solar house which is totally heated by such a system will be built /6/.

Increasing insulation standards, windows with low heat loss coefficients, passive solar architecture and all kinds of solar thermal systems will decrease conventional energy consumption and increase the solar contribution to the energy supply in the FRG.

References

/1/ Erneuerbare Energien, Bundesministerium für Forschung und Technologie, Bonn 1987

/2/ Forschungsstelle für Energiewirtschaft, Daten und Fakten für die Nutzung regenerativer Energiequellen in der Bundesrepublik Deutschland, published by the Ministry for Research and Technology, Bonn 1986

/3/ Sonnenenergie zur Warmwasserbereitung, Fachinformationszentrum Karlsruhe, Verlag TÜV Rheinland, 1987

/4/ Schmidt, Ch., Goetzberger, A., Rommel, M., Schmid, J., 1987, Integrated collector storage systems with highly transparent, highly insulating cover, ISES Solar World Congress Hamburg to be published.

/5/ Goetzberger, A., 1984, Seasonal storage of thermal energy with radiatively heated storage walls, Int. J. of Sol. Energy 2, 521-535

/6/ Goetzberger, A., Stahl, W., Self-Sufficient Solar House 2000, Proc. of 2nd Int. Workshop on Transparent Insulation, p. 74, 1988, Franklin Company

THE ROLE OF ISES - INTERNATIONAL SOLAR ENERGY SOCIETY IN THE DISSEMINATION OF RENEWABLE ENERGY TECHNOLOGIES

Dr. C. Corvi
President of ISES International

ABSTRACT:

Founded in 1954, the International Solar Energy Society has expanded over the years into a truly international organization. It is a non-political non-profit organization dedicated to the advancement of the utilization of solar energy. The Society has members in more than 90 countries worldwide and is ready to cope with the development of the technology of renewables and its introduction into industrialized countries as well as into developing countries.

The major activities of the Society are:
- Publication of newsletters and magazines;
- Organization of International Congresses;
- Publication of the proceedings of the Congresses;
- Identification of end-use energy categories to whom it could be useful to present specific technologies;
- Definition of standards;
- Link research, industry and mass-media.

All these aims are effectively fulfilled by National Sections, of which the Italian one is the second largest in the world and is often taken in the paper as an example.

***

The International Solar Energy Society is a world-wide non-political non-profit organization dedicated to the advancement of the utilization of solar energy. Its interests embrace all aspects of solar energy, including characteristics, effects and methods of use, and it provides a common meeting ground for all those concerned with the nature and utilization of this renewable non-polluting resource.

Founded in 1954, the Society has expanded over the years into a truly international organization, with members in more than 90 countries. It has been accepted by the United Nations as a non-governmental organization in consultative

status and is widely regarded as the most important body of its kind operating in the solar energy field.

The Society is naturally interdisciplinary and its members are world leading figures in solar energy research and development, as well as people whose only qualification is an interest in solar energy and its practical use.

In countries and regions where there exists sufficient interest, Sections of the Society have been established. These Sections, which are largely autonomous, organize meetings, conferences and other local activities and in some cases produce their own publications. For example, the Italian Section publishes its own scientific magazine in Italian: "Energie Alternative-Habitat,Territorio,Energia - HTE". All Society members are eligible to belong to their respective national or regional Sections. In recent years the number of Sections has increased slowly, but steadily.

In the last few years many people from Eastern countries have applied for membership, too and a national section has recently been formed in Jugoslavia, while another national section is going to be formed in the USSR in a short time. This means that the Society is now actually present all over the world and that its action in favour of the dissemination of technology in the field of renewable energies and energy saving can be really effective.

The major activities of the Society are:

- Publication of newsletters and magazines : "Solar Energy", a monthly scientific journal of an archival nature, containing scientific and technical papers on solar energy and its utilization, reviews, technical notes and other items of interest to those working in the field of solar energy; "Sunworld", a less technical magazine issued four times a year; ."ISES News", a quarterly newsletter for members.
- Organization of international Congresses: the last one organized by the Italian Section in co-operation with the European Community Commission was the 8th European Conference on Photovoltaic Solar Energy, which was held in Florence from 9th to 13th May 1988; it was one of the most important events of its kind in the world in the sector of renewable energy sources; 750 scientists and technical experts from 44 Countries attended the Conference.
- Publication of the proceedings of the Congresses: the last ones published were those from the Hamburg World Solar Congress which, also organized by the German Section, was held in Hamburg from 7th to 9th October 1986.
- Identification of end-use energy categories to whom it could be useful to present specific technologies suitable to their energy needs; we try to involve industries in contacting these categories, which could be both interesting for industries themselves and useful for the dissemination of renewable energy technologies.
- Definition of standards: there are various Countries where there exists no standard for renewable energy technologies and such work would be much appreciated by the official standard bodies.
- Link research, industry and mass-media: a very important role is played by ISES in covering the gap existing between

research, development, production on one side and information to public opinion on the other side; in a moment like the present one, in which information often contradictory on the possibility of development and utilization of new sources is diffused through the mass-media, I think that a great care is to be given not to generate in the public opinion easy optimism or expectations which cannot be realistically satisfied, but, at the same time, not to induce them to consider renewable sources just useless and expensive toys for adults; ISES therefore proposes itself as a catalyzing and stimulating element of all the forces operating in this sector, thus contributing in the achievement of significant targets; something of the kind has been done by the Italian Section when it has avoided the formation of an Italian Wind Energy Association, which would have been nothing but another body operating in the field of renewable energy sources, thus generating more confusion in the public: all Italian operators in the field of wind energy became members of ISES and formed the ISES Committee for Wind Energy, instead of a new association.

The Society is ready to cope with any development in the technology of renewables and its introduction into industrialized countries, as well as into developing countries. Very important actions have been undertaken during the last few months to fulfil this last aim. Last April I was in New York and I spoke to the United Nations' Committee on the Development and Utilization of New and Renewable Sources of Energy about solar technology promotion in developing countries. Contacts with United Nations' Agencies, such as UNESCO and UNITAR, are in progress in order to carry on common projects for the diffusion of renewable technologies.

ISES has already involved itself in some initiatives promoted by UNESCO, such as:
- co-publication of an information brochure on autonomous solar electricity supply for rural and remote areas;
- a study on the evaluation of photovoltaic applications for developing countries, to be distributed to interested bodies in Africa and other regions;
- organization of training courses for technicians, engineers and businessmen in the field of small renewable sources of energy.

In addition UNESCO has recently proposed two more topics for cooperation:
- a series of volumes on renewables issued as a joint project UNESCO-ISES;
- organization of a mobile exhibition on autonomous and solar electricity supply to rural and remote areas.

ISES is also in very close contact with UNITAR's Centre on Small Energy Resources (CSER), with which we are exchanging information in our relevant bulletins and are going to co-operate in a promotional programme for rural areas in Africa.

In fact many gaps in knowledge remain, and the funding of R&D in appropriate energy technology is very low in relation to the need. It should be one of the most urgent

tasks on the agenda of aid-giving governments and international agencies to ensure that, at the very least, the technologies enabling energy-needs-strategy to be implemented be readily available to the governments and people of developing countries.

The technologies are disseminated through the mechanism of the market, but in almost every case the market has to be supplemented in several ways.

Thus, R&D and testing are preconditions of a product making its appearance in the market. But neither its appearance, nor detailed information about it, put it in the hands of the rural people. Often the developing people have not enough money, their needs must be translated into effective demand backed by purchasing power. This requires that these people have access to credit enabling them to buy the new equipment. They can then repay the loan out of the increased income they get by using the new technology.

Credit that enables the developing people to become more productive is at the very heart of the process of rural development, of capital accumulation and income generation in rural areas.

Education and training have a role in all the stages of an appropriate technology work, from ''needs identification'' to ''dissemination'', and here again new inputs are required for a strategy of development to be successfully carried out.

New or reoriented programmes of education and training need to be set up, for scientists and engineers, administrators, planners, field workers, and local people in their communities.

Today there is a crippling shortage of people with the intellectual and practical ability required to carry out these programmes, and the appropriate education and training facilities both in the rich and poor countries are scarce.

To summarise my contribution, what is needed now is a major expansion of R&D effort, field testing and demonstration of solar energy technologies, supported by enlarged education and training programmes; the creation of local credit and other facilities enabling everyone to gain access to, and to own and operate this technology; and the removal of administrative and institutional barriers from the spread of appropriate technologies through the market.

I believe that ISES can be a determinant factor in such programmes, because it can help in disseminating much of the know-how gained internationally in this field, and offer a unique opportunity of exchanging experiences at its conferences and seminars.

FEASIBILITY & VIABILITY OF SILICON TECHNOLOGY DEVELOPMENT FOR ISLAMIC COUNTRIES - A PRACTICAL APPROACH

Dr. Atique Mufti,
Director General, *
National Institute of
Silicon Technology,
Islamabad - Pakistan

ABSTRACT

It goes without contentions that Silicon Technology Development is an inescapable reality and the only effective means to meet the challenge of coming Silicon Revolution and Silicon Age which is just around the corner in the 21st century. However, every new and emerging technology requires compatible surroundings, patronizing environment, nourishing parameters and proper inputs for its effective development and growth. Silicon Technology, also, is not an exception, and is heavily dependant upon such pre-requisites. Do the Islamic countries have these demanding pre-requisites to offer this emerging technology for its useful assimilation and utilization or not ? This paper deals, in length, with these ideas and also points out how the Islamic countries which at present are devoid of such infrastructures, can develop them for a congenial growth of their most useful companion of the near future - Silicon Technology.

* * * * *

Silicon Technology Development is a collective name of several processes involved in the extraction of silicon from quartz and converting it into solid state devices such as electronic components, integrated circuits, solar cells etc. These processes are shown in Fig. 1.

In my other lectures and papers [1] I have tried to prove that Silicon Technology Development is very essential for the developing countries provided they have resources or can develop them to join this race. In this paper I shall try to outline the general approach to make this technology development feasible and viable for the Islamic countries. But before that I would like to give an overall picture of the present

---

* Also President, Inter-Islamic Network on Renewable Energy Sources.

status of this technology in the Islamic Countries (Fig.2) for proper understanding and perspective. It may be noted that silicon technology development for the purpose of making electronic components is almost non existant in any Islamic country, however, some activities are going on for harnessing the solar energy through passive methods which is beyond the scope of this paper as they are not included in the Silicon Technology. The only practical step for the development of Silicon Technology has been taken, so far, by Pakistan.

In the light of my experience, I can suggest that the feasibility and viability of silicon technology development depends crucially upon the following few factors:

i) Technical Facilities
ii) Raw Material
iii) Financial Resources
iv) Technical Personnel and Training
v) Political and Government Patronage
vi) Socio-economic conditions and Social Acceptability.

Silicon Technology Development can be visualized like a big inflatable sphere containing several smaller inflatable spheres (Fig.3). In order to inflat the bigger sphere effectively it is extremely important that the inner smaller spheres should be properly inflated to their proper capacity so that a smooth uniform and effective surface of the bigger sphere may be achieved.

Let us now discuss the viability and feasibility of the smaller individual spheres on which the shape of the bigger sphere depends.

1. TECHNICAL FACILITIES

The chart of silicon technology spectrum (Fig.1) clearly shows that this technology can be developed through modular approach which means that the development activities can be initiated from any one stage or process which can be supplemented subsequently by other stages of the chain. This, of course, is a reasonable practical approach and a number of technologists would like to opt this technology in the reverse order in steps and in modules. I fully agree with this philosophy but would like to sound a warning that, although, this modular approach is more practical, yet, unless this piece-meal addition is extended to the whole spectrum, the desired results i.e. low price will not be achieved, because the price of the finished product is proportional to the number of intermediate workers and suppliers.

If the initial raw material is to be imported from some developed country obviously the price of the finished product will include the high price structure of the developed countries which will ultimately nullify the philosophy and determinal viability factor - cheap price.

However, if the raw material can be procured from an equally cheap developing country then there is no harm in curtailing the number of stages for development in any country, but even in this case who is going to guarantee the constant supply of raw material from some external source at an amicable price indefinitely. Hence if any country decides to adopt the modular approach it should not be discouraged because this is a sure way of gradual learning and expansion but to be competetive in the world market this modular approach eventually has to adopt the whole spectrum to produce tangible results and commercial benefits.

This technology is a chain of interdependant stages and the two important factors i.e. cost and efficiency depend upon the total spectrum of development activities. In Islamic countries sometimes the governments are very generous in sanctioning the curtailed stages of facilities by eliminating one or two crucial stages which bogs down the whole show. Since in most of the Islamic countries the bureaucracy consists of non technical personnel it becomes extremely difficult later on to convince them the importance of the missing stages which results in too much loss of time, energy and scientific efforts.

So in order to enter the silicon technology development race successfully it is extremely important to start the work on any stage after getting an unconditional support for the addition of the rest of the stages from the sponsors.

If such kind of extensive activities are not possible at all then the Islamic countries should start a collaborative work by splitting the whole spectrum in the following three phases:-

Some countries should only concentrate and specialise in any one of these activities:

i) Production of polysilicon from quartz.

ii) Production of wafers from polysilicon produced by other brotherly countries as in (i).

iii) Production of solar cells and systems from wafers produced in (ii).

In order to create surety, dependence and understanding some of the Islamic countries rich in finances should be asked to financially support the activities of other countries on reciprocal or mutual basis for technical manpower and resources and vice versa. This kind of collaboration can be implemented either through individual contacts between the countries on bilateral or trilateral basis or under the umbrella of Inter-Islamic Networks which has been recently created under OIC and COMSTECH

2. RAW MATERIAL

One of the firsts before embarking on this programme is to make sure that the country has either sufficient raw material reserves in the

country or have a reliable dependent and steady supplier to keep the supply line in tact under all favourable or adverse circumstances. In the absence of these guarantees one might be stepping into a business like supplying butter in the market at a cheap fixed price without having one's own cows or buffallows or depending upon some milkman who may strangle the supply line at any moment.

Let me sound here a note of warning that in the modern materialistic world, international suppliers, due to large cliental of scientific equipment and supplies are becoming more and more self centred opportunists with less regard to moral or ethical code of business and hence the possibility of exploitation from them at any time cannot be ruled out. So unless it is sure that one can keep a steady supply line of requirements of this technology, an uncalculated jump in Silicon Technology may prove distarstrous and a folly. Rise of raw materail prices to manifold and dishonouring of contracts are just the common happenings. Suppliers do not suffer due to break of contracts and court injunctions as they have employed their legal advisors, but scientific organisations having no such facilities, suffer a lot due to arbitration through court.

3. FINANCIAL ALLOCATIONS

Before a decision is made to enter the race of silicon technology development it is extremely important to make sure that sufficient financial support is available and is likely to continue unabated for about 7 to 10 years. For medium developing countries this figure may be reduced to 6 to 8 years. This figure may sound strange to the scientists of the developed countries for whom 5 years are enough because they are not aware of the bottlenecks which usually crop up typically in the developing countries. If the provision of this fianncial support is less than US$ 10 Million the results may fall short of expectations.

The following two tables are indicative of this expenditure:-

Equipment	Silicon Solar Cells Single Crystal Route (US$ Mills)	Integrated Circuits (US$ Mills)	Remarks
1. Quartz to metallurgical grade silicon	3.0	3.0	Can be avoided if the country has this commercial facility.
2. Metallurgical grade to polysilicon	1.0	1.0	
3. Polysilicon to single crystal	1.0	2.0	
4. Wafering	0.5	0.5	
5. For Cells:			
a) Cell processing, dopping, printing, contact making, photovoltaics	2.0	-	

Equipment	Silicon Solar Cells Single Crystal Route (US$ Mills)	Integrated Circuits (US$ Mills)	Remarks
b) For integrated circuits design, diffusion, alloying, metallization, pattern generation etc.	-	3.5	
6. Encapsulation:			
a) For solar cells	1.0	-	
b) For integrated circuits	-	2.0	
7. Testing & Measurement	3.0	3.0	
8. Building	1.5	1.0	
9. Salaries and Establishment expenditure	2.0	2.0	

Total for 7 years: 13 - 3 = 10 Mills. 18 - 3 = 15 Mills.

With proper experience and guidance the cost for stage (2) to (9) can be reduced by about 10% in equipment and about 15% in building and Establishment charges.

A typical financial phasing is suggested as under:-

	Activities	Allocation Needed (US$ Mills)
1.	Planning, designing of building, recruitment of scientsts	1.0
2.	Placement of orders of equipment, initiation of construction of laboratories building, training of scientists, recruitment of scientists and staff	2.0
3.	Orders of equipment, building construction, trainin g of scientists, recruitment of scientists and staff.	2.0
4.	Completion of building, arrival of equipment, furnishing of laboratories, partial installation of equipment	2.0
5.	Installation and commissioning of equipment	2.0
6.	Scientific activities to start, practical training of scientists and initiation of R & D activities	1.0
7.	Centre fully operational	1.0
8.	Expansion of activities to cover the whole spectrum of silicon technology	?
	Total:	US$ 11+? Mills.

Note: Minor adjustment and overall savings to the tune of 10% is possible depending upon the individual conditions of the country.

4. MANPOWER

In Islamic countries the recruitment of the required manpower is very complicated problem. In some of the Islamic countries, although there are good number of scientists available but due to socio-economic problems they are not prepared to stick to one line of research because their choice is mostly governed by the socio-economic conditions. Since silicon technology is a very specialized branch in which specialized training extending from 2 to 3 years is required hence the scientists of Islamic countries would not like to stick to a specialized branch rather more money even to the extent of one increment can allow them to change their field. Hence like all specialized branches of research silicon technology will face the strange kind of blunt due to influx and outflux of the scientists. In order to cope with this inherent problem and run the project a greater number of scientists as compared to the critical working number have to be recruited. In case a government is not going to realize this difficulty then the project may run with frequent unattended stages in the whole chain and is likely to impair the working of the project as a whole.

Long term training for the degree holder scientists of Islamic countries is not beneficial at all. Of course the non degree holder can be sent abroad for higher degree courses while the degree holders will get almost the practical training in 6 months as they may get in 3 years. This characteristic is due to the socio-economic conditions of the countries which can be elaborated.

External influences for recruitment of interested people from the influential community particularly for a fashionable modern technology such as silicon technology is great in Islamic countries. So while starting this project make sure that you get almost double the number of scientists which are very essential for the project otherwise you will always be short of the critical strength of the scientists to do the work.

No R & D institute can depend indefinitely upon the foreign technical advisors who are extremely busy with their own schedules. So if you think that your scientists in quality and quantity are good enough to take the full load of your project or you can quickly raise them to this standard then start the work otherwise too much reliance on external manpower will not lead you anywhere. As an example let me quote you my experience with foreign advisors.

Never appoint a foreign consultant for less than three months of stay in your country as short term visits merely waste money and no work is accomplished. Let me give you an example of typical foreign advisor's visit to a developing country for two weeks:-

i) Monday evening or Tuesday morning arrival, as he has to leave his country on the weekend.

ii) Tuesday - jet lag and sleep catch up.

iii) Wednesday - Introduction with the local research group.

iv) Thursday - Familiarization with the local research group. Visit to the Embassy. Courtesy call to high officials of the country.

v) Friday - Saturday - Closed holidays.

vi) Sunday - Scientific work - Reconfirmation of travel plans with the airlines and possible change of plans.

vii) Monday - Work but with slow tempo due to stomach disorders.

viii) Tuesday - Work . Afternoon shopping and sight seeing.

xi) Wednesday - Possible disruptions in utilities such as water, electricity etc. which are common in a developing country.

x) Thursday - Wanted to leave on Friday but due to the non-availability of a well known foreign airline flights on Friday he is forced to leave on Thursday.

This exercise will be repeated somehow or the other. Hence if you want to get work out of them then add the working days on the top of these two weeks schedule as given above.

Minimum critical strength of scientific staff for initiation this programme is given below which may swell to 300 at the start of research programme.

	Solar Cells
M.G. to polysilicon	5
Polysilicon to single crystal	5
Wafering	2
Diffusion	5
Printing	2
Photolithography	3
Contacts evaporation	4
Tabbing	2
Lamination	4
Analysis	4
Test and Measurement	6
System design	6
Miscellaneous	2
Total:	50

For expansion to other routes such as polycrystalline and amorphous addition of 5 scientists for each stage is required.

	Integrated Circuit
M.G. to polysilicon	5
Polysilicon to single crystal	5
wafering	2
Design and simulation	5
Epitanial growth	3
Diffusion	4
Alloying	2
Metallization	2
Pattern Generation	5
Test and Measurement	6
Assembly	4
Miscellaneous	2
Total:	45

Again the manpower problem is quite complex in the Islamic countries and I would suggest that instead of thinning our resources we should pool our resources of technical personnel. For this purpose again mutual agreements or using the good offices of Inter_Islamic Network is an effective method.

5. POLITICAL PATRONAGE

Without saying anything about the government systemsof Islamic countries I would conclude it to add that if the active support of the government is disturbed in the course of the project the money already spent will be a mere waste and a folly. So the government should be rest assured that they cannot expect any dent on the socio-economic uplift of the country through this technology before seven years provided all the inputs are provided to it in time and according to its requirements.

It is not very uncommon that most of the officials of the bureaucratic machinary are familiar with the technology to the extent that they have read a popular article on silicon technology in some popular journal such as Readers Digest, Newsweek or Times. So while you are advocating your case of financial allocations and sanction of required manpower they may be running a parallel thought of their information through the articles they have read. Since you being a technical person, might be giving them some true facts and figures they might not be believing you in the light of their recollections. Consequently at the end of the discussions they might throw their verdict that you do not need either that much amount or so many workers. So unless you have some political personality to advocate your case your efforts to start silicon technology may not be fruitful.

6. SOCIAL AWARENESS AND SOCIAL ACCEPTABILITY

In the developing countries social and economic awareness of a technology are tightly coupled with the political awareness. If a few political and influential people are enlightened and are convinced of its usefulness then it is a wisdom to start this work. On the other hand if you can make them convince or enlighten them still it is wise to start this technology. If you have neither of these possibilities then your socio-economic response and acceptability will be very weak because in the developing countries the acceptability of masses carry little weight for a technology as compared to patronage and incentive from the government and influential persons.

From the chart of activities (Fig-2) it is evident that social awareness for this technology do exist in the Islamic Countries. The magnitude of the activities clearly indicate that other factors such as financial, technical facilities and technical manpower and government backing are still lacking. In such circumstances if we go on working on a small scale and on individual basis then our objectives will never be achieved. Hence we have to start the work simultanously on the following fronts even from the grass root.

i) Scientists individual level

ii) University & Organisation level

iii) Government and country level

iv) Islamic Ummah level.

Scientists individual level means that the scientists should work with whatever facilities they may have. Their work could be on megre scale or even may be a repitition of the others work. Once they know the subject then their authetic work is bound to create the interest of their universities or organisation. Good workers even in different departments in the same universities can then join in small groups. They can get some financial support from their organisations which can also be supplemented by other Islamic countries funds such as Kuwait fund and Inter-Islamic Network on Renewable Energy Sources. The only criterian is that the work should be authentic and must contain the germs of promising work.

* * * * *

References

Paper

1 Mufti, A.R. "Development of Silicon Technology in the Developing Countries - A Wisdom or a Folly ? Pakistan Experience"

a) Proceedings of International Symposium-Workshop on Silicon Technology Development and its Role in the Sun-belt Countries, Islamabad, Pakistan, June 14-18, 1987.

b) Proceedings of Third Arab International Solar Energy Conference, Baghdad, Iraq, February 21-24, 1988.

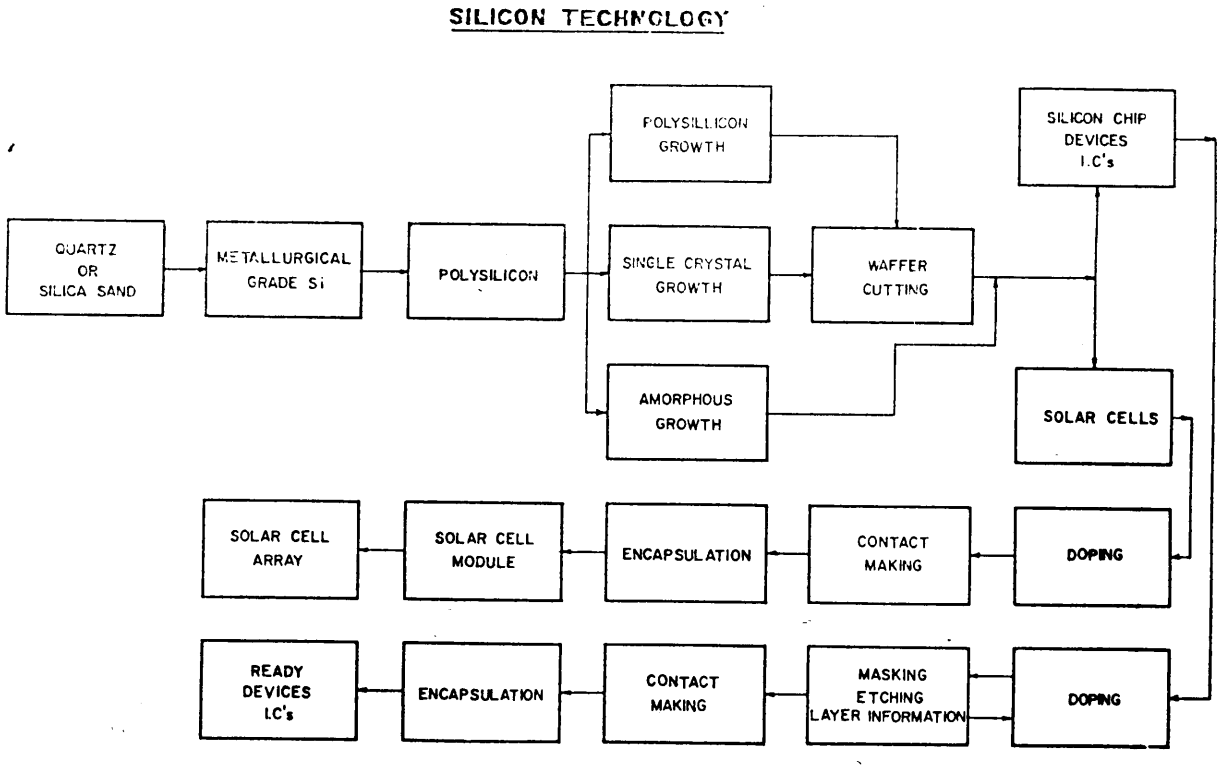

FIG. I

Fig 2(a) Solar Energy Activities in Islamic Countries

(List not conclusive)

Passive Methods

Country	Organisation	Nature of Work
Egypt	Ain Shams University Cairo.	- Solar Radiation
	Alexandira University	- Flat Plate Collector
	Building Research Center Cairo	- Measurements of Solar Radiation
	University of Cairo Cairo	- Solar Air Heating
Iraq	Building Research Center Baghdad	- Cooling and Heating of Buildings
	M. T. C., Baghdad	- Heating & Cooling Load
		- Energy Saving by Ventilation
	National Center for Engineering Consultancy	- Solar Heating
	Solar Energy Research Center, Baghdad	- Cooling Load Calculation
		- Thermal Storage Walls
	University of Mosul Mosul.	- Design of Farm Buildings

Kuwait	Kuwait Institute for Scientific Research, Safat	- Infra Red Sky Radiation - Greenhouse - Solar Cooling Systems
	Ministry of Public Works	- Designing of Solar - Buildings
Libya	Center for Solar Energy Studies, Tripoli	- Thermal Behaviour of Houses
Nigeria	University of Ibadan Ibadan	- Solar Ventilation
Saudi Arabia	King Abdulaziz University Jeddah	- Bioclimatic Design
Tunisia	University of Tunis	- Cooling of Flat Plate Collector
Turkey	Middle East Technical University, Ankara	- cooling of Solar House

Fig 2(b) Solar Energy Activities in Islamic Countries'

(List not conclusive)

Active Methods

Country	Organisation	Nature of Work
Algeria	Centre Des Sciences Et De La Technologie Nucleaire	- Photovoltaics CdS - Cu S Thin Film
Amman	Solar Energy Research Center	- Photovoltaic for Telecommunication and Refrigeration Systems
Egypt	Ain Shams University Cairo	- Single Crystal Si Cells - Wedged Stacked Si Solar Cells - Cu S - CdS Heterojunction
	American University, Cairo	- Si - Cells
	Assiut University, Assiut	- MIS - Tunnel Solar Cells
	Cairo University, Cairo	- Solar Cell & Radiation Distribution
	El - Mansoura University,	- Photovoltaic System under Dynamic Condition
Iraq	Al Mustansiriyah University, Baghdad	- $(2GaAs)_{0.5}$ - $(ZnSiAs)_{0.5}$ Systems
	Solar Energy Research Center, Baghdad	- Cadmium Chalcogens Thin Films - Thin Oxide films by Chemical Deposition
	Solar Research Centre Baghdad	- Hall Mobility and Energy Gaps of a-Si.
	University of Baghdad	- Sn Se/Se Thin Film Solar Cells
Kuwait	Kuwait University	- Amorphous Silicon Selenium Films.
Libya	Center for Solar Energy	- AlGaAs/GaAs Solar Cells. - Optimum - Voltage of Solar Cells.

Libya	Al-Fateh University Tripoli.	- Photovoltaics
Nigeria	University of Ife Ile - Ife.	- CdSn Solar Cells
Pakistan	National Institute of Silicon Technology Islamabad	- Si - Solar Cells & Si - Chips from Indigenous Materials
Sudan	University of Khartoum	- Testing of Si Solar Cells.
Turkey	Firat University, Elazig	- Thermo - Optical Properties for Solar Energy Application.
Tunisia	University of Tunisia	- Solar Cells - Solar Houses and Solar Power
	Laboratoire de Photovoltaique, Tunisia	- Fabrication of $Cd_{1-y}ZnS_y$ - Cu_2S based Solar Cells.

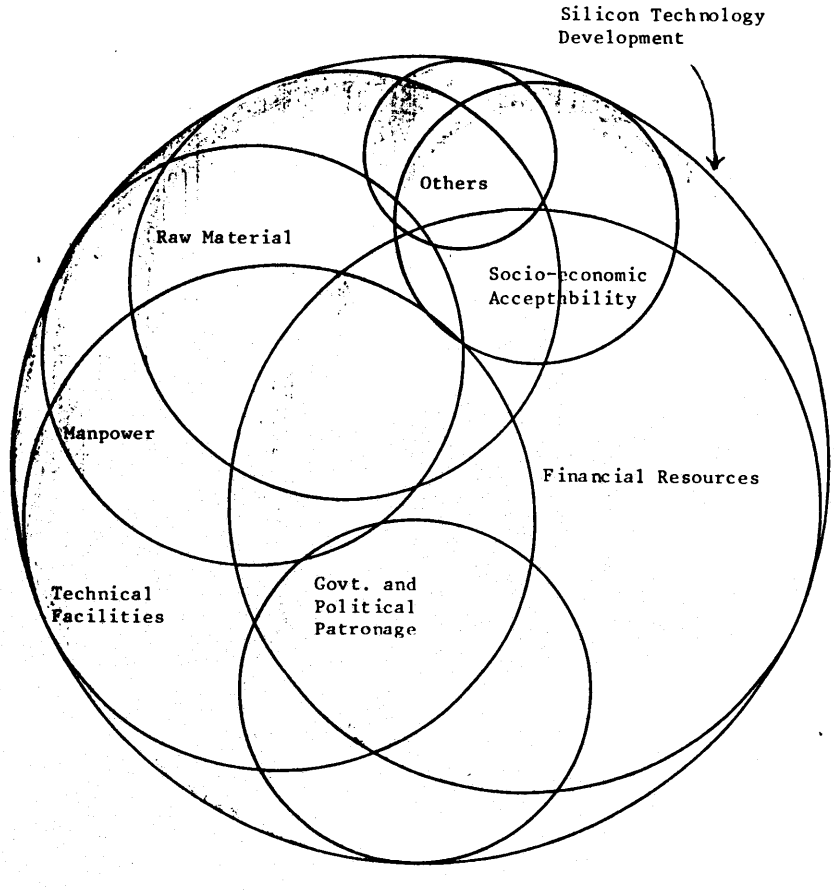

Fig. 3

Inflatable sphere of Silicon Technology Development along with its constituent spheres.

SECTION VIII

THERMAL SYSTEMS

FRUITS SOLAR DRYER MODELING

M. EL HISSE* , M. FOURNIER**

* Laboratoire d'Energétique et Mécanique des Fluides
Dept de Physique - Faculté des sciences
B.P.:S.15 MARRAKECH - MOROCCO

** IMP - CNRS de l'Université de Perpignan
30 Avenue de villeneuve
66025 PERPIGNAN CEDEX - FRANCE

ABSTRACT

The drying process in a SERESOL tipping type agricultural solar dryer is simulated by a mathematical model.

Little unknown parameters were first identified from experiments carried out in the laboratory using a controlled atmosphere ventilated drying tunnel.

The model was then validated during a full scale drying experiment insitu in the solar dryer.

Finally, we give results of drying process simulation with a photo-electric cell powered blower..

1. INTRODUCTION

The agricultural solar dryer prototype presented can dry from 10 to 20 kg of fresh products in 2 or 3 days. This device can operate under natural or forced convection: if the blower is powered by photo-electric cells, the dryer's autonomy is assured.

In this paper,we propose a mathematical model of this dryer, which enables us to simulate its working processes. This work's originality lies mainly in the way in which the problem was tackled: the model discribes the macroscopic processes of the solar dryer while taking into account microscopic phenomena which interne inside the fruit to be dried.

Experimental measurements allowed the identification of some unknown parameters arising in the equations.

2. SERESOL "TIPPING TYPE" SOLAR DRYER

2.1. Description And Working Process

Being an indirect solar dryer (Fig. 1) the fruits to be dried is subjected only to convective thermal transfer [1].

The dryer is composed of 3 different parts:

(i) a fixed part forming the drying chest composed of six horizontal trays of a total surface of $1 m^2$.

(ii) a tipping part designed to enable easy loading and unloading of the trays. Under the transparent cover made of double-skinned extruded polycarbonate panels, there are:

- the botton ($0.72 m^2$) which is in fact the solar absorber. It is made of emulsified polyurethane foam (20 voids per inch) and is blackened through its mass. When the dryer is closed, the porous absorber covers the top of the dryer chest.
- the top ($0.50 m^2$) acts as a solar chimney thanks to the presence of a metallic absober covered in flat black carbon deposit paint. The air passage is behind the metallic absorber.

(iii) another panel, also of porous absorber type is fixed in the lower part of the dryer parallel to the ground and acting as an air preheater ($0.58 m^2$).

If a blower is placed at the entrance to this panel, air can be circulated through the dryer.

2.2. Mathematical Model of The Porous Absorber Type Solar Panel

We choose a simple model, taking only average temperatures into account. The panel's thermal inertia is low, so a model written in the steady state regime is sufficient to represent this hot air generator.

The temperature of the porous matrix is taken to be uniform and the air flow unidimensional.

The matrix thickness is such that no radiation can get right through it (2cm).

Equilibrium of energy in:

- the glass cover.
- the air at the panel entrance.
- the air in the porous matrix.
- the porous material.
- the insulation.
- and in the air at the panel exit, leads to a system of six easily linearisable equations. The solution is determined by a classic triangularization method and allows to deduce of the values of the six unknowns, and in particular, the value of air temperature at the panel outlet as a function of air temperature at its entrance and incident radiation [2].

3. MATHEMATICAL MODEL OF THE DRYING CHEST

3.1. Description of The Drying Phenomenon

Since the publication of SHERWOOD's studies [3], drying phenomenon theory distinguishes 2 successive essential phases, after a brief period of temperature rise.

During PHASE I, the product's internal water evaporation rate is constant. This phase corresponds to the elimination of absorbed water, loosely bound to the solid matter: it is a superficial evaporation phenomenon often imperceptible under usual drying conditions.

PHASE II begins when the previous one ends, when the product's mean water content reaches a critical value W_{cri}. From this point on, the water vaporization front starts to regress towards the product's interior. Internal diffusion of water becomes dominant, leading to a decrease in the rate of drying.

The physical phenomenon occuring in the two phases are different in nature, so we have to propose a set of equations for each phase. The systems main difference lies in the equation giving the drying rate.

3.2. The Model's Equation Systems

The drying chest is composed of 6 superposed trays (Fig.2) each of which can be schematized as a succession of 2 boxes:

- A "full box" containing the product to be dried which is in a current of air.
- An "empty box" above it where the ascending air coming from the full box and the hot dry air arriving sideways through the porous absorber mix together.

This air mixture which then enters the full box of the next tray and so on.

3.3. Hypotheses

-For any given tray, the air temperature humidity and flow rate are homogenous and uniform before and after the mixture. The distribution of the air flow along the side-panel of the chest is determined by calculating the profile of air speeds through the porous absorber [2].

- The exchange surface area between air and fruit remains constant
- All fruit on a given tray is at the same temperature and their initial water content is identical.
- The internal humidity profiles are taken to be identical for all fruits through the drying cycle.

3.4. Formulation of The Model

We have a system of equations for each drying phase. in the evaporation phase (I) water activity in the fruit is greater or equal than one and in the diffusion phase (II) it falls bellow unity (for example Aw = 0.99)

3.5. Model of The Evaporation Phase

* Balance in the "full box" between the fruit layer and the drying air.

(i) For the drying air:

Conservation of energy

The variation in the thermal power of the air during its passage through the fruit layer is equal to the some of the powers exchanged by convection with the fruit and by conduction through the insulating side-panels:

$$Ma\ Cpa\ (Ta_2 - Ta) = -h.S.(Ta - Tf) - ca\ (Ta - Te) \qquad (1)$$

Conservation of mass

-conservation of the air mass going through the fruit layer:

$$Ma_2 = Ma \qquad (2)$$

- Conservation of the water mass leaving this layer

The increase in air humidity comes from water evaporation by the fruit :

$$Ma\ (Xa_2 - Xa) = -\frac{dW}{dt} Ms \qquad (3)$$

(ii) For the fruit layer

Conservation of energy

The variation of the fruit enthalpy is equal to the sum of power exchanged by convection with the air and the power needed to vaporize water inside the fruit:

$$Ms.(1+W)\ Cpf.\frac{dTf}{dt} = h.S.(Ta - Tf) - \Delta Hv\ \frac{dW}{dt} Ms \qquad (4)$$

Conservation of mass or drying rate

The evaporation is regulated by the "pump effect" at the surface whose motor term is best expressed as a pressure difference:

$$\Delta p = p_f(Tf) - p_{va}(Xa)$$

$$Ms.\frac{dW}{dt} = -\beta m \,.S.\,\frac{\Delta p}{rv\,.Ta} \qquad (5)$$

* Equation of the air mixture in the "empty box" (upper part of a tray)

- Conservation of dry air mass flow rate:

$$Ma = Ma_2 + Ma^\circ \qquad (6)$$

-Conservation of airborne water mass flow rate:

$$Ma.Xa = Ma_2 .Xa_2 + Ma^\circ.Xa^\circ \qquad (7)$$

-Enthalpic balance during air mixing

The enthalpy of air leaving the tray is equal to the sum of enthalpies of ascending and lateral air flows less the thermal losses through the insulated back of the chest:

$$Ha = Ha_2 + Ha^\circ - ca(Ta - Te) \qquad (8)$$

3.6. Model of The Diffusional Phase

The transfer of matter inside the fruit is well shown by FICK's diffusional equation applied to a cylinder.

indeed in our case, an apple slice can be easily compared to a cylinder in which drying only occurs on the plane sides while the cylindrical surface (skin) is imervious to the water flux. The thickness of this slice is much less than its diameter. So, the general equation of mass transfer can be written in the case where the coefficient Dm depends only on the fruit temperature.

$$\frac{\partial W}{\partial t} = Dm \,.\, \frac{\partial^2 W}{\partial x^2} \qquad (9)$$

with the initial conditions:

$$W\,(to,x) = W_{in} \qquad (10)$$

and the boundary conditions at the edge of the slice:

$$Dm \,.\, \left.\frac{\partial W}{\partial x}\right|_{x = \pm x_e} = \beta m\,(W_{surf} - We) \qquad (11)$$

another boundary condition can be deducted from the slice symmetry:

$$\left.\frac{\partial W}{\partial x}\right|_{x = 0} = 0 \qquad (12)$$

This reduces by half the amount of calculation needed.

At any given moment, the degree of humidity in any par of the fruit is thus determined as a function of ' convective exchange at the surface.

If we assume that in a layer, all the apple slice: the same degree of humidity (identical slices thickness), then the average value of the degree of humidity of the product layer is obtained at each moment, by integration over the fruit volume of the distribution of the internal degree of humidity. Only this average value is directly measurable experimentally.

$$\bar{W} = \frac{1}{V} \int_{v} W \, .dV \qquad (13)$$

3.7. Determination of The Coefficients Appearing in The Model

The coefficients which appear in the equations of the model can be found either from previously published sources [4-6] or by a parametric identification technique specific to automatics (Powell's method for example).

Thus, the quadratic criteria between the responses of the model and those of the real process subjected to the same stimulation, is minimized.

The experimental results leading to parameter identification are obtained in a ventilated drying tunnel in a controlled atmosphere.

3.8. Solution of The Model and Validation

The equation systems established for each drying phase are discretized and solved using the finite difference method.

The model can be validated by comparing the experimental results with those obtained by the model for identical conditions. The experiment used must be different from that which served to identify the parameters(Fig. 3).

The results are satisfactory, the noted deviations remaining less than 2% [2].

4. SIMULATIONS RESULTS

We compare here the results for two forced convection simulations in summer in Perpignan.

- in one case the blower is continuously powered by mains electricity.
- in the other case, the air flow is regulated by a photoelectric cell panel depending on the insolation.

In figure 4 we drewexperimentally the characteristic curve for the system (photocell panel+blower) i.e. air flow as a function of insolation.

This curve shows an insolation threshold for the fan:

- down to a solar power of 300 W/m^2 the blower does not start.

- when solar radiation decreases the threshold drops to 250 W/m^2.

-It seems interesting to calculate whether this threshold is a handicap for the working process. In figure 5, the water content curves (dry base) as a function of time are represented in both cases:

- discontinuous regime with threshold
- continuous regime corresponding to the maximum possible flow with photoelectric cells.

The two curves obtained are extremely similar. Night ventillation of a product which has reached phase II is not very cost-effective under these conditions.

The difference between the curves obtained for the lowest and highest trays points out again the need for a rotation of the trays during a drying operation.

CONCLUSION

The mathematical model of the solar dryer studied was validated by a drying experiment using sliced Golden apples.

The match between the theoretical and experimental results is satisfactory, proving that the equations developed for the two successive phases of this process represent both superficial evaporation and internal diffusion phenomena.

the parametric identification technique used required simple experiments carried out in a ventilated drying tunnel with a controlled atmosphere [7]. A set of specific parameters, needed for the simulation program is thus determined for each product to be dried.

The model enables us to simulate the drying of a product in different climatic conditions.

When a blower (5 Watts) is used, with an autonomous power source and an air flow modulated by the level of insolation, the drying curves remain close to those obtained with a more conventional steady air flow system. The case for using photoelectric cells is strengthened in spite of their rather high cost at the present time.

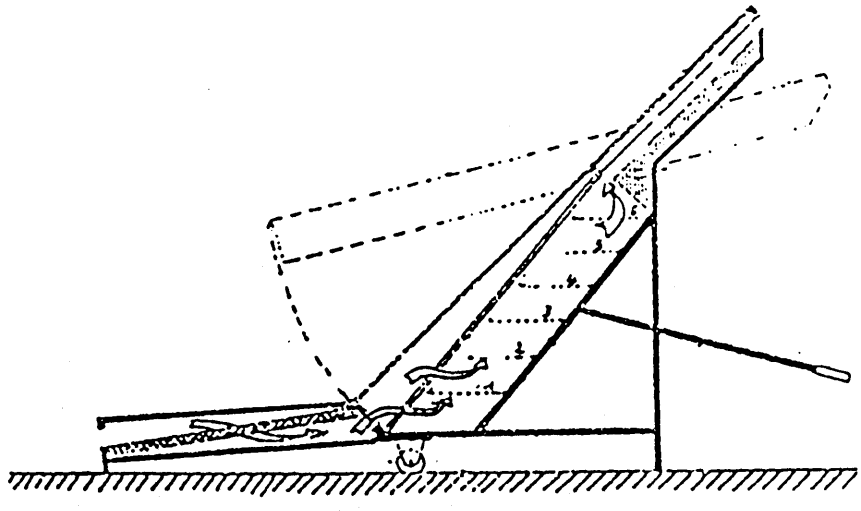

Figure 1. Diagram of the SERESOL solar dryer tipping type

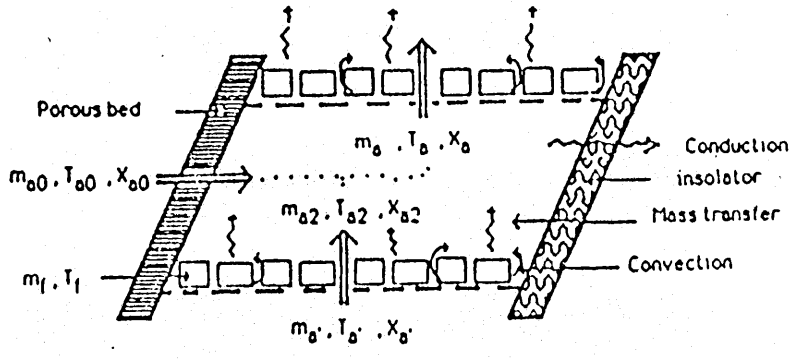

Figure 2. Diagram of a tray with a "full box" and an "empty box"

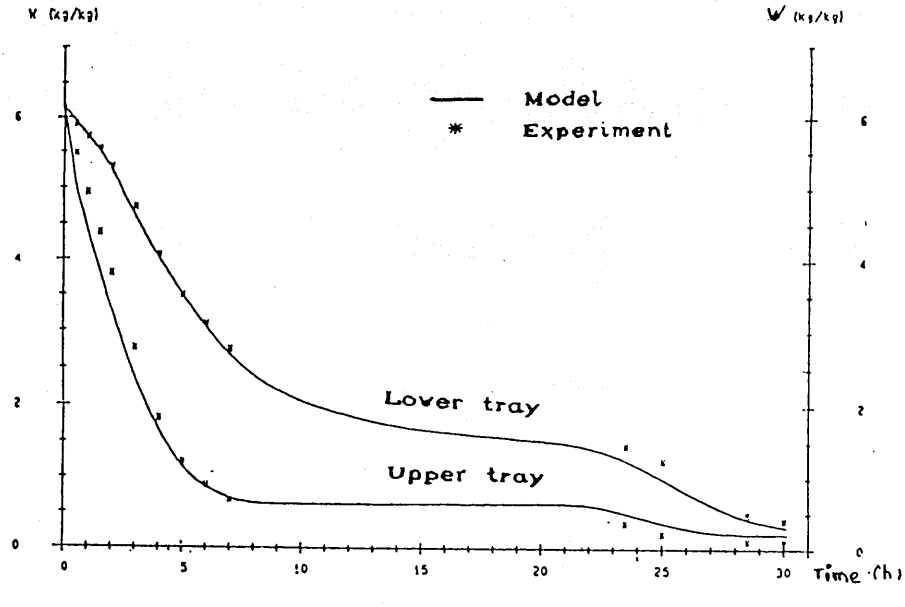

Figure 3. Fruit moisture content Vs. Time

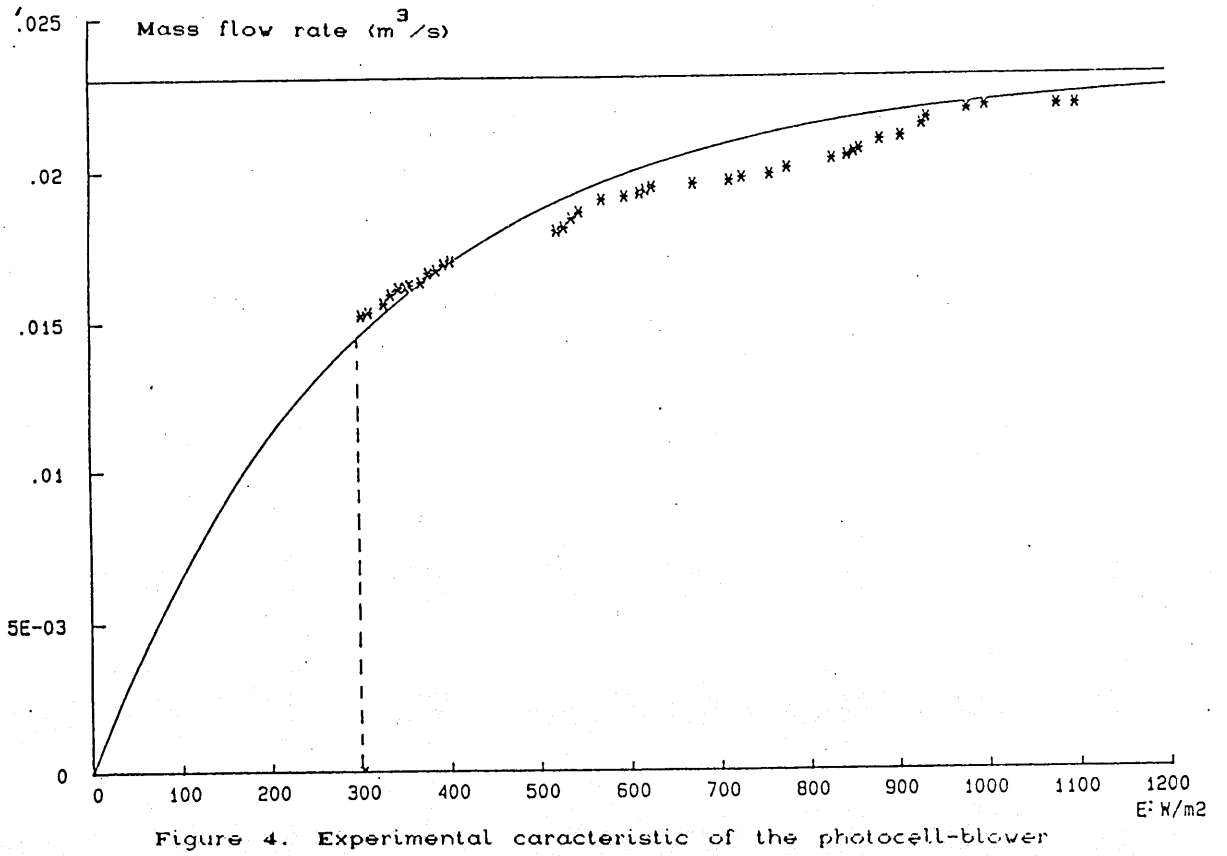

Figure 4. Experimental caracteristic of the photocell-blower system: air flow as a function of insolation.

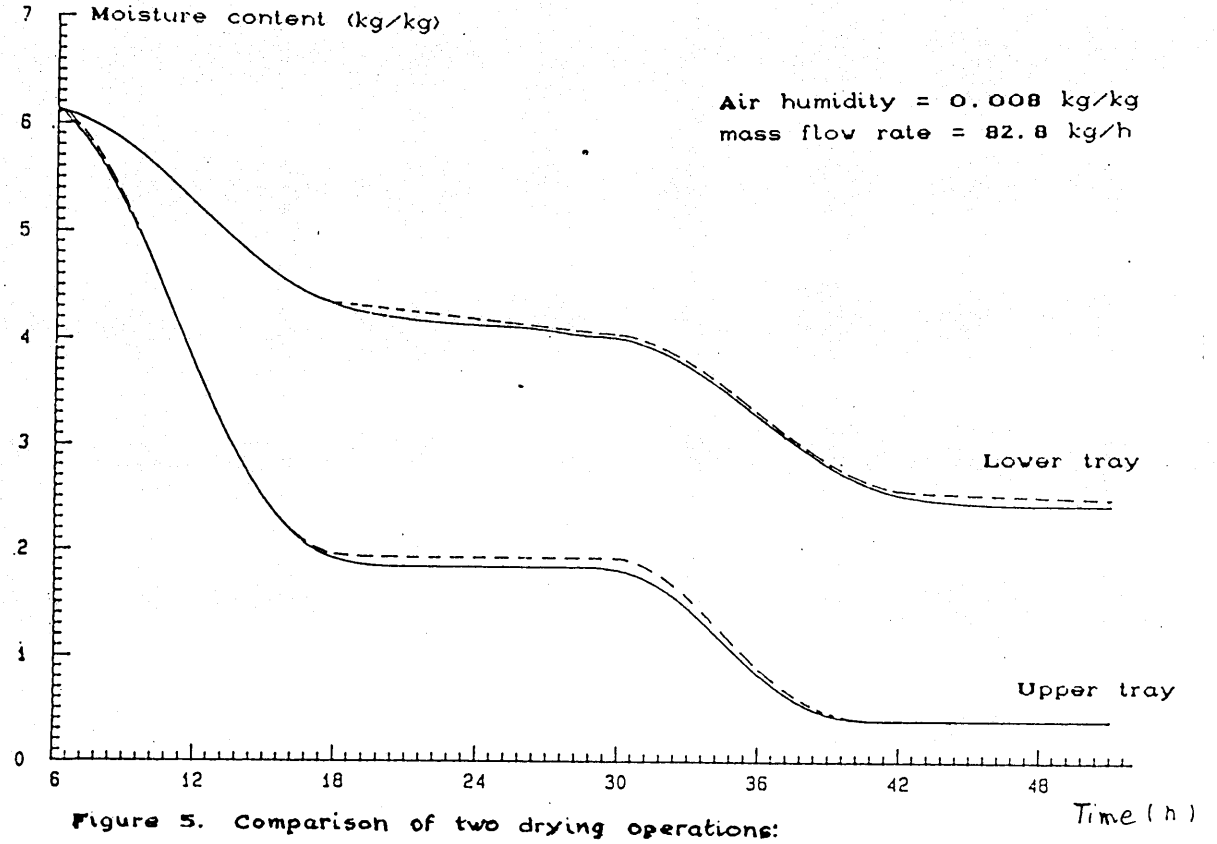

Figure 5. Comparison of two drying operations:
——— continuous regime (mains electricity)
------ discontinuous regime (photocells)

NOMENCLATURE

Capital letters:

AS	: Dry air	
Aw	: Water Activity	(-)
Cpa	:Air specific heat at constant pressure	($J.kg^{-1}°C^{-1}$)
Cpf	:fruit specific heat at constant pressure	($J.kg^{-1}°C^{-1}$)
Dm	:Molecular diffusion coefficient	($m^2.S$)
Ha	:Flux of air massic molar enthalpy	(W/mole)
Ma	:Mass flow rate	($kg.S^{-1}$)
Ms	:Dry mass of fruit	(kg)
Pf	:Water vapour pressure on fruit surface	(Pa)
Pva	:Water vapour pressure on drying air	(Pa)
Pvs	:Satured vapour pressure	(Pa)
S	:Transfer surface area	(m^2)
Ta	:Air temperature	(K)
Te	:Exterior air temperature	(K)
Tf	:fruit temperature	(K)
V	:Volume	(m^3)
W	:Moisture content of fruit (dry base)	(kg/kg.Ms)
$\overline{W}$	:Average moisture content	(kg/kg.Ms)
Xa	:Absolute humidity	(kg/kg.As)

Miniscule:

ca	:heat conductance	(W/K)
h	:Convective heat transfert coefficient	($W.m^{-2}°C^{-1}$)
rv	:Perfect gaz constant	($J.kg^{-1}K^{-1}$)
t	:Time	(S)
x	:Cartesian coordinates	(m)

Grec letters:

βm	:Convective mass transfer coefficient	($kg.m^{-2}Pa^{-1}$)
ΔHv	:Latent heat of evaporation	($J.K^{-1}$)
Δp	:pressure variation	(Pa)

REFERENCES

1. FOURNIER M.,THEMELIN A.,
   Experimentation de séchoirs solaires à fruits de faible capacité : les modèles SERESOL et M5003.
   Séchage solaire et développement rural.
   ENSAM-Bordeaux, pp.105-121, Mai 1983

2. EL HISSE M.,
   Modélisation, Identification et Simulation d'un séchoir solaire agroalimentaire.
   Thèse 3ème cycle, Perpignan-France, Octobre 1987.

3. SHERWOOD T.K.,
Drying of solids.
ind. Engng. chem.
21 (1), p.12-16, 1929
21 (10) p.976-980, 1929
22 (2), p.132-137, 1930
24 (3), p.307-310, 1934.

4. LOF G.O.G.,HAWLEY R.W.,
Unsteady state heat transfer between air and loose solids.
Ind. Engng. Chem. 40, p.106, 1948.

5. BRUHAT G., Thermodynamique.
Masson, Paris? 1968.

6. HENDERSON S.M.,
A basic concept of equilibrium moisture.
Agricultural Engineering 33, PP 29-32 1952.

7. PALLET D., FOURNIER M., THEMELIN A.,
Modélisation, identification et simulation d'un séchoir solaire à bois.
Revue de Physique Appliquée, 22, pp.1397-1407, 1987.

تحليل أداء نظام التبريد الامتصاصي الشمسي باستخدام المواد الماصة الصلبة تحت شروط مدينة بنغازى المناخية ودراسة تأثير سماكة المجمع على الاداء

د . محمد عدنان فرواتي
عضو هيئة التدريس بوحدة بحوث الهندسة الميكانيكية - مركز بحوث العلوم الهندسية بنغازى

الملخص :

ان أنظمة التبريد التي تستخدم المواد الماصة الصلبة هي أبسط أنظمة التبريد الشمسية من الناحية الانشائية. والموضوع الحالي يتناول بالبحث التحليلي نظام التبريد الامتصاصي الشمسي باستخدام ثنائي من الزيوليت (MS - 13X) والماء . ويتألف النظام من ثلاث وحدات أساسية وهي المجمع والمكثف والمبخر وتعمل تحت التخلخل . وقد جرى اعداد برنامج الحاسوب لغرض تحليل أداء النظام تحت شروط مدينة بنغازى المناخية خلال نهار 7/17 لمجمع بمساحة متر مربع واحد وزاوية ميل 20^{o} باتجاه الجنوب وبسماكات مختلفة . فقد تبين لدى تطبيق البرنامج من أجل درجة حرارة تبخر 5 مه ودرجة حرارة تكثف 40 مه بأن المجمع ذو السماكة 3.5 سم يعطي سعة تبريد يومية تبلغ 3.4 ميغاجول بمعامل أداء كلي شمسي 0.16 وأن المجمع ذو السماكة 12 سم يعطي سعة تبريد يومية تبلغ 5 ميغاجول بمعامل أداء كلي شمسي 0.21 ، كما تبين أن سعة التبريد اليومية تبلغ قيمتها العظمى عند زيادة سماكة المجمع (الزيوليت) الى حوالي 12 سم وأنه لاجدوى من زيادة السماكة الى أكثر من ذلك .

الرموز :

COP	معامل الاداء الكلي الشمسي
COP_i	معامل الاداء الكلي الداخلي
C_p	الحرارة النوعية للماء
g_z	كتلة الزيوليت
G_{Tn}	شدة الاشعاع الشمسي الكلي الساقط على المجمع في الفترة الزمنية $\Delta\tau_n$
L	سماكة الزيوليت وهي سماكة وعاء المجمع
LH	الحرارة الكامنة للماء
m	كتلة الماء المتكثف اعتبارا من الشروق وحتى اللحظة τ_N
$(MC)_n$	الحرارة النوعية للمجمع في الفترة الزمنية $\Delta\tau_n$ مع اعتبار فرق درجة الحرارة في الاجزاء المختلفة للمجمع
$(MC)_e$	الحرارة النوعية المكافئة للمجمع في الفترة الزمنية $\Delta\tau_n$
P	ضغط البخار
P_c	ضغط تكثف الماء
P_e	ضغط تبخر الماء
Q_e	سعة التبريد للنظام اعتبارا من شروق الشمس وحتى اللحظة τ_N

Q_c السعة الحرارية للمجمع اعتبارا من شروق الشمس وحتى اللحظة τ_N

Q_r الطاقة الشمسية الساقطة على المجمع اعتبارا من شروق الشمس وحتى اللحظة τ_N

S معدل الطاقة الشمسية التي تم انتقالها الى المجمع في الفترة $\Delta\tau_n$

ST الزمن الشمسي

T درجة حرارة الزيوليت وهي درجة حرارة وعاء المجمع

T_a درجة حرارة الجو

T_{ad} درجة حرارة الامتصاص

T_g درجة حرارة الزيوليت خلال مرحلة التكثف

T_s درجة الحرارة التي يبدأ الزيوليت عندها بطرح البخار

T_s درجة الحرارة التي يبدأ الزيوليت عندها بامتصاص البخار

U_1 معامل الفقد الحرارى الكلي للمجمع

X السعة الامتصاصية للزيوليت

X_a السعة الامتصاصية للزيوليت عند بداية التكثف

X_g السعة الامتصاصية للزيوليت عند نهاية التكثف

Δ مقدار التغير في المتغير خلال الفترة الزمنية $\Delta\tau_n$

η كفاءة المجمع

1 - مقدمة :

ان توافق ازدياد الحاجة للتبريد في فصل الصيف مع ازدياد الاشعاع الشمسي ، وامكانية تشغيل أنظمة التبريد الامتصاصية بالطاقة الحرارية يشجعان على تشغيل أنظمة التبريد الامتصاصية بالاشعة الشمسية وعلى تطويرها عن طريق الابحاث النظرية والعملية. ولعل أنظمة التبريد التي تستخدم المواد الماصة الصلبة هي أبسط أنظمة التبريد الشمسية من الناحية الانشائية نظرا لامكانية استخدام اشعة الشمس بشكل مباشر والاستغناء عن المضخة وبرج التبريد ، هذا بالاضافة الى امكانية استغلال الفائض الحرارى في تسخين الماء [1]. وهناك أبحاث نظرية وعملية كانت تجرى حتى فترة قريبة لتطوير أنظمة التبريد الامتصاصية (الصلبة) الشمسية وذلك في مجال ايجاد أفضل ثنائي امتصاص (مادة ماصة صلبة ـ سائل تبريد) وفي ايجاد أفضل تصميم وشروط تشغيل [2],[3] .

يتركب نظام التبريد الامتصاصي البسيط من ثلاث وحدات رئيسية هي المجمع والمكثف والمبخر ، وهو يؤدى عملية التبريد ليلا . أما نظام التبريد الامتصاصي المركب فهو يضم بالاضافة الى الوحدات الثلاثة الاساسية السابقة وحدة اضافية لاستيعاب البخار أو امتصاصه وذلك لانجاز عملية التبريد نهارا. أما المجمع فهو يعمل كمجمع شمسي مسطح بسيط وكوعاء يحوى المادة الماصة المشبعة بسائل التبريد والمجمع وعلى الاخص ثنائي الامتصاص الذى يحويه المجمع يشكل العنصر الاساسي والهام في نظام التبريد الامتصاصي [1],[4],[5] . ودور المادة الماصة هنا يشبه الى حد كبير دور الضاغط في نظام التبريد الذى يعمل على مبدأ ضغط البخار . ولعل الزيوليت ـ ماء هو أبرز ثنائي أعطى أداء عاليا حتى في حالة استخدام مكثف يعمل بالحمل الطبيعي للهواء [2] , [3] . والزيوليت هو مادة قلوية متوفرة بشكل طبيعي كما أنه يحضر صناعيا [3] , [6] .

ولقد بينت الابحاث المخبرية حول نظام التبريد الامتصاصي ان معامل الاداء الكلي الشمسي يمكن أن يبلغ 0.45 في حال استخدام مجمع مسطح معين بداخله زيوليت طبيعي وباستخدام مكثف يعمل بالحمل الطبيعي للهواء بدرجة تكثف 50 مº [1] . أما في حال استخدام زيوليت اصطناعي فان معامل الاداء ينخفض نتيجة ارتفاع حرارة الامتصاص في الزيوليت الاصطناعي بالنسبة للطبيعي ، ومع هذا

فهو أكبر من معامل الاداء الكلي الشمسي لنظام التبريد الامتصاصي الذى يعمل بمحلول الليثيوم بروميد – ماء تحت شروط مماثلة ، أى باستخدام مجمع شمسي مسطح وبدرجة حرارة تكثف 50 م° .

والبحث الحالي يتناول دراسة أداء نظام التبريد الامتصاصي البسيط باستخدام زيـوليت اصطناعـي ومكثف يعمل بالحمل الطبيعي للهواء وذلك تحت شروط مدينة بنغازى المناخية . كما يتناول البحـث دراسة تأثير زيادة سماكة المجمع (الزيوليت) على درجة حرارة المجمع وبالتالي على سعة التبريـد اليومية ومعامل الاداء .

2 - تركيب النظام ومبدأ عمله :

يتألف النظام هنا من ثلاث وحدات هي المجمع والمكثف والمبخر كما في الشكل 1 ويستخدم فيـه الزيوليت الاصطناعي (MS-13X) والماء كثنائي امتصاص . أما المجمع فيشكل الوحدة الاساسية فـي النظام ويميل 20^{o} مع الافق ومتجه نحو الجنوب ، وذلك لجمع مقدار كبير من الاشعاع الشمسي صيفـا في مدينة بنغازى ذات خط العرض 32.1^{o} شمالا . ويعمل النظام بطورين اثنين خلال اليوم الواحـد ،

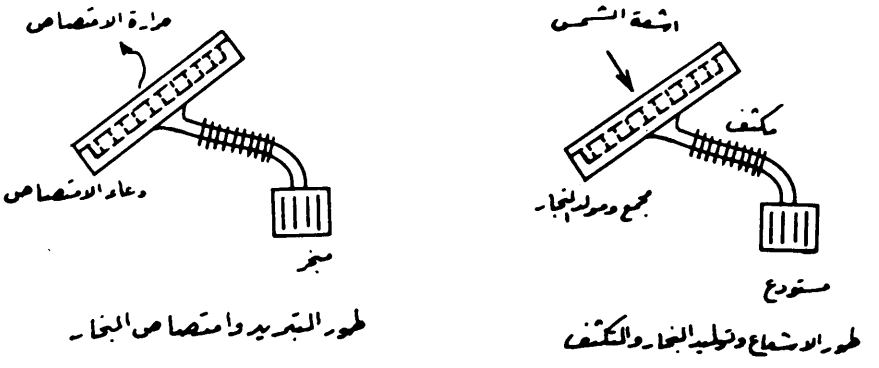

الشكل 1 : تركيب نظام التبريد الشمسي البسيط باستخدام المادة الماصة الصلبة ،ومبدأعمله.

الطور الاول هو طور الاشعاع الشمسي وتوليد بخار الماء وتكثفه ثم يليه الطور الثاني وهو طور التبريـد وامتصاص البخار الناتج بواسطة الزيوليت . أى ان النظام محكم الاغلاق ويعمل تحت التخلخل بيـن ضغط تكثف الماء وضغط تبخره . وعليه فان للمجمع ثلاث وظائف وهي جمع الاشعة وتوليد البخار ثـم امتصاصه وهو بشكل وعاء مسطح من النحاس بمساحة متر مربع واحد مطلي بطلاء أسود ومغطى بلـوح زجاجي واحد . ويوجد بداخل الوعاء فواصل متقاطعة من الالمنيوم تشكل حجرا تحوى الزيوليـت ووظيفتها نقل الحرارة وجعل درجات الحرارة داخل الوعاء أكثر تجانسا ، وكذلك دعم المجمع فـي مقاومته الضغط الخارجي (الجوى) ، وهي مثقبة بشكل يسمح بحركة البخار باتجاه مخرج المجمـع وبالعكس . والوعاء معزول بعازل حرارى من الجوانب والسطح الخلفي . وسماكة الوعاء تساوى سماكـة الزيوليت ويطلق عليها هنا سماكة المجمع . أما المكثف فهو ذو سعة كافية لتكثيف البخار القادم مـن المجمع وذلك بالحمل الطبيعي للهواء . هذا ويسمح المكثف بجريان الماء المتكثف تحت الجاذبيـة الارضية الى المستودع أو المبخر كما في الشكل 1 .

أما الزيوليت الاصطناعي (MS-13X) فهو أحد المركبات القلوية الاصطناعية وهو بحـكـم تركيبه البللورى بشكل X يحوى سطح داخلي كبير يجعله قادر على امتصاص الغازات ذات القطر أصغـر من10 أنغستروم بنسبة امتصاص تصل الى 30 بالمئة من وزنه في درجة حرارة الغرفة . وهو خامل مـن الناحية الكيميائية ويحافظ على قدرته الامتصاصية لفترة زمنية طويلة . ولعل أهم مزاياه في مجـال التبريد هي :

– تعتبر قدرته على امتصاص نسبة عالية من بخار الماء في الضغوط المنخفضة ميّزة أساسية في مجـــال التبريد اذ يجرى امتصاص بخار الماء تحت ضغط التبخر المنخفض المقابل لدرجة حرارة التبخر المنخفضة.
– تتأثر سعته الامتصاصية تأثرا قليلا بضغط البخار المراد امتصاصه وعليه فان ارتفاع ضغط التكثـــف لايؤثر كثيرا على سعته الامتصاصية وبالتالي يمكن استخدام مكثفات بسيطة تبرد بالحمل الطبيعي للهواء مع المحافظة على أداء جيد .
– تغير سعته الامتصاصية تغيرا كبيرا لدى تغير درجة حرارته يسمح باستخدام الاشعة الشمسية مباشـرة وبدون وسائط معقدة [3], [6], [7] .

هذا ويمكن ملاحظة خصائص الزيوليت العملية في منحني العلاقة بين ضغط البخار P وسعـــــة الامتصاص X لدرجات حرارة مختلفة كما هو مبين بالشكل 2 .

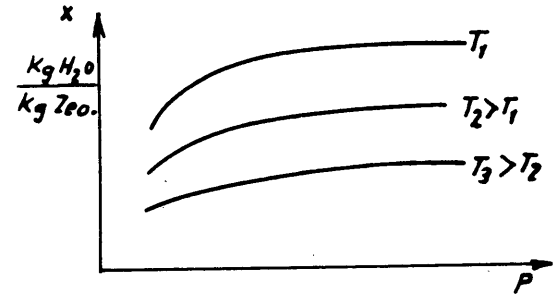

الشكل 2 :منحنيات العلاقة بين سعة الامتصـــاص للزيوليت X وضغط البخار P.

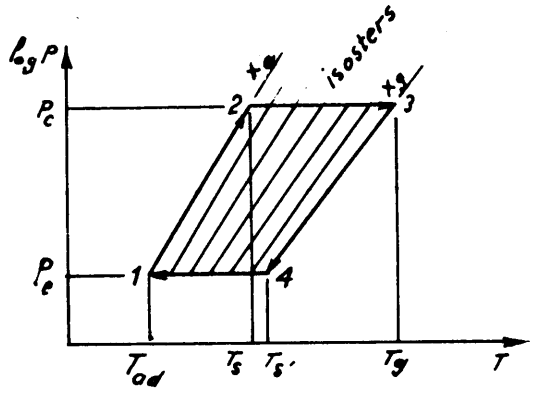

الشكل 3 : دارة التبريد على محورى درجة حـرارة الزيوليت T وضغط البخار P.

3- دارة التبريد :

ترسم دارة التبريد على محورى درجة حرارة الزيوليت T والضغط P السائد داخل النظام لتوضيـح الطورين اللذين يمر بهما النظام خلال اليوم الواحد بما في ذلك المراحل المبينة في الشكل 3 علـــى النحو التالي :

1 – 2 : وهي مرحلة تسخين الزيوليت المشبع بفعل أشعة الشمس التي يحولها السطح الاسود الـى طاقة حرارية . اذ يرافق ذلك ارتفاع درجة حرارة الزيوليت وضغط البخار من T_{ad} و P_e الى P_c, T_s حيث يبدأ طرح البخار وتكثفه . ودرجة الحرارة T_s التي يبدوء عندها الزيوليت بطرح البخار تحسب من العلاقة التالية :

$$T_s = \left[\frac{1}{T_{ad}} - \frac{LH}{\Delta H}\left(\frac{1}{T_e} - \frac{1}{T_c}\right)\right]^{-1} \qquad (1)$$

2 – 3 : وهي مرحلة توليد البخار التي تستمر باستمرار تقديم طاقة الامتصاص اللازمة من الاشعـــة الشمسية حتى يبلغ الزيوليت درجة حرارته القصوى T_g وتنخفض أثناء ذلك سعة الزيوليت أو استيعابـــه للماء من X_a الى X_g. ويرافق ذلك تكثف بخار الماء في المكثف تحت الضغط P_c .

3 – 4 : وهي مرحلة تبريد المجمع بالحمل الطبيعي للهواء ونشر الطاقة المحسوسة الى الوســـط الخارجي اذ تنخفض درجة حرارة الزيوليت وضغط البخار من T_g و P_c الى T_s' و P_e . فتبدأ عمليـة التبريد المطلوبة أى يبدأ الماء المتجمع في المبخر بالغليان والتبخر . أما درجة الحرارة T_s' فهـــي

تحسب من العلاقة التالية :

$$T'_s = \left[\frac{1}{T_g} + \frac{LH}{\Delta H}\left(\frac{1}{T_e} - \frac{1}{T_c}\right)\right]^{-1} \quad (2)$$

4 - 1 : وهي مرحلة التبريد أى تبخر الماء وانتقاله من المبخر الى المجمع ثم امتصاصه من قبل الزيوليت حتى الاشباع · ويرافق هذه العملية نشر طاقة الامتصاص من المجمع بواسطة الحمل الطبيعي للهواء [2] ·

4 - أداء النظام :

يعبّر عن أداء النظام في التبريد بمعامل الاداء وهو نسبة سعة التبريد للنظام على الطاقة التي يزود بها · وفي حال سير العمليات بشكل مثالي فان معامل الاداء يكون تابعا لدرجات الحرارة التي يتم بها انتقال الحرارة ويسمى عندها بمعامل أداء كارنوت ، أى :

$$COP = \frac{T_e(T_g - T_{ad})}{T_g(T_c - T_e)} \quad (3)$$

أما في حال اعتبار LH حرارة تبخر الماء النوعية في المبخر وΔH حرارة الامتصاص النوعية اللازم تقديمها للزيوليت المشبع بصرف النظر عن كميات الحرارة المفقودة والحرارة المخزونة أى اللازمة لرفع درجة حرارة محتويات المجمع فان معامل الاداء تابع الى نوع ثنائي الامتصاص وسعة الامتصاص وهو يساوى نظريا :

$$COP = LH/\Delta H \quad (4)$$

حيث تبقى قيمة LH في هذه العلاقة ثابتة من أجل درجة حرارة تبخر T_e ثابتة للماء بينما تتزايد قيمة ΔH مع تناقص سعة الامتصاص للزيوليت عن حد الاشباع · ونظرا لان تغير سعة الامتصاص عمليا هو قليل خلال طور الاشعاع الشمسي فانه يمكن اعتبار ΔH ثابتة وبالتالي فان COP ثابت أيضا من أجل نوع معين من الزيوليت ·

ولتقييم أداء النظام ككل وتحت تأثير أشعة الشمس كمصدر طاقة لتشغيله فانه يؤخذ في الاعتبار الفقد الضوئي والحرارى والحرارة المختزنة في المجمع بالاضافة الى حرارة الامتصاص (كما هو في المرحلة 2-3) · ولاجراء هذا التقييم يحسب معامل الاداء الكلي للنظام · وهو يعبر عن أداء النظام في التبريد اعتبارا من شروق الشمس وحتى لحظة ما من اليوم · ويمكن مطالعة معامل الاداء هذا كمعامل أداء كلي داخلي ومعامل أداء كلي شمسي على النحو التالي :

$$COP_i = Q_e/Q_c \quad (5)$$

$$COP = \eta \cdot COP_i = Q_e/Q_r \quad (6)$$

حيث يعبر η عن كفاءة المجمع في جمع الاشعة الشمسية وتحويلها الى طاقة مفيدة وهو يساوى :

$$\eta = Q_c/Q_r \quad (7)$$

أما Q_e, Q_c, Q_r فهي على التوالي سعة التبريد والسعة الحرارية للمجمع والطاقة الشمسية الساقطة على المجمع وتحسب بجمع مركبات كل منها خلال الفترات الزمنية المتساوية $\Delta\tau_n$ اعتبارا من شروق الشمس وحتى اللحظة τ_N · وعليه فان :

$$Q_e = \sum_{n=1}^{N} \Delta Q_{en} \qquad Q_c = \sum_{n=1}^{N} \Delta Q_{cn} \qquad Q_r = \sum_{n=1}^{N} \Delta Q_{rn} \quad (8)$$

(9) $$\Delta Q_{en} = \Delta m_n [LH - C_p (T_c - T_e)]$$

(10) $$\Delta Q_{cn} = (MC)_n \Delta T_n + \Delta H . \Delta m_n$$

(11) $$\Delta m_n = g_z (-\Delta X_n)$$

(12) $$\Delta X_n = A(-\Delta T_n)$$

(13) $$\Delta Q_{rn} = G_{Tn} \cdot \Delta \tau_n$$

الثابت A هو ثابت العلاقة بين ΔX_n مقدار التغير في سعة الامتصاص للزيوليت و ΔT_n التغير في درجة حرارته خلال الفترة الزمنية $\Delta \tau_n$. ويعتبر A هنا ثابتا في مجال تغير درجات الحرارة المحدود في مرحلة توليد البخار ، فهو يتراوح عمليا من 50 مم الى 100 مم تقريبا [4] .

ولحساب ΔT_n مقدار تغير درجة الحرارة خلال الفترة الزمنية $\Delta \tau_n$ فانه يحدد تغير درجة حرارة الزيوليت T بالنسبة للزمن τ اعتبارا من شروق الشمس ، وذلك بالاستفادة من علاقة التوازن الحرارى للمجمع في اللحظة τ مع اعتبار تجانس درجات الحرارة في وعاء المجمع نتيجة لوجود نواقل الالمنيوم والنحاس بداخله [8],[9] أى :

(14) $$[(MC) + \Delta H \cdot A \cdot g_z] \frac{dT}{d\tau} = [S - U_1 (T - T_a)]$$

(15) $$(MC) + \Delta H \cdot A \cdot g_z = (MC)_e$$

وبافتراض أن قيم $(MC)_e$ و S و U_1 و T_a تبقى ثابتة خلال الفترة الزمنية $\Delta \tau_n$ فانه يمكن حلّ المعادلة السابقة وحساب T_2 درجة حرارة الزيوليت في نهاية هذه الفترة كالتالي :

(16) $$\frac{S - U_1 (T_2 - T_a)}{S - U_1 (T_1 - T_a)} = EXP[-U_1 \Delta \tau_n / (MC)_e]$$

حيث T_1 هي درجة حرارة الزيوليت في بداية الفترة الزمنية $\Delta \tau_n$.

5 - الشروط المطبقة :

شروط الاشعاع الشمسي ودرجات حرارة الجو التي طبقت على نظام التبريد موضوع البحث تماثل تلك الشروط في نهار 7/17 في مدينة بنغازى حيث صيغت بشكل معادلات رياضية لاستخدامها في دراسة وتحليل أداء النظام خلال فترات زمنية متساوية $\Delta \tau_n = 0.5 hr$ واعتبارا من شروق الشمس حتى غروبها [8],[9],[10],[11] . والمنحنيات التي تمثل شدة الاشعاع الشمسي الكلي الساقط على سطح المجمع G_T ودرجات حرارة الجو T_a حسب تغير الزمن الشمسي ST مبيّنة في الشكل 4 . ولقد اعتبرت درجة الحرارة 40 مم كدرجة حرارة تكثف يمكن أن تحصل لدى استخدام مكثف مناسب يبرد بالحمل الطبيعي للهواء . كما أن اعتبار درجة حرارة التبخر 5 مم يأتي متوافقا مع احتياجات التبريد في مجال تكييف الهواء .

6 - النتائج والمناقشة :

جرى اعداد برنامج الحاسوب لغرض تحليل أداء نظام التبريد الامتصاصي البسيط تحت شروط مدينة بنغازى المناخية المذكورة سالفا . ومن أهم متغيرات النظام التي ترد هنا حسب تغير الزمن الشمسي هي درجة حرارة المجمع وكمية الماء (سائل التبريد) المتكثف وكفاءة المجمع ومعامل الاداء

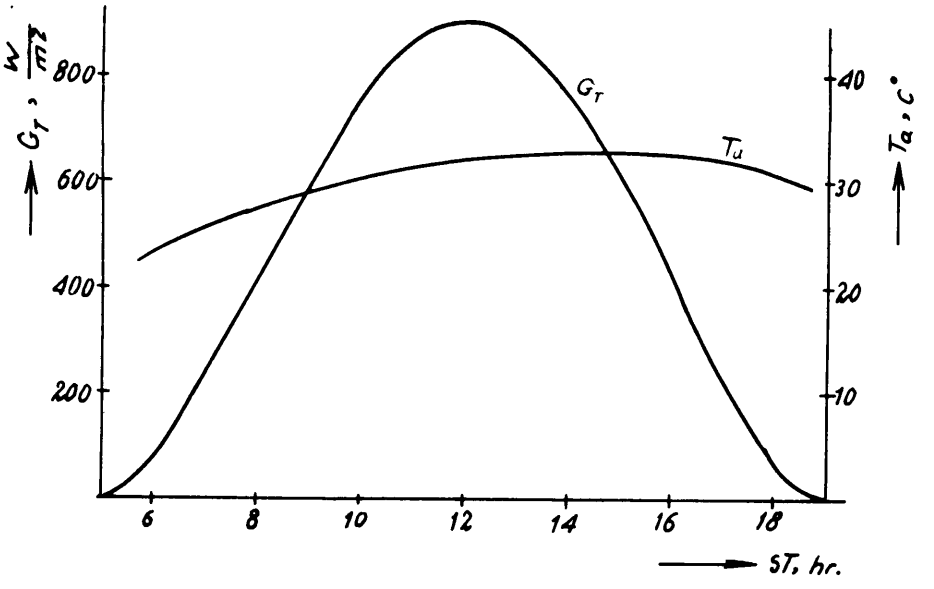

الشكل 4 : شدة الاشعاع الشمسي الكلي الساقط على المجمع G_T ودرجة حرارة الجو T_a حسب تغير الزمن الشمسي ST ·

الكلي الشمسي كما هو مبين في الاشكال 5,6,7,8,9 ·

يلاحظ في الشكل 5 أن ارتفاع درجة حرارة الزيوليت يكون بطيئا في مرحلة التكثف بالمقارنة مع ارتفاعها قبل البدء بالتكثف عند درجة الحرارة T_s وذلك بسبب استهلاك جزء من الطاقة الشمسية في تبخير (طرح بخار) الماء من الزيوليت · كما أن معدل ارتفاع درجة حرارة الزيوليت في المجمع ذو السماكة الكبيرة أصغر مما هو في المجمع ذو السماكة الصغيرة وذلك نتيجة لتأثير السعة الحرارية للمجمع.

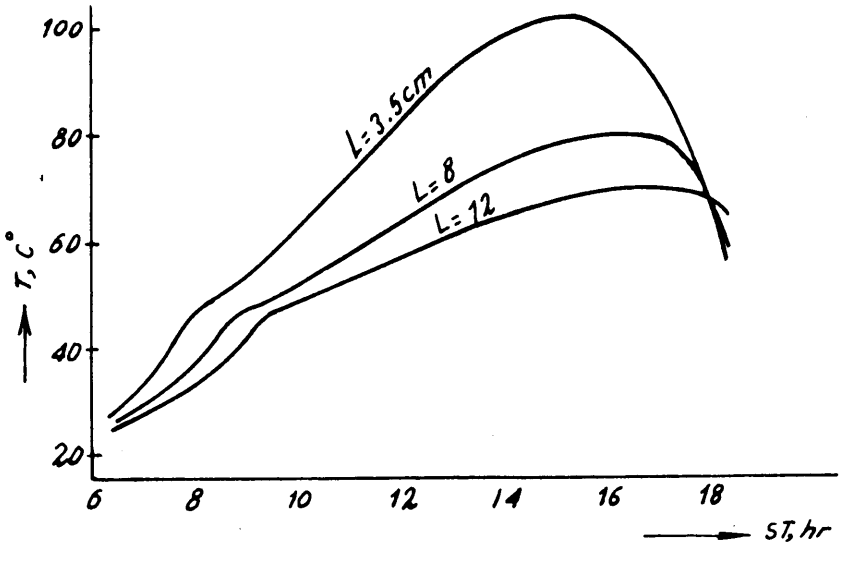

الشكل 5 : تغير درجة حرارة الزيوليت بالنسبة للزمن ولسماكات مختلفة ·

أما تكثف الماء فهو يبدأ عندما ترتفع درجة حرارة الزيوليت الى T_s ويرتفع ضغط البخار داخل النظام الى الضغط المقابل لتكثف الماء في درجة الحرارة 40 مه ويستمر التكثف بمعدل يتناسب مع معدل ارتفاع درجة حرارة الزيوليت ويتوقف عندما يصبح معدل ارتفاع درجة الحرارة صفرا أى عندما تبلغ درجة حرارة الزيوليت نهايتها العظمى كما هو في الشكل 6 · وكمية الماء المتكثف هي مميز هام ويعبر عن سعة التبريد اليومية للنظام · ومن الملاحظ أن ازدياد السماكة أى ازدياد كتلة الزيوليت يؤدى الى تأخر التكثف الا أن معدل الماء المتكثف يكون أكبر مما هو في المجمع ذو السماكة الاصغر · وبما أن درجة حرارة الزيوليت تصل الى نهايتها العظمى مبكرا في المجمع ذو السماكة الصغيرة لذا فان التكثف

يتوقف فيها مبكرا أيضا بالمقارنة مع المجمعات ذات السماكة الكبيرة · وعليه فان طاقة الاشعـــــــاع الشمسي اعتبارا من توقف التكثف وحتى الغروب هي عبارة عن طاقة فائضة يمكن ضمها الى حـــــــرارة التكثف وحرارة الامتصاص والحرارة المخزونة في المجمع ثم الاستفادة من هذا المجموع في تسخين المـاء أو تسخين المجمع تسخينا أوليا في صباح اليوم التالي ·

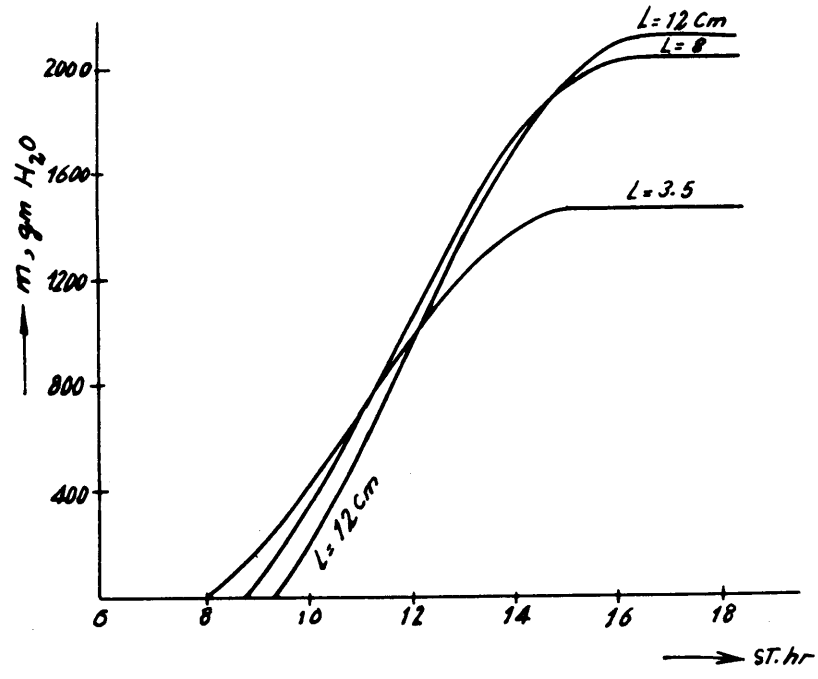

الشكل 6 : كتلة الماء المتكثف لسماكات مختلفة ·

والشكل 7 يبين كفاءة المجمعات الثلاثة في تحويل الطاقة الشمسية الى الطاقة اللازمة لطـــــرح البخار والطاقة الحرارية المخزونة في المجمع ، حيث يؤدى ارتفاع درجة حرارة الزيوليت الى زيـــــادة الفقد الحرارى وانخفاض الكفاءة ·

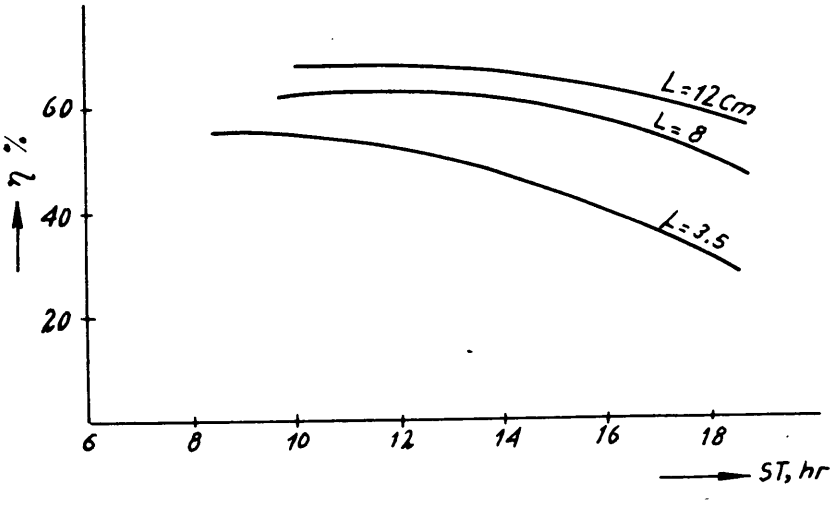

الشكل 7 : كفاءة المجمع لسماكات مختلفة ·

أما بالنسبة لمعامل الاداء الكلي الشمسي فانه يبلغ قيمة عظمى ثم يتناقص مع استمرار الاشعـــــاع الشمسي حتى المغرب كما في الشكل 8 · وفي حالة الاستفادة من طاقة الاشعاع الشمسي بعد توقـف التكثف فان معامل الاداء الكلي الشمسي عند توقف التكثف يصبح المعيار الاساسي لاداء النظام اليومـي اذ يبلغ معامل الاداء الكلي الشمسي اليومي في هذه الحالة 0.21 من أجل مجمع بسماكة 12 سم ·

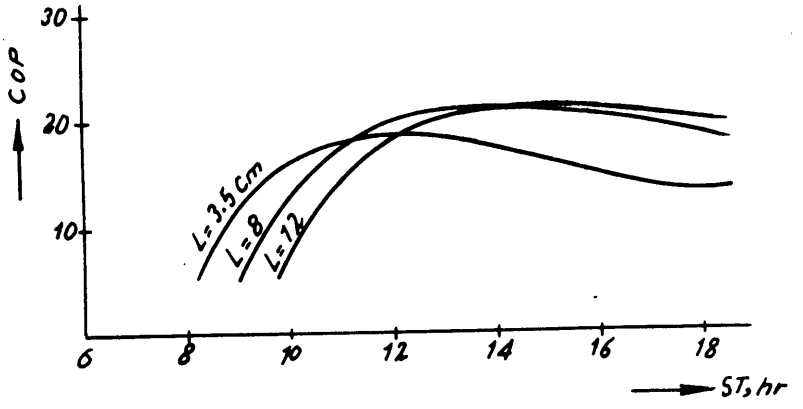

الشكل 8 : معامل الاداء الكلي الشمسي لسماكات مختلفة .

ولعل المقياس المطلق لاداء النظام هو سعة التبريد اليومية · وسعة التبريد اليومية تتناسب طـــردا مع كتلة الماء المتكثف خلال طور الاشعاع الشمسي وبالتالي تتناسب مع كتلة الزيوليت وسماكته في المجمع وعليه فان سعة التبريد تتزايد مع تزايد سماكة الزيوليت على أن لا تؤدى هذه الزيادة في السماكة الـــى خفض درجة حرارته العظمى الى حدود قريبة من درجة الحرارة T_s · فكما هو مبين في الشكـــل 9 ان زيادة السماكة من 3.5 سم الى 12 سم يؤدى الى رفع سعة التبريد اليومية من 3.4 ميغاجول الى 5 ميغاجول · أما زيادة السماكة من 12 سم وحتى 24 سم فان تعادل تأثير زيادة السماكة تقريبا مـــع انخفاض درجة الحرارة يؤدى الى ثبات سعة التبريد تقريبا في هذا المجال · أما زيادة السماكة الـــى أكبر من 24سم فان سعة التبريد تنخفض نتيجة انخفاض درجة الحرارة واقترابها من T_s ·

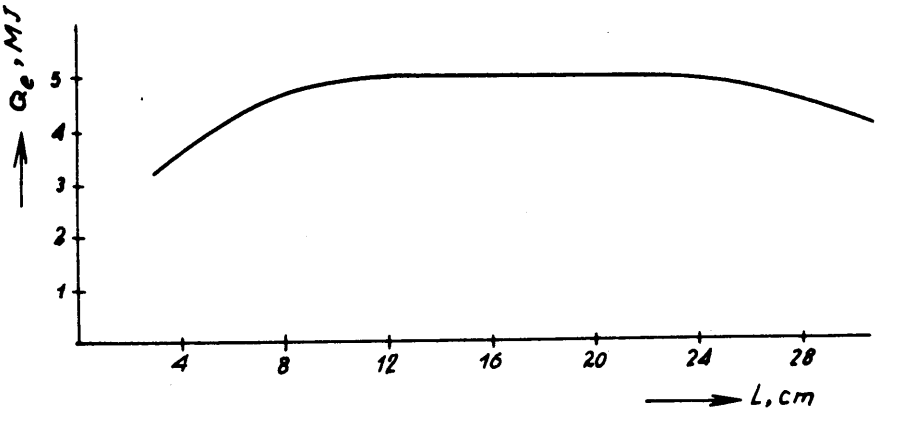

الشكل 9 : منحني العلاقة بين سعة التبريد وسماكة الزيوليت (المجمع) ·

7 - الاستنتاج :

- باستخدام الزيوليت الاصطناعي (MS-13X) والماء كثنائي امتصاص في نظام التبريد الامتصاصـــي البسيط فان معامل الاداء الكلي الشمسي اليومي يصل الى 0.21 تحت شروط مدينة بنغازى المناخيـــة في نهار 7/17 ·

- ان زيادة سماكة الزيوليت في المجمع حتى 12 سم تؤدى الى زيادة سعة التبريد حتى 5 ميغاجـــول من أجل مجمع مسطح بمساحة متر مربع واحد · وان زيادة السماكة الى أكبر من 12 سم لا تؤدى الـــى زيادة سعة التبريد بل تؤدى الى زيادة الكلفة وقد تؤدى الى انخفاض السعة أيضا ·

- ان استخدام المواد الماصة الصلبة والاستفادة من طاقة الاشعاع الشمسي بشكل مباشر يجعل نظـــام

التبريد الامتصاصي بسيطا فهو بذلك لايتطلب استعمال قطع متحركة فيه كالمضخة أو الصمامات ويمكن أن يعمل المكثف بالحمل الطبيعي للهواء ٠

كما أن هذه النتائج تشجع على البحث عن مواد ماصة مماثلة متوفرة محليا والعمل على تطوير هذا النظام لاستخدامه في التبريد والتكييف وايجاد السبل العملية لتصنيعه بأقل كلفة ٠

المراجع :

[1] Sand,L.B.,Mumpton,F.A.,Natural Zoelites,pergamon press,1976.

[2] Meunier,F.,Mischler B.,Solar coolingthrough cycles using microporous solid adsorbents,Proc.Int.sol.Energy Soc.Silver Jubillee congress 1979,V.1.,pergamon,NY,1979.

[3] Tchernev,D.I.,Exploration of molecular sieve zeolites for the cooling of buildings with solar energy,National Technical Information Service,Springfield,1977.

[4] Guilleminot,J.,Meunier F.,Etude experimentale d'une glaciere solaire utilisant le cycle zeolithe 13X-eau,Rev.Gen.Therm., Fr.n°239,Novembre,1981.

[5] Fawati,M.A.,Some aspects of adsorphtion cooling using solar energy,bull.Tech.Univ.Istanbul Vol.38,1985.

[6] Shigeishi,R.A.,Langford,C.H.Hollebone,B.R.,Solar energy Storage using chemical potantial change associated with drying of zeolites,solar energy,V.23,1977.

[7] Union Carbide,Moleuler sieves Catalgue.

[8] Duffie,Beckman,Solar Engineering of thermal processes,John Wiley,Inc,1980.

[9] Kılıç,A.,Öztürk.,A,Güneş Energisi,Kipaş dağıtımcılık,1983.

[10] Jones,W.P.,Airconditioning Engineering,Edward Arnold,1973.

[11] Hawas,M.M.,Muneer T.,Monthly average daily insolation on tilted collectors in LIBYA,Energy Conv.Vol.20,pergamon,1980.

THEORETICAL STUDIES OF A CABINET SOLAR DRYER

G. Datta
Physics Department
Deshbandhu College,
University of Delhi,
Kalkaji, New Delhi-110019, India

H.P. Garg
Centre of Energy Studies
Indian Institute of Technology
Hauz Khas, New Delhi-110016, India

J. Prakash
Physics Department
Ramjas College
University of Delhi
Delhi, India

ABSTRACT

In this paper, a mathematical model has been developed, which predicts the performance of a cabinet type solar dryer. The dryer studied is a simple box type of 1.5 m^2 base area with a 3mm thick glass cover, and a 5cm saw dust insulation at the bottom. A number of holes are drilled in to the sides of the box so that the ambient air can flow in and dry the products placed on a wire mesh tray near the bottom. Drying is therefore by natural convection of heated air.

The transient energy balance equations at the glass cover and grain surface were solved by the finite different method using certain simplified assumptions. The model predicted the instantaneous temperatures inside the dryer, the moisture content, drying rates and overall efficiency for different loads of grain varying from 10 - 40 kgs. for a typical day in late summer.

NOMENCLATURE

C_g specific heat of glass = 670 J/Kg °C

C_p specific heat of plate (weighted average for grain and wood)(J/Kg°C)

h_c convective heat transfer coefficient from grain to ambient air ($W/m^2°C$)

h_r radiative heat transfer coefficient from plate to grain (W/m^2 °C)

h_e evaporative heat transfer coefficient from grain to ambient air (W/m^2 °C)

L latent heat (J/Kg)

M_g mass of glass = 7.5 (Kg/m^2)

M_p mass of wooden plate plus mass of grain (Kg/m^2)

p_1 partial vapour present at T_A (N/m^2)

P_2 partial vapour pressure at T_p (N/m^2)
$s(t)$ solar insolation (W/m^2)
T_p plate temperature (K)
T_g glass temperature (K)
T_A ambient temperature (K)
U_1 heat transfer coefficient from glass to ambient = 30 (W/m^2 °C)
α_p absorptance of plate or grain, dimensionless
α_g absorptance of glass = 0.06, dimensionless
σ stefans constant (W/m^2 K^4)
τ transmittance of glass = 0.9, dimensionless

INTRODUCTION

One of the simplest methods of preservation of farm products used all over the world is by drying. In India and most other developing countries the drying of crops etc. is done out in the open - under the sun. Although this is the simplest method of drying, the dried products are usually of poor quality because of a variety of reasons. Dirt and insects contaminate the products, there may be spoilage by sudden rain, and birds and mice cause wastage. In open air drying there is also no control over the drying rate.

A very much better quality of dried products may be obtained at little extra cost by using solar dryers. They are basically of two types - one in which the natural convection of air is employed. Here the crops are exposed to solar radiation in a box type arrangement which has a glazing at the top. The moisture of the crops is carried away by the air which gets heated in the dryer. The air may leave the dryer by holes or by a chimney at the top of the dryer. Such dryers, generally called cabinet type dryers are simple and inexpensive, and also do not require any other external energy sources.

In order to dry large quantities of agricultural products, natural convection of air may prove insufficient, and so air preheated by a solar air heater is forced to circulate through the products. These systems are expensive, involving the cost of blowers. An external source of energy for driving the blowers is also required, which may not be available in many Indian villages. Therefore for the average Indian farmer, the cabinet type dryer is more feasible.

Lawand [1], Garg and Krishnan [2] have performed some experiments with cabinet type solar dryers. Some details of a simple rice dryer were given by Exell [3]. There has however been very little work on mathematical modelling of solar dryers.

DESIGN DETAILS

Fig. [1] shows the cabinet type solar dryer considered. It consists of a rectangular wooden box with a base area 1.5 Sq. metres covered by a 3mm thick glass cover. The bottom of the dryer is blackened and insulated with 5 cm thick saw dust insulation; holes are drilled into the base so that ambient air can flow into the dryer. The grain to be dried is placed

on wire mesh trays placed about 1 cm above the bottom of the dryer are blackened and holes are provided in them for the moist hot air to escape. The dryer is kept at a tilt of 45° south to receive maximum solar insolation.

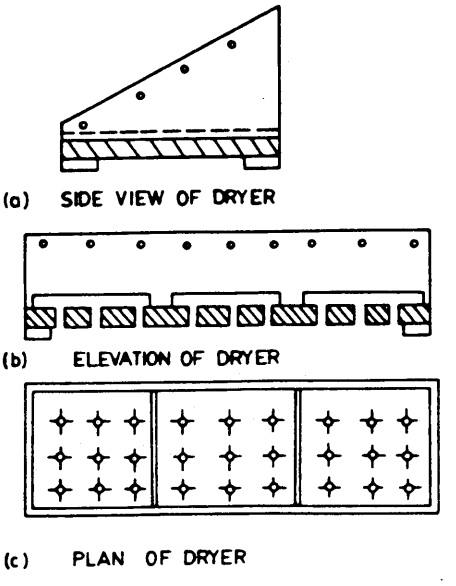

FIG. 1. SCHEMATIC DIAGRAM OF A CABINET-TYPE SOLAR DRIER

MATHEMATICAL MODEL

The transient energy balance equations were considered at the two nodes of the dryer.

They are,

Energy balance at glass cover :

$$M_g C_g \frac{d T_g}{d t} = \alpha_g S(t) + h_r (T_p - T_g) - U_l (T_g - T_a) \qquad (1)$$

Energy balance at grain surface (Plate)

$$M_p C_p \frac{d T_p}{d t} = \tau\alpha_p S(t) - h_r (T_p - T_g) - h_c (T_p - T_a) - h_e (T_p - T_a) \qquad (2)$$

The second equation assumes that the air which enters the dryer gets heated to the plate temperature, and the evaporative and convective heat transfers take place from the grain to the ambient. This assumption implies that the hot moist air at plate temperature escapes from the dryer to the ambient carrying the heat and moisture with it. The heat losses from the bottom being small are ignored.

The transient eqs. (1) and (2) were solved numerically on a digital computer using the finite difference technique. In this, dT/dt was replaced by $(T^{i+1} - T^i)/\Delta t$ where T^{i+1} and T^i were the temperatures at each node after and before a time interval Δt.

The accuracy of the results improved as Δt was reduced. It was found

that Δt = 1 minute gave reasonable convergence. The solar insolation and ambient temperature, which form the inputs of this model were measured by Eppley pyranometer and thermocouples respectively on a half hourly basis and the intermediate values determined by linear interpolation.

Evaluation of Heat Transfer Coefficients h_e, h_c, & h_r.

The convective heat transfer coefficient is given from Dunkle's (4,5) relation

$$h_c = .884 \left[T_p - T_a + \left(\frac{P_2 - P_1}{268.9 \times 10^3 - P_2}\right) T_p\right]^{1/3} \quad (3)$$

and the evaporative heat transfer coefficient h_e (6) is written as

$$h_e = h_c L \left(7.19 \times 10^{-9} \frac{(P_2 - P_1)}{T_p - T_A}\right) \quad (4)$$

The partial pressures P_1, P_2 were determined by taking the values of P from steam table for the temperature range 25-60°C and doing a least square fit.

Since crops, grain etc. are hygroscopic materials and the liquid boundary migrates more and more into the material as drying proceeds, the main amount of drying takes place in the falling rate period. So as drying proceeds more and more heat is required to evaporate the water. This means the heat of vaporization will increase with the process of drying. For a particular crop, wheat, which was considered, Table - 1 shows the variation of heat of vaporization with changing moisture content at 40°C.

TABLE - 1

Moisture content in percentage dry basis.	Heat of Vaporization (L) KJ/Kg
5	2891.724
10	2759.1189
15	2635.8192
20	2470.644

When the moisture content is more than 20% the latent heat of vaporisation is equal to that of water at that temperature. For the lower moisture contents, the values of L from Table - 1 were used in equation (4) thus enabling us to incorporate the falling rate drying into our model.

Radiative heat transfer coefficient h_r was calculated for each time interval from the equation :

$$h_r = \frac{\sigma (T_p + T_g)(T_p^2 + T_g^2)}{\frac{1}{\varepsilon_p} + \frac{1}{\varepsilon_g} - 1}$$

The overall efficiency is defined as

$$\eta = \frac{\text{Total heat evaporated}}{\text{Total solar insolation}}$$

$$= \frac{\text{Mev. L}}{\int_0^t H\, dt} \qquad (5)$$

RESULTS AND DISCUSSIONS

The energy balance equations at glass cover and grain surface were solved for no load conditions and loads ranging from 10-40 Kgs. Inputs for a typical day in late summer were used, which are shown in fig. 2. This figure also shows the variation of plate temperature under no load condition, and with a load of 20 Kg. It is found that maximum temperature of 115°C is the maximum temperature for 20 Kgs. of wheat in dryer. This is expected, for with a load of 20 Kg. wheat most of the heat in the dryer is used to evaporate water from the wheat, and so temperate is less.

Fig. 3 illustrates the fall of percentage moisture content of wheat with time in the cabinet type dryer for different loads. Drying can progress till the equilibrium moisture content is reached - which we took to be 11.5% (dry basis) for a mean temperature inside dryer of 45°C and humidity 50%. It is seen that as the load increases it takes more and more time to dry the wheat to its equilibrium moisture content. For load of 10 Kg. wheat, e.m.c. is reached in about 4 hours, for 15 Kg. wheat six and a half hours, while for load of 20 Kgs. all the sunshine hours are required to dry the product to its e.m.c.

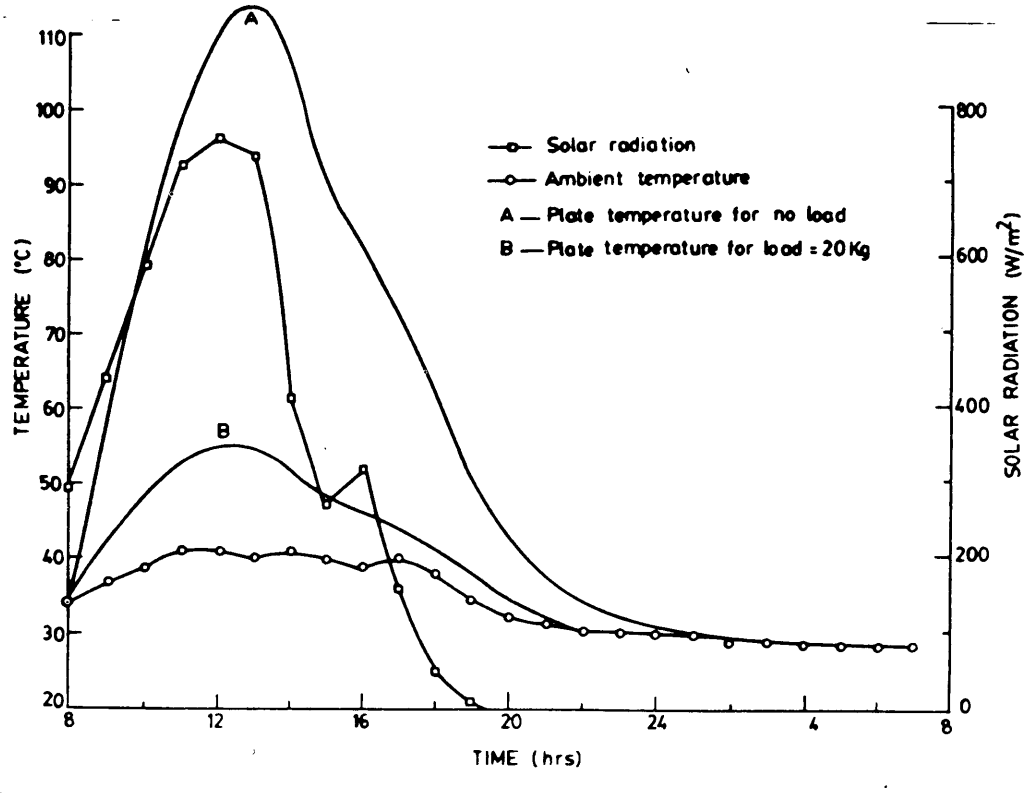

FIG. 2. SOLAR INSOLATION, AMBIENT TEMPERATURE AND TEMPERATURES INSIDE THE SOLAR DRYER

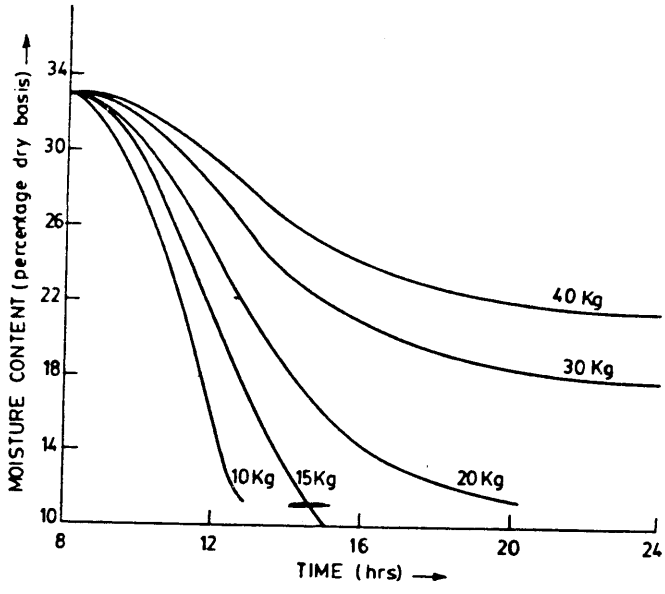

FIG. 3. VARIATION OF MOISTURE CONTENT WITH TIME OF DAY FOR DIFFERENT LOADS.

For loads exceeding 20 Kg. the crop had to be dried the next day also to reach e.m.c.

Fig. 4 gives the variation of overall efficiency of dryer with load, according to eq. (5). Efficiency increases from 31% for 10 Kg. wheat to 45% for 25 Kg. wheat, after which there is a very gradual rise of efficiency.

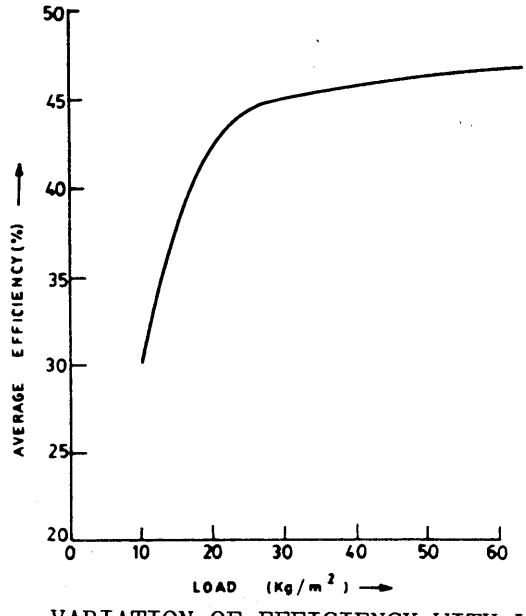

FIG. 4. VARIATION OF EFFICIENCY WITH LOAD

CONCLUSIONS

1. The mathematical model developed in this paper predicts instantaneous performance of cabinet type dryer under transient conditions.

2. This dryer is suitable for drying upto 20 Kgs. of wheat in one day.

For heavier loads drying will have to continue to the next day.

REFERENCES

1. Lawand, T.A., 'A solar cabinet dryer', Solar Energy, 10, 158, 1966.

2. Garg, H.P. and Krishnan, A., 'Solar drying of agricultural products, 1. Drying of chillies in a solar cabinet dryer', Annual of Arid Zone, 13(4), 285, 1974.

3. Exell, H.B., 'Basic design theory for a simple solar rice dryer', Renewable Energy Review Journal, 1(2), 1980.

4. Dunkle, R.V., "Solar water distillation, the roof type still and a multiple effect diffusion still, International Heat Transfer Conference, Part V. Int. Development in Heat Transfer, P. 895, University of Colorado 1961.

5. Dunkle, R.V., 'A simple solar water heat and still', presented at Joint AIRAH-SES Meeting, Perth, May 1971.

6. Baum, V.A. and Bairmmov, R., 'Heat and mass transfer process in solar still of hot box type', Solar Energy, 8(3), 78, 1964.

7. Hall, C.W. 'Drying Farm Crops, Lyall Book Depot, Ludhiana, India, 1970.

SOLAR ENERGY FOR SPACE HEATING IN LIBYA

BY

M.M.MISELLATI
Assistant Professor , Chemical Engineering Department, Green Flag University

AND

A.I. EL-TWATY
Associate Professor , Chemical Engineering Department, Green Flag University

ABSTRACT

During the winter season space heating is required in many parts of Libya. In particular, areas such as Aljabal Al-Akdar and Jabal Nefusa are subject to winter temperatures below 10 C while desert oases experience sub-zero temperatures due to radiation cooling.

The design of buildings does not take into account the minimization of heat losses;therefore cooling loads are partially met by the operation of kerosene and electrical heaters (1-2 Kw). Any attempt to satisfy the cooling load by utilizing solar energy would have to simulate at least the performance of standard heaters now in use. It should not require extensive alteration of the existing household units in addition to being competitive with electric power.

Here a review of the literature pertaining to space heating is made. Several possible modes of solar energy utilization are considered including use of photovoltaic systems, and possible combination of conventional and solar based heating systems so that existing buildings and cost constraints are approached as closely as possible.

1.0 INTRODUCTION

Space heating in sub-Saharan countries like Libya is not given the attention it deserves. Only a few articles and research reports address themselves to this application.

I.Ahmad [1,2] discuss cooling and heating needs in Libya using passive systems. I.Ahmad and R.N.Sheridan [3] as well as M.Zaki [4] describe mathematical models for determining thermal behavior of buildings. Further I.Ahmad [5] discuss six different house models in terms of heating and cooling requirements. The designs are proposed for hot dry climates. In other works by I.Ahmad [6,7] a comparison was made between the indoor temperatures of old and new houses in two locations in Libya; namely Gharian and Ghadames. In Ghadames indoor temperatures for both types of houses in winter indicated the need for space heating. Some data and technical specifications of roof designs typically used in Libya is presented by I.Ahmad [8].

1.1 The Need For Space Heating In Libya.

Simply because a country has a predominantly sub-Saharan geography does not mean that space heating is not necessary. The need for space heating can best be clarified by review of climatological data. Table 2 presents mean daily temperatures [9] for seven locations in Libya, representing coastal,mountain and desert environments. All locations need space heating for the months of December through March. Heating is needed in Shahat and Gharian (mountain locations) in April and November. Table 1 below indicates representative cooling and heating degree-days for four locations,Shahat, Gharian, Tripoli and Hon.

TABLE 1

*Calculated Heating and Cooling Degree-Days Per Year for Some Selected Sites

Location	Type Of Location	Heating Degree-Days	Cooling Degree-Days
Shahat	Mountain	1103	544
Gharian	Mountain	1071	988
Tripoli	Coastal	428	1243
Hon	Desert	651	1563

* $18^{o}C$ was taken as base temperature.

Clearly there is the need for space heating for all types of localities. In particular space heating is more important than space cooling for the mountainous regions. Figure 1 shows monthly degree-days for Tripoli and Shahat;positive numbers are for heating loads and negative numbers are for cooling loads.

TABLE 2

Mean Monthly Temperatures For Selected Sites In Libya

Site	Tubruk	Derna	Shahat	Tripoli	Gharian	Hon	Ghadames
Month							
1	11.6	14.1	9.4	13.2	8.8	11.0	10.5
2	12.9	14.7	10.1	14.2	10.5	13.1	13.1
3	14.9	15.7	11.7	15.9	12.7	16.3	16.7
4	18.1	17.8	14.6	18.4	15.9	20.7	21.1
5	21.5	20.3	18.5	21.4	20.5	24.6	25.8
6	24.6	23.7	22.1	25.0	25.1	28.4	30.8
7	25.5	25.3	22.7	26.4	26.4	28.0	31.2
8	25.7	25.9	23.0	27.0	26.7	27.8	30.8
9	23.9	24.9	21.2	25.8	23.6	26.3	27.9
10	21.2	22.5	18.3	22.4	19.0	21.9	22.1
11	16.9	19.3	14.7	18.2	14.5	16.0	16.1
12	12.9	15.7	11.0	14.5	10.2	12.1	11.4

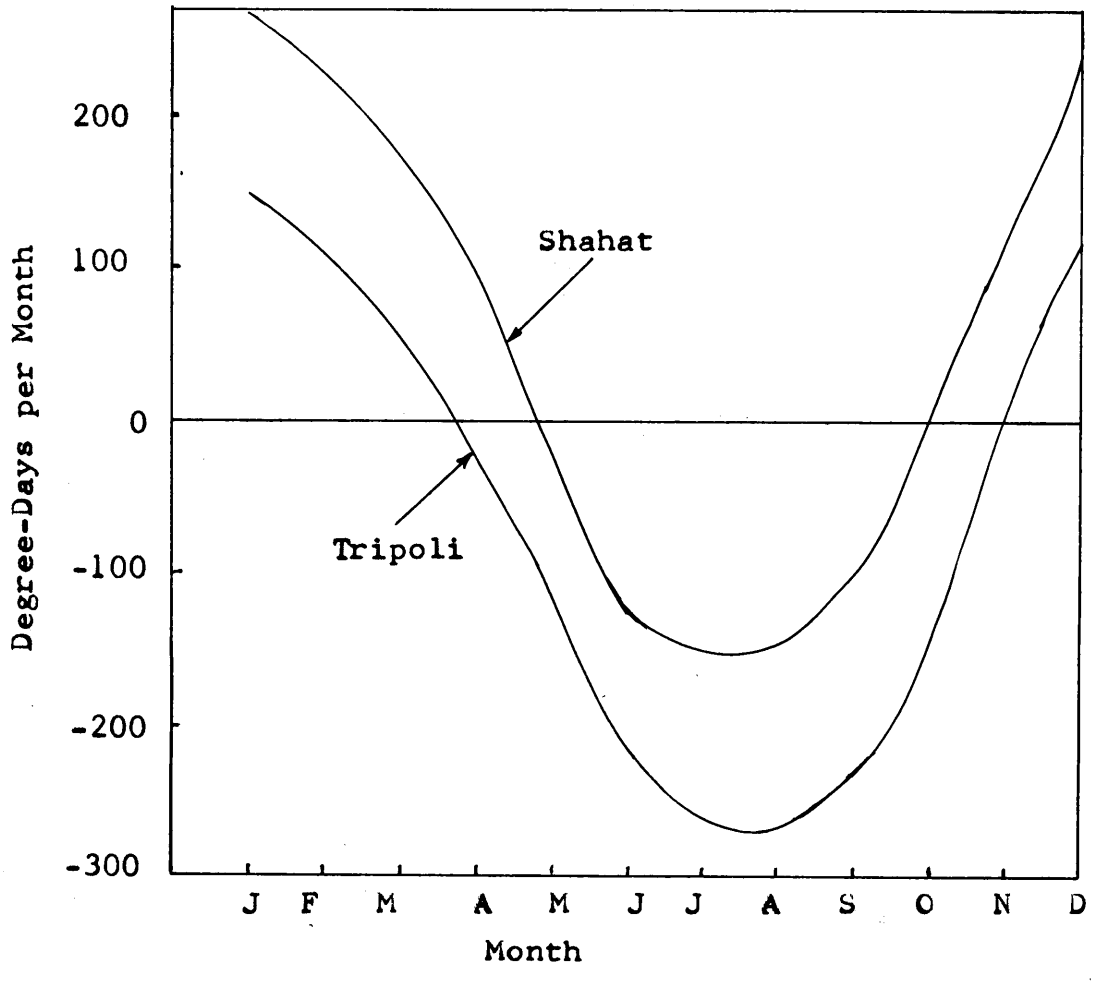

Fig.1 Monthly Degree-Days for selected locations

1.2 Description Of Residential Buildings In Libya.

Conventional buildings are made of a concrete frame, base and roof. Walls are typically of solid brick (20-30cm) or hollow brick of similar dimensions. Window area is typically 1x1.2 m of single pane glass (3mm thick).Roof thickness is 10-12cm concrete covered with a mortar layer of approximately the same thickness.Sometimes a thin tar layer is used as a sealant [8]. Total covered area ranges from 80 to 300 square meter[10,11].There is no typical residential design.Nevertheless living space can be categorised into ; apartments,villas and public housing. Details of the various models is beyond the scope of this paper.

1.3 Present Methods Of Meeting Heating Demands.

Presently the heating demand is partially met through the use of small electric and kerosene heaters in the range of 1-2 Kw. However, these are normally employed in selected rooms while the remainder of the house is generally unheated.Central air-conditioning is limited to public owned places.

1.4 Scope And Objectives.

After reviewing the literature on space heating in Libya, the concept of using solar energy for space heating is developed here through a comparative study of available active and passive systems. The objective is to recommend the best path to follow toward a rational application of solar energy for space heating in Libya.

2.0 SOLAR ENERGY FOR SPACE HEATING

The application of solar energy for space heating has received extensive attention and numerous articles and books have appeared particularly since the early seventies. There is a fair coverage of the subject in the local literature [6,12, 13,14].

Generally solar energy can be utilised for space heating in one of two modes;passive and active systems.

2.1 Passive Systems.

A passive solar system is one in which there is no need for mechanical or electrical energy to achieve the transfer of collected energy to areas of utilisation.A review of the historical development is presented by Robbins [15]. Machina [16] discuss utilisation of passive systems for residential buildings and design parameters and architectural features that should be considered in buildings to enable full use of available sunpower.

Generally passive systems have no separate collector elements and every attempt is made to incorporate the collector into the structure of the external envelope of the building.To what extent this principle can be applied to existing residential buildings,which make up a sizable portion of all buildings in Libya and other countries,is what this paper attempts to

address.

There are several variations for implementing passive systems such as:

(a) Direct gain of solar energy through windows facing south (Northern Hemisphere) with the windows acting as the collector.
(b) Collection and storage of solar energy by a single unit facing south "collector" . Additional storage may be provided by a concrete slab floor.
(c) Energy collection may be achieved via a shallow roof pond [12]. A useful variation of this system is the so called Sky Therm concept[13]. Further details of this system is provided later.

2.2 Active Systems.

For such a system it is essential to supply mechanical or electrical energy in order to transfer the collected energy from the point of collection to the assigned storage or directly to the building interior. The basic components of an active system are: collector,storage medium, auxiliary energy unit, and house or building to be heated, Figure 2 shows one variation of many; this particular example is used for heating.

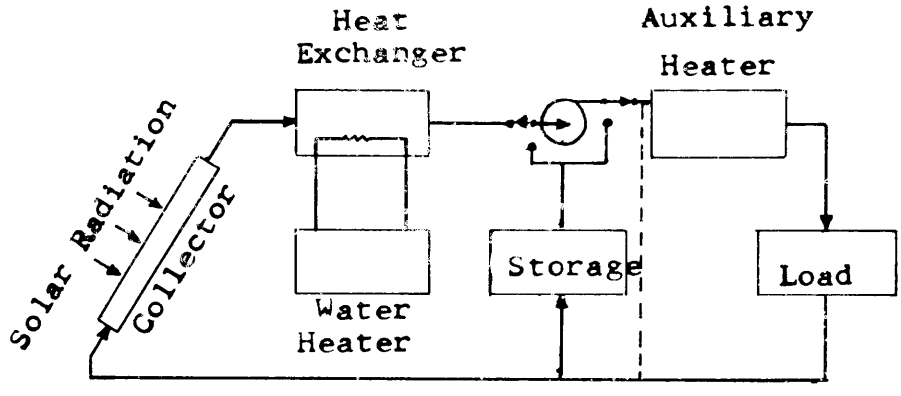

Fig. 2 Typical active solar system for heating

A working fluid is needed for an active system with air and water being the two fluids most commonly used. Further details may be found in the following references[12,13,14].

3.0 SOLAR SPACE HEATING FOR EXISTING BUILDINGS IN LIBYA

Dwellings in Libya, North African and Middle East countries are of the flat roof type. Incorporation of any of the large number of active and passive systems into flat roofed existing buildings is hindered by the necessity for major prohibitive modifications.

Examination of the literature suggested two possible candidate technologies for solar assisted space heating. These are ,the use of photo-voltaic generators and the use of the sky-therm concept[12,13].

3.1 Space Heating By Photo-Voltaic Generators.

Figure 3 shows an integrated system where some of the heat load is supplied by photo-voltaic cells.This figure refers

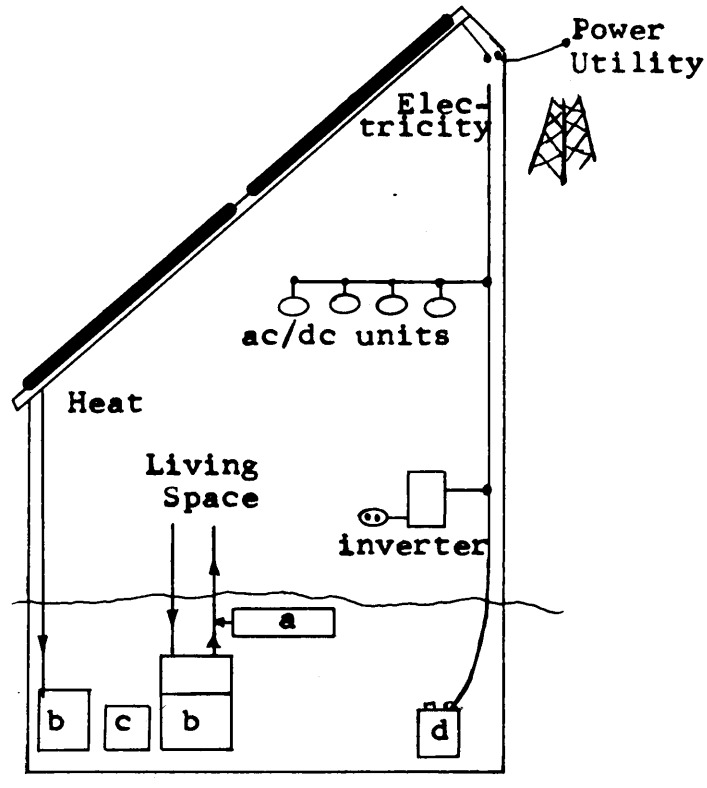

Fig.3 , Delaware House .(a) : aux. heater,(b):heat storage, (c):heat pump, (d): battery

to the experimental Delaware House. Both elecrric and heat energy generated by the solar system are utilized to partially meet the heat load. A connection to the power utility is provided to compliment energy requirements[13].

An examination of data for one location in Libya where space heating is most needed(Shahat) indicated that the minmum available sun-energy is of the order of 2 Kw-hr/m^2-day.This translates into roughly 25 sq.meter of roof space to produce 1 Kw of electric power assuming an overall efficiency of energy conversion of 6%. At \$5/Watt [17] a unit to produce 1Kw of electricity for heating or any other application would cost at least \$5000.Significant cost reduction must be achieved before the full potential of this concept is utilized.

3.2 Sky-Therm Concept.

This system combines collector, radiator and storage capabilities in the basin of water on the horizontal roof of a building.The mode of operation of this concept is illustrated in Figs 4a and 4b, while a schematic drawing of the basic components are shown in Fig. 4c.

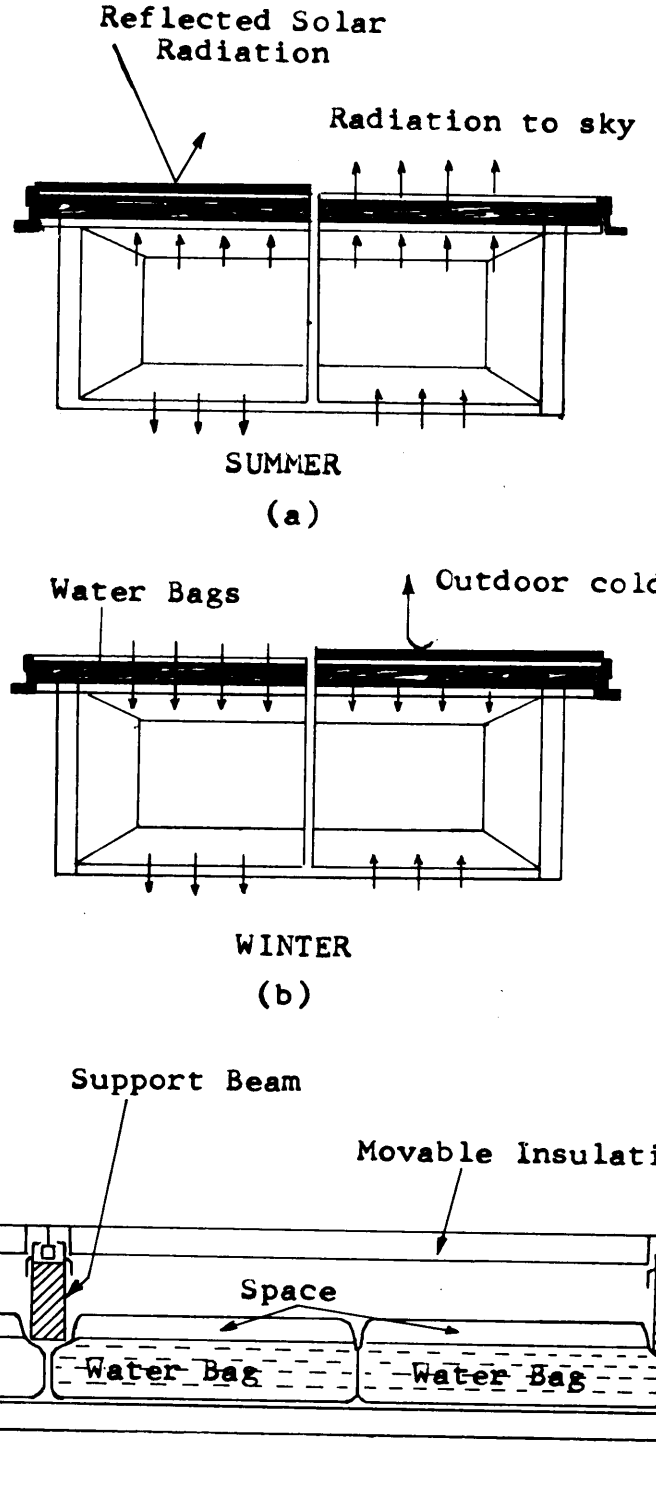

Fig.4 Sky Therm solar system

Water beds fabricated of plastic sheets(polyethylene or PVC) comprise the main element of such a system.Upward thermal losses are prevented by gas(air) cells formed by an additional plastic film suspended above the water bags (Fig.4c). To enable the system to function the dual purpose of heating and cooling, a movable insulation layer(polyurethane panels) is provided above the water beds.

During summer nights the insulation is withdrawn

allowing radiation to the sky to cool the water. At day-time the insulation is pulled in place which prevents the roof from being heated while permiting the cooling of the living space. In winter the action is reversed with insulation removed during the day and put in place for the duration of the night. The arrows in Figure 4 indicate the direction of the heat flow.

The sky-therm system is essentially a passive system. However, there is the need for the removal of the insulation panels which may be considered a departure from the strict definition of a passive system. In reality this movement could be performed manually or by a small electric motor running for a few minutes at a time. A ¼hp motor was found adequate for such a system [13].

Performance and structural details of two such systems are reported in the literature [12,13]. For the Arizona House [13] it is claimed that the use of this system provided sufficient air conditioning that no conventional heating or cooling was required when air temperatures ranged from sub-freezing to 46°C.

4.0 CONCLUSIONS AND RECOMMENDATIONS.

After a review of the pertinent literature, and a consideration of the various types of systems available and bearing in mind that any system chosen should not only be applicable to new buildings but to existing ones as well, it appears that the sky-therm concept possesses the necessary favorable features that qualifies it as the most suitable system. The following advantages are also noted:

(i) Itis suited for flat roofs.
(ii) Plastic sheets and bags required could be manufactured locally or easily obtained.
(iii) Heat transfer is facilitated by conduction through concrete roofs.
(iv) There are no major equipment requirements such as storage tanks etc.
(v) Movement of insulation cover requires a minimum of auxiliary power or could be performed manually.
(vi) The system could be used for both heating and cooling loads.

One shortcoming of the system is that it is limited to top floor and single storey buildings.

Nevertheless, full evaluation of the sky-therm concept under local environmental conditions and on a model housing unit is necessary to supplement the already gained experience for the purpose of local adaptation of the concept.

5.0 REFERENCES.

[1] - Ahmad, I., A.Mokadmy and S.M.Abughres, "Passive Heating And Cooling Strategies for Libya", National Academy for Scientific Research(N.A.S.R.), Center for Solar Energy Studies Report, Tripoli, Libya, 1983.

[2]- Ahmad,I.andS.M.Abughres,"Passive Convective Cooling for Libya", NASR, Center for Solar Energy Studies(CSES), Tripoli,Libya ,1983.
[3]- Ahmad,I.,and R.N.Sheridan,"Modelling the Thermal Behavior of Buildings for Passive Heating and Cooling",NASR,CSES Tripoli,Libya,1983.
[4]- Zaki,M.G.,and K.Hassan,"Thermal Behavior of Buildings Determination andEconomics", NASR,CSES Report.
[5]- Ahmad,I.,"Energy Analysis of Buildings Designs in a Hot Dry Climate",NASR,CSES Report,Tripoli,Lbya,1983.
[6]- Ahmad,I.,S.M.Abughres and K.R.Agha,"Study of the Thermal Behavior of Underground House in Gharian",Therd Arab International Solar Energy Conference,Baghdad,Iraq,1988.
[7]- Ahmad,I.,E.Ketrichand S.M.Abughres,"Thermal Analysis of the Architecture in Old and New Houses at Ghadames", NASR,CSES Report,Tripoli,Libya 1983.
[8]- Ahmad,I.,N.Kabazi and M.Sassi,"Economic and Thermal Performance of Insulated Roofs in Hot Dry Climate",NASR, CSES Report,Tripoli,Libya 1984.
[9]- World Metereological Organization,Office of Meteorology, Tripoli,Libya.
[10]- Ministry of Housing,"Project for 1966 Housing Units in Tripoli and 616 Housing Units in Ghadames",Tripoli,Libya, November 1982.
[11]- Daza,M., Private Communication,1988.
[12]- Sayigh,A.A.M.,Editor,"Solar Energy Application in Buildings,", Academic Press,N.Y.,N.Y. (1979).
[13]- Patton,A.R.,"Solar Energy for Heating and Cooling of Buildings", Noyes Data Corp., London, England,(1975).
[14]- Duffie,J.A.,and W.A.Beckman,Solar Energy of Thermal Processes",John Wiley and Sons,N.Y.,N.Y.,(1980).
[15]- Robbins,C.L.,"A Review of the Historical Development of the Use of Passive Solar Systems", Solar Energy, International Progress,Pergamon Press,1978.
[16]- Machina,M.,and T.El-Dali,"Use of Passive Systems in Residential Buildings", (in Arabic), ELHANDASI No.11 1988.
[17]- Magin,L.M.,"U.S. Photovoltaic Experience;Prospects for Large Power Plants", Proceedings of the 5th E.C. Photovoltaic Solar Energy Conference,D.Reidel Publishing Company,Dorrecht,1983.

DESIGN AND PERFORMANCE STUDIES OF A PASSIVE DIRECT-MODE SOLAR ENERGY DRYER

O.V. EKECHUKWU*; B. NORTON+ and O.A. ODUKWE*

*National Centre for Energy
Research and Development
University of Nigeria, Nsukka
NIGERIA

+Solar Energy Technology Centre
School of Mechanical Engineering
Cranfield Institute of Technology
Bedford MK43 OAL ENGLAND

ABSTRACT

Solar-energy dryers are designed to improve the effectiveness of traditional open-to-sun drying techniques which are widely employed by most rural farmers in the tropics. The shortcomings of the tradition (natural) drying techniques are outlined. Passive (natural-circulation) solar-energy dryers are identified as the most attractive alternative to open sun drying. Passive solar-energy dryers are superior operationally and competitive economically to natural drying techniques. A comprehensive review of integral or direct-mode passive solar-energy dryer designs are presented and the appropriateness of each design for application by rural tropical farmers are discussed.

The behaviour of a large-scale direct-mode passive solar crop dryer appropriate for remote farm drying operations has been studied over the range of weather conditions encountered in a typical tropical climate. The design and a compressive transient performance measurement of the dryer studied in Nigeria are reported and discussed.

1. INTRODUCTION

Solar crop drying techniques can broadly be classified into three main groups.

1.1 Traditional "Open-to-sun" Drying Methods:

Here the product is spread on the ground, mat, cemented floor or placed on either horizontal or vertical shelves and exposed directly to sunlight and natural air currents.

1.2 Active Solar Drying Methods:

Here the product is placed in dryers which employ solar-energy and/or fossil-fuel based heating systems and motorised fans and/or pumps for air circulation.

1.3 Passive Solar Drying Methods:

Here the product is placed in dryers which depend totally on solar-energy for heating and natural convection for air circulation.

Traditional "open-sun" drying though utilized widely in most tropical countries, has inherent limitations: high crop losses can ensue from inadequate drying, fungal attacks and rodent and insect encroachment. In many rural locations in the Third World, supplies of non-renewable sources of energy are either unavailable, unreliable, or for many farmers, too expensive. Thus in such areas, crop drying systems that employ motorised fans or electrical heating are inappropriate. In such conditions, passive or natural-circulation solar-energy dryers appear increasingly to be attractive as commercial propositions.

2. PASSIVE (NATURAL-CIRCULATION) SOLAR-ENERGY DRYERS

The advantages of passive solar-energy dryers that enable them to compete economically with traditional drying techniques are;

(i) they require a smaller area of land in order to dry similar quantities of crop that would have been dried naturally in the open,

(ii) they will yield a relatively high quality of the dry product because insects and rodents are unlikely to infest it during the drying process,

(iii) the drying period is shortened compared with open air drying,

(iv) protection is afforded from sudden downpours of rain,

(v) the relatively low capital and running costs of these dryers and

(vi) the improved quality of the product achieved after drying.

Passive solar-energy dryers can be classified mainly into the distributed or indirect mode and integral or direct mode types. A broad comparison of integral and distributed natural-circulation solar-energy dryers is given in Table 1.

3. INTEGRAL TYPE (DIRECT MODE) PASSIVE SOLAR ENERGY DRYERS

In an integral type natural-circulation solar-energy dryer the crop to be dried is placed in a drying chamber with transparent walls. In this system, the necessary heat is supplied to the crop by direct absorption of solar radiation at the product itself and by convection from the heated internal surfaces of the chamber. The heat abstracts the moisture from the product, while also lowering the relative humidity of the resident air mass thus increasing its moisture carrying capability. Direct absorption of solar radiation enhances the proper colour 'ripening' of greenish fruits by allowing, during dehydration, the decomposition of residual chlorophyll in the tissue [1-4]. For certain varieties of grapes and dates exposure to sunlight is considered essential for the development of the required colour in the dried products. A period of exposure to sunlight of arabica coffee is thought inviolable for the development of full flavour in the roasted bean. Conversely, for some fruits, exposure to sun reduces considerably the vitamin content. Colour retention in some highly pigmented commodities can also be affected adversely by direct exposure to sunlight [5,6].

Integral type natural-circulation solar-energy dryers are both simple and cheaper to construct than those of the distributed type for the same loading capacity. However the potential drawbacks of the former are (i) a liability to localised over-heating and (ii) relatively slow overall drying rates [4]. To overcome these limitations, a "solar chimney" is employed to increase the buoyant force on the air stream and thus provide an increased rate of moist-air removal. Figure 1 illustrates the features of the integral-type natural-circulation solar-energy dryer measurements of whose performance are reported herein. More generally two generic types can be identified, namely: the cabinet dryer and the ventilated greenhouse dryer.

3.1 Natural-Circulation Solar-Energy Cabinet Dryers

A natural-circulation solar-energy cabinet dryer is simply a single - or double - glazed insulated container. Solar radiation is transmitted through the cover and is absorbed on the blackened interior surfaces as well as on the product itself, thus raising the internal temperature. Holes at both the base and upper parts of the cabinet's sides provide ventilation, with warm air leaving via the upper apertures under the action of buoyant forces, drawing in replenishing fresh air at the base. Shallow layers of the product are placed on perforated trays inside the enclosure. Solar cabinet dryers constructed from cheap locally-available materials, are usually relatively small units used to preserve "household" quantities of fruits, vegetables, fish and meat.

The major drawback of cabinet dryers is the poor air circulation obtained, thus resulting in poor moist-air removal (thus reducing drying rate), and very high internal temperatures with a likely overheating of crops. Drying air temperatures as high as between 70°C - 100°C have been reported [7-12]. This is excessive for most products, particularly perishables (fruits and vegetables) for which

cabinet dryers are intended. Relatively large air inlet ducts with appropriately-designed solar chimneys are recommended as the best option to improving circulation within the cabinet and minimising excessive temperatures. The design, construction and testing of a series of natural-circulation solar cabinet dryers were reported by the Brace Research Institute, Canada [11-16]. Fig. 2 illustrates the features of a typical natural-circulation solar cabinet dryer. They are probably the most widely used type of solar dryer. Several designs of similar configurations to those of the Brace Research Institute have been built and tested (for a variety of crops and in various areas), [7, 10, 17-35].

3.2 Natural Circulation Solar-Energy Greenhouse Dryers

Such dryers are larger than most cabinet dryers and are characterised by extensive glazing on their sides. Usually the glazing is on the front side (i.e. sun facing side) of the dryer while the rear side is insulated [36]. Insulant panels may be drawn over the glazing at night to reduce heat losses and heat storage facilities may also be provided. Designed properly, a solar greenhouse dryer allows a greater degree of control over the drying process than the solar cabinet dryer [36] and are more appropriate for large-scale drying.

The design and construction of the earliest form of the natural-circulation greenhouse dryer was the glass-roof solar dryer reported by Lawand et al [10, 13, 15] and Ghosh [37], see Fig. 3.

Typical later designs of natural-circulation solar greenhouse dryers include the widely-reported polyethylene-tent fish dryer built by Doe et al [1, 2, 28, 38-43]. Doe et al [39] noted that the maximum temperature for the drying of fish is 50°C above which the fish will cook. They reported that the achieved internal temperatures of about 45°C, would kill flies and larvae infestations within the fish. Compared with distributed type and with open-sun drying, for tropical fish-drying an integral-type greenhouse tent dryer is probably the best option available [28].

Sachithananthan et al [41], reported the construction of a solar dome dryer, again for drying fish. This integral natural-circulation solar-energy dryer was designed for a capacity of 1000 kg of fresh fish, see Fig. 5. It was reported [41] that the quality and yield of the solar dried fish was considerably higher than that of open sun drying. For an optimal load of between 900 and 1000 kg, the fish would be dried from an unspecified initial moisture content to the 25% (dry basis) required in about 4 days.

Many other practically-realised designs of the natural-circulation solar-energy greenhouse-type dryers have been reported [43-47], however, in most cases essential data is not recorded. Little attempt has been made to quantify their diurnal behaviour. Such data is essential for the validation of simulation models and - ultimately - for the development of design tools.

4. EXPERIMENTAL OBSERVATIONS

A 5 m long, 2.3 m wide and 2.7 m tall experimental greenhouse

type natural-circulation dryer with a 5 m tall solar chimney has been studied extensively in order to gain detailed operational performance data in a tropical environment. The dryer was located at Nsukka, Nigeria, latitude 6.8 degrees North. Taut polythene cladding totally enclosed the drying chamber. A galvanised steel framework was insulated thermally from the polythene cladding by insulant tape. This prevented undesirable localised heating of the cladding which would shorten severely its useful life.

The crops were placed on metal mesh trays, these were hung one beneath another from a horizontal galvanised steel struts. Both banks of and individual trays, were suspended from load cells. Thus moisture loss variations with time during drying could be measured for both the dryer as a whole and for particular locations. Signals from all the sensors were recorded by a modular system. This consisted of the micro-computer, monitor, printer, disc drive, IEEE-488 interface, two multi-application peripheral systems (MAPS), a digital voltmeter and specialised signal conditioners for the air velocity meters. The MAPS scanned the sensor channels and the digital voltmeter then measured the resulting voltage received from each of the 105 channels. Junction boxes containing the cables and their terminal blocks were used to convey the sensor signals to the MAPS. This enabled each of the sensors to be disconnected easily at the dryer (i.e. at the second junction box). The junction boxes could be situated a maximum distance of twenty meters apart. Measurement signals from the crop dryer were conveyed to the building via fourteen lengths of 12-way cable, the micro-computer then converted these signals to appropriate parametric values. These were displayed graphically or in tabulated form on the monitor and stored on disc.

5. RESULTS

For a given set of ambient conditions, the main parameters that influence the temperatures and air flow rates and thus drying rate of the crop within the dryer are the height of the solar chimney, the area and position of the absorbing curtain within the chimney, the length of the dryer, the area of the air intake into the dryer, the packing density of the crop within the dryer and the drying characteristics of the crop being dried. Experimental data has been obtained from the dryer operating under a variety of climatological conditions.

The diurnal variations in the applied (i.e. weather) conditions and the transient performance of the dryer for a test conducted between 13 - 15 December, 1985, are presented in figures 6 to 9. The test commenced at about 12 noon local time on 13 December, 1985, and was undertaken with peeled cassava chips (of volumes between 15-20 cubic centimeters) harvested freshly. It can be seen from figure 6 that the insolation pattern over the test period was fairly constant resulting in little or no fluctuations in the daily drying conditions. The mean insolation value over the test period was about 350 Wm^{-2} with the corresponding ambient temperature and relative humidity being 33°C and 64% respectively. Peak drying air temperature elevation above the ambient of up to 20°C was achieved while the drying air relative humidity was reduced to a mean value of about 38% over the test period.

A moisture content reduction from an initial value of 141% dry

basis to about 18% dry basis was achieved within two days of drying - see fig. 9. This corresponded to about 16 hours of insolation. This relatively rapid drying rate is attributable to low levels of drying air relative humidity. However, nocturnal re-absorption of moisture was recorded after the second day of drying, by which time the crop had been dried to the safe moisture content - as indicated by the horizontal dashed line in fig. 9. No further moisture loss was recorded after the third drying day (i.e. below a moisture content of 6% dry basis). In practice it is unnecessary to dry a crop to moisture levels so far below the safe storage moisture content.

The daily normalised drying efficiencies for five tests are shown in fig. 10. The values were computed over the insolation period of each test and normalised against the total initial crop weight to isolate the effect of different dryer loading densities on the efficiency values. All the tests were undertaken with peeled cassava chips except test 5 for which the chips were unpeeled. It can be seen that the efficiencies for each test decreased as drying progressed which is concommitant with reduced moisture loss over each test period. The efficiencies of tests 1 and 2 undertaken during the dry season showed a more rapid decrease over time compared with tests 4 and 6 for the wet season. The inherent implication of a more rapid decrease in the efficiencies for tests 1 and 2 is a faster drying rate which is attributable to the lower relative humidities encountered during these tests.

Test 5 in which the cassava chips were unpeeled (thus inhibiting moisture migration from the crop surface) showed a very slow decrease with time in the efficiency, but from a much lower initial value than for the peeled cassava.

6. CONCLUSION

The data obtained in this study, of which only a small proportion is represented here, forms a useful database for the validation of theoretical models. This is in addition to its intrinsic value in quantifying the diurnal behaviour of such dryers.

Acknowledgement

The financial support of the Commission of the European Communities, Brussels, Belgium and of the British Council, London, U.K. is acknowledged, as is the contributions of Dr. P.D. Fleming to this project.

REFERENCES

1. FLEMING, P.D., NORTON, B., EKECHUKWU, O.V., ONYEGEGBU, S.O. and PROBERT, S.D., A Large-Scale Facility for Experimental Studies of Natural-Circulation Solar-Energy Tropical Crop Dryers, Proc. Inter. Drying Symp. (Drying 86), Cambridge, Mass. USA, 1986, pp.685-93.

2. FLEMING, P.D., EKECHUKWU, O.V., NORTON, B., and PROBERT, S.D. Experimental Studies of Natural Circulation Solar-Energy Drying of Tropical Crops in Nigeria, Proc. Solar Drying Workshop, IDRC, Dakar, Senegal, 1986.

3. NORTON, B., EKECHUKWU, O.V., FLEMING, P.D., and PROBERT, S.D. Experimental Studies of Large-Scale Natural Circulation Solar-Energy Tropical Crop Dryer, Proc. Int. Workshop on Solar Energy for Rural Dev., Nsukka, Nigeria, 1986.

4. NORTON, B., FLEMING, P.D. and EKECHUKWU, O.V., Passive Autarkic Solar Drying Techniques, Physics and Technology of Solar Energy Proc. Int. Int. Workshop on Physics of Solar Energy, New Delhi, India, 1986, (D. Reidal Publ Co., Netherlands, 1987).

5. BRENNDORFER, B., KENNEDY, L., BATEMAN, C.O.O., KREMA, G.C. and WEREKO-BROBBY, C., Solar Dryers - Their Role in Post-Harvest Processing, Commonwealth Science Council (Commonwealth Secretariat publications), London, 1985.

6. INTERNATIONAL LABOUR ORGANISATION, Solar Drying: Practical Methods of Food Preservation, International Labour Office, Geneva, Switzerland 1986.

7. EZEKWE, C.I., Crop Drying with Solar Air Heaters in Tropical Nigeria, ISES, Solar World Forum, Brighton, UK, 1981, pp.997-1005.

8. BHATIA, A.K., A Simple Solar Fruit Dryer for the Rural Areas, Indian Food Packer, 1978, 32, No. 1, pp.127-9.

9. CHEEMA, L.S. and RIBEIRO, C.M.C., Solar Dryers of Cashew, Banana and Pineapple, ISES Conf., New Delhi, India, 1978, 3, pp.2075-79.

10. KILKIS, B., Solar Energy Assisted Crop and Fruit Drying Systems, Theory and Applications, Proc. Sem. Energy Conserv. & Use of Solar and Other Renewable Energies in Agric., 1981, pp.3907-33.

11. LAWAND, T.A., A Solar Cabinet Dryer, Solar Energy, 1966, 10, pp.158-64.

12. LAWAND, T.A., A Description of Two Simple Solar Agricultural Dryers, Cooperation Mediterraneene pour l'Energie Solair, Bull. 1965, No. 9, pp.51-6.

13. LAWAND, T.A., The Potential of Solar Agricultural Dryers in Developing Areas, UNIDO Conf. 5, Technology for Solar Energy Utilization, 1977, pp.125-32.

14. NAHLAWI, M., The Drying of Yams with Solar Energy, Technical Report, Brace Research Institute, St. James Barbados, West Indies, 1966, No. T27.

15. SAULNIER, B., Survey of Solar Agricultural Dryers, Joint. Conf., Amer. Section ISES & Solar Energy Soc. Canada Inc., 1976, 17, pp.7-21.

16. ANON, How to Make a Solar Cabinet Dryer for Agricultural Produce, DIY Leaflet, Brace Res. Inst. Canada, 1965, No. L6.

17. SHULKA, B.C., Drying of Maize in a Freely Ventilated Crip with Solar Air Heater in Kenya, Tropical Agric. (Trinidad), 1984, 61, No. 1, pp.45-7.

18. BAILEY, P.H. and WILLIAMSON, W.F., Some Experiments on Drying Grain by Solar Radiation, J. Agric. Engng. Res., 1965, 10, pp.191-6.

19. CHEEMA, L.S., Solar Drying of Cassava for Alcohol Production, ISES Conf., New Delhi, India, 1978, pp.1940-44.

20. WAGNER, C.J., COLEMAN, R.L. and BERRY, R.E., A Low Cost, Small Scale Solar Dryer for Florida Fruits and Vegetables, Proc. Fla. State Hort. Soc. (USA), 1979, 92, pp.180-3.

21. WAGNER, C.J., COLEMAN, R.L. and BERRY, R.E., Wind and Radiant Solar Energy for Drying Fruits and Vegetables, Ann. Conf. Amer. Section ISES (Philidelphia USA) 1981, 1, pp.48-50.

22. BHATTA, A.K., and GUPTA, S.L., Solar Dryer for Drying Apricots, Research and Industry, 1976, 21, No. 9, pp.188-91.

23. UMAROV, G.G., and IKRAMOV, A.I., Features of the Drying of Fruit and Grapes in Solar Radiation Drying Apparatus, Applied Solar Energy (Geliotekhnika), 1978, 14, No. 6, pp.55-7.

24. HARIGOPAL, U. and TONAPI, K.V., Technology for the Villages - Solar Dryer, Indian Food Parker, 1980, 1980, 34, No.2, pp.48-9.

25. SHARMA, V.K., SHARMA, S., RAY, R.A. and GARG, H.P., Design and Performance Studies of a Solar Dryer Suitable for Rural Applications, Energy Convers. Mgmt., 1986, 26, No. 1, pp.111-9.

26. DENG, J.C., CHAN, K.V., BAIRD, C.D., HEINIS, J.J., PEREZ, M. and WU, L., Drying Seafood Products with Solar Energy, Proc. 2nd Int. Conf., Energy Use Mgmt., Los Angeles, USA, 1979, pp.1884-92.

27. CLARK, C.S., Solar Food Drying: A Rural Industry, Renewable Energy Rev. J., 1981, 3, No. 1, pp.23-36.

28. CURRAN, C.A., and TRIM, D.S., Comparative Study of Three Solar Fish Dryers, Proc. FAO Expert Consultation on Fish Tech. in Africa, Casablanca, Morocco, 1982, No. 83-32199 (FAO Rome, Italy).

29. ARCHULETA, R., BERKEY, J., and WILLIAMS, B., Research on Solar Food Drying at the University of California, Santa Cruz, Progress in Passive Solar Energy Systems (Amer. Solar Energy Soc. Inc.) 1983, pp.679-83.

30. GUSTAFSSON, G., Solar Assisted Grain Drying in Hot and Humid Areas, Rapport, Sveriges Lantbruksuniversitet, Lund, 1982, 20.

31. McDOWELL, J., Solar Drying of Crops and Foods in Humid Tropical Climates, Caribbean Food and Nutrition Institute Report, Kingston, Jamaica, 1973, No. CFN1-T-7-73.

32. MARTENS, R.W., A Solar Dryer Applied to a Village Food Processing Industry, ADAB News, Bangladesh, 1984, pp.18-23.

33. GARG, H.P., Solar-Drying - Prospects and Retrospects, Proc. Int. Drying Symp. Drying '83 (Mujumda, A.S., Ed.) 1983, pp.353-69.

34. SHARMA, S., RAY, R.A. and SHARMA, V.K., Comparative Study of Solar Dryers for Crop Drying, Invention Intelligence, 1987, pp.105-113.

35. BAIRAMOV, R., Solar Drying of the Agricultural Products, Proc. UNESCO/FAO Working Group Meeting Solar Drying, Perpignan, France, 1984, pp.44-8.

36. BRACE RESEARCH INSTITUTE, Types of Solar Agricultural Dryers, Sunworld, 1980, 4, (6), p.181.

37. GHOSH, B.N., A New Glass Roof Dryer for Cocoa Beans and Other Crops, Proc. ISEC, Paris, 1973, Paper No. V30.

38. SODHA, M.S., BANSAL, N.K., KUMAR, K., BANSAL, P.K., and MALIK, M.A.S., Solar Crop Drying, CRC Press Inc., Florida, USA, 1987, Vol.1.

39. DOE, P.E., AHMED, M., MUSLEMUDDIN, M. and SACHITHANANTHAN, K., A Polythene Tent Dryer for Improved Sun Drying of Fish, Food Tech., in Australia, 1977, 29, pp.437-41.

40. DOE, P., Sun Powered Fish Drying, Australian Fish, 1977, 36, No. 5, pp.24-5.

41. SACHITHANANTHAN, K., TRIM, D. and SPIERS, C.I., A Solar Dome Dryer for Drying of Fish, FAO Fisheries Paper, Rome, Italy, 1983, RAB/81/002/INT/L8.

42. DOE, P.E., The Polythene Tent Fish Dryer: A Progress Report, Energy, Waste & Processing - Proc. Int. Conf. Agric. Engng. in National Dev., Selangor, Malaysia, 1979, 79, (12), pp.250-4.

43. SADYKOV, T.A. and KHAIRIDDINOV, B., A Year-Round Double-Block Greenhouse-Dryers, Applied Solar Energy (Geliotekhnika), 1982, 18, No.1, pp.69-72.

44. PRICE, R.L., SANDS, C.D., LARSON, D.L. and MEILKE, E.A., Fruit Dehydration Using Greenhouse-Like Structures as Solar Heat Collectors, Changing Energy Use Futures - Proc. 2nd Int. Conf. Energy Use Mgmt., Los Angeles, USA, 1979, 4, pp.1910-12.

45. MUTHUVEERAPPAN, V.R., AMBALAVANAN, G., KUNCHITHAPATHAM, M., KAMARAJ, G. and ANANTHANATESAN, ?. Low Cost Plastic Suction Type Greenhouse Grain Dryer, Proc. ISES Cong., INTERSOL 85, Montreal, Canada, 1985, pp.1077-81.

46. YANG, K.C., Solar Kiln Performance at High Latitude, 48°N, Forest Products, J., 1980, 30, No.3, pp.37-40.

47. BAILEY, P.H., Energy Savings from Solar Drying in Agriculture, Span, 1982, 25, (1), pp.18-20.

Table 1 Comparison of Natural-Circulation Solar-Energy Dryers

	Type	
	INTEGRAL	DISTRIBUTED
Principle modes of heat transfer to crop	Radiation (i.e. by direct absorption of solar radiation) and convection (i.e. from heated surounding air).	Convection from preheated air in an air-heating solar-energy collector.
Components	Glazed drying chamber and chimney.	Air-heating solar-energy collector, drying chamber and chimney.
Initial cost	increasing cost →	
Construction, operation and maintenance	Simplicity in both construction (i.e. easy on-the-site construction) and operation. Requires little maintenance.	Consists of comparatively elaborate structures, thus requires more capital investment in materials and large running costs. More operational difficulties of loading and unloading the drying chamber and occasional stirring of the crop (since crops are usually dried in relatively deep layers).
Efficiency	Little information on comparison of performance with distributed-type dryers. Likely to operate at lower efficiencies due to its simplicity and less controllability of drying operations.	Have a tendency to higher efficiency since individual components can be designed to optimal performance.

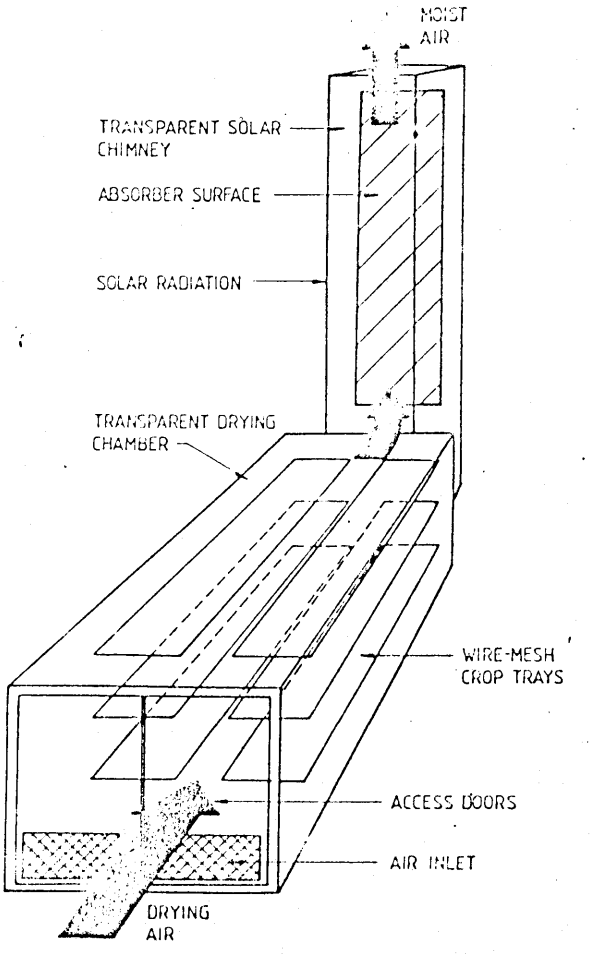

FIG. 1 SCHEMATIC DIAGRAM OF AN INTEGRAL-TYPE NATURAL-CIRCULATION SOLAR-ENERGY DRYER

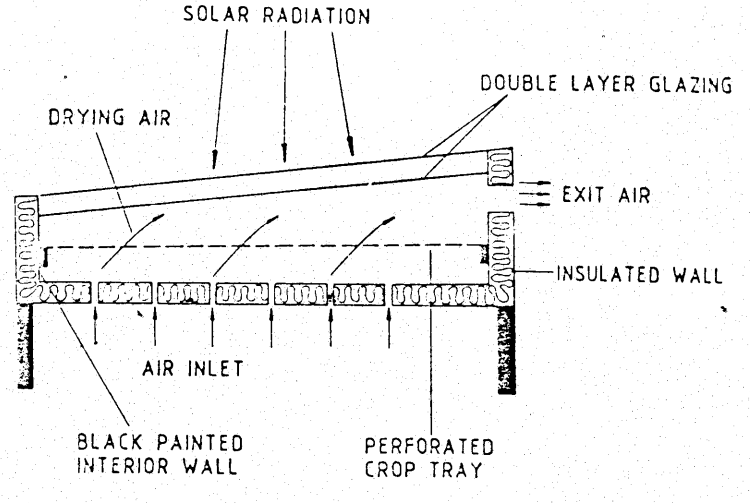

FIGURE 2. SCHEMATIC ILLUSTRATION OF A TYPICAL NATURAL-CIRCULATION SOLAR-ENERGY CABINET DRYER.

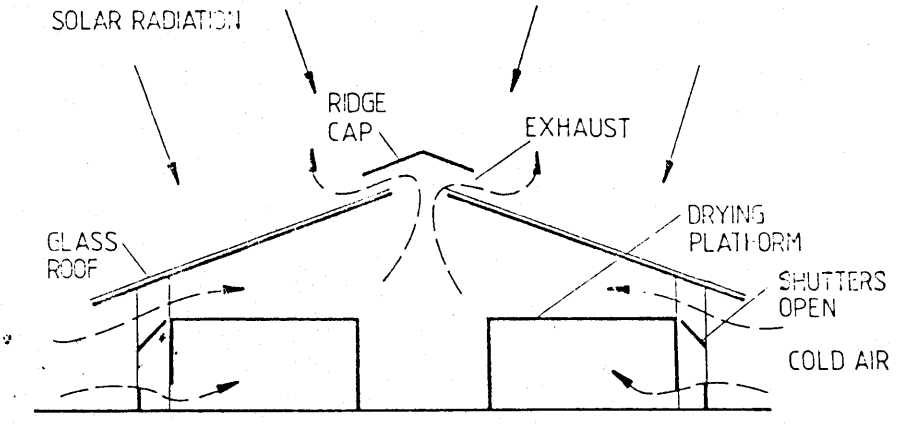

FIG. 3 SCHEMATIC ILLUSTRATION OF THE NATURAL-CIRCULATION GLASS-ROOF SOLAR-ENERGY DRYER

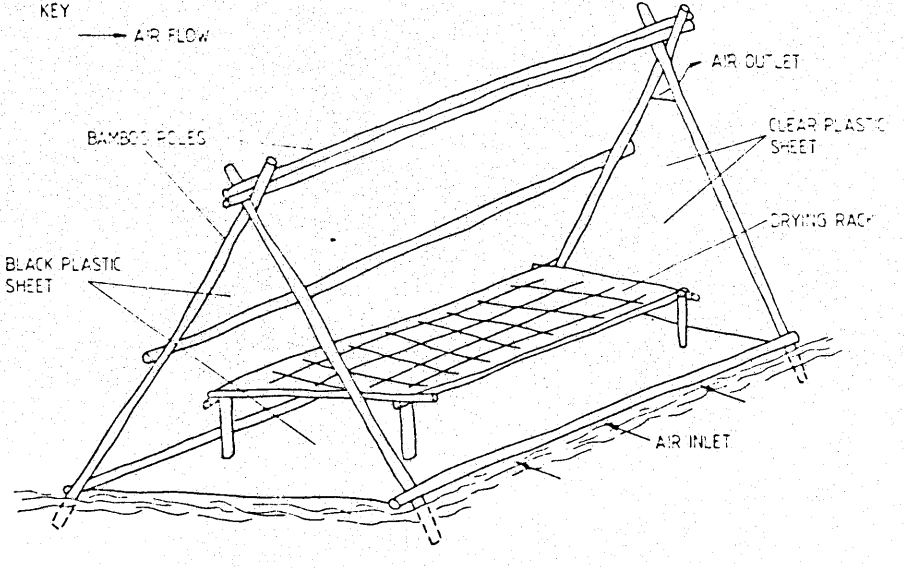

FIG 4 SCHEMATIC DIAGRAM OF THE NATURAL-CIRCULATION INTEGRAL-TYPE POLYTHENE TENT DRYER

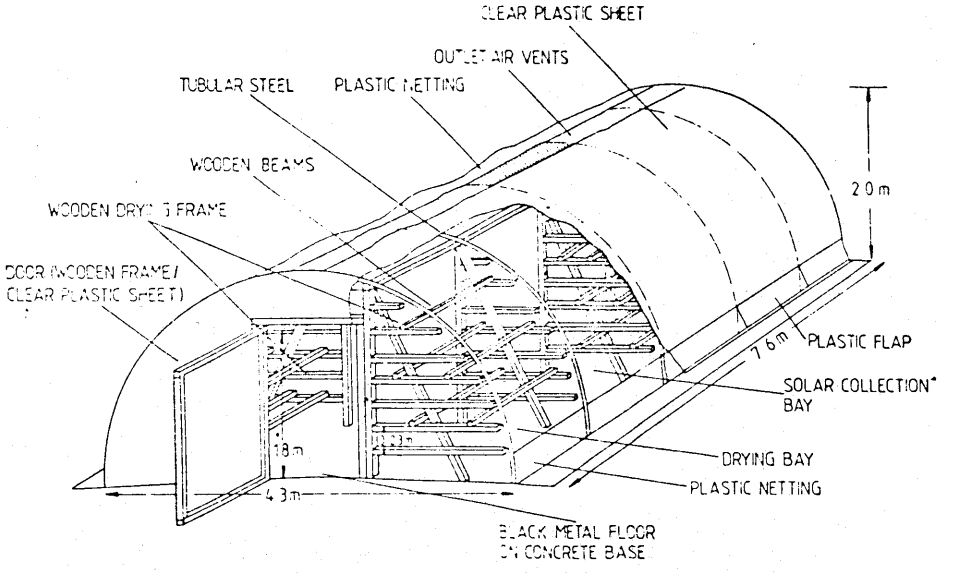

FIG. 5 SCHEMATIC DIAGRAM OF THE NATURAL-CIRCULATION INTEGRAL-TYPE SOLAR DOME DRYER

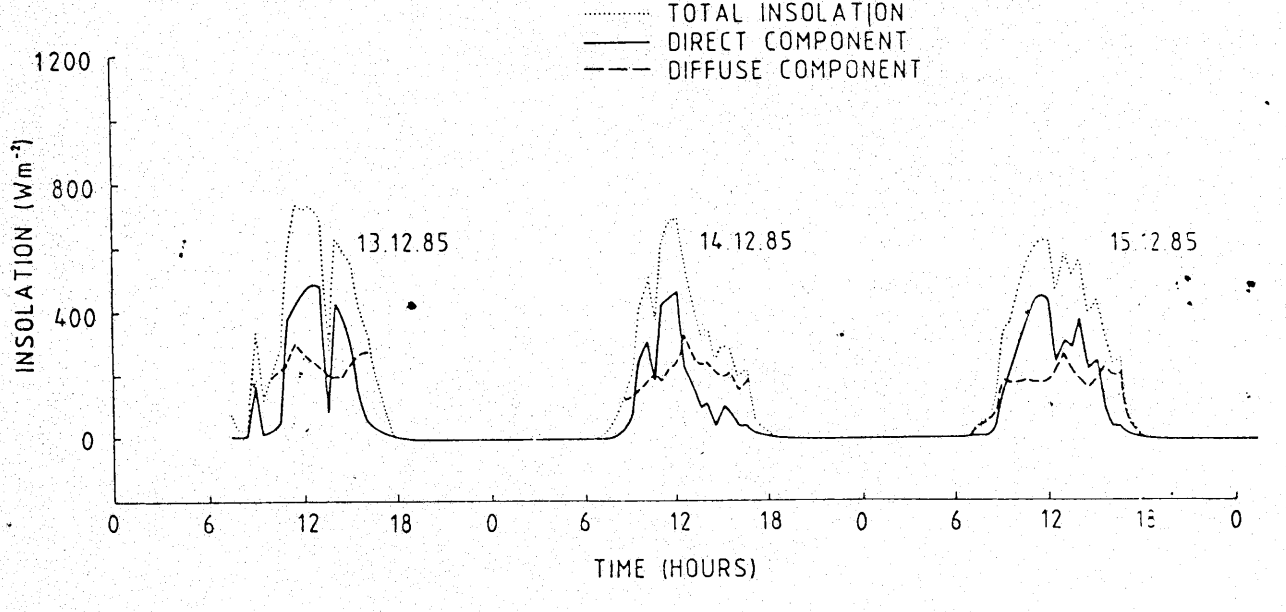

Fig. 6. Diurnal Variations of Insolation for Test 1.

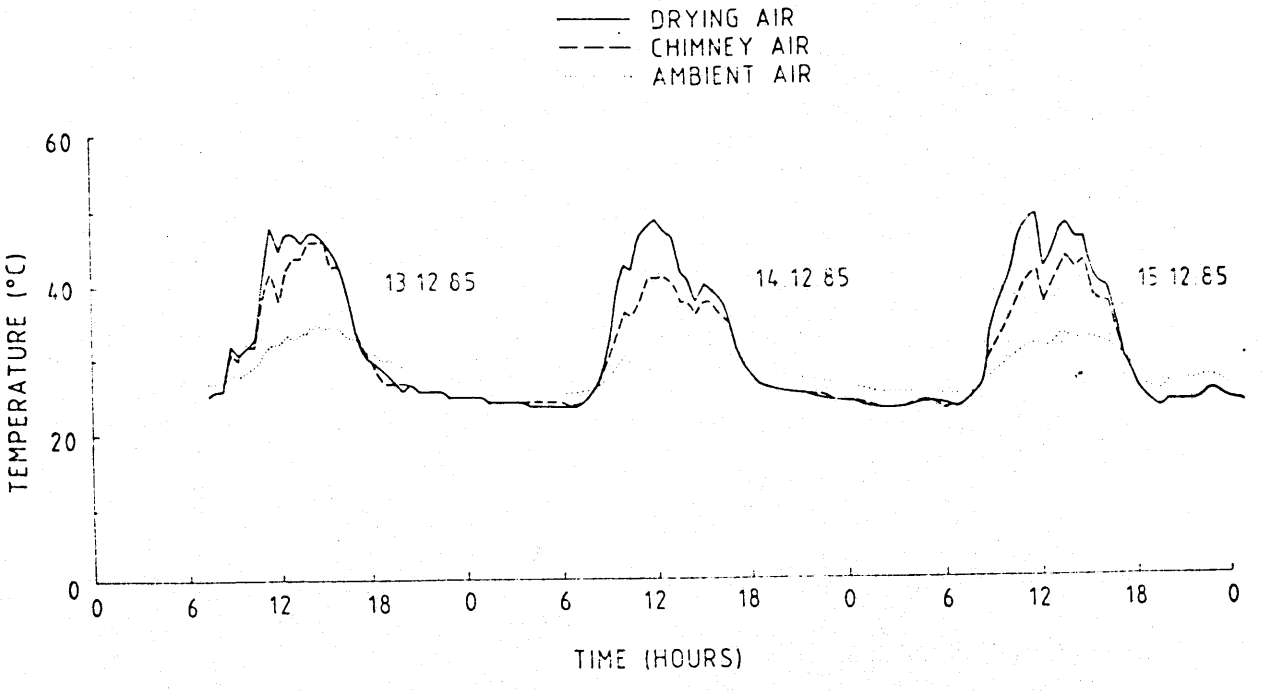

Fig. 7 Diurnal Variations of Drying air, Chimney air and Ambient Air Temperatures for Test 1.

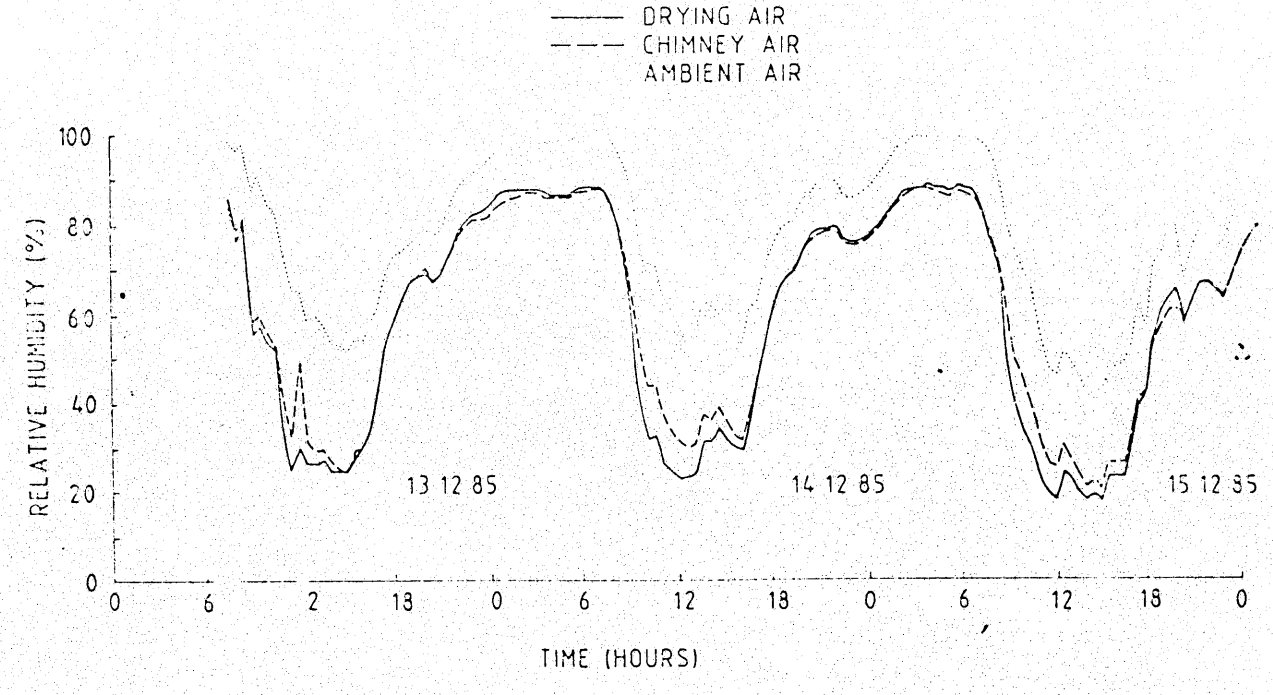

Fig. 8 Diurnal Variations of Drying air, Chimey air and Ambient air Relative humidities for Test 1.

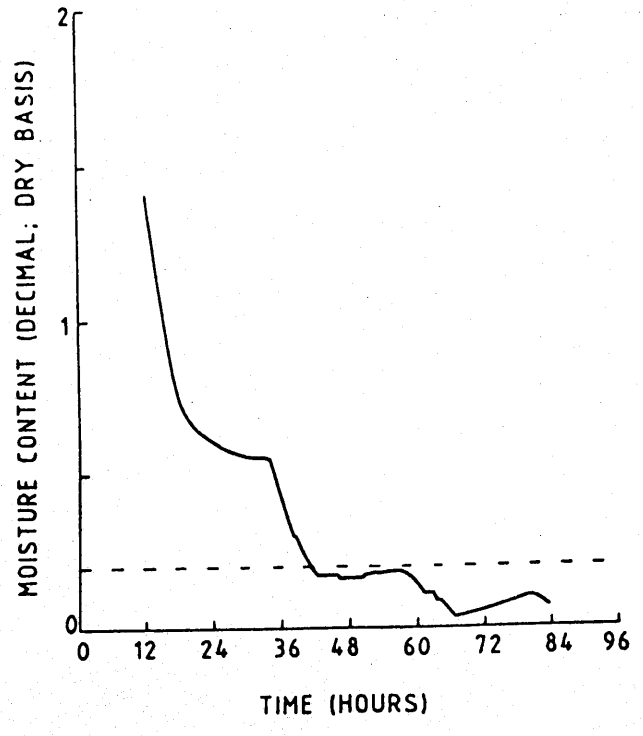

Fig. 9 Mean Drying Curve for Test 1 (13.12.85 - 16.12.86)

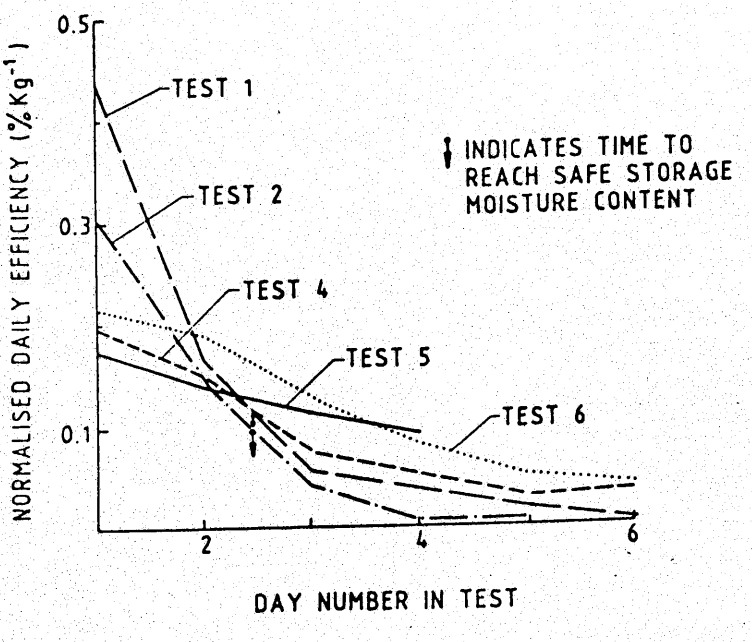

FIG. 10 VARIATION OF NORMALISED DAILY DRYING EFFICIENCIES WITH TIME

SOLAR STILL WITH WATER FLOW IN THE BASIN

Y.P. Yadav

Department of Physics,
C.M. Science College, Darbhanga-846004,
Bihar, India.

SUMMARY

A transient analysis of a solar still with water flow in the basin is presented. Explicit expression for water temperature is derived as a function of time and space coordinates. Explicit expressions for the glass cover temperature, distillate output and efficiency of the proposed system are also developed. Results are shown graphically.

NOTATIONS

b' breadth of the still, m

C_w specific heat of water, J/Kg ^oC

d_w depth of flowing water, m

h_{cga} convective heat transfer coefficient from the glass surface to ambient, $W/m^2\ ^oC$.

h_{rga} radiative heat transfer coefficient from the glass surface to the ambient, $W/m^2\ ^oC$.

h_{cwg} Convective heat transfer coefficient from the water surface to the glass covenn $W/m^2\ ^oC$

h_{rwg} radiative heat transfer coefficient from water surface to the glass cover, $W/m^2\ ^oC$

h_{cwg} evaporative heat transfer coefficient from the water surface to the glass cover $W/m^2\ ^oC$

h_3 convective heat transfer coefficient from the basin liner to water, $W/m^2\ ^oC$

h_4 total heat transfer coefficient from the bottom of the still to the ambient, $W/m^2\ ^oC$.

H_s solar intensity, W/m^2

K_i thermal conductivity of the material of insulation, W/m ^{o}C

L_i thickness of the material of insulation, m

t time-coordinate, S

T_a ambient temperature, ^{o}C

T_g glass cover temperature, ^{o}C

T_p basin-liner temperature, ^{o}C

$\dot{m}_w$ mass flow rate, Kg/S

x space coordinate, m

ρ density of water, Kg/m^3

L latent heat of vaporisation, J/Kg

α_p absorptivity of the basin-line.

INTRODUCTION

Performance studies of solar stills have been of considerable research interest since long. Several solar scientists have studied the performance of solar still. Hirshmann and Roefler [1] and Baun et al. [2] have presented a periodic analysis of a basin-type solar still. Nayak et al. [3] and Sodha et al. [4, 5] also presented a periodic and a transient analysis of a single basin solar still by linearising the Dunkle's relations for convective and evaporative heat losses. With a view to enhance the distillate output, waste hot water available from thermal power plant or chemical laboratories can be used in the basin of the still. Tiwari et al. [6] and Madhuri and Tiwari [7] have presented some analytical investigations on the single basin solar still using waste hot water in the basin. These authors have obtained water temperature as a function of time only; therefore, their analysis are no longer useful for optimization of the still parameters.

This communication presents a transient analytical model of a single basin solar still with water flow in the basin which gives an explicit expression for water temperature as a function of time and space coordinates. In addition to this, explicit expressions for glass-cover temperature, basin-liner temperature, distillate output and efficiency of the proposed system have also been developed. Effects of mass flow rate and still length (space coordinate) on the performance of the proposed system are also studied. The results are shown graphically. Some interesting conclusions follow from this investigation.

TRANSIENT ANALYSIS

The schematic of the proposed system is shown in Fig.1a; Fig. 1b shows the cross-sectional view of the surface over

which water is flowing. Following assumptions were made for energy balance at the various components of the proposed system :

(a) Thermal capacities of the glass cover and the basin-liner are negligible as compared to that of the flowing water in the basin.

(b) There does not exist any temperature gradient along the thickness of the glass-cover, and the depth of the water flowing in the basin.

(c) The glass cover and the water surfaces are parallel.

(d) The fraction of solar energy absorbed by the glass cover and the flowing water in the basin are negligible as compared to that absorbed by the basin-liner.

(e) The glass-cover, flowing water and the basin-liner have the same surface area.

(f) The still is air- and vapor tight.

(g) The still is insulated from the sides and bottom to reduce the conduction losses.

Incorporating the above mentioned assumptions, the energy balance equations at the various components of the proposed system can be written as follows :

Glass-Cover

$$h_1(T_w - T_g) = h_2(T_g - T_a) \qquad \text{--- (1)}$$

where,

$$h_1 = h_{cwg} + h_{ewg} + h_{rwg}$$

and $$h_2 = h_{cga} + h_{rga}$$

Elemental Water Flowing in the Basin

$$b\,dx\,h_3(T_p - T_w) = b\,dx\,\rho_w C_w \frac{\partial T_w}{\partial t} + \dot{m}_w C_w \frac{T_w}{\partial x}\,dx + h_1 b\,dx(T_w - T_g) \qquad \text{--(2)}$$

Basin-Liner

$$\alpha_p I_s = h_3(T_p - T_w) + h_b(T_p - T_a) \qquad \text{--- (3)}$$

where, $$h_b = \left[\frac{L_i}{K_i} + \frac{1}{h_4}\right]^{-1}$$

Equations (1-3) subject to the transformation relation,

$$x + \frac{t}{A} = \xi \quad \text{and} \quad x - t/A = \eta,$$

and boundary and initial conditions

$$T_w(x=0;\ t=0) = T_{wo},\ \text{give}$$

$$T_w = T_{wo} \exp\left[-\frac{b}{2}(x+t/A)\right] + T_{ssa}\left[1-\exp\left\{-b/2(x+t/A)\right\}\right] \qquad \text{--- (4)}$$

where,

$$T_{ssa} = \frac{c}{b} H_s + T_a$$

$$b = \frac{b'}{\dot{m}_w C_w}(h+h')$$

$$c = (h'\alpha_p h')/(\dot{m}_w C_w h_b)$$

$$h = \left(\frac{1}{h_1} + \frac{1}{h_2}\right)^{-1}$$

$$\text{and } h' = \left(\frac{1}{h_3} + \frac{1}{h_b}\right)^{-1}$$

The hourly distillate output and the efficiency of the proposed system can be written as

$$\dot{m}_e = \frac{h_{cwg}(T_w - T_g)}{L} \times 3600 \qquad \text{--- (5)}$$

and efficiency

$$n\ \% = \frac{\left(\sum_1^{24} \dot{m}_e\right) \times L}{A_b\left(\sum_1^{24} H_s\right) \times \delta t} \times 100 \qquad \text{--- (6)}$$

where δt = time-interval over which the intensity is measured, and L = latent heat of vaporisation of water.

RESULTS AND DISCUSSIONS

Equations (4), (5) and (6) are the required explicit expressions for water-temperature, hourly distillate output and the efficiency of the proposed system. As Eq. (4) gives the water temperature as a function of both time and space coordinate, it can be used to depict the transient and quasi steady state behaviour of the system. For quantitative assessment of the analytical results obtained so far, numerical calculations were made using the meteorological

parameters of a typical day at Delhi (Fig. 2). Values of the relevant parameters are as follows :

$L_i = 0.05m$, $K_i = 0.04$ W/m °C, $h_1 = 16.76$ W/m^2 °C
$h_2 = 40.88$ W/m^2 °C, $h_3 = 135.04$ W/m^2°C,
$h_4 = 6.17$ W/m^2 °C, $h_{cwg} = 8.85$ W/m^2 °C, $=1000.0$ Kg/m^3,
$C_w = 4190.0$ J/Kg m^3, $L = 2.297 \times 10^6$ J/Kg.

Figure 3 shows the effect of mass flow rate on hourly variation of distillate output. It follows from the results of this figure that the distillate output of the still increases with decreasing mass flow rate. This is expected result and it happens because decreasing mass flow rate corresponds to decreasing thermal capacity of flowing water in the basin. This result is useful for optimization of the mass flow rate for a typical solar still. The effect of still-length (i.e. space coordinate) on the distillate output is shown in Fig. 4. The results of this figure reveal that the performance of the still improves upto a typical still length; this result is also expected one because increasing still-length amounts to increasing absorber surface area.

CONCLUSIONS

1. The present thermal model of the still can be used to predict the transient, quati-steady-state and the periodic performance of the proposed system.

2. The distillate output and hence the efficiency increases with decreasing mass flow rate.

3. The distillate output and hence the efficiency increases with increasing space coordinates.

REFERENCES

1. Hirshmann, J.R. and Roefler S.K., Thermal Inertia of Solar Stills and its Influence on Performance, Proceedings of International Solar Energy Congress, Melbourne (1980) 402.
2. Baum, V.A., Bagaramov, B.B. and Malevsky, Y.N., Solar Still in the desert, Proceedings of the International Solar Energy Congress, Melbourne (1970) 426.
3. Nayak, J.K., Tiwari, G.N. and Sodha, M.S., Periodic theory of Solar Still, International Journal of Energy Research, 4 (1980) 41.
4. Sodha, M.S., Singh Usha, Kumar Ashvini and Tiwari, G.N., Transient analysis of solar still, Energy Conversion and Management, 20 (1981) 191.
5. Sodha, M.S., Nayak, J.K., Singh Usha and Tiwari, G.N., Thermal performance of Solar Still, Journal of Energy, 5(6), (1981) 331.
6. Tiwari, G.N., Garg, H.P. and Madhuri, Effect of water flow over the glass cover of a single basin solar still with intermittent flow of waste hot water in a basin, Energy Conversion and Management, 25(1985) 315.

7. Madhuri and Tiwari, G.N., Performance of Solar Still with intermittent flow of waste hot water in the basin Desalination, 52 (1985) 45.

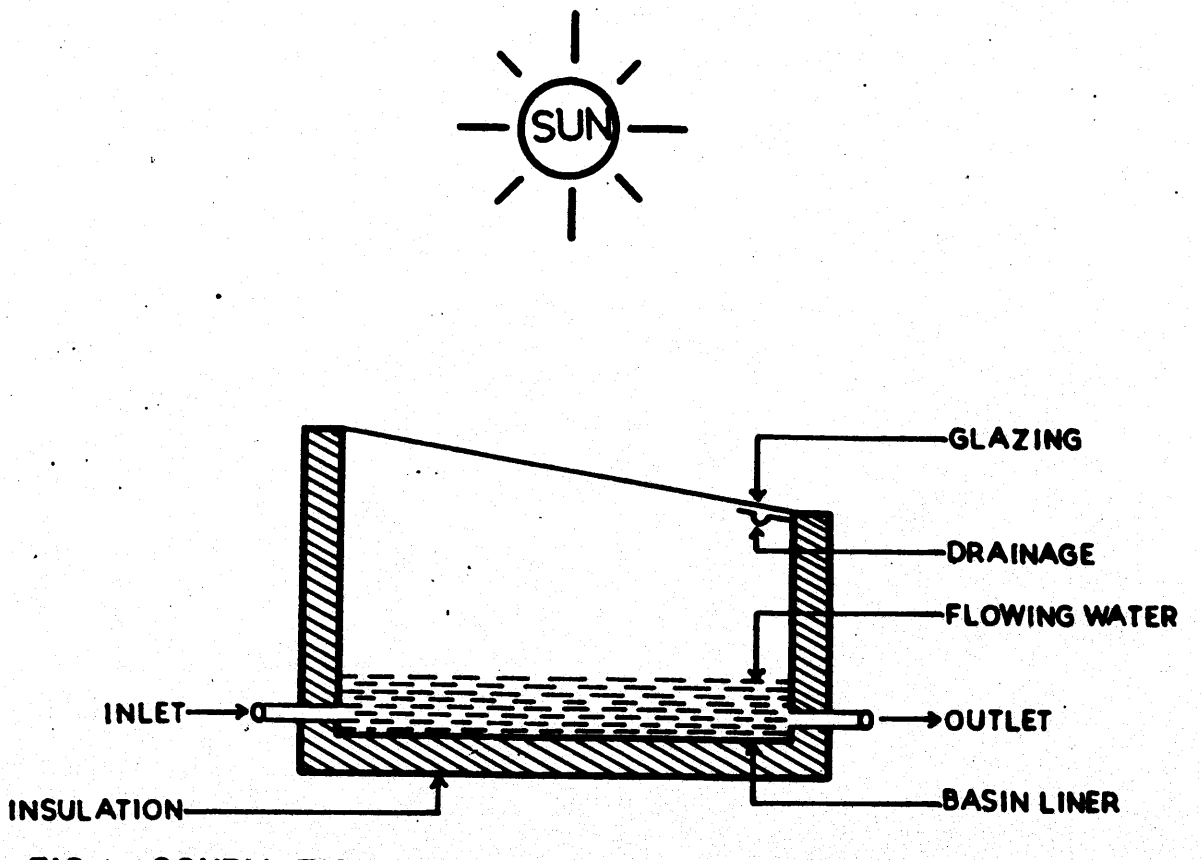

FIG.1a. SCHEMATIC OF A SINGLE BASIN SOLAR STILL WITH WATER FLOW IN THE BASIN.

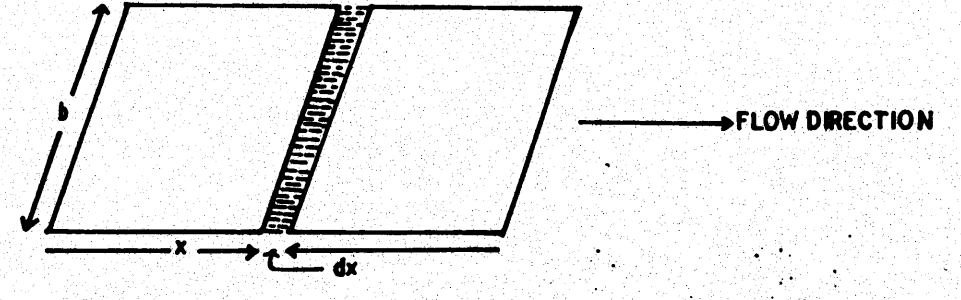

FIG.1b. CROSS-SECTIONAL VIEW OVER WHICH THE WATER FLOWS.

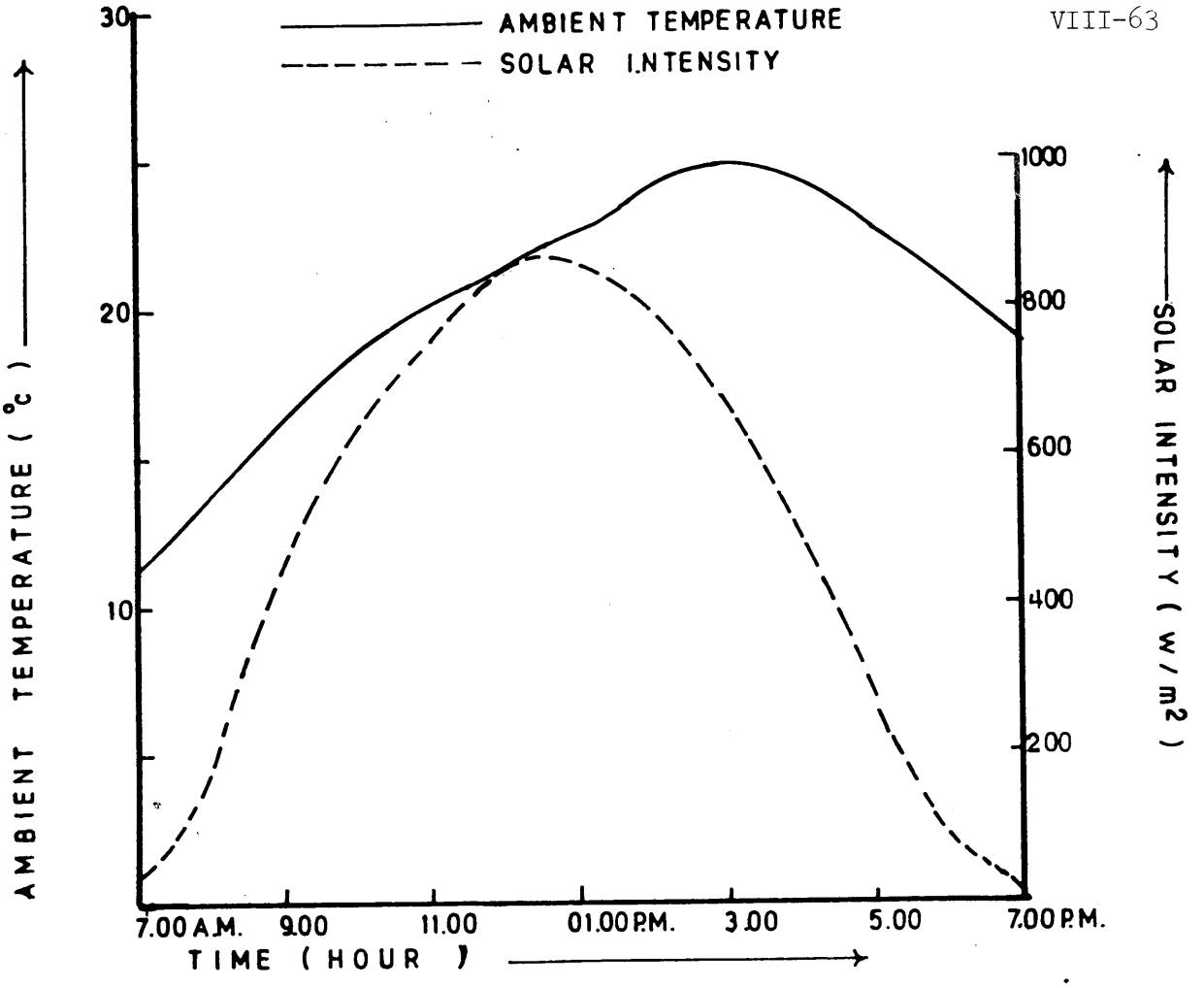

FIG.2. HOURLY VARIATION OF SOLAR INTENSITY AND AMBIENT TEMPERATUR.

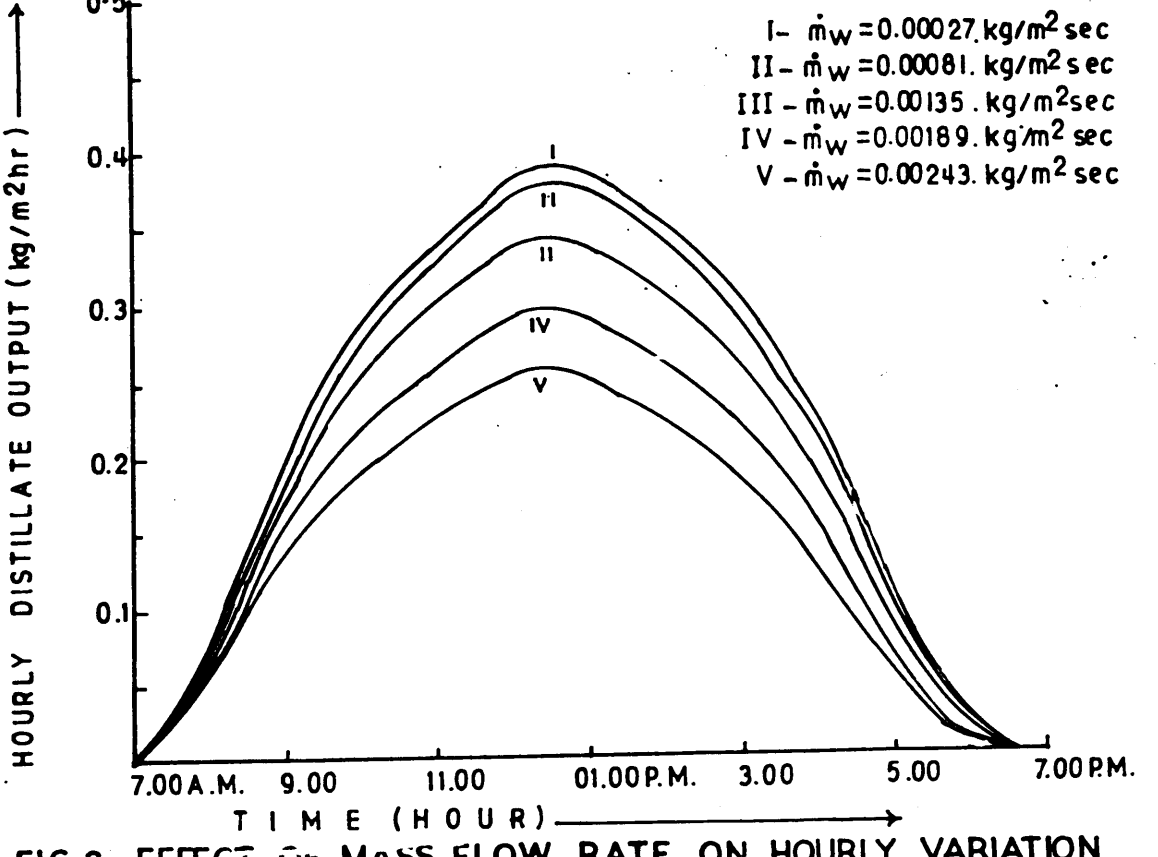

FIG.3 EFFECT OF MASS FLOW RATE ON HOURLY VARIATION OF DISTILLATE OUTPUT.

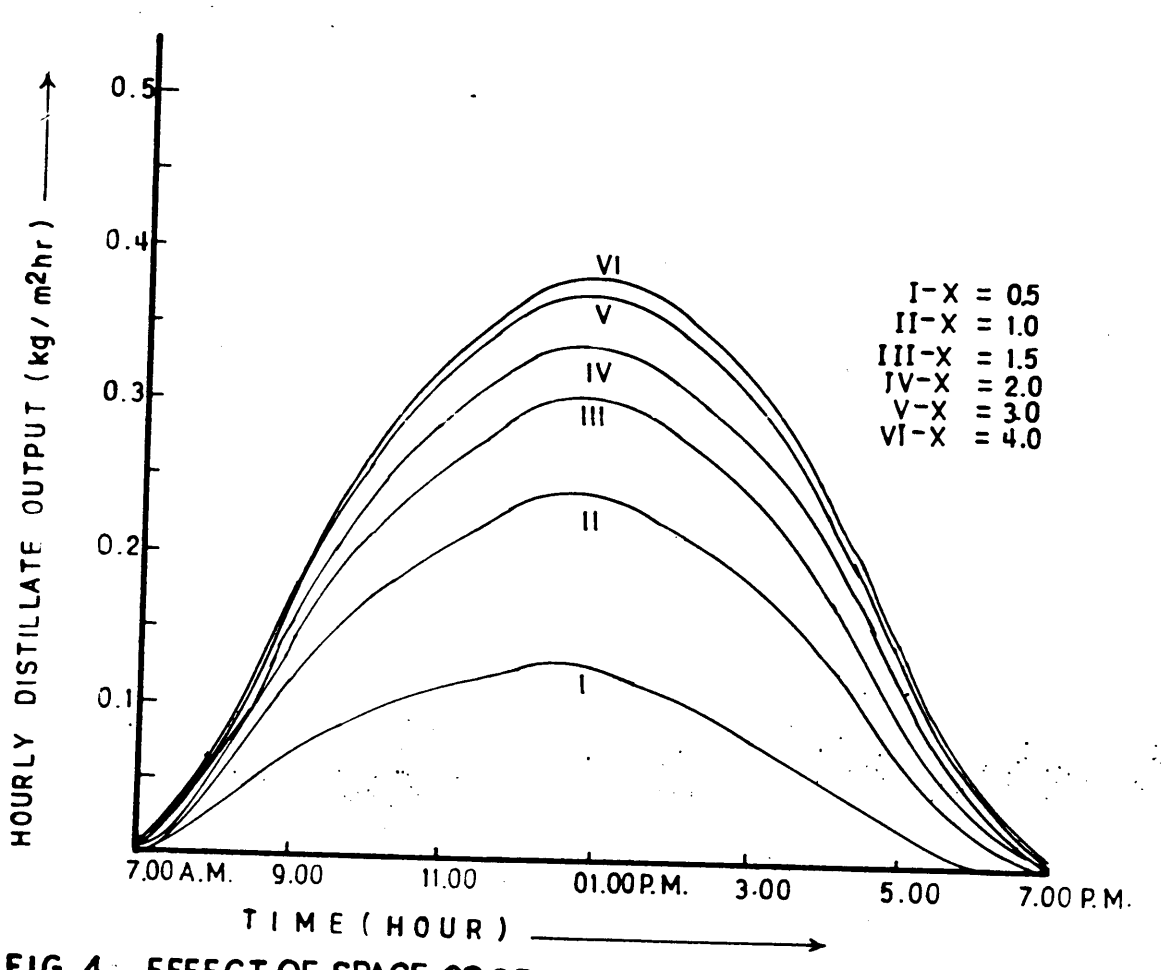

FIG. 4 EFFECT OF SPACE CO-ORDINATE ON HOURLY DISTILLATE OUTPUT.

HEATING OF CHARGED PARTICLES OF THE PLASMA BY WAVE OF ORDINARY MODES

GEORGES F. MALEK and MOHAMAD K. BERRO

Dept. of Physics, Sabeh Men April University, Zawia, Libya

A high frequency electromagnetic wave of ordinary mode is considered to propagate in plasma, perpendicular to the magnetic field. When the condition of resonance is satisfied, the equation of motion of the charged particles are solved in the relativistic and nonrelativistic cases. In nonrelativistic case, the longitudinal energy of the charged particle is constant, while the tranverse energy grows proportional to the square of time. The energy growth on the fundamental and second harmonic resonance is analysed . In relativistic case the energy of the charged particle has an oscillating form. In this case,in order to accelerate the charged particle,an external magnetic field varying synchronically with the variation of energy of the charged particle can be used.

1. INTRODUCTION

The problem of controled thermonuclear fusion has been intensively studied lately, The interest to this problem is due to the possibility of getting a new source of energy without any negative results on our surroundings.

In order to realise the controled thermonuclear fusion, we have to solve a lot of theoretical and experimental problems. The most important one is the problem of plasma heating up to the temperature of thermonuclear fusion. There exist many differents methods of plasma heating, one of the important methods is the high frequency heating.

In the case of resonance a HF electromagnetic wave propagating in magnetized plasma gives rise to the energy of the plasma particles, as a result plasma can be heated. There are many theoretical and experimental works where different types of waves are used and different resonance conditions are considered [1 - 7] .

In nonrelativistic case, there exist contradictory results about the growth rate of transverse energy of particles in the wave of ordinary mode, propagating perpendicular to the external magnetic field [2, 4] . In this work the revised theory is proposed with taking into account relativistic effects.

2. BASIC EQUATIONS

The ordinary electromagnetic wave propagating perpendicular to the uniform magnetic field $\vec{B}_0 = (0, 0, B_0)$ has the component

$$\vec{E}_\sim = (0, 0, E \cos\theta)$$
$$\vec{B}_\sim = (0, -\frac{ck}{\omega} E \cos\theta, 0) \qquad (1)$$

Here $\theta = -\omega t + k x$ is the phase of the ordinary wave, ω and k, respectively, the frequency and the wave vector.

Applying the averaging method of Bogoliubov [8] for a multi-periodic system of equations, the equations of motion for electron are averaged over the fast gyrophase ψ_0 and phase ψ, connected with phase θ by the relation [1].

$$\psi = \theta - \frac{K P_\perp}{m\omega_0} \sin\psi_0 \qquad (2)$$

Here $P_\perp$ is the transversal component of the momentum of the particle,

$\omega_0 = \frac{\Omega_0}{\gamma} = \frac{eB_0}{m_0 \gamma c}$ is the relativistic cyclotron frequency,

Ω_0 - the classical cuclotron frequency and γ is the relativistic factor

$$\gamma = [1 + (P_\perp^2 + P_\parallel^2)/m_0^2 c^2]^{1/2}$$

The averaged equations of motion have the form :

$$\frac{dP_\parallel}{dt} = -eE\left(1 - \frac{N\Omega_0}{\gamma\omega}\right) J_N(R) \cos\phi_N$$
$$\frac{dP_\perp}{dt} = -eE \frac{P_\parallel N\Omega_0}{P_\perp \omega\gamma} J_N(R) \cos\phi_N \qquad (3)$$
$$\frac{d\gamma}{dt} = -eE \frac{P_\parallel}{m_0 c^2 \gamma} J_N(R) \cos\phi_N$$
$$\frac{d\phi_N}{dt} = -\omega + \frac{N\Omega_0}{\gamma} + eENK \frac{v_\parallel}{P_\perp} J_N'(R) \sin\phi_N$$

Here $P_\parallel$ is the parallel component of the momentum, N- integer, $J_N(R)$ is the Bessel's function, $J_N'(R) = dJ_N(R)/dR$, $R = Kv_\perp/\Omega_0$

$\phi_N = \psi + N\psi_0$ is the resonant difference of phases.

3. NONRELATIVISTIC CASE

In nonrelativistic case($\gamma = 1$) under the condition of exact resonance ($\omega = N\Omega_0$), the system of equation (3) seems as follows :

$$\frac{dv_\parallel}{dt} = 0 \qquad (4\text{-a})$$

$$\frac{dv_\perp}{dt} = -\frac{eE}{m_0}\frac{v_\parallel}{v_\perp} J_N(R)\cos\phi_N \qquad (4\text{-b})$$

$$\frac{d\phi_N}{dt} = \frac{eE v_\parallel K}{m_0 v_\perp \Omega_0} J_N'(R)\sin\phi_N \qquad (4\text{-c})$$

where $v_\parallel$ and $v_\perp$ are the longitudinal and trasversal components of velocity.

From the first equation of system (4), we can notice that the longitudinal component of the velocity remains constant. Taking the derivative of the second equation and taking into account the third equation of system (4) we get

$$\frac{d^2 v_\perp^2}{dt^2} = 2\left(\frac{eEv_\parallel}{m_0}\right)^2 \frac{K}{\Omega_0 v_\parallel} J_N(R) J_N'(R) \qquad (5)$$

In nonrelativistic case ($R = Kv_\perp/\Omega_0 \sim v_\perp/c \ll 1$) [4] by decomposing Bessel'ssfunction, for fundamental harmonic resonance ($\omega = \Omega_0$, N=1) equation (5) seems as follows:

$$\frac{d^2 v_\perp^2}{dt^2} = \left(\frac{eEKv_\parallel}{m_0\Omega_0}\right)^2 = \alpha^2 \qquad (6)$$

while for the second harmonic resonance ($\omega = 2\Omega_0$, N=2), equation (5) becomes

$$\frac{d^2 v_\perp^2}{dt^2} = \frac{\alpha^2}{8}\left(\frac{Kv_\perp}{\Omega_0}\right)^2 \qquad (7)$$

The obtained equations (6) and (7) are simple differential equations, we can easily solve them. Their solution gives

$$v_\perp^2 = \frac{\alpha^2}{2}t^2 - 2\alpha v_{\perp 0}\cos\phi_{10}\, t + v_{\perp 0}^2$$

for N = 1

$$v_\perp^2 = v_{\perp 0}^2\left(\mathrm{ch}\,K\alpha t/\sqrt{8}\,\Omega_0 - \cos\phi_{20}\,\mathrm{sh}\,K\alpha t/\Omega_0\sqrt{8}\right)$$

for N = 2, where

$$\cos\phi_{10} = (\psi + \psi_0)_{t=0}$$

$$\cos\phi_{20} = (\psi + 2\psi_0)_{t=0}$$

On the first sight, it follows, from equations (8, 9), the transverse energy on the second harmonic resonance increases by an exponential law [4]

but this conclusion is rong. Comparing(6) and (7) we notice that the right side of (7) is less than that of (6) by the factor R/8 , so equation (9) is valid for a short interval of time $(\kappa a t/\sqrt{8}\Omega_0 \ll 1)$. Therefore, in both cases the energy increases by the law t^2 . However, the increase of energy for N= 2 occurs slower than that for N= 1. This conclusion is confirmed by numerical calculations, where the numerical solution of system (4) is shown graphically (fig. 1).

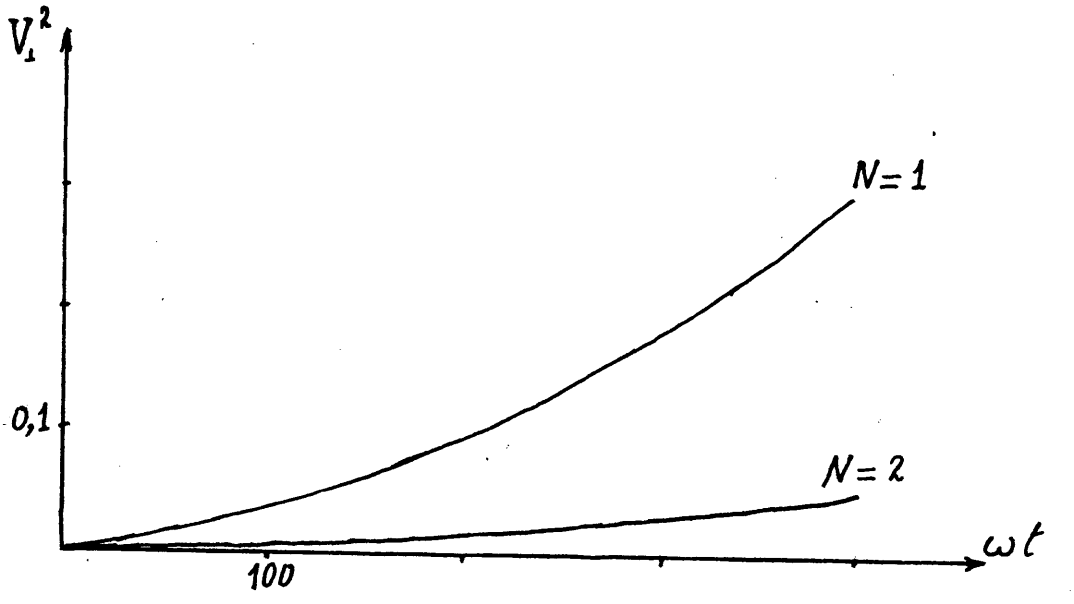

Fig. 1. Variation of $V_\perp^2$ by the time t .

$eE/mc\omega = 0,1$, $V_{\parallel 0} = v_{\parallel 0}/c = 0,05$, $V_{\perp 0} = v_{\perp 0}/c = 0,01$
$ck/\omega = 0,9$, $\psi_{10} = \psi_{20} = \pi$

4. RELATIVISTIC CASE

In relativistic case, when the velocity of electron is comparable with the velocity of light, as it happens in hot plasma, from the initial system of equations of motion of electrons we get :

$$\gamma = \frac{N\Omega_0}{\omega} + \left[\left(1 - \frac{N\Omega_0}{\omega}\right)^2 + P_\parallel^2\right]^{1/2} \qquad (10)$$

$$P_\parallel = \frac{eE}{m_0 c\omega} J_N(R) \sin\phi_N + Const \qquad (11)$$

where $P_\parallel = p_\parallel/m_0 c$. From (10) and (11), in contrast to nonrelativistic case, we notice that the longitu dinal momentum of the particle and its energy can not increase unlimitly. The character of the variation of energy with time can be determined by means of approximate equation

$$\frac{d^2\phi_N}{dt^2} - \nu_N^2 \cos\phi_N = 0 \qquad (12)$$

where $\nu_N = [e E N \omega_0 P_{\parallel} J_N(R)/\gamma^2]^{1/2}$ is the frequency of the nonlinear oscillations of the particle in the wave. From equation (12) one can get the approximation integral of energy

$$\frac{1}{2}\left(\frac{d\varphi_N}{dt}\right)^2 - \nu_N^2 \sin\varphi_N = const. \qquad (13)$$

so the energy of the particle oscilates with frequency ν_N. This conclusion is provrd by the numerical solution of the system (3).(fig. 2). Early, such a result was obtained for the extraordinary mode [5].

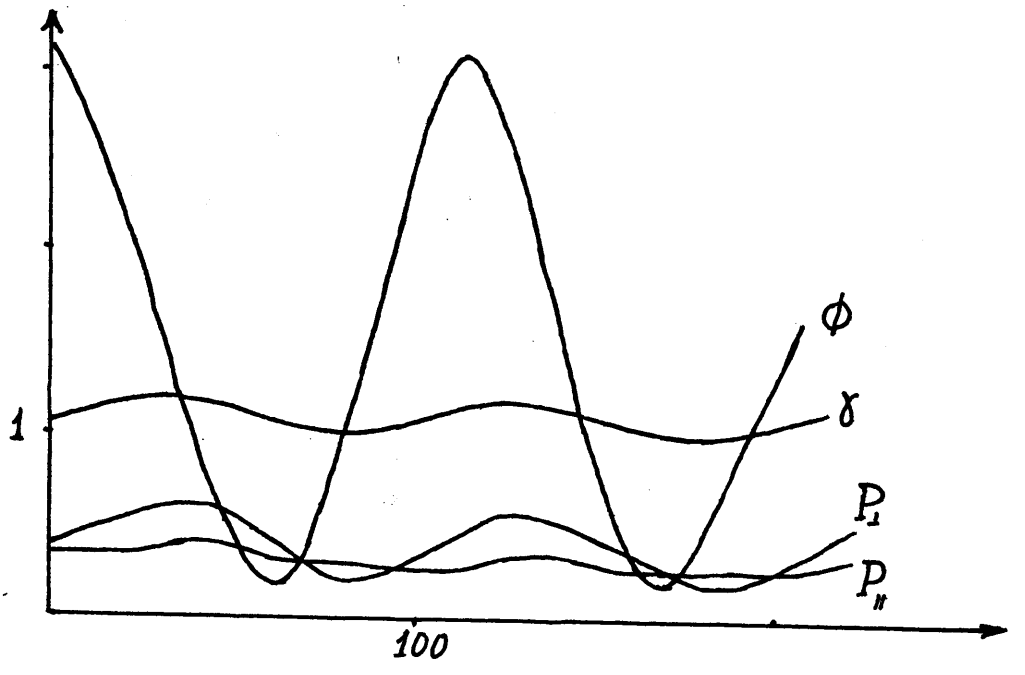

Fig. 2. Numerical solution of system (3).

$$eE/m_0 c\omega = 0,1 \;,\; ck/\omega = 0,9 \;,\; P_{\parallel 0} = 0,3$$
$$P_{\perp 0} = 0,4 \;,\; \gamma_0 = 1,118 \;,\; \psi_{10} = \pi \;,\; N = 1$$

In order to conserve the resonant condition at all the time of motion of the particle, an external magnetic field, varying synchronically with the variation of energy of the particle, can be used. Then the energy of the particle should increase continuously [9]. We consider the magnetic field as being increased slowly by a linear law

$$B(t) = B_0 (1 + At) \qquad (14)$$

Using the field (14) system (3) is numerically solved on the computer (fig.3). It is supposed that the cyclotron resonance at the initial moment takes place.

Figure (3) illustrates that the energy of the particle is growing with time by an oscillating form.

In the case of standing wave, a similar problem was discussed in [9]

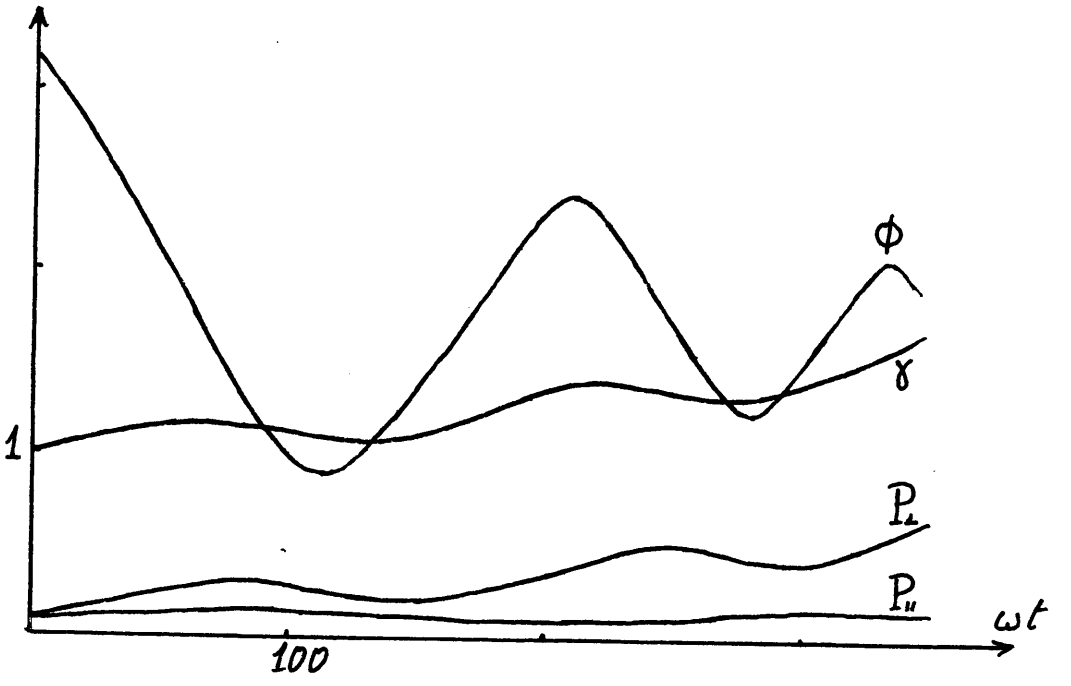

Fig. 3. Numerical solution of system (3) by taking into account the variation of the magnetic field.

$eE/m_0c\omega = 0,1$, $ck/\omega = 0,9$, $A = 0,00045$,
$P_{\parallel 0} = P_{\perp 0} = 0,1$, $\gamma = 1,0099$, $\psi_{\perp 0} = \pi$.

REFERENCES

1 - Roberts, C.S., and Buchsbaum, S.J.," Motion of a charged particle in a constant magnetic field and a transverse electro-magnetic wave, propagating along the field", Phys. Rev., vol. 135, A381- A389, 1964.

2 - Rawlands, J., and et. al.," Quasilinear damping theory of EM waves in magnetised plasma", Zh. Eksp. Teor. Fiz. 50, 994, 1966.

3— Schmitt, J.P.M., La Pierre, Y.," Resonant wave-particle interaction at the half-integer cyclotron harmonics", Plasma Phys., 20, 95-105, 1978.

4 - Kuo, S.P., Cheo, B.R.," Perpendicular electron cyclotron resonance heating by ordinary modes", Phys. Fluids, 24, 785-786, 1981.

5 - Milantiev, V.P.," Theoretical treatment of the interaction between the resonant particles of a magnetised plasma and a high -frequency wave packet", Zh. Eksp. Teor. Fiz. 85, 132-140, 1983.

6 - Karnilovich, S.P., Malek, G.F., Milantiev, V.P.," Gyrokinetics of particles of a magnetised plasma in the range of the half-integer cyclotron resonances and resonances on the beats of two waves packets", Proc. of the 6th InterConf. on Plasma Physics, 2, 246, 1984.

7 - Karnilovich, S.P., Malek, G.F., Milantiev, V.P.," Gyrokinetics of resonant particles in a collisionless plasma", J. Plasma Physics, 34, part 2, 177-189, 1985.

8 - Bogoliubov, N.N., Mitropolsky, Yu.A.," Assymptotic methods in the theory of nonlinear oscillation", Naouka, Moscow, 1974.

9 - Golovanivsky, K. S., " Autoresonant acceleration of electrons at non-linear ECR in a magnetic field which is smoothly growing in time ", Phys. Scr. , 22,126-133, 1980.

MINI SCALE SOLAR POND ACTIVATED BY HALOGENIC LAMP

Dr.Hasan Külünk
Kocaeli Engineering Faculty,İzmit,Turkey

ABSTRACT

In order to study dynamic temperature profile of salt stratified solar pond a number of laboratory experiments are carried out using a glass tank of dimensions 0,188x0,190x0,137 m3. Tank is filled with four brine layers of densities 1000-1102-1153-1197 kg/m3 each having 0,04 m thickness. Brine solution tank which is insulated at the sides and bottom is then heated using 200 watt halogenic lamp. The effect of PVC plate and clear oil layer floating on the brine surface on evaporation rate have also been studied. It is concluded that with the present device density gradient can be set up and convection currents can be prevented to yield nearly 80 ^{o}C at the bottom zone. Preliminary results are encouraging for further studies with larger ponds.

1.INTRODUCTION

The salt stratified solar pond system is proposed as a device for collecting and storing solar energy [1] , power generation [2] and numerous other applications [3] . Solar pond system is actually a body of water in which the salinity at the bottom is greater than the salinity at the surface.The depth may change in the limits of 0,5 to 2 meters. Generally it consists of thin convective layer at the top and thick convective layer at the bottom. These two zones are separated by a nonconvective gradient zone in which salinity and temperature gradients occurred. Small pond experiments which are undertaken can be seen in literature [4] . On the other hand, experimental studies on a shallow solar pond which have very different thermal characteristics can be seen in literature [5]. The detailed present status of mathematical modelling and practical aspects of solar pond are also reviewed by Ortabaşı [6] .

The rate of solar energy collection and heat loss, and the total heat storage capacity at the bottom convective zone

determine the utility of solar ponds for collecting and storing solar energy. The cost of maintaining the nonconvective zone which provides the thermal insulation together with its durability are also effective on the reliance of solar ponds.

In this study, the thermal behaviour of a miniature salt stratified solar pond is considered experimentally. However, it's theoretical aspects are rather complicated and left to an another study.

2.EXPERIMENTAL METHOD

The set up of the device used in experiments and it's main dimensions are shown in Fig.1. NaCl solutions in different capes are then poured into the glass tank by means of pipe attached to a cork floating on the surface of the solution as shown in Fig.2. The width of each brine zone is 0,004 m and the density gradient produced in the pond varies from the surface to bottom as 1000-1102-1153-1197 kg/m3. To minimize heat loss from the pond to the enviroment, sides and bottom of the glass tank is surrounded with 0,04 m thick insulation material. Brine solution is then heated by using 200 watt halogenic lamp instead of sun. During the heating operation a certain amount

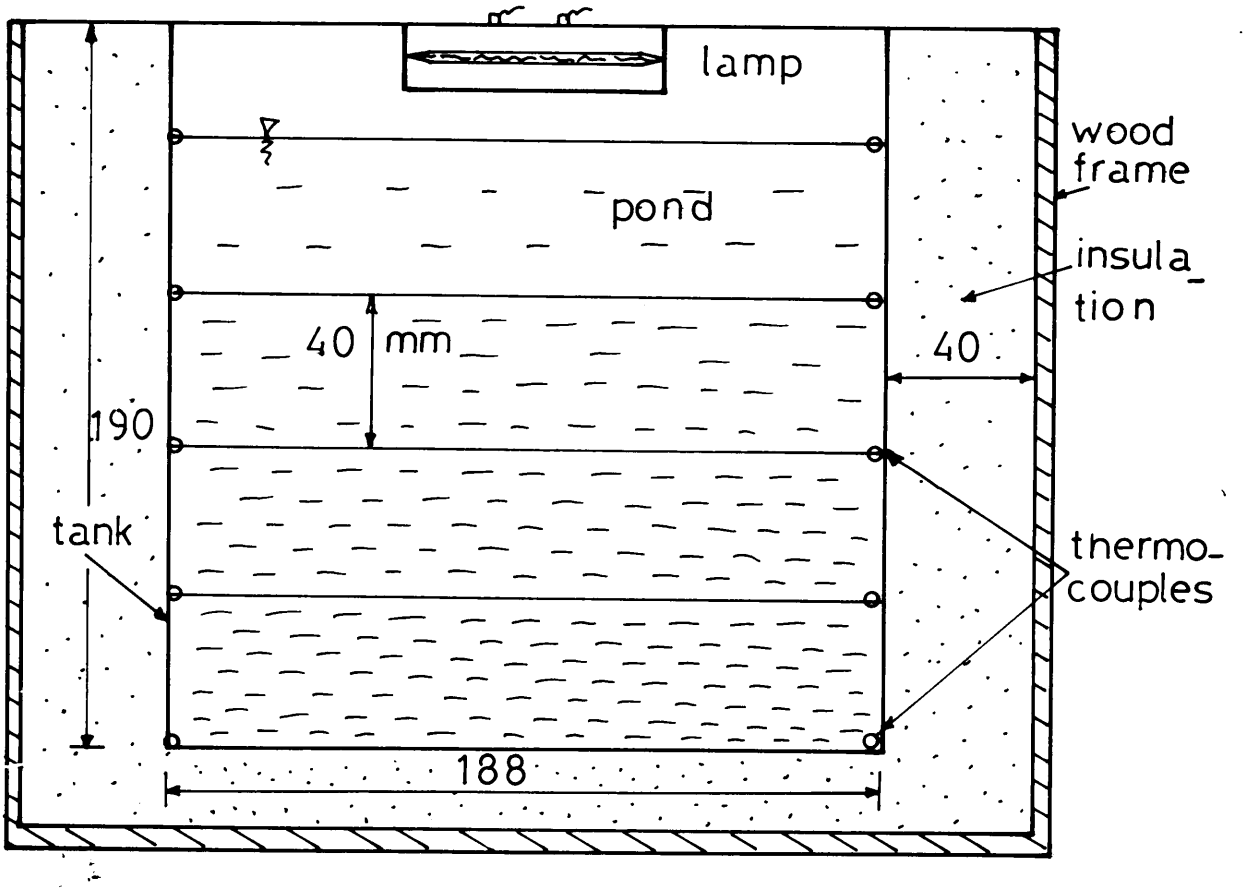

Fig.1. The experimental set up used to investigate the thermal behaviour of mini scale solar pond

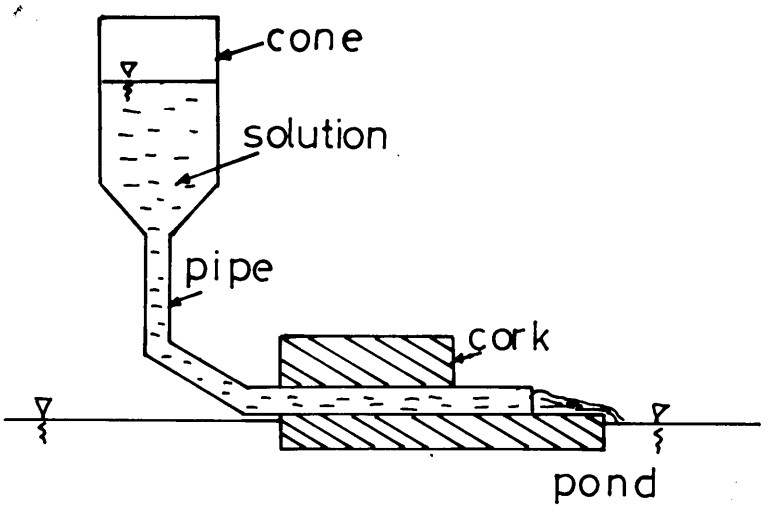

Fig.2.Floating mechanism used to fill the tank

of water is added occassionally at the top again by floating mechanism to compensate evaporation . To see the effect of PVC plate (with thickness 1,5 10^{-4} m and transmission coefficient 860 1/m) and clear oil (with thickness 5 10^{-3} m and transmission coefficient 2,9 1/m) on evaporation the surface of the pond solution is covered with these transparent substances at seperate experiments. Results obtained are presented in the following section.

3.RESULTS AND DISCUSSION

Fig.3 shows the heating operation of solar pond. By the inspection of it, one sees that during the first 10 hours

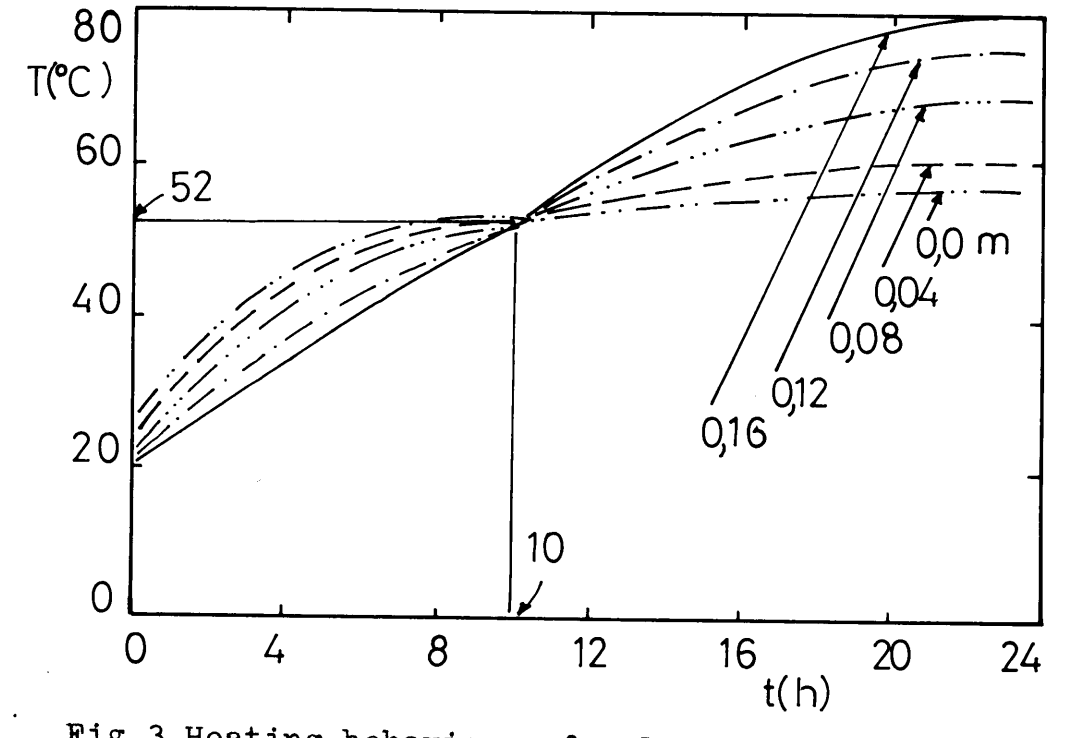

Fig.3.Heating behaviour of solar pond at various depths

upper layers absorb energy at a higher rate compared with lower layers. However, in about 10 hours the whole body of pond solution attains temperature of about 52 °C. Therefore average efficiency during 10 hours is estimated as:

$$\text{Efficiency} = \text{Energy Stored/Input Energy} \qquad (1)$$

$$= \frac{4{,}6\ \text{kg} \cdot 4180\ \text{J/kg}\ ^{\circ}\text{C} \cdot (52-22)\ ^{\circ}\text{C}}{200\ \text{J/s} \cdot 10 \cdot 3600\ \text{s}}$$

$$= 8{,}0\ \%$$

The effect of temperature and concentration on specific heat is ignored in the computation of efficiency. In following 14 hours, lower layers absorbe and store thermal energy at a higher rate compared with upper zones and finally bottom zone reaches peak temperature of 80 °C.

The variation of temperature with depth for selected time of heating is depicted in Fig.4. By the close inspection

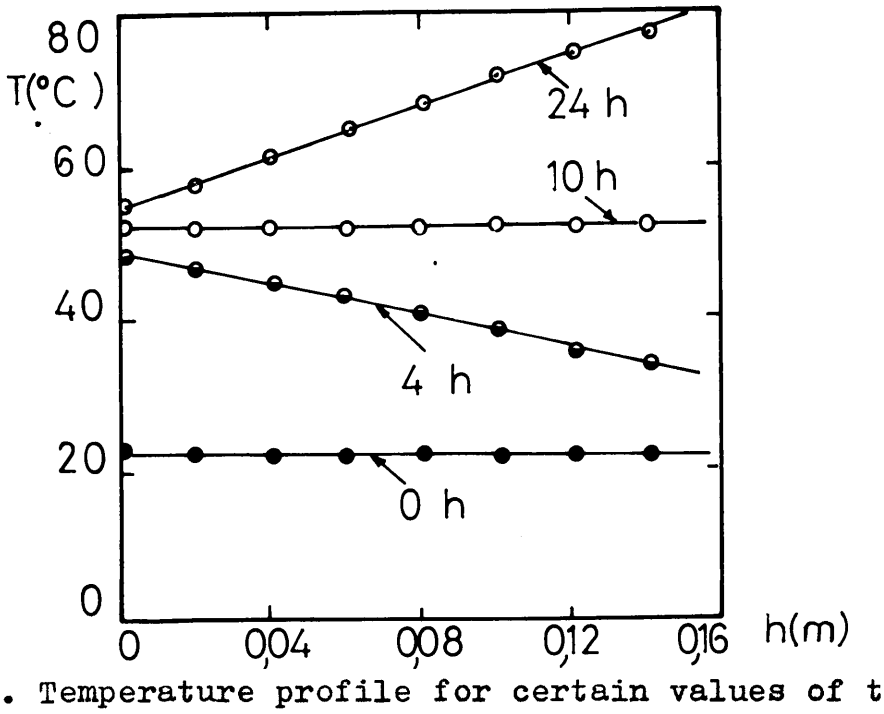

Fig.4. Temperature profile for certain values of time

of Fig.4 at times 0 and 4 h pond has uniform temperatures of 22 and 52 °C respectively. However, at times 4 and 24 h temperature change nearly linearly with depth obeying:

$$\text{for } t=4\ \text{h};\quad T(^{\circ}\text{C}) = -106\ h(\text{m}) + 48 \qquad (2)$$

$$\text{for } t=24\text{h};\quad T(^{\circ}\text{C}) = 156\ h(\text{m}) + 55 \qquad (3)$$

On the other hand, using the data given above, the thermal energy stored at the bottom zone can be estimated as:

$$Q = m.c.\Delta t \qquad (4)$$

$$= (0{,}188.0{,}137\text{m}^2).0{,}04\text{m}.1197\text{kg/m}^3.4180.(80-22)$$

or $$Q = 0,3.10^6 \text{ J}$$

is obtained where Q(J), m(kg), c(J/kg °C) and Δt denote stored energy, mass of brine , specific heat of water and temperature increase respectively.

Fig.5 shows the dynamic temperature behaviour of cooling of solar pond at various depths. Layers at the bottom cools at a lower rate compared with upper zones which predict exponential character rather than linear. This is of course expected due to enviroment.

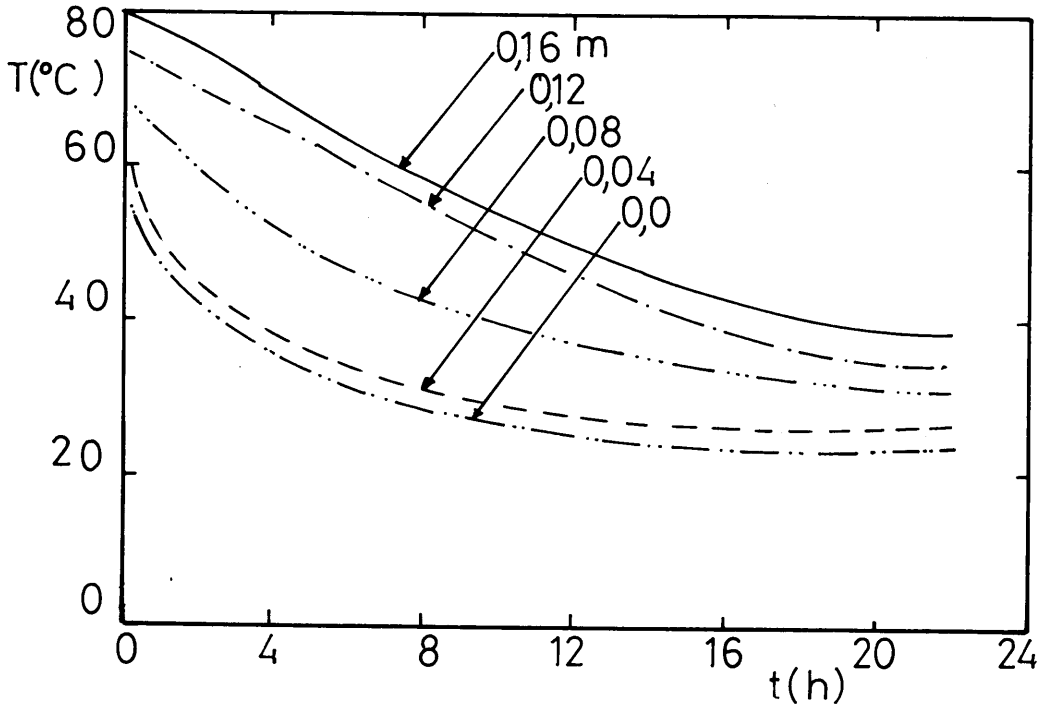

Fig.5.Cooling behaviour of solar pond at various depths

Finally Fig.6 shows heating and cooling movements of solar pond at depth h=0,12 m. Again nearly linear relationships are encountered between temperature and time.

4.CONCLUSIONS

General trend of the heating process shows that variation of temperature at a given depth with time changes nearly linearly except the periods of first and last 4 hours. After 24 h heating is ceased since no more thermal energy is stored but incoming energy has only compensated the losses. Maximum temperature reached is 80°C and average efficiency during first 10 h is about 8% which seems reasonable under present conditions.

About 1 kg of water is added to keep the solution at level 0,16 m due to evaporation. However, when the experiment is repeated with $5\ 10^{-3}$ m thick oil the evaporation rate

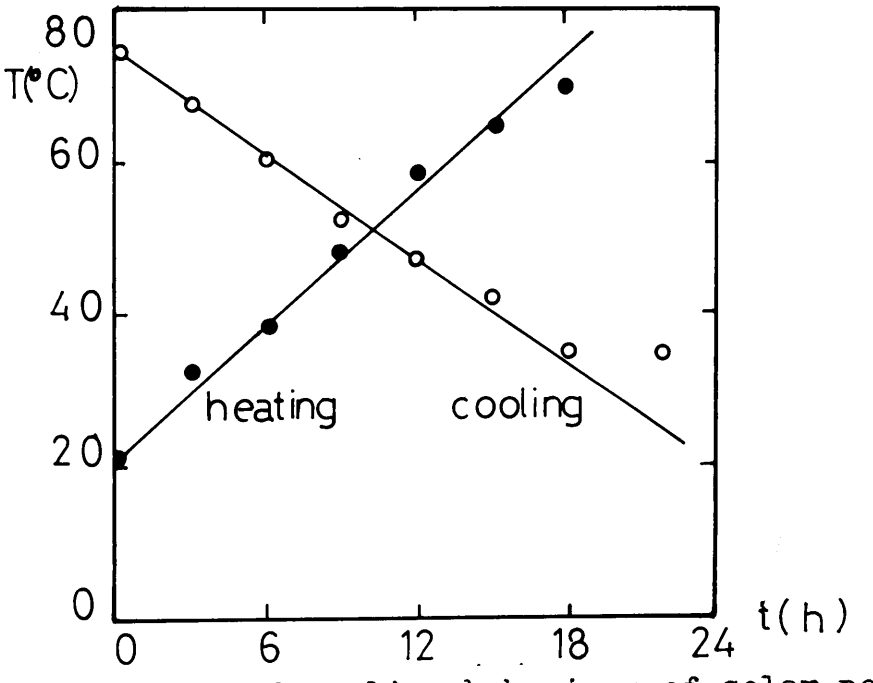

Fig.6. Heating and cooling behaviour of solar pond at depth 0,12 m.

is reduced by a factor of 10 while 2 with PVC plate. However extra work is needed in this aspect since water is one of the most important ingredient used in solar ponds. It is believed that same technique may well be adopted to large scale applications and saves the amount of water used.

Halogenic lamp used instead of sun provides artificial solar intensity equal to 200watt/0,188.0,137 m^2 = 7765 w/m^2 which implies 7765/1353= 5,73 times concentrated sun's energy where 1353 w/m^2 represents solar constant. Of course part of this energy is wasted to heat up enviroment. In future work, a lamp immersed in the pond will be considered to eliminate this drawback.

Finally, it is concluded that with this device general principle of salt stratified solar pond can be verified to encourage tests for larger systems together with theoretical aspects of the heating and cooling processes.

5.REFERENCES

1 - Nielsen,C.E.,"Salt Gradient Solar Ponds for Solar Energy Utilization", Environmental Conservation, 2,289-292, 1975.

2 - Tabor,H.,"Solar Ponds",Solar Energy,7,189-194,1963.

3 - Tabor,H.,Matz,R.,"Solar Pond Project",Solar Energy, 9,177-182, 1965

4 - Nielsen,C.E.,et.al.,"Flow System for Maintenance of Salt Concentration Gradient in Solar Ponds", Solar Energy, 19, 763-766, 1977.

5 - Ali,H.M., Akhlaghi,M., "Experimental Study in a Shallow Solar Pond", Solar and Wind Technology, 4, 425-430, 1987.

6 - Ortabaşı,U., Gürgenci,H.,"An Overview of Solar Ponds for Process Heat and Power Generation", International Symposium Workshop on Renewable Energy Sources , Lahore, Pakisten, March, 87-138, 1983.

ITALIAN R&D ACTIVITY ON SOLAR ENERGY CONVERSION

Dr. C. Corvi
ENEL - Italian Electricity Board
R&D Department

ABSTRACT :

The paper deals with the opportunities offered by different solar energy conversion options. The use of solar energy at low temperature for hot water and hot air production is technologically mature but up to now solar collectors have not been very successful in Italy because of the great availability of methane at very low prices and a bad offer organization.

The cost of plants which could use solar heat at high temperature is very high, while the experiments made at Adrano on thermodynamic conversion of solar heat to produce electricity have been substantially negative.

Photovoltaic conversion is much more promising because the technology is relatively new and therefore allows for potential cost reduction. It can industrially develop even in case of low demand because photovoltaic cells are already economically convenient in other fields. An improvement in cell technology, mainly due to the use of amorfous silicon, can dramatically increase their efficiency and therefore reduce land occupation.

The paper ends with a short report on Italian activities in the field of wind energy.

***

1. THE ENERGY SITUATION IN ITALY

The Italian GDP (Gross Domestic Product) increased at an average annual rate of 3% from 1983 to 1987.

New economic expansion determined considerable recovery in the energy demand both in Italy and in other Countries.

Total demand of energy passed, over four years, from 97.2 Mtoe in 1983 to 105.3 Mtoe in 1987 (+8.1 Mtoe), while electricity demand passed from 181 billion kWh in 1983 to 210 in 1987 (+29 TWh).

The average annual rate in rise of the electricity demand was thus 3.8% against a rate of 2.1% for all forms of energy.

In particular, the evolution in electricity demand reported in 1987 marked a great rise in electricity intensity compared to 1986 (+2.3%, as the difference between +4.9% in demand and +2.6% in GDP). This was due above all to great increases in electricity consumption by tertiary services (about +8%), domestic services (+5.5%) and agriculture (about +5%). Electricity consumption by industry has increased on the whole by about 3%.

The close link between economic growth and energy consumption (electricity in particular) can also be confirmed for Italy, especially during economic expansion phases. The electricity demand also reported greater evolution compared to economic growth due to modernization that is under way in the production sector and, in particular, in services. In fact, Italy is still at lower levels compared to other bigger industrialized Countries both in terms of electricity intensity of production sectors and of consumption and in terms of per capita electricity consumption.

As regards long term forecasts, the National Conference on Energy held in February 1987 pointed out an almost total convergence on an essential element: an average annual growth rate of the GDP by 2.5% as far as the year 2000 is a minimum value not to aggravate the economic situation.

These rates of economic growth are considered compatible with the potentials of the Italian production system and with the evolution of the international scene that envisages (with regard to prices of energy sources) gradual recovery at the end of the century from the minimum levels reached in 1986 to values already reported at the beginning of 1980. This expected rise in prices can only be gradual if industrialized Countries will continue to make the effort to save energy, maximize internal sources and diversify the sources of supply.

A very detailed sectorial analysis was carried out with the help of an economy-energy model that was jointly prepared by ENEL and ENI.

The main social and economic features may be summarized as follows:

- extremely restrained demographic growth;
- further restraint on the weight of products that are ''energy-intensive'' within the industrial sector of ''Intermediate Goods'';
- tendency towards re-equilibrium of rises in productivity among different production sectors and, in particular, modernizing plans for the tertiary sector;
- gradual success in the action for expanding transport over one's territory (railway, underground) including sea transport.

In future there is to be an increase in the tertiary service sector (from 58% of the GDP in 1986 to 63% in the year 2000), as well as faster growth (within industries for ''Intermediate Goods'') of branches having high value added and low energy intensity (for example, ''fine'' chemistry).

From a technological point of view, evaluations were carried out taking into account rapid rise (compared to current trends) of conservation and a more rational use of energy.

The total results of the above mentioned assumptions can be reported briefly in terms of evolution envisaged on electricity intensity.

Table 1 reports the results of the forecast by sector and destination of the ''end'' use of energy (thermal use at certain temperatures, ''necessary use'' of electricity and fuel), while fig. 1 reports an evaluation on ''useful'' energy that is linked to the above ''final'' consumption. This is done bearing in mind the yield of utilization equipment by users.

It was reported compared to 1986 that:

- the structure of ''final'' uses is directed towards restraining the amount of thermal use, in particular at low and high temperature;
- the effect of ''final'' consumption of different sectors over the total consumption turns towards tertiary service and transport sectors;
- in terms of total energy efficiency (the ratio between ''useful'' energy and ''final'' energy) the system improves, going from 53% in 1986 to 58% in the year 2000;
- the effect of electricity (for necessary and non-specific uses) increases in all sectors, going in the total final uses from 15.5% in 1986 to 20.9% in the year 2000 (table 2);
- the amount of ''non-specific'' electricity consumption in the field of ''civil uses'' (residential and of tertiary services) falls from 31% in 1986 to 26% in the year 2000.

Great changes towards activities having less energy intensity have already been considered recently in Italy, both with regard to the structure of the production system (minor effect than industry and agriculture to the advantage of tertiary service) and to the structure of the industrial system with restraints on basic industries.

Coverage of envisaged needs of electricity will be shared among the various energy sources according to the outline in table 3, thanks to the management programme (summarized in table 4) of the generation plants.

Currently the energy policy in Italy is among the priority topics being discussed by the new Government.

Following the November 1987 referendums that were against the development of nuclear power, heated debates took place in political surroundings, in the mass-media and in public opinion.

The new National Energy Plan has recently been presented by the Government to the Parliament. The intention is to give up any electricity generation by means of nuclear power plants, leaving just an opportunity in the future for any inherent safe nuclear reactor, which might be technologically ready in the next century.

The gap of generating power thus opened will be filled mainly by burning more coal and methane.

On the other hand an important development for renewable energy sources is planned. As an example wind turbines for a capacity of 300 to 600 MW are to be installed by the year

2000 and PV plants mainly for stand-alone users for a global capacity of 25 MW are to be installed by the year 1995.

2. THE ROLE OF RENEWABLE ENERGY SOURCES

Strengthening as far as possible the contribution of national renewable energy sources is the primary aim in order to lower the degree of dependency from abroad, especially where this is considered pursuable (in particular for hydroelectric energy and geothermoelectric power) with a minimum impact on the environment and over the territory (table 5).

Results that can be obtained in the hydroelectric and geothermoelectric field by the year 2000 (specified below) are the maximum assumable and are essentially based on conventional technologies.

This great effort for the development of renewable sources will lead on the whole to an availability increase by 27.4 TWh, of which 17.4 is hydro, 6 geo and 4 biomass, photovoltaic and wind, to be compared to the rise in demand by 105 TWh from now till the year 2000.

2.1. Solar Energy

Production of heat at low temperature.

At the end of 1986 about 300,000 m^2 collector installations were operational and had fuel saving equal to 80,000 tons of equivalent oil. Experience acquired in Italy in recent years confirmed the greater convenience that is advisable with installations for group users than for individual ones and the need to improve total efficiency of the plants and of technical and economic issues formed by distribution and installation.

In recent years simplified collectors were quite successful especially for agricultural applications (where methane is generally less available) as well as in cases where the trend for heat demand corresponds to the availability of solar energy.

An area of great applicational interest due to growing possibilities of commercialization for agriculture and building (certain sectors) uses is the field of hot air production through solar systems based on the formation of air spaces obtained by overlapping transparent plastic coverings over industrial sheds according to suitable shapes.

In addition, this technology proved to be adequate for other innovative uses of solar energy, such as treatment for evaporation of polluted water and drying of agricultural products.

Production of heat at high temperature - Thermodinamics conversion.

Italy's experience matured with the 1 MW power station at Adrano, in Sicily, which is the first power station of its kind in the world that is linked to the electricity network implemented by ENEL and Ansaldo according to an EEC programme.

As a general conclusion, we may state that the experimental operation of the plant demonstrated the possibility of generating electric power and sending it out to the network through operational procedures that are widely similar to those envisaged for conventional thermal power plants, but placed in evidence the heavy limitation on power producibility. This is mainly due to the cloudiness and high stresses to which the subsystems and components are subject under continuous transient operation. If we consider in addition the moisture and dust present in the atmosphere, which cause a degradation of the direct irradiation and the following fall in steam production, together with the need for frequent maintenance and adjustments typical of an experimental plant, we can understand the low power production globally obtained at the end of the experimental operation.

The results, which were also confirmed by the operational experience of similar plants subsequently put into operation throughout the world, together with the current high plant costs characterizing this technology made the EEC decide to close the experiment in 1986.

Photovoltaic Conversion.

Photovoltaic Conversion in Italy is currently the subject of a vast research and demonstration programme. In 1986 expenses for government and private research equalled 36% of research expenses for ''new'' renewable sources.

Also in Italy the sector's strategy envisages the development of the following main lines of research: monocrystalline, polycrystalline and amorphous silicon and gallium arsenide cells technology.

In the field of amorphous silicon a high effort is being done by ENEA (Italian Commission for Nuclear and Alternative Energy Sources), which has built a Research Centre fully dedicated to this technology in Portici, near Naples. In this Centre a pre-industrial plant for the manufacturing of amorphous silicon photovoltaic modules will be built, too. This technology should enable us to drastically cut down the module cost.

Applications that envisage development in the next few years are the ones for feeding certain users that are isolated by the electricity network by high connection costs.

A series of demonstration and experimental plants (for a total power of 0.6 MW saving the equivalent of 300 tons of petroleum a year) have been set up in Italy in order to check on site and on the market the performance of photovoltaic plants.

Delphos 300 kW PV plant.

The main result obtained in the development and implementation of prototypes is the completion and the beginning of the experimental running stage of the first section (about 300 kW in peak) of the Delphos plant (Demonstration Electric Photovoltaic System) implemented by ENEA.

The plant was parallely connected to the grid for the first time in August 1986.

The Plant is run directly by ENEA through the Photovoltaic Research Centre of Portici (Naples).

The system's main characteristics are shown in Table 6. The photovoltaic modules have been supplied by Italsolar, Ansaldo, Helios Technology respectively in the amount of 150, 100 and 50 kW.

Giglio Island 45 kW PV plant.

Another important application is the one set up in Giglio Island. The plant, located at Allume powers a 300 m^3 refrigerator for the preservation of easily perishable foodstuffs, and a system for the production of ozone to sterilize well water.

Both usages, typical of islands, are characterized by a peak demand in the summer, which favours the photovoltaic option for the production of electric energy.

The implementation of the plant was financed by the Regional Administration of Tuscany, the EEC and ENEA, which also performed the technical review of the project and supervision of construction.

Several companies associated (namely, Italsolar, Oto Melara and Nuovo Pignone) were responsible for the design and the plant installation.

In particular, Italsolar performed the system design, supplied the modules and realized the photovoltaic array; Oto Melara contributed for the refrigeration system and the control electronics connected, while Nuovo Pignone set up the ozone generator's control system and the data acquisition system of the entire plant.

The 45 kW photovoltaic array is made of 864 monocrystal silicon modules and is subdivided into two section, respectively of 30 kW and 15 kW, the first one to feed the refrigerator, and the second one the ozone generator.

Vulcano island PV plant.

Another important initiative was the implementation by ENEL (the Italian Electricity Board) in 1984 of the photovoltaic plant at Vulcano according to an EEC programme. According to this programme a copy of the data recorded by the data acquisition system is transmitted every month to ESTI laboratories in Ispra.

The power generated by this plant can supply either a group of 54 domestic users in the neighbourhood or a 20 kV distribution network already existing on the island and connected to a 3,000 kVA diesel-power station.

The annual average plant productivity was evaluated around 150,000 kWh on the basis of an average daily solar energy density of 5 kWh/m^2 that is typical of the area.

The main features of the plant are summarized in Table 7.

The major goals pursued through the experimental operation of the Vulcano plant are:

- evaluation of the reliability and degradation of photovoltaic modules with time;

- evaluation of the power supply continuity in stand-alone operation;
- evaluation of the plant producibility during synchronized operation over the different seasons;
- operation data analysis to draw up monthly and annual energy balances for the whole plant and any of its components (photovoltaic field, storage battery and converter efficiency).

The experience acquired so far will permit a concrete evaluation of the prospects for the utilization of the photovoltaic technology in the situations characterized by high costs of power from conventional sources that are peculiar to small islands.

The annual production of electricity, referred to the period from June 1985 to May 1986, was 90,540, kWh versus a theoretical generation capacity of 131,000 kWh in the same period. The difference between the two values is due mainly to the limitation of the storage capacity, in addition to a few plant shutdown to trim the conversion electronics.

The electrical characteristics of the modules, on the basis of measurements made by sampling, were found to remain unaltered and therefore it is reasonable to affirm that the degradation of the performance of the photovoltaic field is practically nil. It was also observed that atmospheric pollution (dust, sand, etc.) has little effect on the module performance and thus on the production of energy; this is also due to the natural washing of the glass panes covering the modules by rain.

Standard 100 kW photovoltaic plants are envisaged within the next two years for the production of electricity on some smaller islands.

Isolated users PV installations.

Another initiative is the ''Scattered Housing'' Project, whose initial stage envisages feeding ten isolated houses (shelters, staff quarters) belonging to certain protection organizations (such as WWF, CAI - Italian Alpine Club, National Parks) with small volume photovoltaic installations (with reference to kW).

More specifically, in the years 1985-1986 plants were built in the WWF protected area at Orbetello and in the Zannone island of the Circeo Park, and seven huts were electrified. These jobs were performed in collaboration with Italian manufacturers of the sector.

In the plants built for the Scattered House Project use was made of PV modules manufactured in Italy, which have better technological characteristics than those supplied in 1983-1984 for the Vulcano plant. Substantial progress was made in the cell fabrication technology (for instance, the front electrode has been improved) and in cell assembly by means of automatic welding equipment. Also more reliable is the method of incapsulation, which should ensure a longer component life.

The plants built in the high-mountain huts are subject to very low ambient temperatures that are quite severe for all the components and particularly for the accumulators. Cost considerations have also suggested evaluating the

possibility of using the traditional lead-acid accumulator also in such climatic conditions. However, it was necessary to fill some of the gaps in the knowledge about the behaviour of these accumulators at low temperatures (down to 30°C) by means of specific tests in a climatic chamber.

The satisfactory result of the test determined the decision to use lead accumulators at almost all the sites.

At any rate, in order to have a reference for the life of the lead accumulators, also a Ni-Cd accumulator was installed, which is notably more suited for cold climates but much more expensive than the Pb accumulator. It will thus be possible, in a few years, to appraise the behaviour of the two types of accumulators and consequently the actual incidence of storage on the plant operating cost.

The utilization of electricity in all the plants is typical or rural dwellings where it is necessary to cover at least the priority needs (lighting, frigidaire, radio and TV sets, water pumps for sanitary uses, supply of small two-way communication systems). The use of direct-current or alternating-current equipment to meet these needs was evaluated.

Notwithstanding the obvious advantages afforded by alternating-current appliances which are relatively cheap and easy to find on the market, it turned out to be more appropriate to opt for d.c. equipment in order to dispense with the conversion from d.c. to a.c. which is very expensive energy wise (conversion losses may take about 20% of the total energy supplied). Furthermore, the use of d.c. makes it possible to use high-efficiency fluorescent lamps for room lighting with approximately 50% savings in the supply of lighting power over the cost with the traditional incandescent lamps.

The two aforesaid advantages allow the relative higher cost of the appliances to be compensated by the drastic reduction in the overall plant cost because the required number of photovoltaic modules - which are at present the most expensive component - is reduced.

In fact, the second stage of the Project envisages experimenting a system that can meet the energy needs required by isolated houses based on a photovoltaic kit (having limited power hardly exceeding 300 W) connected in certain cases to a thermal kit provided with about 2 m² of solar panelling for producing hot water.

The first kits were installed last August in Stromboli, one of the Eolian islands in Sicily.

As a conclusion, we can say that photovoltaic generation will have a more important role in feeding the national electricity network only when new technologies will make it possible to greatly reduce plant costs.

Following the recent 8th European Photovoltaic Solar Energy conference, which was held in Florence on May 9-13, 1988 thanks to the sponsorship of the Commission of the European Communities and the Italian Section of ISES, this is not any more merely a hope, as very important achievements have been reported, as far as module efficiency and manufacturing processes are concerned.

2.2. Wind Energy.

As regards wind energy, there is an organized national programme formed by public enterprises and industries coordinated by the Ministry for Industry where each one carries out specific roles. Till now activities are mainly aimed at carrying out anemological investigations in order to determine suitable sites for installing wind energy plants and experimenting wind generators having power up to several hundred kWs.

According to the anemological investigations some locations situated on the islands and along the coast appear to have interesting wind energy resources (average annual speed of wind being greater or equal to 5.5 m/s).

However, these values are far below the ones existing in other north European Countries.

As regards experiments on wind generators, over 20 prototypes whose size is between 3 and 40 kW are operating. Most of them are installed in ENEL's test zones at S. Caterina (Cagliari) and in ENEA's test areas at Casaccia (Rome).

In 1984 ENEL set up a wind power station in Sardinia formed by eight units having 50 kW each. Many modifications and improvements, that greatly affected the full operation of the plant, had to be carried out during the experimental stage of this power station.

A 225 kW MEDIT wind generator having a two blade rotor (with a 32 m diameter) implemented by ENEA is currently being experimented on the site of the power station.

As regards large-size units, an order has already been made for the purchase of GAMMA prototype (whose power ranges from 1 to 1.8 MW) that will be built by a Consortium headed by Aeritalia, and for a subsequent purchase of two pre-series machines after the prototype will have totalled 1,000 operating hours. This prototype will be constructed with a contribution of the EEC and is expected to start operating by 1990.

This project has innovative aspects compared to similar machinery already implemented, such as the following: variable speed, a control system for variable speed, power control linked to rotation of the shuttle compared to the direction of the wind.

In addition to the above described activities that tend to stimulate the construction of prototypes by Italian industry, the possibility of setting up a wind power station of ''wind farm'' is being examined. This power station should include tested machinery and have a unit power around 300 kW for a total power of 10 MW.

Taking into account the present knowledge about site availability, turbine characteristics, associated costs and restraints due to environment and to the electric grid management, Italy's wind potential is estimated to be 10 TWh, referred to 1.5 MW machinery and 5 TWh, referred tio 225 kW machinery.

The territorial commitment corresponding to this potential is enormous (1,000 km^2 equal to 1/300 of the whole national area).

Taking into account the above, the maximum contribution that can be expected from wind energy in Italy until the year 2000 appears to be quite limited and this is due to objective technological, economic and environmental ties.

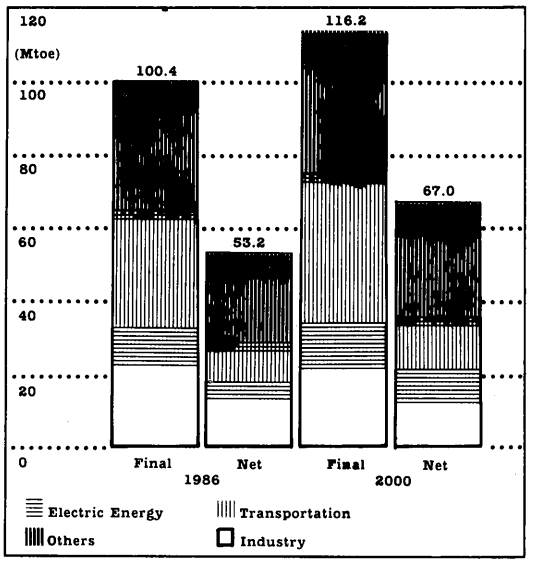

Fig. 1

ENERGY END USES IN 1986 AND FORECAST FOR THE YEAR 2000 (M toe) **TAB. 1**

	Agriculture	Industry	Transportation	Services	Residential	Total
1986						
Thermal uses	0.6	23.1	—	5.6	23.5	52.8 (53)
— Low temperature	0.6	2.7	—	5.3	21.8	30.4 (30)
— Medium temperature	—	3.9	—	0.3	1.7	5.9 (6)
— High temperature	—	16.5	—	—	—	16.5 (17)
Specific electric uses	**0.3**	**8.2**	**0.5**	**2.4**	**2.1**	**13.5 (13)**
Fuels	**1.7**	**0.8**	**31.6**	—	—	**34.1 (34)**
TOTAL	**2.6 (3)**	**32.1 (32)**	**32.1 (32)**	**8.0 (8)**	**25.6 (25)**	**100.4 (100)**
2000						
Thermal uses	**0.5**	**19.8**	—	**6.1**	**25.4**	**51.8 (45)**
— Low temperature	0.5	2.0	—	5.8	23.4	31.7 (28)
— Medium temperature	—	3.8	—	0.3	2.0	6.1 (5)
— High temperature	—	14.0	—	—	—	14.0 (12)
Specific electric uses	**0.5**	**11.7**	**0.7**	**4.8**	**3.7**	**21.4 (18)**
Fuels	**1.7**	**1.0**	**40.3**	—	—	**43.0 (37)**
TOTAL	**2.7 (2)**	**32.5 (28)**	**41.0 (35)**	**10.9 (10)**	**29.1 (25)**	**116.2 (100)**

NOTE: Percentages are in brackets

ENERGY-END-USE SHARES OF VARIOUS SECTORS AND ELECTRIC ENERGY PENETRATION

TAB. 2

	1975			1986			2000		
	Total Energy (Mtoe)	Electric Energy (Mtoe)	Electric Penetration (%)	Total Energy (Mtoe)	Electric Energy (Mtoe)	Electric Penetration (%)	Total Energy (Mtoe)	Electric Energy (Mtoe)	Electric Penetration (%)
Agriculture	2.3	0.1	6.2	2.6	0.3	11.5	2.7	0.5	18.5
Industry	37.6	6.6	17.6	32.1	8.2	25.5	32.5	11.7	36.0
Transportation	24.6	0.4	1.6	32.1	0.5	1.6	41.0	0.7	1.7
Services	6.1	1.3	21.3	8.0	2.6	32.5	10.9	5.0	45.9
Residential	24.0	2.4	10.0	25.6	3.9	15.2	29.1	6.4	22.0
TOTAL	**88.9**	**10.8**	**12.1**	**100.4**	**15.5**	**15.4**	**116.2**	**24.3**	**20.9**

COVERAGE OF ELECTRIC ENERGY NEEDS (TWh)

TAB. 3

Net production	1987	2000
Thermoelectric	145.6	250.8
Hydroelectric	42.1	59.5
Geothermoelectric	2.9	9.0
Nuclear	0.2	
Renewables	—	4.0
Total	190.8	323.3
Exchange with foreign countries	+23.1	—
Pumping consumption	-4.2	-8.3
Demand	**209.7**	**315.0**

ENEL GENERATING POWER PLANTS FOR THE COVERAGE OF 2000 ELECTRIC ENERGY NEEDS (MW)

TAB. 4

Plants	Coal and Oil	Nuclear	Turbogas	Geo	Hydro	Total
In service in 1987	28311	1120	1364	378	11876	43069
Under construction	8958	—	528	123	1956	11565
Repowering, combined and gas-turbines	1300	—	176	—	—	1476
Multifuel	11300	—	—	—	—	11300
Turbogas, Hydro, Geo not yet authorized	—	—	176	587	1841	2604
Decommissioned	-3710	-1120	-349	—	—	-5179
Total	46159	—	1915	1088	15673	64835

1987 TAB. 5
ITALIAN GOVERNEMENT BUDGET:

Energy RD + D: 1296 Million US$
New sources RD + D: 32.5 " "

Solar heating and cooling	:	15%
Photo electric	:	28%
Wind	:	23%
Biomass	:	26%
Geothermal	:	8%

MAIN CHARACTERISTICS OF DELPHOS FIRST SECTION **TAB. 6**

SOLAR ENERGY COLLECTION SYSTEM	a) fixed plant photovoltaic field
OPERATION	a) connected to the national electric network
	b) in connection with stand-alone users
PEAK POWER RATING	300 kW
VOLTAGE RATING	a) 800 V
	b) 660 V
NUMBER OF PHOTOVOLTAIC MODULES	5760
AREA OF PHOTOVOLTAIC FIELD	3917 m²
TILT ANGLE OF MODULES	20°

MAIN CHARACTERISTICS OF VULCANO PV PLANT **TAB. 7**

Rated power output of the array	80 kW
Rated battery voltage	260 V dc
Plant altitude	345 m o.s.l.
Tilt angle of the modules	38°
PV ARRAY	
• Area of PV arrays	1200 m²
• Total area covered by the PV field	appr. 4.000 m²
• Number of sub-arrays	2
• Encumbrance of each sub-array	85 x 25 m
Ansaldo modules: number	1.344
material	polycrystalline silicon
peak power	33,8 W
Pragma modules: number	672
material	single-crystalline silicon
peak power	58 W
INVERTERS	
Stand-alone operation	40 kVA (380 V, 3 ph, 50 Hz)
Grid-connected operation	140 kVA (20 kV, 3 ph, 50 Hz)
LEAD-ACID STORAGE BATTERY SYSTEM	
• Number of modules	130
• Total storage capacity	1.500 Ah
• Energy stored	400 kWh

OPTIMUM DESIGN OF EVAPORATORS FOR HEAT PUMPS WORKING AIR/AIR, (AIR+LIQUID)/AIR

Kemal Altinisik
Selcuk University,
Engineering Faculty, Konya, Turkey

ABSTRACT

In this study, the optimum design for evaporators of heat pumps, working air/air and (air + liquid)/air has been investigated. In calculation, in particular, the following objectives were considered:

a) The transfer of maximum heat from the minimum surface,
b) The minimum length, height and weight of evaporator,
c) The minimum cost price.

For the calculation of the evaporator the fouling of inner surfaces of pipes used in the evaporator design has been considered.

List of Symbols

Qc	Heat load of cold medium	kjh^{-1}
Ql	Heat load received from the liquid	"
Qa	Heat load received from the air	"
q	Amount of heat flowing from unit surface	kjm^{-2}
K	Coefficient of overall heat transfer	$W\,m^{-2}\,k^{-1}$
ΔTm	Temperature difference	K

A	Unit surface	m^2
Tl	Temperature of the liquid	^oC
Tr	Temperature of the refrigerant	^oC
Ta	Temperature of the air	^oC
Kl	Coefficient of overall heat transfer of the liquid-side	$W\ m^{-2}\ k^{-1}$
Ka	Coefficient of overall heat transfer of the air-side	"
kf	Thickness of the fin	m
α_a	Coefficient of surface film for the air-side	$W\ m^{-2}\ k^{-1}$
α_R	Coefficient of surface film for the refrigerant-side	"
n_{L-a}	Efficiency of surface for the air-side	
n_{R-a}	Efficiency of surface for the refrigerant-side	
GR	Mass flow of the refrigerant	$kg\ h^{-1}$
D	Diameter of the pipe	m
μ	Dynamic viscosity	$kg\ m^{-1}\ s^{-1}$
A_R	Surface area of the refrigerant-side	m^2
Gc	Mass flow of the air passing-from the unit surface per unit time	$kg\ m^{-2}\ s^{-1}$
A_a	Surface area of the air-side	m^2
A_s	Cross-section, which is vertical to the flow	m^2
A_m	Mean surface area of A_R and A_a	m^2

$\dot{G}_a$	Mass flow of the air	$kg\ h^{-1}$
λ	Thermal conductance	$W\ m^{-1}\ k^{-1}$
R_{R-i}	Thermal fouling resistance of the refrigerant	$m^2\ W^{-1}\ K$
R_{a-i}	Thermal fouling resistance of the air	"
V_t	Total volume	m^3
Z	Numbers of fins	
y	Distance between two fins	m

1. INTRODUCTION

It is well-known that heat pumps are not advantageous at low ambient temperatures. The heat is received by evaporators from the surroundings, so optimum design of evaporators are essential.

The evaporator used in this experiment consists of two pipes: one of the pipes, having a different diameter, is inserted into the other one. The liquid flows through inner pipes and the refrigerant flows between each of two pipes. The liquid, which consists of glycol, water and salt, is circulated in the exchanger, and exchanger is placed 1.2 m below surface of the ground.

2. CALCULATION OF THE EVAPORATOR SURFACE AREA

Figure 1 shows the design of the evaporator and Fig. 2 shows the cross-section of the evaporator. The heat received by the evaporator is given by the following equation:

$$Q_c = Q_l + Q_a \qquad (1)$$

As seen in Fig. 3 temperature gradient has to be known, so that the heat received by the evaporator can be calculated.

As shown in Fig. 4 the unit surface A, which is defined by the broken line is considered.

The heat flux from the unit surface A is as follows:

$$q = K \Delta T_m \tag{2}$$

Equation (2) can be rewritten in the following form:

$$q = \left(\frac{T_L - T_R}{1/K_L} + \frac{T_a - T_R}{1/K_a} \right) \tag{3}$$

In equation (3) the values of $1/K_L$ and $1/K_a$ should be known, for the extended surfaced exchanges. K_a is given by the following equation (1,2,3):

$$\frac{1}{K_a \cdot A} = \frac{1}{\alpha_a \cdot A_a \cdot \eta_{L-a}} + \frac{\Delta x}{\lambda A_m} + \frac{1}{\alpha_R A_R \eta_{L-R}} \tag{4}$$

In this equation if A is replaced by A_a the following equation is obtained:

$$\frac{1}{K_a} = \frac{1}{\alpha_a \cdot \eta_{L-a}} + \frac{X}{\lambda(A_m/A_a)} + \frac{1}{\alpha_R \eta_{L-R} \cdot (A_R/A_a)} \tag{5}$$

The thickness of the copper pipe may be neglected because, the resistance of the copper pipe is too small so the value of η_{L-R} can be assumed as 1. From this point the above equation can be restated by the following equation:

$$\frac{1}{K_a} = \frac{1}{\alpha_a \cdot \eta_{L-a}} + \frac{1}{\alpha_R \cdot (A_R/A_a)} \tag{6}$$

In order to calculate this equation, it is necessary to know the values on the right hand side of the equation. The refrigerant changes the phase in the horizontal pipe, so the coefficient of heat transfer (4) is:

$$\alpha_R = \frac{\lambda^2 M_R \cdot \Delta T}{d_{wet}} \qquad (7)$$

For the outside of the horizontal pipe, equation (8) can be written as follows (5):

$$\alpha = \frac{St.Pr^{2/3} \cdot G_c \cdot c_p}{\left(\frac{\mu c_p}{k}\right)^{2/3}} \qquad (8)$$

$St.Pr^{2/3}$ can be found by means of R_e number and the number of fins per cm. If R_e is considered for the metal plates and not the pipe, for the compressible liquids, R_{eL} is given by

$$R_{eL} = \frac{Gc \cdot D}{\mu} \qquad (9)$$

For the mass flow of the air, the following equation can be written:

$$m_a = G_c \cdot A_s \qquad (10)$$

The value of the massflow is either known or may be roughly estimated. After calculating the values of α_R and α_a, the calculation of the efficiency of the fins and the surface area of the fins can be obtained. For the efficiency of the fins, the following equation can be written (6):

$$\eta_f = \frac{\tanh (mr\ \Phi)}{m r\ \Phi} \qquad (11)$$

For Φ, the following equation is given:

$$\Phi = \left(\frac{Re}{D} - 1 \right) \left[1 - 0.35 \ln \left(\frac{Re}{D} \right) \right] \qquad (12)$$

and for (Re/D) given in equation (12), the following expression can be written:

$$\left(\frac{Re}{D} \right) = 1.27 \cdot \psi \cdot (\beta - 0.3)^{1/2} \qquad (13)$$

In order to calculate the value of β the following equations are written respectively. Figure 5 shows the design of pipes and its fins.

$$\beta = \frac{L_\ell}{M} \qquad (14)$$

$$M = \frac{X_a}{2} \qquad (15)$$

$$L = \frac{[(X_a/2)^2 + X_b{}^2]^{1/2}}{2} \qquad (16)$$

the ψ is given by

$$\psi = \frac{M}{D} \qquad (17)$$

Finally, for the value of m, the following equation can be used,

$$m = \frac{2 \cdot \alpha_a \cdot L_\ell}{k_f \cdot L_\ell \cdot y} = \left[\frac{2 \cdot \alpha_a}{k_f \cdot y} \right]^{1/2} \qquad (18)$$

Where, k_f is the thickness of the fins, which is attached to the pipe, y is the distance between each fin. After having calculated the value of n_f, the efficiency of the fin surface area was obtained by the following equation:

$$n_s = 1 - \frac{A_f}{A}(1 - n_f) \tag{19}$$

where, it was supposed that:

$$A = A_f + A_b \tag{20}$$

A_b is the surface area of the pipe

A_f is the extended fin surface area

If α is defined in the following form, that is:

$$\alpha = \frac{A_a}{V_t} \tag{21}$$

It is also necessary to know the value of A_R/A_a. For the calculation of A_R/V_t, equation (22) is used:

$$\frac{A_R}{V_t} = \frac{D_R \cdot \pi}{X_a \cdot X_b} \tag{22}$$

The same equation can be rewritten as follows (6):

$$\frac{A_R}{A_a} = \frac{A_R}{V_t} / \frac{A_a}{V_t} = \frac{\pi D_R}{X_a X_b \alpha} \qquad (23)$$

The value of Ka is the theoretical value, we also have to consider the fouling resistance, because the refrigerant flows in the pipe and the air flows over the pipe. The fouling can be expressed as follows:

$$\frac{1}{K_{a-i}} = \frac{1}{K_a} + (R_{R-i}) + (R_{a-i}) \qquad (24)$$

Where:

R_{R-i} is 0,0002 $m_2^2\ C^0\ W_{-1}^{-1}$

R_{a-i} is 0,0004 m $C^0\ W^{-1}$

K_{a-i} is the thermal resistance of the refrigerant (2).

As a result, the overall heat transfer coefficient between the refrigerant and the air can be calculated. In order to calculate the overall heat transfer coefficient between the liquid and the refrigerant, the following equation is utilized:

$$\frac{1}{K_L} = \frac{1}{\alpha R} + R + \frac{1}{\alpha L} \qquad (25)$$

For α_L the following equation can be used:

$$\alpha_L = \frac{Nu \cdot k}{D} \qquad (26)$$

For the flow in pipes and ducts, if R_e is > 2300 >

$$Nu_D = 0.023\ Re_D^{0.8} \cdot Pr^n \tag{27}$$

If Re is < 2300 the following equation is used:

$$Nu_D = 3.66 + \frac{0.668\ (D/L) \cdot Re_D \cdot P_r}{1 + 0.04\ [(D/L) \cdot Re_D\ P_r]^{2/3}} \tag{28}$$

In this calculation, the resistance of the pipe material has been neglected, because of its negligible value.

As shown in Fig. 4 for the surface of the liquid-side, the following equation can be defined respectively:

$$A_L = y \cdot \pi \cdot D \tag{29}$$

$$A_a = A_{plate} + A_L \tag{30}$$

Before designing the evaporator the amount of heat received from the heat source has to be known. For that reason, the following equation can be used:

$$A_{total} = \frac{Q\ cold}{q} \tag{31}$$

If Z is the number of fins, then Z can be expressed as:

$$Z = \frac{A\ tot}{A\ unit} \tag{32}$$

Assuming that, y is the distance between two fins, the total pipe length, can be written as follows:

$$L_t = y \cdot Z \tag{33}$$

It is important that the number of pipes should not exceed five or six rows, otherwise, the coefficient of heat transfer for the air-side, the

efficiency of the fins and the mass flow of the air may change [7].

3. CONCLUSION

The evaporator is an important part of a heat pump. Because of this, the optimum design of evaporator was the basis of this study of heat pump working air/air and (air+liquid)/air.

As shown in Fig. 2 the liquid flows through the inner pipe and the refrigerant flows between the two pipes. The liquid consists of glycol, salt and water. The liquid is circulated in an exchanger which is underground and its depth is about 1.2 m. Even if the system is run at low ambient temperature less than $0^{0}C$, the temperature of the liquid never drops less than $9^{0}C$. Thus, this system, especially for small houses, may be used during the heating period of the houses.

References

1. Suces, T., "Heat transfer", Simon and Schuster, Inc. New York, 1975.

2. Cornwell, K., "The Flow of Heat", U.N. Reinhold Co., Edinburg, 1977.

3. McQuiston, F.C., and Parker, J.D., "Heating, Ventilating and Air Conditioning, New York, 1982.

4. Reay, D.A., Mac Michale, D.B.A., "Heat Pumps, Design and Application", Pergamon Press, Oxford, 1979.

5. Kew, P.A., "Development in Vapour Compression Heat Pumps", ASI Heat Pumps Fundamentals, Espinho, Portugal, Dec. 1-12, 1980.

6. Holman, J.P., McGraw-Hill, Kogakusta Ltd, Tokyo, 1976.

7. Sontag, R.E., and Wan Wylen, G.S., "Fundamentals of Classical Thermodynamics", John Wiley and Sons, Inc., U.S.A., 1976.

8. Paikert, P., "Calculation and Optimization of Condensers and Evaporators for Heat Pumps", ASI Heat Pumps Fundamentals, Espinho, Portugal, Dec. 1-12, 1980.

9. Arora, C.D., "Refrigeration and Air Conditioning", Data McGraw-Hill Publishing Co. Ltd, New Delhi, 1983.

10. Stocker, W.F., "Refrigeration and Air Conditioning", McGraw-Hill Co., 1982.

11. Born, P., and B. Hapwanani, J., "Heat Pumps/Control Functions", Heat Productions, June, Part III, 1981.

12. Rinch, T., Bivalente Warme Pumpen - Heizung, Technischer Ausbau, Essen, W. Germany, 1982.

13. Cematini, E., and Kester, T., "Heat Pumps and their Contribution to Energy Conservation, Noordhoof, London, 1976.

14. Altinisik, K., and Altintop, N., "Thermodynamics Analysis of Heat Pumps", 8th Miami Int. Conf. on Alternative Energy Sources, Dec.14-16, 1987, U.S.A.

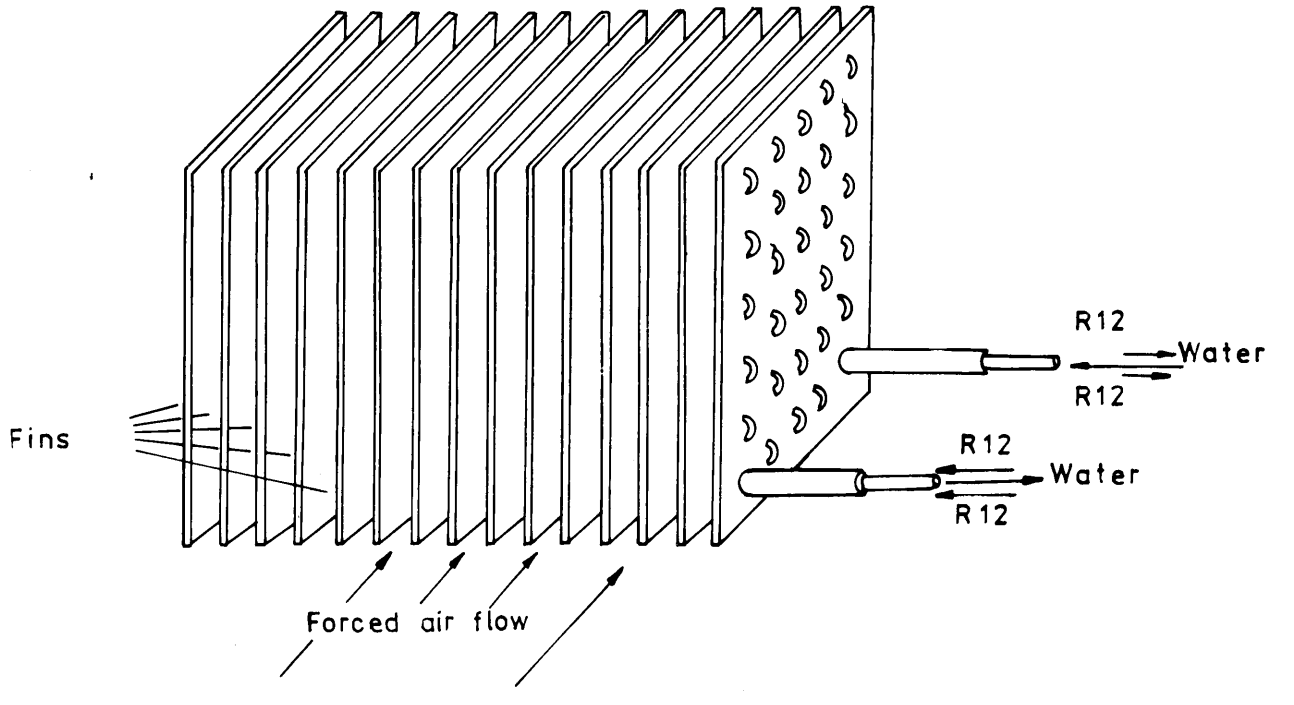

Figure 1. The View of evaporator used in experimental study

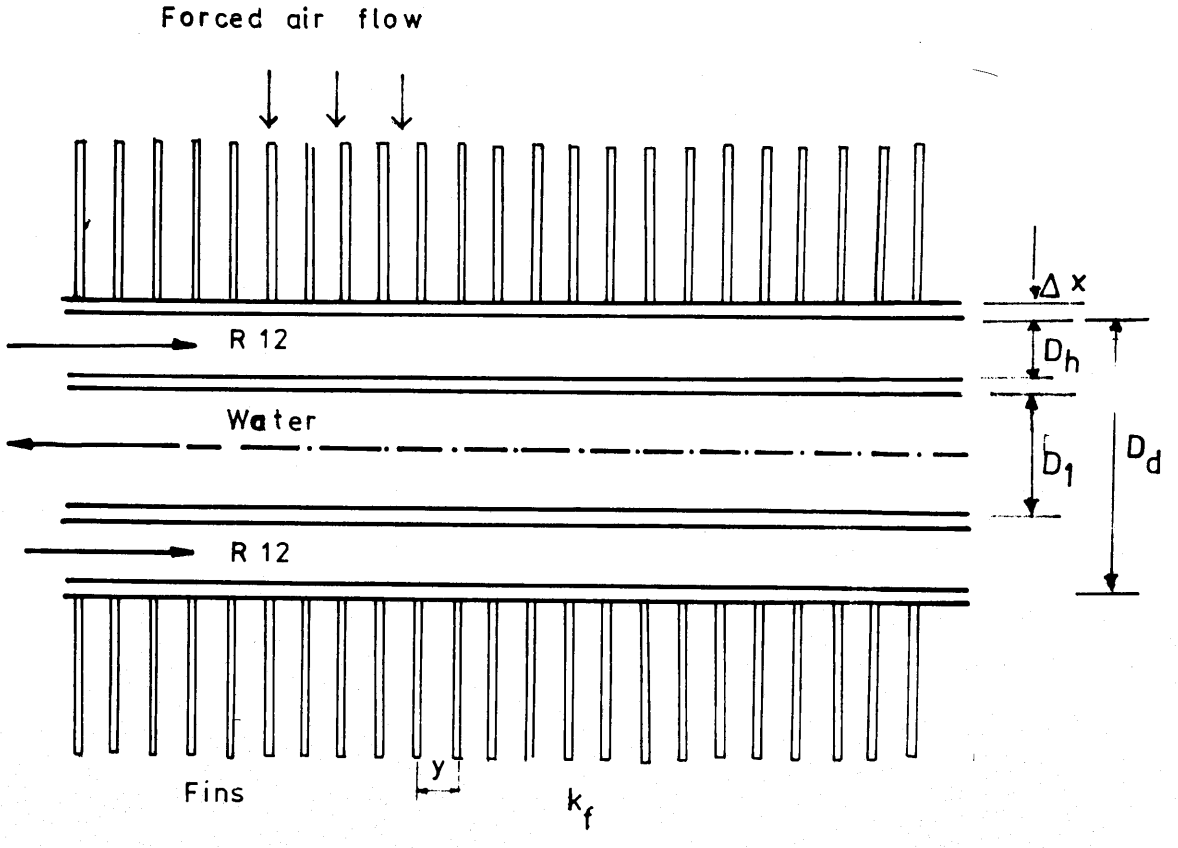

Figure 2. Cross-section area of evaporator

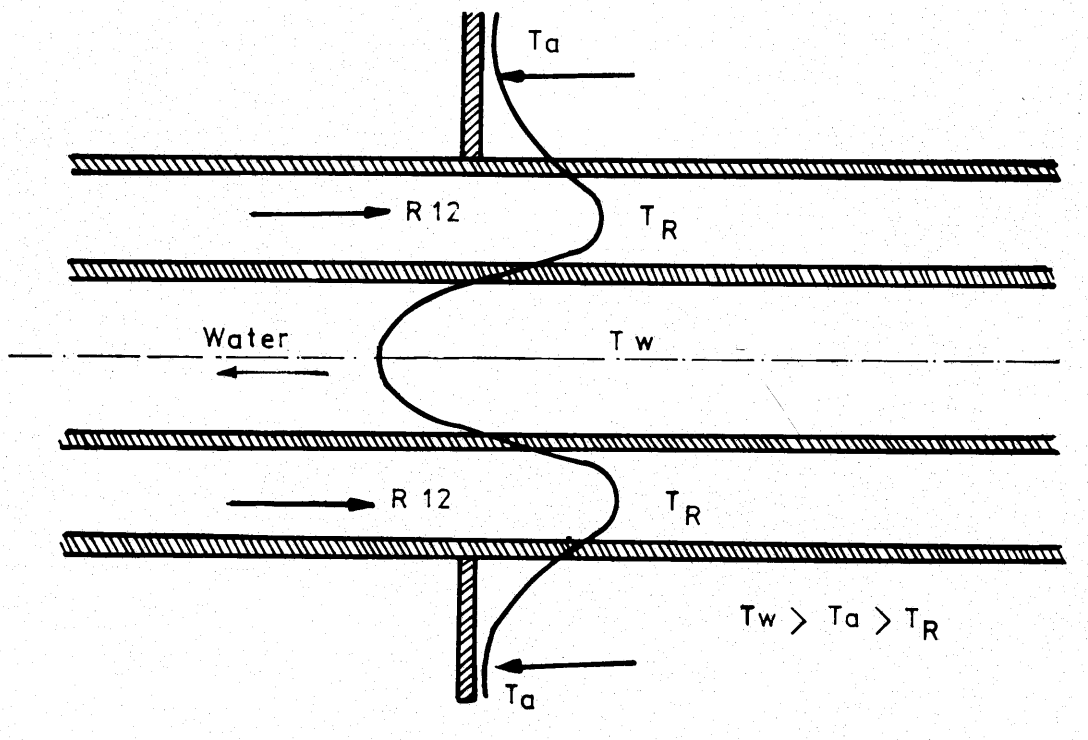

Figure 3. Temparature gradiant in the evaporator

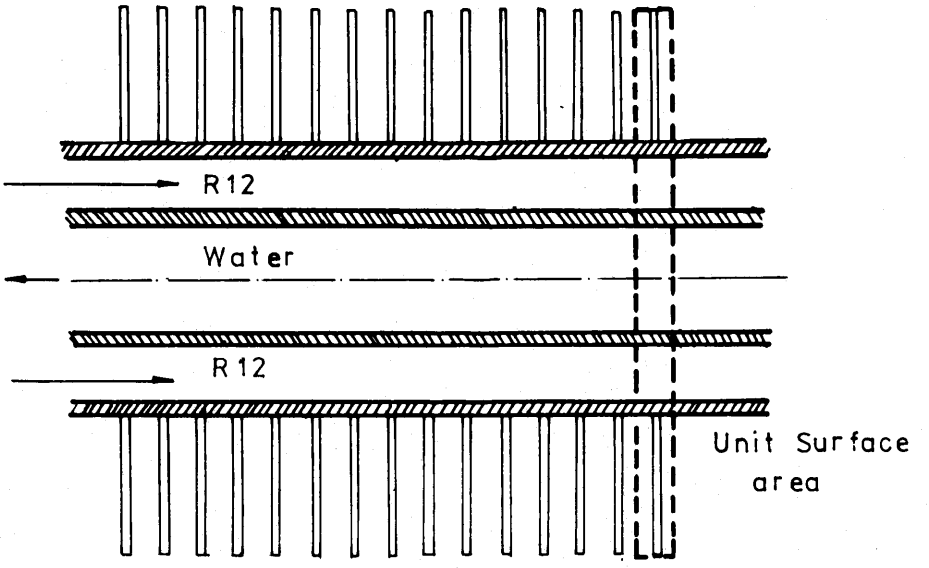

Figure 4. Unit surface area of evaporator for calculations

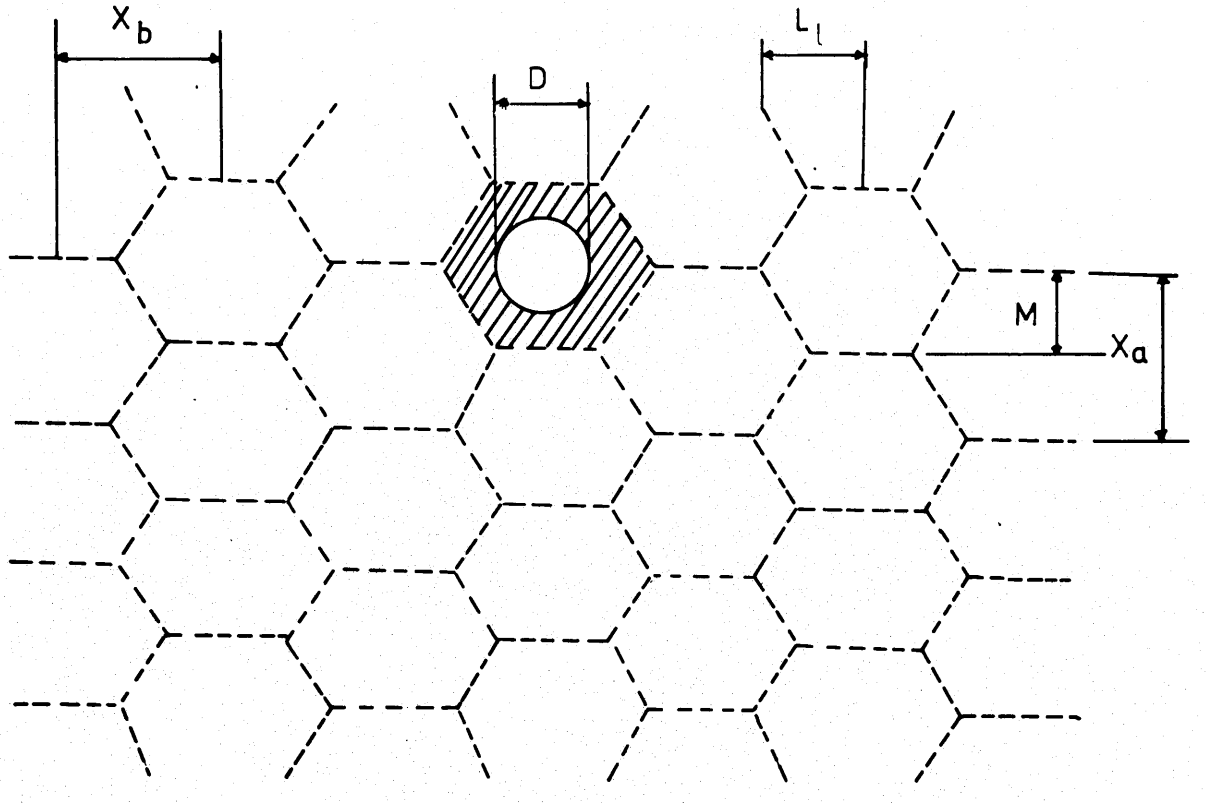

Figure 5. The design of pipes and its fins

SECTION IX

SOLAR COLLECTORS

MATHEMATICAL MODELLING AND EXPERIMENTAL EVALUATION OF AN NATURAL CONVECTION TYPE SOLAR CABINET DRYER

V.K.Sharma*, Sanjay Sharma and R.A.Ray

Centre of Energy Studies
Indian Institute of Technology
Hauz Khas, New Delhi - 110016
India

*Visiting scientist at ENEA-DIPARTIMENTO FARE,
21020 Ispra (Varese), ITALY

ABSTRACT

General objective of the investigation described in this research communication is to discuss the design methodology, performance studies and analytical solution of an cabinet-type solar dryer. Experimental results of different experiments conducted with different products, at New Delhi climate are included in this paper. The analytical solution is based on the principle of simultaneous heat and mass-transfer.

KEY WORDS

Solar drying, Moisture content, Air temperature, Fruits & vegetable drying.

1.0 INTRODUCTION

As an economically viable solar energy device, solar dryer seems to be the most promising way for preservation of various agricultural products such as foodgrains, fruits, vegetables, medical plants, etc. A great deal of experimental work over the last few years has already demonstrated that agricultural products can be satisfactorily dehydrated using solar energy. Various designs for small scale solar dryers have been proposed for their applications in developing countries, in the past [1-5] and still a good deal of work is going on in this direction. But still solar drying units are not readily available, commercially and those that are available are not

functioning properly. The non-uniform temperature distribution, no control over drying temperature, non availability of technical-know-how, etc. are some of the major problems associated with the drying phenomenon. In a controlled cabinet type drying process, the external parameters that affect the drying process are controlled carefully to provide the desired drying rate compatible with the attainment of the desired product quality. The authors in the present research papers presents an simple analytical model, experimental results and design methodology for an solar cabinet dryer in the conventional mode of operation.

2.0 THEORETICAL CONSIDERATION

When air at a particular temperature and relative humidity is used for drying, a part of the heat energy travels into the interior of the product, causing a rise in temperature and formation of water vapours whereas the remaining amount is utilized in the evaporation of the moisture from the surface. The moisture and the water vapour from the interior diffuses to the surface to replace the loss of moisture by evaporation. The analytical model discussed below is based on the principle of simultaneous heat and mass transfer at the product and includes the effects of relative humidity, wind speed, etc. The heat balance equation for the inside air temperature may be written as

$$(\alpha_p.\tau_g).I(t) = G_a.C_a \frac{\partial T_{ai}}{\partial x} + h_{ai}(T_{ai}-T_p) + \varrho p.h_{fg} \cdot \frac{\partial M}{\partial t} \quad \ldots (1)$$

whereas the heat balance equation for the product temperature to be dried may be written as

$$(\alpha_p \cdot \tau_g)\ I(t)+h_{ai}(T_{ai} - T_p) = (\varrho_p.C_f + \varrho_p.C_v.m)\frac{\partial T_p}{\partial t} \quad \ldots (2)$$

similarly the equations for the determination of the moisture content and humidity of air inside the dryer can be written as:

$$\frac{M - M_{eq}}{M_o - M_{eq}} = e^{-Kt} \quad \ldots\ldots\ldots (3)$$

and

$$G_a \frac{\partial W}{\partial x} = -\varrho_p \cdot \frac{\partial M}{\partial t} \quad \ldots\ldots\ldots\ldots (4)$$

The equations can be solved using Laplace technique with the conditions as T_{ai} (o,t) = T_{ai} (in), W(o,t) = W_{in} and T_p(x,o) = T_{po}, to obtain the expression for product temperature, air temperature inside the dryer, moisture content of the product in the dryer and air humidity ratio etc..

3.0 DESIGN CONSIDERATION

The designing of an solar energy dryer can be considered under two major headings namely (i) thermodynamical design considerations and (ii) mechanical design considerations. Thermodynamical details refers to all heat, mass and humidity calculations and fixes the major parameter such as (1) amount of water to be evaporated, (2) quantity of heat required, (3) mass of air needed and finally the volume of air needed for drying the product. Mechanical designs considerations on the other hand involves detailed studies regarding the area of absorber required, cabinet size, tray dimensions, depth of the material to be loaded, etc.. Local climatic conditions and geographical locations are others factors to be examined seriously, to make a solar dryer techno-economically feasible.

3.1 MOISTURE CONTENT

The amount of moisture in a product is designated on the basis of the weight of water and is usually expressed as a percentage. The initial and final moisture content in percentage for a wet basis can be calculated by dividing the weight of water present in the material by the total weight of the material using the relation

$$M.C.\% \text{ (wet basis)} = 100\ (W-d)/w \quad \ldots\ldots\ldots (5)$$

where w = mass of wet sample and d = mass of the dry material.

3.2 QUANTITY OF WATER TO BE REMOVED

The amount of water to be extracted from the material is calculated using the expression given below provided we know the initial and desired final moisture content of the product i.e.

$$m_w = W\ (M_i - M_f)\ /\ (100 - M_f) \quad \ldots\ldots\ldots\ldots\ (6)$$

where W = initial mass of sample and M_i, M_f = initial and final moisture content.

3.3 VOLUME OF AIR NEEDED FOR DRYING

The calculation of the volume of air needed for drying is possible either using psychrometric chart or by making use of energy balance equation. Knowing the amount of water to be extracted, specific latent heat of vaporisation, specific

heat capacity of air, etc.. we get the mass of air needed, by using the relation

$$m_w h_{fg} = (T_f - T_i)\, m_a\, C_p \quad \ldots\ldots\ldots\ldots (7)$$

where m_w = weight of water to be evaporated, m_a = weight of air to be circulated, h_{fg} = latent heat of evaporisation, C_p = specific heat of air and T_f, T_i = final and initial air temperatures. The corresponding volume of air can be calculated using the gas law as follows.

$$V_a/m_w = (m_a/m_w).RT/P \quad \ldots\ldots\ldots\ldots\ldots (8)$$

The procedure adapted to calculate the volume of air needed for drying few vegetables has already been discussed in earlier publication by the author [6].

3.4 AMOUNT OF HEAT REQUIRED

The removal of water from a surface requires an amount of heat equal to the latent heat of vaporization of water, plus a current of air moving past the surface to carry away the water vapour produced so:

Amount of heat required = amount of water to be extracted x specific latent heat of vaporization. .... (3.8')

3.5 AREA OF ABSORBER REQUIRED

The area required to collect sufficient energy to dry a given product can be determined by using the expression as follows:

$$Q = (\tau\alpha)_e \cdot I_{Tt} \cdot A \cdot \eta_{av} \quad \ldots\ldots\ldots\ldots (9)$$

where Q = amount of heat required as calculated in eqn. (3.8'), $(\tau\alpha)_e$ = effective transmittance-absorbstance product, I_{Tt} = quantity of solar radiation falling on the unit, A = area of the absorber required and η_{av} = average efficiency of the dryer.

4.0 DRYING EQUATION

The drying of product is essentially the rate of evaporation of water which may be written as

$$\frac{dm_w}{dt} = \frac{K_f . A}{h_{fg}} [T_{ai}(t) - T_a(x=o,t)] \quad \ldots\ldots\ldots (10)$$

or

$$\frac{dM}{dt} = \frac{I}{Wm} \frac{K_f . A}{h_{fg}} [T_{ai}(t) - T_a(x=o,t)] \quad \ldots\ldots\ldots (11)$$

This equation is applicable only during the first phase of the drying when the surface of the product behaves like water surface. However, in the falling rate period - the expression becomes as

$$\frac{dM}{dt} = -K (M - M_{eq}) \quad \ldots\ldots\ldots (12)$$

where K = thin layer drying constant

t = drying time

M_{eq} = Equilibrium moisture content

solution of the above equation yield

$$\frac{M - M_{eq}}{M_o - M_{eq}} = \exp(-Kt)$$

or

$$t = \frac{I}{K} \log e \left(\frac{M - M_{eq}}{M_o - M_{eq}} \right) \quad \ldots\ldots\ldots (13)$$

5.0 EXPERIMENT

A cabinet-type solar dryer designed & fabricated at IIT Delhi was experimented at IIT Delhi in winter season. The dryer consists of an quadrilateral shaped cabinet, trays for the product and single layered transparent glass at the top. The observation of solar intensity, inlet and outlet air temperatures, instantaneous weight of the product under experimentation, etc.. were recorded at a regular interval of an hour. Precaution was taken for the free passage of air through the product to ensure uniform drying.

6.0 RESULTS AND DISCUSSION

No device is useful unless it is economically viable. A major question regarding solar energy devices is whether these are cost effective. The economic feasibility of these devices, however, depends on the optimization of the trade-off between their performance under specified design

conditions and low material and fabrication cost. Keeping this point in view attempts have been made to fabricate the experimental set up under investigation in such a way that in actual field installation the same can be fabricated out of readily available and indigenous materials. The present study is an attempt towards this goal. The analytical model suggested and the various design steps described in the paper can be used to design and evaluate the performance of the drying unit, without much difficulty. Based upon the calculation, a solar cabinet type dryer shown in Fig.1 was fabricated at IIT Delhi. A series of experiments were conducted and the results obtained are included here to discuss about the system's applicability. The solar dryer was tested in the winter season. Figure 2 shows the variation of the meteorological parameters like ambient temperature and solar intensity along with the exit air temperature of the solar dryer as a function of time of the day and with & without load conditions. From the graph we see that as the day progresses the outlet air temperature rises, peaks at noon and then decreases in the afternoon. Also the air temperature remains always higher in no load operation than the case when the dryer was operated with load. Here also the air temperature inside the dryer is a function of the product to be dried, environmental conditions and the load in the dryer. The performance of solar dryer while loaded with different vegetables is presented in Figs. 3-5. The graphs shows the amount of water lost per unit time as a function of drying period in hours. It is evident from the figures that the drying in the first few hours is very rapid. This is because of the fact that the surface of the product behaves like a water surface and hence drying occurs under constant rate period. However, after that the drying occurs under a falling rate period & hence the drying rate is considerably lower. Apart from the initial moisture content of the product, thickness also plays a major role in determining the drying rate. It has also been observed experimentally that the products dried in solar cabinet dryer are of much superior quality and can be preserved for longer duration as compared to open sun drying. It is therefore concluded that the solar cabinet dryer described in this communication can be used successfully for drying a variety of agricultural products, especially, fruits and vegetables, to prevent spoilage and retaining nutritional value of the material.

REFERENCES

[1] Buelow, F.H., U.N. Conference, New Sources of Energy, 5, 267 (1964).

[2] Kapoor, S.G. and Agarwal, H.C. Proceedings International Congress, The Sun in the Service of Mankind, Paris, vol.29 (1973).

[3] Exell R.H.B., Sun World, 4, 186 (1980).

[4] Bansal, P.K. and Kaushika, N.D. Energy Convers. And Mgmt., Vol.21, pp.81 (1981).

[5] Vanarsdell, W.B. et al., Food Dehydration, Vol.1, Drying, Methods and Phenomena, AV1, Westport, Conn. (1975).

[6] SHARMA, V.K. et al., Design and Performance Studies of a Solar Dryer Suitable for Rural Applications, Energy Convers.Mgmt., Vol. 26 (1), pp. 111-119 (1986).

ACKNOWLEDGEMENT

One of the authors (VKS) is grateful to ENEA and ICTP for the financial support and also wishes to thank G.Rizzi and G.De Giorgi for timely help.

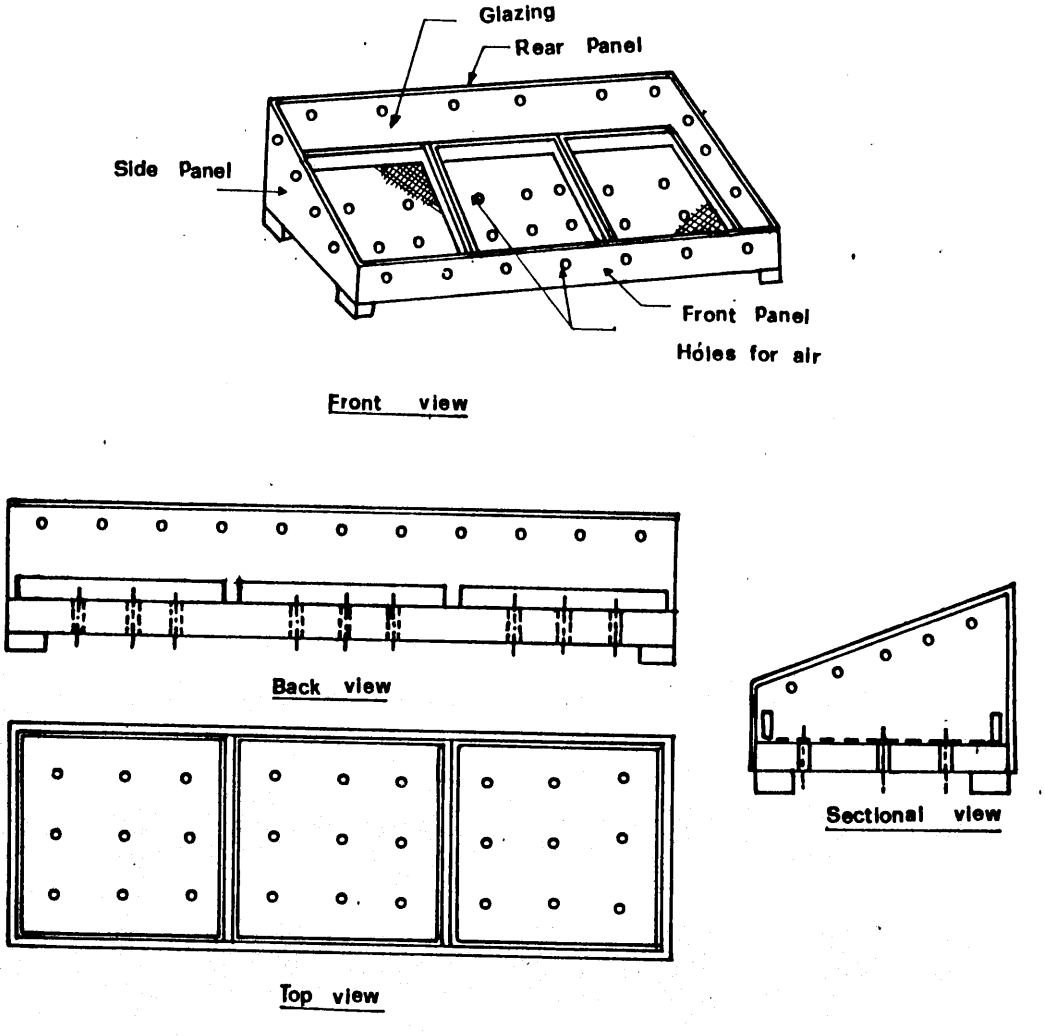

FIG.1 Sectional view of cabinet dryer

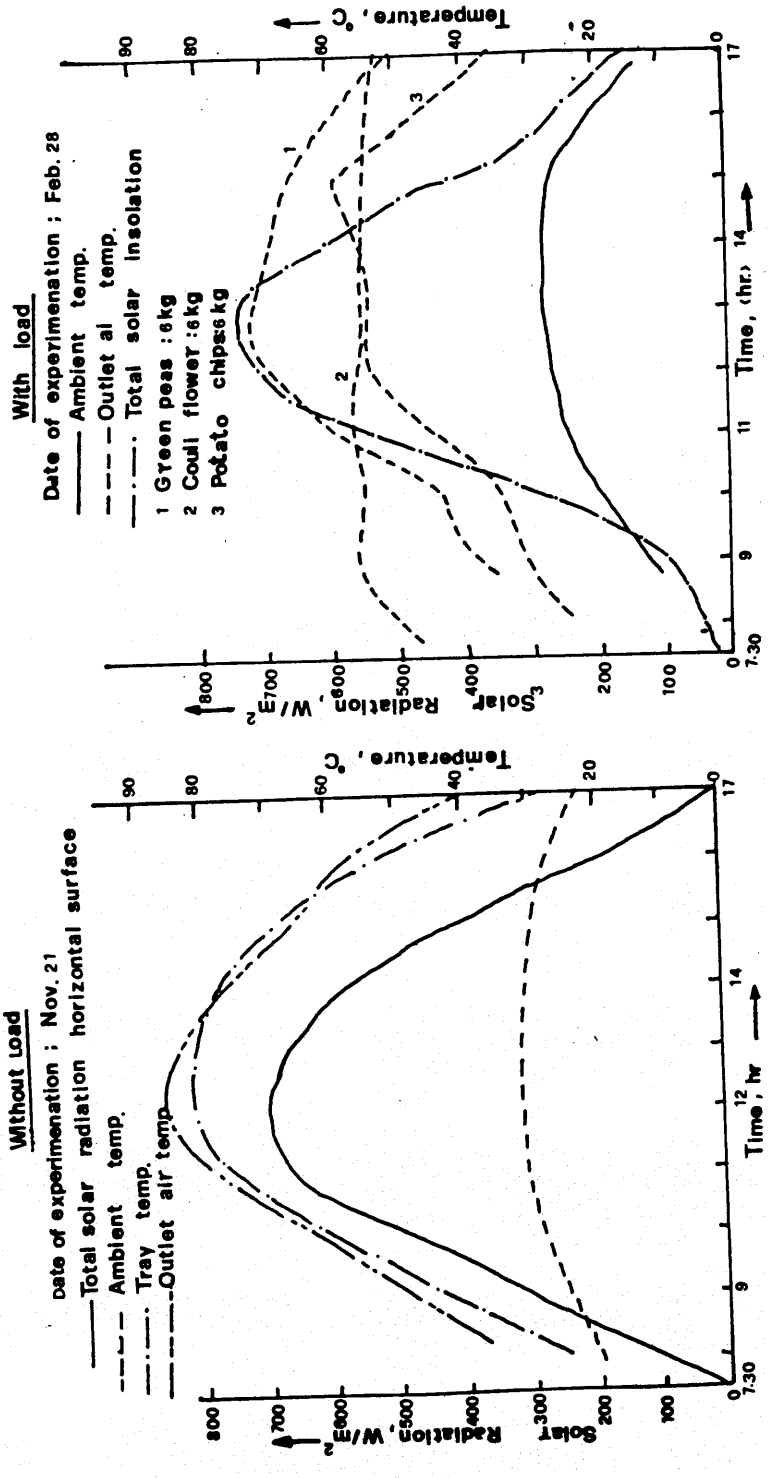

FIG. 2 DIURNAL CURVES FOR SOLAR CABINET DRYER

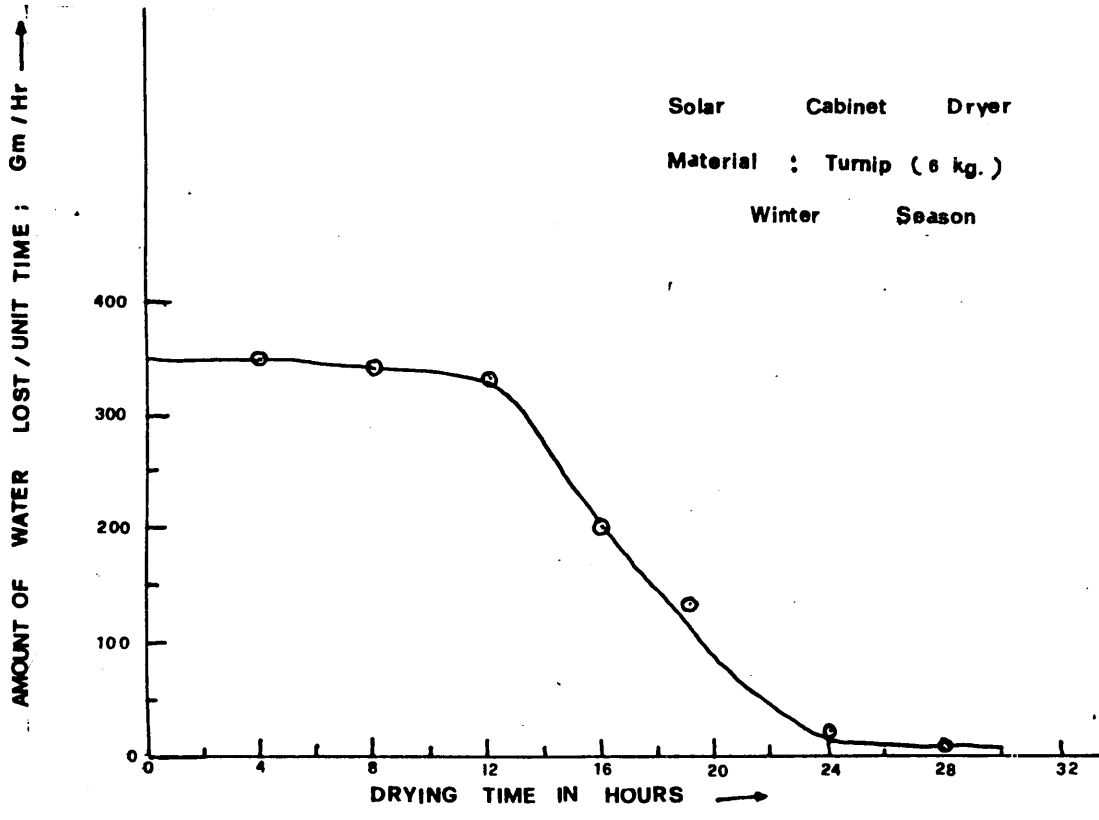

FIG. 3 DRYING CURVE FOR TURNIP

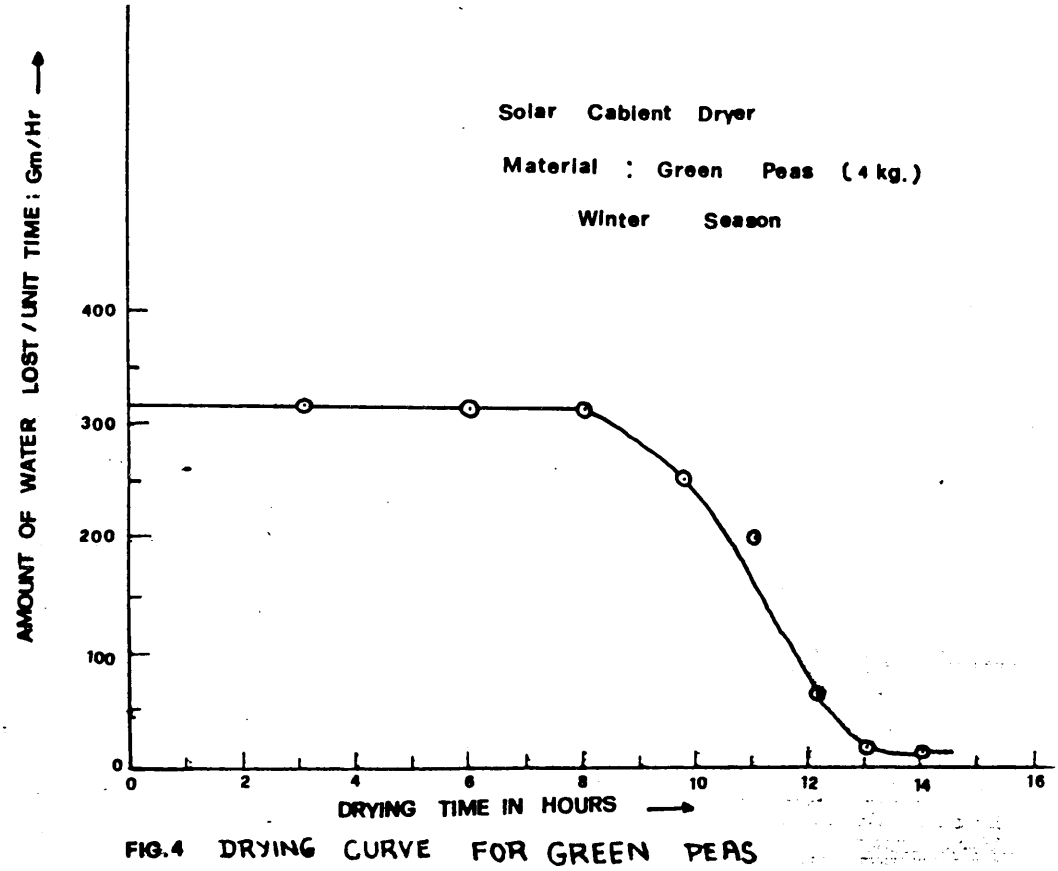

FIG. 4 DRYING CURVE FOR GREEN PEAS

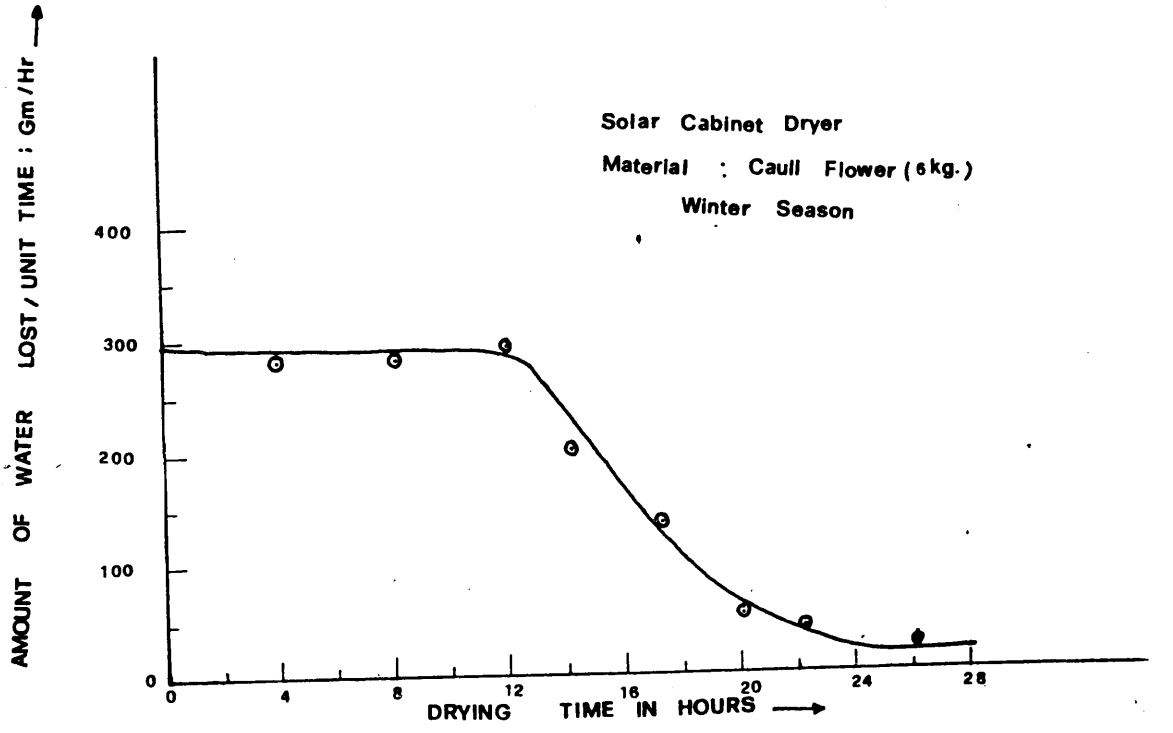

FIG. 5 DRYING CURVE FOR CAULI FLOWER

COMPARATIVE STUDY OF EXPERIMENTAL PERFORMANCE OF A PLASTIC FLAT-PLATE SOLAR COLLECTOR USING WATER AS THE HEATING FLUID.

N. KASBADJI and M. MERZOUK
HCR/CDER, route de l'observatoire, BP 62, Bouzareah
Alger, ALGERIE

ABSTRACT

A flat-plate solar collector using plastic material has been tested in outdoor conditions following ASHRAE standard completed by European recommendations. Comparing with a plastic flat-plate collector using glass cover, the difference can be neglected when using polycarbonate or glass as a cover. Comparaison has been made with a Al-Cu flat-plate collector in the range of domestic applications, it can be said that the plastic flat-plate collector represents an acceptable solution in this case.

NOMENCLATURE

I_g : solar radiation, W/m^2
m : mass flow rate, Kg/s
T_a : ambient temperature, K
T_i : inlet fluid temperature, K
V : wind velocity, m/s
X : $(T_i - T_a) / I_g$, $K\ m^2 / W$
η : instantaneous efficiency of the collector
η_p : instantaneous efficiency of the plastic flat-plate collector
η_a : instantaneous efficiency of the Al-Cu flat-plate collector

1. INTRODUCTION

Nowadays, economical crisis and the important fall of oil prices have caused research in the field of renewable energy in general to be confronted to numerous economical problems, which led to the situation where the majority of projects have been given up.
However, this could be avoided by reducing extra cost introduced in the capital investment of a solar or renewable energy installation in general.
In this concept, the use of flat-plate solar collectors to satisfy domestic needs of hot water, can represent an interesting solution.
The object of the present paper is to confirm this assumption, from experimental results obtained with a flat-plate solar collector made fully of plastic. These results are compared to those obtained with a classical flat-plate collector.

For the rest of the text, the two collectors will be respectively called "Plastic" and "Al-Cu".

2. DESCRIPTION OF BOTH COLLECTORS

Fig. 1 and 2 show schematic presentation of both collectors. Adding to the difference in dimensions and materials, the two collectors also differ by the design of their respective absorbers.
In the case of the Plastic collector, the absorber is composed of a double serpentine made of black polypropylene [2], whereas in the case of Al-Cu collector, the absorber is composed of a black aluminium sheet and copper tube water solar heater [3]. See all thermophysical characteristics of both collectors in table 1.

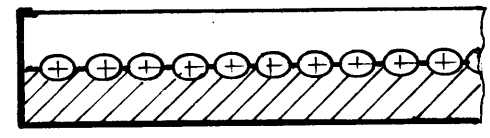

Fig. 1a : Schematic view of the Plastic collector.

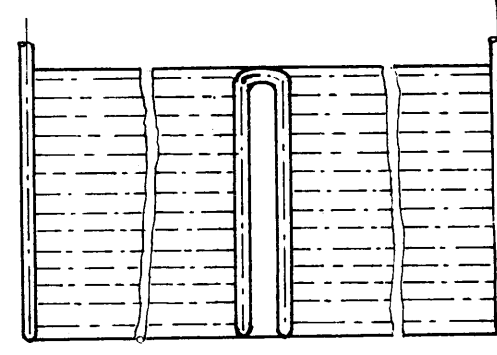

Fig 1b : Schematic design of the Plastic absorber.

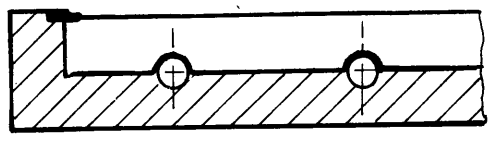

Fig 2 : Schematic view of the Al-Cu collector.

Table 1. Thermophysical caracteristics of the two collectors

Designation		Plastic collector	Al-Cu collector
Dimensions	(m)	.35 x 1.7	.92 x 1.80
Gross area	(m^2)	.6	1.70
Cover		Polycarbonate (or glass)	Glass
Cover thickness	(mm)	5	5
Absorber		Polypropylene	Aluminium
Tubes		Polypropylene	Copper
Insulation		Polyurethane	Polyurethane
Edge insulation thickness	(mm)	———	30
Back insulation thickness	(mm)	25	30
Box		Glass resin	Aluminium-Steel
Maximal temperature	(C)	75	———

3. TEST METHODS

3.1 Testing Loops

The Plastic collector (in both versions) has been tested with the aid of a test bench of a closed loop, having a control and regulation system. Operation of the installation, acquisition processing and storage of data are fully automatic [4], see schematic drawing in fig. 3.
The Al-Cu collector has been tested with the aid of an open loop made at the CDER [5], see fig. 4. It is composed of :
- a storage tank to preheat the working fluid using an electrical resistance

- an open tank, used to supply the collector with the fluid at constant flow rate
- and a circulator supplying the open tank from the preheat tank.

Acquisition of data is performed using potentiometric recorder, (with discontinous tracing for the different temperatures and a continous tracing for data of the difference in temperature of inlet-outlet and global solar radiation).

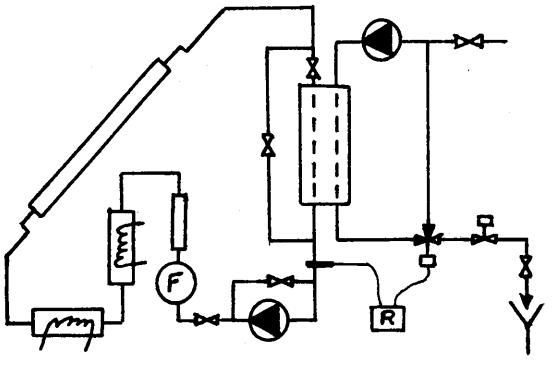

Fig. 3 : Closed testing loop

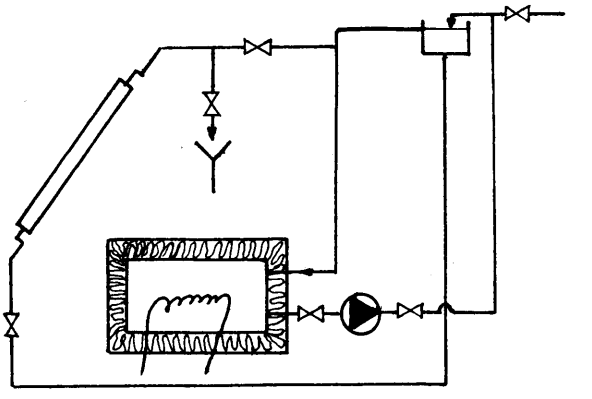

Fig. 4 : Open testing loop

3.2 Experimental Conditions

Experimental tests have been performed followed ASHRAE standard [6], completed by European Recommendations, [7] made for the same matter. Experimental conditions recorded while performing tests relative to the three flat-plate solar collectors [2], [8], are reported in Table 2.

Table 2. : Experimental conditions variation range.

Parameter		Plastic	Plastic (glass)	Al-Cu
I_g	(W/m^2)	780 to 897	685 to 830	830 to 1040
$\dot{m}^g$	(kg/s)	.0119 to .0166	.0106 to .0156	.01 to .02
V	(m/s)	.9 to 3.	.1 to 3.6	.2 to 2.5
T_a	(°C)	28 to 34	31 to 37	30 to 40

4. RESULTS AND DISCUSSION

4.1 Plastic Cover Effect

Figure 5 shows experimental points with curves representing the evolution of the instantaneous efficiency of the Plastic collector as function of X depending whether the cover is in glass or polycarbonate.
Both curves practically coinciding which leads to say that polycarbonate represents an excellent solution, because of its price and the glass being too fragile (the problem of operational life is largely compensated by this last criterium).

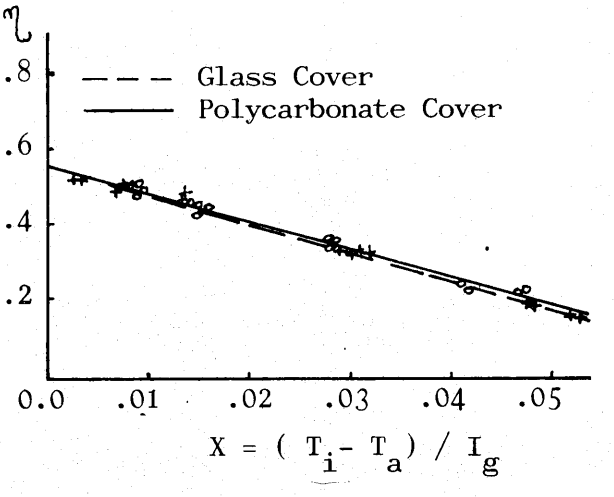

Fig. 5: Instantaneous efficiencies of Plastic using glass or polycarbonate as a cover.

4.2 Operating Conditions

For the purpose of a solar installation destinated to satisfy at a very low cost domestic needs, supplying hot water at temperature approaching 50 to 60 °C is certainly a reasonable choice. Also, considering the average ambient temperature of Algiers [9], varying between 15 to 35 °C, during operational periods of the collector and for a solar radiation of 800 to 900 W/m^2, an operational range (relative to variable X=(Ti-Ta)/Ig) lying between .02 and .04 K m^2/W is obtained.

4.3 Efficiencies Comparaison

Experimental data and curves representing the respective evolution of instantaneous efficiencies of Al-Cu and Plastic collectors in function of X are shown in figure 6.
By noting the operational range in figure 6., (hatched region), we can notice a difference of 20 to 30% between respective efficiencies of both collectors (see table 3).
The use of a polycarbonate cover (instead of a glass cover) having a small effect on the Plastic collector efficiencies recorded differences can only be justified by differences in :
- absorber (material)
- insulation (thickness)

table 3. : Collector efficiencies Plastic and Al-Cu to limits of domestic range

X	η_p	η_a	$\frac{\eta_a-\eta_p}{\eta_a}$
.02	.4	.5	.20
.04	.27	.38	.29

And because of the limited influence of material conductivity (see figure 7) on the instantaneous efficiency of flat-plate solar collector [10], a small increase in thickness at the insulation (particulary lateral) will lead, at a small cost, to a better improvment in the performance of Plastic collector

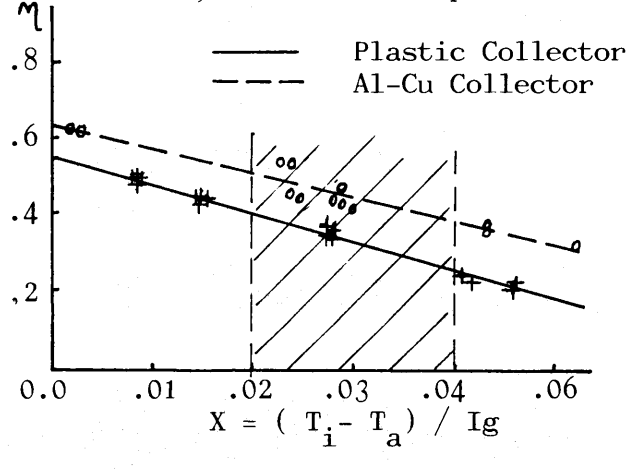

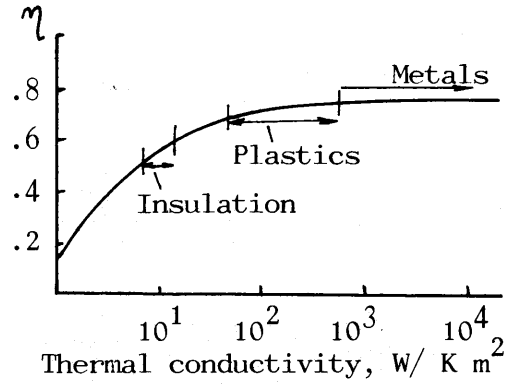

5. CONCLUSION

Although, the choice of the operational range to satisfy hot water needs by using solar collectors can always be a subject of discussion, it still represents a good approach at least for the site under consideration.
In this range, the Plastic collector is, in the worst case and without the recommended improvment, 30% less efficient than a conventional collector. This deficit is largely compensated by the difference in the cost.
In effect, and despite the lack of capital cost study, it is evident that the price of a square meter of a collector can easily double or even triple from Plastic to Al-Cu, bearing in mind, not only the difference in material cost, but also and above all production methods (Plastic is produced with

minimum operation and machinery).

REFERENCES

[1]- Duffie, J. A. and W. A. Beckman, Solar Engeneering of Thermal Processes Willey and sons, New York, 1980.
[2]- Kasbadji, N., Etude Theorique et Experimentale des Performances Instantanees de Trois Capteurs Solaires Plan a Eau, Thesis, CDER, Alger 1986.
[3]- Menasseri, K., Etude Experimentale des Performances d'un Chauffe-Eau Solaire, Final year engineer's project, ENITA-SEES, Alger, 1986.
[4]- Grinzato, E. and R. Lazzarin, "La prova dei collectori solari a tubi evacuati", Energia Alternativa Hte, 5-14, Italy, 1986.
[5]- Merzouk, M. and N. Kasbadji, "Banc d'essai capteurs plans en boucle ouverte", Internal repport, CDER, Alger, December 1987.
[6]- ASHRAE, Standard Commitees, ASHRAE Standard 93-77, Methods for Testing to Determinate the Thermal Performance of Solar Collectors, USA, 1977.
[7]- Commission of the European Communities, Recommendations of European Solar Collectors Test Methods, Derrick A. and W. B. Gillet, 1980.
[8]- Kasbadji, N. and M. Merzouk, "Capteur solaire plan Premier", Internal Technical Repport, CDER, Alger, December, 1987.
[9]- ONM, Recueil de donnees Climatologique, Alger, 1970.
[10]-O'brien-Bernini, F. C. and J. G. McGowan, "Performance modelling of non metallic flat-plate collectors", Solar Energy, 3/4, 305-319, 1981.

SECTION X

PHOTOVOLTAIC

STUDIES ON ELECTROLYTE SEMICONDUCTOR JUNCTION SOLAR CELLS

M. SALEEM

DEPARTMENT OF PHYSICS, NAGPUR UNIVERSITY, NAGPUR, INDIA.

ABSTRACT :

A photo-electrochemical solar cell (PESC) is a semiconductor-electrolyte interface. The charge transfer takes place at this interface resulting in a band bending. This paper seeks to report the characteristics of some semiconductor-electrolyte junction solar cells developed by chemical bath deposition technique. The CdS photo-electrochemical solar cells with varying concentration of PbS in CdS are prepared with intention to bring down the band gap of deposited $Cd_xPb_{1-x}S$ films to increase the efficiency. The best efficiency has been found for solar cell with 0.0005M $Pb(NO_3)_2$ doped in CdS.

1. INTRODUCTION :

Solar energy conversion devices have recently renewed interest due to the likely energy crisis. The total solar radiation is spread in the visible/U V region (51%) and I.R. region (49%). Various solar thermal devices like solar heating and cooling systems, drying units etc use the infrared part of the radiation. Many scientists have worked on solar energy conversion by photo-voltaic solar cell using visible/U V part of the solar spectrum [1-6]. These devices essentially use p - n junctions between similar and dissimilar semiconductors known as homojunction and heterojunction solar cells respectively. Gerischer [7] and Ellis et al [8] demonstrated direct conversion of solar energy into electrical energy using a semiconductor--electrolyte interface. These cells are known as electrochemical "photo--voltaic cells" or "wet photo-voltaic cells". In general, the solar cells based on semiconductor - electrolyte interface are termed as "photo-electro--chemical solar cells" (PESC). In PESC the junction is between a semiconductor and an electrolyte. The photo induced charge transfer at the semiconductor - electrolyte interface is responsible for the photocurrent and photo-voltage [9]. This cell has advantages of easy fabrication, the possibility of solar energy storage [10] and low cost.

In this CdS photo-electrochemical solar cells with varying concentration of PbS in CdS are prepared by chemical bath deposition technique [11-14] The band gap of CdS is 2.4 eV while the optimum bandgap for the maximum

efficiency is $\sim$ 1.6 eV. As such PbS (bandgap = 0.3 eV) of varying concentration is incorporated to bring down the bandgap and satisfactory results are found. It has been observed that various compounds with composition $Cd_xPb_{1-x}S$ for different values of x differ in bandgap. The bandgap has been measured by optical absorption studies. It has been demonstrated that efficiency of CdS photo-electrochemical solar cells can be improved by alloying PbS into CdS.

2. EXPERIMENTAL :

CdS and $Cd_xPb_{1-x}S$ films were deposited on conducting glass substrates by chemical bath deposition technique. The experimental arrangement is shown in figure 1. The reaction cell was an ammonical solution of

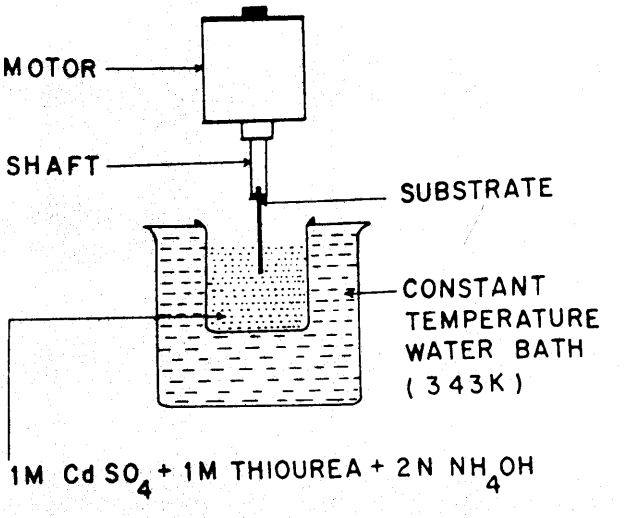

Fig.1 Schematic diagram of Chemical bath deposition arrangement.

1M $CdSO_4 8/3\ H_2O$(5ml), 1M $CS(NH_2)_2$ (5ml), 2N NH_4OH(10ml) for CdS film and 0.00001M, 0.00005M, 0.0001M, 0.0005M, 0.001M, 0.005M, 0.01M $Pb(NO_3)_2$ solution was added every time before adding NH_4OH in above solution for preparing PbS doped films of CdS. The temperature of the solution was kept at 343K throughout the film preparation. The conducting glass plate was suspended from a shaft (dipped in solution) which was being rotated by a motor with the speed of N200 r.p.m. for 30 minutes for each film. The freshly grown film was thoroughly washed by water jets, dried and kept in dissicater.

Optical absorption spectra of all the films was taken at 303K using a Hitachi spectrophotometer.

To study J-V characteristics of the solar cells the current and voltage obtainable from each cell at different loads and without load were measured under illumination, 55 mW/cm^2, by dipping the film in sulphur/sulphide redox couple (S^{2-}/S_2^{2-}) as shown in figure 2.

3. RESULTS AND DISCUSSION :

Figure 3 shows optical absorption spectra of all the samples. It is clear that there is a shift of absorption towards higher wavelength side due to PbS-doping. The dependence of absorption coefficient, α, on the photon energy can be expressed as :

$$\alpha = \frac{h\,(E - E_g)^n}{E} \qquad \ldots\ldots\ldots\ldots\ldots\ldots \quad (1)$$

where A, E and E_g are a constant, photon energy and bandgap respectively.

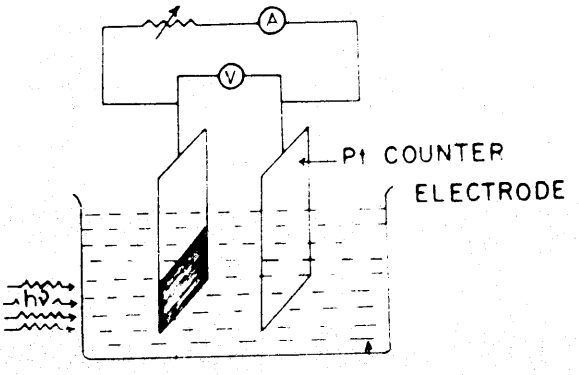

Fig.2

The experimental arrangement for studying J-V Characteristics of the interface of PESC.

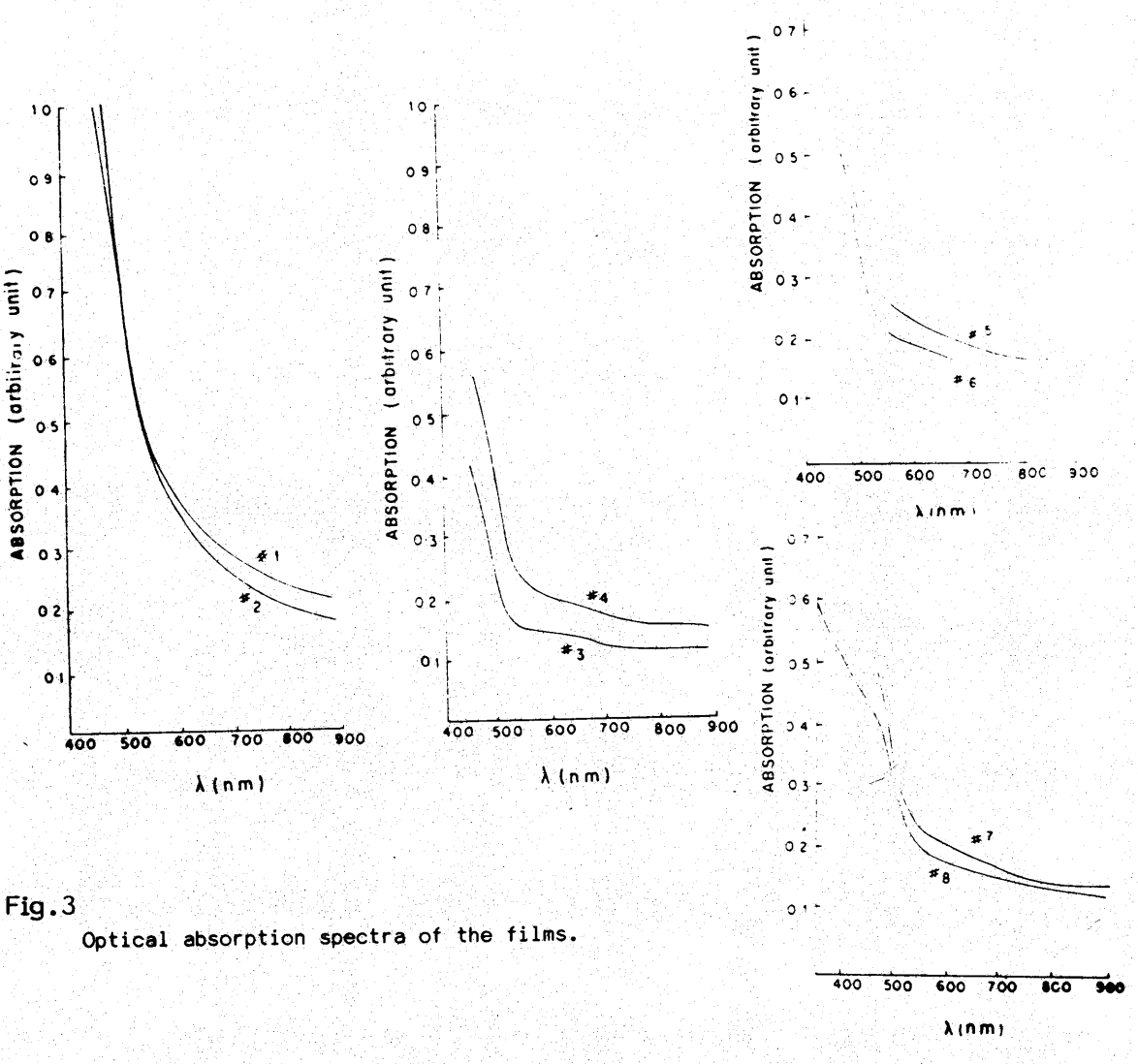

Fig.3

Optical absorption spectra of the films.

For direct bandgap materials n = $\frac{1}{2}$. As CdS is a direct bandgap material a plot of α^2 Vs E or λ would yield a straight line which gives the value of bandgap by extrapolating to zero absorption. These graphs are plotted for all the films and bandgap is determined (see table 1).

TABLE 1

Photo-electrochemical solar cell parameters for CdS and $Cd_xPb_{1-x}S$ films.

PESC No.	Composition $Cd_xPb_{1-x}S$ forming chemical bath.		Band gap eV	Solar cell behaviour			
	$CdSO_4$	$Pb(NO_3)_2$		Voc m Volt	Jsc mA/cm^2	η	Fill factor
#1	1M	0.01M	1.77	580	0.152	0.07	0.436
#2	1M	0.005M	1.65	575	0.146	0.07	0.436
#3	1M	0.001M	1.77	570	0.121	0.05	0.422
#4	1M	0.0005M	1.91	595	0.246	0.11	0.418
#5	1M	0.0001M	1.97	600	0.142	0.06	0.413
#6	1M	0.00005M	2.0	590	0.189	0.08	0.378
#7	1M	0.00001M	2.07	580	0.155	0.06	0.417
#8	1M	0.0M	2.30	555	0.141	0.05	0.36

Figure 4 shows the plot for samples #2, #4 and #8.

J-V characteristics of photo-electrochemical cell are drawn for different solar cells when illuminated with a light intensity of 55 mW·cm^{-2} (figure5). The efficiency and fill factor of each cell is calculated from the graph (see table).

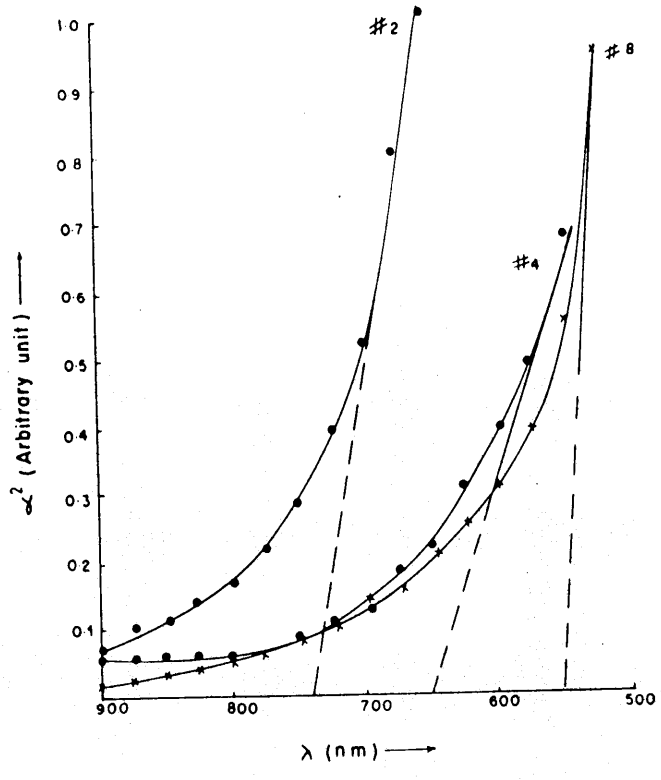

Fig.4

A plot of (absorption coefficient)^2 Vs photon wavelength.

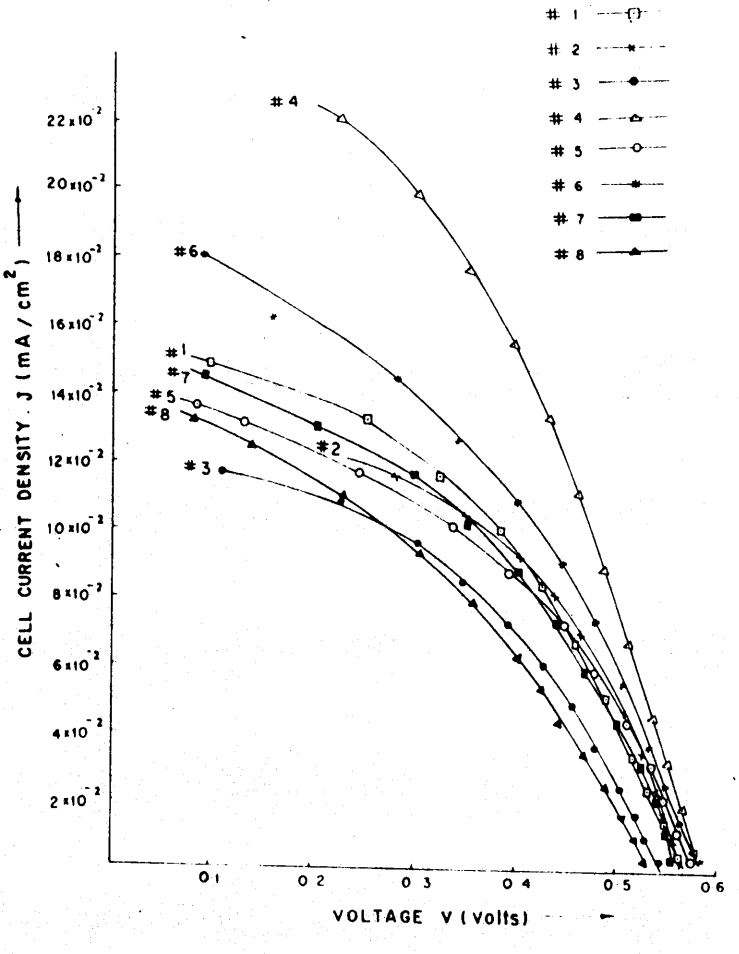

Fig.5

J-V characteristics of PESC under illumination (55 mW cm^{-2})

It is obvious from the above results that band gap decreases with increase in doping concentration. The minimum bandgap, 1.65eV, is found for sample #2 with doping concentration 0.005M. This sample has efficiency 0.07. The experimentally found efficiencies of different bandgap solar cells are in agreement with the predicted conversion efficiency of PESC with

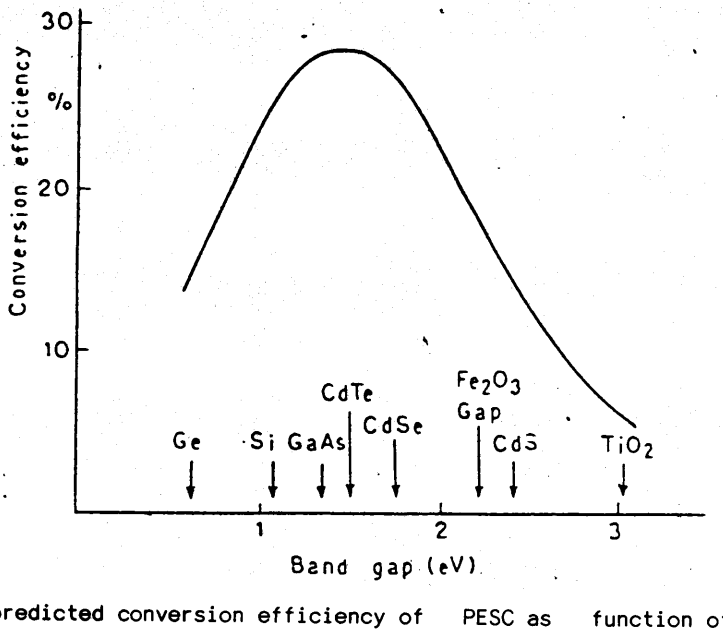

Fig.6

The predicted conversion efficiency of PESC as function of bandgap.

respect to its bandgap [15]. According to this (figure 6) the maximum efficiency is expectef for the materials with bandgap 1.6 eV and the materials with bandgap between 1.2 to 2.0 eV are quite satisfactory.

ACKNOWLEDGEMENT :

The author is thankful to Prof. S. Chandra for his constant encouragement. He is also thankful to Mr. Harimohan, Mr. Ajay and Mr. Hashmi for their assistance throughout the work.

REFERENCES :

[1] Hill, R., Thin Film Active and Passive Devices, P.487 - 602, Ed.T.J.Cotis, Academic Press, 1978.
[2] Coutis, T.J., Thin solid films, 50, 99, 1978.
[3] Coutis, T.J., Phys. Technol.,9, 254, 1978.
[4] Boer, K.W., Phys. Stat. sol.,40 , 355, 1977.
[5] Boer, K.W., and Rothwarf, A., "National Science Foundation, Research Applied to National needs", Grant AER 72-03489, P.303, 1976.
[6] Chandra, S., and Neeraj Khare, Semicond. Sci. Technol., 2, 220,1987.
[7] Gerischer, H., J. Electroanalyt. Chem., 58, 263, 1975.
[8] Ellis, A.B., Kaiser, S.W., and Wrington, M.S., J.Amer. Chem. Soc., 98, 1635, 1976.
[9] Chandra, S., Photoelectrochemical Solar Cells, P.104 - 113, Gordon and Breach Science Publishers, 1985.
[10] Manassen, J., Hodes, G., and Cahen, D., J. Electrochem. Soc., 124, 532, 1977.
[11] Pavaskar, N.R., Menzes, C.R. and Sinha, A.P.B., J. Electrochem. Soc., 124, 743, 1977.
[12] Chandra, S., Pandey, R.K., and Agrawal, R.C., J.Phy.D., 13, 1757, 1980.
[13] Lokhande, C.D. Uplane, M.D., and Pawar, S.H., Solid State Commun., 43, 623, 1982.
[14] Sahu, S.N., and Chandra, S., Solar Cells, 22, 163, 1987.
[15] Chandra,S., "Photoelectrochemical Solar Cells", P.145, Gordon and Breach Science Publishers, 1985.

SOLAR CELLS POTENTIAL IN RURAL AREAS IN THE ARAB WORLD

F.R. Akkari, M. M. Mousa, A. S. Akki
Department of Electrical Engineering,
Engineering Research Centre
Arraya Al-Khadra School of Engineering,
Tripoli, Libya

ABSTRACT

Attention is given to the vital and other justified needs of rural areas in the Arab World. The required power to satisfy these needs is estimated. Accessible energy sources are compared against evaluation parameters and degree of satisfying the needs. These comparisons prove that solar cells are the most suitable energy source for development of the rural areas in the Arab World. General specifications and recommendations are also provided to ensure proper implementation of such technology.

I. INTRODUCTION

The least developed areas in the Arab countries are rural and desert communities. Therefore a special attention is given to the needs of these communities in order to raise the standard of living, introduce new means of technical and social development, and utilize renewable energy sources using existing technologies. Based on the above the required power is estimated and the proper energy source is identified. In satisfying the requirements certain care is given to two factors; first the living habits of the consumers, second the fact that solar energy is evenly distributed both in time and space. Therefore its suitable utilization in the areas of applications should obey the two factors.

In this paper the basic needs of desert and rural areas are defined taking into consideration the degree of satisfying such needs in the present, the living habits and the goal of raising the living standard and modernize and develop these communities. The power requirements to meet such needs are calculated and the best fit energy source is determined. Comparison of the possibly available energy sources against both evaluation parameters and degree of satisfying the needs is conducted to choose the most suitable energy source for rural areas in the Arab countries.

II. ENERGY DEPENDENT BASIC NEEDS

Energy dependent basic needs in rural areas in the Arab world are mainly water, food cooking, lighting, refrigeration, and information and

educational services. These needs will be classified according to three main categories, namely Family needs, Community needs, and General needs. These will briefly be introduced with emphasis on their current status.

1) Family Needs

a - Food Cooking

Daily meals of rural inhabitants are prepared using primitive means of energy sources like wood, animal manure or oil products. Yet no modern source is being introduced.

b - Lighting

At night some form of lighting is needed depending on their limited night activities. Current sources are primitive lighting with oil. Availability of an electricity lighting is rare.

c - Refrigeration

Refrigeration is required for both cooling and food saving. At present saving is possible through open air drying methods, and cooling is through evaporation methods. Use of refrigerators operated by electricity are not yet possible.

d - Information Services

Information services such as Television and radio sets are required for each family in rural areas. The lack of such services is mainly due to the lack of power sources in these areas.

2) Community Needs

A group of families living in the same location constitute a community. Common community needs include:

a - Water

Drinking water, and water for other uses in rural areas is obtained from wells or springs. Community needs are not currently satisfied employing modern methods.

b - Health Care Requirements

Part of its requirements are saving of medicine, and vaccine, beside water and lighting. Non existence of proper care facilities implicate primitive means only.

c - Information & Educational Requirements

TV and radio based educational, informative and entertaining programmes, though can accelerate development process of desert and rural areas, yet they are not available due to the lack of suitable power sources.

3. GENERAL NEEDS

Other needs not included in the above catagories but beneficial to the general public in the area are called General Needs. They include:

a - Gas Stations:

Gas stations are required along the roads in desert and rural areas. Some sort of power is required for gas pumping, lighting, and battery charging.

b) Rest Areas:

Rest areas are essential along the roads in rural and desert areas. They can be within or nearby the gas stations, power is required for water pumping, lighting, entertainment, refrigeration, and cooking. The lack of such facilities is mainly due to the lack of power source.

c - Check Points:

Chech points are encountered along rural and desert areas, power is required for lighting, water pumping, cooking and entertainment.

d - Oil and Military Camps:

Military and oil camps are frequently encountered in rural and desert areas. Their needs are mainly water, cooking, lighting, refrigeration, and communications.

e - Unmanned Stations:

Unmanned stations such as repeater stations, transmitter/receiver stations, VOR stations, car based VOR stations are essential in rural and desert areas. Power availability is a vital need of such stations.

III.BASIC NEEDS - POWER REQUIREMENTS

To estimate the power requirements in rural areas, it is first necessary to define categories of these areas with typical examples, and to study their living habits.

- Examples of Rural Areas:

Rural areas are remote and scattered with low population. One family or more or a group of people may constitute the solely temporary inhabitants in a given location in the rural areas. Another component of rural area is a collection of families forming a community. Typical examples of these areas are (1) Small village and oasis, (2) Gas stations, (3) Rest areas, (4) Remorte border cross points, (5) unmanned stations, and (6) Car VOR like stations, (7) Oil and military camps and car-based VOR stations.

- Living habits:

The living habits and activities of people in rural areas either inhabitants or travellers differ for different seasons. Table 1 shows type and time of activities during summer and winter seasons.

Table 1 : Time table of activities in Rural desert areas

Season	Possible Outdoor Activity	Possible Indoor Activity	Possible Travelling time
Summer March to September	6 A.M to 12 A.M 5 P.M to 8 P.M	12 A.M- 3 P.M 8 P.M-10 P.M	6 P.M to 10 A.M
Winter October to February	7 A.M to 6 P.M	6 P.M-10 P.M	Day time

The power requirements of rural areas are classified into three main categories (1) family requirements, (2) Community requirements and (3) Other requirements.

(1) Family Requirements:

A family in a rural area comprises from 6 to 8 persons on the average. They live in a house of an area about 100 m^2. A typical house consists of a living room, two bed rooms, and a kitchen. The bathroom is usually located outside the house. Its power requirements include the following:

a - Cooking:

Cooking is a basic need of the rural area inhabitants. Lunch, dinner and three tea breaks are expected daily. The following table shows the average cooking times for a given meal and the corresponding power requirements.

Meal	Time for Cooking	Power required KW/hr
Lunch	2 hrs.	1.500
Dinner	1 hr.	1.5
Tea (three times)	0.5 hr. each	0.5
Daily energy requirements per family		6 Kw.h

The average power requirement per hour is given by $\frac{6}{4.5}$ = 1.33 KW

b - Lighting:

To estimate lighting requirement, a typical house is assumed to consist of three rooms, kitchen, with a roofed area per house about 60 m^2. The power requirements are as follows:

Item	Power Requirements (upper limit)
. Rooms (4)	4 x 60 W = 240 W
. Desk Lamp (1)	40 W
. Outdoor Lighting (1)	40 W
. Portable Light (1)	20 W
Total Power	340 W

With the assumption of lighting period to be 4 hours. Then total energy requirement is 4 x 340 = 1.36 Kw.hr.

c - Refrigeration

To up-grade the standard of living in rural areas, refrigeration is to be introduced for water cooling and food saving. A typical refrigerator consumes 150 W. Therefore if assuming a single refrigerator per family, the power requirement is 150 Watt.

d - Information Services:

To provide information services for the families, radio and TV sets are to be introduced to each house. Typical power requirement for operation of radio and TV sets is about 80 watts.

(2) Community Requirements:

a - Daily Water Needs:

To estimate the daily water needs of families in rural areas to cover drinking, washing, cooking and animals water needs. The following assumptions are made:

- Average family size	m	persons
- Daily water consumption per person	l	litres
- Daily average consumption per animal	d	litres
- Number of animals per family	a	
- Power required to pump one m^3 of water at a depth of one meter	P	KW
- Water head (Well-depth)	H	meters
- Number of families per community	M	
- Total power required for water pumping to satisfy daily needs of M-families.	P_w	
- Total sunshine period	h	

Accordingly, the total power required for water pumping from a well of H meters depth to satisfy the daily needs of M families is given by:

$$P_w = (m.l + d.a)\ M.\ P.H. \times 10^{-3} \quad KW/day.$$

Thus the power required to pump this water quantity per one hour of sunshine period is given by

$$P_w = \frac{(m.l + d.a)\ M.\ P.H \times 10^{-3}}{h} \quad KW/hr$$

Thus the pump power rating is P_W. KW.

Example:

For m = 8, l = 37 litres*
d = 4 litres
a = 25, M = 25

Family consumption = 396 litres
For 25 families community = 9.9 m^3
Water consumption.

For P = 0.02 Kw/m^3 at 1 m depth (Estimated from Ref. 1)
h = 12 hrs., H = 25 m
P_W = 412 W
Pump rating is to be > 412 W

---

*This figure is estimated assuming 5 litres for drinking, 2 litres for cooking, 30 liters for washing.

b - Health Care:

Health care center in rural area is assumed to include two rooms and a path room. One room for service and the other is used for storage purposes. Basically it requires lighting and refrigeration at a total consumption of 350 W.

c - Battery Charger:

A battery charger is needed and it is estimated to require in the order of 60 W.

d - Information and Education Services:

The information and education services include a school of two classrooms, a mosque with a selected public lighting. They are estimated to consume a total of 600 W.

(3) General Requirements:

These include gas stations, unmanned station, rest areas, oil and military camps, remote border check points. Their power requirements are given in Table 2. The assumptions made in estimating these values are based on the number of persons and their daily activity; in addition to general assumptions made in parts 1 and 2 above. However, for un-manned station only power required to operate the equipment is introduced in the Table. The demand factor as can be seen in the table ranges from 20% to 100% according to practical experiences of operation and time span of the electric energy requirements.

Table 2 : Estimated Power Requirements of Desert Rural Areas

Consumer / Service	Family	Community	Others					
			Gas Station	Rest Areas	Check Points	Unmanned Station		
						Trans. Recei-ver	Repe-ater	VOR
Lighting per hour	300 W	950 W	160 W	120 W	80 W	20 W	20	20
Pumping/hr.	-	412 W	Manual &/ or 300 W	300 W	300 W	-	-	-
Refrigeration/hr	150 W	-	120 W	240 W	120 W	-	-	-
Entertainment/hr	80 W	-	80 W	80 W	80 W	-	-	-
Battery Charger/24 hr	-	60 W	60 W	60 W	60 W	-	-	-
Power for operation/hr	-	-	-	-	-	140 W	140 W	140 W
Total Power Assuming 100%	530 W	1422 W	720 W	800 W	640 W	160 W	160 W	120 W
Demand Factor	40 %	25 %	50 %	40 %	20 %	100 %	100 %	100 %
Actual Total Consumed Power	212 W	355 W	360 W	320 W	128 W	160 W	160 W	120 W

IV.COMPARISON OF USABLE ENERGY SOURCES:

The implemented methodology in comparing the different energy sources is through comparison of the degree of satisfaction of weighted basic needs in one aspect, and comparison of the energy sources against different evaluation parameters as the second. (Fig. 1) presents a block diagram of the model used to obtain the overall evaluation of the energy sources.

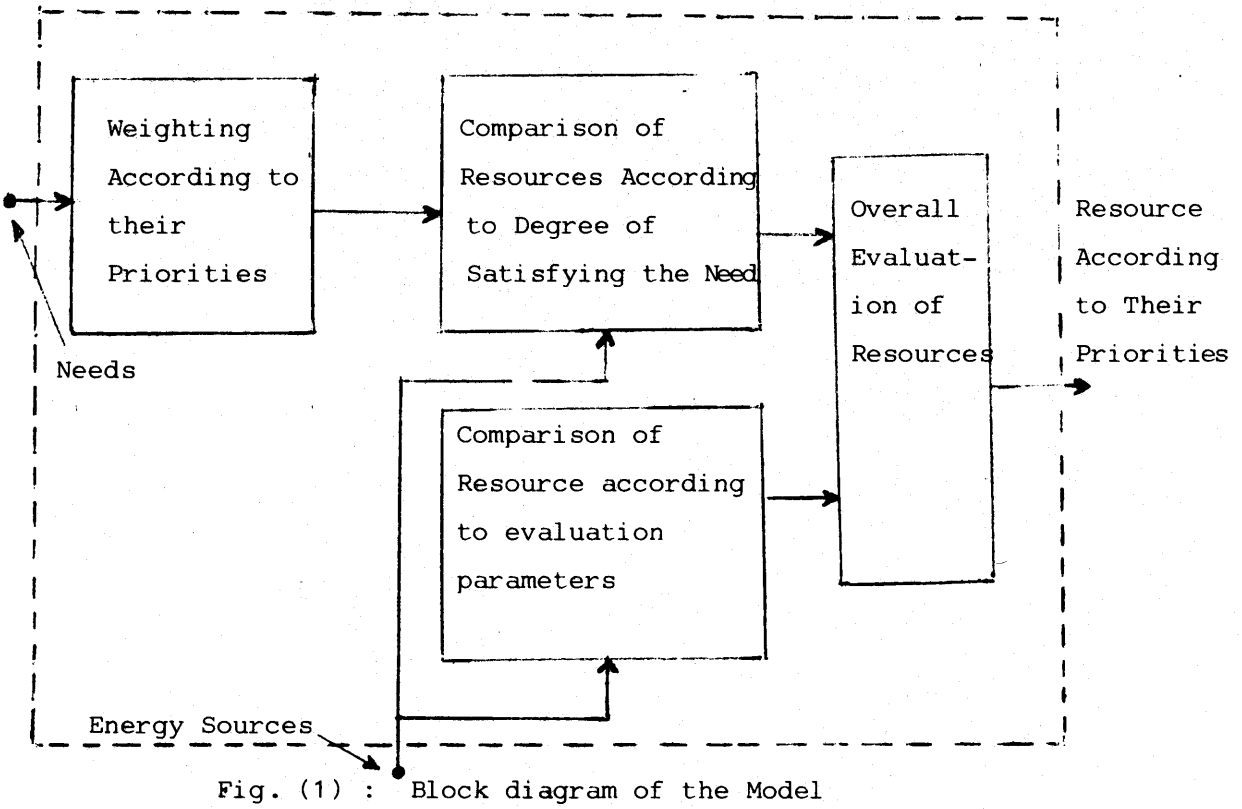

Fig. (1) : Block diagram of the Model

Comparison of energy resources according to the degree of satisfying a selected need is introduced first, then the overall comparison is developed.

1 - Comparison according to degree of satisfying a selected need:

The potential of different energy sources according to degree of satisfying specific needs is developed in Table (3). In this table a 5 points scale is used, and the given grades are according to analysis made for basic needs.

Table 3 : Potential of different energy sources according to degree of satisfying basic needs of rural areas

Energies / Services	Diesel	Oil Products	Primittive	Solar Thermal	Wind	Solar Cells
Cooking	1	5	5	3	1	1
Lighting	5	3	1	1	3	5
Water Pumping	5	1	1	1	3	5
Refrigeration	5	3	3	3	3	5
Radio & T.V Information & Ed.	5	1	1	1	3	5

Analysis of Table 3 according to a specific basic need, the following tabulated result is obtained. It can also be noticed that 80% of needs

Need	The most suitable power source	The least suitable power source
Cooking	. Oil products . Primitive source	Wind, Diesel, Solar Cells
Lighting	Solar cells Diesel generator	Primitive source
Water Pumping	Solar Cells Diesel generator	.Oil products .Primitive sources .Solar thermal
Refrigeration	Solar Cells Diesel generator	. Wind, Oil products . Solar thermal . Primitive sources
Information & educational (Radio & TV)	Solar Cells Diesel generator	. Oil Products . Primitive sources . Solar thermal

can be covered by either solar cells or diesel generator while only for cooking solar cells is one of the least sources.

2 - Overall Comparison

The energy sources are compared against 13 evaluation parameters, and a score is obtained for each of these sources as shown in Table (4). In this evaluation 5 points scale is used, and points are distributed as 1, 3 or 5. It can be seen from the table that solar photovoltaic cells has the highest score followed by solar thermal, and diesel generator get the lowest score.

Since rural areas inhabitants and travellers have different priorities to their basic needs, a questionaire answered by 25 people in order to grade importance of their needs is made. The normalized result in this questionaire according to services is given as:

Service	Cooking	Lighting	Water Pumping	Refrigeration	Information & Education
Weight	0.58	0.43	0.94	0.65	0.65

To obtian the overall score of energy sources from importance point of view. We will multiply their scores in (table 3) by the row vector of the weights as given below:

$$[0.58 \quad 0.43 \quad 0.94 \quad 0.65 \quad 0.65] \times \begin{bmatrix} 1 & 5 & 5 & 3 & 1 & 1 \\ 5 & 3 & 1 & 1 & 3 & 5 \\ 5 & 1 & 1 & 1 & 3 & 5 \\ 5 & 3 & 3 & 3 & 3 & 5 \\ 5 & 1 & 1 & 1 & 3 & 5 \end{bmatrix}$$

Table 4 : A comparison table of utilizing different energy sources in desert areas through use of 13 different evaluation parameters

Energy sources \ Evaluation parameters	1	2	3	4	5	6	7	8	9	10	11	12	13	Points Score
Diesel Generator	5	3	1	1	1	1	3	1	3	3	5	3	3	33
Solar cells	5	5	5	5	3	3	5	5	5	5	5	5	5	61
Solar thermal	5	3	5	5	3	3	5	5	3	3	5	5	3	53
Wind	1	3	3	5	3	3	3	5	1	1	5	5	1	39
Oil Products	5	5	3	5	5	3	5	1	3	1	5	3	1	45
Primitive sources	5	5	5	5	5	3	1	1	1	1	5	1	1	39

1. Possibility of usage
2. Reliability
3. Manpower operational requirement
4. Fuel Operational requirement
5. Maintenance
6. Relative cost
7. Life time
8. Environmental effect
9. Flexibility
10. Modularity
11. Technology accessability
12. Technology trend
13. Limitations

The result of this multiplication is given in Table 5 as the potential of energy sources in satisfying basic needs according to their weights.

Table 5 : Potential of energies in satisfying basic needs according to their weights

Energy	Score	Normalized Score
Diesel	13.93	0.83
Solar Cells	13.93	0.83
Oil Products	7.53	0.45
Primitive Sources	6.77	0.40
Solar thermal	5.71	0.34
Wind	8.59	0.51

The overall evaluation of the different energy sources from both degree of their importance and yielded scores of evaluation is given in Table 6. From this table it is clear that solar cells has the highest overall score that is 50.6 followed by diesel generator 27.4, and oil products as the lowest. This result is expected since the main available energy source in the rural areas of the Arab world is the sun which shines daily for 10 hours during winter, and 14 hours during summer.

Table 6 : Overall Evaluation of Energy Sources

Energy Sources	Points from table (4)	Normalized score from Table (5)	Overall evaluation of resources
Diesel Generator	33	0.83	27.4
Solar Cells	61	0.83	50.6
Solar thermal	53	0.45	23.9
Wind	39	0.40	15.6
Oil products	45	0.34	15.3
Primitive Sources	39	0.51	19.9

V. GENERAL SPECIFICATIONS & RECOMMENDATIONS

1. General Specifications:

In this section through different energy profiles the average energy consumption every day and night for family, community and others is calculated. Accordingly the estimation of the proper solar panel dimensions that can cover the consumption is proposed assuming guaranteed obtainable panels efficiencies.

Fig. 2 shows the energy profile per family consumption. According to Figure (2) then

Total night time consumption per family = 3x120+3x300+12x25+5x80
= 1.96 KWH

Total day time consumption per family = 25 x 12 + 40 x 8
= 0.62 KWH

Family total 24 hrs. consumption = 1.96 + 0.62 = 2.58 KWH

Figure 3 shows the energy profile for community consumption. According to the figure then

Total night time community consumption = 3x240+1x80+3x160+12x60+12x25 + 6x160
= 3.26 KWH

Total day time community consumption = 12x412+12x60+12x25+6x160
= 6.924 KWH

Community total 24 hrs. consumption = 10.184 KWH.

Similarly the 24 hours energy requirement for general needs can be calculated according to table 2 and other assumptions related to practical consumption made before.

Now generation by solar cells panels have to meet such consumption, and in order to come with a modular panel size that ought to be portable, easily installed, and reasonable size for single family usage and implementation. A ½ m^2 panel (100 cm x 50 cm) is recommended.

On the assumption that guaranteed solar cells panels can generate out of every KWH solar energy a total of 0.14 KWH usable electric energy, that is 14% efficiency, for every 1 square metre, therefore, our recommended panel will give 70 W. Accordingly, the no. of panels needed can be calculated based on the assumption of a 10 hours sunshine period daily throughout the year. Table below shows the energy consumption, energy generated and the saving according to panel size proposed.

Table : Solar cells energy consumption and generation

Item	24 hrs. energy consumption	Energy generated daily by 70 W panel	No. of Panels	Saving KWH
Family	2.58 KWH	0.7 KWH	4	0.220
Community	10.184 KWH	"	15	0.316

2 - Recommendations

Based on the comparisons made above, energy requirements calculations and the desired objective of rural area developments, the following general recommendations are presented:

a) Solar energy as being evenly distributed over space and time. Therefore distributed systems for applications are highly recommended.

b) In all applications conservations of natural resources, and national culture is highly recommended.

c) A flexible, easy to install, easy to operate and maintain system design is needed.

d) A modular, portable unit panel array is desirable

e) A portable modular solar cell powered multipurpose power supply is recommended.

f) Introduction of practical implementation of solar cell powered system in rural areas is recommended to help in building a national experience in such developing field.

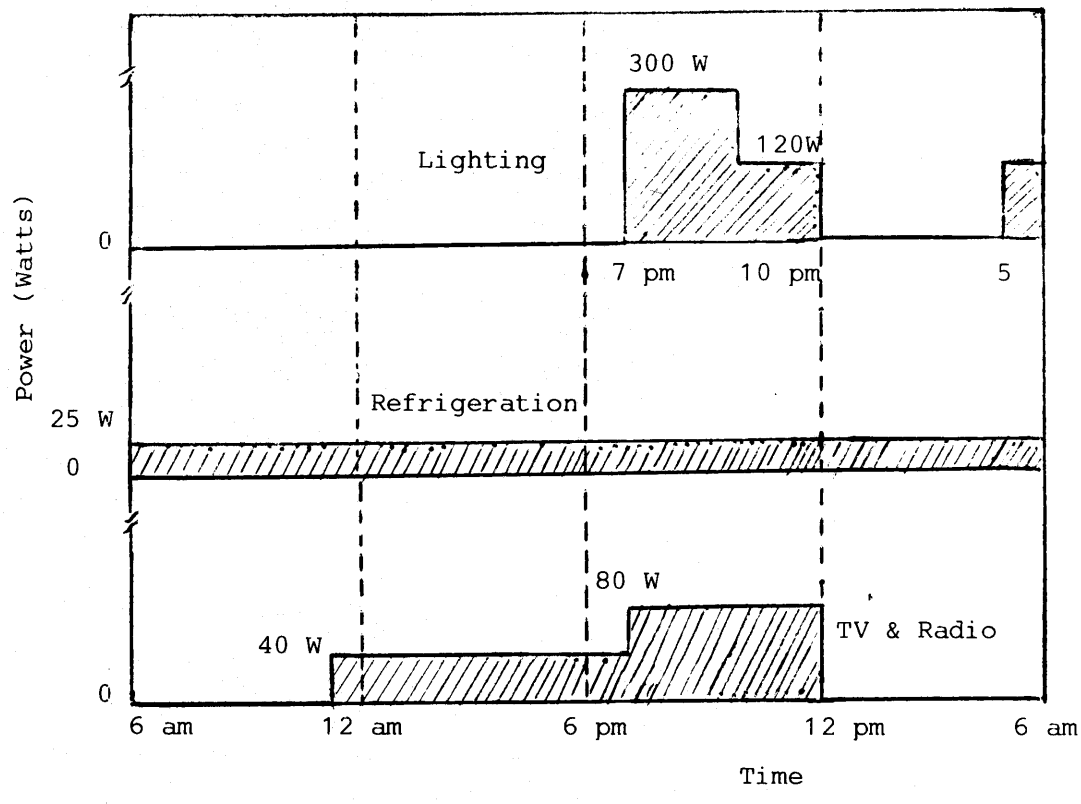

Fig. 2 : Family Consumption Profile

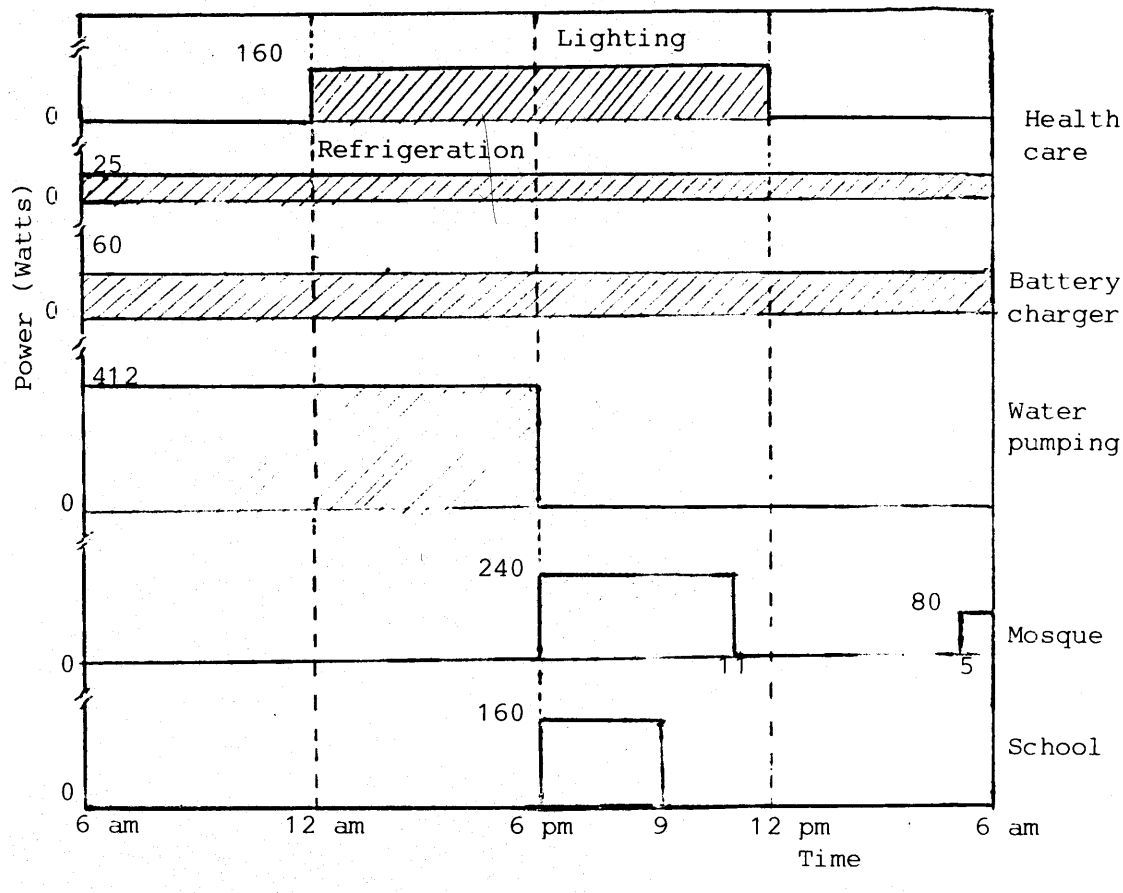

Fig. 3 : Community Consumption Profile

Conclusion:

In conclusion solar cells are found to be the most suitable energy source to satisfy the basic energy needs of rural areas in the Arab world. In designing these systems two factors are to be respected. First, conservation of the rural areas culture, second is that solar energy is evenly distributed naturally both in time and space.

Practical implementation of systems based on such technology in the rurals of the Arab World is important and essential to build up a national and a regional practical experiences, in addition to reduce reliance on oil and oil products as the solely energy sources.

References:

1. "Development of Renewable Energy Sources Applications in Morocco", By Fakahary A, Berday M, and Bakry M., 3rd Arab International Solar Energy Conference Proceedings, pp 9-41, 21-24 Feb, 1988.

2. "Solar Cooking Technology" By Garg H.P. 3rd Arab International Solar Energy Conference Proceedings, pp 0-20, 21-24 Feb. 1988.

3. "Photovoltaics vs Diesel: A grounded cast study of Water Pumping Options for Botswana By Danley D.R. and Bucciaralli, 2nd Arab International Solar Energy Conference, Bahrain, p. 258-263, 12-15 Feb. 1986.

4. "Solar Energy Economy and Prospective", By Sayigh M.A. 2nd Arab International Solar Energy Conference, Bahrain, p.2-25, 12-15 Feb.1986.

5. "Solar Cell a Suitable Power Source to Modernize Desert Areas in the Developing Countries", By F. Akkari,A. Akki, and M. Mousa. International Conference on Energy Options and the Rural Sector in Developing Countries, Italy, 28-29 June, 1988.

ATOMIC-LEVEL ANALYSIS OF PHOTOVOLTAIC DEVICES

Lawrence L. Kazmerski
Solar Energy Research Institute,
Golden, Colorado 80401 USA

The methods and techniques for chemical, compositional and structural analysis of grain boundaries and other micro-features in polycrystalline solar cells are reported. These analyses cover the spatial resolution regime from several hundred microns to single atoms. Emerging analysis techniques, including volume-mapping surface analysis and spectroscopic scanning tunneling microscopy, are introduced for diagnostic applications. The limitations and interpretation of data obtained by these characterization approaches are evaluated, especially the limits of spatial resolution. Examples are provided for the neutralization of shallow impurities at Si grain boundaries by hydrogen, and the incorporation of oxygen at internal defects in $CuInSe_2$.

1. INTRODUCTION

Increased understanding and control of impurities in semiconductor material and at internal interfaces have contributed significantly to the improvements in photovoltaic device performances, including the demonstration of better than 20% single-crystal cells and polycrystalline thin-film cells exceeding 11%[1-5]. Whether the impurities are purposely-placed (such as dopants) or result inadvertently during the processing, the control of such atomic and molecular species depends largely on the ability to detect them—not only with respect to concentration levels and their exact spatial location within the solar cell structure, but also their precise chemical nature (such as bonding). The behavior of hydrogen in single-crystal, polycrystalline and amorphous Si solar cells[6] provides an example of the requirements to correlate the events which occur on the microscale with the macro-electrical and optical properties of the materials/devices. The uncertainties of the role of oxygen in polycrystalline compound semiconductors used in thin-film solar cells require accurate measurements on the Angström-resolution regime to fully understand the processing events on the centimeter scale. The purpose of this paper is to introduce and discuss chemical and compositional characterization techniques for semiconductor devices, emphasizing the role of ultra-microanalysis for the fundamental understanding and diagnosis of processes that occur on the several microns through the atomic-level within such materials and structures. The limits of resolution (spatial and detection) are examined. Specifically, surface analysis voluming-mapping techniques are utilized for subsurface identification of chemical interactions at grain boundaries on the tens-of-microns to the tenths-of-microns scales using secondary ion mass spectrometry (SIMS) and scanning Auger electron spectroscopy (AES), respectively. Results of these studies are supported at the atomic-level by scanning tunneling microscope (STM) investigations. Spectroscopic STM is introduced to provide differential imaging of specific atomic species at defects, with better than 2

Å resolution. These techniques are utilized in the examination of the electrical neutralization processes involving the interaction of hydrogen with shallow acceptors at Si grain boundaries. In addition, the incorporation of oxygen at defects within polycrystalline $CuInSe_2$ solar cells is evaluated. The results of both these important impurity-related problems demonstrate the needs for evolving characterization methods--as well as the diagnostic applications and importance of the techniques themselves.

2. MICROANALYSIS TECHNIQUES

This section serves as an introduction to the microanalysis techniques used in the experimental portions of the investigations of Si and $CuInSe_2$ for this paper. The conventional surface analysis methods are not discussed, since several excellent sources are available to the reader[7-9]. However, those modifications and technique developments which provide special analysis capabilities are explained. In addition, the recently-developed STM is briefly introduced.

2.1 Volume-Indexed Surface Analysis: Mapping

The detection of impurity species is routinely accomplished using a variety of surface analysis methods. Two, SIMS and AES, are particularly-well suited for the mapping of elemental or ionic species at surfaces due to the controllability and relatively small size of the incident probes[7-9]. The detection and mapping at subsurface features is often hampered by the ability to know exactly where these features are located. Fracturing the sample in order to expose the analysis regions has been shown to be difficult and uncertain[8]. Conventional depth-profiling using sputtering provides a method to detect species essentially along a line from the surface through the feature. The detection may be missed if the feature is small or the distribution of impurities is not uniform and of sufficient concentration. Sputtering, of course, is very disruptive to such analyses—and is prone to provide artifacts for misinterpretation of the data[10]. Recently, volume-mapping methods have been introduced which provide for the optimization that sub-surface compositional and chemical information can be obtained during a single analysis run[11,12]. Volume mapping, schematically represented for a grain boundary in Fig. 1, provides the digital acquisition of AES or SIMS data throughout a selected microvolume, coding this information for elemental or ionic species, spatial location within the selected region, and concentration. That is, this indexed information is obtained at each point in the chosen microvolume during a single depth-profile operation by control of the analyzer and beam, with a spatial resolution of 5000-8000Å for SIMS and 300-500Å for AES. The best depth resolution is in the range 100-1000Å for each case. The software permits the operator to selectively display the information for any point, along any line, or on any plane within the analysis microvolume after a single-analytical operation. The technique minimizes the occurrences of missed or lost information encountered in the routine depth-profile analysis and in fracturing or cleaving operations.

2.2 Auger Difference Spectroscopy

One limitation of AES is its ability to detect hydrogen directly. Although SIMS has this important analysis capability, it lacks the spatial resolution of the electron probe techniques. It is beneficial to utilize the smallest available input probe to maximize the spatially-resolved distribution of the detected species. The utility of AES to detect H (or other selected species) is based upon the effect on the observed valence AES transition that the element has in bonding to the host species. This is illustrated in Fig. 2, which shows the Si-LVV transitions for both elemental and hydrogenated Si. Peak shape differences and energy position differences are apparent. Such differences are also apparent in the B-transitions for elemental and H-treated cases [13]. By taking the difference between the measured transition and the elemental transition, for instance, the degree of hydrogen bonding in the sample can be ascertained[13]. If the difference-result is a straight line, the detected

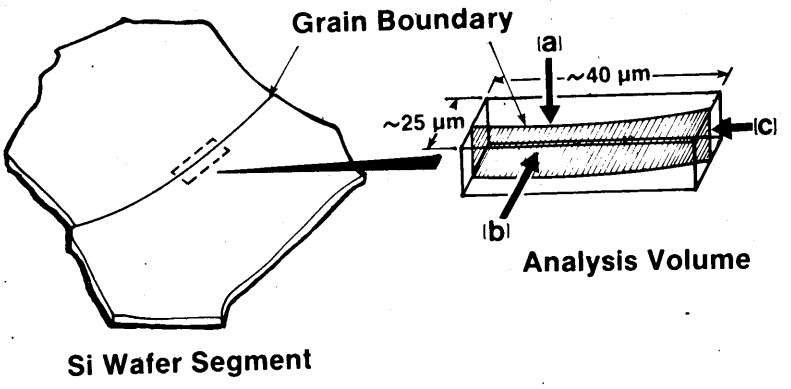

Fig. 1. Schematic representation of volume-indexed surface analysis

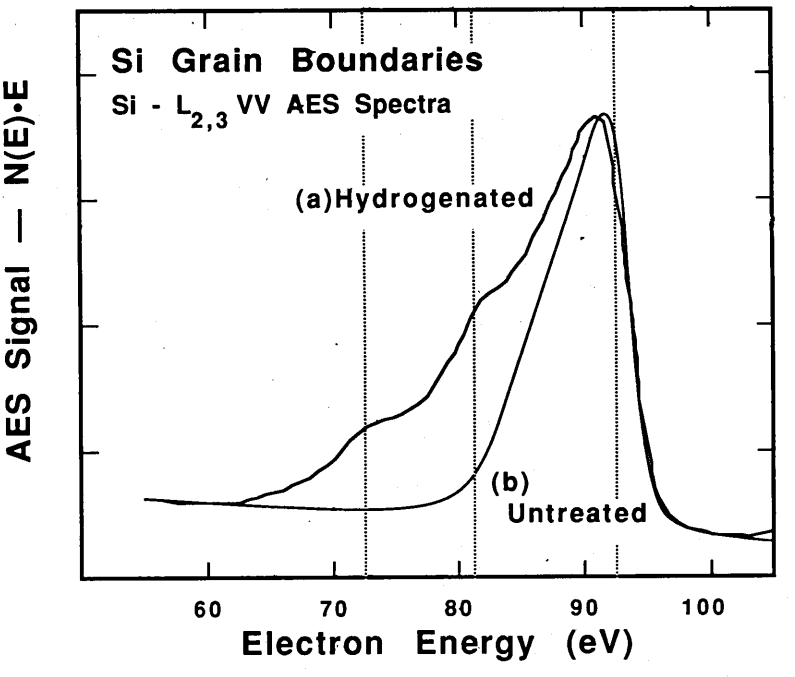

Fig. 2. Si-LVV Auger transition for (a) hydrogen-treated grain boundary, showing chemical effects on peak shape and energy position relative to (b) elemental Si-LVV signal

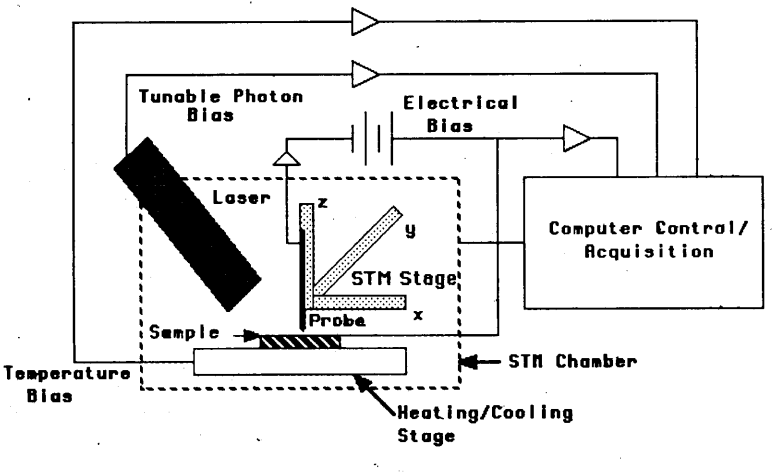

Fig. 3. Schematic representation of spectroscopic STM. Conventional STM is portion enclosed by dashed lines.

species is elemental. If the difference-characteristic is structured, some other bonding (or elemental transition) is detected. The power and ability of this method to combine with volume-mapping to provide information on the chemistry of hydrogen in Si are illustrated later.

2.3 Scanning Tunneling Microscopy

The STM is an extremely high-resolution instrument, capable of structural, electronic and spectroscopic imaging of surfaces and interfaces on a scale that extends to atomic dimensions[14-16]. This recently-developed characterization technique provides atomic imaging, information on topography, electronic and chemical structure. It has lateral resolutions better than 2Å, and can be used on metals, semiconductors and insulators. Its operation is not confined to vacuum (in which the highest resolutions are possible), but can be used on gas/solid and liquid/solid environments as well. This characterization technique is still in its infancy, and its applications and strengths for electronic device diagnostics are only starting to be explored.

With the STM, a final metal tip (usually an electrochemically-prepared tungsten or platinum-rhodium probe) is brought within 3-10Å of the sample surface to permit electronic tunneling between the tip and surface. Typically, the tunneling currents are of the order of 1 nA. At these extremely small distances, the wavefunctions of the atoms at the sample surface and on the fine probe overlap, and by applying a voltage difference between them (in the range of 1 mV to 1 V), the electrons can tunnel from the probe tip to the sample (or vice-versa). The tunneling is actually between a single atom on the probe and the sample surface, under the desired conditions. In the STM, the probe is mounted on three orthogonal piezoelectric transducers, which allow positioning vertically and movement horizontally with respect to the surface. Two common modes of operation are used. The *first* monitors changes in the tunnel current to reflect changes in the distances between the tip and surface. These are used to monitor the probe surface separation. The *second* mode is more common. The variations in tunnel current are monitored by a feedback circuit, which applies a feedback voltage to the vertical control piezoelectric transducer so that a constant tunnel current is maintained while scanning. This voltage correction is measured during the horizontal raster scan and presented as a real-space image of the surface corrugations, providing a topographic replica. These data can be further processed to provide three-dimensional and color-coded images of the atomic arrangements. Figure 3 provides a schematic representation of the spectroscopic STM, a modification of the original instrumentation. This system utilized coordinated and integrated electrical, photon and temperature biasing to provide the selective atomic and structural imaging with Angstrom-level resolution. This biasing, involving potential differences between the probe and sample surface, wavelength-tunable laser excitation and temperature control, provides for the differential, direct and selective imaging of atomic species not gained in conventional STM.

3. SHALLOW IMPURITIES AT SILICON GRAIN BOUNDARIES

In crystalline Si, spreading resistance profiles have been used to show that there is an interaction between the acceptor concentration of the Si and the hydrogen introduced into the semiconductor. Treatment with atomic hydrogen increases the resistivity of p-Si, and the resistance profile suggests that the higher the acceptor background, the greater the interaction between the H and the acceptor. Both the H-Si and H-acceptor bonding models could be used to support the H-diffusion behavior[17-19]. The electrical effect of the acceptor neutralization has been reported in EBIC studies of grain boundaries. In general, the degree of neutralization follows the bond strength trend B>Ga>In[20]. The aluminum case is not analogous. The EBIC response and the spreading resistance data are anomalous compared to the results for the other three shallow acceptors--indicating the chemistry of incorporation might be different.

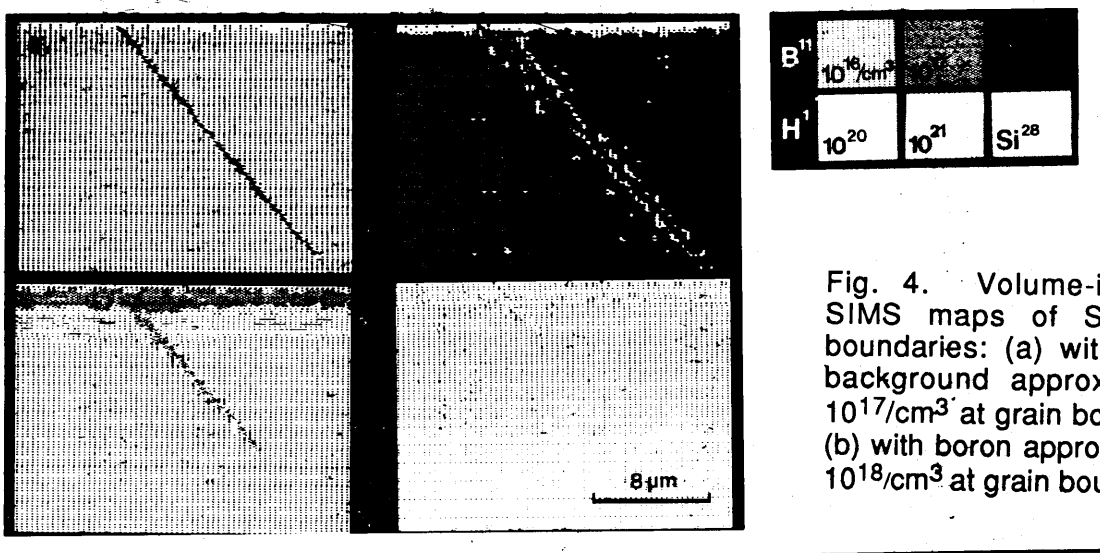

Fig. 4. Volume-indexed SIMS maps of Si grain boundaries: (a) with boron background approximately $10^{17}/cm^3$ at grain boundary; (b) with boron approximately $10^{18}/cm^3$ at grain boundary

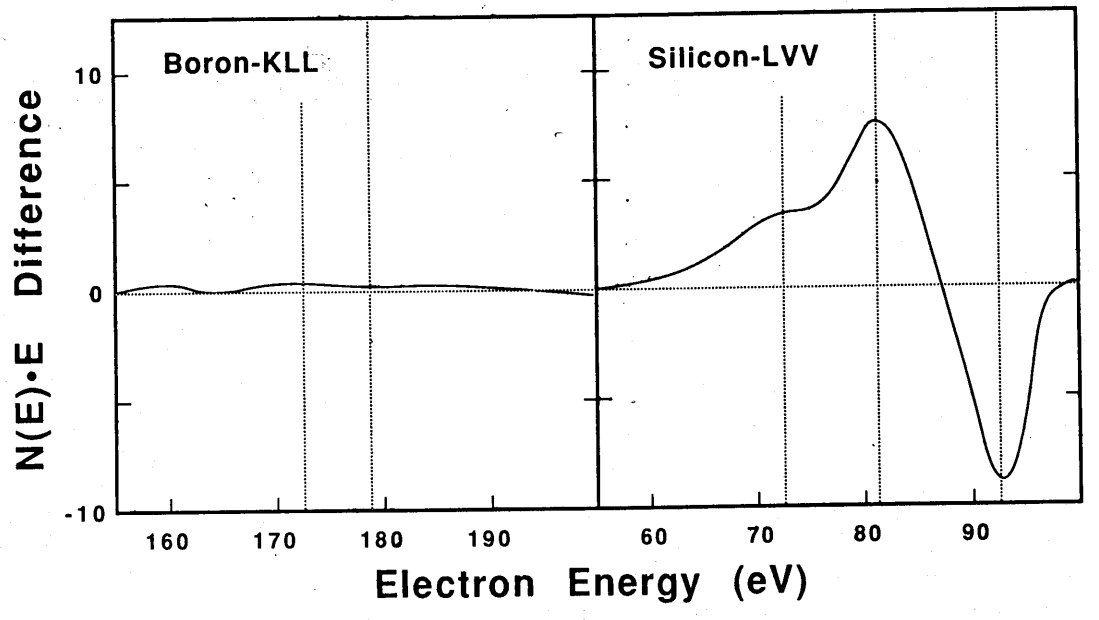

Fig. 5. AES difference spectra for B-KLL and Si-LVV transitions

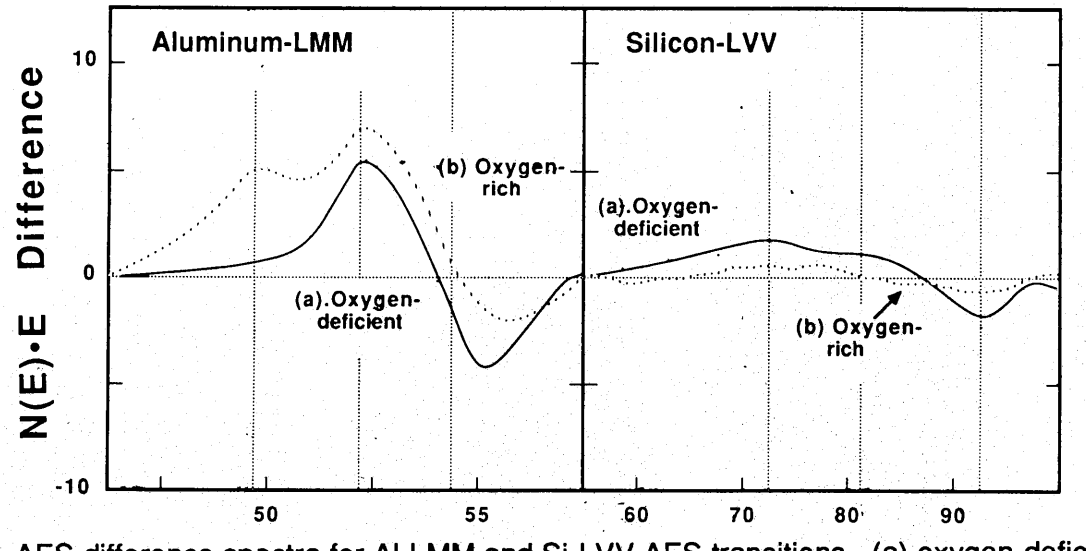

Fig. 6. AES difference spectra for Al-LMM and Si-LVV AES transitions. (a) oxygen-deficient grain boundary; (b) oxygen-rich grain boundary

3.1 Surface Analysis Results: Micron to Submicron Imaging

As indicated previously, the *direct* detection of hydrogen requires SIMS. SIMS volume-indexed maps, such as that presented in Fig. 4, have been used to argue the bonding mechanisms involved[18]. However, two potential problems exist. *First*, the image presented is actually magnified. The grain boundary in Fig. 4 appears to have concentrations of B and hydrogen several microns in width across the defect—a dimension that is considerable larger than expected. *Second*, the ion-products detected utilizing SIMS can only be construed as possible representing the chemistry present in the grain boundary. Since the sputtering process is extremely disruptive on the microscale, it is possible to perform more chemistry during the analysis than actually is present. In order to increase the spatial resolution, indirect analysis using the electron-beam input of AES is required. (Care must be exercised in these analysis to minimize damage or artifact generated by the electron beam.) The ability to discern chemical variations, such as hydrogen-bonding, is afforded by Auger difference spectroscopy—as has already been demonstrated in the data of Fig. 2 Figure 5 presents AES difference spectra for a B-rich grain boundary, similar to that investigated in Fig. 4. The difference spectrum for the B-KLL transition is essentially a straight line of zero magnitude, indicating that the B-detected (at about $10^{19}/cm^3$) is nearly elemental in chemistry. In turn, the Si-LVV spectrum shows Si-H bonding, supporting the model of Pankove *et al.* If the B were bonding directly to the B, the B-KLL spectrum would be affected in a manner analogous to that presented in Fig. 2. Similar AES difference data have been reported for Ga and In. That is, the Si-H bonding dominated during the electrical neutralization process.

The case involving Al neutralization is more complex. The AES difference spectra in Fig. 6 show an apparent direct Al-H bonding mechanism, corresponding with a substantial decrease in the Si-H component. The resistivity for the Al-doped and H-neutralized samples also has been reported to have several anomalous features[17,20]. For example, the resistivity of layers has been shown to increase significantly more than for B, Ga or In-doping. Part of the explanation may have to do with alloying of the Al with the Si. However, such data also exist for samples processed well below the alloying temperature for this couple. The data of Fig. 6 indicate that the incorporation of the H may indeed be different—with the direct bonding of the hydrogen to the Al as proposed by Sah *et al.*[18] Another explanation may be that some degree of hydroxyl bonding may take place[21]. This effect is observable in the oxygen-rich grain boundary data of Fig. 6, in which the oxygen content is approximately $10^{19}/cm^3$. The AES difference spectrum, Fig. 6b, contains measurable AlO(OH) and $Al(OH)_3$ components—species which are indistinguishable by AES or XPS but are known to exist in Si oxides treated by H. Such a transition is absent from the oxygen-deficient ($\sim 10^{17}/cm^3$ oxygen from SIMS estimates) AES difference spectrum of Fig. 6a. Therefore, it is likely that this Al-H bonding may be responsible for the anomalous results in the electrical measurements.

These AES difference data can be incorporated into the volume-mapping previously introduced in order to provide chemical maps illustrating the neutralization process. The benefits to utilizing AES are twofold: *First*, the spatial resolution is better due to the use of a focused beam. *Second*, the analysis is more rapid, minimizing instrument variations and stability/vibration problems. The simple subtraction of data is also significantly more rapid than the more complex deconvolution methods that have been previously employed. Figure 7 presents a comparison of the chemical species for two cases. In the boron-doped case, the Si-H bonding clearly dominates, with no detected B-H bonding. The B is observed to be accumulated or segregated at the grain boundary region. In contrast, the Al (also accumulated at the grain boundary) shows far less Si-H bonding (indicated by the intensity of the mapped species), but significant acceptor-H bonding. Thus, these volume-indexed chemical maps give further evidence to the results of the previous electrical and surface analysis investigations, and show directly the penetration of the neutralizing complex down the grain boundary plane.

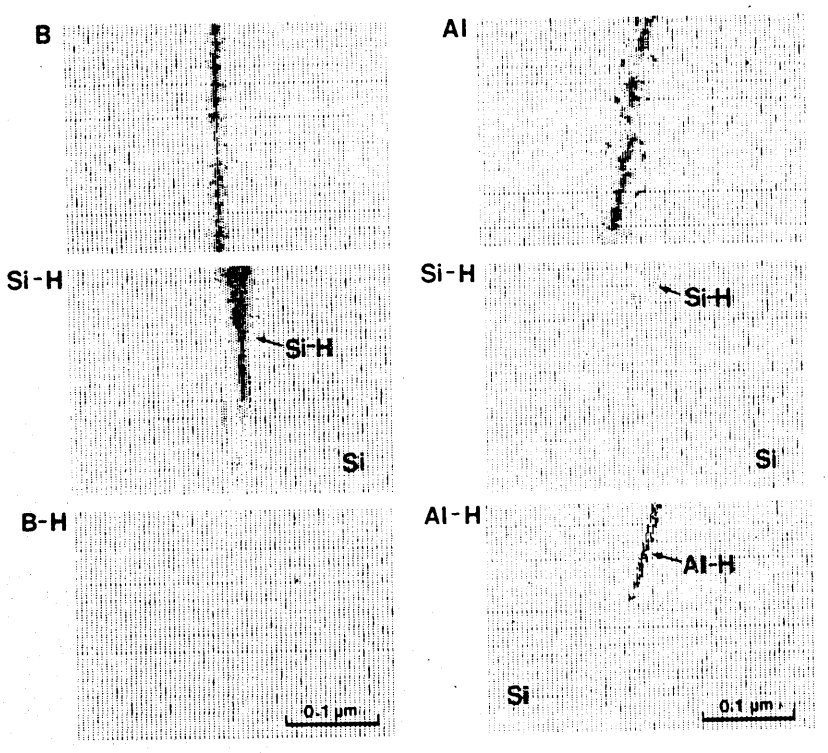

Fig. 7. Volume-indexed AES sequence comparing B-doped with Al-doped grain boundary. Maps are obtained using the difference spectra of Figs. 8 and 9. Although H cannot be detected directly, its presence can be evaluated from chemical effects on the Si and B AES valence transitions

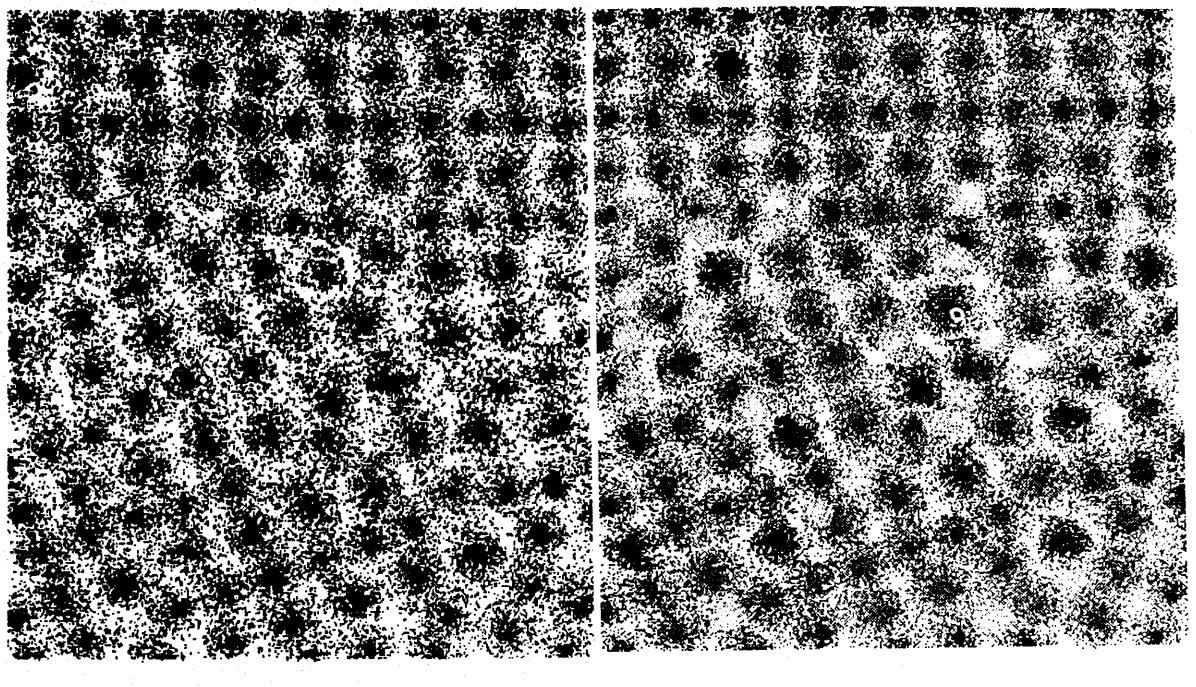

Fig. 8. Scanning tunneling microscope images of Si grain boundary doped with B: (a) conventional STM image; (b) spectroscopic STM image showing B and H locations

3.2 Scanning Tunneling Microscope Investigations: Atomic-Level Images

These data can be further supported by utilizing the atomic-level imaging capabilities of the STM. Grain boundaries of the same samples characterized by the surface analysis methods were prepared for STM examination by fracture in UHV in order to expose the region with minimal external contamination and to produce a flat surface for evaluation. A conventional STM image of a fractured region in the vicinity of a grain boundary is presented in Fig. 8. The image clearly shows the positions of the atomic species—on the (110) Si-plane. The atomic planes can be seen to be ordered at the top of the image and at the bottom--with about a 28° mismatch in the planes (medium-angle grain boundary). The region in-between can be observed to be very disordered, but with the disorder extending over perhaps a hundred Angstroms rather than several microns from the SIMS data or several hundred Angströms from the AES results. This density of states image provides little distinction between the species, although a close examination can provide some indication of variations due to distortions in the density-of-states representations. With the application of proper positive and negative DC electrical bias of a predetermined magnitude, and the inclusion of photon bias to excite the impurity species, various atomic species can be tuned in—and from an evaluation of the STM current-voltage characteristics, a spectroscopic image of the various atoms can be obtained. The image in Fig. 8b shows the same region as that in Fig. 8a, but with the boron and hydrogen atoms spectroscopically-imaged at their positions at the grain boundary. The H-atoms are spatially co-located with the Si atoms, not with the B—giving direct confirmation on the atomic level that the neutralization process involves the bonding of the H to the Si, leaving the Si and B fully satisfying in their chemical configurations. Similar spectroscopic STM images show the same process to occur in grain boundaries containing Ga and In.

The case for the Al-doped region presented in Fig. 9a. For the H-neutralized region, a significant amount of Al-H bonding is observed—giving direct evidence for this process, but on the atomic scale. It should be noted that the H can also be seen to be associated with Si in the grain boundary region, as might be expected in the passivation of the grain boundary containing no additional impurity species. An interesting observation is also provided in the spectroscopic STM image of a grain boundary containing excess oxygen in addition to the Al and the H (Fig. 9b). The possible presence of the predicted hydroxyl-bonding (i.e., OH groups), in addition to direct Al-H and Si-H bonding, can be interpreted. The existence of these OH groups supports modeling of HANSEN et al.[21] for Si having oxygen excesses. Therefore, these fundamental spectroscopic STM results give direct evidence for the mechanisms involved in the electrical neutralization processes for shallow acceptors at Si grain boundaries, and for the first time, measurements at the basic atomic-level have been used to ascertain macroscopic models of electrical transport and chemical processing.

4. COPPER-INDIUM-DISELENIDE: OXYGEN AT DEFECTS

Polycrystalline $CuInSe_2$ thin films form the basis for one of the current leading candidates for economic, medium-efficiency and stable solar cells[22-24]. Devices in excess of 11% conversion efficiency have been confirmed, and modules with inherent reliabilities exceeding those from other thin-film technologies have been initially demonstrated[22-24]. However, some cell processing involves the inclusion of impurity species at interfaces and exposure to oxygen to enhance both open-circuit voltages and short-circuit currents. The direct detection of these impurity species, especially the oxygen, is critical to the eventual explanations required for the performance of this cell type. The STM has been applied for the first time for diagnostic studies at grain boundaries in a ternary semiconductor material in order to correlate atomic-level observations with macroscopically-measured performance.

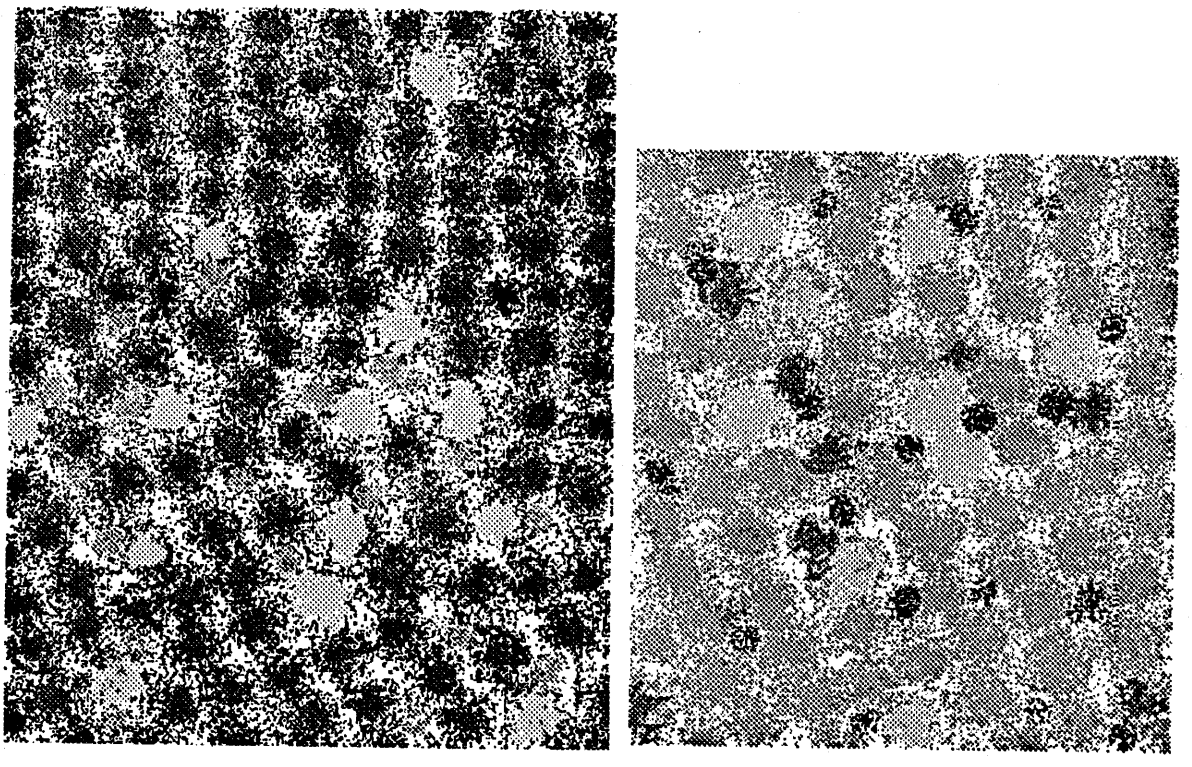

Fig. 9. Spectroscopic STM images of Al-doped Si grain boundary: (a) oxygen-deficient case; (b) oxygen-rich case

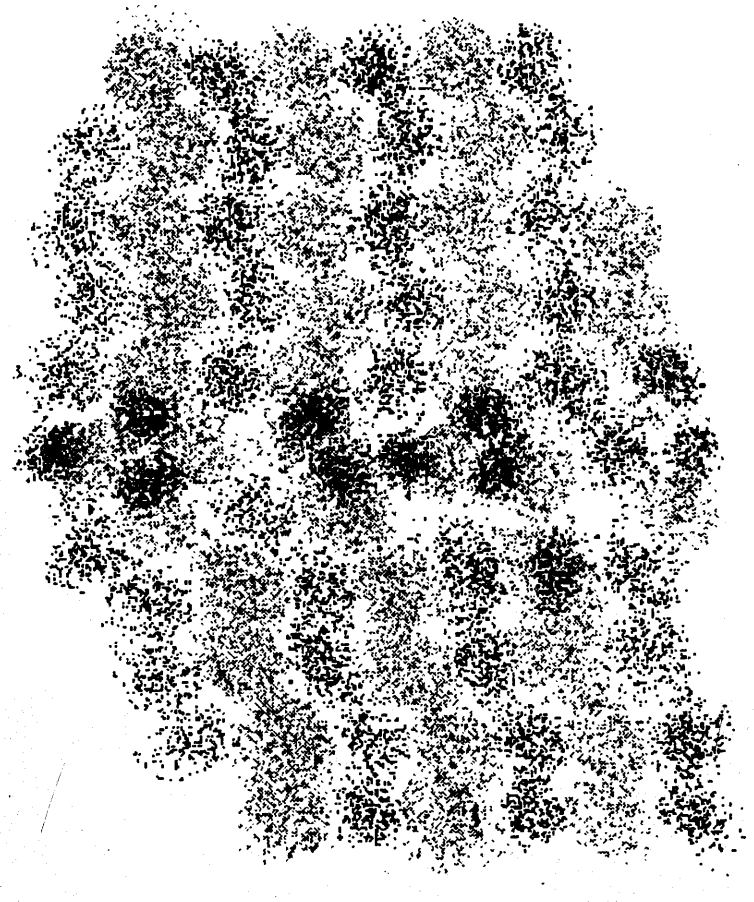

Fig. 10. Spectroscopic STM image of grain boundary in oxygen heat-treated $CuInSe_2$, showing oxygen localization with In at Se sites

The major purpose of these investigations has been to provide a partial explanation of how oxygen might affect the carrier properties of this polycrystalline semiconductor. The as-fabricated solar cells contain $CuInSe_2$ layers that are less than dense. Therefore, for the purpose of these STM investigations, special structures were grown on large-grain polycrystalline $CuInSe_2$ bulk-grown samples. Otherwise, the structures were subjected to the same depositions, the same processing and the same post-deposition treatments as the normal solar cells. The structure was fractured in vacuo, and examined on this cleaved and clean surface by the STM. Before the post-deposition annealing in oxygen, no oxygen localization could be observed in several samples analyzed in the STM. After a 40 min., 250°C oxygen treatment, oxygen localization could be imaged on refractured surfaces using the spectroscopic STM technique. Figure 10 presents such an STM spectroscopic micrograph of a defect (likely a grain boundary) region in the deposited $CuInSe_2$ layer. The positions of the Cu and In atoms on the (112) chalcopyrite plane are clearly visible. (The Se was not imaged, but is located 1/3 lattice spacing below the represented plane.) The oxygen level in the bulk was estimated to be $4x10^{18}/cm^3$ by SIMS, but the positions of the oxygen at the defect are evident. The bonding from this direct atomic-level imaging can be inferred to be primarily with the In--supporting the proposal of CAHEN and NOUFI[25]. In addition, recent spectroscopic images of other planes in this material indicate that a large population of the oxygen is at Cu sites (Cu-vacancies), providing some confirmation of the origin of the p-type characteristics of these films after the oxygen heat treatments. This oxygen incorporation at defects has been observed in more than 12 samples prepared separately for evaluation. However, attempts at observing this bonding directly in the films used for normal devices has not been successful due to the roughness and porousness of those layers. Therefore, the application of the STM to such thin-film electronic device problems might be limited due to the problems involved in preparing suitable surfaces for characterization.

5. SUMMARY AND CONCLUSIONS

The use and applications of microanalytical chemical, compositional and structural techniques from the several micron to the single-atom level for the investigation of grain boundaries in polycrystalline semiconductors have been demonstrated. Specifically, (i) evolving electron and ion beam analysis methods have been introduced and described with respect to their application to micro-feature analysis in polycrystalline semiconductors; (ii) volume-indexed surface analysis mapping techniques and scanning tunneling microscopy have been emphasized for their diagnostic analysis potential; (iii) a new analytical method, spectroscopic STM, has been developed to differentially and specifically image selected atomic species using coordinated electrical, photon and temperature biasing; (iv) examples of the applicability have been presented. These were for the neutralization of shallow acceptors at Si grain boundaries using hydrogen, and the incorporation of oxygen at defects in polycrystalline $CuInSe_2$. In these studies, the requirements and needs for evolving analytical characterization techniques was emphasized.

Acknowledgements. The author gratefully acknowledges the SERI Director's Development Fund which supported the instrument developments reported in this paper. This work was performed under U.S. Department of Energy contract DE-AC02-83H10093 with the Solar Energy Research Institute.

[.] - G. Harbeke, ed.: Polycrystalline Semiconductors, Springer Ser. Vol. 57 (Springer-Verlag, Heidelberg 1985)
[2] - H.J. Leamy, G.E. Pike and C.H. Seager, eds.: Grain Boundaries in Semiconductors, Vol. 5 (North Holland, New York 1982)
[3] C.H. Seager, D.J. Sharp, J.K.G. Panitz and J.I. Hanoka: J.Phys. C1 43, 103 (1982)
[4] - Martinuzzi, S., M.A. Sebbar and J. Gervais: Appl.Phys.Lett. 47, 376 (1985)
[5] - J.A. Roger, J.A., R. Baruch, D. Bernard, J.P. David, J. Guerin, A. Mounguegi and S.

Nopurredine: Proc. Sixth Photovoltaic Solar Energy Conf. (D. Reidel Publ. Co., Dordrecht 1986) pp. 98-102.
[6] - See, for example, K. Takahashi and M. Konagi: Amorphous Silicon Solar Cells (Wiley Interscience, New York 1986)
[7] - Benninghoven, A., F.G. Rüdenauer and H.W. Werner: Secondary Ion Mass Spectrometry (Wiley-Interscience, New York 1987)
[8] - Kazmerski, L.L., In Advances in Solar Energy, ed. by K. Boer, Vol. 3 (Plenum Publ. Co., New York 1986)
[9] - Kazmerski, L.L., J.R. Dick and R.J. Matson: J.Vac.Sci.Technol. A2, 1120 (1984)
[10] - Kazmerski, L.L., Solar Cells 24, 387 (1988)
[11] - Kazmerski, L.L., J.Vac.Sci.Technol. A4, 1570 (1986)
[12] - Kazmerski, L.L., Rev. Bras. de Vacuo 5, 271 (1985)
[13] - Kazmerski, L.L., Proc. 8th European Photovoltaic Solar Energy Conf. (D. Reidel Publ. Co., Dordrecht 1988) in-press
[14] - Binnig, R., H. Rohrer, Ch. Gerber and E. Weibel: Phys.Rev.Lett. 50, 120 (1983)
[15] - Garcia, N., ed.: Scanning Tunneling Microscopy '86 (North-Holland, Amsterdam 1987)
[16] - Feenstra, R.M., Ed.: J.Vac.Sci.Technol. A6 257-554 (1988).
[17] - Pankove, J.I., R.O. Wance and J.E. Berdeyheiser: Appl.Phys.Lett. 45, 1100 (1984); Also, J.I. Pankove, P.J. Zanazucchi and C.W. Magee, Appl.Phys.Lett. 46, 787 (1985)
[18] - Sah, C.T., J.Y.C. Sun and J.J. Tzou: Appl.Phys.Lett. 43, 204 (1983); Also, C.T. Sah, J.Y.C. Sun and J.J. Tzou: Appl.Phys.Lett. 55, 1525 (1984)
[19] - Pearton, S.J., Phys.Rev.Lett. 53, 855 (1984)
[20] - Kazmerski, L.L., A.J. Nelson, R.G. Dhere, A. Yahia and F. Abou-Eltotouh: J.Vac.Sci.Technol. A6, 1007 (1988)
[21] - Hansen, W.L., S.J. Pearton and E.E. Haller: Appl.Phys.Lett. 44, 606 (1984)
[22] - Mickelsen, R.A., and W.S. Chen: Proc. 15th IEEE Photovoltaic Specialists Conf. (IEEE, New York 1981) pp. 800-805
[23] - Mitchell, K.W., C. Eberspacher and J. Ermer: Proc. 8th European Photovoltaic Solar Energy Conf. (D. Reidel Publ. Co., Dordrecht 1988) in-press
[24] - Morel,D., W. Bottenberg, L. Fabick, B. Felder, M. Gardenier, D. Jumamoto and R. Rifai: Proc. 8th European Photovoltaic Solar Energy Conf. (D. Reidel Pulb. Co., Dordrecht 1988) in-press
[25] - Tuttle, Y., D. Albin, J. Goral, C. Kennedy and R. Noufi, Solar Cells 24, 67 (1988)

SECTION XI

RADIATION DATA

CORRELATION OF BEAM IRRADIATION WITH SUNSHINE DURATION AND THE LINKE TURBIDITY FACTOR

M. Hussain
Physics Department and Renewable Energy Research Centre
University of Dhaka, Dhaka-1000, Bangladesh.

ABSTRACT

Monthly average data of daily beam irradiation on a horizontal surface I has been correlated with bright sunshine duration s of seven locations in north and central India using the relation $(I/I_0)=b_o(s/S')$ where I_0 is the monthly value of extraterrestrial irradiation over a day, S' is the corresponding duration over which Campbell-Stokes type sunshine recorders remain sensitive and b_o is the regression constant. Station independent but period and region dependent values of b_o could be assigned to a large part of India using data of seven stations. Monthly estimates of beam radiation using the assigned values of b_o show that for the seven stations r.m.s. errors are within 3-6%. Tests made for two other stations in India also gave good estimates. Hence the present correlation which does not involve data on global radiation should give satisfactory estimates of beam irradiation for stations in a large part of the Indian subcontinent. The correlation technique may prove useful for other countries too.

It has been possible to use Linke's picture for the attenuation of beam radiation in the earth's atmosphere to explain the main features of our results. The beam irradiation is related to Linke turbidity factor T_L and b_o turns out to be equal to $\exp(-md_RT_L)$ where m is the relative air-mass d_R is the Raleigh optical thickness and T_L is the Linke turbidity factor.

$\bar{I}$ = monthly averaged daily value of solar beam irradiation on a horizontal surface on earth.

I_0 = monthly averaged daily solar beam irradiation on a horizontal surface outside the atmosphere i.e., extraterrestrial horizontal irradiation.

s = monthly averaged daily bright sunshine duration

S = monthly averaged day length

S' = monthly averaged period of the day over which Campbell-Stokes type sunshine recorders remain sensitive.

a,b,c = regression parameters

a_o,b_o = regression parameters

m = relative air mass, monthly average value

d = Raleigh optical thickness, monthly average value

T_L = Linke turbidity factor, monthly average value.

h = solar attitude, monthly average value

θ_z = zenith angle of the sun, monthly average value

w = precipitable water amount, monthly average value

β = Angstrom's turbidity parameter.

1. INTRODUCTION

Information on the direct or beam radiation from the sun at a place is required for both concentrating and non-concentrating collectors. For concentrators the output depends almost solely on the direct radiation. For flat collectors data on direct radiation are needed to estimate the amount of solar radiation reaching them which are kept tilted towards the sun. But data on direct radiation are not usually available. For a few locations only global and diffuse radiation data are available and direct radiation values can be obtained from them. For most places the direct irradiation has to be estimated.

Fairly satisfactory techniques for the estimation of diffuse irradiation D in terms of global radiation G have been developed [1-3]

MiSSING Page

type sunshine recorders remain active replaces the day length S. As there is no beam radiation when there is no sun, a_o must be equal to zero. Hence let us try the relation.

$$I/I_0 = b_o(s/S') \quad \ldots\ldots\ldots \quad (2)$$

The very simple relation should allow us to find monthly values of $b_o = (I/I_0)/(s/S')$. We used available data [6-8] on I and s for seven sea-level stations in north and central India to determine the monthly values of b_o. The sunshine data are averages over periods around twenty years while data on I obtained from the difference between values of global and diffuse irradiation are averages over a period of 100 to 255 months. The stations Ahmadabad, Bhavnagar and New Delhi lie in a semi-arid region, region 1, while Bombay, Nagpur and Vishkhapatnam belong to the **wet-and-dry region, region 2**, having a higher rainfall. Calcutta belongs to wet-and-dry zone but it has a higher atmospheric turbidity compared to all other stations 9 and we consider this station to belong to a separate region, region 3. Table 1 gives the monthly values of b_o for the stations.

Table 1 Monthly values of $b_o = (I/I_0)/(s/S')$

Month	Region-1			Region-2			Region-3
	Ahmada-bad	Bhav-nagar	New-Delhi	Bombay	Nagpur	V. patnam	Calcutta
Jan	0.56	0.56	0.56	0.56	0.55	0.55	0.48
Feb	0.56	0.58	0.56	0.56	0.54	0.55	0.49
Mar	0.64	0.62	0.67	0.59	0.56	0.55	0.52
Apr	0.59	0.55	0.59	0.56	0.56	0.53	0.47
May	0.56	0.53	0.60	0.56	0.51	0.50	0.47
June	0.44	0.42	0.56	0.46	0.48	0.50	0.48
July	0.34	0.34	0.44	0.45	0.38	0.46	0.42
Aug	0.37	0.32	0.45	0.33	0.35	0.40	0.46
Sept	0.52	0.54	0.57	0.45	0.53	0.50	0.48
Oct	0.56	0.56	0.57	0.50	0.57	0.54	0.49
Nov	0.55	0.54	0.55	0.55	0.55	0.54	0.48
Dec	0.55	0.57	0.55	0.56	0.56	0.56	0.51

An examination of Table 1 shows that

a) For any station b_o can not be considered to be a constant over the year i.e. under clear sky condition ($s/S'=1$), I/I_0 or the atmospheric transparency varies over the year,

b) for all stations b_o values are lowest for June and July when the humidity level is high and it increases for months having low precipitable amount of water and

c) for certain groups of months b_o may be considered to be constant for a region and b_o values may be assigned to such groups.

Table 2 shows the assigned values of b_o. For June, July and August the sunshine data have relatively larger errors and we consider that the data are not accurate enough to show regional effects. For September we consider that b_o values for regions 2 and 3 can not distinguished.

Table 2 Assigned values of b_o.

Months	Region 1	Region 2	Region 3
Jan-Feb	0.56	0.55	0.49
Mar	0.64	0.55	0.49
Apr-May	0.56	0.55	0.49
June	0.48	0.48	0.48
Jul-Aug	0.40	0.40	0.40
Sept	0.55	0.49	0.49
Oct-Dec	0.55	0.55	0.49

The r.m.s errors in the computation of monthly values of I/I_0 using the assigned values of b_o for each station are compared below in Table 3 with those of Garg and Garg[5]. The present technique gives much lower errors (3-6%) for these stations. As a direct check on the method we compute I/I_0 for Pune and for Jodhpur using our parameters for the semi-arid region (Table 2) although Jodhpur lies in the arid zone. We find the r.m.s errors to be 6% and 7% respectively. Hence, one expects that the use of Table 2 should enable one to make satisfactory estimates of the beam radiation at sea-level locations in the

MISSING PAGE

MISSING PAGE

4. CONCLUSION

We find that the period and region dependent correlation $I/I_0 = b_o(s/S')$ allows one to obtain satisfactory estimates of the beam radiation from sunshine data. The correlation is in line with Linke's picture of atmospheric transmission.

Values of b_o have been obtained for a large part of India and one reasonably expects that a determination of b_o values for other parts of the world will also give good estimates for the beam radiation.

5. REFERENCES

1. Liu, B.Y.H. and R.C. Jordan, "The Interrelationship and Characteristic Distribution of Direct, Diffuse and Total Solar Radiation", Solar Energy 4, 3, 1960.

2. Page,J.K.,"The Estimation of Monthly Mean Values of Daily Total Short-Wave Radiation on Vertical and Inclined Surfaces from Sunshine Records for Latitudes 40°N-40°S, Proc. U.N. Conf. on New Sources of Energy, U.N., New York, 1964.

3. Collares-Pereira,M. and A. Rabl, "The Average Distribution of Solar Radiation - Correlations Between Diffuse and Hemispherical and Between Daily and Hourly Insolation Values",Solar Energy, 22, 155, 1979.

4. Iqbal,M., "Correlation of Average Diffuse and Beam Radiation with Hours of Bright Sunshine, Solar Energy, 23, 169, 1979.

5. Garg, H.P. and S.N. Garg, "Correlation of Monthly Average Daily Diffuse and Beam Radiation with Bright Sunshine Hours", "Energy Convers. Magmt., 25, 409, 1985.

6. Mani,A. and S. Rangarajan, Solar Radiation Over India, Allied Publishers Limited, New Delhi, 1982.

7. Mani,A., Handbook of Solar Radiation Data for India, Allied Publishers Limited, New Delhi, 1980.

8. Mani,A. and S. Rangarajan, "Techniques for the Precise Estimation of Hourly Values of Global, Diffuse and Direct Solar Radiation", Solar Radiation", Solar Energy, 31, 577, 1983.

9. Mani,A., C. Chacko and S. Hariharan, "A study of Angstrom's Turbidity Parameters from Solar Radiation Measurements in India" Tellus XXI, 6, 1969.

10. Kondratyev, K.Ya., Radiation in the Atmosphere, Academic Press, New York, 1969.

11. Dogniaux, R. and M. Lemoine, "Classification of Radiation Sites in terms of Different Indices of Atmospheric Transparency", Intern. Daylighting Conference-General Proceedings, Phoenix, Arizona, 1983.

****

MISSING PAGE

MISSING PAGE

2. THE DATA BASE AND SITE

The data used for this study, were recorded in electronic and instrumentation laboratory in Marrakech university. The characteristics of our site climate are presented in [7]. The measurements analysed in this paper were done from September 83 to August 1987 between 6^h:00 and 20^h:00 (the irradiation rates outside this time interval are negligible even during the summer). We denote by H(h,j) the hourly global irradiation received in hour h, day j and for a given month k. The variable h varies from 1 to 15;(h=1 corresponds to hour 5-6,...,h=15 corresponds to hour 19-20).

3. NECESSITY OF A STATIONARY PROCESS

To have a descriptive model for the irradiation process, we need to apply a set of statistical methods such as the average, the variance and the autocorrelation function. For this, it's necessary to have a stationary random variable of second order. The variable H(h,j) does not satisfy this condition because the average $\bar{H}(h)$ and the standard deviation $\sigma(h)$ vary with time h (see Fig. 1). To make this variable stationary, we construct a reduced variable Y(h,j) defined for each hour h in day j and for a month k by the equation :

$$Y(h,j) = \frac{H(h,j)-\bar{H}(h,k)}{\sigma(h,k)} \qquad (1)$$

Where $\bar{H}(h,k)$ is the hourly average value for the month k of the irradiation H(h,j) calculated by the unbiased and consistent estimation :

$$\bar{H}(h,k) = \frac{1}{N_k} \sum_{j=1}^{N_k} H(h,j) \qquad (2)$$

and $\sigma(h,k)$ is the standard deviation of hour h for the month k defined by the unbiased and consistent estimation :

$$\sigma(h,k) = \left\{ \frac{1}{N_k-1} \sum_{j=1}^{N_k} \left[H(h,j)-\bar{H}(h,k)\right]^2 \right\}^{1/2} \qquad (3)$$

N_k : The number of the days in the month k for four years.

This classical transformation gives a centred and normed variable. Then, the stationarity of the process Y(h,j) is determined by the study of the autocorrelation function R(h,p) of this new variable :

$$R(h,p) = \frac{1}{N_k} \sum_{j=1}^{N_k} Y(h,j).Y(h+p,j) \qquad (4)$$

To eliminate the seasional climatic effects, we perform this study month by month. For a stationary process, R(h,p) depends only on p. Consequentely, to test the independence of R(h,p) with time h, we have plotted (see Fig. 2) the values R(h,p) versus h and for p=1,2 for the September month. We remark that the slope of linear regression line is very small for all months, this result allows to conclude that the process described by the reduced variable Y(h,j) is stationary to second order. In table.1, we give the autocorrelation coefficients $\rho(p)$, month by month defined by :

$$\rho(p) = \frac{1}{15-p} \sum_{h=1}^{15-p} R(h,p) \qquad (5)$$

With :p=1,...,5
15 :Number of hours between 6^h:00 and 20^h:00.

Table. 1: Autocorrelation coefficients $\rho(p)$ p=1,...,5, relative to the reduced variable Y(h,j) for each month.

$\rho(p)$	JAN	FEB	MAR	APR	MAY	JUN	JUL	AUG	SEP	OCT	NOV	DEC
$\rho(1)$	0.83	0.82	0.79	0.80	0.86	0.88	0.82	0.81	0.79	0.82	0.79	0.80
$\rho(2)$	0.60	0.70	0.69	0.67	0.70	0.77	0.62	0.60	0.62	0.71	0.62	0.61
$\rho(3)$	0.48	0.60	0.54	0.48	0.59	0.66	0.49	0.43	0.41	0.48	0.47	0.44
$\rho(4)$	0.39	0.54	0.45	0.36	0.47	0.52	0.38	0.27	0.33	0.39	0.38	0.29
$\rho(5)$	0.28	0.42	0.37	0.23	0.36	0.38	0.27	0.14	0.27	0.31	0.27	0.15

It seems that $\rho(p)$ decreases slowly with the increase of the order p. We think that, this weak decrease is from a mixture of a days with a different statistical properties, that the days with a high (or low) sunshine having a positive (or negative) Y(h,j) for every hour h, possess high contribution in the autocorrelation coefficient R(h,p). But the days with a average sunshine, give a low contribution in R(h,p). For this reason, it is useful to study the behaviour of Y(h,j) during the day.

The average value of Y(h,j) during the day j and for the month k, is defined as follows :

MISSING PAGE

MISSING PAGE

Table.2 : Autocorrelation coefficients $\rho(p)$ p=1,...,5, relative to the reduced variables $Y_B(h,j)$ et $Y_M(h,j)$.

mois	JAN	FEB	MAR	APR	MAY	JUN	JUL	AUG	SEP	OCT	NOV	DEC
B $\rho(1)$	0.58	0.64	0.64	0.73	0.79	0.90	0.78	0.80	0.67	0.7	0.69	0.65
M $\rho(1)$	0.75	0.74	0.68	0.70	0.77	0.83	0.71	0.72	0.68	0.6	0.65	0.68
B $\rho(2)$	0.39	0.49	0.53	0.58	0.61	0.72	0.64	0.56	0.43	0.5	0.49	0.43
M $\rho(2)$	0.52	0.53	0.48	0.48	0.58	0.67	0.49	0.46	0.45	0.4	0.40	0.48
B $\rho(3)$	0.26	0.40	0.44	0.39	0.43	0.52	0.47	0.37	0.25	0.4	0.34	0.22
M $\rho(3)$	0.33	0.38	0.35	0.30	0.43	0.53	0.34	0.25	0.25	0.2	0.29	0.29
B $\rho(4)$	0.13	0.33	0.28	0.19	0.24	0.29	0.32	0.17	0.10	0.3	0.14	0.00
M $\rho(4)$	0.23	0.25	0.28	0.19	0.31	0.38	0.31	0.06	0.19	0.1	0.22	0.10
B $\rho(5)$	0.05	0.23	0.18	0.01	0.07	0.04	0.17	0.05	0.06	0.1	0.04	0.10
M $\rho(5)$	0.17	0.17	0.18	0.06	0.18	0.27	0.07	0.04	0.08	0.0	0.11	0.06

the identification procedure involves two stages :

(1) To decide the order m of the process.

(2) Given m, to estimate the parameters $\mu,\alpha_1,\ldots,\alpha_m$.

5.2 Determining the Order of the (AR) Process.

The suitable order m of process (8) is determined by using the maximum likelihood estimation of AR process, assuming that the error (noise) z(t) has a normal distribution. The residual variance σ_z^2 is approximated by [9] :

$$\sigma_z^2(m) = \frac{N-m}{N-2m-1}\left\{ C_{xx}(0)-\alpha_1 C_{xx}(1)-\ldots-\alpha_m C_{xx}(m)\right\} \qquad (9)$$

C_{xx}: The autocorrelation function of the serie X(1),...,X(N).

If an insufficient number of terms have been fitted in the model (8), the estimation of the residual variance (9) will be inflatted by those terms not yet included. Only, when correct number of terms has been included a valid estimation of σ_z^2 will be obtained. Also, the minimal value of $\sigma_z^2(m)$ corresponds to the correct order of the process.

5.3 Estimation of the Parameters of the Process

The autocorrelation function of the AR prcess (8) is defined by Jenkins [6] as follows :

$$C_{xx}(p) = \sum_{i=1}^{m} \alpha_i C_{xx}(p-i) \qquad (10)$$

by using the effect that the autocorrelation function is even, the parmeters α_i will be determined by resolving the system :

$$\begin{aligned}
C_{xx}(1) &= \alpha_1 C_{xx}(0) + \alpha_2 C_{xx}(1) + \ldots + \alpha_m C_{xx}(m) \\
C_{xx}(2) &= \alpha_1 C_{xx}(1) + \alpha_2 C_{xx}(0) + \ldots + \alpha_m C_{xx}(m-1) \\
&\vdots \qquad\quad \vdots \qquad\qquad \vdots \qquad\qquad\quad \vdots \\
C_{xx}(m) &= \alpha_1 C_{xx}(m-1) + \alpha_2 C_{xx}(m-2) + \ldots + \alpha_m C_{xx}(0)
\end{aligned} \qquad (11)$$

6. RESULTS

The purpose of this study is to elaborate a prediction model of the hourly solar irradiation by using the autoregressive process :

$$Y(h,j) = \alpha_1 Y(h-1,j) + \alpha_2 Y(h-2,j) + \ldots + \alpha_m Y(h,j) + z(t) \qquad (12)$$

We can deduce the hourly irradiation H(h,j):

$$H(h,j) = \sigma(h,k) Y(h,j) - \bar{H}(h,k) \qquad (13)$$

$\bar{H}(h,k)$ and $\sigma(h,k)$ are calculated by equations (2) and (3).

The application of minimisation of the residual variance principle to the serie Y(h,j), shows that the correct order of the process varies between one and five, from one month to another. After the separation between beautiful weather and bad weather, this order is between 1 and 3 for the group B and between 1 and 2 for the group M. To appraise this, we give the obtained values of the residual variance σ_z^2 for January, April, July and October in table.3. The underlined values correspond to the minimal variance and the convenient order of the model. In table.4, we present the parameters α_i relative to the found orders and for the group B and M,for each month.

6.1 Use of the Model for Forecast

The prediction objective in our study is to estimate the values H(h,j) such as the previous values are known. The model already elaborated can be applied only to a given weather type (beautiful or bad) and a given month. Hence, it must be necessary to predict the group type. To test the validity of the model, we work on the previous days by using two methods already used by G.Boch and al.[10].

The method (1) uses the days which we know if the weather is beautiful or bad, but this method isn't interesting because it is contrary to the principle prediction.

MISSING PAGE

for the group B, and :

$$\varepsilon_M(h,k)=\frac{1}{N_M}\sum_{j=1}^{N_M}\left[H_p(h,j)-H_M(h,j)\right]^2 \qquad (15)$$

for the group M.

N_B, N_M: The number of days in group B for each month.

$H_B(h,j)$,$H_M(h,j)$: The observed values of H(h,j) for B and M.

$H_p(h,j)$: The hourly irradiation calculated by the model.

To examine the pertinence of the model, we have evaluated the ratios ε_B/σ_B and ε_M/σ_M for each predicted hour and for all month using method (1) and (2) (see table.5). We remark that, the method (2) gives the best results than the method (1). Also, the estimation of the hours corresponding to group B gives a small error than this corresponding to the hours of group M. In figure.6, we represent simultaneously the predicted and observed values by applying the method (2) to days which are not used in the elaboration of the model chosen arbitrarly to test the model.

7. CONCLUSION

We have analyzed the time series H(h,j) of four years of hourly global irradiation data collected in Marrakech site.

We have shown that this time series can be identified by a autoregressive process with the order and the parameters depend on the weather type and the month.

We have described a method which uses a maximum likelihood estimation principle to determine the suitable order and the parameters of the process.

The test of the validity of the model using two methods gives an acceptable results in spite of the monthly reduced samples used in the treatement.

Table. 4 : Ratios ε_B/σ_B and ε_B/σ_M for the predicted hours, using methods (1) and (2).

		method (1)						method (2)					
h		JAN	MAR	MAY	JUL	SEP	NOV	JAN	MAR	MAY	JUL	SEP	NOV
7	B	–	–	–	0.04	0.04	–	–	–	–	0.03	0.19	–
	M	–	–	–	0.07	0.04	–	–	–	–	0.10	0.04	–
8	B	–	–	–	0.04	0.05	–	–	–	–	0.06	0.12	0.10
	M	–	–	–	0.06	0.14	–	–	–	0.06	0.05	0.11	0.07
9	B	–	–	0.04	0.04	0.08	0.07	0.61	0.20	0.08	0.07	0.23	0.17
	M	–	–	0.10	0.06	0.20	0.16	0.83	0.17	0.10	0.05	0.12	0.17
10	B	0.18	0.08	0.08	0.07	0.19	0.04	0.80	0.23	0.09	0.08	0.34	0.10
	M	0.15	0.17	0.20	0.10	0.24	0.19	0.17	0.16	0.21	0.09	0.15	0.16
11	B	0.07	0.06	0.10	0.05	0.19	0.05	0.13	0.09	0.11	0.06	0.59	0.18
	M	0.12	0.14	0.34	0.18	0.36	0.20	0.20	0.21	0.33	0.14	0.22	0.17
12	B	0.15	0.08	0.08	0.06	0.13	0.17	0.29	0.82	0.26	0.06	0.29	0.22
	M	0.20	0.27	0.25	0.21	0.24	0.19	0.23	0.24	0.23	0.19	0.20	0.19
13	B	0.14	0.16	0.18	0.04	0.18	0.07	0.19	0.14	0.39	0.04	0.15	0.23
	M	0.21	0.18	0.37	0.22	0.19	0.25	0.22	0.33	0.34	0.21	0.15	0.23
14	B	0.15	0.10	0.13	0.07	0.07	0.11	0.14	0.10	0.58	0.18	0.24	0.34
	M	0.22	0.23	0.57	0.46	0.25	0.37	0.26	0.20	0.51	0.39	0.22	0.30
15	B	0.17	0.14	0.26	0.06	0.18	0.13	0.17	0.10	0.30	0.58	0.38	0.17
	M	0.19	0.23	0.42	0.31	0.28	0.28	0.27	0.22	0.41	0.28	0.29	0.29
16	B	0.12	0.11	0.23	0.10	0.26	0.19	0.11	0.05	0.32	0.13	0.29	0.14
	M	0.13	0.24	0.36	0.29	0.19	0.12	0.17	0.31	0.36	0.29	0.17	0.18
17	B	0.10	0.09	0.16	0.04	0.16	0.10	0.09	0.05	0.17	0.37	0.16	0.13
	M	0.07	0.11	0.22	0.27	0.16	0.10	0.09	0.35	0.24	0.19	0.14	0.10
18	B	0.07	0.06	0.14	0.03	0.08	0.02	–	0.04	0.10	0.11	0.06	0.02
	M	–	0.05	0.16	0.13	0.05	–	–	0.13	0.20	0.11	0.14	–
19	B	–	–	0.10	0.03	0.04	–	–	0.09	0.06	0.04	0.04	–
	M	–	–	0.13	0.06	0.03	–	–	–	0.17	0.06	0.03	–

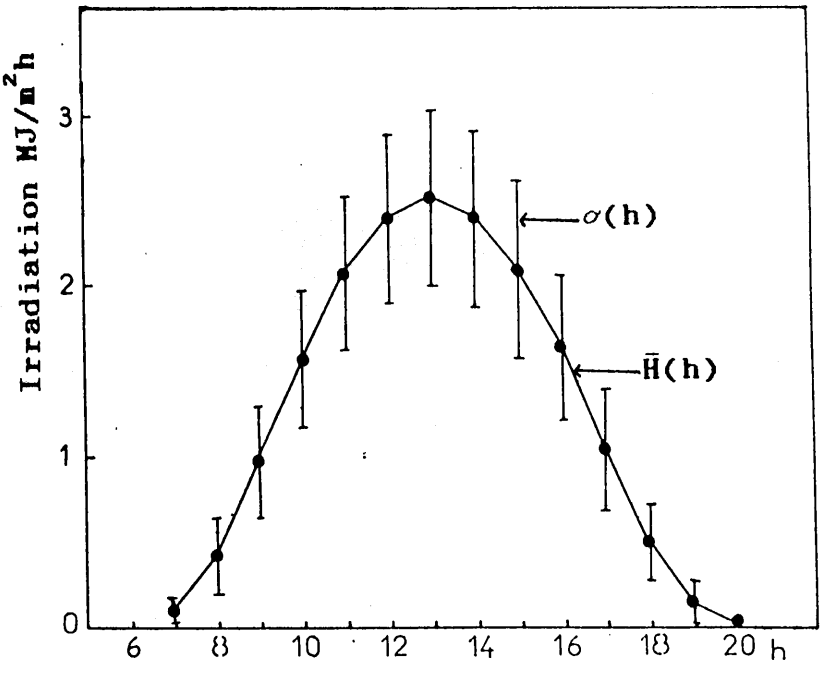

Fig. 1: Evolution of hourly average irradiation $\bar{H}(h)$ and standard deviation $\sigma(h)$ with time h (hours).

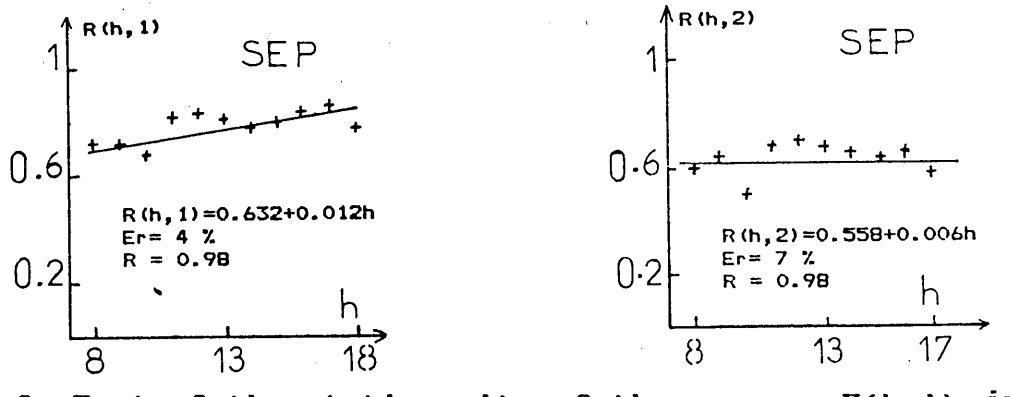

Fig. 2: Test of the stationarity of the process Y(h,j) in September (E_r:Relative error, R:Correlation coefficient)

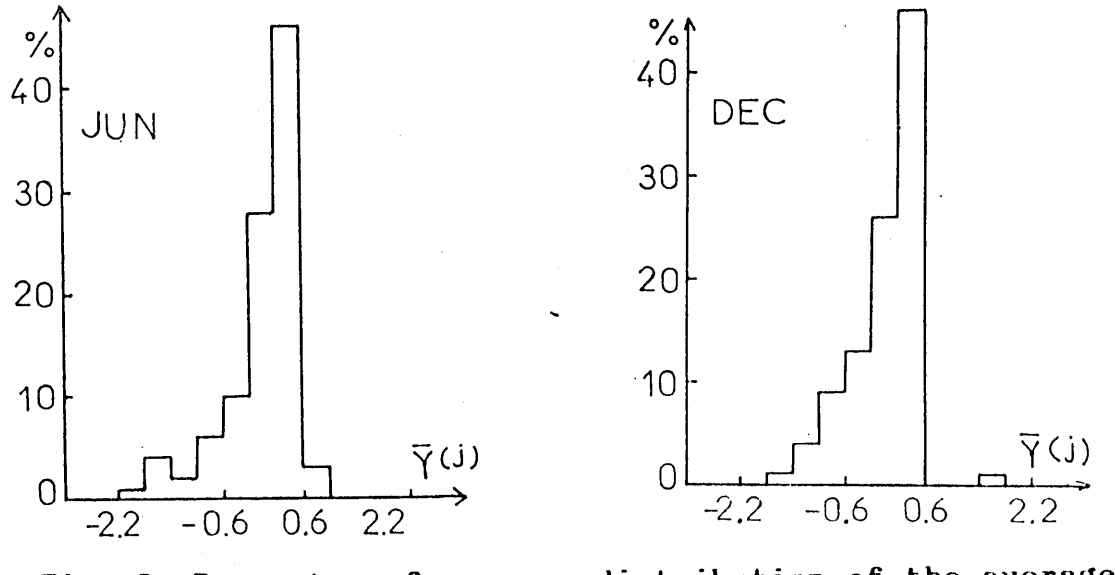

Fig. 3: Percentage frequency distribution of the average $\bar{Y}(j)$ in June and December.

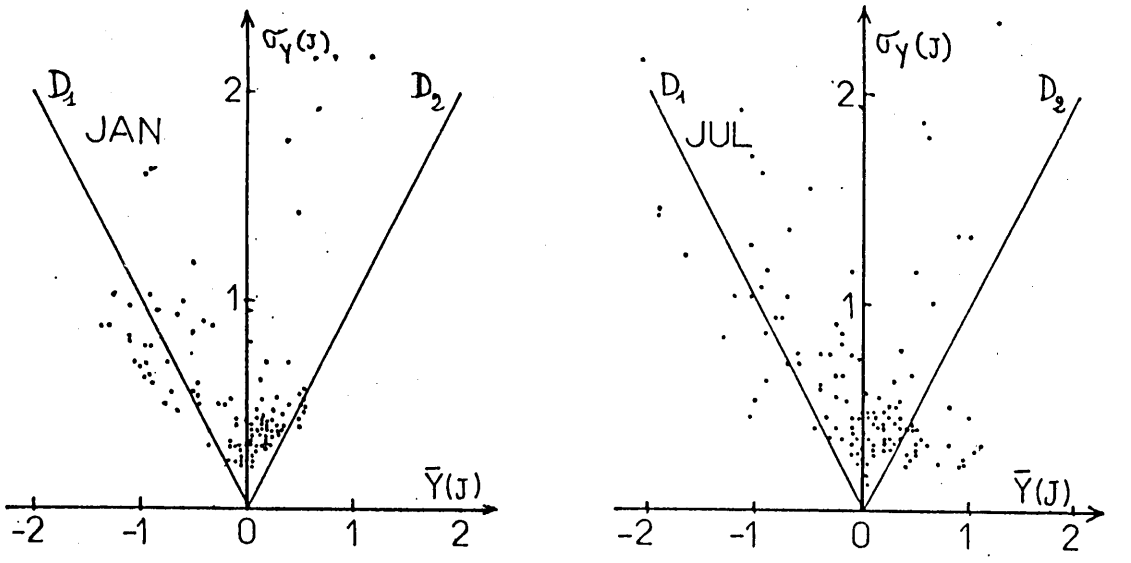

Fig. 4: Dot distribution to examine the stability of the days in January and July.

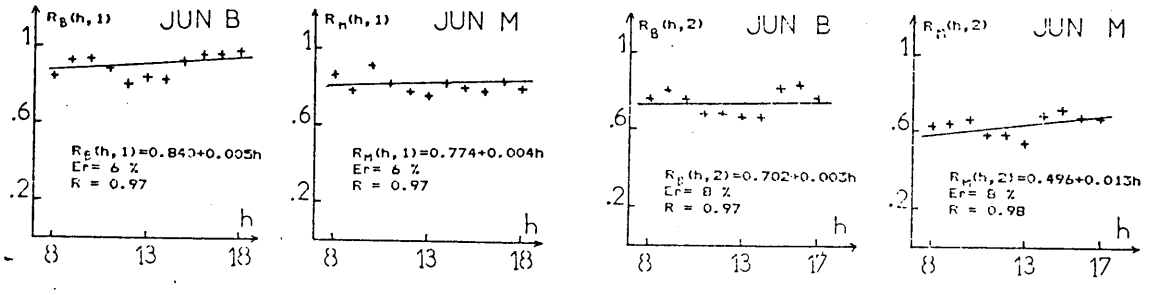

Fig. 5: Test of the stationarity of the reduced variables $Y_B(h,j)$ and $Y_M(h,j)$ in June for the order p=1,2.

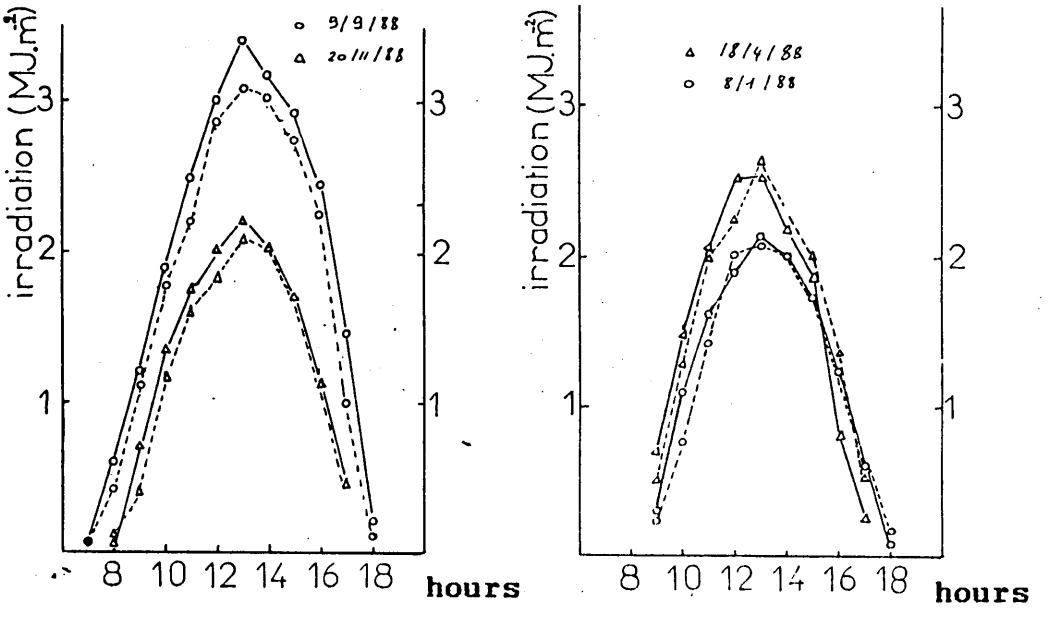

Fig. 6: Comparison between the predicted values (----) and observed values (——) of hourly irradiation for 4 arbitrary days.

REFERENCES

[1] - B.J.Brinkworth, "Autocorrelation and stochastic modeling of insolation sequences". Solar Energy 19, 343-347 (1977).

[2] - E.Boileau, "Discussion d'un modèle statistique en météorologie solaire". Rev. Phys. Appl 14, 145-152 (1979).

[3] - E.Boileau et B.Guerrier, "Comparaisons the modèles statistiques saisonniers et non saisonniers en météorologie solaire ". La météorologie VI^{e} série, pp. 115-130 (1979).

[4] - B. Guerrier, E. Boileau and C. Benard, "Analyse statistique temporelle de l'irradiation solaire quotidienne:Modélisation d'une variable réduite à l'aide de modèles statistiques ARMA Rev. Phys. Appl 15, 93-102 (1980).

[5] - R. T. Chin, J. Y. C. Jau, J. A. Weinman, " The application of time series Models to Cloud Field Morphology Analisis". Journal of climate and applied meteorology, Vol 26,Mar.1987.

[6] - E.Boileau, " Use of some simple statistical models in solar meteorology ", Sol. Energy, Vol 30,No 4, 333-339 (1983).

[7] - A.Zeroual and A. Ait ouahman , " Contribution to the study of hourly and daily solar radiation measurements in dry climate in Marrakech - Morocco ". Proceedings of Third Arab International Solar Energy Conference, Baghdad, Iraq, 21-24 February 1987.

[8] - C. Benard, A. Wirgin, Y. Body and D. Gobin, "Caracterisation de la stabilité de l'intensité solaire par l'analyse temporelle de séries aléatoires en France et au Pérou ". La météorologie VI^{e} série, 53-71 (1979).

[9] - Jenkins & Watts, " Spectral analysis and its applications ", Holden -Day, California (1968).

[10]- G.Boch, E.Boileau et C.Benard, "Modélisation de l'irradiation solaire au pas de temps de l'heure", Rev. Phys. Appl 16, 237-247, (1981).

DEVELOPMENT OF INSOLATION MAPS FOR PAKISTAN USING SATELLITE DATA

A. Q. Malik*, H. W. Hiser** and A. R. Mufti*

* National Institute of Silicon Technology, Islamabad, Pakistan.

** Remote Sensing Laboratory, University of Miami, Coral Gables, Florida, USA.

1. ABSTRACT

Climetological data for a geographic region varies from year to year and a solar year model for each country is a basic requirement to predict the performance of solar systems installed within that particular country. In Pakistan solar radiation data is collected at meteorological stations in five major cities i.e. Karachi, Lahore, Multan, Peshawar and Quetta. These stations are too sparse for a country like Pakistan (Area 796096 Sq. Kms.)to determine important mesoscale differences that can be of major significance in solar power plant location. The present paper describes the development of a method based on the Geostationary Operational Environmental Satellite (GOES) cloud imagery technique to monitor the seasonal and mesoscale geographic distribution of solar energy reaching the earth's surface in Pakistan. Models for converting the satellite measured radiance to equivalent solar radiation falling on the earth's surface are discussed. The method is still being improved and the technique will be used to generate solar maps showing geographic distribution of solar radiation on the mesoscale.

2. INTRODUCTION

Pakistan is located in so called Sun-belt region of the globe. But unfortunately the importance of the geographic location of our country has not been fully appreciated. Presently our country is facing the acute problem of energy shortage so it is very important and urgent to think about alternative energy sources. The solar energy which is abundantly available and reliable through out the country is the possible solution of the present energy crises.

Utilization of solar energy in applications such as rural electification, water pumping, electric power generation, cooling and heating will be quite helpful for the development of the country, specially in the remote areas.

A knowledge of the solar radiation which reaches the earth's surface is necessary both to avail of it as well as for climatological studies. Inspite of the fact that Pakistan is located in the sun-belt region there is no proper insolation data available. However, number of meteorological stations have been established in Pakistan which record standard meteorological data such as temperature, humidity, pressure, sunshine duration and wind speed and direction. But only five of these stations at Karachi, Lahore, Multan, Peshawar and Quetta are equiped with Pyranometers/radiometers for measurements of global solar radiation. The geographic location of these stations is tabulated in table 1. These meteorological stations are too sparse for a country like Pakistan (Area 796096 Sq. Kms.) to produce accurate estimates of solar radiation at all loaction of interest. The knowledge of amount of global solar radiation at a site is very much essential for the proper design and assessment of solar energy photovolatic systems. The only practical source of such high resolution data is GOES because these satellites can provide measurements at half hourly intervals throughout the day and hence a good space and temporal resolution can be achieved [2-4].

The objective of present study is to develop and test new and improved models using satellite data to evaluate amount of solar radiation falling in the territory of Pakistan and to set up the procedures and software packages which can be use for actually producing data for any point in the Countary. The data for this project is being collected from a geostationary operational environmental satellite "INSAT".

3. SATELLITE AND METEOROLOGICAL DATA

A geostationary satellite is that which has an orbit directly above the equator at a height of 22300 miles and an orbital velocity that matches the rotation velocity of the earth. In this way the satellite appears to remain stationary in the sky with respect to a point on earth. From this position in the space the satellite can see about a third of the earth's surface. A 'full disk' image from INSAT gives the cloud cover with in the 20 degree elevation circle which is depicted in figure 1. The primary instrument on INSAT, a Visible Infrared Spin Scan Radimeter (VISSR), makes observations in the visible region (0.55 - 0.75 micrometer); the data set obtained is called a Picture. Visible data are in the form of digital counts, ranging from 0 to 255, which is a measure of relative brightness. The data available for the present studies are 512 X 512 matrix for a full image. By plotting this matrix over the full disk coverage area on an eastern hemisphere map, it is possible to extract the desired geographic area.

The maximum time resolution on INSAT in one full disk image is 30 minutes. However, only two images per day are presently available for the present studies. These are at 0600 Greenwich and 1200 Greenwich time which corresponds to 1100 and 1700 solar time on the 75th Meridian East, in the area of interest. We plan to use hourly satellite image for hours 0800 through 1700 75th Meridian time. This will provide measurements of solar radiation reaching the earth as a function of time of the day at a given place.

4. THE MODEL

In the present studies radiative transfer model due to Dedieu et. al. [1] is being used and modifed according to the requirement. This states that solar irradiance at the earth's surface 'E_o'can be calculated using following relationship:

$$E_o = Ed^{-2}\cos(\theta_s)T(\theta_s)(1-A)/(1-A_s) \qquad (1)$$

where E is the solar constant, d the radius vector (the ratio of actual to mean sun-earth distance), θ_s the solar zenith angle, $T(\theta_s)$ a clear sky transmission factor accounting for gaseous absorption and rayleigh and Mie scattering, A the planetary albedo viewed by satellite and A_s is the surface albedo. $T(\theta_s)$ is estimated from climatological values of atmosphric conditions. We can improve this by using standard meteorological balloon sounding measurements of water vapor content for the day and region under investigation.

$$A = (\bar{R}-R_a)/[T_a+S_a(\bar{R}-R_a)] \qquad (2)$$

where R_a and S_a are atmosphric reflectance and spherical albedo, respectively, for molicular and aerosol scattering and T_a is the transmission factor for absorption and scatterings integrated over the short wavelength bandpass of the INSAT instrument. $\bar{R}$ in equation 2 is the satellite derived equivalent reflectance given by:

$$\bar{R} = \bar{L}/\bar{E}d^{-2}\cos(\theta_s) \qquad (3)$$

where $\bar{L}$ is the radiance measured by satellite and defined as:

$$\bar{L} = \alpha(X - X_o) \qquad (4)$$

$\bar{L}$ is obtained from the digital count, X, using the calibration coefficient α = 7.30 Wm Sr counts and the offset , X_o , which will be obtained from the manufacture of the INSAT radiometer in the United States. X_o is near or equal to zero for INSAT. $\bar{E}$ is the equivalent solar constant in the INSAT visible channel bandpass defined by:

$$\bar{E} = \int E(\lambda).F(\lambda)d\lambda \Big/ \int F(\lambda)d\lambda \qquad (5)$$

where $E(\lambda)$ is the spectral solar constant and $F(\lambda)$ is the spectral response of the instruments. $F(\lambda)$ can be obtained from the instrument manufacturer.

5. RESULTS AND DISCUSSION

This is a collaborative project between Natinal Institute of Silicon Technology, Pakistan and University of Miami, USA duration of which is three years. This project has three major parts. Firstly, the collection of ground truth data for global solar radiation from five different meteorological stations in Pakistan (see table 1); secondly, the development of models for conversion of satellite data into radiance by taking into account the attenuation of solar radiation in atmosphere and thirdly, correlating of ground truth data with the satellite data. At the present research is being conducted on the first and second part of the project.

The first part of the project demands the collection of solar data measured at ground stations e.g. global radiation and radio sonde data. The global radiation data has been collected form the Pakistan Meteorological Department for a period of 20 years (1960 - 1982). This data has been compiled , analysed and the yearly average is taken over 20 years which is tabulated in Table 2. The Radio Sonde data which provides information on pressure, temperature, dewpoint depression, wind direction and wind speed has been collected and is being analysed. This data will be used to develop models to simulate solar radiation attenuation conditions in the atmosphere over Pakistan.

The second part of the project deal with the solution of equation 1 through different set of conditions which had alredy been discussed in section 4. The satellite data for a period starting from April 1985 to February 1986 has been collected and is being analysed and simulated on VAX 8650, NORSK DATA 851446 and IBM PS/2 computers. The location of Pakistan on 512 X 512 matrix for full disk image of INSAT data has been compiled and identified. The brightness solar map of Pakistan has been simulated and is depicted in figure 3. The numbers in this figure represent values of 'X' of equation 4. In order to highlight the Arabian sea region all counts representing clear sky conditions over the water are taken as zero. The highest numbers in this figure represent the presence of clouds in that particular area, intermediate numbers indicate the land area and the lowest number correspond to the existence of water. For example figure 3 demonstrates the presence of a lot of clouds in the northern area of Pakistan and a clear and bright day in the remaining parts of the countary. However, the amount of solar radiation falling varies from point to point which can be very easily analysed from the brightness map of pakistan. Similarly work is in progress to develop brightness solar maps of Pakistan in order to determine surface albedo value 'A ' and cloud albedo value 'A '.

The reflectance 'R' which can be evaluated by solving equation 3 is dependent of the solar zenith angle of the location. Computer packages have been developed to simulate the variation of solar zenith angle with days of the year and

with the hour angle. The results of these variation are summarised in table 3 for eight different locations in Pakistan.

At the present, conversion of satellite brightness data to equivalent solar radiation reaching the territory of Pakistan is in process. The effects of attenuation factors present in the atmosphere are being explored. The hourly satellite images for hours starting from 0800 through 1700 time will be arranged in order to increase both space scale and temporal resolution per day. This will allow us to produce more detailed mapping of small areas which shall provide information about the variation of the amount of solar radiation with time.

6. REFERENCES

[1] - Dedieu, G., P. Y. deschamaps and Y. H. Keer, "Satellite Estimation of Solar Irradiance at Surface of the Earth and of Surface Albedo using Physical Model Applied to Meteosat Data", J. Climate and Appl. Meteor., Vol 26, 1978, 79-87.

[2] - Hiser, H. W., "Satellite Mapping of Solar Radiation Reaching the Earth's Surface In Pakistan", Proceeding of International Symposium - Workshop on Silicon Technology Development and its role in the Sun - Belt Countries, 14-18 June 1987, Islamabad, Pakistan edited by A. Mufti and T. N. Veziroglu, N-1, N-12.

[3] - Malik, A. O., A. Mufti and H. W. Hiser, "Computer Simulation of Satellite Data for Solar Radiation in Pakistan", Proceeding of International Symposium - Workshop on Silicon Technology Development and its role in the Sun - Belt Countries, 14-18 June 1987, Islamabad, Pakistan edited by A. Mufti and T. N. Veziroglu, CI-1, CI-22.

[4] - Mufti, A., A. Q. Malik and H. W. Hiser, "Insolation Estimation of Pakistan From Satellite", Proceeding of Third Arab International Solar Energy Conference 21-24 February 1988, Baghdad, Iraq, edited by N. I. Al-Hamdani et. al., 1-82, 1-86.

TABLE 1. Geographic location of five meteorological stations in Pakistan which record global solar radiation.

Location Number	Name of Location	Latitude (North) Degrees	Longitude (South) Degrees	Elevation (Meters)
1.	Karachi	24.90	67.10	22.00
2.	Lahore	31.60	74.30	214.00
3.	Multan	30.20	71.50	123.00
4.	Peshawar	34.00	71.60	359.70
5.	Quetta	30.20	67.02	179.90

TABLE 2. Average Global Radiation in M.J/m for five Meteorological stations in Pakistan. Average is taken over 20 years.

S.No.	Month	Karachi	Lahore	Multan	Peshawar	Quetta
1.	Jan.	15.83	10.72	12.69	11.26	14.11
2.	feb.	17.96	13.94	15.41	14.65	16.58
3.	Mar.	21.02	18.21	18.76	18.30	20.35
4.	Apr.	22.48	20.89	22.73	21.73	23.95
5.	May	23.45	22.82	24.20	25.10	27.46
6.	Jun.	22.73	22.31	23.53	25.96	29.68
7.	Jul.	19.17	20.56	23.19	23.45	26.88
8.	Aug.	17.83	18.76	21.73	21.35	26.42
9.	Sep.	19.84	18.25	20.39	19.38	24.20
10.	Oct.	19.43	15.11	16.75	15.87	20.35
11.	Nov.	16.81	12.43	13.86	12.73	16.16
12.	Dec.	14.86	10.21	11.56	10.47	13.60

Table 3. Variation of solar zenith angle [$\cos(\theta_s)$] with days of years of five cities of Pakistan at A(1100) and B(1700) hours.

Days	Karachi		Lahore		Multan		Peshawar		Quetta	
	A	B	A	B	A	B	A	B	A	B
1.	0.60	0.14	0.55	0.17	0.55	0.15	0.50	0.11	0.53	0.09
31.	0.64	0.15	0.60	0.19	0.60	0.15	0.56	0.14	0.58	0.10
59.	0.74	0.22	0.71	0.29	0.70	0.24	0.68	0.24	0.66	0.17
65.	0.75	0.24	0.74	0.31	0.75	0.29	0.70	0.26	0.72	0.22
80.	0.82	0.31	0.80	0.38	0.80	0.35	0.77	0.33	0.77	0.28
90.	0.85	0.34	0.84	0.42	0.84	0.39	0.81	0.38	0.81	0.34
95.	0.86	0.36	0.86	0.45	0.86	0.42	0.84	0.41	0.84	0.36
120,	0.92	0.44	0.93	0.54	0.91	0.48	0.91	0.51	0.90	0.45
130.	0.93	0.47	0.95	0.57	0.94	0.54	0.93	0.54	0.92	0.47
151.	0.93	0.48	0.96	0.59	0.95	0.55	0.94	0.56	0.93	0.49
158.	0.93	0.48	0.96	0.59	0.95	0.55	0.94	0.56	0.93	0.50
173.	0.93	0.47	0.96	0.59	0.95	0.55	0.94	0.56	0.93	0.49
181.	0.93	0.47	0.96	0.58	0.95	0.54	0.94	0.55	0.92	0.49
187.	0.93	0.46	0.95	0.57	0.94	0.53	0.94	0.54	0.92	0.48
212.	0.92	0.44	0.94	0.55	0.93	0.51	0.92	0.52	0.91	0.45
219.	0.91	0.43	0.92	0.53	0.91	0.49	0.90	0.49	0.89	0.42
243.	0.88	0.40	0.88	0.49	0.88	0.45	0.86	0.45	0.87	0.39
248.	0.88	0.39	0.88	0.48	0.87	0.44	0.85	0.44	0.84	0.38
264.	0.85	0.37	0.82	0.44	0.82	0.41	0.79	0.39	0.80	0.35
273.	0.82	0.35	0.80	0.42	0.80	0.39	0.76	0.37	0.77	0.33
279.	0.81	0.34	0.77	0.40	0.77	0.37	0.74	0.35	0.75	0.31
304.	0.73	0.29	0.67	0.32	0.68	0.29	0.63	0.27	0.66	0.24
310.	0.71	0.27	0.63	0.29	0.68	0.29	0.60	0.23	0.63	0.21
334.	0.63	0.20	0.58	0.22	0.58	0.20	0.53	0.17	0.56	0.14
339.	0.62	0.18	0.56	0.21	0.57	0.19	0.52	0.15	0.55	0.13
355.	0.60	0.15	0.55	0.18	0.55	0.16	0.50	0.12	0.53	0.10
365.	0.60	0.14	0.55	0.17	0.55	0.14	0.51	0.11	0.53	0.09

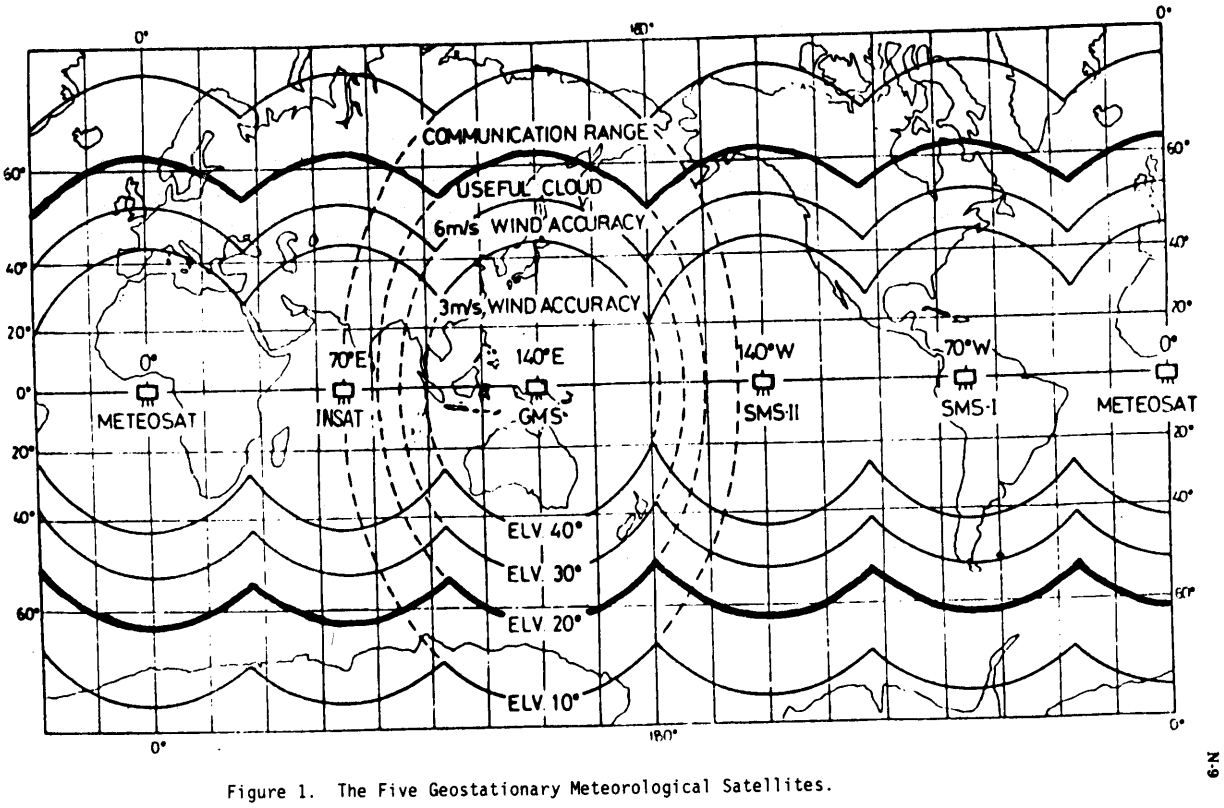

Figure 1. The Five Geostationary Meteorological Satellites.

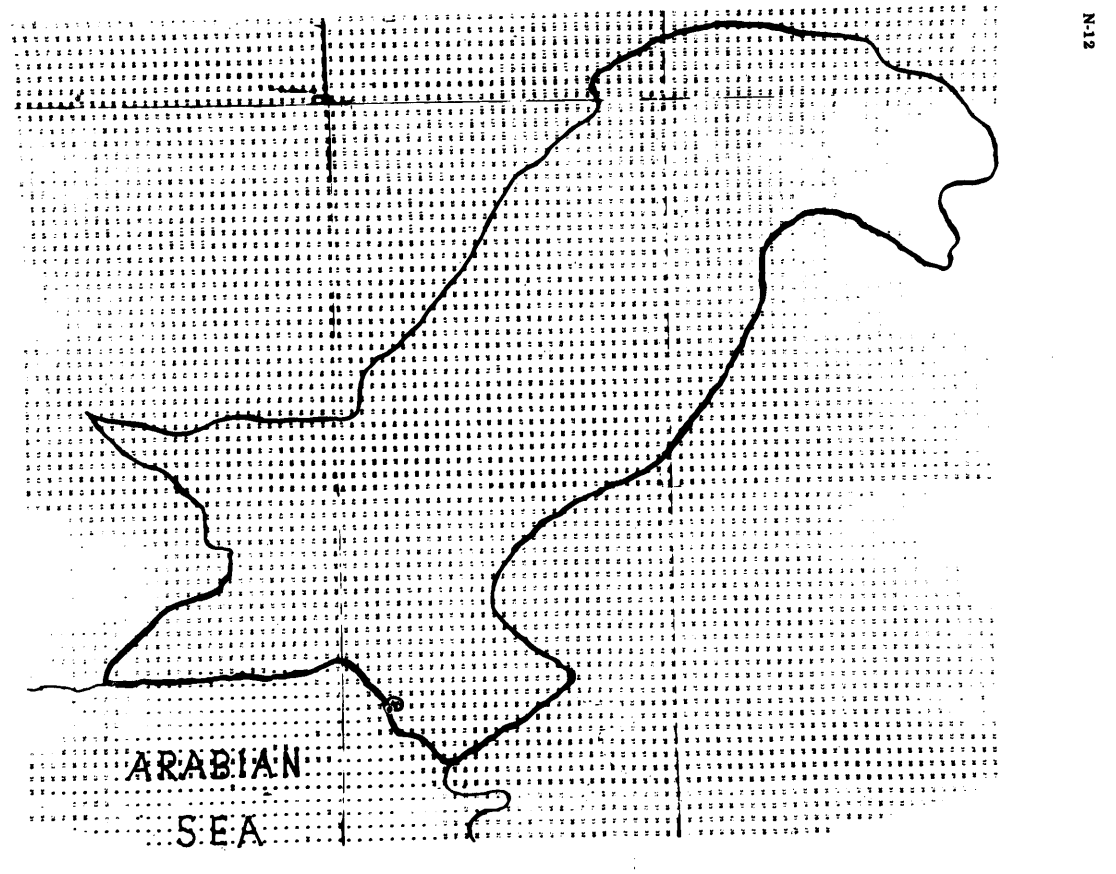

Fig.2 Satellite brightness data over Pakistan.

ON THE MODELLING OF THE DIRECTIONAL DISTRIBUTION OF THE DIFFUSE RADIANCE

F.M.F. SIALA† , M.A. ROSEN‡ AND F.C. HOOPER†

† Department of Mechanical Engineering, University of Toronto, Toronto, Ontario, Canada
‡ Department of Mechanical Engineering, Ryerson Polytechnical Institute, Toronto, Ontario, Canada

ABSTRACT

The physical characteristics of the angular distribution of diffuse sky radiance, and several traditional and recently proposed models for this distribution, are reviewed. The rationales for the development of the models are also discussed. As a demonstration of the importance of considering the directional distribution of the diffuse radiance in collector design, the errors introduced by not accounting for the directional variability of the diffuse radiance are illustrated for a compound parabolic collector (CPC).

1. INTRODUCTION

The diffuse component of solar radiation is important to many disciplines. The magnitude of the diffuse solar radiation incident on the surface of the earth is greater than is usually perceived. Although it is substantial at all locations, the diffuse component constitutes a higher fraction of the total incident solar radiation at higher latitudes, where the average optical path length through the atmosphere is higher. In sites located between latitudes 40° N and 60° N, the diffuse fraction is on average between 0.4 to 0.6 [1]. Whereas, in Tripoli, Libya (33° N), for example, the average diffuse fraction, calculated with 1981 solar radiation data [2], was found to be only 0.30.

The principal present interest in the diffuse component, however, is not in its magnitude but in its directional distribution over the sky hemisphere. The diffuse radiation arises as a consequence of the complex processes of interaction between the solar radiation which enters the earth's atmosphere and the particulate matter within it. The phenomena of single and multiple scattering and absorption which occur, together or separately, at all wave lengths, modify the incident radiation field and redistribute the energy of the nearly parallel solar beam. These processes lead to a directional distribution of the diffuse radiance which is highly non-uniform. The physical concepts of the aforementioned phenomena have long been well understood. Lord Rayliegh, in 1871, discovered the physical law which governs light scattering by very small particles, and Mie, in 1908 [3], proposed his theory for scattering by a spherical particle.

Application of the concept of energy conservation to a differential element of an absorbing-emitting-scattering medium, such as the earth's atmosphere, leads to the equation of radiative transfer [4], which, when solved, describes the angular distribution of the monochromatic diffuse radiance. The simple form of the equation is, however, misleading. The required detailed information about the physical state and chemical make-up of the atmosphere, which are usually not available, combined with the inherently complex calculations involved in Mie scattering, render attempts to solve the equation in its most general form futile. Even with the introduction of a number of simplyfing assumptions, such as single scattering in a plane-parallel atmosphere, substantial computing resources must be used to obtain the directional distribution of the total, or integrated (over wave length or frequency), diffuse radiance. Dave [5] reported the

availability of about 35-40 million monochromatic diffuse radiance datapoints calculated for a limited number of clear sky model atmospheres.

From the viewpoint of solar energy systems applications, the anisotropy of the distribution of the diffuse radiance implies that a horizontal surface is seldom the orientation which receives the maximum input of solar radiation. Yet, most of the measurements of the diffuse radiation are performed precisely for this particular inclination. The lack of measurements for other geometries, and the inability to solve the equation of radiative transfer in the earth's atmosphere, have led solar system designers to utilize a number of simple models to assess the solar resource. A number of the most widely used models describing the angular distribution of the diffuse radiance are reviewed in this paper, and these certainly do no constitute an exhaustive list.

2. CHARACTERISTICS OF THE DIFFUSE SKY RADIANCE DISTRIBUTION

Experimental observations have permitted a good understanding of the qualitative characteristics of the angular distribution of diffuse sky radiance to be obtained for several sky conditions. The principal factors affecting the distributions include solar position, amount and type of cloud cover, atmospheric turbidity, and season [6]. There are many peculiarities in sky radiance, especially in relation to cloud cover [7]. A discussion of the general characteristics of the diffuse sky radiance distribution is now given for the following sky conditions: clear, opaque overcast, non-opaque overcast, and partially cloudy (including multiple cloud layers). Figure 1 illustrates typical radiance distributions for several sky conditions.

The radiance distribution for clear skies exhibits a maximum intensity in the region near the sun, the "circumsolar" region, due to the "forward" elongation of the scattering phase function of the atmospheric particulates, and there is an increase in intensity towards the horizon, or "horizon brightening", due to the increasing optical thickness of the atmosphere at increasing zenith angles [7]. The relative intensity of the radiance distribution is dominantly dependent on the degree of turbidity of the atmosphere [8,9]. A symmetry of the distribution exists relative to the vertical plane along the solar azimuth, or the solar vertical plane [7,10,11].

The radiance distribution for opaque overcast skies exhibits a maximum intensity in the direction of the zenith [10]. A monotonic decrease in intensity towards the horizon [6], or negative horizon brightening, is exhibited due to the increasing absorption of opaque clouds with increasing optical thickness. The distribution is symmetric about the zenith as no dependence on solar position exists.

Non-opaque overcast skies exhibit some of the characteristics of both the above two cases, depending on the degree of opacity of the overcast. In general, as the opacity of the overcast increases, the circumsolar component becomes relatively less intense, and the horizon brightening component decreases and eventually inverts to a negative horizon brightening component. The overall magnitude of the radiance values may increase or decrease, depending on whether increased scattering or increased absorption is predominant in the cloud type. The radiance distribution for hazy clear skies exhibits similar characteristics to that for low-opacity overcast skies.

The angular distribution of the diffuse radiance from partially cloudy skies, and skies containing multiple cloud layers, is extremely complex [7,12]. Since the positions of clouds in such skies can change dramatically in very short time intervals, there exists no typical spatial distribution of diffuse radiance across the sky. However, regularities do exist in the way clouds affect the transfer of shortwave radiation through the atmosphere [13]. First, the spatial distribution of the intensity of shortwave radiation, which has been scattered through an isolated cloud (at a certain position in the sky), exhibits qualitative characteristics very similar to the spatial distribution for an overcast cloud layer of similar opacity, which has previously been described. Second, the shortwave radiation "reflected" from a cloud surface to the observer is a maximum when the cloud is opposite to the luminary [13]. The greater the optical thickness of the cloud in the observer's line of sight, the stronger the reflected radiance [10]. The manner in which a cloud reflects radiation is very difficult to classify as it is neither purely diffuse, nor purely specular, nor indeed any simple combination of these.

3. MODELS FOR THE DIRECTIONAL DISTRIBUTION OF THE DIFFUSE RADIANCE

Many investigations into the quantitative aspects of the angular distribution of diffuse radiance have been done. Almost all of the work in this field has concentrated on the development of empirical models. A

discussion of attempts to model the diffuse radiance is now given.

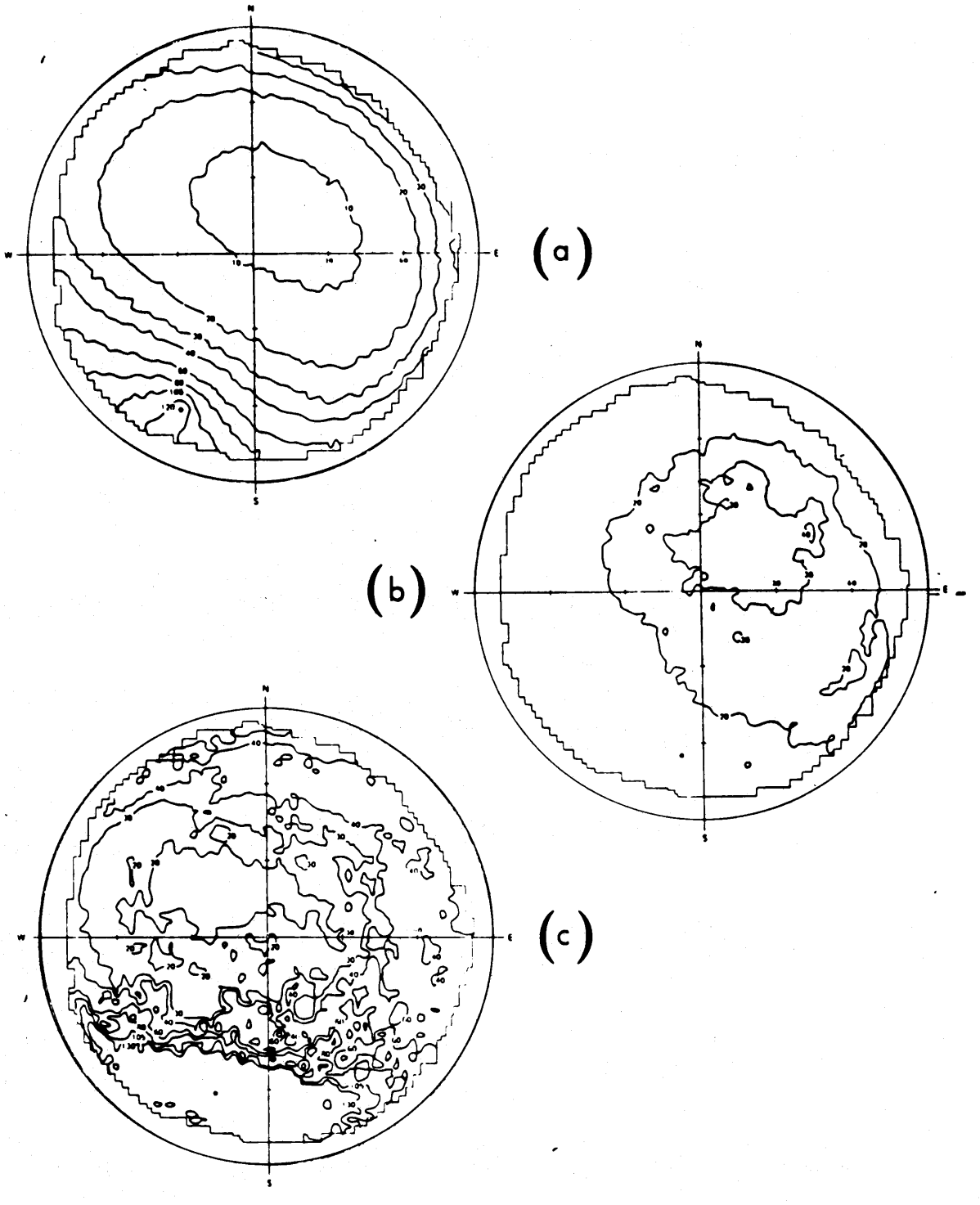

Fig. 1 Typical diffuse sky radiance (W m^{-2} sr^{-1}) distributions for (a) a clear sky, (b) an opaque overcast sky, and (c) a partly cloudy sky. Distributions produced by McArthur and Hay [12] from photographic negatives taken in February, 1978 ($\theta_o \approx 65°$).

3.1 The Isotropic and Heliocentric Models

Traditionally, solar energy system designers have normally assumed that diffuse radiation originates either uniformly from all over the sky, the isotropic assumption, or from the circumsolar region, the heliocentric assumption. The two methods lead to substantially different results. For example, for a surface

inclined at an angle α from the horizontal, the heliocentric assumption results in the following equation for the incident diffuse radiation

$$D_s = D_h \frac{\cos \theta_i}{\cos \theta_o} \tag{1}$$

where D_h is the diffuse irradiance on the horizontal, θ_i is the angle of incidence of the direct radiation on the inclined surface and θ_o is the solar zenith angle. For the same geometry, the isotropic assumption leads to

$$D_s = D_h \frac{1 + \cos \alpha}{2} \tag{2}$$

In general, the heliocentric assumption overestimates, while the isotropic assumption underestimates, the diffuse radiation incident on any surface other than a horizontal surface. Both assumptions represent limiting cases and neither is accurate. Obviously, more realistic models are needed. The fact that the isotropic assumption is far from being valid was recognized at least as early as 1960 [14].

3.2 The Fixed Combinational Model

This model, one of two proposed by Hay [15], combines the isotropic assumption and the heliocentric assumption. Half of the diffuse radiation is assumed to be isotropically distributed and the remaining half is assumed to originate directly from the the direction of the sun. This model leads to the following expression for D_s

$$D_s = 0.5 D_h \left[\frac{1 + \cos \alpha}{2} + \frac{\cos \theta_i}{\cos \theta_o} \right] \tag{3}$$

3.3 The Variable Combinational Model

The second model proposed by Hay is an overall improvement to the fixed combinational model. Instead of assuming equal contributions from the isotropic and the heliocentric models, Hay defined an anisotropy index, k_h

$$k_h = (I/I_o)^{1/m} \cos \theta_o \tag{4}$$

where I and I_o are the direct solar radiation at the earth's surface and the top of the atmosphere respectively and m is the optical air mass. Application of the anisotropy index to the isotropic and heliocentric models results in the following expression for D_s

$$D_s = (1 - k_h) D_h \left[\frac{1 + \cos \alpha}{2} \right] + k_h D_h \left[\frac{\cos \theta_i}{\cos \theta_o} \right] \tag{5}$$

3.4 Clear Sky Models

Pokrowski [16], as cited by Walsh [17], proposed the following formula for the distribution of clear sky radiance:

$$d(\theta, s) = q\{(1 + \cos^2 s)/(1 - \cos s) + k\} \{1 - \exp(-p \sec \theta)\} \tag{6}$$

where θ is the zenith angle, s is the scattering angle (i.e. the angle which the scattered radiation direction makes with the direction of the sun), q is a scaling factor, p is the scattering coefficient of air, and k is an empirical constant to allow for multiple scattering. The values of q, k and p, as suggested by various authors and summarized by Steven [18], are presented in Table 1. Steven notes further that the values of p and k could vary by 0.2 and 1, respectively, without significantly altering the goodness of the fit. Also, as expected, the fitted values of the coefficients for radiance and luminance data were quite different. In general, none of the fits was found to be particularly satisfactory. A similar clear sky model developed by Dogniaux [19] suffered from similar difficulties.

Table 1 The coefficients in the clear sky radiance distribution formula (given in equation 6) as suggested by various authors.

Source	q	k	p
Pokrowski [16]*	-	5	0.32
Hopkinson [20]*	-	0	0.32
Steven [18]**	0.49	11.7	0.92

* Based on luminance data.
** Based on radiance data.

3.5 Overcast Sky Models

Steven and Unsworth [21] summarized several authors' attempts to describe the radiance distribution from opaque overcast skies by the equation

$$d(\theta) = d(0)\,(1 + b\cos\theta)/(1 + b) \tag{7}$$

or in terms of D_h instead of $d(0)$,

$$d(\theta) = D_h\,[1 + b\cos\theta]/[\pi(1 + 2b/3)] \tag{8}$$

where $d(0)$ is the radiance at the zenith and b is an empirically determined constant. The values of b suggested by various authors are listed in Table 2. Although Steven and Unsworth [21] found b varied widely from one overcast sky to the next, they also found that b was approximately independent of season and of the total amount of diffuse radiation incident on a horizontal surface. Overall, the fit of the observed data was found to be very good.

Table 2 The b coefficient values in the opaque overcast sky radiance distribution formula (given in equations 7 and 8) as suggested by various authors.

Source	b
Kondratyev [7] (isotropic sky)	0
Moon and Spencer [22]	2.0
Fritz [23]	1.0 to 1.23
Walsh [17]	1.5
Goudriaan [24]	1.14 to 1.5
Steven and Unsworth [21]	1.23

3.6 The Three-Component Continuous Distribution Model

Although the clear and overcast sky models, which attempted to present a more realistic distribution of the diffuse sky radiance, did usually provide more accurate and realistic results when used to calculate diffuse irradiance on slopes, they were found to be very inflexible. Thus, a new model was required every time a new sky was considered. In hopes of obtaining a more realistic sky radiance distribution model, flexible enough to fit all sky conditions, Hooper and Brunger [1] proposed the Three-Component Continuous Distribution (TCCD) model. The general equation defining this model is

$$d(\theta,\phi) = A_0 + A_1(\theta/90)^f + A_2\exp(g.s) \tag{9}$$

where A_0, A_1, A_2, f, and g are empirically determined constants, ϕ is the azimuth angle, and s is the angular distance between the solar position (θ_o,ϕ_o) and an arbitrary point (θ,ϕ) in the sky. The three anisotropy coefficients, A_0, A_1, and A_2, can be expressed in normalized form as

$$A_i' = A_i/D_h\ ,\quad i = 0,1,2 \tag{10}$$

The first term in the TCCD equation represents the isotropic contribution, the second term the horizon brightening contribution and the third term the circumsolar contribution.

Using clear sky radiance data of several authors, Hooper, Brunger and Chan [25] were able to calibrate the TCCD model for clear skies. The results of this calibration are presented in Table 3. Rosen [28] has found that, based on Hooper and Brunger's [29] radiance data, which represents one of the only data sets available for the complete range of cloudiness, the TCCD model could be made to fit the radiance distributions smoothly for the complete range of cloudiness by using the values of f and g obtained by fitting Steven's data and recalibrating the values of the three anisotropy parameters.

Table 3 Parameters in the TCCD model formula.

TCCD Eqn. Coeffs.	Data Source		
	Steven [27]	Chan [26]	Chan [26]
f	2	2	$1.31 + .02297\,\theta_o$
g	$-.0145e^{.0232\theta_o}$	$-.0145e^{.0232\theta_o}$	$.0114e^{.0172\theta_o}$
A'_0	–	$.00549\,\theta_o - .288$ †	$-.752 + .439e^{.00803\theta_o}$
A'_1	–	$-.00368\,\theta_o + .636$ †	$.616 - \lvert.800 - .465e^{.00937\theta_o}\rvert$
A'_2	–	$.0144\,\theta_o + .582$ †	$.840 + .0123e^{.0603\theta_o}$

† Functional relations determined by Rosen [28].

3.7 Another Continuous Distribution Model

The model proposed by Brunger [30] is a continuous distribution model which combines, linearly, an isotropic term, a horizon-brightening term and a circumsolar term. The model parameters are allowed to vary with the clearness index, K_T, and the diffuse fraction, K, which are used to parametrize the sky conditions, to provide enough flexibility for the model to represent the full range of diffuse radiance distributions. In the work carried out by Brunger, the model parameters were obtained for the Toronto, Canada, site in the form of matrices corresponding to a discrete partition of the $K_T - K$ space.

3.8 The Three Discrete Radiance Components Model

Since, at an instant in time, the distribution of diffuse radiance over a partly cloudy sky is not continuous, the previously developed models are inappropriate for study of short-term transient effects in the instantaneous distribution of diffuse sky radiance. The Three Discrete Radiance Components (TDRC) model, proposed by Rosen [28,31], can represent both the instantaneous and time-averaged distributions of diffuse sky radiance.

The TDRC model assumes that the diffuse radiance from a partly cloudy sky is made up of three components: clear, scattered and reflected. The clear component is comprised of radiation received from cloud-free regions of the sky, the reflected component of radiation received from that part of the side of a cloud which is exposed to direct solar radiation, and the scattered component of radiation received from both that part of the side of a cloud which is not exposed to direct solar radiation and from the cloud base.

The TDRC model further assumes that: each radiance component has a distribution across the sky; each component distribution can be modelled using the TCCD equation; the contributions of each of the components to the total radiance distribution for a general sky are discrete; the radiance of a given component at a particular point in the sky is independent of cloud amount; the reflected radiance from a cloud surface which has been shaded from direct solar radiation by another cloud is part of the scattered component; and the radiance from the thin, bright edges of a cloud of moderate to great optical thickness is part of the reflected component.

The TDRC model expresses the instantaneous radiance distribution for a general sky as

$$d(\theta,\phi,t) = d_i(\theta,\phi,t) \tag{11}$$

and the time-averaged distribution, $\bar{d}$, as

$$\bar{d}(\theta,\phi) = \sum_{i=1}^{3} d_i(\theta,\phi)\, x_i(\theta,\phi) \tag{12}$$

where t denotes time, and the parameters x_i represent the fraction of time the radiance component d_i is at a position (θ,ϕ) in the sky. For the clear component, $i = 1$; for scattered component, $i = 2$; and for the reflected component, $i = 3$. The time-averaged TDRC model has been successfully calibrated for several sky conditions [32].

3.9 A Semi-Empirical Model

This model, introduced by Siala [33], is based on a mixture of physical and empirical reasoning. It is a regression-type model, with the form of the base functions derived from physical principles. The approximation of successive orders of scattering, which is used to circumvent direct computations of multiple scattering in the solution of the monochromatic equation of radiative transfer, is adopted in this model to describe the directional distribution of the integrated diffuse radiance. Calibration of the model using the diffuse radiance data measured by Brunger [30] indicates that inclusion of scattering orders higher than the first increases the complexity of the model tremendously, but does little to increase the accuracy. The proposed final form of the model is, therefore, similar to the analytical solution of the monochromatic equation of transfer which is obtained using the single scattering approximation in a plane-parallel atmosphere.

The model, in its present stage of development, describes the angular distribution of the diffuse radiance averaged over all weather conditions and, therefore, does not account for variations in the distribution with sky conditions.

3.10 Stochastic Models

The models described so far in this paper overlook the very important characteristic of the diffuse radiation that the physical processes giving rise to it are essentially stochastic. Because of the statistical behaviour of the matter in the atmosphere, the diffuse radiance also exhibits a statistical behaviour. The diffuse radiance at any given position in the sky has associated with it a statistical distribution function, which assigns probabilities of occurence to every value in the diffuse radiance range at that position. Moreover, values of the diffuse radiance occuring at the same position at successive instants of time, and also values occuring at adjacent positions at the same or different instants of time, may not be statistically independent. The only apparent way to describe this behaviour is through the introduction of a stochastic component in the directional distribution model.

Based on a linear realtionship proposed between the standard deviation and the mean of the diffuse radiance [34], a stochastic model was suggested [33,35] to account for the correlation structure of the diffuse radiance.

4. APPLICATION TO A CPC COLLECTOR

As a demonstration of the importance of considering accurate models for the angular distribution of the diffuse radiance, consider the calculation of the fraction, f_{acc}, of diffuse radiation accepted by a compound parabolic concentrator (CPC) with an acceptance half angle θ_{acc}. Evaluating f_{acc} is straightforward in the case of an isotropically distributed diffuse radiance. For a CPC oriented such that the trough axis is aligned in the East-West direction and the aperture is inclined at an angle β from the horizontal,

$$f_{acc} = \frac{\int_0^{2\pi}\int_0^{\pi/2} G(\theta_s,\phi_s,\theta_{acc})\, d(\theta_s,\phi_s)\cos\theta_s \sin\theta_s \, d\theta_s \, d\phi_s}{\int_0^{2\pi}\int_0^{\pi/2} d(\theta_s,\phi_s)\cos\theta_s \sin\theta_s \, d\theta_s \, d\phi_s} \tag{13}$$

where $d(\theta_s,\phi_s)$ is the diffuse radiance in the direction (θ_s,ϕ_s), $G(\theta_s,\phi_s,\theta_{acc})$ is a geometric parameter which determines whether $d(\theta_s,\phi_s)$ is intercepted by the receiver. In the above expression, θ_s and ϕ_s are zenith and azimuth angles evaluated with respect to the inclined surface of the CPC's aperture, and are related to θ and ϕ by

$$\theta = \cos^{-1}(-\sin\beta \sin\theta_s \cos\phi_s + \cos\beta \cos\theta_s) \tag{14}$$

and

$$\phi = \sin^{-1}(\sin\phi_s \sin\theta_s / \sin\theta) \tag{15}$$

Obviously, f_{acc} is a function of the acceptance half-angle, the inclination angle and the angular distribution of the diffuse radiance. It is seldom explicitly mentioned that, in the case of an isotropic distribution, the expression $f_{acc} = 1/CR$, where CR is the concentration ratio of the CPC, is only valid if $\beta = 0$. For the general case, for an isotropic distribution, equation 13 can be integrated to give

$$f_{acc} = \begin{cases} \dfrac{2}{CR\,(1+\cos\beta)} & \text{if } \beta + \theta_{acc} \le \pi/2 \\ \dfrac{1+CR\cos\beta}{CR\,(1+\cos\beta)} & \text{if } \beta + \theta_{acc} > \pi/2 \end{cases} \tag{16}$$

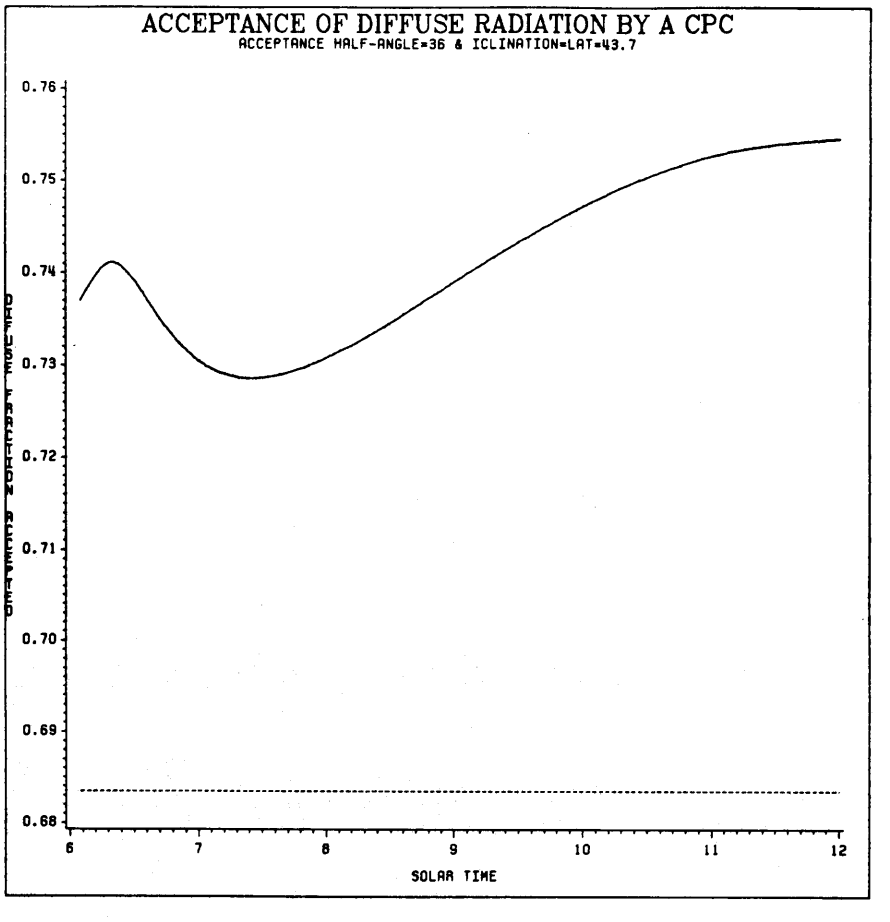

Fig. 2 The fraction of diffuse radiation intercepted by a CPC calculated using the semi-empirical model (solid line) and the isotropic model (dashed line).

Figure 2 illustrates f_{acc} calculated using the isotropic model and the semi-empirical model described in Section 3.9. The CPC is oriented such that its axis lies in the plane of the apparent diurnal path of the

sun. In this case f_{acc} calculated using the heliocentric model would be unity, and would not be a function of the time of the day. While f_{acc} calculated using the isotropic model is also constant, that calculated using the semi-empirical model depends on time through the dependence of the diffuse radiation distribution on the solar position. From Fig. 2 it is found that the values obtained from the semi-empirical model are up to 10% above those for the isotropic model. Similar calculations performed for the same geometry, but for $\beta = 0$, indicate that the semi-empirical model gives values as much as 15% below those for the isotropic model.

5. CLOSURE

This paper has reviewed several models proposed for the angular distribution of diffuse sky radiance, and the physical characteristics of the distributions for a wide range of skies. Models are in general required because the physical processes which give rise to the angular distribution are too complex to manipulate. A wide range of models is required to be able to predict the radiance distribution for the wide range of sky conditions encountered in reality. The different models possess differing degrees of accuracy, complexity, reality, practicability, usefulness, and precision. The selection of a model for a particular application depends on the the nature of the application, the parameters of interest, the degree of accuracy required and the amount of effort to be expended, as well as on other factors.

Acknowledgements – Financial support provided by the Natural Sciences and Engineering Research Council of Canada, and by the Centre for Solar Energy Studies, Tripoli, Libya, and is gratefully acknowledged.

REFERENCES

1. F.C. Hooper and A.P. Brunger, "A Model for the Angular Distribution of Sky Radiance", *Transactions of ASME*, Vol. 102, 1980, pp. 196-202.
2. Centre for Solar Energy Studies, *Solar Radiation Meaurements*, National Academy for Scientific Research (Libya), 1981.
3. G. Mie, "Beigrade zur Optik truber Medien, speziell kolloidaler Metallosungen", *Ann. Physik*, (4) Vol. 25, 1908, pp. 377-445.
4. S. Chandrasekhar, *Radiative Transfer*, Dover Publications, London, 1960.
5. J.V. Dave, "Extensive Datasets of the Diffuse Radiation in Realistic Atmospheric Models with Aerosols and Common Absorbing Gases", *Solar Energy*, Vol. 21, 1978, pp. 361-369.
6. A.P. Brunger, *The Development of an Empirical Model for the Angular Distribution of Sky Radiance*, M.Eng. Project Report, Department of Mechanical Engineering, University of Toronto, 1981.
7. K. Ya, Kondratyev, *Radiation in the Atmosphere*, Academic Press, New York, 1969.
8. K.L. Coulson, *Solar and Terrestrial Radiation*, Academic Press, New York, 1975.
9. C.W. Morris and J.H. Lawrence, "The Anisotropy of Clear Sky Diffuse Solar Radiation", *ASHRAE Trans. Part II*, Vol. 77, 1971, pp. 136-141.
10. N. Robinson, *Solar Radiation*, Elsevier Publishing, Amsterdam, 1966.
11. M.D. Steven and M.H. Unsworth, "The Diffuse Irradiance of Slopes under Cloudless Skies", *Quart. J. R. Met. Soc.*, Vol. 105, 1979, pp. 593-602.
12. L.J.B. McArthur and J.E. Hay, "A Technique for Mapping the Distribution of Diffuse Solar Radiation over the Sky Hemisphere", *J. Appl. Meteor.*, Vol. 20, No. 4, 1981.
13. World Meteorological Organization, *International Cloud Atlas – Volume I, Manual on the Observations of Clouds and Other Meteors*, Geneva, Switzerland, 1975.
14. K.J. Kondratyev and M.P. Manolova, "The Radiation Balance of Slopes", *Solar Energy*, Vol. IV, 1960.
15. J.E. Hay, "Measurement and Modelling of Shortwave Radiation of Inclined Surfaces", Third Conference on Atmospheric Radiation, American Meteor. Soc., Davis, California, June 28-30, 1978, pp. 150-153.
16. G.I. Pokrowski, "Uber eien scheinbarach Mie-Effect ad seine mogliche Rolle in der Atmospharenoptik", *Zeitchrift fur Physik*, Vol. 53, 1929, pp. 67-71. (As cited in reference 7, p. 122).

17. J.W. Walsh, *The Science of Daylight*, MacDonald, London, 1961.

18. M.D. Steven, "Standard Distributions of Clear Sky Radiance", *Quart. J. Roy. Meteor. Soc.*, Vol. 103, 1977, pp. 457-465.

19. R. Dogniaux, "Variations Geographiques et Climatiques des Expositions Energetiques Solaires sur des Surfaces Receptrices Horizontales et Verticales", *Inst. Roy. Met. Belg.*, Misc. ser. B, No. 38, 1975.

20. R.G. Hopkinson, "Measurements of Sky Luminance Distribution at Stockholm", *J. Opt. Soc. Am.*, Vol. 44, 1954, pp. 455-459.

21. M.D. Steven and M.H. Unsworth, "The Angular Distribution and Interception of Diffuse Solar Radiation Below Overcast Skies", *Quart. J. R. Met. Soc.*, Vol. 106, 1979, pp. 57-61.

22. P. Moon and D.E. Spencer, "Illumination from a Non-Uniform Sky", *Trans. Illum. Engng. Soc. N.Y.*, Vol. 37, 1942, pp. 707-726.

23. S. Fritz, 1955, "Illuminance and Luminance under Overcast Skies", *J. Opt. Soc. Amer.*, Vol. 45, 1955, pp. 820-825 (As cited by reference 6).

24. J. Goudriaan, *Crop Micrometeorology: a Simulation Study*, Centre for Agricultural Publishing and Documentation, Wageningen, Netherlands, 1977.

25. F.C. Hooper, A.P. Brunger and C.S. Chan, "A Clear Sky Model of the Diffuse Sky Radiance", *ASME Solar Energy Division*, 4th Annual Technical Conference, Albaquerque, 1982.

26. C.S. Chan, *The Measurement and Modelling of the Distribution of the Diffuse Sky Radiance*, M.A.Sc. Thesis, Department of Mechanical Engineering, University of Toronto, 1979.

27. M.D. Steven, *Angular Distribution and Interception of Diffuse Solar Radiation*, Ph.D. Thesis, Department of Physiology and Enviromental Studies, University of Nottingham, School of Agriculture, 1977.

28. M.A. Rosen, *The Characterization and Modelling of the Angular Distribution of Diffuse Sky Radiance*, M.A.Sc. Thesis, Department of Mechanical Engineering, Universty of Toronto, 1983.

29. F.C. Hooper and A.P. Brunger, *Observation of the Sky-diffuse Shortwave Solar Radiation*, Final Report, Prepared for the Atmospheric Enviroment Service (Canada), 1982.

30. A.P. Brunger, *The Magnitude, Variability, and Angular Characteristics of the Shortwave Sky Radiance at Toronto*, Ph.D. Thesis, Department of Mechanical Engineering, University of Toronto, 1987.

31. M.A. Rosen and F.C. Hooper, "A Model for the Instantaneous Distribution of Diffuse Sky Radiance", *Proc. 11th Canadian Congress of Applied Mechanics*, 31 May-4 June, Edmonton, Alberta, 1987, pp. E104-E105.

32. M.A. Rosen and F.C. Hooper, "A Calibration of the Three Discrete Components Model", *Proc. 10th Biennial Congress of the Int. Solar Energy Soc.*, 13-18 September, Hamburg, West Germany, 1987.

33. F.M.F. Siala (Private Communication), 1988.

34. F.M.F. Siala, M.A. Rosen and F.C. Hooper, "An Investigation of the Statistical Nature of Sky Radiance: the Relation between Mean and Standard Deviation" , *Proc. 10th Biennial Congress of the Int. Solar Energy Soc.*, 13-18 September, Hamburg, West Germany, 1987.

35. F.M.F. Siala and F.C. Hooper, "Stochastic Modelling of the Angular Distribution of the Diffuse Radiance", *Proc. 10th Biennial Congress of the Int. Solar Energy Soc.*, 13-18 September, Hamburg, West Germany, 1987.

DEVELOPMENT AND APPLICATION OF PASSIVE SOLAR ENERGY TECHNOLOGY FOR THE HOT_DRY ZONES

Said M. S. Bukamur

P.O.Box 906 Tripoli Libya

ABSTRACT:

The goal of this paper is to provide architects who work in Hot_dry climate zones,with a better understanding of potential design strategies for the building envelope and its relation to certain environmental control guide lines to achieve human comfort inside residential buildings. The other aim, is to help reduce per capita consumption of energy in housing projects, through effective conservation practices.These practices are based on passive solar energy design methods applied in the architectural design proposed by the outhor for the 3000 dwelling project in Sebha.

1_Analysis and discusion of climatic data & details of design:

Sebha, is one of the hot arid regions in the southern part of Libya. Undesirable winds blow from almost all directions. Besides, it is not appropriate to achieve comfort indoors using mechanical and electrical solutions,becuase of sand migration and lack of maintenance services. Hence, more attention was payed to climatic control through architectural design of the previous mentioned project in Sebha.

To give a clear review ofthe annual climatic situation of Sebha, combined temperature and relative humiditiy are plotted on the bioclimatic chart (fig.1).
To present the yearly needs during daytime hours,percentages of the registred climatic data of each month were calculated according to their location on the chart. Results were as follows: 21% required sun heat, 79% shade, 39% wind protection, 25% breeze for cooling and ventilation, 27% other additional cooling methods ; and 9% of the time falls within the comfort zone (1).

Like wise from the summary of design strategies chart, one can realize that both cooling and heating design stategies are needed for Sebha to achieve comfort indoors (fig.2). However, just cooling design strategies are emphasized in the next part of this paper, as a dominant requirement of desgin in Sebha.

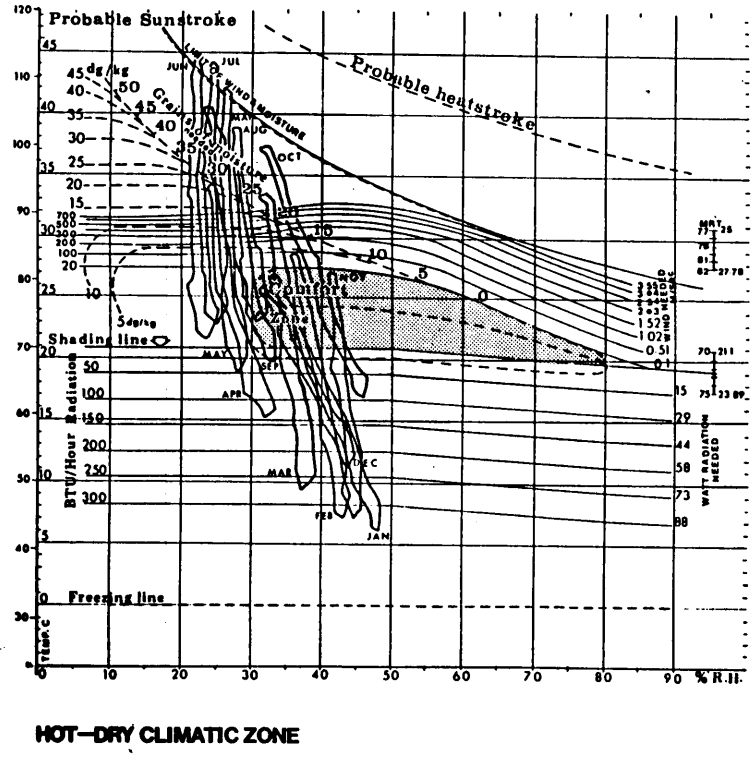

Fig.1. Evaluation of Sebha zone "bioclimatic registration of climatic data".

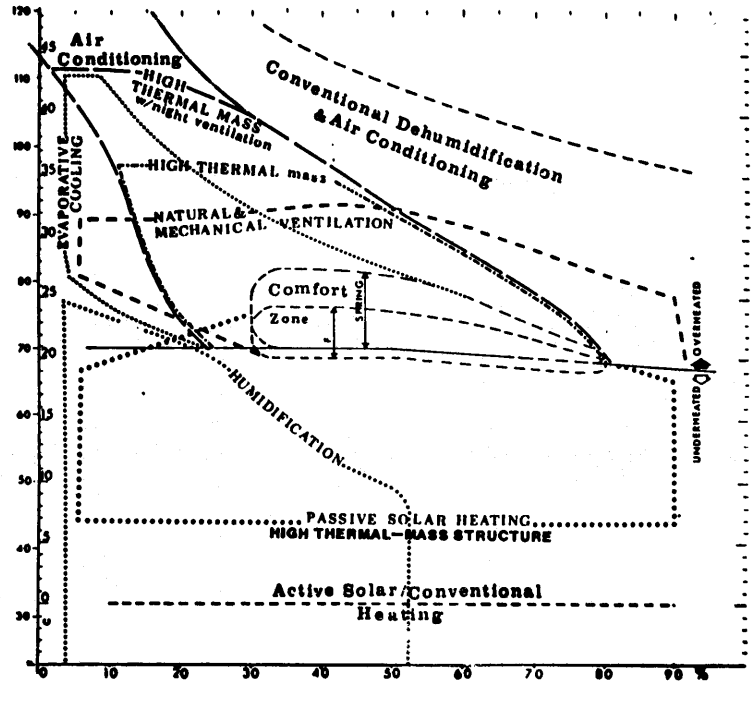

Fig.2. Summary of design strate[illegible] "combined method".

COOLING DESIGN STRATEGIES:

(A): Passive cooling of high_mass structure:

This strategy takes care of the high marked variatin of temperature between day and nighttime for the over heated period curves within its limits. The thermal mass of buildings required to this phenomena in Sebha is estemated by 3000 Kg/m^2 of the floor area (2). This is achieved through compactness of building design,thick walls of local mud and self_shaded structure.

The macro unit of design consistes of four houses,two in the ground floor and two in the first floor connected with a semi covered pedestrian pathways composed of overhang rooms. This element works as a deep shading device connected together with two open spaces in each unit to prevent trpped air and heat build_up. The first floor is designed so taht its elements create four colonaded arcades surrounding the courtyard of the ground floor with no windows facing the neighbors courtyard.

(B): Passive cooling of high_mass structure with programmed nighttime ventilation:

The main concept of this strategy is to cool the building interior mass using the prevailing nighttime breeze and to close it during the hot daytime. In Sebha the estimated daily potential for convective cooling using night air is between 5 and 7 mjm^2_day, which is almost appropriate to achieve comfort indoors (3). For the efficiency of this strategy, more attention is payed to the criterion of optimum orientation, wind protection and solar insulation, during the proposed design of the project.

a. Criterion of optimum orientation:

Using Olgyays method to determin the optimum orientation for dweelings, the total annual solar radiation incident on a diffrently oriented vertical walls is calculated for the underheated and overheated period and plotted on the chart (fig.3).

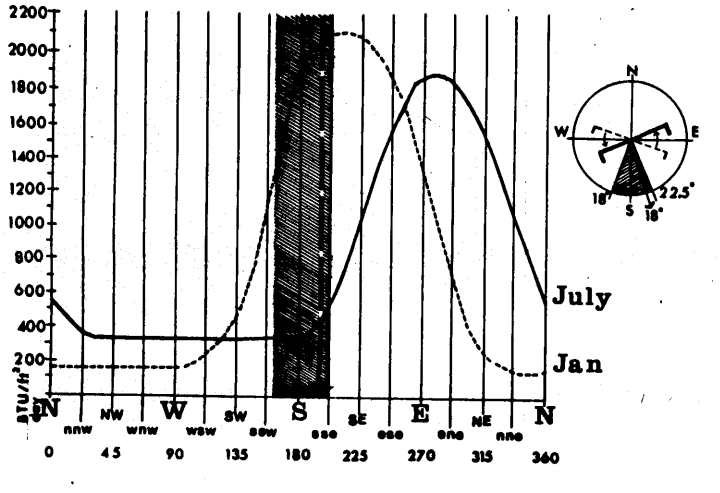

Fig.3 The optimum orientation for housing design in Sebha.

The line connecting between the maximum solar radiation gained by the vertical walls in winter and the minimum solar radiation gained by some walls in summer is ranging between due south and 18 to east of south.Likewise, the desirable orientation is between 18 west of south and 22.5 east of south. However; recognizing the other factros of wind directions and effect of sand, the optimum orientation applied for the project is from south to 10 west of south.

b. Wind Protection:

The undesirable wind in Sebha blow from almost all directions. the previously mentioned orientation from optimal solar radiation control exposes the building to the same axis as the most undesirable ~ghibly~ wind which associated with blowing sand and high temperature. Likewise the optimum direction of the N_NNE_NE, desirable breeze falls within the same axis of the S_SSW_SW hot winds of speed reeching 6_9m/sec, while the speed of breeze do not exeed 2 m/sec, (5) .

Solving this problem, rooms are organized surrounding its own courtyard open to the sky and connected to the backyard and suitable oriented to provide sufficient wind speed to the prevailing night time breeze inside the interior spaces Location and size of windows are carefully designed to catch prevailing breeze and oriented twoards the open courtyards in the ground and first floor. Each house is also provided with a private terrace roof for the family activities. The estimated potential for convection cooling using this element vary from 150_400 kjm^-2_h. (6).

c.Solar insulation:

The total amount of solar radiation on clear days, striking the differently oriented vertical walls, is illustrated for 27 N latitud of Sebha (fig.4). From the chart , it is clear that the south_facing side recieves the maximum amount of direct solar radiation in winter and the minimum amount in summer.

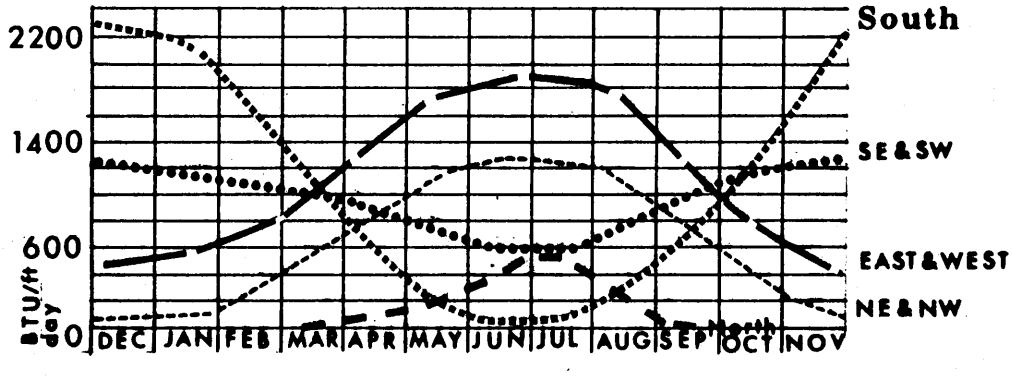

Fig.4. Direct solar radiation incident on different oriented walls in BTU/ft^2/day for clear days throughout the year.

The maximisation of shade and the minimisation of the wall surfaces exposed to the sun required are achieved through a self _shaded structure and self_ventilated overhangs to prevent the heighest amount of solar radiation occurs between 9:00 am (morning)and 4:00 pm (afternoon). Moreover, all rooms are organized to open direct to the open courtyard. Windows of guestrooms and living rooms facing south are provided with deep horizontal overhangs and vault roofing in the first floor. In order to form the brick work roof vaults ofthe upper guestroom, precast fiber_reinforced cement shells are proposed to act as formwork. The other rooms take advantage of every morning and late afternoon sun (Fig.5&6).

(C):Natural and Mechanical Ventelation For Cooling:

AS stated previously, about 25% of the overheated period of Sebha climatic data falls within the limit of natural and mechanical ventelation design strategy. Cool breeze have 25% yearly prevalence during summer and winter from N_NE direction with speed of 1.5m/sec. The most undesirable hot sandy winds of SE_S is called ~ghibly~ with a high speed of 30_45 knots (4 to 6msec), and yearly prevalenc ranging between 4 and 21%.

Laboratory and field studies, observed that the courtyard house is very good dust barrier for such conditions to improve living(7). The inlet and outlet windows are designed of almost equal size facing the courtyard on a wall of 35cm thickness of local mud.

(D): Evaporative cooling:

The concept of the evaporative cooling design strategy is based on using the surounding air temperature to evaporate water. However; becuase the lack of water in Sebha, some social means are adopted to surve this strategy replacing old Arabic fountain in the courtyard.

The required water of the common daily use, is provided through a water tap over a concreate washtub. It is located in the oped area connecting between the main courtyard and the backyard which acts as a cloth dreyer area facing the prevailing cool breezes. The washtub is designed so that a suitable amount of water is always remain below the waste pipe to be evaporated.Vapour of cloth dryer, green plants and the vapor of the remaining water of the wash tub, then is drived by the prevailing breezes twards the rest of the house.

3_ Conclusion:

The most effecient design criteria for the hot_dry climte are based on three critical points . First, is to minimise solar heat penetration and maximize reflective outsisde vertica surfaces. Then, is to use thermal in a structure to delay the effect of the intense solar radiation during daytmie to give it back or reject it to the interior 12 hours later to decrease the effect of cold nights during the early morning period. Finaly, is to chose the best orientation of building allowing the cool prevailing breezes and preventig the builing from the sand hot winds.

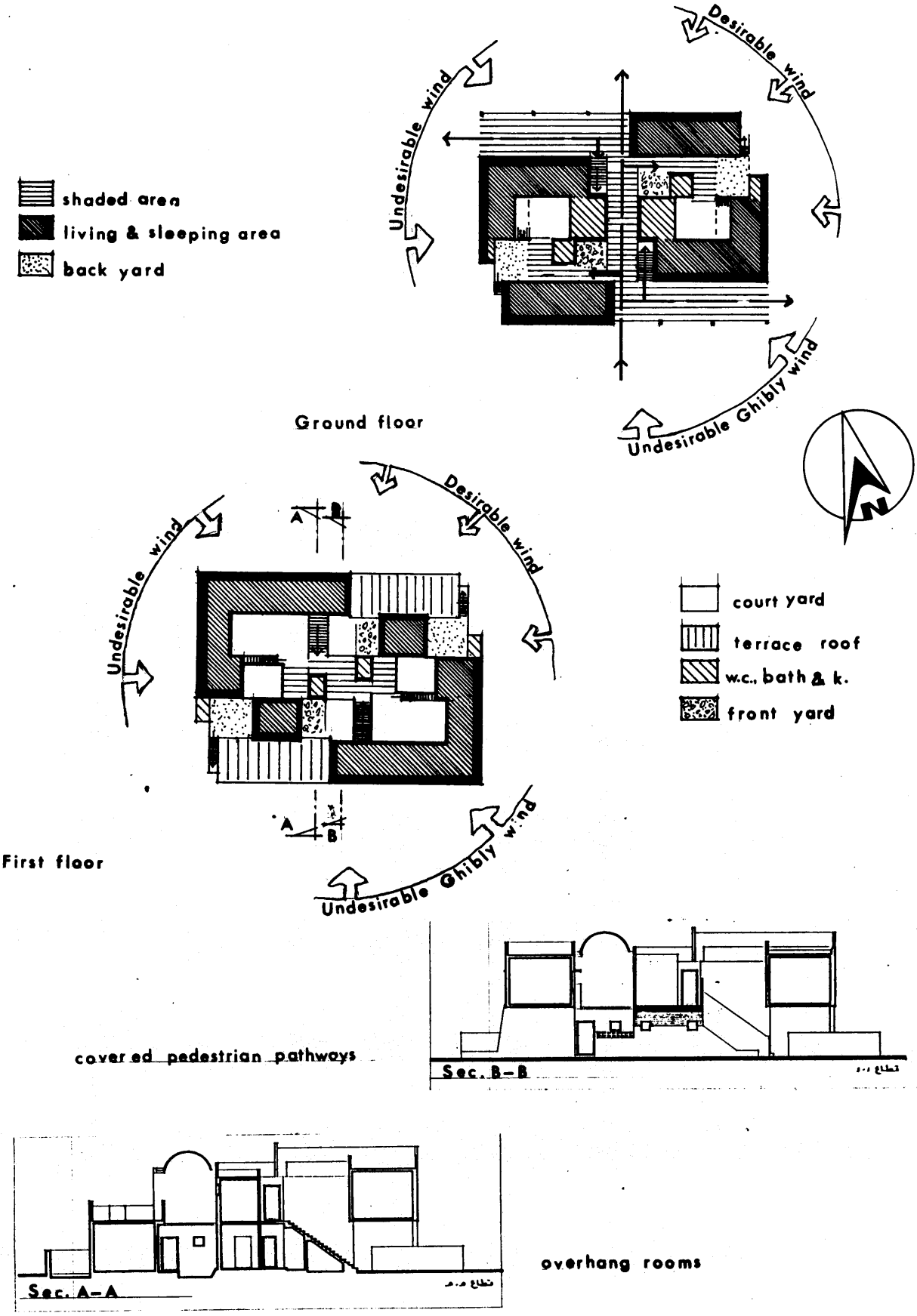

Fig.5. Orientation, solar insulation and wind protection for the macro unit of design.

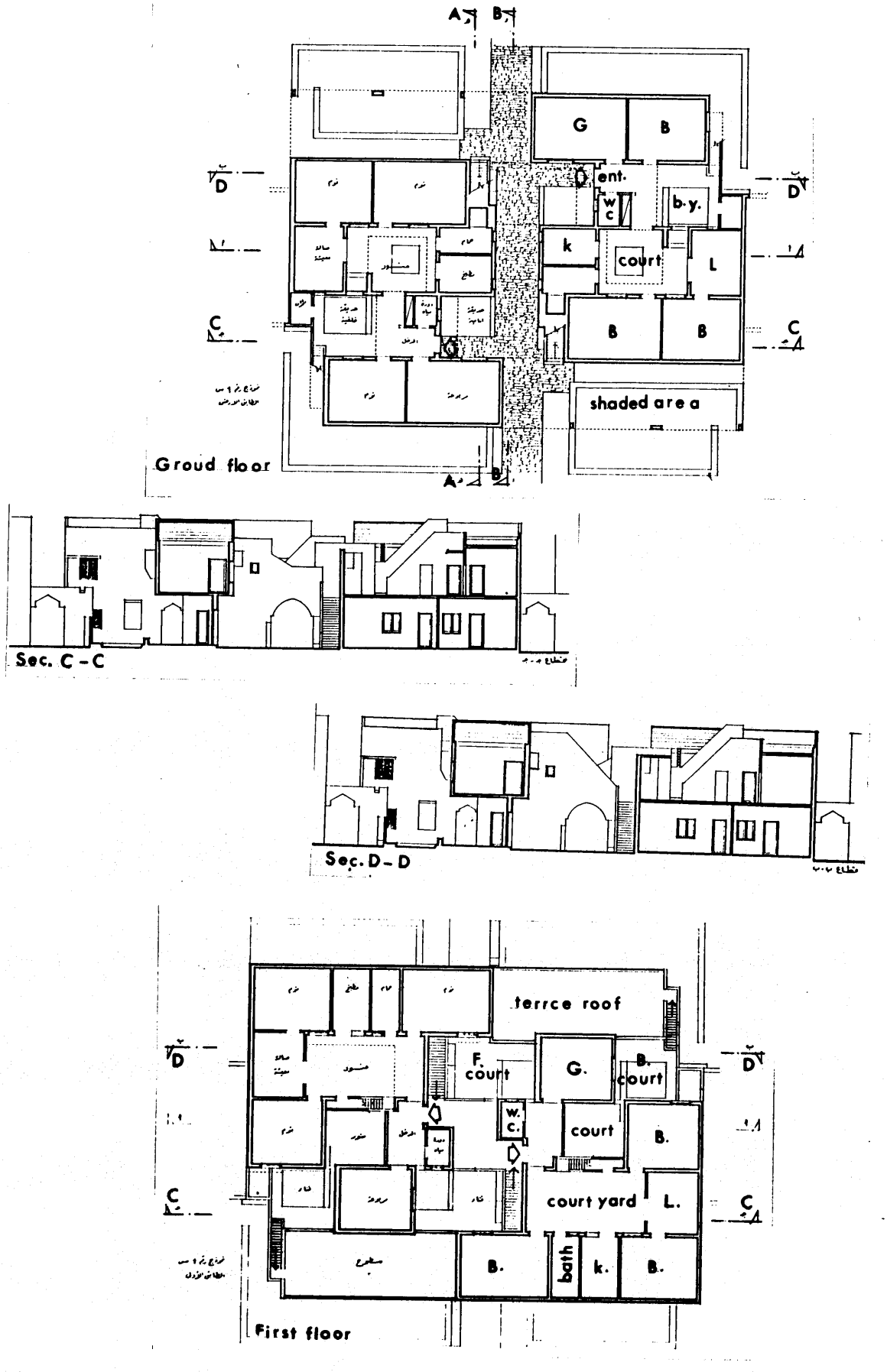

Fig.6. Plans and sections showing the arrangement of rooms.

REFRENCES:

(1)_ Bukamur,Said m.,Design Guidelines For Housing In Libya Based On Climatic and Social Critiria,University Of Microfilms International,Ann Arbor, Michigan, U.S.A.,1985.

(2)_ Ahmad,I.and Abughres,S.M.,Passive Convective Cooling For Libya,Center Of Solar Energy Studies,Tripoli, Libya, Sep.1984.

(3)_ Olgyay,Alador,"Solar Control And Orientation To Meet Bioclimatic Requirements",In Housing And Building In Hot_humid And Hot_dry climates,Research Comfrence Report no.5, National Academy Of Science, 1953.

(4)_ Olgyay,Victor,Design With Climate,Bioclimatic Approach to Architectural Rigionalism,Princeton University Press, Princeton, New Jersy, Fourth printing, 1973.

(5)_ Anderson,abruce, The Solar Home Book:Heating,Cooling And Design With Sun, Brick House Publishing Co., Inc., Massachusttes, 1976.

(6)_ Mashina,M.A.,And Addaly,A.R.,"Applications Of Passive Solar Energy In Residential Buildings",In Alhandasy, Tripoli Libya,Apr. 1988.

(7)_ AIA,Development Of Improved Design Criteria To Better Resist Effects Of Extreme Winds For Low_rise Buildings In Developing Contries, U.S. Government Printing Office , Washington, D.C, 1974.

ON TILTED SOLAR RADIATION IN NORTH AFRICA

DR. M.S. SMEDA

Civil Aviation and Meteorological Office
P.O. Box No. 5069, Tripoli, Libya.

Abstract: Measured global radiation on the horizontal for selected stations in Libya and Morocco have been used as input data to calculate direct radiation received on the horizontal and inclined planes. Measured data revealed that yearly daily average is of order 5 Kwh/m^2 and over 70% of the total received in a direct form. Direct radiation received on inclined planes facing South is presented. The model in use is still to be verified when measurements of direct radiation and measurements on inclined planes are obtained in areas under consideration.

Symbols

Isc	:	Solar constant = 1353 Watt
h	:	Hour angle
n	:	Day of the year (Starting first of January)
ϕ	:	Latitude
δ	:	The solar declination
α	:	Tilt angle to the horizontal
H	:	Daily average radiation on a horizontal plane
H_o	:	Extraterrestial radiation on a horizontal palne.
H_d	:	Diffuse radiation
$\overline{K}$	:	Recalculation factor.
N	:	Number of years

1. INTRODUCTION

During recent years and specially after the oil crisis in the Seventies, the problem involved in finding other sources of energy have become topics of increasing interest to many disciplines. To solve diverse problems in solar energy applications, it is essential to have a basic data on the radiation regime of oriented surfaces of different angles. Data of [illegible]tion on inclined planes are extremely rare and none of such measurements took place in our area. However, measurements of global radiation on horizontal planes have recently started and the available data have been used for calculating diffuse and hence direct radiation, where

Liu-Jordan method has been used. In estimation of radiation components on inclined plane, the recalculation factor at the earth surface is assumed to be equal to that value at the top of the atmosphere (air mass = 0). The short period observations as totals of one hour, for example, is not available and hence our computations are restricted to the daily average of the month and the recalculation factor for the monthly mean has been used which is less dependent on cloud amount and atmospheric transparancy.

2. THE MODEL

a) The daily extraterrestial radiation on a hoizontal plane is given by:

$$H_o = \frac{24}{\pi} \text{Isc} \quad (1 + .033 \cos \frac{2\pi n}{365}) \; (h \sin\phi \sin\delta + \cos\phi \cos\delta \sin h) \quad (1)$$

When the surface is inclined by an angle on the horizontal, then ϕ should be replaced by $(\phi - \alpha)$ in the above equation.

Following Liu-Jordan, the daily diffuse radiation is computed by the formula:

$$H_d = K_T \; (1.390 - 4.027 \; K_T + 5.531 \; K_T^2 - 3.108 \; K_T^3) \quad (2)$$

$$\text{where } K_T = H/H_o \quad (2a)$$

and hence the short wave direct radiation reaching the earth's surface on a horizontal plane is obtained by substracting the diffuse from the observed total H.

The next step in the computation is to calculate the direct bean radiation on inclined surfaces. The Main assumption here is that the recalculation factor at the top of the atmosphere is the same as that of the earth's surface and for a surface facing the equator, the recalculation factor is given by:-

$$\bar{K} = \frac{H_o(\alpha)}{H_o} = \frac{h \sin(\phi - \alpha) \sin\delta + \cos(\phi - \alpha) \cos\delta \cosh}{h \sin\phi \sin\delta + \cos\phi \cos\delta \cosh} \quad (3)$$

Equations (1), (2) and (3) is a closed system and can be solved to produce the three unknowns H_o, H_d and $\bar{K}$ in terms of ϕ, α, δ, h, Isc and the measured global radiation H at the surface.

b) After having values of $\bar{K}$ and H_d, B and $B(\alpha)$ are computed by

$$B(\alpha) = \bar{K} \; B \quad (4)$$

$$\text{Where } B = H - H_d \quad (4a)$$

The calculation of total radiation on inclined surface requires knowledge of the ground albido. An approximate value of 0.2 has been used in the computation. In addition, an isotropic approximation for the diffuse and reflected radiation from the ground is assumed and hence the total

radiation on inclined plane is given by:

$$H(\alpha) = B(\alpha) + H_d(1+\cos\alpha)/2 + 0.2\,H(1-\cos\alpha)/2 \qquad (5)$$

Equations (4) and (5) produce values of direct solar and global radiation received on inclined planes over the earth's surface.

3. INPUT DATA

The only measured available data used in the computation is the daily global radiation at the earth's surface on a horizsontal plane. All the computations are carried out for the daily total average for each month. Five stations have been selected in Libya, two over the coast Tripoli and Shahat, three in the south; Kufra in the east, Ghat in the west, and Hon somewhat in the middle. The data is of four years period (1981-1984). A sixth station in the Casa Blanca is considered also specially this latter has a fourteen years data record (1970 - 1983) and almost at the same latitude as the Libyan coast. The input data is summarized in the following table.

Observed daily average of global radiation for each month on a horizontal plane received at the earth's surface (Kwh/m^2)

Station (lat) \ Month	JAN	FEB	MAR	APR	MAY	JUN	JUL	AUG	SEP	OCT	NOV	DEC	N
Tripoli (32° 54')	3.0	4.1	5.2	6.1	6.7	7.3	7.3	6.6	5.6	4.0	3.1	2.4	4
Shahat (32° 49')	2.2	3.0	4.3	5.5	6.3	6.9	6.6	6.4	5.2	3.8	2.8	2.0	4
Hon (29° 08')	3.7	4.5	5.4	6.4	6.8	7.4	7.3	6.9	6.1	4.7	3.9	3.4	4
Kufra (24° 13')	4.6	5.6	6.5	7.1	7.3	7.6	7.3	7.3	6.7	5.9	5.0	4.1	4
Ghat (24° 57')	4.3	5.0	5.9	6.5	6.4	6.9	7.3	6.6	6.4	5.1	4.5	3.7	4
Casa Blanca (33° 34')	2.7	3.5	4.7	5.8	6.5	6.8	6.9	6.3	5.5	4.1	3.0	2.5	14

4. RESULTS AND DISCUSSIONS

The main task of this work is to find out values of solar radiation over inclined planes where no such measurements have been taken. Two main runs have been performed:

(i) To compute the daily average of extraterrestial radiation for each month and to find out the horizontal diffuse radiation using Liu-Jordan method.

(ii) To deduce the beam radiation on the horizsontal and to compute values of monthly daily average of measured global radiation and deduced beam radiation on different inclined planes mainly on 30, 60 and 90°.

The measured total radiation on the horizontal and computed on inclined planes facing south are shown in figures 1, 2, 3, 4, 5 and 6 for the corresponding choosed stations. Observed data indicate that the yearly daily total average is of order 5 Kwh/m^2, with highest value occurs during June and July and of order 7 Kwh/m^2.

Calculations have shown that the yearly daily direct solar radiation represents 70% of the received total on the horizontal over coastal stations as Tripoli and Casa Blanca, and it is of order 75% of the total in stations situated in the south as Ghat and Kufra. We may observe also that more heat would be received on inclined planes during cold months (Sept-March) than that received on the horizontal and less heat received in summer time.

ACKNOWLEDGEMENT:

The author would like to thank Miss Suad Mazeg from the Libyan Met. Department for her help in executing the computer programme of this work.

Data supplied by Met. Department of Morocco, used in this study, is highly appreciated. Also we thank AGIP Exploration Company for providing computer facilities.

REFERENCES

S.A. Klein, "Calculation of monthly average Insolation on tilted surfaces", Solar Energy Vol. 19, pp 325-329, 1977.

WHO Technical note No. 172, "Meteorological Aspects of the Utilization of Solar Radiation as an Energy Source", 1981.

M.S. Smeda, "Solar radiation and wind measurements in Libya", Libyan Met. Department internal report, presented in Conference on appropriate utilization of solar energy in the Arab World, Tripoli, April 23-26, 1984.

Fig:1

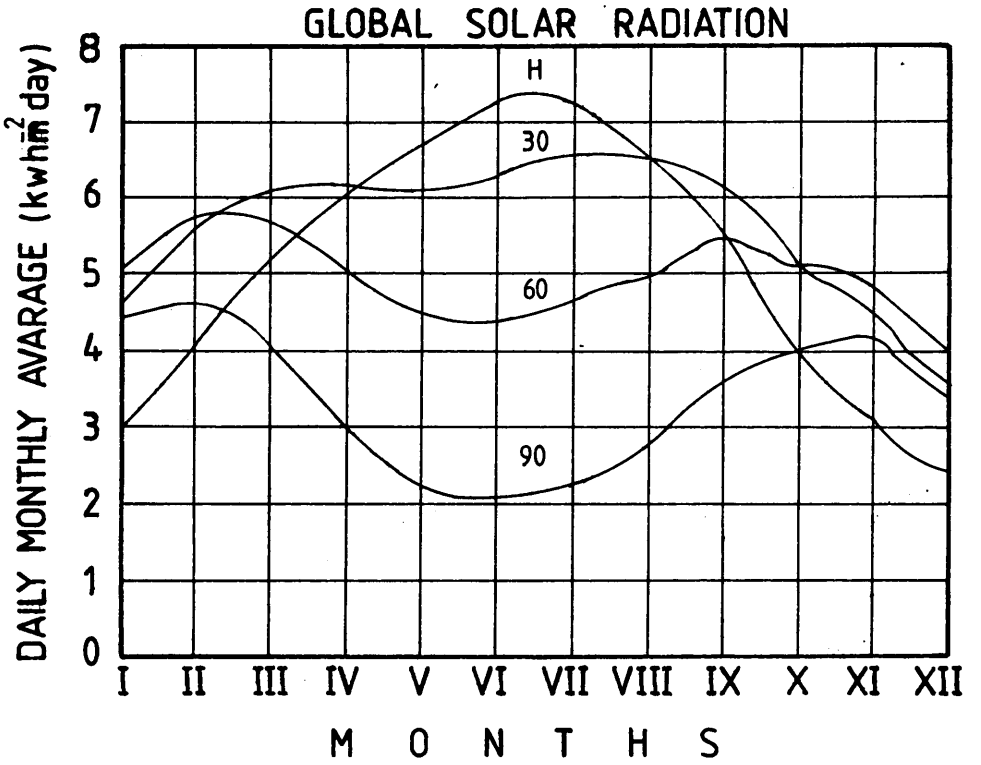

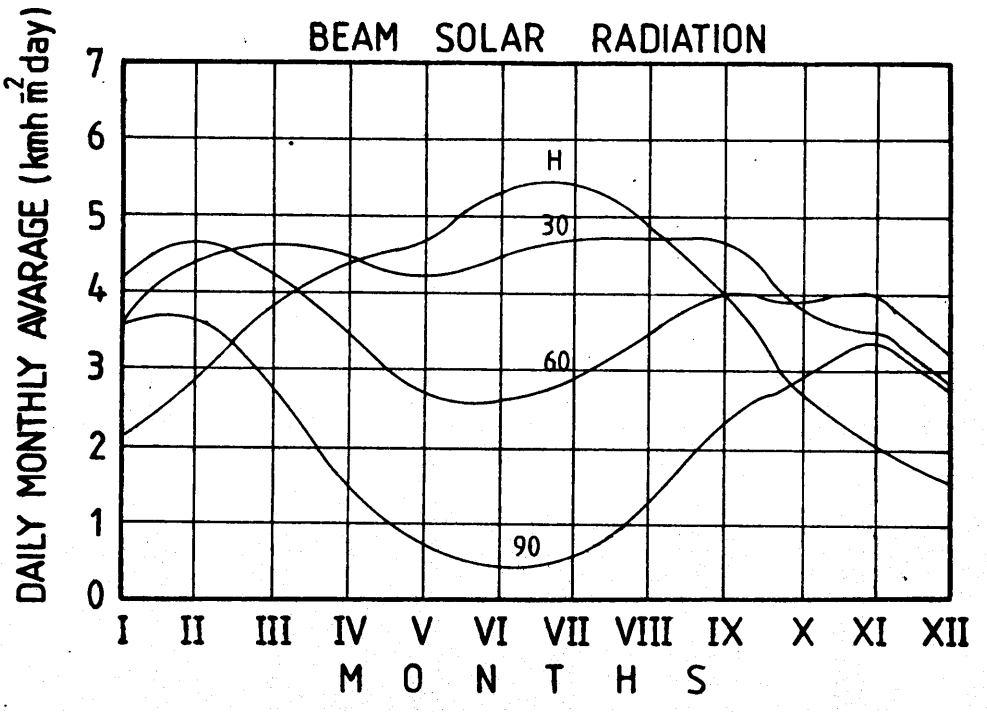

STATION : TRIPOLI

Fig: 2

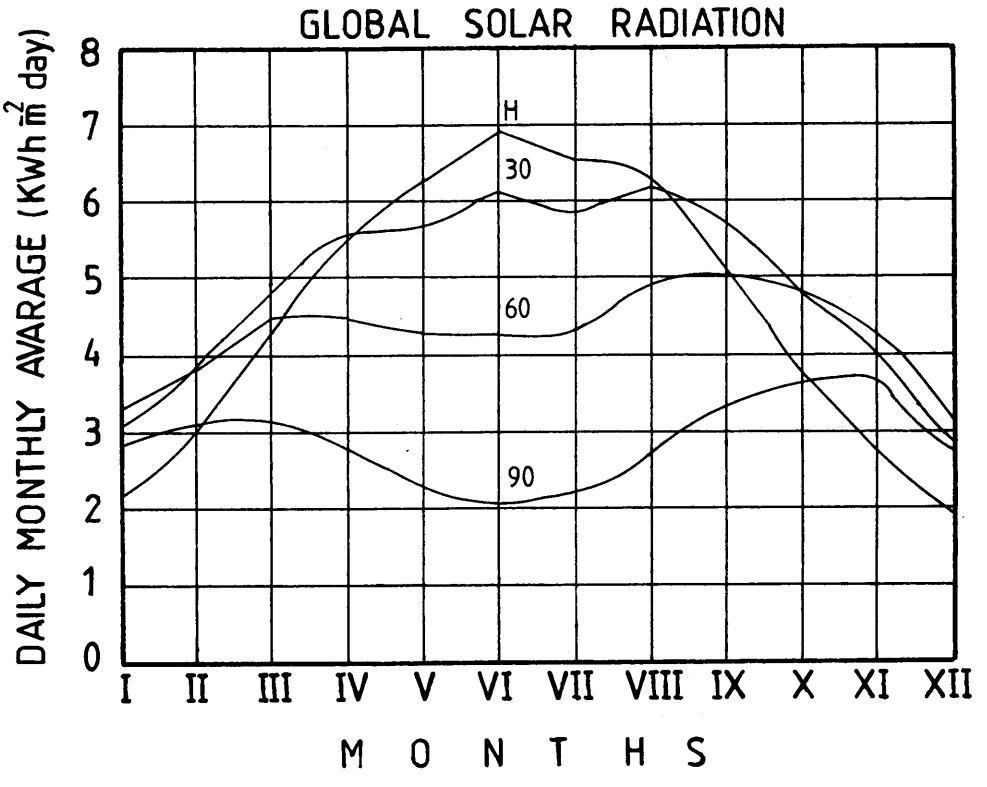

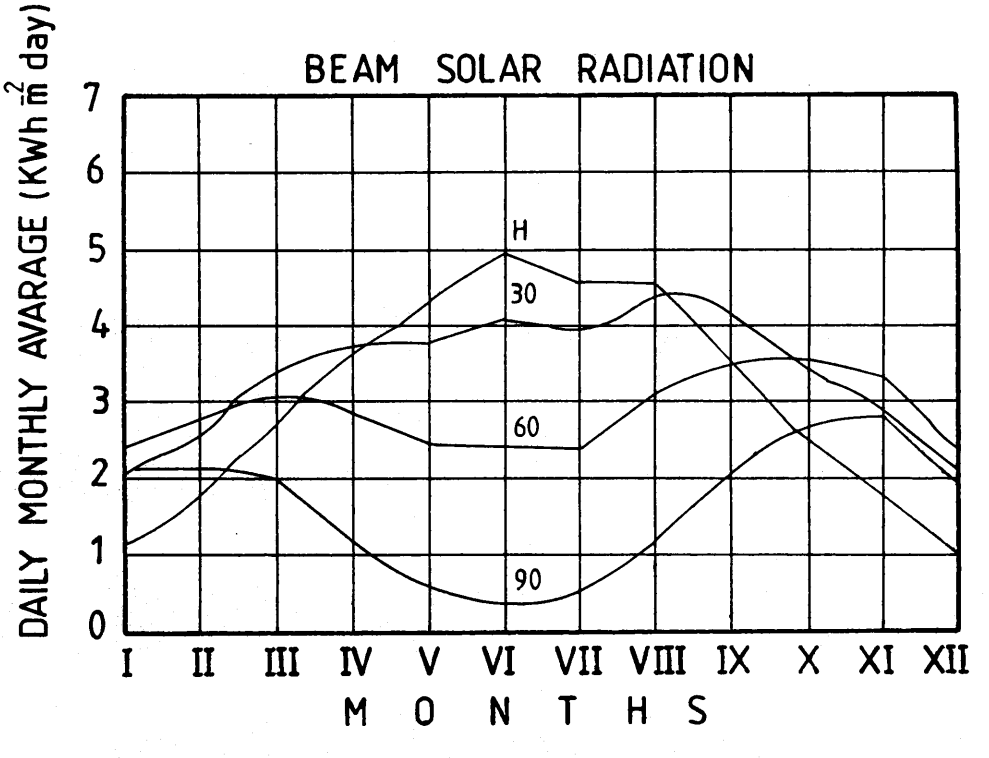

STATION : SHAHAT

Fig : 3

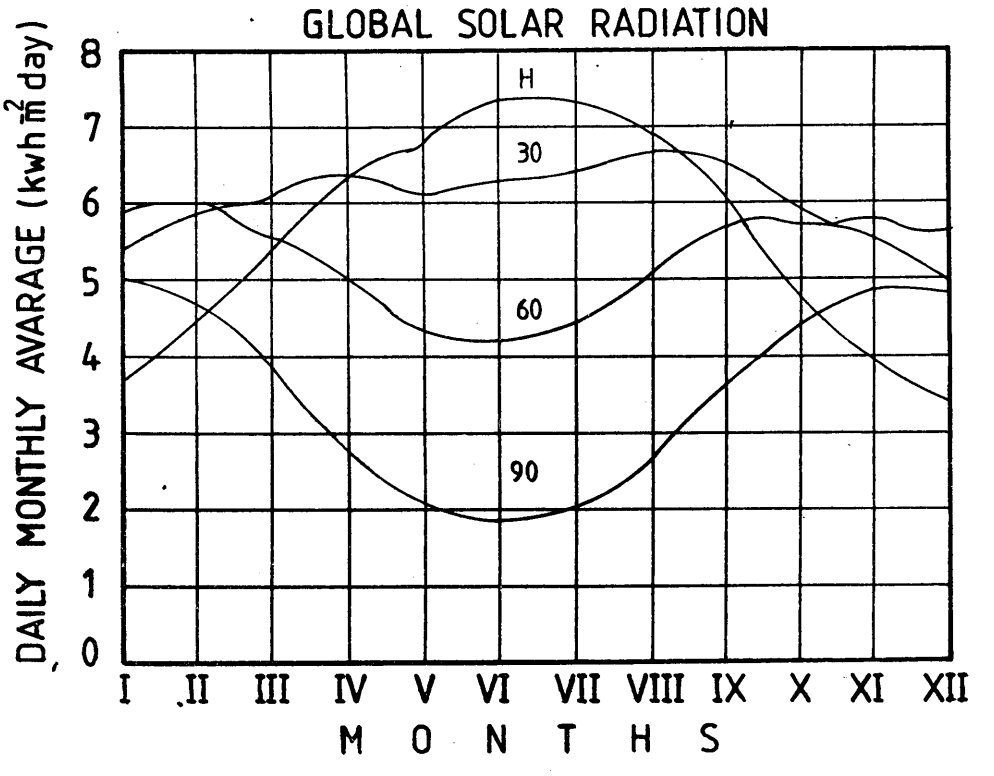

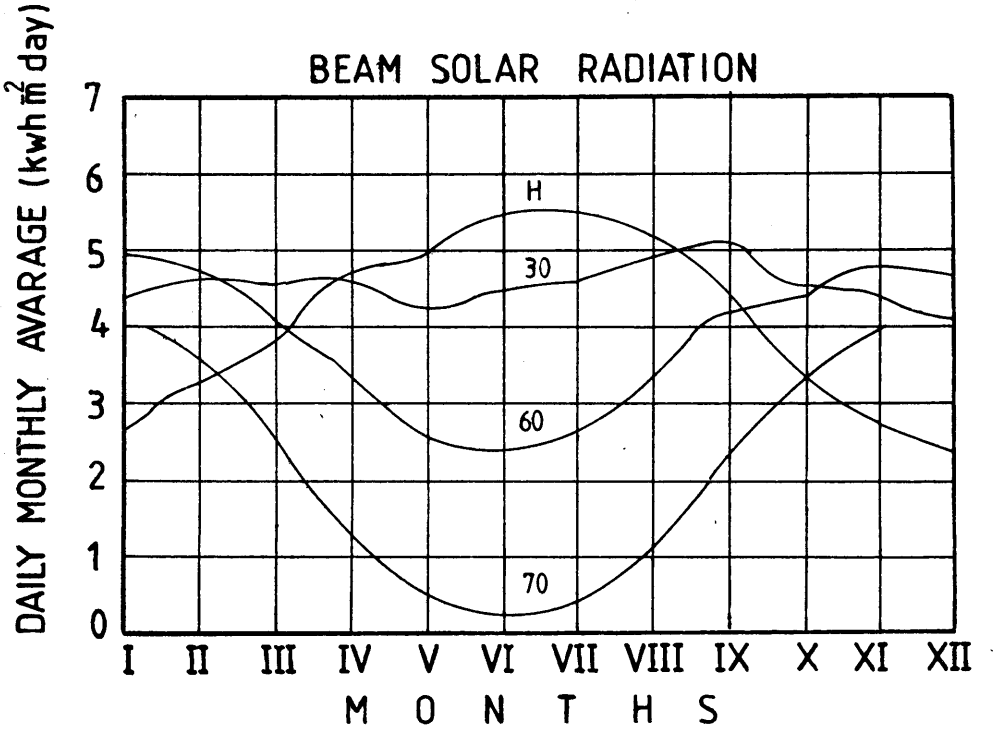

STATION : HON

Fig : 4

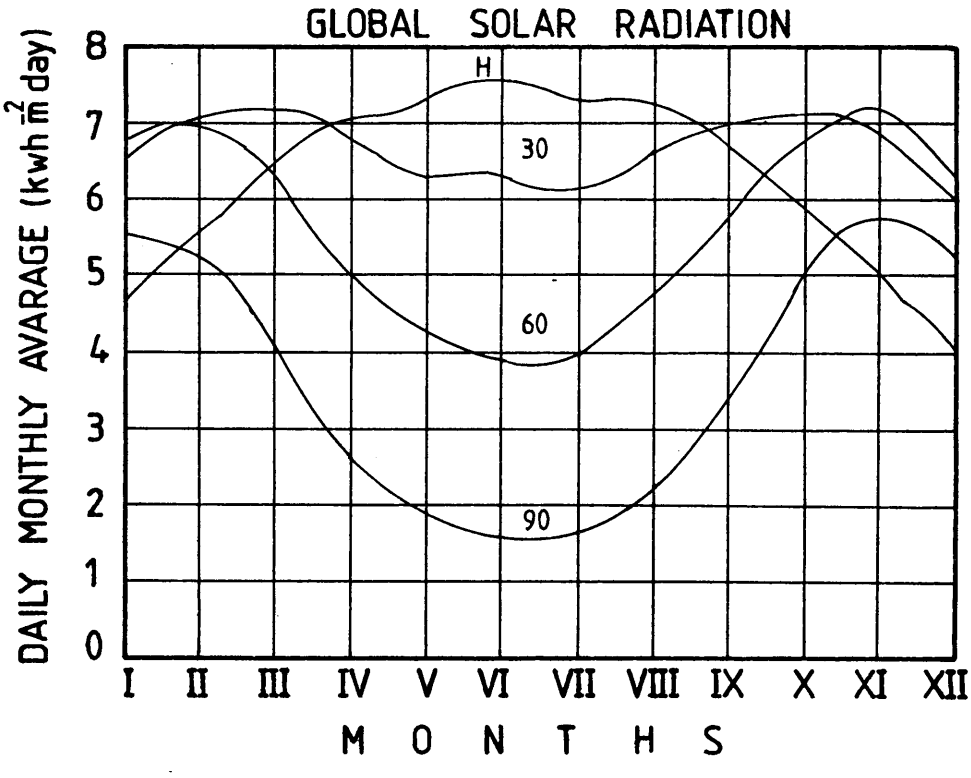

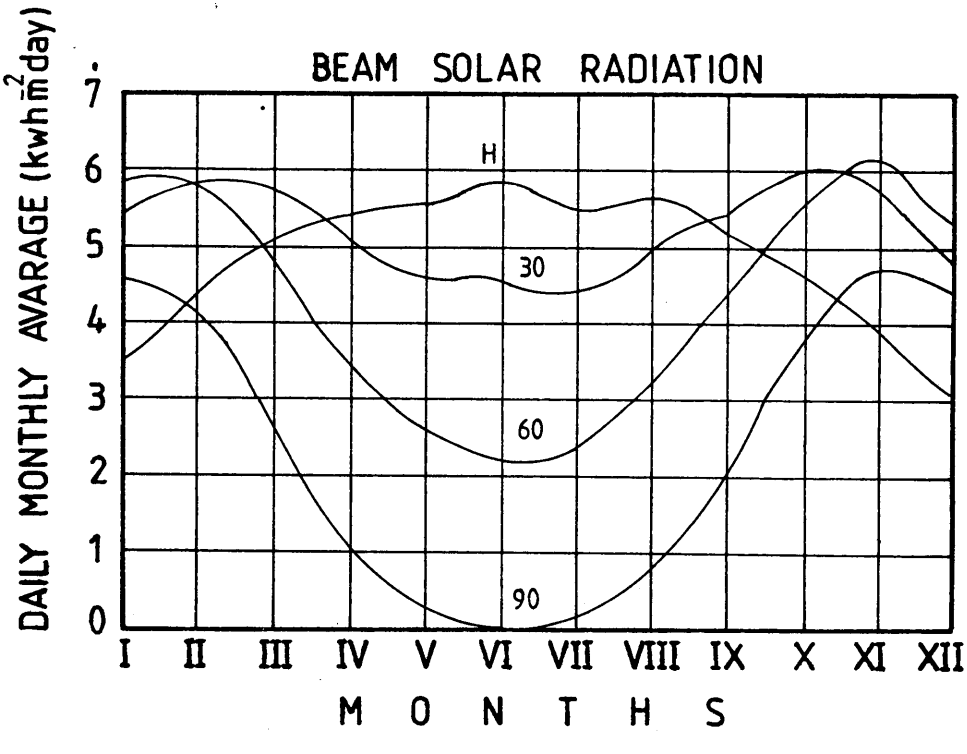

STATION : KUFRA

Fig : 5

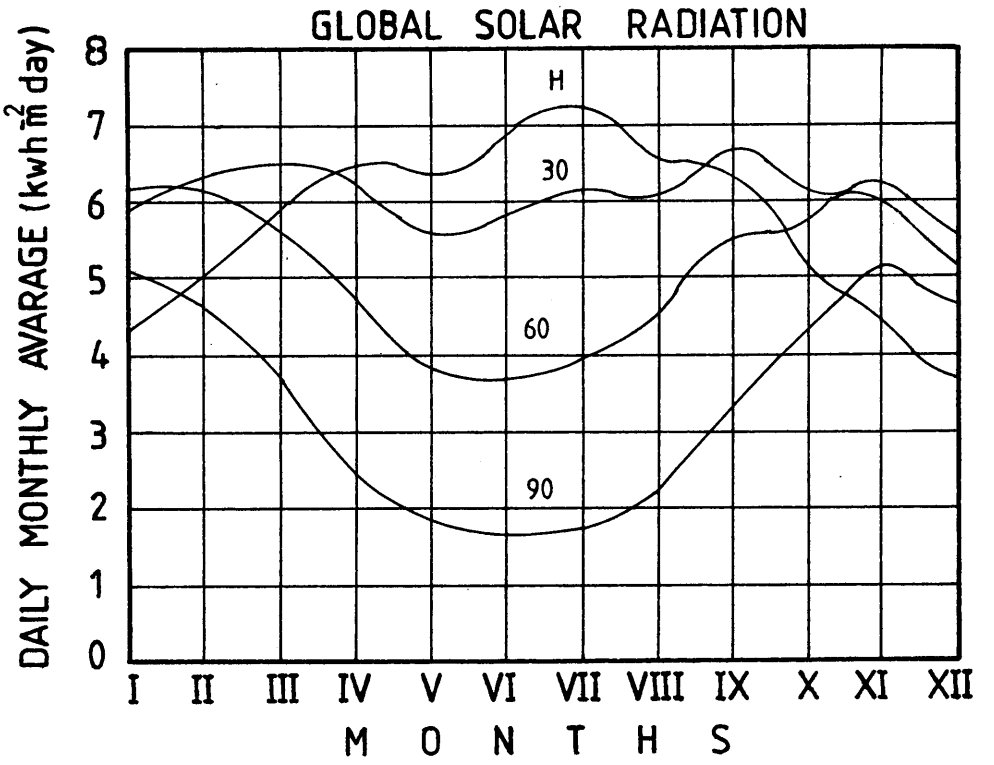

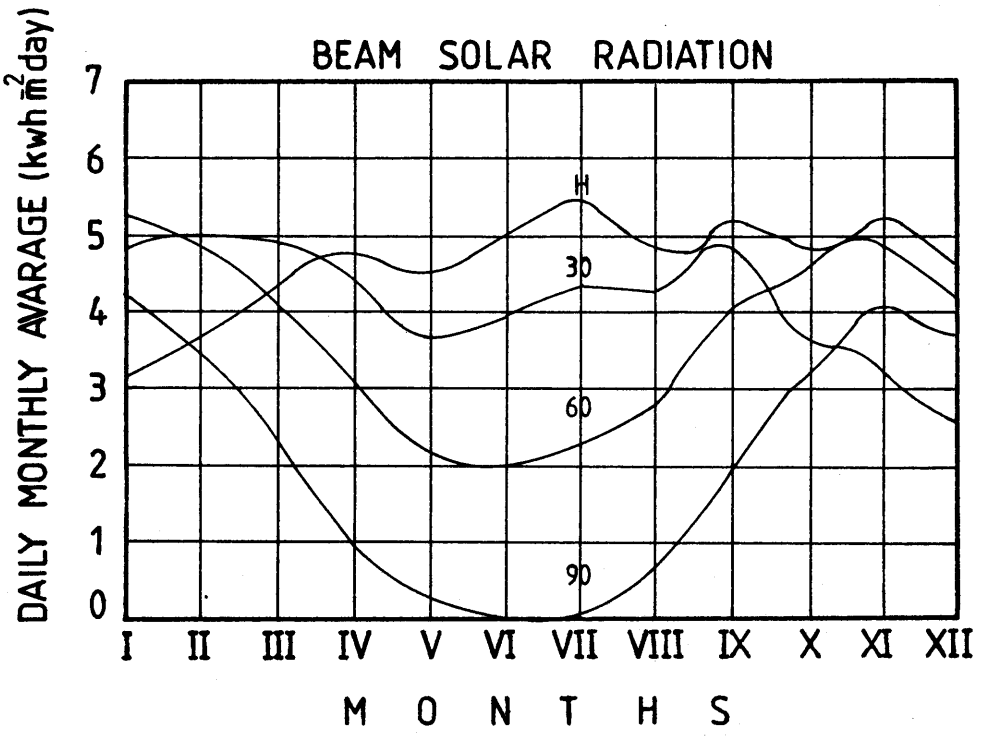

STATION : GHAT

Fig: 6

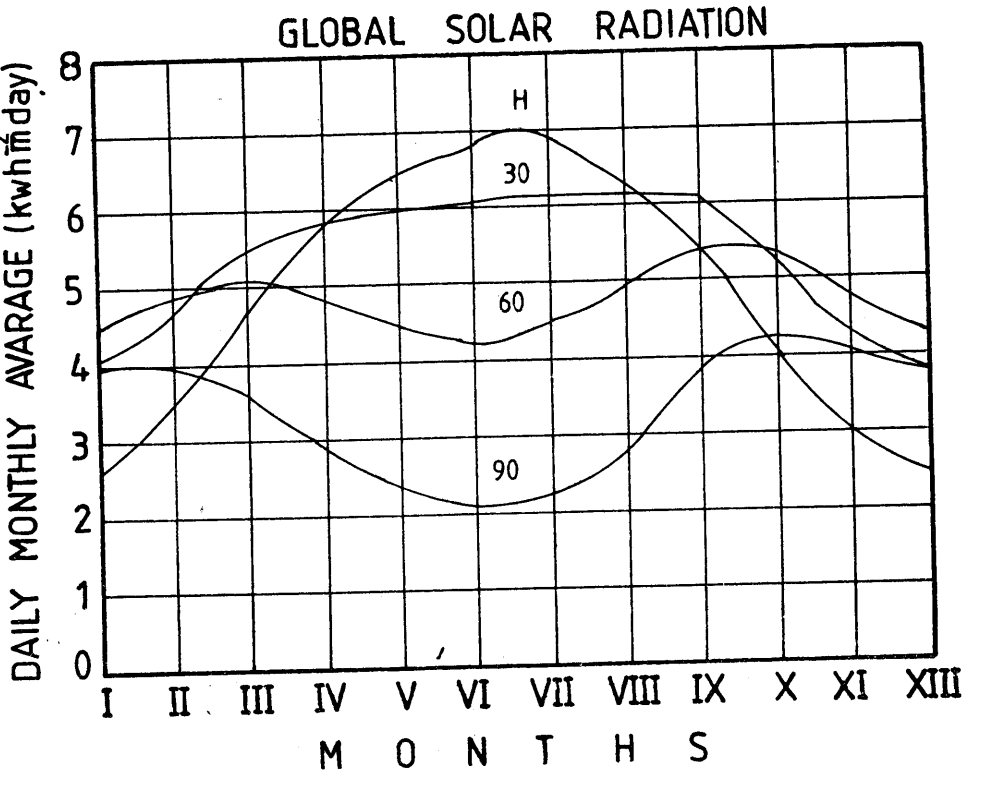

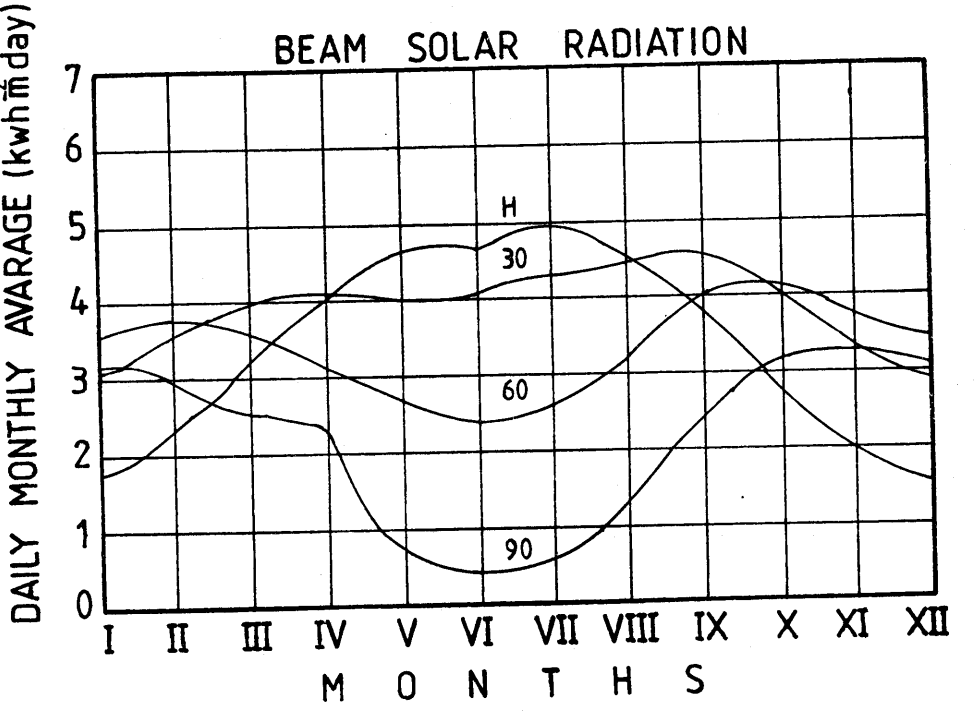

STATION : CASABLANCA

MODELLING OF HOURLY GLOBAL AND DIFFUSE IRRADIATION ON HORIZONTAL PLANE

P.C.Jain

Physics Dept., The University of Zambia, P.Box 32379, Lusaka, Zambia.

ABSTRACT

A general method for obtaining horizontal monthly average hourly global and diffuse irradiation from the respective daily values has been developed. The method seeks to consider some of the finer aspects so as to be useful in more refined system modelling in solar energy. The method is based on the two parameter β-distribution which is symmetric if the values of the two parameters are equal and asymmetric otherwise. This is the first approach that is able to consider the subtle morning-afternoon asymmetries of the instantaneous radiation by allowing variations in the values of the two parameters.

Using the hourly irradiation data of three French and one Canadian location, the performance of the method has been tested and compared with those of the well known existing methods. The method is found to be highly accurate, convenient and advantageous.

1. INTRODUCTION

An accurate estimation of solar radiation on surfaces of various tilts is needed in several applications and system optimization in solar energy. With increasingly refined system modelling, there is a growing need for more accurate data bases and theoretical methods.

The usual method for estimating the daily global irradiation on a tilted plane involves the obtaining of the horizontal hourly beam and the hourly diffuse irradiation. This is done by converting the horizontal daily global as well as diffuse irradiation into the respective hourly values. The method of Collares-Pereira and Rabl [1] for the hourly global and that of Liu and Jordan [2] for the hourly diffuse irradiation are commonly used.

A common feature of the existing methods is their symmetry, i.e. they estimate exactly the same values for the two hours situated symmetrically about the solar noon. However, asymmetries of more or less magnitude in the radiation for the morning and the afternoon hours do exist. From a study of hourly irradiation data of Canadian locations, Iqbal [3] observed that in

Vancouver the global irradiation througout the year is substantially more in the afternoon than in the morning and that deviations of up to about 10% from the mean exist. For a more refined work it is important that these asymmetries be taken into account. In this paper a general method recently developed by Jain, Jain and Ratto [4] for estimating both the hourly global and the diffuse irradiation from the respective daily values is presented. This method can incorporate the morning-afternoon asymmetries of the radiation and has the flexibility to consider the spatial and the temporal variations in the hourly irradiation.

2. THE DEVELOPMENT OF THE EXPRESSION

2.1 The β-distribution

The density of the β-distribution, a function of two parameters α and β, is defined as

$$g(x;\alpha,\beta) = \begin{cases} C(\alpha,\beta)\, x^{\alpha-1}\,(1-x)^{\beta-1} & : \alpha,\beta>0;\ 0\leq x\leq 1 \\ 0 & : \text{elsewhere} \end{cases} \qquad (1)$$

where x is any variable and $C(\alpha,\beta)$ is a normalization constant given by

$$\int_0^1 g(x;\alpha,\beta)\,dx = 1 = C(\alpha,\beta)\int_0^1 x^{\alpha-1}\,(1-x)^{\beta-1}\,dx \qquad (2)$$

Or in terms of the gamma function

$$C(\alpha,\beta) = \frac{\Gamma(\alpha+\beta)}{\Gamma(\alpha).\Gamma(\beta)}\ , \qquad (3)$$

where

$$\Gamma(\alpha) = (\alpha-1)! \qquad (4)$$

2.2 The β-distribution function over a day length

To define the β-distribution over the day length S_o, i.e. from the sunrise hour $(12-S_o/2)$ to the sunset hour $(12+S_o/2)$ we change x in eqn (2) by the transformation

$$x = \frac{t-(12-S_o/2)}{S_o} \qquad (5)$$

and obtain the density function

$$f(t;\alpha,\beta) = \frac{\Gamma(\alpha+\beta)}{\Gamma(\alpha)\,\Gamma(\beta)\,S_o^{\alpha+\beta-1}}\left[\frac{S_o}{2}+(t-12)\right]^{\alpha-1}\left[\frac{S_o}{2}-(t-12)\right]^{\beta-1} \qquad (6)$$

2.3 Evaluation of the Normalization Constant

For non-integral values of α and β the normalization constant $C(\alpha,\beta)$ in eqn (6) can be found using the relation

$$\frac{\Gamma(\alpha)\Gamma(\beta)S_o^{\alpha+\beta-1}}{\Gamma(\alpha,\beta)} = \int_{12-S_o/2}^{12+S_o/2} \left[\frac{S_o}{2} + (t-12)\right]^{\alpha-1} \left[\frac{S_o}{2} - (t-12)\right]^{\beta-1} dt \qquad (7)$$

Though the numerical evaluation of the above integral using computer is not difficult, a simpler analytical approach is possible. For non-integral values of the argument, we rewrite the gamma function as

$$\Gamma(\alpha) = (\alpha-1)(\alpha-2).....(x!) \quad : 0 \leq x \leq 1. \qquad (8)$$

For example, $\Gamma(4.8) = 3.8 \times 2.8 \times 1.8 \times (0.8!)$.

The value of $x!$ for $0 \leq x \leq 1$ can be evaluated to almost 100% precision using the polynomial approximation [5]

$$\Gamma(1+x) = x! = 1 + a_1 x + a_2 x^2 + a_3 x^3 + a_4 x^4 + a_5 x^5 \qquad (9)$$

where the coefficients are given by

$$a_1 = -0.57486,\ a_2 = 0.95124,\ a_3 = -0.69986,\ a_4 = 0.42455,\ a_5 = -0.10107 \qquad (10)$$

Eqn (6), with gamma functions given by (8), (9) and (10) and the parameters α and β to be determined, is proposed to give the ratio of the monthly average irradiances I and I_d to the monthly average daily values H and H_d, respectively.

3. DATA BASE

The French data used in the present study are from Carpentras, Millau and Marignane. These are well known for their accurate data base. The relevant station details are provided in Table 1. The five-year hourly data (5 years) x (365 days) x (12 hours) of each of the three locations for the

Table 1. Brief description of the selected sites and the data

Site	Latitude	Longitude	Elevation above the sea level	Duration of the data used
Carpentras	44° 05'N	5° 03'E	99m	Jan 1979 - Dec 1983
Marignane	43° 27'N	5° 13'E	6m	Jan 1980 - Dec 1984
Millau	44° 07'N	3° 01'E	715m	Jan 1980 - Dec 1984
Montreal	45° 30'N	73° 40'W	-	Oct 1964 - Dec 1975

diffuse and the global radiation were used in our analysis and comparison. Both the global and the diffuse radiation were measured on the horizontal surface with Kipp-Zonen pyranometers; the shadow-band used to intercept the direct radiation for the measurement of the diffuse radiation had a width of 6 cm and the diameter of 90 cm.

The monthly average hourly global and the diffuse irradiation data of Montreal were used. The data has been used earlier by Iqbal [3]. The data and the details are given in his book [6].

4. PERFORMANCE TESTS AND RESULTS

4.1 Estimation of Parameters

The parameters α and β that minimised the root mean square error (rmse) of the computed hourly values from those of the measured values were computed in two different ways: (1) Site dependent, and (2) Independent of site. For both the categories, the parameters could be expressed as simple linear functions of the day-length.

The computed hourly values for both the global and the diffuse radiation were obtained by integrating (i) the expression (6), (ii) the relevant expression of the Collares-Pereira and Rabl method, and (iii) that of the Liu and Jordan method, over a given solar hour from 4 upto 20 hours. The values of S_o were readily obtained for each location from their latitude values using the accurate tables prepared by Jain [7].

4.1.1 Site dependent parameters

Monthly sets of the parameters for each location for the diffuse and the global radiation that best fitted the corresponding measured data were generated for the two cases, viz. (a) when the method is used as an asymmetric one, i.e. α and β are allowed to vary independently, and (b) when the method is used as symmetric, i.e. $\alpha=\beta$. This was done with the aims of testing the accuracy of the method in recreating the existing hourly values and its ability to account for the morning-afternoon asymmetries.

The monthly best-fit values of the two parameters together with the corresponding rmse and the % rmse values for a representative location are presented in Tables 2 and 3 for the global and the diffuse radiation, respectively. Table 4 gives the yearly average % rmse for all the four locations. It is seen from the small values of the % rmse, which is mostly around 2%, that the fits are excellent for all the places. Fig 1 is representative of the performance test for the symmetric case. It shows the plot of the estimated values (solid line curve) vs. the measured values (marked ⊙) for the month of November for Carpentras (global radiation). Tables 2,3 and 4 also show that with the consideration of asymmetry the average reduction in rmse is about 25% with respect to the case when $\alpha=\beta$. Larger improvements are expected for locations that have larger morning-afternoon asymmetries. The largest asymmetry (deviation from the mean) in our study was only 3.4% for April for Millau (diffuse radiation).

To establish the day-length dependence of the parameters, the sixteen (4 sites x 2 parameters x 2 kinds of radiation) sets of 12 values of the two parameters for the asymmetric case were each fitted into the following simple linear functions of the day length

Table 2. Best-fit monthly values of α and β and the corresponding rmse for the asymmetric and symmetric cases for Carpentras (global radiation).

month	α	β	rmse	% rmse	$\alpha=\beta$	% rmse
1	2.38	2.41	0.19	1.9	2.40	2.2
2	2.49	2.49	0.18	2.1	2.49	2.1
3	2.52	2.50	0.11	1.3	2.51	1.6
4	2.62	2.67	0.13	1.8	2.64	2.6
5	2.71	2.72	0.12	2.0	2.72	2.0
6	2.70	2.72	0.06	1.0	2.71	1.3
7	2.71	2.72	0.07	1.1	2.72	1.2
8	2.64	2.66	0.09	1.2	2.65	1.5
9	2.58	2.58	0.12	1.6	2.58	1.6
10	2.49	2.54	0.13	1.6	2.51	2.7
11	2.46	2.42	0.16	1.6	2.44	2.5
12	2.43	2.41	0.20	2.0	2.42	2.3

Table 3. Same as Table 2 but for the diffuse radiation

month	α	β	rmse	% rmse	$\alpha=\beta$	% rmse
1	2.01	2.04	0.23	2.3	2.02	2.7
2	2.12	2.16	0.21	2.5	2.14	3.4
3	2.07	2.04	0.17	2.0	2.05	2.6
4	2.15	2.18	0.16	2.2	2.16	2.6
5	2.19	2.19	0.13	2.1	2.19	2.1
6	2.15	2.16	0.13	2.1	2.16	2.2
7	2.06	2.07	0.08	1.2	2.07	1.3
8	2.11	2.08	0.12	1.7	2.10	2.2
9	2.04	2.09	0.18	2.5	2.06	3.6
10	2.06	2.09	0.20	2.4	2.07	2.8
11	2.02	2.00	0.21	2.1	2.01	2.4
12	2.05	2.09	0.33	3.3	2.06	3.8

Table 4. Yearly average errors for the four locations

Location	Yearly average % rmse			
	Global		Diffuse	
	$\alpha\neq\beta$	$\alpha=\beta$	$\alpha\neq\beta$	$\alpha=\beta$
Carpentras	1.6	2.0	2.2	2.6
Marignane	1.3	1.9	2.0	2.6
Millau	1.9	2.5	2.2	2.9
Montreal	1.6	2.1	2.5	2.8
Overall Average	1.6	2.1	2.2	2.7

$$\alpha = a + b\, S_o \qquad (11)$$

$$\beta = a' + b' S_o \,, \qquad (12)$$

where the constants a, b, a' and b' were evaluated by the least square regression analysis of the data.

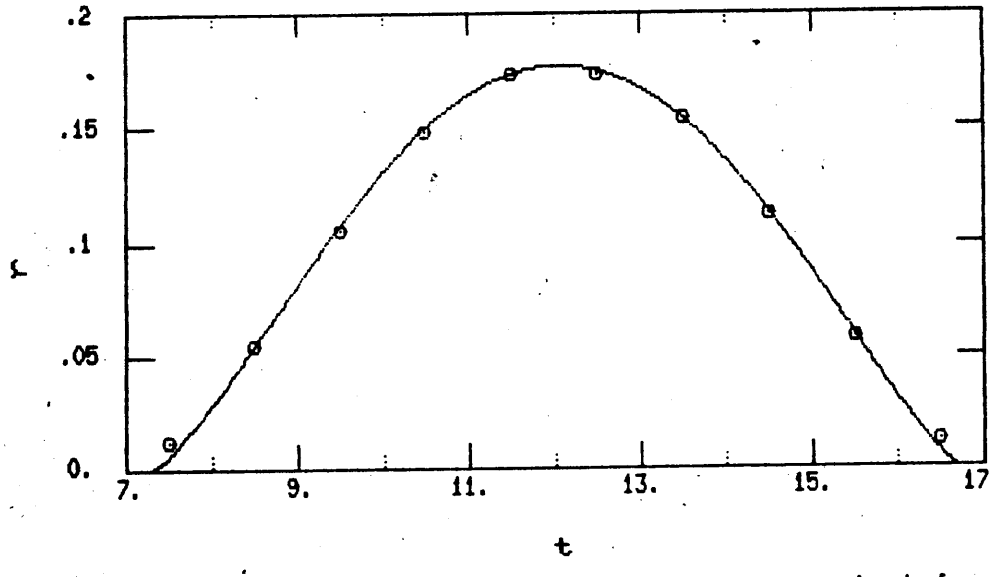

Fig.1. Representative diagram of the performance test for the site and day-length dependent (asymmetric) category. ● represent the measured values and the solid line curve the computed values using eqn (6) and α=2.46, β=2.42. (Location: Carpentras; month: November; radiation: global).

Table 5. Computed values of the best-fit coefficients in eqns (11) and (12) and the correlation coefficient ρ.

Location	For eqn (11)			For eqn (12)		
	a	b	ρ	a'	b'	ρ
GLOBAL RADIATION						
Carpentras	1.98	0.048	0.98	1.94	0.052	0.98
Marignane	2.11	0.036	0.91	2.11	0.035	0.93
Millau	2.02	0.037	0.92	2.03	0.037	0.90
Montreal	2.19	0.028	0.82	2.10	0.036	0.96
DIFFUSE RADIATION						
Carpentras	1.89	0.016	0.67	1.94	0.013	0.50
Marignane	2.04	0.003	0.10	2.03	0.003	0.09
Millau	1.85	0.026	0.69	1.97	0.016	0.55
Montreal	2.00	0.024	0.83	2.06	0.019	0.72

The computed values of the constants in eqns (11) and (12) and the values of the correlation coefficient are given in Table 5. As may be seen the fits for the global radiation are fairly good for all the four locations with the value of the coefficient of correlation ρ ranging from 0.82 to 0.98. For the diffuse radiation, though there exist positive correlation, the fits are not as good as those for the global radiation. The computed values of the % rmse when the parameters are given by eqns (11) and (12) are given in Table 6 (see under II). As expected this results in a little increase in the errors over the case when actual monthly parameters are used but the results are still very accurate. The maximum errors for the global

and the diffuse radiation are only 2.8% and 3.3%, respectively.

Table 6. Results of the performance test and comparison

Location	% RMSE			
	CR*/LJ**	Our Method+		
		I	II	III
G L O B A L R A D I A T I O N				
Carpentras	3.0	1.6	2.1	2.3
Marignane	3.2	1.3	2.0	2.2
Millau	3.3	1.9	2.8	3.3
Montreal	3.1	1.6	2.2	2.5
Average % Error	3.2	1.6	2.3	2.6
Decrease in Error	-	50%	28%	20%
D I F F U S E R A D I A T I O N				
Carpentras	3.6	2.2	3.0	3.5
Marignane	4.6	2.0	3.0	3.5
Millau	3.4	2.2	3.3	3.5
Montreal	4.6	2.5	3.1	4.9
Average % Error	4.1	2.2	3.2	4.0
Decrease in Error	-	45%	22%	1%

* Collares-Pereira and Rabl Method
** Liu and Jordan method
+I : Using the monthly parameters
II : Using the site dependent parameters
III : Using the site independent parameters

4.1.2 Site independent parameters

To determine the common set of the best-fit values of the constants in eqn (11) or (12) (for the case $\alpha=\beta$) for all the four locations for the global radiation, the 96 values (=12x2x4) of the parameters α and β for the global radiation were all combined together and plotted as functions of S_o. The best-fit linear equation was then obtained by least square fitting. The best-fit common set of the constants for the case of the diffuse radiation was obtained similarly by using the 96 values of the constants for the diffuse radiation. The aim of this was to obtain equations with possible applicability to any location, in general, without any hourly radiation measurements. For the global radiation the following best-fit correlation with $\rho=0.86$ was obtained

$$\alpha = \beta = 2.061 + 0.0385\ S_o . \qquad (13)$$

For the difuse radiation, we obtained

$$\alpha = \beta = 1.969 + 0.0153\ S_o , \qquad (14)$$

with ρ = 0.33. The corresponding % rmse values obtained upon using (13) and (14) are given in Table 6 (see under III). Again, as expected the errors are a little more compared to those for the previous cases, but the consistently low values of the % rmse, with maximum values of 3.3% and 4.9%, respectively, for the global and the diffuse radiation, still show excellent results. The diagram in Fig.2 is representative of the performance test for this category. This shows the estimated values (solid line) vs. the measured values (marked ⊙) of the ratio r for the month of April for Montreal (global radiation).

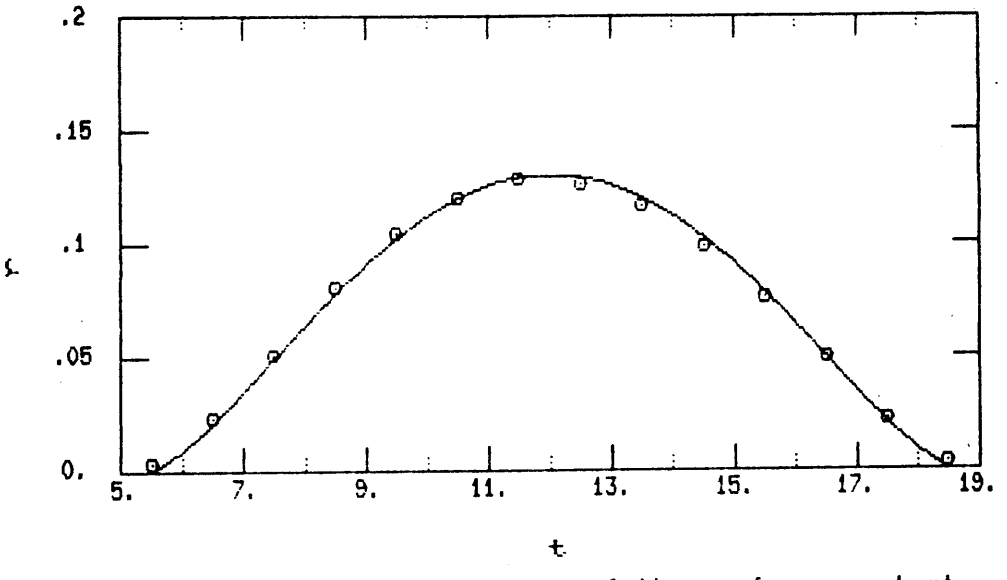

Fig.2. Representative diagram of the performance test for the independent category. ⊙ represent the measured values of r and the solid line curve the computed values using eqn (6) and $\alpha=\beta=2.58$ as given by (13). (Location: Montreal; month: April; radiation: global).

Whether eqns (13) and (14) can be applicable to any location in general may be open to question. Admittedly, the data used in the present study are from a narrow latitudinal zone 43°27′N to 45°30′N. Therefore it may be desirable to check the validity of these eqns for a more varied data for different latitudes. Nevertheless the climate of Montreal is much different from milder climates of the French locations and Marignane being on the Mediterranean coast is in a different situation than Carpentras and Millau which are about one hundred kilometers away from it. Furthermore, the range of S_o covered by each of these four locations is about 8 hrs to 16 hrs which appears fairly adequate for obtaining relationships like (13) and (14). Therefore it may be appropriate to suggest the use of these equations for locations without hourly radiation measurements.

4.2 Comparison With Known Methods

We compared the performance of our method with that of the Collares-Pereira and Rabl [1] for the hourly global and that of the Liu and Jordan [2] for the hourly diffuse radiation. As is seen in Table 6, the errors for all the three categories and cases of our method are less than those for the two methods. However, as our data is fitted exactly to the data of the four locations used in the analysis, a further comparison using

independent and more varied data set would be desirable before concluding that our method provides more accurate results than the two methods.

5. CONCLUSIONS AND SUGGESTIONS

The two parameter β-distribution based equation (6) with the normalization constant being evaluated by (8), (9) and (10) is found to fit accurately the hourly global as well as the diffuse irradiation values. The performance test done by using the hourly data of Carpentras, Marignane, Millau (France) and Montreal (Canada) in two ways, viz. (1) site dependent, and (2) site independent, show that this method is very accurate. For the four locations studied here, the maximum yearly average % rmse for the site dependent category are 1.9% and 2.5%, respectively, for the global and the diffuse radiation. For the site independent category, these figures are 3.3% and 4.9%, respectively.

For locations without any hourly measurements, the use of eqns (13) and (14) may be adequate to find the values of α and β. For places where the measurements of hourly irradiation exist, an analysis of the kind done here can be performed to establish the values of the two parameters on the monthly basis and then possibly their fitting into convenient equations of the form (11) and (12). The values of the two parameters obtained above in either of the two manners together with eqns (6), (8), (9) and (10) should then provide the desired radiation values with good accuracy.

As further studies it would be desirable to (i) make a comparison of this method with the known methods using independent data set, (ii) to check the validity of eqns (13) and (14) using varied data set, (iii) to study the method's ability to account for the morning-afternoon asymmetries in locations with larger asymmetries such as Vancouver, and (iv) to investigate the working of the method in case of the instantaneous beam radiation.

ACKNOWLEDGEMENTS

This work was carried out with the financial support of the "ICTP Programme for Training and Research in Italian Laboratories, Trieste, Italy". The facilities provided by the Physics Department, University of Genova and the sabbatical leave granted by the University of Zambia are highly appreciated. Dr. R. Festa helped in various computational matters arising from time to time.

NOMENCLATURE

H	monthly average daily hrizontal global irradiation
H_d	monthly average daily horizontal diffuse irradiation
I	monthly average instantaneous horizontal global radiation
I_d	monthly average instantaneous horizontal diffuse radiation
r	(monthly average hourly)/(monthly average daily) horizontal global ratio
r_d	(monthly average hourly)/(monthly average daily) horizontal diffuse ratio
S_o	monthly average daily day length
t	solar time in hours
ρ	coefficient of correlation
α,β,a,b,a',b'	parameters

REFERENCES

[1] - Collares-Pereira, Manuel and Rabl, Ari , "The Average Distribution of Solar Radiation - Correlations Between Diffuse and Hemispherical and Between Daily and Hourly Insolation Values". Solar Energy 22, 155-164 (1979).

[2] - Liu, B.H.Y. and Jordan, R.C., "The Interrelationship and Characterstic Distribution of Direct, Diffuse and Total Solar Radiation". Solar Energy 4, 1 (1960).

[3] - Iqbal, M., "A Study of Canadian Diffuse and Total Solar Radiation Data - II Monthly Average Hourly Horizontal Radiation". Solar Energy 22, 87-90 (1979).

[4] - Jain, P.C., Jain, S. and Ratto, C.F., "A New Model for Obtaining Horizontal Instantaneous Global and Diffuse Radiation from the Daily Values". To be published.

[5] - Abramowitz, M. and Stegun, I.A. (Eds.), Handbook of Mathematical Functions, Page 257, Dover Publications, Inc., New York (1972).

[6] - Iqbal, M., An Introduction to Solar Radiation, 220-229, Academic Press, Canada (1983).

[7] - Jain, P.C., "Accurate Computations of Monthly Average Daily Extra-terrestrial Irradiation and the Maximum Possible Sunshine Duration". Solar and Wind Technology 5, 41-53 (1988).

"COMPARISON OF MEASURED AND ESTIMATED MONTHLY AVERAGE DAILY GLOBAL SOLAR RADIATION ON HORIZONTAL SURFACE AT KARACHI,PAKISTAN".

FIROZ AHMAD and S.A.HUSAIN

Solar Energy Research Group,Institute of Pure and Applied Physics,University of Karachi, Karachi,Pakistan.

ABSTRACT An estimate of monthly average daily global solar radiation on horizontal surface is made via six different correlations.The comparison with the measured data suggest that the Angstrom equation and the relation by Frere et al. predicts the radiation value better as compared to the relations of Rietveld,Glover & McCulloch,Hay and Reddy.The regression constants calculated are in close agreement with the values of Modi and Sukhatme for areas of Pakistan. Correlation coefficients,Coefficient of Determination, root mean square errors and mean bias error have also been computed to test the validity of the prediction formula.

1.INTRODUCTION: In order to evaluate the performance and efficiency of any solar thermal device,adequate information and knowledge of the incoming solar radiation is of basic importance.The solar radiation data is available for most of the part of the world,but meteorological departments in developing and underdeveloped countries record only parameters such as sunshine hours,humidity,maximum & minimum temperatures,number of rainy days etc.Therefore in the absence of solar radiation data,different empirical formula using the above mentioned climatological parameters are employed for the estimation purpose (1-8)

In this paper attempt is made to estimate the solar radiation data for Karachi through the correlation making use of the sunshine hours as input parameter. Comparison of the estimated data with the measured values will enable us to establish the superiority of one correlation over the other,to use it for the places where solar radiation data is not available.

2. PREDICTION OF GLOBAL SOLAR RADIATION $\bar{H}$:

Making use of the bright sunshine hours ,an attempt has been made to predict the monthly average daily global solar radiation on horizontal surface at Karachi.The empirical formula employed for the relationships of Angstrom(9),Rietveld(10) Glover & McCulloch(11),Reddy(12) and Hay(13).Besides this the regression constants evaluated by Frere et al.(14) is also used to predict the insolation.All the correlation needs sunshine hours as an input parameter for prediction purpose.

Out of the various models which is used to determine the global solar radiation on horizontal surface, Angstrom equation is the simplest,presented below;

$$\frac{\bar{H}}{\bar{H}_0} = a + b \left(\frac{\bar{n}}{\bar{N}} \right) \quad \ldots\ldots\ldots (1)$$

where $\bar{H}$ is the monthly average daily global solar radiation, $\bar{H}_0$ is the monthly average extraterrestrial radiation, $\bar{n}/\bar{N}$ is the percentage of available sunshine(n is sunshine hours and N being the daylength).The constants a and b are the regression constants.

The second formula due to Rietveld(10) is given as;

$$\frac{\bar{H}}{\bar{H}_o} = 0.18 + 0.62 \left(\frac{\bar{n}}{\bar{N}} \right) \quad \ldots\ldots\ldots\ldots (2)$$

Further attempts to improve the solar radiation-sunshine relationship were made by Glover and McCulloch(11).They included the lattitude effect and presented the following correlation;

$$\frac{\bar{H}}{\bar{H}_0} = 0.29 \cos \phi + 0.52 \left(\frac{\bar{n}}{\bar{N}} \right) \quad \ldots\ldots\ldots (3) \qquad \text{For } \phi < 60^0$$

where ϕ is the lattitude of the place.

Reddy(12) has developed a formula for the setimation of daily total solar radiation as

$$R_t = K \frac{(1+0.8\ s)(1-0.2t)}{} \quad \text{cal/cm}^2\text{/day} \quad \ldots\ldots (4)$$

where $K = (\lambda N + \psi \cos \phi)\sqrt{h} \times 10^2$ cal/cm^2/day
$\lambda = 0.2/1+0.1\ \phi)$,known as lattitude factor.
ϕ= lattitude of the place.
ψ= seasonal factor
N=mean length of the day
s=n/N,where n=mean hours of bright sunshine per day during a month.
t=r/M,where r=number of rainy days & M=number of days in a month.
h=mean relative humidity per day in a month.

Reddy formula ,makes use of the bright sunshine hours, alongwith the additional climatological parameters such as seasonal factor ψ lattitude factor λ ,number of rainy days relative humidity factor.

Hay(13) developed a generalized proceedure and suggested a site independent correlation

$$\frac{\bar{H}}{\bar{H}_0} = \frac{0.1572+0.556\ (\bar{n}/\bar{N}_j)}{1-\rho\left[\rho_a\ (\bar{n}/\bar{N}_j) + \rho_c(1-\bar{n}/\bar{N}_j)\right]} \quad \ldots\ldots\ldots(5)$$

where ρ is the ground albedo, ρ_a is the cloudless sky albedo and ρ_c the cloud albedo. N_j is the modified day length and excludes the fraction during which solar zenith angle is greater than 85^0. The modified daylength is obtained from the relation

$$\bar{N}_j = 1/7.5\ \frac{\cos^{-1}\left(\cos 85 - \sin\phi \sin\delta_c\right)}{\left(\cos\phi\ \cos\delta_c\right)} \quad \ldots\ldots(6)$$

δ_c is the characteristic declination and ϕ is the lattitude. The value of ρ_a and ρ_c in equation are assumed to be 0.25 and 0.60 respectively, and the ground albedo is taken to be 0.20 for Karachi.

Frere et al.(14) proposed a graphical relationship between the regression constants a and b and the annual average of $\bar{n}/\bar{N}$. This relationship was obtained with values of constants a and b for several stations with lattitude ranging from 50N to 35°S as published by many authors. The regression constants based on $\bar{n}/\bar{N}$ values for Karachi are obtained and then used to predict the monthly average global solar radiation.

3. RESULTS AND DISCUSSIONS:

Presented in Table:1 are the parameters which are used to calculate the monthly average global solar radiation from sunshine data. The first coulmn of the Table represent the measured data of global solar radiation at Karachi, $\bar{H}_0$ is the extraterrestrial radiation while $\bar{n}/\bar{N}$ is the ratio of the bright sunshine hours to daylength and the solar declination for each month. The daylength is obtained from Cooper's formula(15) by inserting the values of n from Klien's(16) recommended days for each month. The modified daylength $\bar{N}_j$ due to Hay(13) is presented in Table:2. In Table:3 the estimated values of monthly average of global solar radiation obtained through various correlations are presented, alongwith the measured values for comparison. These estimated values of global solar radiation are plotted in Fig:1 with the measured values. As the various correlation which have been employed

to predict the monthly average global solar radiation makes use of the parameters $\bar{n}/\bar{N}$, therefore a plot of the monthly variation of this parameter alongwith $\bar{H}$ and $\bar{H}/\bar{H}_0$ is shown in Fig:2.

The percentage difference between the estimated and observed values are given in Table:4. To get a more meaningful assesment of the data, root mean square error (RMSE), mean bias error (MBE), Correlation Coefficient (C.C) and Coefficient of Determination (C.D) have been computed. Statistical tests of these models show that the Angstrom correlation and the Frere et al. method are most appropriate for the estimation purpose having low values of MBE, RMSE and high Coefficient of Correlation (r) and Coefficient of Determination (r^2). The equations suggested by Rietveld, Hay, Glover and McCulloch do not behave well. The formula suggested by Reddy fails miserably with a poor correlation coefficient and high MBE and RMSE.

The regression constants a and b obtained through the methods of Rietveld, Angstrom and Frere et al. gives us

a= 0.326	b= 0.405	.....Angstrom
a= 0.265	b= 0.504	.....Rietveld
a= 0.310	b= 0.410	.....Frere et al.

The correlation coefficients for these are Angstrom (r=0.994), Rietveld (r=0.91) and Frere at al. (r=0.99). The values of a and b are in close agreement with the predicted values of Modi and Sukhatme (17) for locations in Pakistan. The average from these three methods of a and b for Karachi is 0.300 and b=0.44. Comparing it with the coastal station; Bhavnagar (a=0.28, b=0.47), Goa (a=0.30, b=0.48) and Poona (a=0.31, b=0.43) of India we observe a fine agreement.

4. CONCLUSIONS:

This study is done only for one station i.e Karachi, therefore it is difficult to ascertain the superiority of one correlation over other. However a more extensive work is underway for five stations of Pakistan (18), initial analysis of which has indicated that Angstrom and Frere et al. methods ranks high in the list of empirical relations.

5. ACKNOWLEDGEMENT

The authors are thankful to Pakistan Meteorological Department, Geophysical Centre, Quetta for providing the global solar radiation data of Karachi & the climatological parameters. Helpful discussions with Dr. A.A, Qidwai, Physics Department, Karachi University, is also gratefuly acknowledged.

Table:1 Parameters required to calculate the monthly average daily Global solar radiation at Karachi, from sunshine data. Lattitude: 24.9^0 N

MONTHS	$\bar{H}_0$	$\bar{H}$	$\bar{n}/\bar{N}$	δ	$\sin\delta$	$\cos\delta$
JAN	23.98	15.89	0.80	-20.84	-0.355	0.934
FEB	28.18	18.09	0.77	-13.32	-0.230	0.973
MAR	32.96	21.16	0.76	- 2.40	-0.041	0.999
APR	37.07	22.57	0.73	9.46	0.164	0.986
MAY	39.29	23.56	0.74	18.78	0.322	0.946
JUN	39.94	22.73	0.59	23.04	0.391	0.920
JUL	39.49	19.21	0.38	21.11	0.360	0.932
AUG	37.78	17.91	0.39	13.28	0.229	0.973
SEP	34.34	19.84	0.60	1.97	0.034	0.999
OCT	29.50	19.35	0.81	- 9.84	-0.170	0.985
NOV	24.92	16.68	0.83	-19.02	-0.326	0.945
DEC	22.72	15.04	0.83	-23.12	-0.392	0.919

Table:2 Modified Daylength for Karachi.
Calculated from Hay(13) .

MONTHS	MODIFIED DAYLENGTH	BRIGHT SUNSHINE HOURS TO MODIFIED DAYLENGTH $\bar{n}/\bar{N}_j$
JAN	9.84	0.885
FEB	10.45	0.842
MAR	11.14	0.882
APR	11.85	0.788
MAY	12.42	0.790
JUN	12.70	0.637
JUL	12.60	0.395
AUG	12.11	0.414
SEP	11.46	0.658
OCT	10.74	0.879
NOV	10.05	0.908
DEC	9.73	0.906

Table:3 Predicted value of the monthly average daily Global solar radiation on horizontal surface at Karachi (lattitude 24.9° N)

MONTHS	H_0	ANGSTROM	RIETVELD	GLOVER & McCULLOCH	HAY	FRERE et al.	REDDY	MEASURED
JAN	23.98	15.64	16.28	16.34	16.54	15.35	17.20	15.89
FEB	28.18	18.04	18.63	18.78	18.78	17.70	19.42	18.09
MAR	32.96	20.91	21.50	21.70	21.60	20.51	21.39	21.16
APR	37.07	23.16	23.64	23.98	23.62	22.71	21.26	22.57
MAY	39.29	24.63	25.17	25.51	25.07	24.14	20.42	23.56
JUN	39.94	22.64	21.92	22.86	22.10	22.12	18.67	22.73
JUL	39.49	18.96	16.43	18.20	16.40	18.41	14.65	19.21
AUG	37.78	18.28	15.93	17.60	16.11	17.75	15.78	17.91
SEP	34.34	19.56	18.99	19.78	19.40	19.12	18.54	19.84
OCT	29.50	19.39	20.27	20.30	20.25	19.03	19.92	19.35
NOV	24.92	16.57	17.41	17.40	17.50	16.27	19.80	16.68
DEC	22.72	15.05	15.78	15.78	15.93	14.77	17.41	15.04

Table:4 Percentage difference between Measured and Predicted values of Monthly Average Global Solar Radiation through various correlations at Karachi.

MONTHS	ANGSTROM	RIETVELD	GLOVER & McCULLOCH	HAY	FRERE et al	REDDY
JAN	1.57	2.45	2.83	4.09	3.39	8.20
FEB	0.27	2.98	3.81	3.81	2.15	7.35
MAR	1.18	1.60	2.55	2.08	3.07	1.08
APR	-2.61	4.74	6.24	4.65	0.62	5.80
MAY	-4.54	6.83	8.27	6.40	2.46	13.32
JUN	0.39	3.56	0.57	2.77	2.68	17.86
JUL	1.30	14.47	5.25	14.60	4.16	23.73
AUG	-2.06	11.05	1.73	10.00	0.89	11.90
SEP	1.40	4.28	0.30	2.21	3.62	6.55
OCT	-0.20	4.75	4.90	4.65	1.65	2.94
NOV	0.66	4.37	4.31	4.92	2.45	18.70
DEC	-0.05	4.92	4.92	5.91	1.79	15.75
MBE	0.045	-0.006	0.517	0.105	-0.346	0.633
RMSE	0.399	1.267	0.917	1.240	0.509	2.488
C.C(r)	0.994	0.91	0.97	0.91	0.99	0.497
C.D(r^2)	0.988	0.83	0.94	0.83	0.98	0.247

REFERENCES:

1. Sabbagh,J.A,Sayigh,A.A.M,& El-Salam:"Estimation of the total solar radiation from meteorological data". ISES Conference,Los Angeles,1975
2. Sayigh,A.A.M:"Formula for total and diffuse solar radiation",3rd course in Solar Energy Conversion International College of Applied Physics,Alghero, Sarolinia,1976.
3. Sayigh,A.A.M:"Solar Energy availability prediction from climatological data";2nd Conference on Solar Energy conversion,International College of Applied Physics Naples,Italy,1975
4. Swartman,R.K,Ogunlade,O :"Solar radiationestimates from common parameters" Solar Energy,11,170-172(1967)
5. Sabbagh,J.A et al.:"An estimation of total radiation from meteorological data" Solar Energy,19,307-311(1971)
6. Norris,D.J;"Correlation of Solar radiation with clouds" Solar Energy,12,107 (1968)
7. Bennett,I:"Correlation of daily insolation with daily total sky cover,opaquecover and percentage of possible sunshine" Solar Energy,12.3 (1969)
8. Goldberg :"A comparison of some simple model used to predict solar irridiance on a horizontal surface". Solar Energy,23,81-83 (1979)
9. Angstrom,A:"Solar and terrestrial radiation" Q.J.R.Met.Soc.50,121 (1924)
10. Rietveld,M.R:"A new method for estimating the regression coefficient in the formula relating solar radiation to sunshine". Agr.Meteor,19,243-252(1978)
11. Glover,J & McCulloch,S.G:"The empirical relation between radiation and hours of sunshine",Q.J.R.Met.Soc,84,172, 1958.
12. Reddy,S.J:"An empirical method for the estimation of total solar radiation" Solar Energy,13,289-290(1971)
13. Hay,J.E:"Calculation of monthly mean solar radiation for horizontal and inclined surfaces, Solar Energy,23(4)301-307(1979)
14. Frere et al:"Estudio agroclimatologico de la zona ondina"Informe Tecnico,FAO/UNESCO/OMM,Rome.1975
15. Cooper,P.I:"The absorption of solar Radiation in Solar stills"Solar Energy,12,p.3(1969)
16. Klien,S.A :Calculation of monthly average insolation on tilted surface". Solar Energy 19,325-329(1977)
17. Modi,V and Sukhatme,P:"Estimation of daily total and diffuse insolation in India from weather data". Solar Energy,22,407-411(1980)
18. Ahmad,F et al."Comparison of various correlations on horizontal surface for five stations in Pakistan" (in preparation,1988)

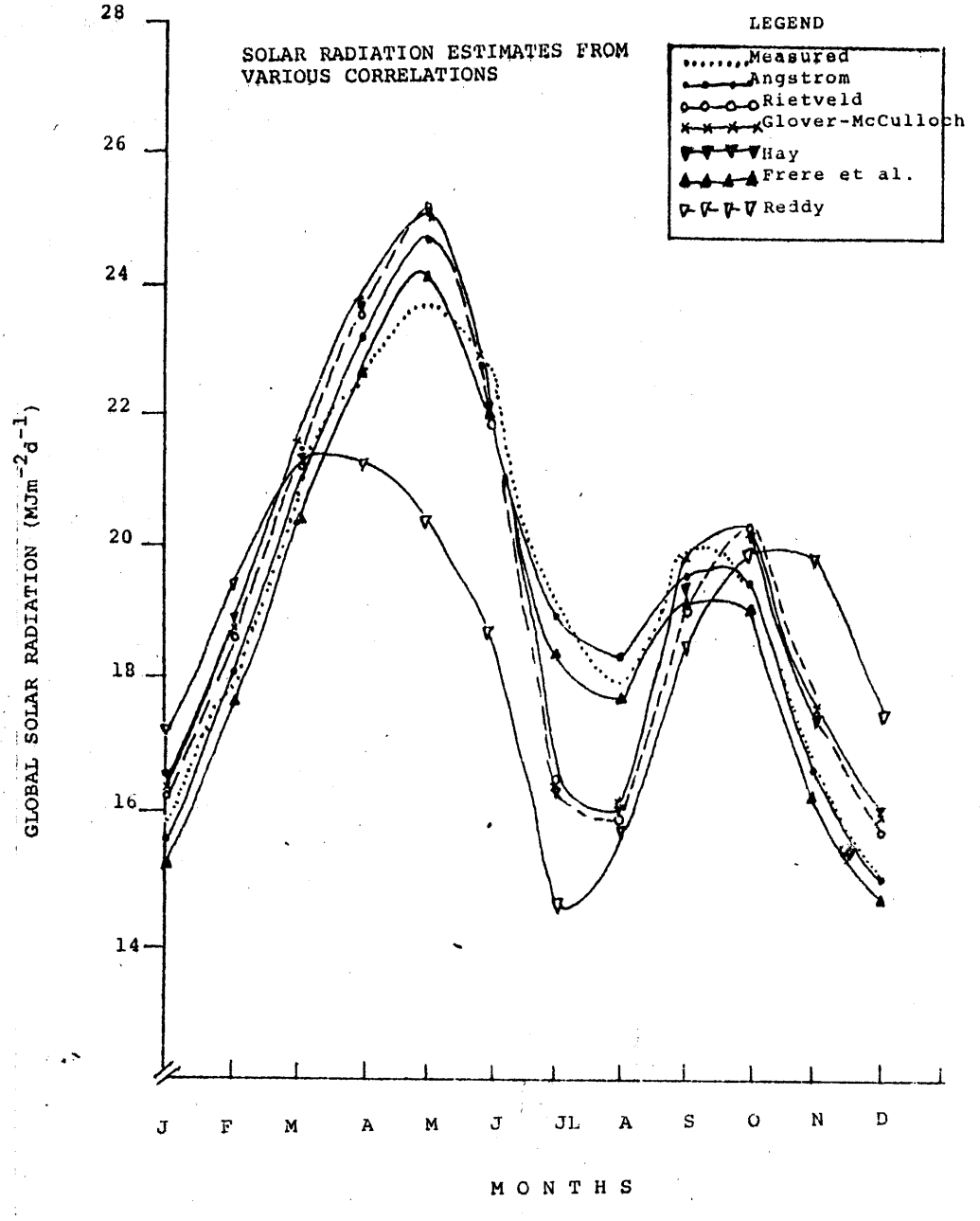

Figure:1. Global Solar Radiation Estimates from Various correlations at Karachi,Pakistan.

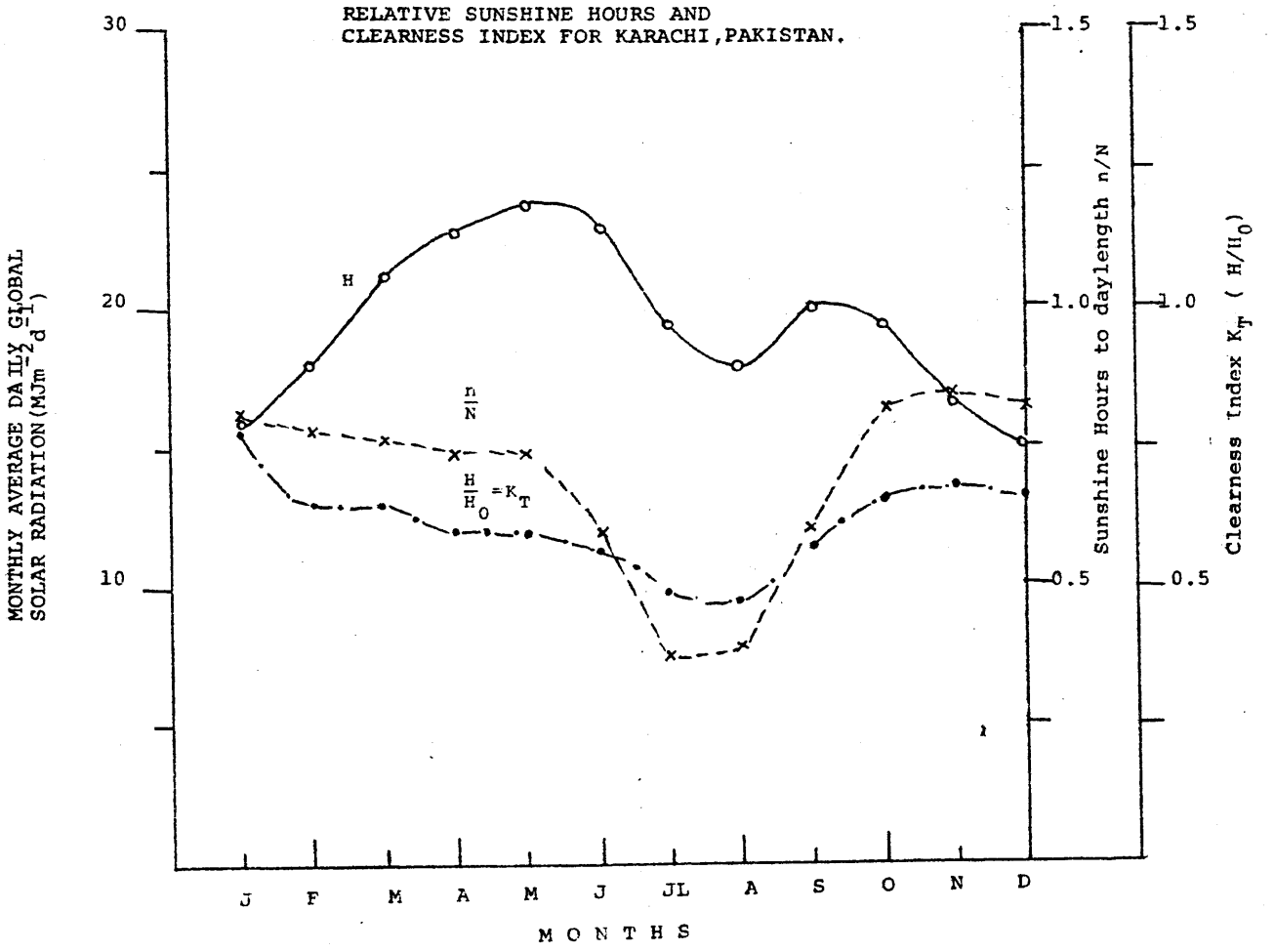

Figure:2 Relative Sunshine Hours and Clearness Index for Karachi,Pakistan.

OPTIMUM SLOPE OF FLAT-PLATE SOLAR COLLECTOR FOR DIFFERENT APPLICATIONS

S.M.Abughres, Y.M. Elegely and M.B. Elalu
Centre For Solar Energy Studies
P.O. Box 12932, Tripoli Libya.

ABSTRACT

The work presents the results of an optimization analysis for the inclination of a stationary flat-plate solar collector for six applications in Libya. The optimum inclination is found to depend on the prevailing climatic conditions , the time period of the application and the site -location. Whereas this optimum rises up to 26 degrees above and falls down to 31 degrees below the latitude angle for winter and summer applications respectively, it approaches the latitude angle for all year-round applications. Exceptions of the latter are those cases of domestic water heating in locations known for their frequent cloud overcast where the optimum falls dowen to about 8 degrees below the latitude angle. In general ,it is recommended to calculate the optimum inclination, taking into account the various controlling factors as those mentioned earlier , rather than relying on approximate methods as the commonly used Rule of Thumb for space heating installation .

1. INTRODUCTION

It is essential in the design and installation of solar systems, employing stationary flat plate collector ,to seek the best inclination of the collector's surface that will ensure the maximum interception of solar insolation within a pre-specified time period during the year. The total solar insolation on an inclined surface is generally expressed as a sum of direct beam radiation, the diffuse radiation from the sky dome, and the radiation reflected from the ground and surroundings. A number of reports are available in the literature on the calculation of solar insolation on inclined surfaces [1-6]. However,these reports are either of non-specific application, or they are meant for other locations different from what is considered in the current work.

This paper presents the findings of an exercise whereby the collector slope of six applications at 23 locations in Libya

has been optimized for pre-specified time period. The data of insolation used in the optimization analysis have been taken either from measurements records of up to six years or calculated from a mathematical model developed at the centre [4,7]. The applications have been chosen in such a way so to represent different seasonal utilities during the year of which the time durations have been specified on the basis of the frequency of the energy demand. For this purpose, two summer applications,namely;space cooling and irrigation water pumping, and one winter application for space heating have been selected. In addition, three all year round applications,namely ; domestic water heating ,potable water pumping, and the powering of a relay-station have also been considered.

2. FORMULATION AND ANALYSIS

The solar insolation,at the locations where measurements records are not available, is calculated using a total cloud based model. The model is formulated in details in references [4] and [8], where the monthly average daily total insolation on a horizontal surface ($\bar{H}$) is expressed as ;

$$\bar{H} = \bar{H}_o \ [1+(\bar{\tau}-1)]/[1-\rho_g . \rho_c . CA] \qquad \ldots\ldots (1)$$

and the corresponding ratio of difuse ($\bar{D}$) to total insolations as ;

$$(\bar{D}/\bar{H}) = 1-(1- CA)*(\bar{I}_o/\bar{H}_o) \qquad \ldots\ldots (2)$$

where($\bar{H}_o$) and ($\bar{I}_o$) are the monthly average daily clear sky total and direct beam insolation on a horizntal surface respectively, (CA) is the fraction of the sky-dome that is covered by clouds, ($\bar{\tau}$) is the atmospheric (cloud) transmittance, and (ρ_g) and (ρ_c) are the ground and cloud base reflectances respectively.

It should be noted that the available measurements records give the total solar insolation in 15 of the 23 locations considered and the total cloud amount in all of these locations. Figure 1 shows a distribution of these locations throughout the country. As the diffuse component of the solar insolation is not measured, it is calculated by means of equation (2). Procedure of detailed analysis and justification of the radiation model are given in references [7] and [9] where satisfactory correlation between measured and calculated total solar insolation on a horizontal surface was found with a root mean square error and mean bias error of 5.3 % and -0.2 % respectively . Also, the ratio of diffuse to total insolations on a horizontal surface as calculated by equation(2) was in close agreement with those predicted by the method of Liu and Jordan [10].

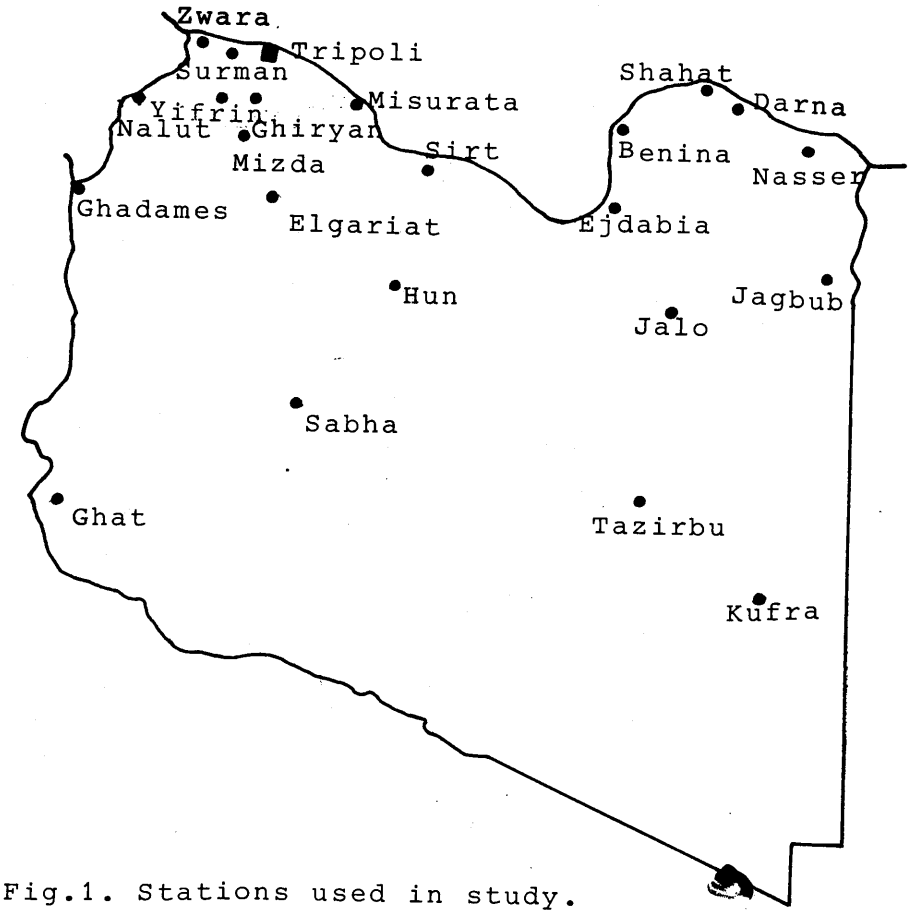

Fig.1. Stations used in study.

The monthly average daily total insolation on an inclined surface ($\bar{G}$) is estimated by individually considering the direct beam, diffuse and reflected components of radiation incident on inclined surface. Assuming diffuse and reflected radiation to be isotropic, Liu and Jordan [11] have proposed that $\bar{G}$ can be expressed as ;

$$\bar{G} = (\bar{H}-\bar{D}).\bar{R}+\bar{D}.(1+\cos\beta)/2+\bar{H}.\rho_g(1-\cos\beta)/2 \qquad \ldots\ldots (3)$$

where ($\bar{R}$) is the tilt (iclination) factor defined as the ratio of monthly average daily direct beam radiation on the tilted surface to that on a horizontal surface , (β) is the angle of inclination of the surface from the horizontal and (ρ_g) is the ground reflectance, as defined before, ranging from 0.2 to 0.7 depending on the snow cover .For the ground surface in Libya, a reflectance of 0.2 is considered a most likely value.

Liu and Jordan [11] have also suggested that $\bar{R}$ can be estimated to be the ratio of extraterrestrial radiation on the tilted surface to that on a horizontal surface for the month. For surfaces facing directly towards the equator;

$$\bar{R} = \frac{\cos(L-\beta).\cos\delta.\sin h_s+(\pi h_s/180)\sin(L-\beta).\sin\delta}{\cos L.\cos\delta.\sin h_r+(\pi h_r/180)\sin L.\sin\delta} \qquad \ldots\ldots(4)$$

where (L) is the solar latitude angle, (δ) is the solar declination angle , (hr) is the sunrise hour angle for horizontal surface, given as ;

$$h_r = \arccos(- \tan L \,.\tan\delta) \qquad .....(5)$$

and (h_s) is the sunset hour angle for the tilted surface which is expressed as;

$$h_s = \min\{ h_r , \arccos [- \tan(L-\beta).\ \tan\delta]\} \qquad .....(6)$$

Thus the optimum inclination can be found by calculating $\bar{G}$ for different values of and summing all values of $\bar{G}$ during the application period until a maximum value of ($\Sigma \bar{G}$ .d/Σ d) is achieved. d here is the lenght of the application period in days. An explicit expression giving an optimum is not possible during the period when arcos(- tan L.tanδ) is greater than arcos[-tan(L-β). tanδ] due to the resulting complicated mathematical expression which needs to be differentiated for maximum values. However, this is possible during the heating season as it has been demonstrated by Chiou and El-Naggar [6].

3- RESULTS AND DISCUSSIONS

Table 1 summarises the results for the six different applications at the 23 locations considered. These results are also presented in graphical form in Figs.2 to 24. Examination of the results shows that the optimum inclination for domestic water heating (DWH) varies from about the latitude angle to 8 degrees below the latitude. This is attributed to the prevailing climatic conditions, as it is evident that optimum inclinations below latitude angles correspond to regions known with frequent cloud overcast. In other words, the proportion of inceased diffuse component of solar insolation becomes more significant, thus leading to lower optimum inclination. This is in line with the findings of Chiou and El-Naggar [6]. In thier study on the optimum slope during the heating season, they found that the optimum decreases with decreasing direct beam component of solar insolation .

It is obvious from the assumption incorporated in deriving relationship (3) that; as the diffuse component of solar insolation increases, the optimum inclination decreases till it reaches zero. In this relationship, the diffuse component of solar insolation ($\bar{D}$) and that reflected from the ground ($\bar{H}.\rho_g$) are assumed to be isotropic. therefore under conditions of complete cloud overcast, that is ; when the direct beam component of solar insolation ($\bar{H}-\bar{D}$) is zero, the optimum position of the surface is the horizontal plane. This leads to the conclusion that for domestic water heating, the optimum inclination of flat-plate collctor does not depend on location only, but also on prevailing cloud conditions.

Table (1). Duration of the application and the optimum inclination of the stationary flat plate solar collector.

Location	DWH		Cooling Season		Heating Season		Irri.Wa. Pumping		Pota.Wa. Pumping		Pow. of Re. Sta.	
	Du.	Op. Tilt	Du.	Op. Tilt	Du.	Op. Tilt	Du.	Op. Tilt	Du.	Op. Tilt	Du.	Op. Tilt
TRIPOLI Lat.32.87	All Year	30	0 Mon.	-	5 Mon.	50	6 Mon.	10	All Year	30	All Year	30
BENINA Lat.32.1		25	0	-	5	50	6	10		30		30
DERNA Lat.32.76		25	0	-	5	40	6	10		30		30
EJDABIA Lat.30.72		25	0	-	5	50	6	10		30		30
ELGARIAT Lat.30.38		30	3	0	5	50	6	5		30		30
GHADAMES Lat.30.13		30	4	5	5	50	6	5		30		30
GHAT Lat.24.95		25	5	0	3	50	6	0		30		30
GHIRYAN Lat.32.18		30	2	5	6	45	6	5		30		30
HUN Lat.29.13		30	3	0	5	50	6	5		30		30
JAGBUB Lat.29.82		30	3	0	5	50	6	5		30		30
JALO Lat.29.03		30	4	5	5	50	6	5		30		30
KUFRA Lat.24.22		25	5	0	4	50	6	0		25		25
MISURATA Lat.32.3		25	2	5	5	40	6	5		30		30
MIZDA Lat.31.45		25	3	0	5	50	6	5		30		30
NALUT Lat.31.87		30	2	5	6	45	6	5		30		30
NASSER Lat.31.87		30	0	-	6	45	6	10		30		30
SABHA Lat.27.02		25	5	5	4	50	6	5		25		25
SHAHAT Lat.32.82		25	0	-	6	40	6	5		25		25
SIRT Lat.31.2		25	0	-	4	50	6	5		30		30
SURMAN Lat.32.87		30	0	-	6	45	6	5		30		30
TAZIRBU Lat.25.77		25	5	0	4	50	6	0		30		30
YIFRIN Lat.32.06		25	2	5	6	45	6	10		30		30
ZWARA Lat.32.93		30	0	-	6	45	6	10		30		30

In the other two cases of all year round applications ; potable water pumping and the powering of relay-station, the optimum inclination is approximately equal to the latitude

angle. The collectors in these applications consist of photo-voltaic panels which are reckoned to be mainly sensitive to the direct beam component of solar insolation. In such applications, the site location or latitude angle is therefore, themain parameter determining the optimum inclination. The increase in optimum inclination with latitude angle is due to the increase in the incidence angle of solar insolation as the site location moves further away from the equator , thus necessitating higher inclination for maximum possible interception of solar insolation.

As for seasonal applications, the results show the optimum inclination reaches a maximum of about 26 degrees above the latitude angle during the heating season and a minimum of about 31 degrees below the latitude angle for summer applications. The extreme values on both sides of latitude angle occur when the time period of application is shortest and when the solar system is operated near the sotistial condition, that is; when the position of the sun in sky-dome is lowest in winter and highest in the summer. However, the optimum inclination is also influenced by other factors such as the prevailing climatic conditions for reasons explained earlier. This is a likely explanation why the optimum inclination is not the same at location with the same length of period of application. In conclusion, although the results of the heating season are in agreement with those of Chiou and El-Naggar [6], they are generally higher than those recommended by the commonly used Rule of Thumb for space heating installation [12]. The latter normally suggests an inclination at approximately 10-15 degrees greater than the latitude angle.

4. CONCLUSIONS

The optimum inclination of a stationary flat-plate solar collector is determined for six applications at 23 locations in Libya. The optimum is found to rely on the prevailing cloud conditions, the time of application during the year and the site location or latitude angle. Whereas an increase in cloud overcast reduces the optimum inclination, the time of application affects this optimum in a way depending on its occurance in the year. Optimum inclinations of up to 26 degrees above and down to 31 degrees below the latitude angle are achieved for winter and summer applications respectively.

For all year round application, the optimum inclination appears to take an average value reching approximately the latitude angle. Exceptions are those cases of domestic water heating in locations known for their frequent cloud overcast. In these places , the optimum is about 8 degrees below the latitude angle .

The site location affects the optimum inclination by virtue of its latitude angle. Increasing the latter means moving further away from the equator wich necessitates higher inclination to ensure the maximum possible interception of solar rays. In general , the optimum inclination should be always determined on the basis of such controlling factors as

the prevailing climatic conditions, time of application and site location. Approximate means as the commonly used Rule of Thumb for space heating installation should be avoided.

5. ACKNOWLEDGEMENTS

The work is a part of a project funded by the Centre for Solar Energy Studies under contract number SEC/MD/VA/RPP/1986. The authors are grateful to the Centre for providing the computer facilities and the permission to publish the work, and also to the Meteorological Department for the provision of the data.

6. REFERENCES

[1]- Klein,S.A "Calculation of Monthly Average Insolation on Tilted Surfaces ", Solar Energy, Vol. 19, 325-329, 1977.

[2]- Iqbal,M."Hourly vs Daily Methods of computing Insolation on Inclined Surfaces " , Solar Energy ,Vol. 21, 485-489 1978 .

[3]- Hawas,M.M and Muneer,T."Monthly Average Daily Insolation on Tilted Collectors in Libya " ,Energy Conv. and Mgmt. Vol. 2 , 213-218, 1980 .

[4]- Abughres, S.M " Monthly average Daily Insolation For Horizontal and Inclined Surfaces ", Solar and Wind Technology, Vol. 1 , 119-139, 1985 .

[5]- Muntasser, M.A. and Bawany,A.D " Optimal Tilts for Flat-Plate Collectors in Libya " , Libyan Journal of Energy, Vol. 2, 21-41, 1985 .

[6]- Chiou, J.P. and El-Naggar ,M.M." Optimum Slope for Solar Insolation on a Flat Surface Tilted Towards thr Equator In Heating Season " , Solar Energy , Vol. 36, 471-478, 1986 .

[7]- Abughres, S.M. and Bishti,S.A. " Cloud Amount-Sunshine Duration relationship and The Calculation of Solar Irradiance and Components " , Proceedings of the 24th International Conference (Solar Energy-New Energetic Technologies for Environment and Agriculture), Verona, Italy, Sep. 28- Oct. 2, 1986 .

[8]- Monterith,J.L." Attenuation of Solar Radiation :A Climatological Study ", Q.J.R.Met. Soc. , Vol. 88, 508 - 521, 1962 .

[9]- Abughres,S.M. " Correlating the Fraction of Possible Sunshine to the Total Cloud Amount for the Purpose of Solar Radiation Prediction "Proceedings of the 3rd. Arab International Solar Energy Conference, Bagdad, Iraq . Feb. 21-24, 1988 .

[10]- Liu,B.Y.H. and Jordan, R.C. " The Inter-Relationship and Characteristic Distribution of Direct,Diffuse, and Total Solar Radiation " ,Solar Energy , Vol. 4, 1-19, 1960 .

[11]- Liu,B.Y.H. and Jordan,R.C. "Daily Insolation on Surfaces Tilted Towards the Equator " Trans. ASHRAE. 526-541,1962

[12]- Kreider,J.F. and Kreith,R.C." Solar Heating and Cooling" Hemisphere Publishing Corporation, New York, 1982 .

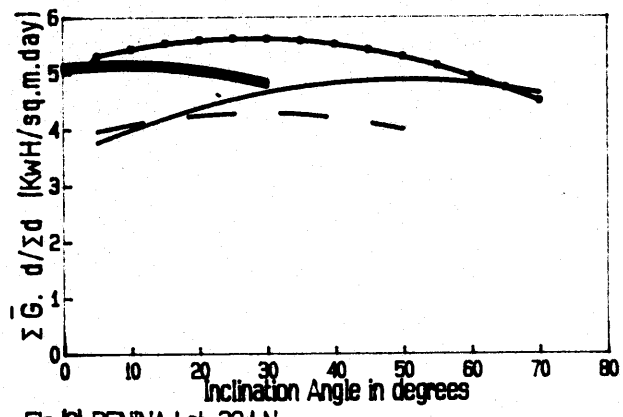

Fig.[2] BENINA Lat. 32.1 N

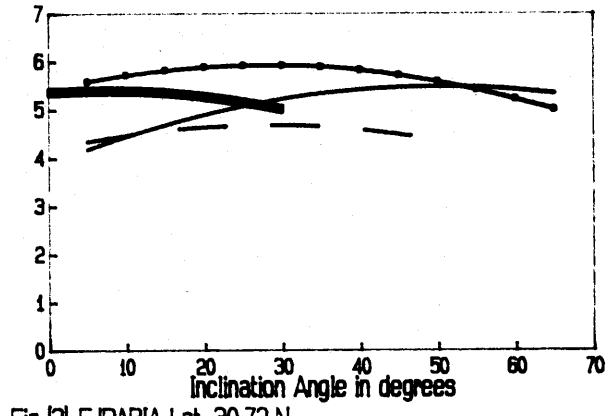

Fig.[3] EJDABIA Lat. 30.72 N

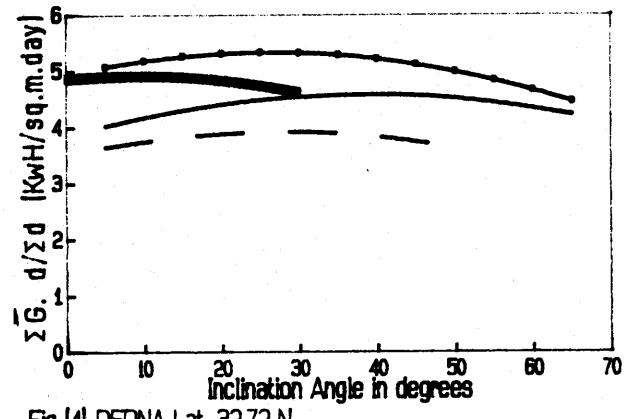

Fig.[4] DERNA Lat. 32.72 N

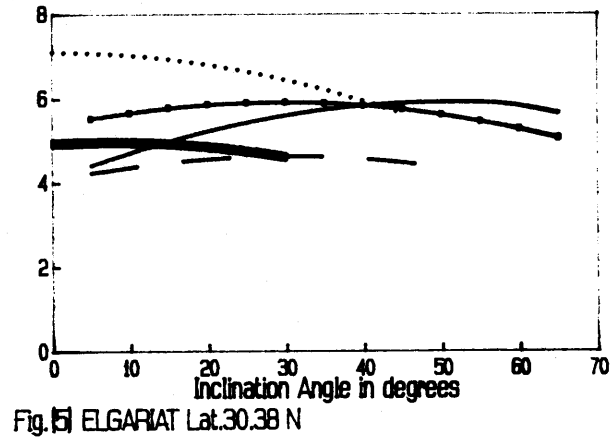

Fig.[5] ELGARIAT Lat.30.38 N

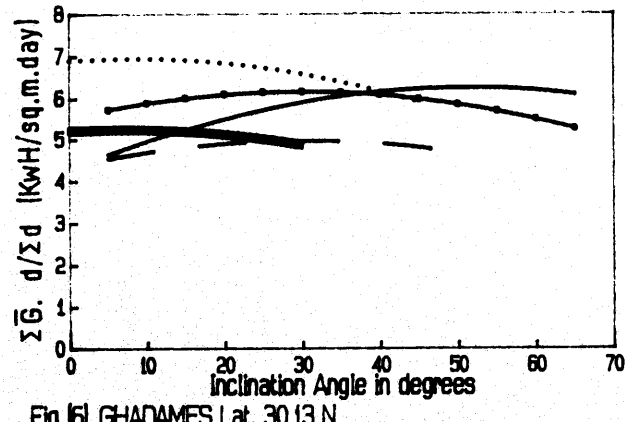

Fig.[6] GHADAMES Lat. 30.13 N

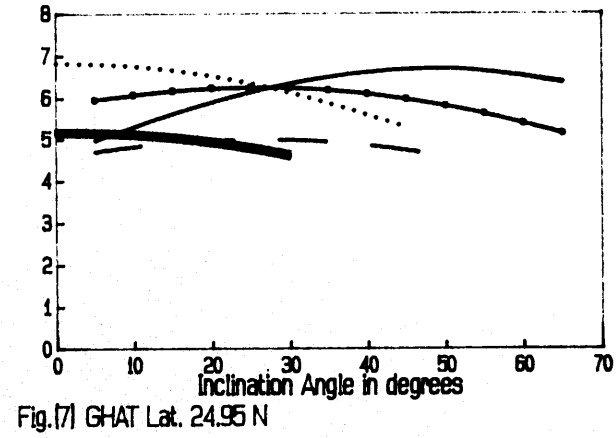

Fig.[7] GHAT Lat. 24.95 N

DWH Season — Heating Season — Irrig.W Pumping
Cooling Season — — Pot.W P & Relay Stations

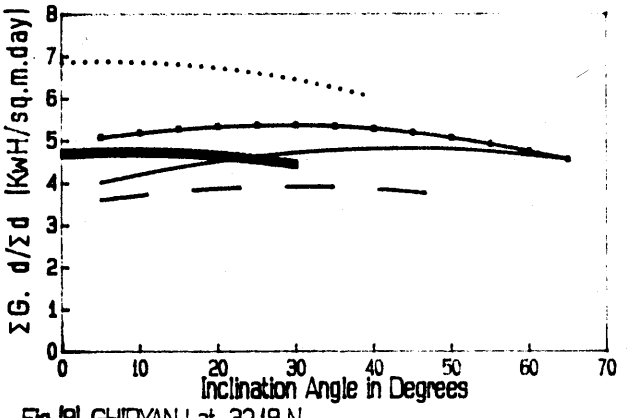

Fig.[8] GHIRYAN Lat. 32.18 N

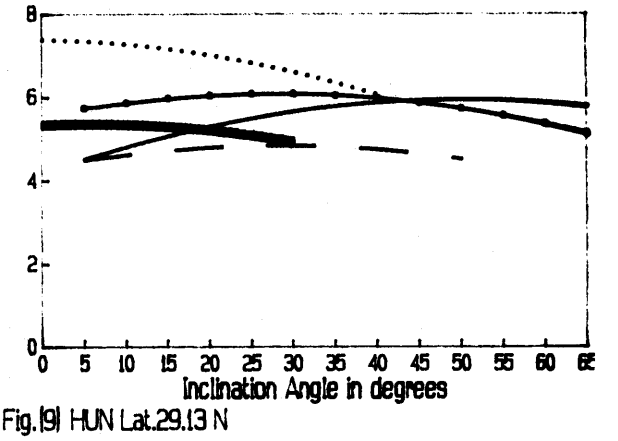

Fig.[9] HUN Lat.29.13 N

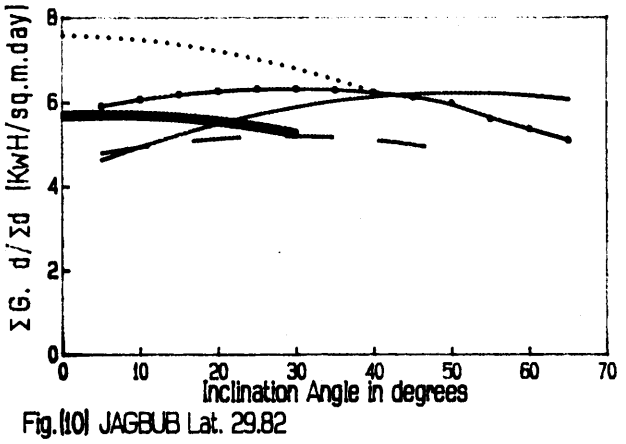

Fig.[10] JAGBUB Lat. 29.82

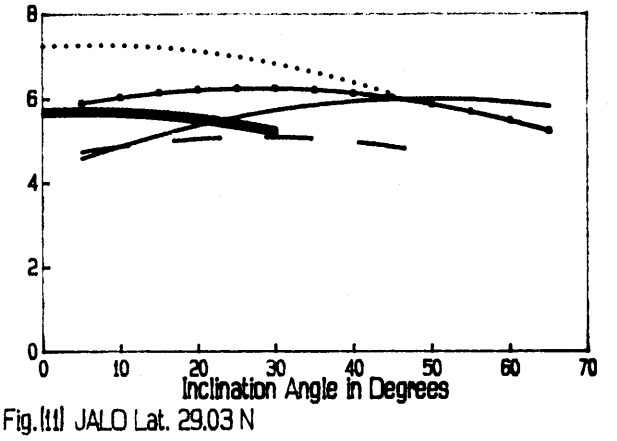

Fig.[11] JALO Lat. 29.03 N

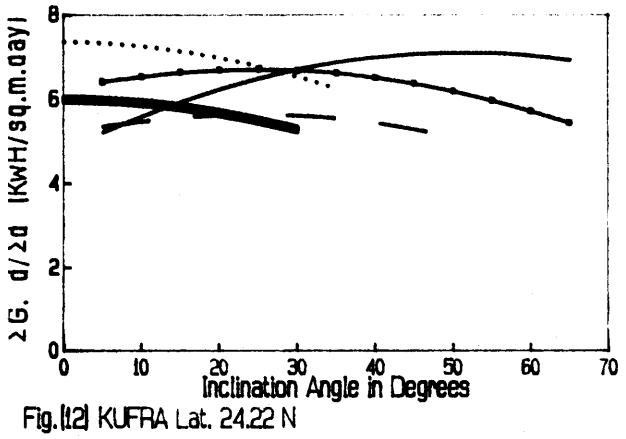

Fig.[12] KUFRA Lat. 24.22 N

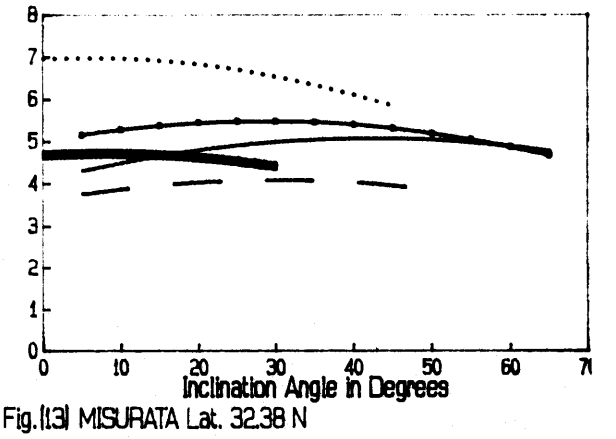

Fig.[13] MISURATA Lat. 32.38 N

DWH Season — Heating Season — Irrig.W Pumping
Cooling Season — — Pot.W P & Relay Stations

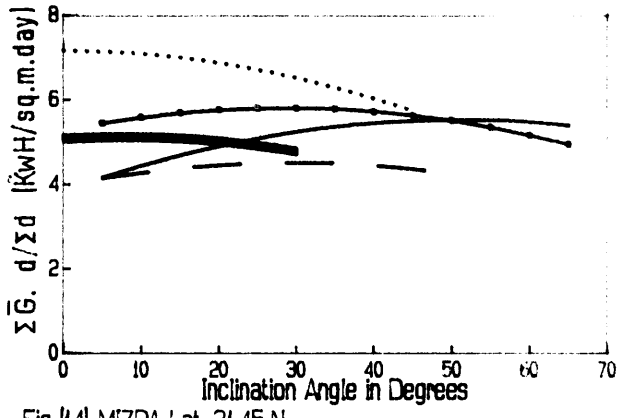

Fig.[14] MIZDA Lat. 31.45 N

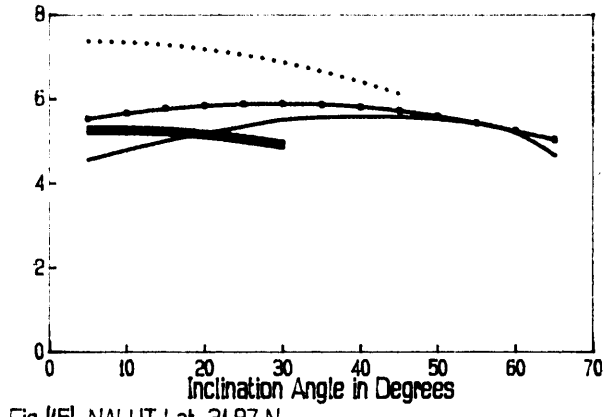

Fig.[15], NALUT Lat. 31.87 N

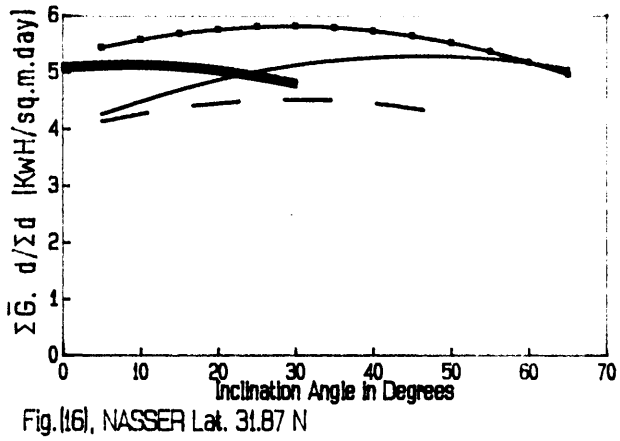

Fig.[16], NASSER Lat. 31.87 N

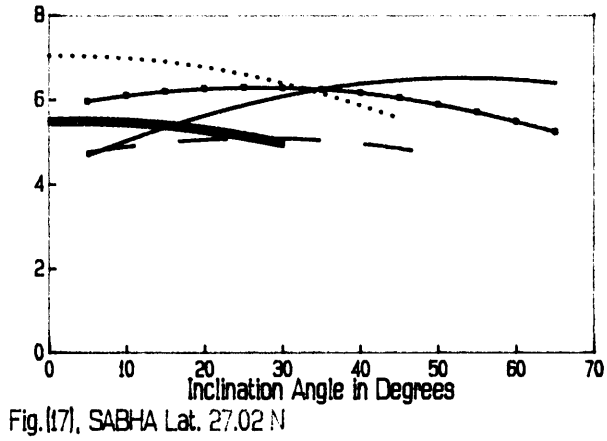

Fig.[17], SABHA Lat. 27.02 N

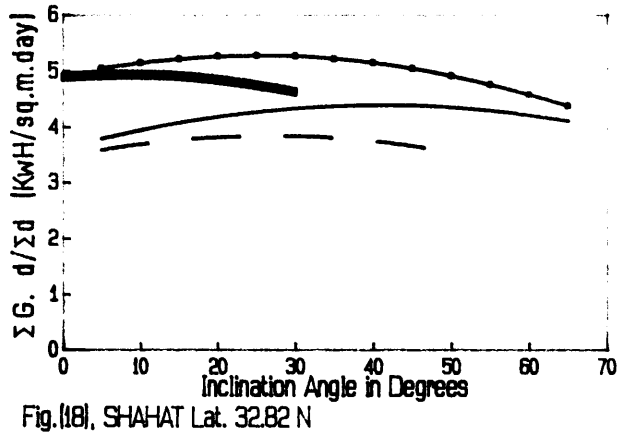

Fig.[18], SHAHAT Lat. 32.82 N

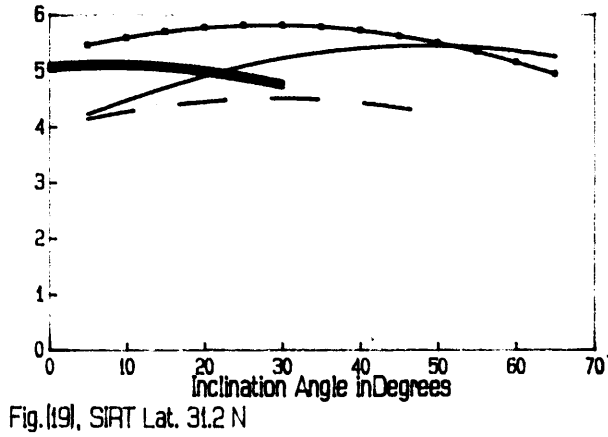

Fig.[19], SIRT Lat. 31.2 N

DWH Season — Heating Season — Irrig.W Pumping
Cooling Season — — Pot.W P & Relay Stations

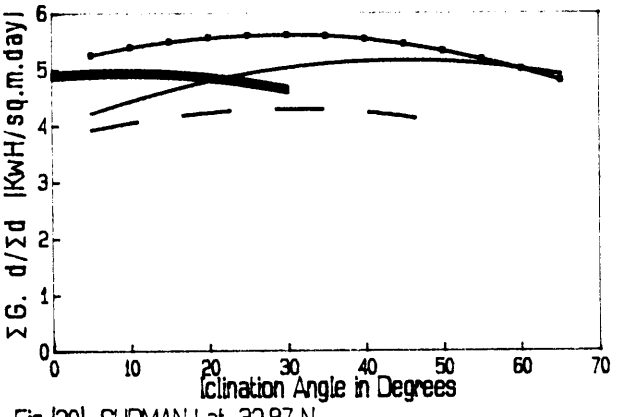

Fig.(20), SURMAN Lat. 32.87 N

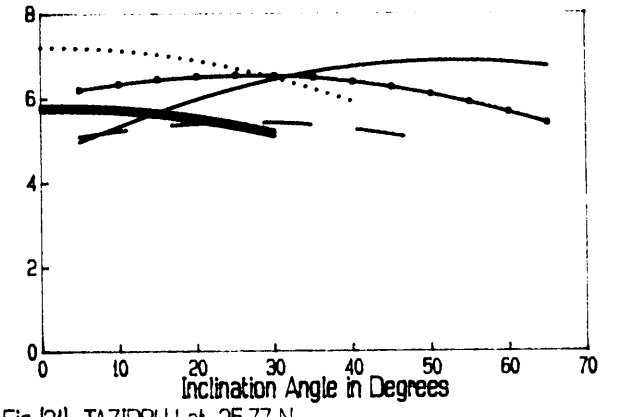

Fig.(21), TAZIRBU Lat. 25.77 N

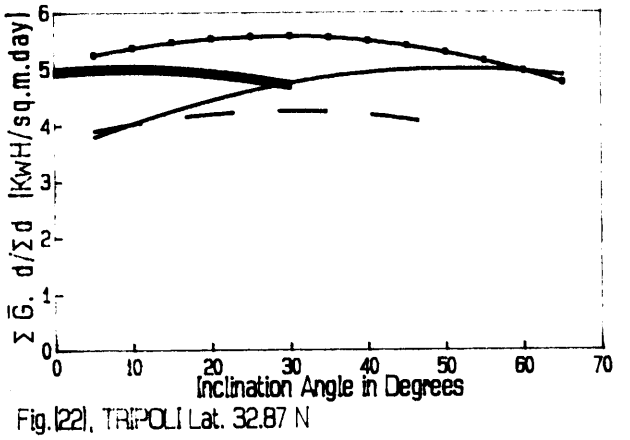

Fig.(22), TRIPOLI Lat. 32.87 N

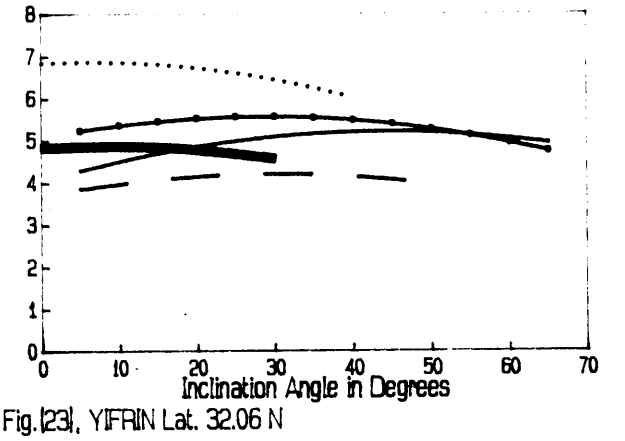

Fig.(23), YIFRIN Lat. 32.06 N

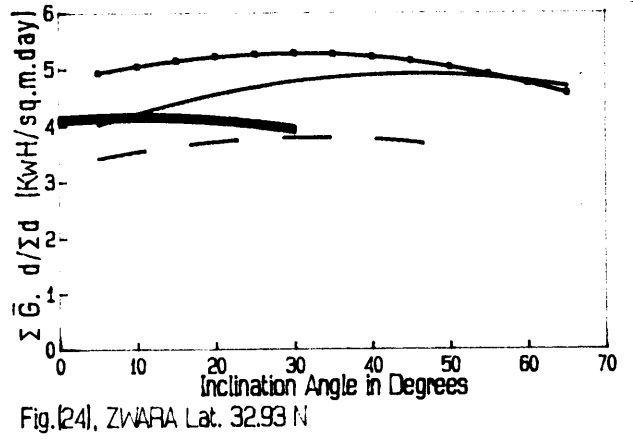

Fig.(24), ZWARA Lat. 32.93 N

—•— DWH Season
—— Heating Season
▬▬ Irrig.W Pumping
····· Cooling Season
— — — Pot.W P & Relay Stations

SOLAR RADIATION IN DHAKA

Md. Maksud Helali, Dr. Musharrif Hussain Khan and
Dr. A. M. Aziz-ul Huq.

Department of Mechanical Engineering
Bangladesh University of Engineering & Technology, Dhaka,
Bangladesh

ABSTRACT :

Solar radiation data in Bangladesh are very scarce. The daily total horizontal solar radiation was measured continuously by a pyranometer, located at the Bangladesh University of Engineering and Technology, Dhaka (Latitude 23°45' N) for four years, starting from March 1982. The data has been analysed and presented here. The daily diffuse radiation in Dhaka has also been estimated. The estimated results has been compared with some measured values and also with those suggested by other authors.

NOMENCLATURE :

H	Daily total radiation on a horizontal surface on earth.
H_o	Daily total extraterrestiral radiation on a horizontal surface [3]
H_d	Daily diffuse radiation on a horizontal surface on earth.
I	Hourly total radiation on a horizontal surface on earth.
I_o	Hourly total extraterrestrial radiation on a horizontal surface [3]
I_d	Hourly diffuse radiation on a horizontal surface on earth.
K_T	Clearness index, day basis, that is the ratio of a particular days total radiation to the total extraterrestrial radiation for that day.
$\bar{K}_T$	Clearness index, monthly average daily basis, that is the ratio of monthly average daily total radiation to that monthly average daily extraterrestrial radiation of that month.
k_T	Clearness index, hourly basis, that is the ratio of hourly total radiation on a horizontal surface to the hourly totoal extraterrestrial radiation for that hour.
ω	Hour angle, that is the angular displacement of the sun East or West of local meridian.
ω_s	Sun set hour angle.

INTRODUCTION :

Utilization of solar energy for a wide varity of application like solar thermal, solar photovoltaic cell etc. is increasingly becoming popular and in some situation very much cost effective. For optimum design and efficient performance of the appliances, the information of the solar insolation data at site (or region) is very important.

In Bangladesh some research organization measured total insolation data in a discrete way. In the department of Mechanical Engineering, Bangladesh University of Engineering and Technology, Dhaka (latitude 23°45' N), continuous and systimatic measurement of instantaneous and daily total solar radiation was done for a period of nearly four years from March 1982 to December 1986 under the supervission of Dr. Hossain A. [4].

The aim of the present work is mainly to present the solar data for Dhaka and to compare the data and generalised curves given by different authors with the data and curves the authors generated by actual measurement.

As diffuse radiation is significant in design of solar energy collection devices the calculated diffuse radiation data from daily total insolation data has also been presented here.

CORRELATION USED AND METHODOLOGY FOLLOWED :

The frequency of occurance of days with various daily clearness index (H/H_o) and the cumulative frequency of occurance of those days are calculated and presented graphically for Dhaka. The 'Monthly $\bar{K}_T$ curves' are drawn for different values of monthly average daily clearness index and compared with the results obtained by Liu and Jordan [5]. The hourly clearness index for Dhaka are also calculated and presented.

The following correlation of Collares-Pereira & Rabl [1] were used to determine the daily diffuse radiation.

$$
\begin{aligned}
H_d/H &= 0.99 && \text{For } K_T \leq 0.17 \\
H_d/H &= 1.188 - 2.272\,K_T + 9.473\,K_T^2 - 21.865\,K_T^3 + 14.648\,K_T^4 && \text{For } 0.17 \leq K_T \leq 0.75 \\
H_d/H &= 0.54\,K_T + 0.63 && \text{For } 0.75 < K_T \leq 0.80 \\
H_d/H &= 0.2 && \text{For } K_T > 0.80
\end{aligned}
\qquad (1)
$$

The hourly total and hourly diffuse radiation is calculated with the help of the equations given by Collares-Pereira and Rabl [1] and Orgil and Hollands [7]. These equations are given below.

$$
I/H = \frac{\pi}{24}\,(A + B\,\mathrm{Cos}\,)\,\frac{\mathrm{Cos}\,\omega - \mathrm{Cos}\,\omega_s}{\mathrm{Sin}\,\omega - \frac{2\pi}{360}\,\omega_s\,\mathrm{Cos}\,\omega_s} \qquad (2)
$$

Where,

$$A = 0.409 + 0.5016\,\mathrm{Sin}\,(\omega_s - 1.047)$$

$$B = 0.6609 + 0.4767\,\mathrm{Sin}\,(\omega_s - 1.047)$$

$$
\begin{aligned}
I_d/I &= 1.0 - 0.249\ k_T && \text{For } k_T < 0.35 \\
I_d/I &= 1.557 - 1.84\ k_T && \text{For } 0.35 \leqslant k_T \leqslant 0.75 \\
I_d/I &= 0.177 && \text{For } k_T > 0.75
\end{aligned} \qquad (3)
$$

The results are compared with some actual measured values recorded by the authors.

INSTRUMENTS USED :

Kipp & Zonen Pyranometer model CM5 has been used with integrator CC-1 to measure the daily and hourly total radiation on a horizontal surface. The diffuse radiation on a horizontal surface was measured by Kipp & Zonen Pyranometer model CM5 with Epphy integrator.
Pyranometer with the shadowring is calibrated against the Kipp & Zonen Pyranometer model CM5.

RESULTS AND DISCUSSIONS :

The results obtained are presented and discussed below.

The daily total radiation on a horizontal surface recorded in $cal.cm^{-2}.day^{-1}$ during four year in Dhaka has been considered. The average yearly total radiation is found to be 1368.6 $kw.m^{-2}.year^{-1}$. The four year average daily total radiation were calculated. It is found that the mean monthly average daily total radiation in Dhaka varies from 2.95 $kw.m^{-2}day^{-1}$ in December to 4.73 $kw.m^{-2}.day^{-1}$ on april (Table 1). The annual mean is 3.76 $kw.m^{-2}.day^{-1}$ for Dhaka. Table 1 also includes the predicted values of Mani [6] and Dejong [2] . The values of Mani and Dejong are higher than the measured values for Dhaka obtained by the authors. Mani may have considered the data of Shillong (latitude 25°34' N, longitude 91°53' E) and Calcutta (latitude 22°39' N, longitude 85°27' E) for predicting the values for Dhaka. The differences between the actual measurement and predicted values of Mani may be due to climatic condition of Dhaka, particularly the water particles present in the atmosphere. From the relative humidity (RH) data it is seen that Shillong has the RH range from 34% to 90%. Whereas about 50% of the days in a year it lies between 70% to 90%. But RH of Dhaka range from 60% to 99% with the 80% of days having a value between 70% to 90%.

The elevation of Bangladesh from the sea level is another factor, Dhaka is almost at the sea level (7.68 from msl) whereas the elevation of Shillong is 1600 m from mean sea level.

Figure 1 shows the frequency of occurances of days with various clearness indices and the cumulative frequency of occurencess of those days. It is observed that during 68% days of the year the clearness index values are between 0.3 and 0.5 and there are no days when the values of clearness index are above 0.57 and below 0.15. The frequency of occurence curve is slightly skewed towards the right.

Figure 2 shows the Monthly $\bar{K}_T$ curves' these curves are drawn for monthly average clearness index $\bar{K}_T$ values of 0.32, 0.40 and 0.50. It is seen that 50% of the days of the months having $\bar{K}_T$ of 0.50 will have $K_T \leqslant 0.53$. Liu and Jordan [5] claimed that these curves are general and valid for widely separated localities but the present work indicates that the curves for Dhaka are different from those obtained by Liu and

Jordan. It is found that for $\bar{K}_T$ 0.5 there are no days in the month having K_T below 0.39 in Dhaka, whereas the curve of Liu and Jordan suggested $K_T \leq 0.19$ for 30% of the days. This indicates that generalization may not be possible and there might be some seasonal and geographical dependence of these distributions.

Calculated values of the daily total diffuse radiation are presented in Table 1. It is observed that the mean annual values of daily diffuse radiation is significant (2.69 kw.m^{-2}.day^{-1}) and the annual diffuse radiation is 981.4 kw. m^{-2}. year^{-1}, which is 72% of the total yearly radiation. The maximum and minimum daily diffuse radiation is 3.4 kw.m^{-2}. day^{-1} and 1.51 kw. m^{-2}.day $^{-1}$ respectively. Maximum occurs during the month of July whereas the minimum is in the month of November.

Due to the onset of the monsoon during the later half of May water vapor gradually increases in the atmpsphere causing an increase in diffuse radiation (diffuse radiation is about 75% of the total radiation in May). The effect of water vapor and cloud persists for the months of June, July, August and September. During these month 80% to 90% of the total radiation is of diffuse nature. In the remaining months of the year the diffuse component is about 55% of the total in these months.

The measured values of diffuse radiation after necessary shadowring correction are plotted (Fig. 3). It is found that the curves are in good agreements with the curves drawn with estimated data.

A comparison between the diffuse radiation data for Dhaka given by Mani [6] and that obtained by authors are given in Table 1. It is found that for the months June, August and September the data have good agreement.

Monthly average hourly diffuse and hourly total radiation are calculated. These values were measured on some days. A comparison in Fig.4 shows that for lower $\bar{K}_T$ values the calculated values are 16% higher and for higher K_T values it is 30% lower. But for the middle values of K_T which is more frequent in Bangladesh, the deviation is less. This observation is to be conformed by taking many readings of hourly diffuse and hourly total radiation.

CONCLUSIONS :

The information available as of today indicates that prospect of solar energy in Bangladesh is reasonably good. It appears that simple extrapolation in the case of prediction of solar radiation might not be appropriate.

From estimation and measurement it appears that percentage of diffuse radiation is high in Dhaka, Bangladesh and this should be considered for the design of solar energy collection devices.

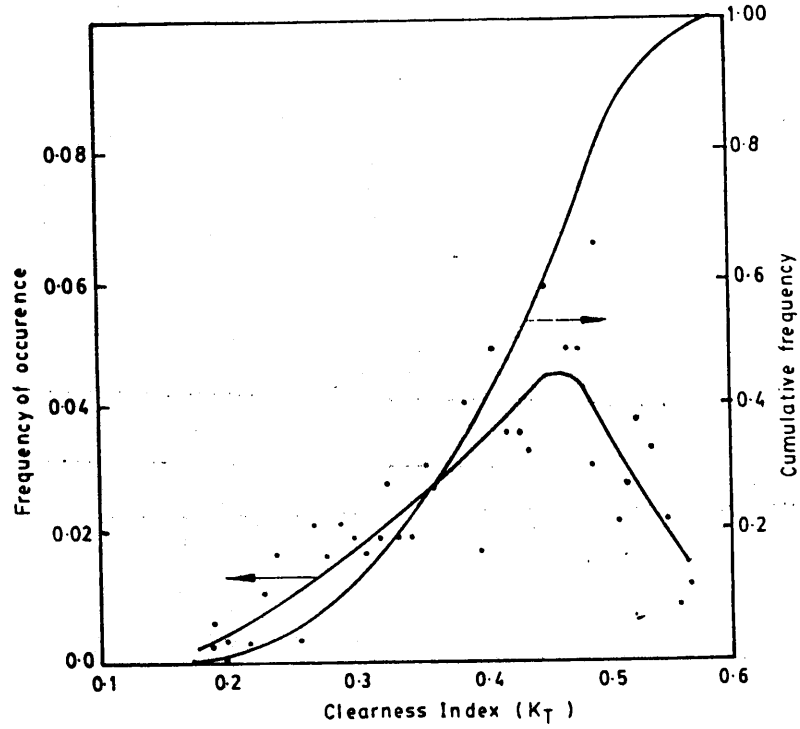

FIGURE.1. . FREQUENCY OF OCCURRENCE OF DAYS WITH VARIOUS CLEARNESS INDEX AND THE CUMULATIVE FREQUENCY OF OCCURRENCE OF THOSE DAYS.

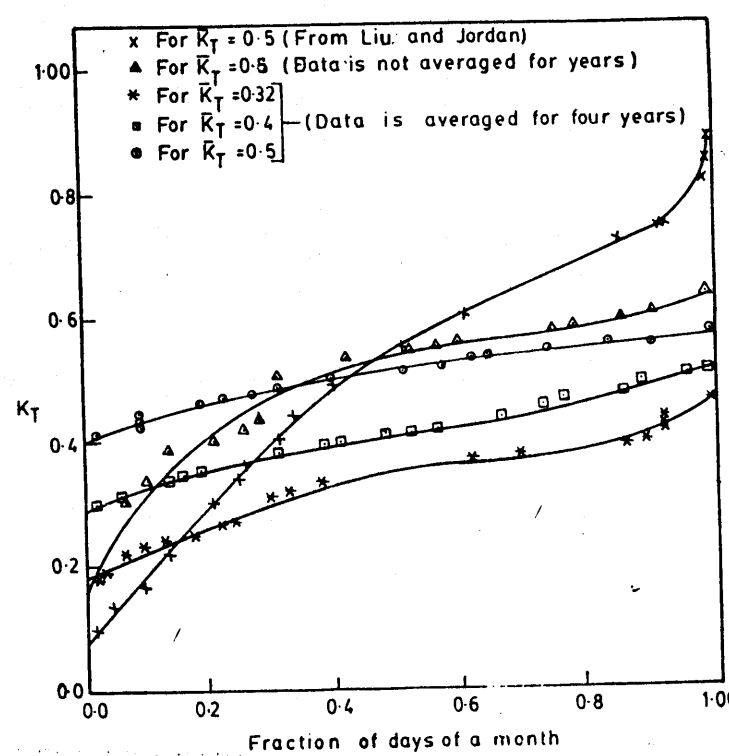

FIGURE.2. FRACTION OF DAYS OF A MONTH HAVING DIFFERENT VALUES OF K_T AS A FUNCTION OF $\bar{K}_T$

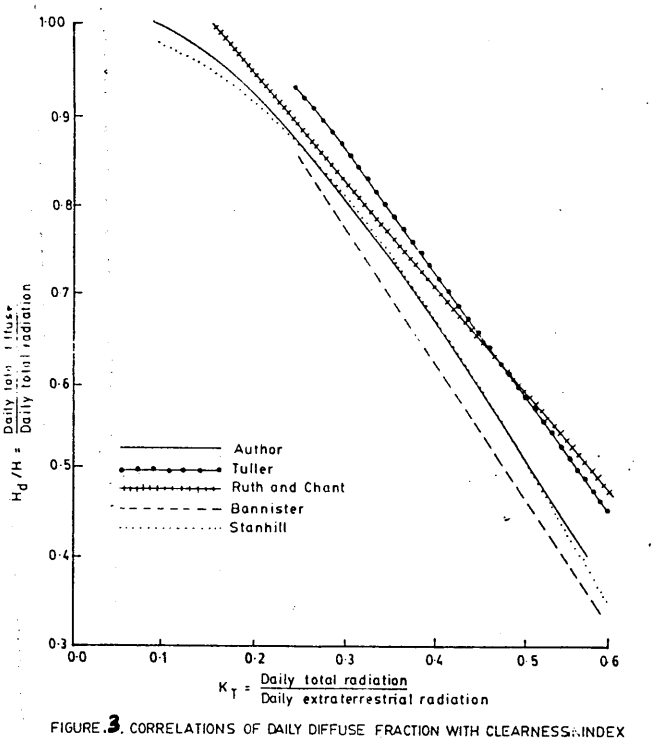

FIGURE 3. CORRELATIONS OF DAILY DIFFUSE FRACTION WITH CLEARNESS INDEX

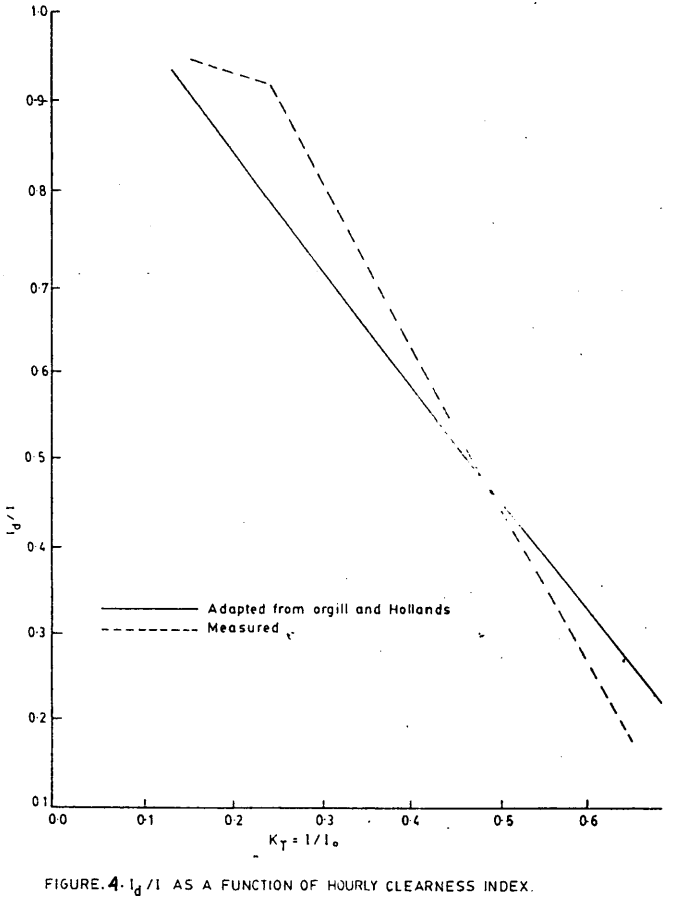

FIGURE 4. I_d/I AS A FUNCTION OF HOURLY CLEARNESS INDEX.

Table - 1

Monthly average daily radiation on a horizontal surface in Dhaka obtained by different authors

Month	Monthly average daily total radiation (kw. m^{-2}. day^{-1})			Monthly average daily diffuse radiation ($Kw.m^{-2}$. day^{-1})	
	By Author	By Mani	By Dejong	By Author	By Mani
January	3.12	4.29	-	2.14	1.50
February	3.72	5.39	-	2.37	1.80
March	4.67	5.80	5.52	2.73	2.30
April	4.73	6.20	-	3.14	2.60
May	4.41	6.39	-	3.29	3.00
June	3.52	4.80	3.23	2.98	3.10
July	3.72	5.09	-	3.07	3.10
August	3.42	5.00	-	2.86	3.00
September	3.41	5.06	4.65	2.71	2.70
October	3.64	5.20	-	2.51	2.20
November	3.64	4.70	-	2.07	1.60
December	2.95	4.29	4.07	2.01	1.60

REFERENCES :

1. Collares Pereira, M. and Robl, A., " The Average Distribution of Solar Radiation - Correlation Between Diffuse and hemispherical and Between Daily and Hourly Insolation Values.". Solar Energy,22,1975.
2. Dejong, B., " Net Radiation Received by a Horizontal Surface at the Earth." Monograph published by Delf-University press, Netherland (1973).
3. Duffie, J. A. and Beckmen, W. A., Solar Engineering of Thermal processes. John Wiley ' Sons, New York, 1980.
4. Helali,M.,"Solar Radiation in Bangladesh" M. Sc. Thesis (1986)
5. Liu, B. Y. H. and Jordan, R. C. " The Internationalship and Characteristic Distribution of Direct, Diffuse and total Solar Radiation". solar Energy, 4 (3) 1960.
6. Mani, A. and Rangarajan, S. Solar Radiation over India, Allied Publishers Private Limited. New Delhi. 1982
7. Orgil, J. F. and Hollands, K.G.T., " Correlation Equation for Hourly Diffuse Radiation on a Horizontal Surface." Solar Energy, 19. 357 (1977).

CALCULATION OF MONTHLY MEAN SOLAR RADIATION FOR INCLINED SURFACES

Dr Gamil M. Abdul Aziz,
Assistant Professor, Basic Sciences Dept.
College of Technology, Maalla, Aden, University of Aden,

Dr Aboubakr Abdul Rashid,
Lecturer, Physics Dept.,
Higher College of Education, Khormaksar, Aden, University of Aden,

Ahmed Salem Nasser
Basic Sciences Dept.,
College of Technology, Maalla, Aden, University of Aden.

A B S T R A C T

Several applications of solar energy require monthly average meteorological data. Monthly averages of solar radiation incident on a horizontal surface are available. However, radiation data on tilted surfaces are generally not available. A simple method for calculating the monthly average radiation for tilted surfaces facinf directly towards the equator, presented by Liu and Jordan (1) has been used in this study.

The monthly average values for the fraction of diffuse radiation have been calculated by using the empirical relationships derived by Liu and Jordan and Page. These results are used to evaluate the ratio of the total insolation rate on a tilted surface to that on a horizontal surface.The experimental results and those obtained from empirical relationship agree acceptably.

1. INTRODUCTION

The increasing demand for information on the availability of solar radiation for use as a supplement to the more conventional and non-renewable sources of energy has highlighted the inadequacy of the current observational networks. This inadequacy occurs in three basic ways:

- Limited spatial coverage,
- Limited length of record,
- And predominance of data for horizontal surface

while inclined surface date are more appropriate to solar energy evaluations (2).

In a previous work (3), measurements of global and diffuse solar radiation made by the Meteorological Department of the Civil Aviation Authority in Aden during the period 1958 - 1965 were used to verify some well-known empirical relations of prediction. The agreement with measurements for horizontal surfaces was within 5 per cent. For diffuse radiation, acceptable results were also obtained. The error remains with 15 per cent.

This paper presents a simple method for calculation of monthly average insolation on tilted surfaces facing directly towards the equator for Aden.

The results obtained in this paper will be of immense use for utilization and applications of solar energy in P.D.R.Y.

2. CALCULATION OF MEAN MONTHLY RADIATION IN SURFACES FACING DIRECTLY TOWARDS THE EQUATOR

The average daily radiation for each calender month on a tilted surface, H_T, can be expressed:

$$\bar{H}_T = \bar{R}\,\bar{H} = \bar{R}\,\bar{K}_T\,\bar{H}_o \qquad (1)$$

where $\bar{H}$ is the average daily radiation on a horizontal surface. The ratio $K_T = \bar{H}/\bar{H}_o$ is the clearliness index or the fraction of the mean daily extraterrestrial radiation $\bar{H}_o$ on a horizontal surface. H_o is given by:

$$(H_o)_n = \frac{24}{\pi} I_{sc}\left[(1 + 0.033 \cos \frac{(360n)}{365}\right] \times \left[\cos \phi \cos \delta \sin w_s \left(\frac{2\pi W_s}{360}\right) \sin \phi \sin \delta\right] \qquad (2)$$

where I_{sc} is the solar constant taken as 4871 $KJhr^{-1}$ m-2, n the day of the year, ϕ is the latitude and δ is the solar declination which can be approximately expressed:

$$\delta = 23 . 45^{o} \sin (360 (284 + nn) / 365) \qquad (3)$$

W_s is the sunset hour angle:

$$\cos W_s = -\tan \phi \tan \delta \qquad (4)$$

H_o can be conveniently estimated from eqn (2) by selecting for each month, the day of the year for which the daily extraterrestrial radiation is nearly the same as the monthly mean value. In our calculation, the recommended days proposed by Klein (4) are used.

Table 1 gives the recommended average day for each month and the monthly average daily extraterrestrial radiation.

Table 1. RECOMMENDED AVERAGE DAY AND MONTHLY AVERAGE DAILY EXTRATERRESTRIAL RADIATION, FOR EACH MONTH.

Month	Day of the year	Date	H_o ($MJ.m^{-2}$)
January	17	17 January	30.31
February	47	16 February	33.27
March	75	16 March	36.20
April	105	15 April	37.60
May	135	15 May	38.70
June	162	11 June	37.50
July	198	17 July	37.40
August	228	16 August	37.50
September	258	15 September	36.60
October	288	15 October	34.20
November	318	14 November	31.10
December	344	10 December	29.40

$\bar{R}$ is defined to be the ratio of the daily average radiation on a tilted surface to that on a horizontal surface for each month. This ratio can be measured directly or may be calculated by means of equations which are valid under certain conditions. The limits imposed on these equations are due to the nature of the diffuse component of the total radiation. It is impossible to determine accurately the angular correction factor for converting diffuse radiation rates on a horizontal surface to that on a tilted surface. This is a result of the indeterminate nature of the diffuse radiation, vis, its distribution over the sky is generally unknown.

Assuming diffuse and reflected radiation to be isotropic, Liu and Jordan (1) have proposed that $\bar{R}$ can be estimated by individually considering the beam, diffuse, and reflected components of the radiation incilence on the tilted surface and can be expressed:

$$\bar{R} = (1 - \bar{H}_d/\bar{H})\ \bar{R}_b + \bar{H}_d/\bar{H}\left(\frac{1 + \cos S}{2}\right) + \rho\left(\frac{1 - \cos S}{2}\right) \qquad (5)$$

where $\bar{H}_d$ is the monthly average daily diffuse radiation, $\bar{R}_b$ is the ratio of the average beam (direct) radiation on the titled surface to that on a horizontal surface, ρ is the ground reflectance, and the quantities in parentheses are the view factors for the diffuse component and reflected radiation respectively.

Liu and Jordan suggest that $\bar{R}_b$ can be estimated to be the ratio of extraterrestrial radiation on the tilted surface to that on a horizontal surface for the month. For surfaces facing directly towards the equator,

$$\bar{R}_b = \frac{\cos(\phi - S)\cos\delta \sin W'_s + (\pi/180)\, W'_s \sin(\phi - S)\sin\delta}{\cos\phi\cos\delta\sin W_s + (\pi/180)\, W_s \sin\phi\sin\delta} \qquad (6)$$

where W is the hour angle which is 15^{o} X (hours from solar noon), afternoons, positive, mornings negative and W'_s is the sunset hour angle for the tilted surface which is given by:

$$W'_s = \min\left[W_s, \text{ar cos}\left[-\tan(\phi - S)\tan\delta\right]\right] \qquad (7)$$

In our particular case, we possess experimental data for 8 years, from 1958 to 1965 for global and diffuse radiation, these data where supplied by the Meteorological Department of the Civil Aviation Authority in Aden. We have no information or direct experimental measurements for solar radiation on tilted surfaces.

The calculation of the monthly average solar radiation on tilted surface will be given by transforming the solar radiation data for horizontal to in inclined surface by using eqn(5). The results will be then compared by using the empirical relations reported by Liu and Jordan,

and Page which give the diffuse radiation fraction, $\bar{H}_d/\bar{H}$ as a function of $\bar{K}_T$. These relationships can be expressed:

$$\bar{H}_d = 1.390 - 4.027\ \bar{K}_T + 5.531\ \bar{K}_T^2 - 3.108\ \bar{K}_T^3 \qquad \text{LIU and JORDAN (8)}$$

$$\frac{\bar{H}_d}{\bar{H}} = 1.00 - 1.13\ \bar{K}_T \qquad \text{PAGE (9)}$$

3. RESULTS AND DISCUSSION

Table 2. gives the results for $\bar{R}_b$, $\bar{R}$ and $\bar{H}_T$ with $\rho = 0.2$ for Acen (Lat. 13° N), and this for different angles of inclinaison. The average daily radiation on a tilted surface $\bar{H}_T$ facing directly towards the equator is plotted in fig. 1.

It is seen from Table 2 and Fig. 1 that during winter months, October-March, a maximum solar radiation over tilted surfaces is obtained with s = 30°. During summer months, this maximum is given for horizontal surfaces, s = 0°.

In Table 3, the experimental measurements for $\bar{H}$ and H_d are used to evaluate $\bar{R}$ and are compared with values estimated from eqn 5 with $\rho = 0.2$ using the diffuse radiation fraction relationships of Liu and Jordan (eqn 8) and Page (eqn 9).

Based on this experimental data, it appears that the estimated values given by Liu and Jordan eqns (5) and (8), and Page eqns (5) and (9) agree acceptably.

Month	s = 0° R_b	s = 0° $\bar{R}$	s = 0° $\bar{H}_T$	s = 15° $\bar{R}_b$	s = 15° $\bar{R}$	s = 15° $\bar{H}_T$	s = 30° $\bar{R}_b$	s = 30° $\bar{R}$	s = 30° $\bar{H}_T$	s = 45° $\bar{R}_b$	s = 45° $\bar{R}$	s = 45° $\bar{H}_T$	s = 60° $\bar{R}_b$	s = 60° $\bar{R}$	s = 60° $\bar{H}_T$	s = 75° $\bar{R}_b$	s = 75° $\bar{R}$	s = 75° $\bar{H}_T$
JAN.	1	1	18.60	1.204	1.134	21.09	1.326	1.209	22.48	1.358	1.219	22.68	1.297	1.165	21.67	1.148	1.049	12.52
FEB.	1	1	20.90	1.129	1.087	22.72	1.182	1.118	23.36	1.154	1.089	22.77	1.047	1.004	20.99	0.869	0.868	18.15
MAR.	1	1	24.00	1.044	1.030	24.72	1.017	1.006	24.15	0.920	0.930	22.33	0.761	0.808	19.39	0.550	0.647	15.53
APR.	1	1	25.00	0.958	0.968	24.20	0.853	0.888	22.19	0.691	0.764	19.10	0.486	0.607	15.17	0.254	0.429	10.72
MAY	1	1	24.50	0.894	0.923	22.61	0.734	0.805	19.72	0.532	0.655	16.04	0.307	0.485	11.89	0.089	0.320	7.83
JUN.	1	1	22.90	0.864	0.916	20.97	0.680	0.797	18.24	0.463	0.651	14.91	0.235	0.494	11.31	0.035	0.351	8.03
JUL.	1	1	21.40	0.877	0.930	19.91	0.704	0.825	17.66	0.494	0.693	14.83	0.266	0.544	11.65	0.057	0.401	8.59
AUG.	1	1	22.50	0.930	0.956	21.50	0.801	0.869	19.55	0.621	0.746	16.79	0.405	0.598	13.45	0.175	0.437	9.84
SEP.	1	1	23.40	1.009	1.004	23.50	0.950	0.958	22.42	0.826	0.864	20.21	0.648	0.728	17.04	0.422	0.561	13.12
OCT.	1	1	23.50	1.101	1.079	25.35	1.127	1.098	25.80	1.076	1.057	24.84	1.952	0.958	22.51	0.762	0.808	18.98
NOV.	1	1	20.20	1.184	1.141	23.04	1.288	1.218	24.61	1.303	1.228	24.81	1.230	1.169	23.61	1.073	1.044	21.09
DEC.	1	1	18.70	1.227	1.155	21.59	1.369	1.248	23.33	1.419	1.273	23.80	1.372	1.229	22.98	1.231	1.119	20.92

Table 2. VALUES OF F_b, R and H_T FROM EQN 4.

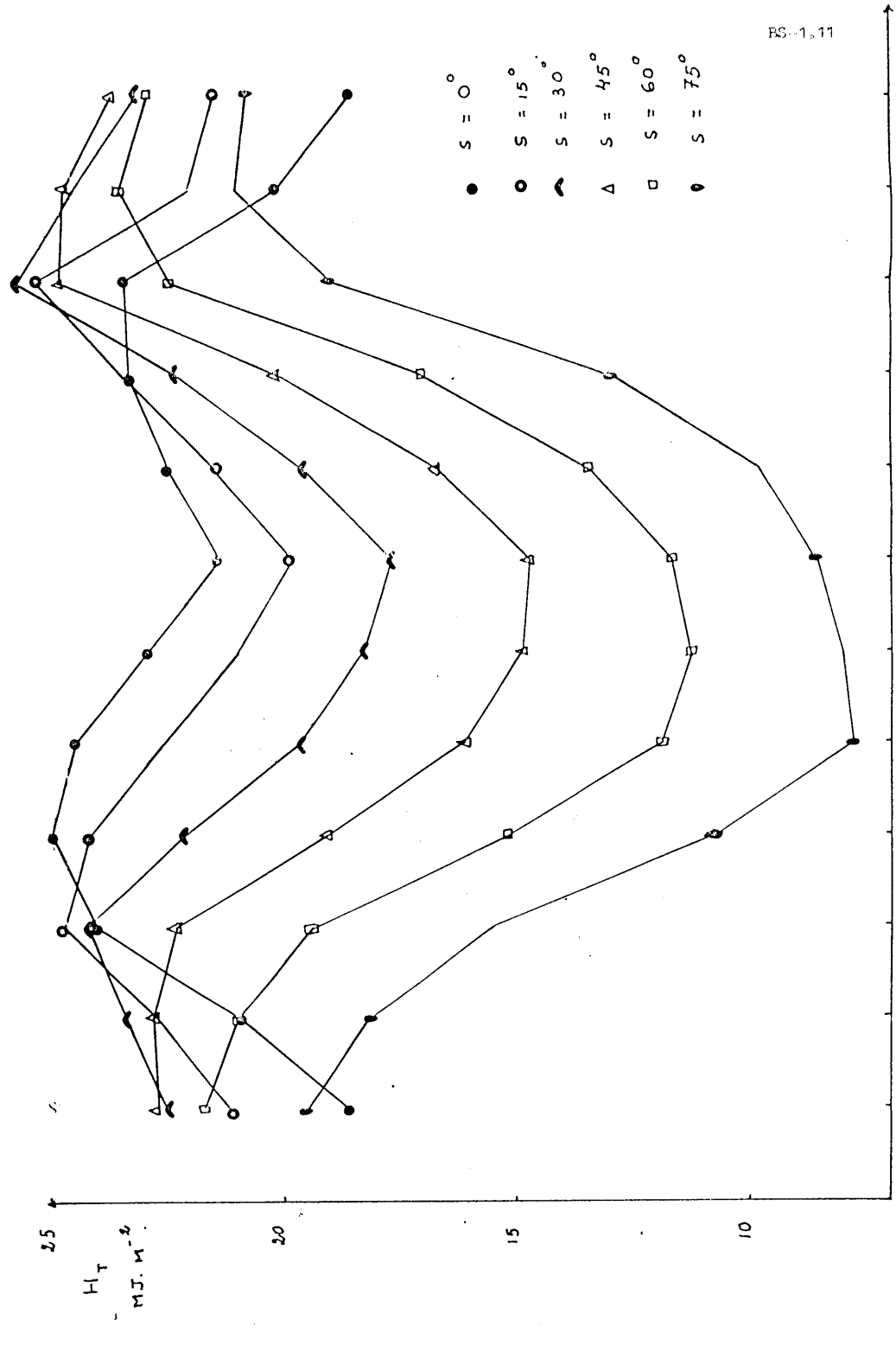

FIG. 1. SOLAR RADIATION AT DIFFERENT INCLINED SURFACES FACING SOUTH IN ADEN

Month	K_T	s = 15°			s = 30°			s = 45°		
		$\bar{R}$ experimental	$\bar{R}$ estimated eqn 5 and 8	$\bar{R}$ estimated eqn 5 and 9	$\bar{R}$ experimental	$\bar{R}$ estimated eqn 5 and 8	$\bar{R}$ estimated eqn 5 and 9	$\bar{R}$ experimental	$\bar{R}$ estimated eqn 5 and 8	estimated eqn 5 and 9
JAN.	0.5963	1.134	1.142	1.135	1.209	1.236	1.223	1.219	1.271	1.254
FEB.	0.6252	1.087	1.093	1.090	1.118	1.131	1.126	1.089	1.112	1.106
MAR.	0.6638	1.030	1.032	1.032	1.006	1.010	1.009	0.930	0.934	0.933
APR.	0.6660	0.968	0.966	0.968	0.888	0.886	0.886	0.764	0.760	0.761
MAY.	0.6341	0.923	0.921	0.922	0.805	0.800	0.804	0.655	0.647	0.653
JUNE	0.6109	0.916	0.901	0.904	0.797	0.766	0.772	0.651	0.604	0.613
JULY	0.5733	0.930	0.914	0.918	0.825	0.789	0.798	0.693	0.636	0.650
AUG.	0.6005	0.956	0.949	0.951	0.869	0.853	0.857	0.746	0.725	0.725
SEP.	0.6393	1.004	1.006	1.005	0.958	0.959	0.959	0.864	0.863	0.863
OCT.	0.6898	1.079	1.078	1.078	1.098	1.099	1.100	1.057	1.062	1.063
NOV.	0.6466	1.141	1.124	1.133	1.218	1.198	1.216	1.228	1.215	1.238
DEC.	0.6381	1.155	1.166	1.162	1.248	1.284	1.277	1.273	1.342	1.333

Table 3. COMPARISON OF EXPERIMENTAL AND ESTIMATED VALUES OF $\bar{R}$ FOR SURFACE FACING SOUTH AT ADEN. LAT. 13° N.

$s = 60^{\circ}$			$s = 75^{\circ}$		
$\bar{R}$ experimental	$\bar{R}$ estimated eqn 5 and 8	$\bar{R}$ estimated eqn 5 and 9	$\bar{R}$ experimental	$\bar{R}$ estimated eqn 5 and 8	$\bar{R}$ estimated eqn 5 and 9
1.165	1.248	1.229	1.949	1.180	1.159
1.004	1.037	1.031	0.868	0.916	0.910
0.808	0.809	0.809	0.647	0.645	0.645
0.607	0.600	0.601	0.429	0.419	0.421
0.485	0.476	0.483	0.320	0.308	0.316
0.494	0.432	0.444	0.351	0.279	0.293
0.544	0.468	0.486	0.401	0.310	0.333
0.598	0.556	0.566	0.437	0.383	0.396
0.728	0.723	0.725	0.561	0.551	0.554
0.958	0.969	0.808	0.808	0.879	0.829
1.169	1.176	1.203	1.044	1.091	1.119
1.229	1.340	1.329	1.119	1.293	1.282

C O N C L U S I O N

A simple method for calculating the average daily radiation for each calender month on tilted surfaces facing directly towards the equator presented by Liu and Jordan, has been used in our study.

During winter months, maximum value of radiation is oobserved for s = 30^{o}. For summer months the maximum value of solar radiation is obtained over horizontal surfaces.

For fixed tilt surfaces, an average value of s = 15^{o} can be taken for the whole year.

R E F E R E N C E S

(1) B.Y.H. Liu, R.C. Jordan, DAILY INSOLATION ON SURFACES TILTED TOWARD THE EQUATOR, Trans. Ashrae 526-541 (1962),

(2) John E. Hay, SOLAR ENERGY, Vol. 23, pp 301-307, 1979.

(3) Gamil M. Abdul Aziz, Mohammed A. Moqbel, CONFERENCE IN RENEWABLE ENERGY, Halab University Syria, 29 sept-2-Oct. 1986.

(4) S.A. Klein, SOLAR ENERGY, Vol. 19, pp 325-329, 1977.

SOLAR ENERGY DISTRIBUTION OVER EGYPT USING CLOUDINESS FROM METEOSAT PHOTOS

M.A.Mosalam Shaltout and A.H.Hassan

National Research Institute of Astronomy and Geophysics

Helwan - Cairo - Egypt

ABSTRACT

In Egypt, there are ten ground stations for measuring the global solar radiation, and five stations for measuring the diffuse solar radiation. Every day and at noon, the Meteorological Authority in Cairo receiving three photographs for the cloudiness over Egypt from Meteosat artificial satellite, one in the visible, and two in the infra red bands (10.5 - 12.5 μm) and (5.7 - 7.1 μm) . The monthly average of the cloudiness for 24 sites over Egypt are measured and calculated from Meteosat observations during the period 1985 - 1986 .

Correlation analysis between the cloudiness observed by Meteosat and global solar radiation measured from the ground station are carried out . It is found that , the correlation coefficients are about 0.90 for the simple linear regression, and increase for the second and third degree regressions. Also , the correlation coefficients for the cloudiness with the diffuse solar radiation are about 0.80 for the simple linear regression, and increase for the second and third degree regression. Models and empirical relations for estimating the global and diffuse solar radiation from Meteosat cloudiness data over Egypt are deduced and tested. Seasonal maps for the global and diffuse radiation over Egypt are carried out.

1.INTRODUCTION

As solar energy use increases, mapping the geographical and temporal distribution of surface insulation will become increasingly important, in order to size collecting surfaces, as a function of energy needs. In recent years, satellite data have been increasingly used to measure solar energy at the earth's surface. The major Strength of this approach lies in its wide area coverage, specially over ocean or desert.

Tarpley (1) related surface insulation to GOES 2 Satellite visible channel brightness measurements over U.S.A. through a statistical model. Peal (2) determined empirical formulas for the calculation of the relative global radiation over Hungary from values of Cloud coverage using Meteosat Satellite pictures and from other meteorological parameter (visibility). A system for mapping the mesoscale distribution of insulation from GOES Satellite data has become operational at the University Wisconsin Space Science and Engineering Center(3) . Nullet (4) found two methods for estimating insulation over the tropical pacific using cloud cover from satellite observations. Nunez (5) used visible reflectivity data from the Japanese meteorological satellite to estimate the daily global radiation in Tasmania, Australia.

The principle aim of present study is to develop and test new and improved models for using Meteosat cloudiness data to evaluate the amount of solar radiation (global and diffuse) reaching Egypt on the monthly average.

2. DATA

2.1 Satellite Data :

Meteosat Satellite is stationed in a geostationary orbit at nearly 36,000km above the equator and the Greenwich meridian (0 degrees N, 0 degrees E). The principle payload of the satellite is a multi spectral radiometer (6). This provides the basic data of the Meteosat system as visible and infra - red radiance producing images of the full earth's disk visible from geostationary orbit. The three channel radiometer includes :

- Two identical adjacent visible channels in the 0.4 - 1.1 μm spectral band.
- A thermal infra - red (window) channel in 10.5 - 12.5 μm band .
- An infra - red (water vapour) channel in the water - vapour absorption band (5.7 - 7.1 μm), which can be operated in place of one of the two visible channels.

The possible sets of images in any one half hour period are :

- Either 2.5 km resolution visible, with 5 km infra - red (11μm), or 5 km resolution visible with 5 km infra red (11μm) and 5 km water - vapour (6 μm).

Every day and at L.M.T. 11^h, the Meteorological Authority of Egypt at Cairo, receiving two images from the artificial satellite Meteosat for the cloudiness over Egypt and the surrounding Countries. One image in the visible spectral band (0.4 - 11 μm), and the other in the thermal infra - red window (10.5 - 12.5 μm). Beside, third image in the water vapour absorption band (5.7 - 7.1 μm). The brightness of a resolution element as seen by the satellite is interpreted as an index of atmospheric opacity, which in turn enables the calculation of surface insulation using models or empirical relations (7) . We classified the brightness to five degrees (very dark area is

zero, while very bright area is four), and measured the daily brightness of the three images for 24 sites in Egypt (see map 1) . The available images were for two years only (1985 - 1986) . The measurements are multiplied by 2 to convert it from four fold scale to eight fold scale as the cloudiness measured from ground (in Oktas). There are missing data for some days during the period (1985 - 1986). The available visible, infra - red and water vapour images cover 62%, 94% and 89% from the total period respectively.

2.2 Ground Data :

There are ten ground stations for measuring the global solar radiation in Egypt, beside five stations for measuring the diffuse radiation (see table 1). Also, we used the available data of solar global radiation from the ground station at Aqaba in Jordan.

The insulation data of the Egyptian Stations are available from the Meteorological Authority of Egypt at Cairo. Data of Aqaba are available from (8). The data of Sidi Barani and Bahtim are not used in our analysis, because the first are available for short period and cloudiness data observed by Meteosat for Bahtim have the same value for Abbasiya station at Cairo area.

Table (1)
Ground stations for measuring global and diffuse solar radiations

No.	Station	Code	Climatic region	Coordinates of Station		
				Lat.N	Long. E	Elev. (m)
1	Sidi Barani	SID	Mediterranean	31° 38`	25° 28`	21.0
2	Matruh	MAT	Mediterranean	31° 20`	27° 13`	28.3
3	Tahrir	TAH	Nile Delta	30° 39`	30° 42`	15.6
4	Bahtim	BAH	Cairo Area	30° 08`	31° 15`	16.9
5	Abbasiya	ABB	Cairo Area	30° 05`	31° 17`	34.4
6	Asyout	ASY	Middel Egypt	27° 03`	31° 01`	234.7
7	Aswan	ASW	Upper Egypt	23° 58`	32° 47`	200.0
8	Kharga	KHA	Western Desert	25° 27`	30° 32`	77.8
9	Owienat	OWI	Western Desert	22° 28`	28° 42`	274
10	El Arish	ARI	North Sinai	31° 16`	33° 45`	15.0
11	Aqaba	AQA	South Sinai	29° 33`	35° 00`	51.0

- All the stations measure global radiation.
- Stations (No. 2 , 3 , 5 , 7 and 8) measure diffuse radiation.
- Code name is special code for the present work only.

3. ANALYSIS AND DISCUSSION

Considerable difficulties were encountered in obtaining three images (visible, infra - red, and water vapour) per day on a regular basis from Meteosat. Some difficulties from the operation of the reception facilities at the Meteorological Authority in Cairo, and others from poor quality and low contrast of the images. The monthly average of the cloudiness for the three spectral bands are determined for 24 sites of map(1) . The monthly average of the global radiation for 11 ground station of table (1), and the monthly average of diffuse radiation for 5 ground Station of table (1) are obtained.

A regression analysis are carried out for correlations between solar radiation measured at ground and cloudiness observed by Meteosat on the forms :

1^{st} degree $Y_i = a_o + a_1 X_j$

2^{nd} degree $Y_i = b_o + b_1 X_j + b_2 X^2_j$

3^{rd} degree $Y_i = C_o + C_1 X_j + C_2 X^2_j + C_3 X^3_j$

Where i = 1 , 2 , and j = 1 , 2 , 3

Y_1 is the monthly average of global radiation, and

Y_2 is the monthly average of diffuse radiation.

also,

X_1 is the monthly average of the cloudiness in the visible band.

X_2 is the monthly average of the cloudiness in infra - red band.

X_3 is the monthly average of the cloudiness in water vapour band.

The coefficients of multiple correlations are calculated for each regression and the results for the global radiation are given in table (2) .

Table (2)

Multiple correlation coefficients for global radiation measured from the ground with cloudiness observed by Meteosat in three spectral bands.

Station	degree	Correlation coefficients		
		visible	infra - red	water vapour
Matruh	1	0.363	0.947	0.821
	2	0.680	0.947	0.849
	3	0.596	0.948	0.856
Tahrir	1	0.214	0.943	0.791
	2	0.650	0.950	0.810
	3	0.672	0.962	0.842
Abbasiya	1	0.019	0.940	0.804
	2	0.605	0.941	0.819
	3	0.599	0.943	0.845
Asyout	1	0.557	0.916	0.792
	2	0.765	0.921	0.795
	3	0.776	0.922	0.859
Aswan	1	0.496	0.868	0.719
	2	0.506	0.931	0.722
	3	0.638	0.934	0.735
Kharga	1	0.583	0.947	0.770
	2	0.611	0.963	0.770
	3	0.610	0.963	0.781
Owienat	1	0.661	0.952	0.832
	2	0.694	0.953	0.837
	3	0.704	0.958	0.840
El Arich	1	0.476	0.939	0.801
	2	0.520	0.953	0.821
	3	0.520	0.956	0.873
Aqaba	1	0.461	0.931	0.820
	2	0.560	0.943	0.835
	3	0.563	0.945	0.871

The coefficients of multiple correlations between the diffuse radiation measured from the ground and cloudiness observed by Meteosat in the three spectral bands are given in table (3).

Table (3)
Multiple correlation coefficients for
diffuse radiation measured from the ground
with cloudiness observed by Meteosat in three spectral bands.

Station	degree	Correlation coefficients		
		visible	Infra - red	water vapour
Matruh	1	0.229	0.764	0.516
	2	0.620	0.770	0.689
	3	0.617	0.773	0.723
Tahrir	1	0.168	0.784	0.483
	2	0.439	0.786	0.591
	3	0.536	0.843	0.666
Abbasiya	1	0.187	0.775	0.540
	2	0.584	0.784	0.636
	3	0.601	0.807	0.699
Kharga	1	0.394	0.758	0.476
	2	0.476	0.799	0.498
	3	0.476	0.812	0.519
Aswan	1	0.575	0.754	0.543
	2	0.692	0.854	0.562
	3	0.573	0.855	0.564

From tables (2) and (3), we can notice that :

a) The best correlation coefficients for regression between solar radiation and cloudiness, are for cloudiness observed in Infra - red (10.5 - 12.5 μm) band. The poor correlation are between radiation and cloudiness observed in visible (0.4 - 1.1 μm) band. This is right for both global and diffuse solar radiation.

b) The correlation increase with increasing the degree of the regression equation.

The poor correlation between solar radiation and cloudiness observed in the visible band can be interpret by the following :

- 38% from the length of the period (Jan. 1985 to Dec. 1986) without data in the visible band.
- The poor quality of the images in the visible band at Cairo.
- The short diminches of the visible images (relative to the infra - red images) lead to difficulties in measurements, and affecting on the accuracy.

The constants of regression for the third degree regression equation between radiation and cloudiness observed in infra - red are given in table (4) .

Table (4)

The constants of regressions of the third degree equation
for relation between solar radiation and cloudiness observed in infra - red

Station	Type of radiation	Constant of regression				r
		C_o	C_1	C_2	C_3	
Matruh	G	9.211	-0.976	-0.284	0.045	0.948
	D	2.688	0.219	-0.219	0.024	0.773
Tahrir	G	7.972	0.541	-1.195	0.198	0.962
	D	1.898	1.502	-0.945	0.135	0.843
Abbasiya	G	7.970	-0.752	-0.317	0.057	0.943
	D	2.231	0.433	-0.365	0.051	0.807
Asyout	G	8.639	-2.096	0.387	-0.039	0.922
Aswan	G	9.340	-4.480	1.580	-0.189	0.934
	D	2.556	-1.086	0.163	0.023	0.855
Kharga	G	8.612	-1.684	-0.0003	0.044	0.963
	D	2.505	-0.092	0.0892		0.812
Owienat	G	6.592	-0.193	-0.644	0.153	0.958
El - Arich	G	7.612	-1.227	-0.183	0.049	0.956
Aqaba	G	7.542	-1.077	-0.171	0.053	0.945

- G means global radiation .
- D means diffuse radiation .
- r means correlation coefficient .

Table (5)

Errors of estimations (%)

station code	Type	J	F	M	A	M	J	J	A	S	O	N	D	mean *
MAT	G	-5.2	17.6	18.6	-7.4	10.7	-1.8	5.4	1.2	-9.0	-12.0	-25.6	-10.9	10.4
	D	-10.3	26.2	19.3	7.7	21.9	0.3	4.8	-8.3	-23.0	-26.0	-27.3	-18.2	16.1
TAH	G	-8.9	17.6	-1.2	-0.3	11.0	0.1	3.5	-3.0	-12.4	1.9	-8.1	-9.1	6.7
	D	-11.1	20.9	7.8	11.6	18.3	5.8	-4.4	-10.8	-25.6	-17.5	-11.2	-7.3	11.8
ABB	G	-2.7	15.9	15.5	-1.8	13.1	2.0	-1.4	0.3	-9.6	-10.0	-17.4	-19.2	9.0
	D	-4.1	15.3	18.8	10.9	15.9	-0.8	1.6	-7.6	-17.6	-26.1	-18.5	-15.1	12.4
ASY	G	-0.2	12.2	17.6	-4.6	4.6	-2.6	8.2	5.3	-6.0	-15.3	-11.9	-21.7	9.2
ASW	G	0.6	11.6	4.8	-6.2	11.0	-2.7	3.5	4.3	-6.3	-10.2	-8.3	-7.6	6.4
	D	1.9	20.4	6.8	3.2	23.7	-4.4	-6.7	-5.5	-11.2	-14.3	-17.5	-18.3	11.1
KHA	G	0.9	9.5	6.4	-0.9	7.9	-0.9	0.6	-2.0	-0.7	-10.5	-8.7	-5.4	4.5
	D	-2.6	15.8	18.4	10.6	12.2	-3.9	-2.1	-5.2	-24.6	-25.8	-12.4	0.7	11.2
OWI	G	-2.3	10.6	-3.2	-4.7	-2.1	1.1	5.5	3.3	2.1	-4.8	-0.1	-7.5	4.0
ARI	G	-0.9	10.8	5.7	-2.2	13.3	0.8	2.7	-3.6	-10.1	-6.9	-3.4	-13.3	6.1
AQA	G	3.3	7.6	10.3	-2.8	13.1	1.2	3.6	-2.6	-12.6	-7.1	-6.1	-17.0	7.2

* Mean means the average value of the absolute values of the errors of estimation of the 12 months of the year.

The constants of the empirical relations (Models) in table (4) are tested, by calculating the errors of the estimations for global G and diffuse D radiation using the Cloudiness observed in infra - red band by Meteosat, as seen from table (5). The average of the mean errors of estimation of G for the different ground stations is equal to 7.0%, while it is equal to 12.5% in the case of D estimation. This can be interpret by the level of correlation, Where the mean correlation coefficient for all ground Stations for G with Cloudiness is r = 0.948, while it is r = 0.818 for the correlation of D with Cloudiness, see table (4).

4. Estimating Solar Energy

As we mentioned before, the cloudiness are measured from meteosat photos for 24 sites in Egypt, nine of them are the ground stations of measuring the global and diffuse solar radiation. The remain fifteen sites have uniform distribution over Egypt, in the different climatic regions. Foe each one of the fifteen sites, we applied the model of the nearest station to estimate the global and diffuse solar radiation at the site.

The estimated values of the radiation are monthly values in kwh / m^2 / day. Mapping the geographical and seasonal distribution of global and diffuse solar radiation are carried out. The seasons are defined on the basis of :

Winter is (Dec., Jan., Feb.),

Spring is (Mar., Apr., May),

Summer is (Jun., Jul., Aug.), and

Autumn is (Sept., Oct., Nov.).

Maps (2 to 5) give the seasonal distribution of the global radiation G over Egypt, while maps (6 to 9) give the seasonal distribution of the diffuse radiation D over Egypt.

From maps (2 - 5) we can notice the following :

1) There is regular increase for G from the north to the south of Egypt for all seasons. There are exceptional droop in two areas, Cairo area due to air pollution (9), and Owienat area due to sand storms and tropic clouds (10, 11).

2) The variation of G from north to south of Egypt have wide range (3.7 to 5 kwh / m2 / day) at winter, and narrow range (8 to 8.3 kwh / m2 / day) at summer. The transit seasons have intermediate range.

3) The seasonal variation of G over Egypt is clear. It varying from winter to summer in wide range (3.7 to 8 kwh / m2 / day) at north, and in narrow range (5 to 8.3 kwh / m2 / day) at south of Egypt.

4) Generally, solar energy potential of Egypt is very high. The utilization of solar energy as alternative and renewable energy must be take strongly into consideration in the future, specially in remote areas (12).

From maps (6 - 9) we can notice the following :

1) The diffuse radiation D decrease from the north to the south of Egypt.

2) The diffuse radiation D have regular seasonal variation over Egypt.

3) Owienat area in the west - south desert have high level of diffuse radiation due to the sand rising and storms in the deep desert. Beside the effect of the tropic clouds (11).

4) The diffuse fraction KD (ratio of diffuse to global) varying from 0.34 to 0.43 at the north of Egypt from summer to winter. KD approximately constant at the level 0.25 at the south of Egypt. This confirm our results in (13), than our results in (14).

5. CONCLUSION

In this study empirical formulas (Models) were determined for the estimation of the global and diffuse radiation over Egypt, from cloud coverage obtained from satellite Meteosat photos. The new models are tested and reliable. The average of the errors of estimations is 7.0% for global radiation, and 12.5% for the diffuse radiation. The Knowledge and forecast of the incoming solar radiation is very important for economical application of the solar energy. Mapping the geographical and seasonal distribution of global and diffuse solar radiation are carried out, and many conclusions from its are obtained, see section (4). All the conclusions lead to higher conclusion of :

The utilization of solar energy at Egypt as alternative and renewable energy must be take strongly into consideration in the future, specially in developing the desert and remote areas, where Egypt is on of the most rich countries of solar energy.

6. REFERENCES

1) Tarpley, J.D., Estimating incident solar radiation at the surface from geostationary Satellite data, J. Appl. Meteor. 18, 1172 - 1181, (1979).

2) Paal, A.R., Determination of global radiation from Satellite pictures and Meteorological data, Solar Energy vol.31, No. 1, pp. 79 - 84, (1983).

3) Diak, G.R., and et al., An operational system for mapping insulation from GOES Satellite data, Solar Energy vol. 28, No. 5, pp. 371 - 376, (1982).

4) Nullet, D., A Comparison of two methods of estimating insulation over the tropical pacific Ocean using Cloudiness from Satellite observations, Solar Energy, vol.39, No.3, pp. 197 - 201, (1987).

5) Nunez, M., A Satellite - based solar energy monitoring system for Tasmania - Australia, Solar Energy vol. 39, No. 5, pp. 439 - 444, (1987).

6) Morgan, J., Introduction to the Meteosat system, European Space Operations Centre ESOC, Darm Stadt, Federal Republic of Germany, (1978).

7) Bahm, R.J., ed., Satellite and Forecasting of solar radiation, International Solar Energy Society, 76 - 85, (1981).

8) Sayigh, A.A.M., The iso - radiation map for the Arab region, solar & wind Technology vol.4, No.2, pp. 163 - 177, (1987).

9) Mosalam Shaltout, M.A., Solar radiation and air pollution in Cairo, Proceedings of Third Arab International Solar Energy Conference, ed. N.AL Hamadani and et al., Baghdad, Iraq, 21 - 24 February (1988).

10) Mosalam Shaltout, M.A., and A.H.Hassan, Solar Energy Potential Two Owienat, Advances in Solar Energy Technology, Pergamon Press, Oxford, UK, (1987).

11) Mosalam Shaltout, M. A., and A.H.Hassan, Solar energy potential to Owienat from measured data, Proceedings of Cairo international symposium on renewable Energy Sources, ed. A.EL - Sharkawi, Cairo, Egypt, 13 - 16 June (1988).

12) Mosalam Shaltout, M.A., Solar energy input and photovoltaic water Pumping in the Western Desert Oases of Egypt, Advances in Desert and Arid land Technology and development. vol. 5, ed. A. Bishay and H.R.Dregne, Harwood Academic Publishers, New York, U.S.A., (1988).

13) Mosalam Shaltout, M.A., Atmospheric transmission and diffuse fraction of solar energy over Egypt, Proceedings of International Symposium on Applications of Solar & Renewable Energy ASRE'86, ed. A. Mobarak and H. El - Agamawi, Cairo, Egypt, 23 - 26 March, (1986).

14) Mosalam Shaltout, M.A., Estimation of the different components of the solar radiation over Egypt from the meteorological data, Solar & Wind Technology vol.1, No.3, pp. 175 - 185, (1985).

FIGURES

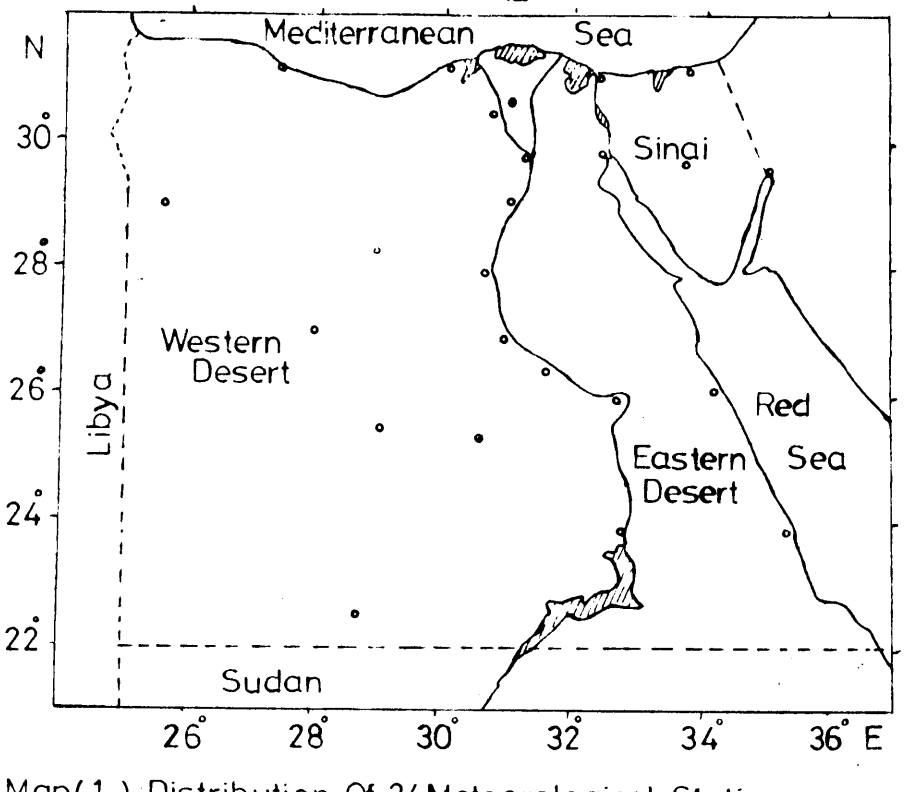

Map(1) Distribution Of 24Meteorological Station

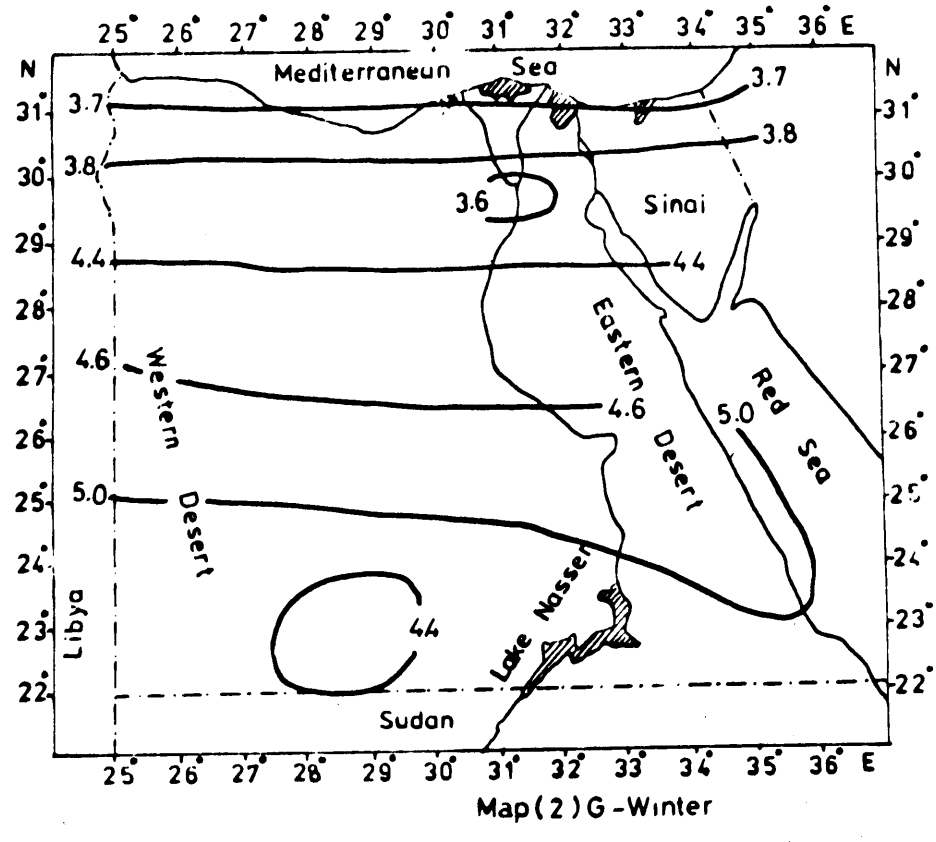

Map(2)G-Winter

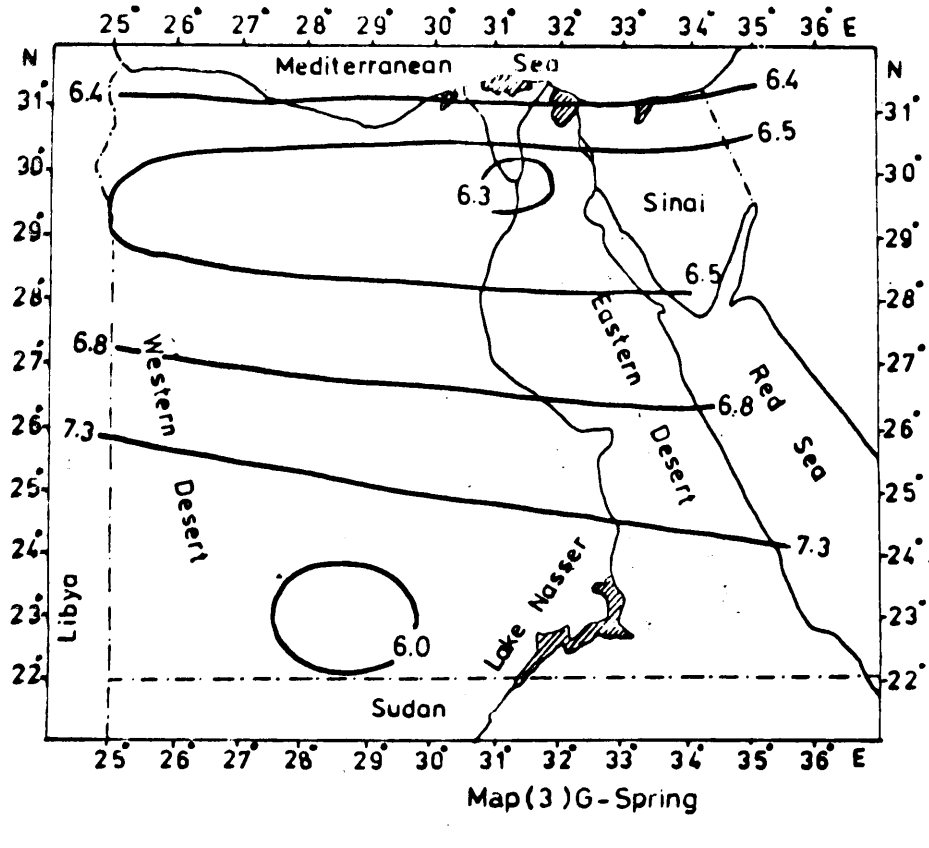

Map(3)G-Spring

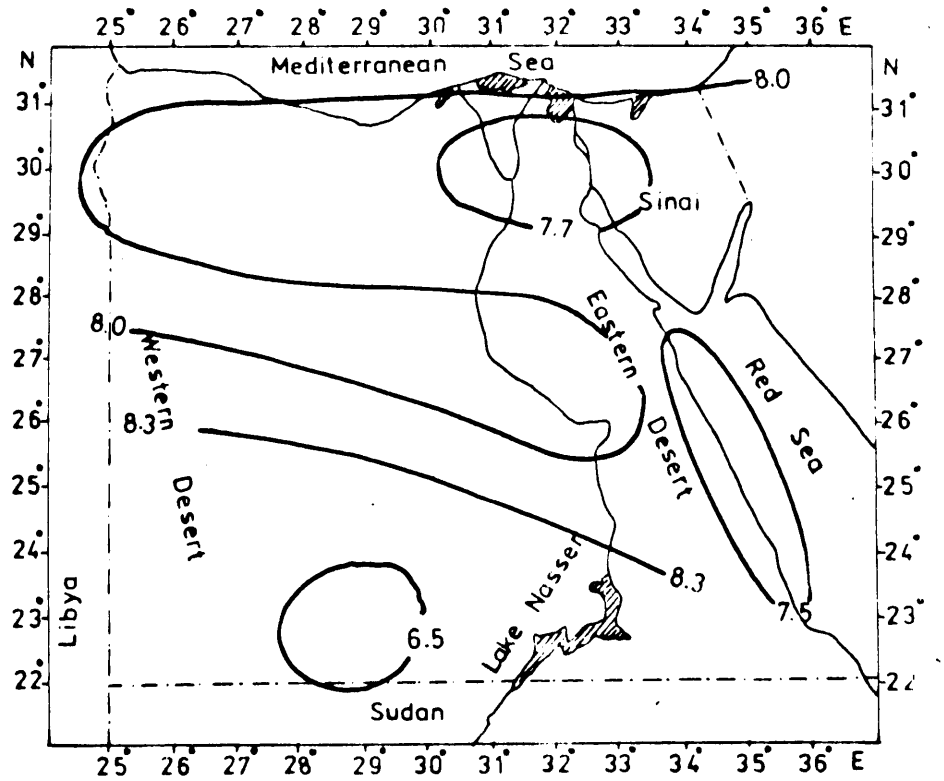

Map (4) G - Summer

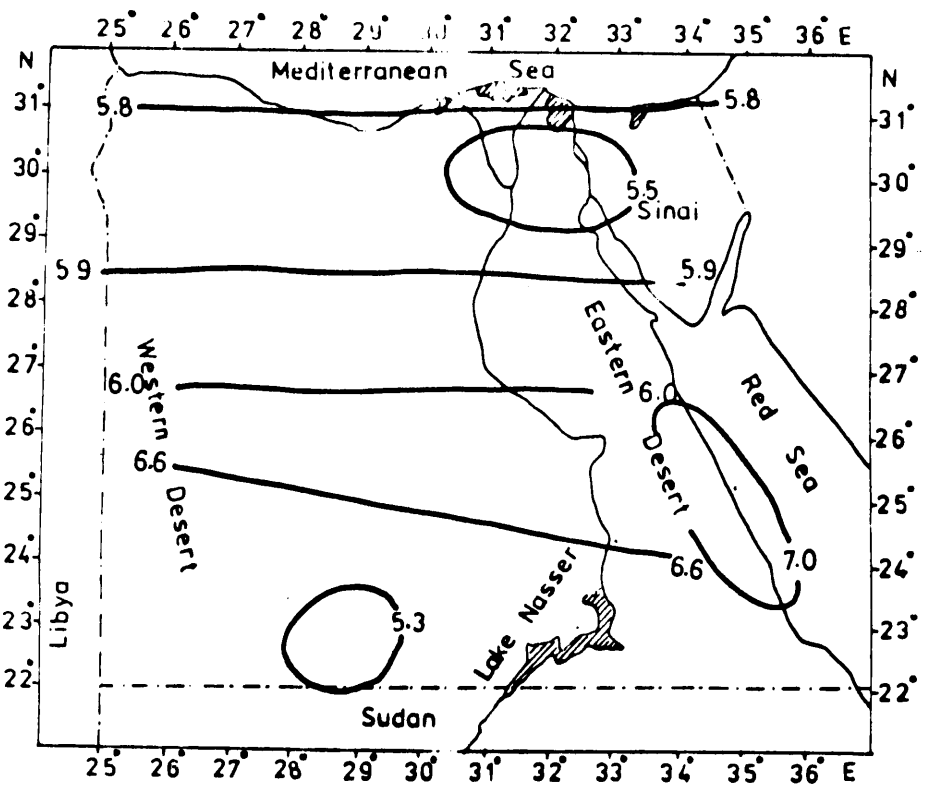

Map (5) G - Autumn

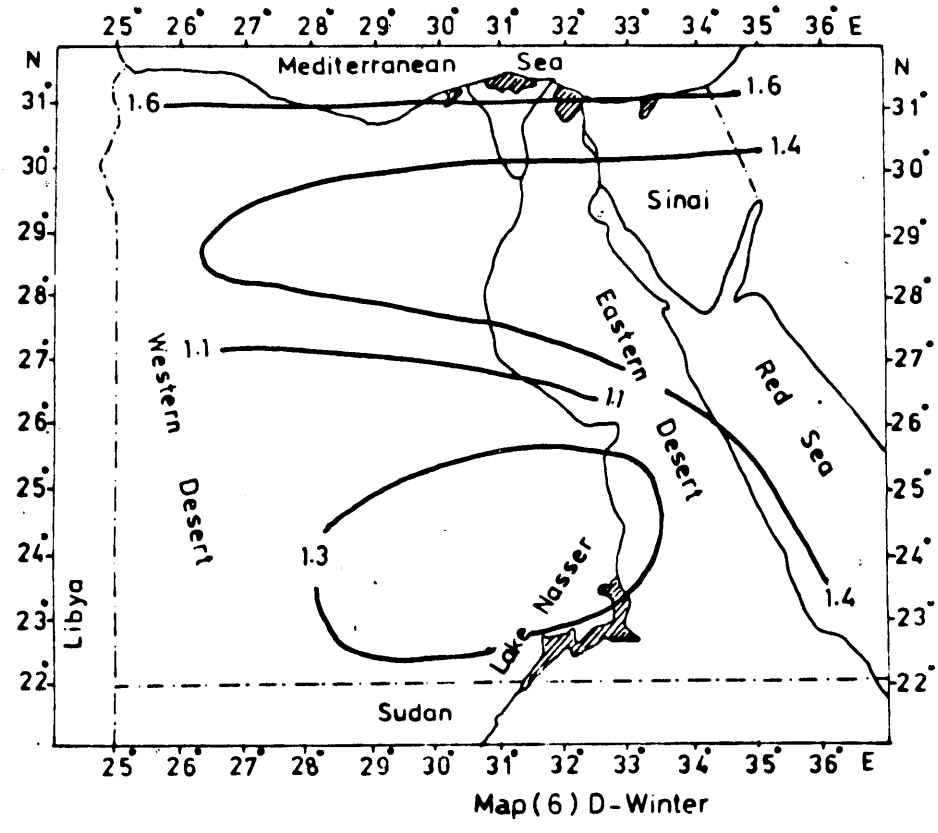

Map (6) D-Winter

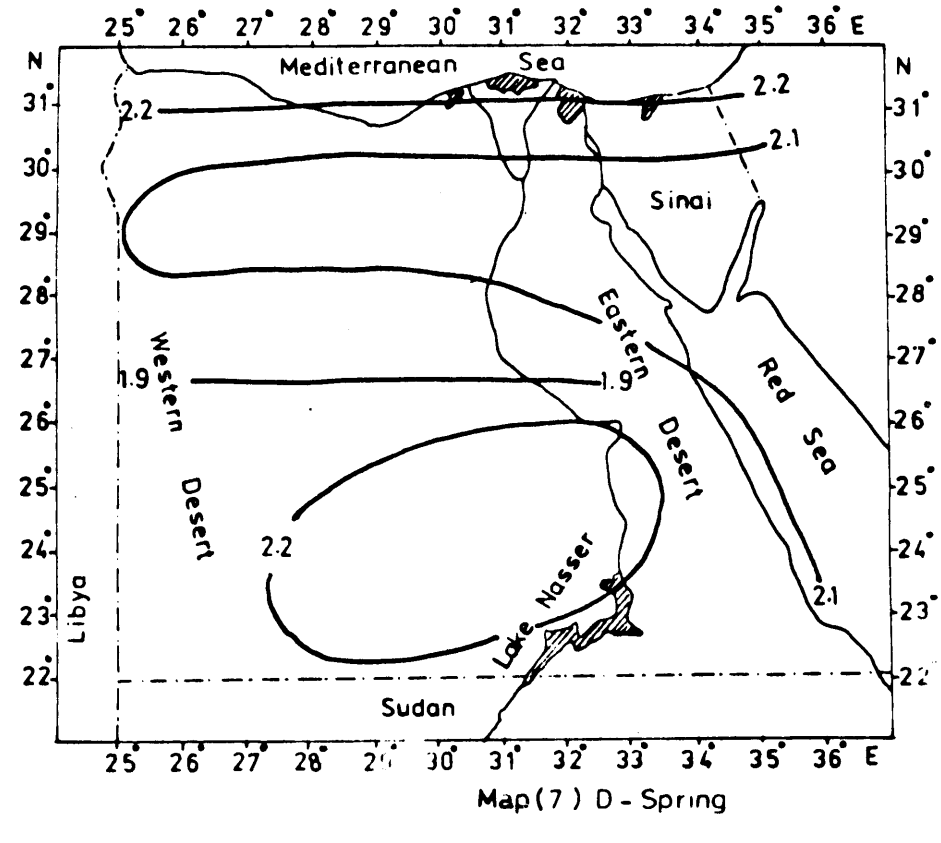

Map (7) D - Spring

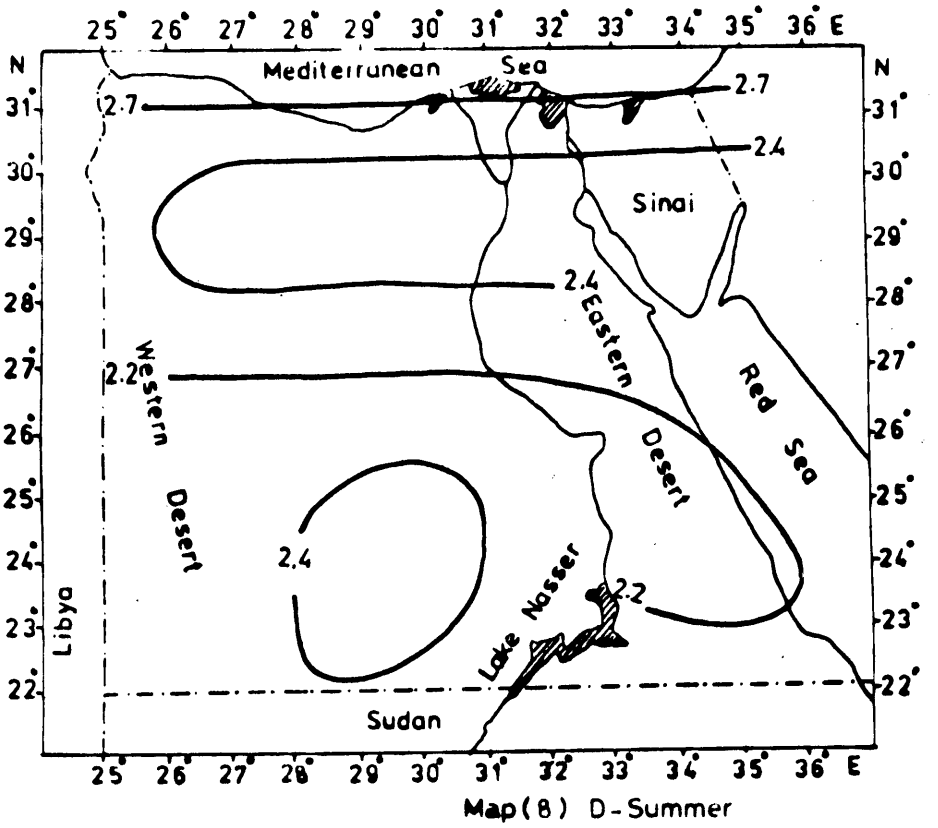

Map(8) D-Summer

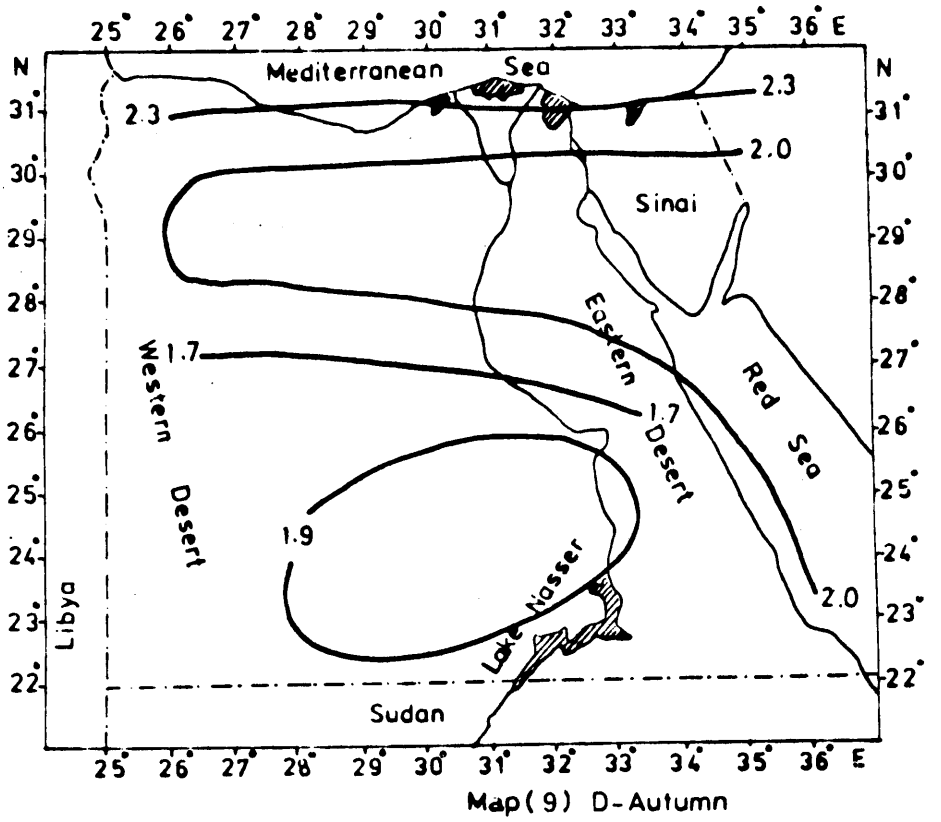

Map(9) D-Autumn

SECTION XII

PASSIVE SYSTEMS

PASSIVE - DESIGN FEATURES OF THE VERNACULAR BUILDINGS IN THE YEMEN ARAB REPUBLIC

M.K.Al-Motawakel

Department of Physics, Faculty of Science
Sana'a University, Sana'a, Yemen Arab Republic

ABSTRACT

The Passive - Design Features of the vernacular buildings in the Yemen Arab Republic, developed over thousands of years and coming from the observations and experiences handed on from generation - to - generations, are reviewed and analyzed.

It was evident, based on the reviewed thermal qualities, that a real renewed growth in the climate - responsive designs would come from the translation of the traditional passive features in a studied and well defined approach. The new "language" of such translation is presented in form of a multi-stage program and is defined as one of particular historic, artistic, economic, and environmental values. Until the implementation of the proposed translation scheme, we provide designers with a number of correlations which can be used to evaluate the climate requirements of thermal resistance and heat capacity. In the absence of any kind of standards or codes, the use of the developed correlations (presented in form of design graphs) would limit the wide spread of the climate insensitive or combative designs and consequently minimizes the consumption of oil, gas, and electricity used in heating and cooling the newly built houses.

INTRODUCTION

Yemen Arab Republic lies between 12.4 and 17.3 north latitude and includes elevations from sea level to more than 3500 m [1]. The country can be divided into three distinct climatic zones. The tropical and desert climatic zones, zone I and III in Fig.1, divide the warmer regions of the country with zone I being warmer and more humid than zone III. The temperate and subtropical climatic zones, represented by zone II in Fig.1, comprise the higher elevations of the country where temperatures are considerably lower than in zones I and III. The monthly mean values, averaged over the period 1983 to 1987, of the weather parameters characterizing these zones are presented in Fig.2 [2]. The differences in climate for each zone are significant for the design and the selection of materials to adapt buildings to climate. It is clear, from Fig.2, that the passive systems in zones I and III should be designed to avoid overheating in summer. However, in zone II the importance of heat storage and heat retention increases. In section I we review the passive design features of the vernacular buildings in the Yemen Arab Republic. The issue of using the comfort producing aspects of the traditional Yemeni architecture as the bases of developing modern planning construction and design strategies is investigated in section II. Section III outlines the general conclusions and recommendations.

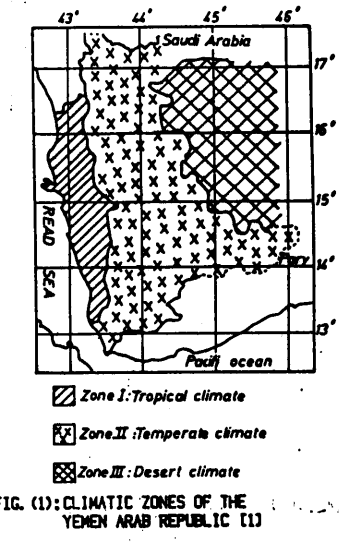

FIG. (1): CLIMATIC ZONES OF THE YEMEN ARAB REPUBLIC [1]

SECTION I : PASSIVE DESIGN FEATURES OF THE VERNACULAR BUILDINGS IN THE YEMEN ARAB REPUBLIC

1.1 Passive-Design Features In Zone I

The predominance of high humidity in zone I, see Fig.2, necessitates a corresponding high air velocity to increase the efficiency of sweat evaporation. Continuous ventilation is therefore the primary comfort requirement and affects all aspects of building design in this region. In the traditional redbrick houses, see Fig.3, continuous ventilation is provided by south-facing large openings shaped in form of rawshan, wooden canopies, latticed windows, and friezes and perforated arched parapets [3]. In the reed houses, continuous ventilation requirements are provided by open spaces between the domed or sloped roofs and the mud or straw walls or by ventilation holes located in the mud or straw walls, see Fig. 3. Solar heat gains are controlled by minimizing the total area exposed to the sun and using light reflective external colours, see Fig. (3).

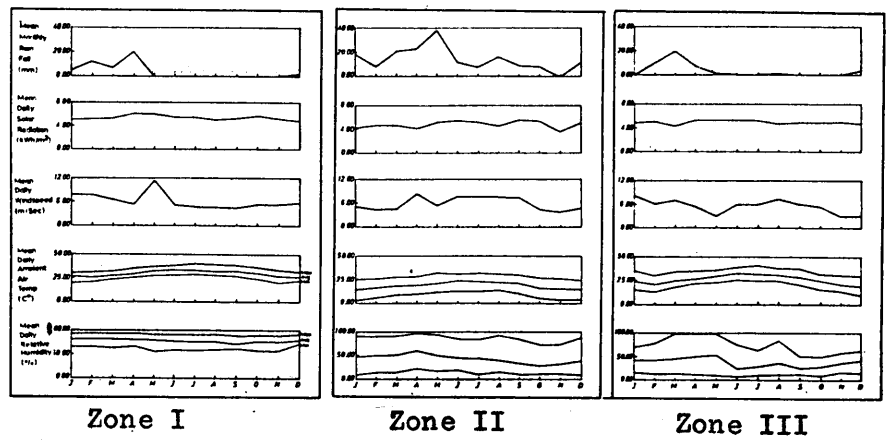

FIG.(2): CLIMATIC GRAPHS OF THE CONSIDERED CLIMATIC ZONES

The proper selection of building materials forms the third principle of passive design in this region. High thermal resistance - low heat storage capacity materials such as reed and redbrick are commonly employed in constructing the traditional houses in both rural and urban areas of zone I. Unfortunately, the design of the newly built houses in this region is in direct conflict with the climatic conditions of zone I. This is caused by the availability of concrete and the absence of the building's codes. Instead of promoting the heat losses and minimizing overheating, the newly built houses are designed with thin concrete walls (of thickness 20 to 30cm and thermal resistance between 0.2 and 0.4 $m^2 C^o/W$), and large volume to surface area ratios [4] . Daily observations have indicated that the problems such designs create for themselves internally become sever than the influence of the outside climate. This fact is reflected in the wide use of window and central airconditioners particularly in the large town centers of zone I. The absence of information made it difficult to estimate the exact impact of using airconditioners for space cooling on the energy consumption and/or the recently discovered oil. However, the interpretation of the 1982 energy survey figures [5] , adapted for 1988, indicates that the space cooling costs the house owner 0.22 U.S.dollar per day. On the assumption that the average percapita income is 500 U.S.dollar per year [6] , then the above daily cost of the space cooling load is responsible for 16% of the owner's percapita yearly income.

FIG. (3): TRADITIONAL PRINCIPLES OF CONTINOUS VENTILATION EMPLOYED IN THE REED AND REDBRICK HOUSES OF ZONE I

1.2 Passive-Design Features in Zone II

The variability of climate in this zone, see Fig.2, presents a good example to apply different approaches and architectural solutions. As a result, buildings in region II are so designed and built to provide not only the protection from heat in summer and cold in winter but also to reflect the artistic heritage of the traditional Yemeni architectures which have been published on a worldwide bases by authors such as Lewcock, Varanda, and others [3] .

Traditional buildings in this zone are designed in two architectural styles which can be classified into the following main two groups : -

Group I : Includes single and multi - storey houses built wholley using any of walls types 1 to 5 in Fig.(4) ;

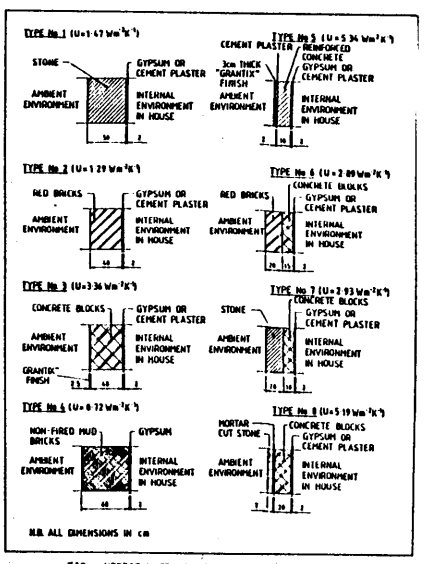

FIG.4 : VERTICAL CROSS-SECTIONS OF SOME COMMONLY EMPLOYED TYPES OF WALLS IN THE YEMEN ARAB REPUBLIC

Group II : Includes multi - storey houses built in dissimilar types of walls per each storey. A multi - storey house in this group is traditionally constructed with stone (wall type 1 in Fig.4) for the ground floor walls, followed by redbrick (wall type 2 in Fig.4), or concrete blocks (wall type 3 in Fig.4) for successively higher storeys in decreasing order of popularity.

As an example, Fig.5 illustrates the artistic features, the spatial organization, and the passive principles characterizing a typical traditional Yemeni house in zone II. Visual observations indicate that the preferred materials, as far as the indoor climate is concerned, depend on the size and shading efficiency of the windows. The absence of windows in the ground-floors of multi-storey houses means that the heat flowing across the walls of the ground floors is the main source of heat gain. Accordingly, the thermal resistance is relatively more important than heat capacity in minimizing the rate of daytime heating. This explains why stone, in addition to its structural strength, is the preferred building material for the ground-floor walls in a large number of multi-storey houses in this region. As one goes up, the relative area of the windows increases and reaches its maximum at the top floor where the social gathering rooms are located — see Fig.(5). In this way a significant portion of the heat gain is coming from the windows either by conduction, transmission, or hot outdoor air infiltration. Under such condition heat capacity assumes much greater importance because of the fact that light weight materials are heated by the absorped solar insolation more than heavier materials. As a result Yemeni used redbrick (wall type 2 in Fig.4) or mud (wall type 4 in Fig.4) for constructing the external walls of the successive higher storeys.

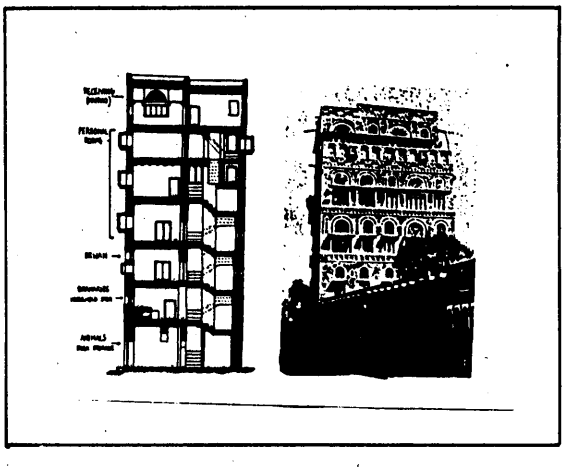

FIG. (5): ARTISTIC SPATIAL ORGANIZATION AND PASSIVE-DESIGN CONCEPTS AHARACTERIZING A TYPICAL TRADITIONAL HOUSE IN ZONE II

In this way, a balance between the heat gain and the thermal insulation properties of the traditional houses was accomplished. In fact the walls when wetted by the rains are cooled by evaporation due to the wind; their external surface temperature drops below the outdoor ambient air temperature; while at the same time their thermal resistance becomes weaker. The choice of higher thermal resistance materials to construct the walls of the higher storeys would allow for such reduction with the added advantage of resisting the heat flow during the hot summer spells. The rate of heat loss from a house of n storeys in Group I and Group II was taken as a measure for the thermal insulation efficiency of the traditional multi-storey houses built in zone II. In the notations of a previous study [4], the difference in the rate of heat loss from a multi-storey house belonging to Group I and a similarly designed multi-storey house but belonging to Group II is given by : -

$$\dot{Q}_{II} - \dot{Q}_{I} = \left(\frac{\sum_{i=1}^{n} U_{(i+1)}}{(n-1)\, U_1} - 1 \right) (n-1)\, \dot{Q}_1 \qquad \ldots (1)$$

where

$\dot{Q}_{II}$ and $\dot{Q}_{I}$ respectively represent the rate of heat loss from a similarly designed multi-storey houses in Group II and Group I.

$\dot{Q}_{1}$ refers to the rate of heat loss from ~~the~~ ground floor of the considered multi-storey houses.

n refers to the number of storeys.

U_1 and $\sum_{i=1}^{n} U_{(i+1)}$ respectively represent the external walls heat transfer coefficient of the ground storey and the sum of the U-values of all the successive higher storey's walls.

Accordingly and for $n \geq 2$, we have the following conditions :

IF $\sum_{i=1}^{n}\left(U_{(i+1)} / U_1(n-1)\right) < 1$ then $\dot{Q}_{II} < \dot{Q}_{I}$;

IF $\sum_{i=1}^{n}\left(U_{(i+1)} / U_1(n-1)\right) > 1$ then $\dot{Q}_{II} > \dot{Q}_{I}$;

IF $\sum_{i=1}^{n}\left(U_{(i+1)} / U_1(n-1)\right) = 1$ then $\dot{Q}_{II} = \dot{Q}_{I}$

By reference to Fig.(4), one can prove that the condition $\dot{Q}_{II} < \dot{Q}_{I}$ is satisfied when a multi-storey house is built of the veracular arrangement of walls constructed from stone (wall type 1 in Fig.4) for the ground floor walls, and redbrick (wall type 2 in Fig.4) or mud (wall type 4 in Fig.4) for all the successive higher storey's walls. Under such case the use of dissimilar materials per each storey has improved the thermal insulation efficiency of the house. On the other hand, the condition $\dot{Q}_{II} > \dot{Q}_{I}$ is satisfied when a multi-storey house is built of the arrangement of walls constructed from stone for the ground-floor walls, concrete (wall type 3 in Fig.4) or reinforced concrete (wall type 5 in Fig.4) for all the successive higher storey's walls. For all other storey-by-storey sequences of the locally available materials, Fig.(6) illustrates the effect of different vertical layers of materials on the rate of heat loss.

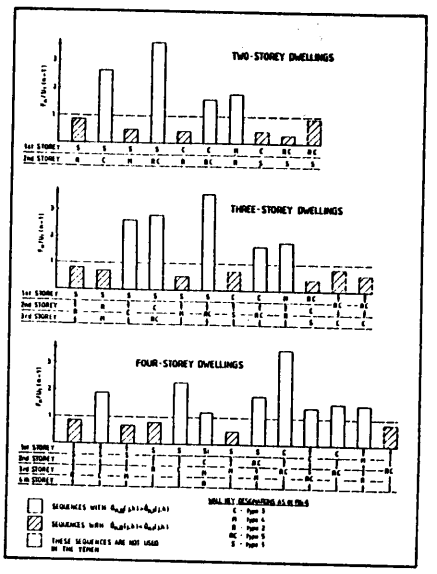

FIG. 6 INDICATIONS OF THE RATES OF HEAT LOSS FROM DWELLINGS IN THE YEMEN ARAB REPUBLIC : EFFECTS OF DIFFERENT VERTICAL LAYERS OF MATERIALS IN THE WALLS

1.3 Passive-Design Features Of Buildings In Zone III

Buildings in the desert region of the country, Zone III in Fig.1, are traditionally designed with white-washed flat roofs, thick mud walls, and very small unglazed window openings --- See Fig.(7). North-south orientations and rectangular shapes are also employed to minimize solar heat gains. It is clear that the aim of this type of design is to lower the day-time temperatures as far as possible. The stabilizing influence of thick walls results in flattening the temperature-variation curves of the internal wall's surfaces [4]. The white-washed external surfaces help in limiting the contribution of the direct and reflected solar radiation which are the most intensive sources of heating in desert areas. This potential control of internal temperature variations is aided by keeping both windows and shutters closed during the day. Natural lighting is provided by small apertures located in the walls

and ceilings of the house [3].

SECTION II : PROGRAM OUTLINE FOR TRANSLATING THE TRADITIONAL DESIGN FEATURES INTO MODERN PLANNING AND DESIGN STRATEGIES

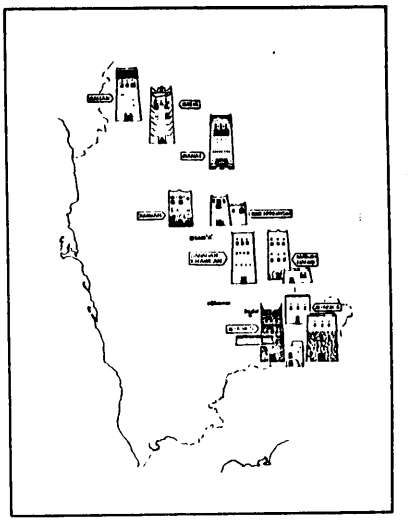

FIG. (7): TYPICAL MUD ARCHITECTURES OF THE EASTERN AND NORTH-EASTERN REGIONS OF THE COUNTRY (3)

The indigenous architectural heritage of Yemen is internationally respected for both its artistic and thermal qualities. The artistic heritage has been published on world wide bases by authors such as Lewock, Varanda, and others [3]. Unfortunately, there are very limited numbers of studies concerning the comfort producing aspects of traditional Yemeni architecture [4, 5, 7, and 8] . These studies, though limited in their presentation to certain thermal qualities, have endorsed the concept of investigating the comfort producing aspects of traditional Yemeni architectures as the bases of developing modern planning construction and design strategies. The ESCWA report [8] had reflected this fact by saying :

" When People Talk About Bioclimatic Designs and Working With and Not Against The Environment, Buildings Architecture in the Yemen Arab Republic should be A REAL GUIDE TO THEM. The Establishment of Architectural School in Yemen Arab Republic may be the most efficient way to achieve it. "

Thus for cultural as well as economic reasons, translation of traditional principles into modern applications is imperative. The new "language" of translation will allow : -

- The articulation of plans to integrate the already existing vernacular buildings and environments with new structures and environments ;
- The establishment of city and national master plans, zonning standards, and building codes ;
- The development of particular building materials industries and new built environments which achieve a coherent integration with the historic architectures and at the same time take into account the functional requirements of the modern society ;
- The implementation of legal and financial incentives which would encourage the climate-responsive designs and the conservation of the Yemeni architecture identity.

The program outline suggested for achieving such goals is presented in Table (1). Because of the far reaching potentials of such a plan, the general principles and methodology involved in the choice of the building materials as a function of the ambient conditions are the considerations of the present paper.

The physical properties of principal interset are the thermal resistance and the heat storage capacity. The thermal resistance of a wall or roof (R) required to create a nominal indoor air temperature (T_i), a nominal indoor air-to-surface temperature

difference (Δt_i), can be calculated as a function of the design minimum outdoor air temperature ($T_{o,min}$) and the internal air-film heat transfer coefficient (h_i) by the following expression [9] : -

$$R = \left(\Delta T / (h_i \Delta t_i) \right) \quad ...(2)$$

where

$$\Delta T = T_i - T_{o,min}$$

Eq.(2) does not take into account the effect of the heat storage capacity in moderating the influence of the outdoor climate on the interior environment. For standards building materials such as concrete, bricks, stone, etc., the thermal damping effect of the heat storage capacity is proportional to the weight per unit area of the external walls. Thus inclusion of such effect in Eq.(2) would be approached by compensating for the increase in the heat storage capacity with a corresponding modification of the design minimum outdoor temperature. In doing so, the heat storage capacity (Q) is not referred to as the product of specific heat, density, and thickness of the walls, but is expressed in terms of the "Equivalent Weight" per unit area of the external walls (W in Kg/m^2). This equivalence allows the following modification for $T_{o,min}$;

$$T'_{o,min} = T_{o,min} + f W \quad .. (3)$$

Table(1): PASSIVE HEATING AND COOLING FOR YEMENI BUILDINGS
A Program Outline

1. Planning:
   - A. Goals
   - B. Task Definition
   - C. Participants
   - D. Collect documents of previous similar efforts
   - E. Assess existing data base
   - F. Contributors: human and financial
   - G. Timeline Planning
   - H. Financial Budgeting

2. Investigating:
   - A. Surveying and documenting the physical aspects of selected passive features.
   - B. Researching related aspects of the passive features including the effect of social stability, customs, traditions, and needs, external influence (particularly Turkish), and the variation of the climatic conditions on the historical development of the surveyed and documented passive features.
   - C. Develop climatic data base at both mezzo (urban and regional) and micro (building site) level.
   - D. Develop performance criteria and comfort standards, (existing and proposed).

3. Evaluating:
   - A. Examination and evaluation of the suitability of existing and historical passive heating and cooling features to the regional variations in the climatic conditions. This can be accomplished by developing mathematical models and design methods which facilitate the estimation of the following:
     1. the solar contribution to the building's heating requirements.
     2. the amount of solar energy captured per day that exceeds the house's daily heating load and which must be vented to prevent overheating.
     3. the variation with time of the temperature within the building.
     4. passive cooling potentials and similar quantification
   - B. A parallel examination and evaluation of similar topics in typical recent or modern construction to establish a comparative basis and a definition of opportunity.

4. Hypothesis:
   - A. Quantification and evaluation of various proposals at improving the thermal performance of buildings, such as:
     1. increasing the building's thermal insulation.
     2. optimizing the window and door sizes.
     3. decreasing the air leakages.
     4. insulating the shading devices properly and correctly.
     5. designing, insulating, and maintaining the passive heating and cooling features.
     6. utilizing the building structure's storage capacity more fully.
     7. avoiding single story construction.
     8. idealized dimensions and orientations of courtyards.
   - B. Quantification and evaluation of various recommended thermal proposals in terms of economic or social costs:
     1. the added costs for materials, construction, and maintenance which would be incurred.
     2. satisfying the local building regulations and the architectural traditions, as well as the indigenous life-styles of the occupants.
   - C. Synthesis of preferred methods and assemblies and evaluation of their interactive responses. Integration within a series of urban planning, architectural and thermal models.

5. Implementation: Realization of various goals by dissemination, additional studies or research or other activite: information transfer, demonstration, training, economic and legal incentives assuring continuity feedback and upgrading. Potential activities might involve:
   - A. City and National Master Plans, zoning standards, building codes.
   - B. Development of particular building materials industries.
   - C. Development of particular construction or design or analytic skills.
   - D. New or remodeled construction of models as physical demonstrations.
   - E. Implementation of legal or financial incentives or disincentives.
   - F. Transference or program efforts from one building type or climatic focus to other.
   - G. A program of local or national competitions or awards to identify role models or exemplary means of reaching goals.

Dimensionally the equivalence factor (f) is the reciprocal of the heat storage capacity multiplied by the heat content of one kilogram and is typically taken as $0.01 (m^2\ ^oC/Kg)$ [10] .

With this value of f and taking into consideration Eq.(3), Eq.(2) becomes :

$$R = \left[(T_i - T_{o,min} - 0.01\ W) \ / \ (\Delta t_i\ h_i) \right] \quad ... (4)$$

The indoor air temperature (T_i) satisfactory for thermal comfort is about 20 to 22 °C . As far as air-surface temperature difference (Δt_i) is concerned, Gormossev [10] suggested a maximum value of 3 °C.

With these values of T_i and Δt_i and taking the value of h_i as 8.13 $W/m^2\ ^oC$ [4], Eq.(2) can be rewritten as :

$$R = \left[(20 - T_{o,min} - 0.01\,W) / 24.39 \right] \qquad \ldots (5)$$

The desired R values in ($m^2\ ^oC/W$) which satisfy the above nominal indoor climate are correlated to the weight per unit area of the external walls, for $T_{o,min} = -30\ ^oC$ to $10\ ^oC$, in Fig.(8). Thus by knowing the weight per unit area of the external walls, designers can use the correlations of Fig.(8) to calculate the required value of R. The blackened dots on Fig.(8) correspond to the R-values of the currently used external walls. It is clear that the vernacular walls (types 1, 2, and 4 in Fig.4) were designed to stand weather conditions characterized by $T_{o,min} < 0$. On the other hand, modern walls (types 3 and 5 through to 8) were designed to stand weather conditions characterized by $T_{o,min} > 0$.

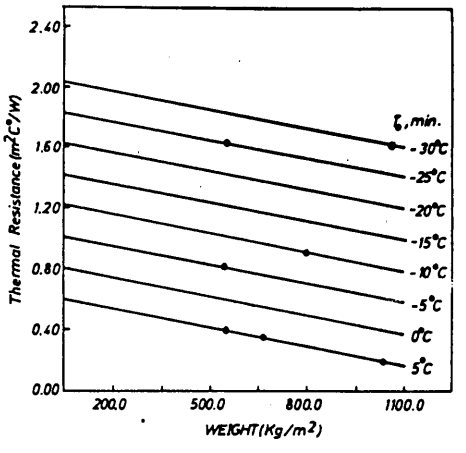

FIG. (8): CORRELATION OF THERMAL RESISTANCE TO THE WEIGHT PER UNIT AREA OF EXTERNAL WALLS

In another words, the economic benefits expected from the introduction of the modern walls might be negligible when compared to the cost of the heating loads consumed in heating the modern-adopted structures.

At present, no standards or codes are available for evaluating the climate requirements of thermal resistance and heat storage capacity. By correlating the thermophysical properties of the currently used building materials [4] to the temperature differences between the maximum and the minimum outdoor air temperature values observed in the considered climatic zones during the period 1983 to 1987 [2], we were able to develop the following mathematical formulae which can be used as a tentative guide in selecting the suitable building materials in the considered climatic zones; i.e.

$$R = \left(0.0386\ \Delta T_o\right)\left(1 + \left((T_{o,max} - T_i)/\Delta T_o\right) + 0.415\left(\Delta T_s/\Delta T_o\right)\right) \qquad \ldots (6)$$

$$Q = \left(4.075\ \Delta T_o\right)\left(1 + 0.4\left(\Delta T_s/\Delta T_o\right)\right) \qquad \ldots (7)$$

The difference (ΔT_o) between the expected maximum and minimum outdoor air temperatures and the increase in the surface temperature (ΔT_s) of the external walls caused by the absorption of the solar insolation are respectively defined by : -

$$\Delta T_o = T_{o,max} - T_{o,min}$$

$$\Delta T_s = (\alpha\ I_{max} / h_o) \qquad \ldots (8)$$

where

$T_{o,max}$, $T_{o,min}$ = values of the expected maximum and minimum outdoor air temperatures.

α = absorption coefficient of the external walls (taken here between 0.2 and 0.8)

I_{max} = maximum observed solar insolation.

h_o = external surface air-film heat transfer coeff.

For indoor climate characterized by T_i = 20 °C , and outdoor environment characterized by $T_{o,max}$ = 25°to 35°C, ΔT_o = 5° to 20°C and ΔT_s = 0° to 20°C, Fig.(9) plots the correlations of the R, Q, and RQ values to ΔT_o. Thus by knowing the temperature difference between $T_{o,max}$, and $T_{o,min}$ and by specifying the increase in the surface temperature of the outside walls, designers can use the correlations of Fig.(9) to calculate the climate requirements of thermal resistance and heat storage capacity.

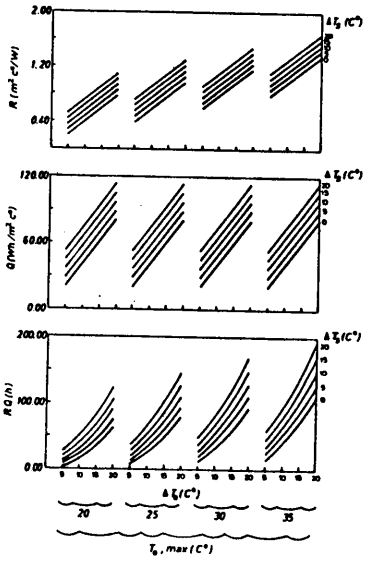

FIG. (9): CORRELATION OF THE THERMAL RESISTANCE, HEAT STORAGE CAPACITY, AND THEIR PRODUCT TO THE AMBIENT CONDITIONS OF NORTH YEMEN

SECTION III : CONCLUSIONS AND RECOMMENDATIONS

We might agree on the fact that the passive design features developed by observations and experiences or by the latest 20 th. century computer - simulation methods tell designers who want to be energy conscious and climatically correct to : -

- Promote solar gains and resist heat losses during the cold seasons ;
- Resist solar gains and promote heat losses during the hot seasons .

Physically we know how to accomplish these two conflicting messages. The first involves delaying the periodic heat flow and promoting solar gains and at the same time minimizing conductive and external heat flows as well as infiltration. The second message demands minimizing conductive heat losses and solar gains, delaying periodic heat flows, and promoting ventilation as well as radiant and evaporative coolings.

Depending on the experimental trial and error process is very expensive and slow. Furthermore there is no certainty that such an experimental process can converge to optimum solutions which take into account the rapid evolution of technologies and the increasing availability of the new building materials . On the other hand, the use of the latest 20 th. century design tools depends on the answers to the following set of questions :-

- What can/cannot such tools analyze ?
- How difficult are they to learn ?
- Are the solutions proposed by such tools suitable from the social and cultural points of views ?

With the tendency for surrendering to the power of the 20 th. century designs tools, there is a feeling for a certain type of evasion through climate-insensitive designs and climate-combative designs. The climatic-insensitive designs feature houses with very thin walls and large volume to surface area ratios. In some of these designs, the interior spaces are completely dependent on artificial lighting. In short, the problems such designs create for themselves internally become severe than the influence of the outside climate. It is sad to say that some residential houses, hotels, and commercial buildings in the Yemen and elsewhere are climatic-insensitive designs. The climatic-combative designs regard climate as an enemy which can not be employed to condition the indoor environment. This understanding

introduces the "Supper Insulated" buildings (walls u-value $<0.25\ W/m^2C^\circ$, window u-value $1\ W/m^2C^\circ$). Thus orientation becomes unimportant and the building site is only important for determining the thickness of the insulation that is necessary to pack the house envelope with. The problem with such designs is that they do not go far enough. They end when climate changes from being an enemy to being a resource that can be tapped to condition the indoor climate.

It is clear that evasion through climate-insensitive or combative designs does not solve the energy costs of buildings. Success comes from imposing "CLIMATE-RESPONSIVE" designs whose enclosures act as filters rejecting adverse climatic forces and admiting beneficial ones. As a first step towards accomplishing this goal, we recommend the use of the correlations plotted in Figs. (8 and 9) and described by equations (6), (7), and (8).

REFERENCES : -

1) Central Planning Organization, "Final Report on the Airphoto Interpretation Project Of The Swiss Technical Co-operation Service", Berne, Zurich, April 1978.

2) Unknown, "Annual Climatological Summeries", Civil Aviation And Met. Authority, Sana'a, Yemen Arab Republic.

3) Varanda, F., "Art Of Building In Yemen", MIT Press, Cambridge, Massachusetts, London, England, 1982.

4) Al-Motawakel, M.K., and et.al., "Thermal Behaviour Of The Vernacular Buildings In The Yemen Arab Republic", Applied Energy, Vol.24, pp. 245-276, 1986.

5) Al-Motawakel, M.K., and et.al., "Energy As Used Domestically In The Yemen Arab Republic", Applied Energy, Vol.24, pp.185-219, 1986.

6) Central Planning Organization, "Statistical Year Book", Statistic Department, Central Planning Organization, Sana'a, Y.A.R.

7) Al-Motawakel, M.K., and et.al., "Solar Energy Harnessing Performance Of Direct gain and non-vented Trombe Walls Under Yemeni Weather conditions", Applied Energy Vol.26, pp.159-181, 1987.

8) Central Planning Organization, "Energy Conservation In The Housing sector of the ESCWA Region", Economic and Social Commission For Western Asia, Natural Resources, Science And Technology Division, E/ESCWA/NR/86/10, July 1987.

9) Kreider, J.F., and Kreith, F., "Solar Energy Hand Book", McGraw-Hill Book Company, N.Y., 1981

10) Goromossov,M.S., "The Physiological Basis Of Health Standards For Dwellings", World Health Organisation", Public Health Papers, No.33,Geneva,1968

EXPERIMENTAL STUDY OF THE THERMAL PERFORMANCE OF AUTOMATED VENETIAN BLIND WINDOWS

S. Rheault and E. Bilgen

Ecole Polytechnique
P.O. Box 6079, Station "A",
Montreal, Quebec H3C 3A7, CANADA

ABSTRACT

This study presents an experimental study on automated venetian blind window systems which consist of horizontal pivoted louvers installed and hermetically sealed between two glass panes. The experimental study was carried out using a test cell of 2.43 m high, 1.48 m wide and 1.92 m deep. Various parameters were measured instantaneously and recorded using a data acquisition system: inside and outside air temperatures, various surface temperatures and total and direct solar radiations. A linearized numerical model was used to verify the experimental results.

INTRODUCTION

The automated venetian blind systems with pivoted louvers installed horizontally and hermetically sealed between two glass panes are versatile devices to optimize solar heat gains. In addition to the beneficial effects due to control of solar heat gains, they also provide high thermal resistance. The latter characteristics can further be improved using new materials such as heat absorbing glass, low emissivity glass, etc. without affecting the control benefits of the louvers. A theoretical analysis on the heat transfer through an automated venetian blind window system has been recently reported [1]. The results of this study on the overall system performance using case studies indicated that the auxiliary energy to maintain comfort conditions can be reduced by about one third during winter and about one half during summer. These overall results have been verified experimentally [2]. Further experimental studies were however necessary to determine the thermal resistance characteristics and shading coefficients of the louvered system and to identify new window materials for its improvement [3].

In the following sections, a large scale experimental study will be outlined and the results will be analyzed using the theory developed earlier [1].

SYSTEM DESCRIPTION

The system studied is shown in Fig. 1 and consists essentially of horizontal pivoted louvers installed and sealed between two glass panes. The louvers are fixed at both ends to the side of the window unit and can rotate around the z axis; the fully open position corresponds to a louver angle of $\beta = 0°$ from the x-z plane; they can rotate by means of a mechanical system outside the window seal clockwise to -90° or anti-clockwise to +90° from that plane. The louvers are made of aluminium coated with a white paint; their width L is the same as the distance separating them in the y direction.

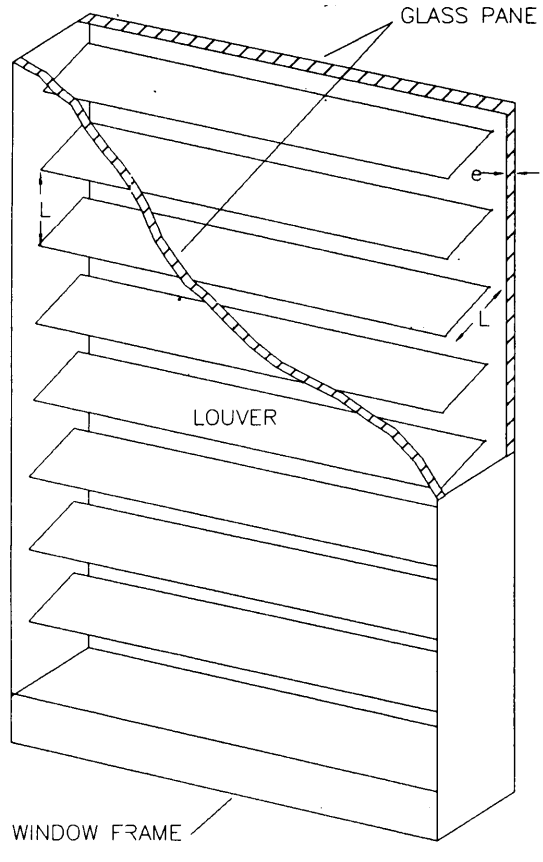

Figure 1 : System schematic.

THEORETICAL CONSIDERATIONS

The theoretical analysis will only outline the major steps of the equations involved in the solution of the system since a complete description of the mathematical model has already been published in [1]. Three major heat exchanges are present: radiative exchange both in infra-red and solar radiation band, convective exchange outside the glass panes as well as inside the cavity defined by the two glass panes and finally conductive exchange in the walls of the building where the venetian blind window system is installed. The heat exchange in the system was analysed within a fictive domain formed by two louvers and the surrounding glasses except those of natuaral and forced convection which require the full size of the window unit.

For all the radiative exchanges, the net radiation method was used; the method consider every elements of the system as a radiative node and the solution is carried out in an energy balance equation. Knowing the equations for radiosity, solar irradiance and incident solar radiation for all the surfaces, it is possible to obtain a system of simultaneous equations and find the radiosities R_k and the irradiances E_k for all the elements k, leading to the net solar radiation absorbed by each surface:

$$\Phi_{k\,s} = R_{k\,s} - E_{k\,s} \qquad (1)$$

Following the assumption that the surfaces are considered gray-diffuse surfaces in the infra-red radiation band, the radiosity

and the irradiance equations for all the elements are first written; the resulting system of simultaneous non-linear equations which cannot be solved explicitly, will be solved with an iterative scheme based on the energy balance on each elements of the system. The infra-red radiation absorbed by all the surfaces can be expressed in the same way as for solar radiation:

$$\Phi_{kr} = R_{kr} - E_{kr} \qquad (2)$$

The convective exchanges are evaluated using standard correalations available in the litterature for both the outside and inside surfaces, while for the convective exchanges inside the window cavity, the louvers were considered to be in the core region where almost no temperature gradient is present.

The solution of the system using an iterative scheme was carried out with energy balance on each element of the system used as a convergence criterion for all the unknown temperatures involved in the equations. The energy balance for the outside glass, the louvers and the inside glass were calculated as:

$$\Phi_{kc} + \Phi_{kr} + \Phi_{ks} = 0 \qquad (3)$$

where k stands for outside glass, louvers and inside glass.

After all the energy balances and the temperatures of the different elements have been determined, it is possible to evaluate the total solar heat gain transmitted to the room which includes the solar, radiative and convective exchanges. The total solar heat gain is then used to determine the shading coefficient associated with the tested window. The shading coefficient is evaluated by comparison with a reference glazing material which is a double-strenght sheet glass (DSA, ASHRAE). The shading coefficient, SC, is defined as the ratio of the solar heat gain through the system to the solar gain through the reference glass. Knowing the energy balances for all the elements of the system, it is possible to evaluate the global thermal resistance R_{top} of the system based on the thermal nodes involved.

EXPERIMENTAL STUDY

The large scale experimental study was carried out in one of the test cells of the solar laboratory [4]. It is 2.43 m high, 1.48 m wide and 1.92 m deep and it has an overall $U_w A_w$ = 13 W/C. The inside surface of the cell is painted black with $\epsilon = \alpha$ = 0.94. The only surface exposed to outside conditions is the test window, all the other being exposed to the air of the solar laboratory. The opening for test windows is 2.25 m high by 1.15 m wide. The prototype window was 2.25 m high by 1.15 m wide and had regular glasses both at the interior and the exterior. The common geometrical parameters of the system were: louver length = 35 mm, glass to glass distance = 50 mm and glass thickness = 6 mm.

The inside air temperature of the test cell was not thermostatically controlled; hence, there was no need to measure the energy to maintain the air temperature constant. By measuring

the floating air temperature it was possible to relate the instantaneous gain to the other measured parameters and evaluate the required thermal characteristics and shading coefficients of the test windows.

It is clear that the test cell used in this study constitute a variable temperature calorimeter which serves as a constant temperature calorimeter for a small period of time when all the instantaneous thermal parameters are measured. This may be compared to the standard calorimetric procedure using hot boxes [5,6] in which the inside air temperature must be kept constant all the time so that the solar heat gain and the thermal characteristics of a window can be evaluated from experimental data. The theoretical treatment for both types of calorimeter will be outlined in the next section.

A data acquisition system (Omega) was used to collect the experimental data. Copper-constantan thermocouples were used to measure the outside temperature (T_a), the floating inside air temperature (T_e), the outside glass temperature (T_o), the inside glass temperature (T_i) and the louver temperature (T_L). An Eppley pyranometer was used to measure the total horizontal solar radiation (I_T) and a pyrheliometer to measure the direct solar radiation (I_b). In addition to the above parameters, the solar laboratory air temperature (T_l) and the total transmitted solar radiation (I_g) were also measured and recorded.

The experimental error in radiation measurements was estimated to be ± 2.1 % of which 0.1 % due to data acquisition system; the experimental error in temperature measurements was estimated to be ± 1 °C which is the sum of ± 0.5 °C due to thermocouples, ± 0.4 °C due to radiation effects and ± 0.1 °C due to data acquisition system.

In a variable temperature calorimeter, the indoor temperature variation is used to evaluate the net energy transferred. The variation of the air temperature can be defined as a function of the solar heat gain and the different heat losses from the box and the test window. The equation for the solar heat gain is then defined as:

$$SHGF = [(T_e^{i+1} - T_e^{i})\rho c_p V]/\Delta t + (U_v A_v + U_w A_w)(T_e - T_a) \quad (4)$$

The only difference between variable and constant temperature calorimeter is the first term on the right: in the constant temperature calorimeter, it is the required energy to maintain the inside air temperature while in the variable temperature calorimeter it is the energy required to obtain a certain inside air temperature variation from time t^i to t^{i+1}. The main advantage of the variable temperature calorimeter is the simplicity of the experimental set-up which does not require any control system to maintain a constant air temperature.

RESULTS AND COMPARISON

From the solar radiation measurements, the diffuse component of

radiation (I_d) was calculated and then I_b, I_d and T_a were used as input for a numerical simulation. With the theoretical model, the different temperatures T_o, T_i, T_L and T_e were evaluated and compared to experimental values. Using the theoretical model, the thermal resistance (R_{top}) and shading coefficient (SC) of the system were calculated, based on a simplified linear model and the thermal network of the system with all different temperatures taken from the experiment.

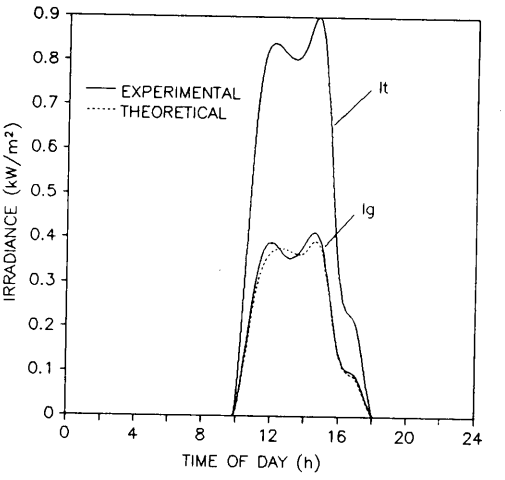

Figure 2 : Solar Transmission.

The large scale experimental study in the test cell was carried out for several weeks, from October to November 1986 and for various louver angles. Typical results for the test day of November 4,1986 are presented in Figs. 2 and 3 for a louver angle of $\beta = 0°$. Fig. 2 shows the relative difference between the predicted and the measured radiation through the window system which is about 6 % in average with a maximum of 8 %. Theoretical and experimental floating room temperatures (T_e), glass pane surface temperatures (T_o and T_i) are presented as a function of time in Fig. 3 which shows that the relative difference between predicted and measured temperatures was about 7 % in average with a 18 % maximum.

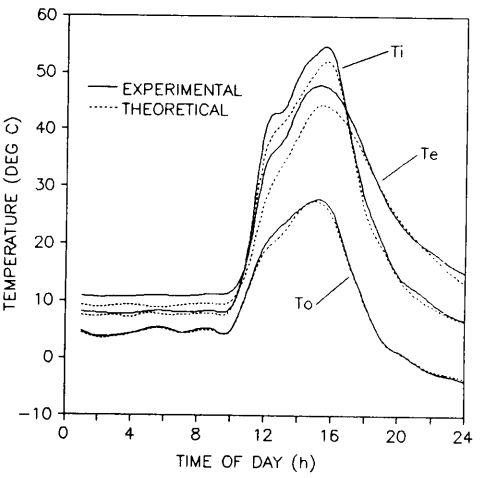

Figure 3 : Temperature.

The system performance in terms of its thermal resistance (R_{top}) and shading coefficient (SC) is evaluated using the theoretical model. The results of the performance calculation are shown in Fig. 4 for both the winter and summer period as a function of the louver angle. As it can be seen, the thermal resistance of the system varies only a little with the louver angles but the shading coefficient varies a great deal. This situation will be helpful for an eventual control strategy of the whole system according to the different outside and inside conditions for a given period.

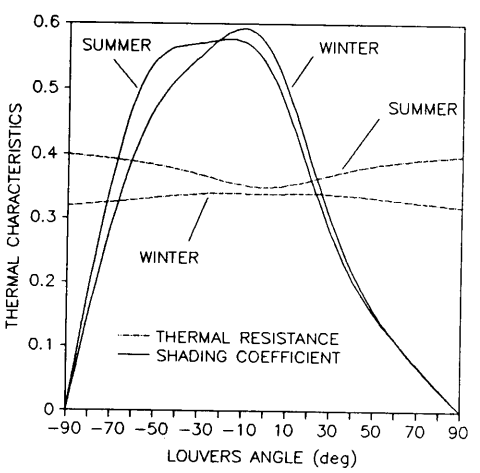

Figure 4 : Thermal characteristics.

CONCLUSION

It can be seen that the use of experimental data and a simple model (linear system) greatly simplifies the evaluation of the thermal resis-

tance and the shading coefficient of the louvered window systems. It can also be seen that the variable temperature calorimeter can be used with confidence to evaluate these characteristics. With the results of performance calculation, an evaluation of the economy of auxiliary energy requirements was made, showing about 30% possible economy during winter and 50% during summer.

NOMENCLATURE

A : Surface area (m^2)
C_p : specific heat (J/kg K)
E_k : irradiance of the surface k (W/m^2)
I : incident solar radiation (W/m^2)
R_k : radiosity of the surface k (W/m^2)
R_{top} : thermal resistance (m^2 K/W)
SC : shading coefficient (-)
SHGF : rate of solar heat gain (W)
T : temperature (°C)
U : overall thermal conductance (W/°C)
V : test cell volume (m^3)
ϵ : emissivity (-)
α : absorptance (-)
Φ : net energy rate absorbed (W)
β : louver angle (deg)
ρ : density (kg/m^3)

subscript

a : outside
b : beam
e : inside air
g : transmitted
i : inside glass
k,s : solar on element k
k,r : radiative on element k
k,c : convective on element k
l : solar laboratory
L : louver
o : outside glass
T : total
v : venetian system
w : test cell walls

REFERENCE

1. Rheault, S. and Bilgen, E., On the heat transfer through an automated venetian blind window system, ASME/JSME Conference, Solar Engineering, Honolulu, Hawaii, pp. 745-755, 1987.
2. Rheault,S. and Bilgen, E., Heat transfer optimization of an automated venetian blind window system, ASES 12th National Passive Solar Conference, Portland, Oregon, pp. 122-128, 1987.
3. Rheault,S. and Bilgen, E., Experimental study of the thermal performance of automated venetian blind windows, Solar and Wind Technology, (to be published).
4. Bilgen, E. and Michel, J., Integration of solar system in architectural and urban desing, in Solar Energy Application in Buildings, edited by Sayigh, A. A., Chap 9, Academic Press, New-York, 1979.
5. Parmelee, G. V., Warren, W. and Aubelee, W., Solar and total heat gain through double flat glass, ASHVE Research Bulletin no 1348, 1948.
6. Parmelee, G. V., Warren, W. and Aubelee, W., Overall coefficients for flat glass determined under natural weather conditions, ASHVE Research Bulletin no 1351, 1949.

DESIGN AND MATHEMATICAL MODELLING OF A ROOF-TOP WICK-TYPE SOLAR STILL

Magal B.S. (Professor) and Gaunekar A.S. (P.G. Student)
Department of Mechanical Engineering
Indian Institute of Technology, Powai, Bombay-400076
INDIA

ABSTRACT

For the present investigation, the high output, high efficiency wick-type tilted solar still has been chosen. Situated on the roof of the house, the still is characterised by simplicity of design, very low installation and maintenance costs, with no requirement of extra land-area outside that of the house. The design of the still has been made keeping in mind availability of local materials in India and could be modified to suit the needs of any other tropical region of the world.

Made of concrete, the thermal interia of the still is quite high. The daily yield on a moderately hot sunny day is expected to be around 3 to 4 kg and the daily efficiency in the range of 40 to 60% depending upon the conditions of solar insolation, wind-velocity, ambient temperature etc.

A unit of the still has been fabricated and is ready for thorough testing. Initial trial runs have shown encouraging results. However, the scope of this paper is limited only to the design, modelling and development of a flexible computer software.

1. INTRODUCTION

Lack of adequate quantities of fresh potable water could become one of the most serious problems confronting mankind, in the decades to come. The conventional desalination processes such as multiple effect evaporation, multi-stage flash evaporation, thin film distillation, reverse osmosis and electrodialysis are not only energy intensive, but also uneconomical for low and medium demands of fresh water. In the wake of the worldwide energy crisis and consequent increase in the cost of conventional fuels, SOLAR-DISTILLATION appears to be a very attractive alternative to the other

methods. The technology required is simple and so is the maintenance. In certain remote arid regions, this may be the only alternative.

A project has been undertaken at the I.I.T. - Bombay, with the purpose of investigating the technical feasibility of utilising solar energy to provide pure drinking water. The scope of this paper is limited to the designing, mathematical modelling and developing a computer program for simulating the daily performance of the still.

2. SELECTION OF STILL

A wick-type inclined solar still has been selected for investigation. The selection has been made keeping in mind its merits over the other still-types, such as follows:-

(i) Its cost has been found to be considerably lower than the basin type solar still.

(ii) The water surface can be effectively oriented by selecting an appropriate still-slope (β), so as to maximise solar radiation absorbed over a certain period.

(iii) Minimum shadowing effect due to small height of side-walls; unlike in the case of basin-type stills.

(iv) Only a small amount of brine is contained in the tray at any instant; so better response and higher efficiency.

3. STILL-DESIGN

The designing of a suitable solar still has been done keeping in mind the following important factors:-

(i) Supply of pure water at minimum cost.

(ii) Use of cheap locally available materials.

(iii) Use of already available roof space so that no extra land area is required to build the still.

(iv) Ease of construction, maintenance and handling.

A prototype of a roof-top solar still (the schematic of which is shown in Fig.1) has been fabricated fully out of concrete. It is in the form of a reinforced slab, 10 cm thick, this being found to be the average thickness of standard housing roofs in the semi-rural regions of India. Changes in the material suggested and the slab-thickness may be made according to material availability and suitability of the region concerned. Care should however be taken to see that the material selected is leak-proof and non-degradable when in prolonged contact with water. Four walls of height and thickness as low as 7 cm are built on the slab to enclose an area of about 0.8 square meters. The height of the walls was selected keeping in mind that the wall-height determined the absorber-cover distance, as the cover is placed directly on top of the four walls. The other dimensions of the wall (thickness and length) were decided upon, considering the standard dimensions of the cover materials available

(viz. perspex and glass) and requirements of clamping. These wall dimensions may be suitably modified to suit locally available materials and conditions.

4. WORKING OF THE STILL

The wick, made of a black, fibrous material, easily absorbs water from the brine-trough at the top of the slab. It acts as the evaporator, by absorbing the solar radiation incident on it. The condenser is in the form of a 3 mm thick cover made of glass, perspex or any other strong, transparent material. The film of water on the wick continually evaporates, to be replenished by brine from the trough by capillary and gravitational forces. The vapours condense on the underside of the cover and the distillate slides down in a collecting channel, to be led out in a flask, through an S.S. - tube.

5. THEORETICAL ANALYSIS

The theoretical analysis of the working of the still is done by considering the various heat flow modes possible in the different sections of the device and forming energy balance equations for the various capacitive elements therein. For convenience, the conventional solar still with a single sloped cover is analysed and then a modified model, suitable for a wick-type solar still is discussed.

The net irradiation on the still is mainly the beam and diffuse component of incoming solar radiation viz. I_b and I_d respectively. The reflected component is neglected, for simplicity, as it is very small. The fraction of the total incident radiation, productively absorbed in the still (S) and that absorbed by glass (S') are given as follows:-

$$S = [I_b R_b (\tau\alpha)_b + I_d R_d (\tau\alpha)_d] A_w \qquad ...(1)$$

$$S' = [I_b R_b \alpha_{gb} + I_d R_d \alpha_{gd}] A_g \qquad ...(2)$$

Of the total energy absorbed by wick, brine and slab, some fraction is lost to the surroundings by conduction through the sides and bottom of the slab ($Q_s + Q_b$). Of the remaining, some heats up the brine and the rest is lost to the cover by convection, radiation and evaporation. Of the net energy incoming on the cover, some goes to heat it up and the rest is lost to the surroundings by convection and radiation.

(i) Heat balance for water-mass

$$S = \kappa_b + \kappa_s + \kappa_{rl} + \kappa_{cl} + \kappa_e + C_w \cdot \frac{dT_w}{dt} \qquad ...(3)$$

where the various modes of heat-transfer are given as follows:

(a) Base and side heat losses:

$$\kappa_b = A_w U_b \cdot (T_w - T_a) \qquad ...(4)$$

where $U_b = \frac{K_i}{b}$

and $Q_s = A_w U_s (T_w - T_a)$

where $U_s = \frac{(L_1+L_2)\, L_3 K_1}{L_1 L_2}$ ...(5)

(b) Radiative loss:

$$Q_{r1} = \left[\frac{1}{\varepsilon_w} + \frac{1}{\varepsilon_g} - 1\right]^{-1} . A_w . \sigma . [(T_w+273)^4 - (T_g+273)^4] \quad ...(6)$$

(assuming parallel plates configuration)

(c) Convective loss: The model becomes complex as convective heat transfer is coupled with mass transfer from the heated water surface.

Dunkle's relationship to account for these simultaneous phenomena is:

$$Q_{c1} = A_w h_{ci} (T_w - T_g) \quad ...(7)$$

$$\text{where } h_{c1} = 0.884 (T_w - T_g) + \frac{(P_w - P_g)(T_w+273)}{(268.9 \times 10^3 - P_w)}^{1/3}$$

Experimentation has shown that this expression is valid for the working of the wick-type still [1].

(d) Evaporative loss:

$$Q_e = 16.36\, A_w\, h_{c1}\, (P_w - P_{wg}) \quad ...(8)$$

(ii) Heat balance for cover:

$$S' + Q_{r1} + Q_{c1} + Q_e = Q_{r2} + Q_{c2} + C_g \frac{dT_g}{dt} \quad ...(9)$$

where

(a) Radiative loss:

$$Q_{r2} = \varepsilon_g \cdot \sigma \cdot A_g [(T_g+273)^4 - (T_{sky}+273)^4] \quad ...(10)$$

(b) Convective loss:

$$Q_{c2} = A_g \cdot h_{c2} \cdot (T_g - T_a) \quad ...(11)$$

where $h_{c2} = 5.7 + 3.8\, V$ (for low wind velocity V)

The above analysis for a conventional solar still can be readily applied to the present case of a wick-type solar still with a few minor modifications. The important features of the wick-type still to be kept in mind vis-a-vis the conventional basin type still are the following:

(i) At any time of consideration the water mass in the still being exposed to the incident solar radiation is very small. It is in the form of a thin broken film rather than a pool.

(ii) It is assumed that there exists no temperature gradient across the thin wick layer.

(iii) The temperatures at all points on the still absorber surface are considered equal to T_w.

(iv) The heat fraction required to raise the temperature of the water-mass from its initial temperature to the operating temperature is neglected.

6. THE PROGRAM LOGIC

The eleven equations (eqns. 1 to 11) can be reduced, by proper substitution, to two linear, simultaneous differential equations in two unknowns viz. water temperature (T_w) and glass temperature (T_g). Hence a numerical solution is resorted to, using specific time intervals, for a 24 - hour period. The flowchart of the program is shown at the end.

For better understanding of the logic of the software developed, it would be of interest to study the day-long variation of temperatures T_w, T_g and T_A as obtained in some preliminary test-runs of the still which is shown in Fig.2. along with the variations in the solar insolation and distillate - output for the day.

We see that there is a gradual rise in the temperature in the early hours of the day, an increase in the rate towards noon and peaking at around 1400 hours. The decrease is more or less of a similar nature with a final flattening, much after sunset.

Turning to Fig.3. (which represents qualitatively the variation of just one general temperature-variable for simplicity), we choose a small time interval t, for investigation of the simultaneously occuring heat-gain and heat-loss effects.

As a first approximation, the change in glass temperature ΔT_g is calculated basing the heat losses on the initial temperatures T_{wi} and T_{gi} at time t_i. This increase is compared with a certain limit-value TGG. If ΔT exceeds TGG, then the next approximation is based on a value in between T_i and T_f given by $T_{av} = T_i + (\Delta T/2)$. This iterative process is followed until a point when the T_{av} - value used for calculating the losses yields a ΔT within practical limits. Then the value of $T_f = T_i + \Delta T$ is printed as the predicted final value of temperature for that interval which is also the

initial value for the next.

The distillate-output for the interval is computed based on Q_E of the final iteration, and cumulative addition is done upto each interval. The output for the day is also printed.

Due to high thermal inertia of the still it is not very meaningful to speak of still-efficiency for an interval. Hence the efficiency of the still is computed based on its performance throughout a whole 24 - hour cycle.

7. CONCLUSIONS

(i) The wick-type roof-top solar still scores over the conventional stills in terms of economy and efficiency. The former is simpler, in design and construction and it lends itself to easy maintenance.

(ii) The importance of mathematical modelling of such a device and development of a computer software based on the model, for prediction of its performance, cannot be overstressed.

(iii) Trial-runs of the still showed encouraging results. The temperature-values predicted on the computer show a trend similar to that shown by experimental values. The program is in the process of further refinement in order to make it more flexible.

(iv) A large number of such still modules will have to be built and rigourous experimentation be done for an exhaustive validation of the software developed.

REFERENCES

[1] Malik, M.A.S., Tiwari G.N., Kumar A., Sodha M.S., Solar Distillation, Pergaman Press (1982).

[2] Gaunekar A.S., 'Design and Testing of a Roof - Top Solar Still', M.Tech. Dissertation, (Stage - I), Dept. of Mech. Engg., I.I.T., Bombay (1988).

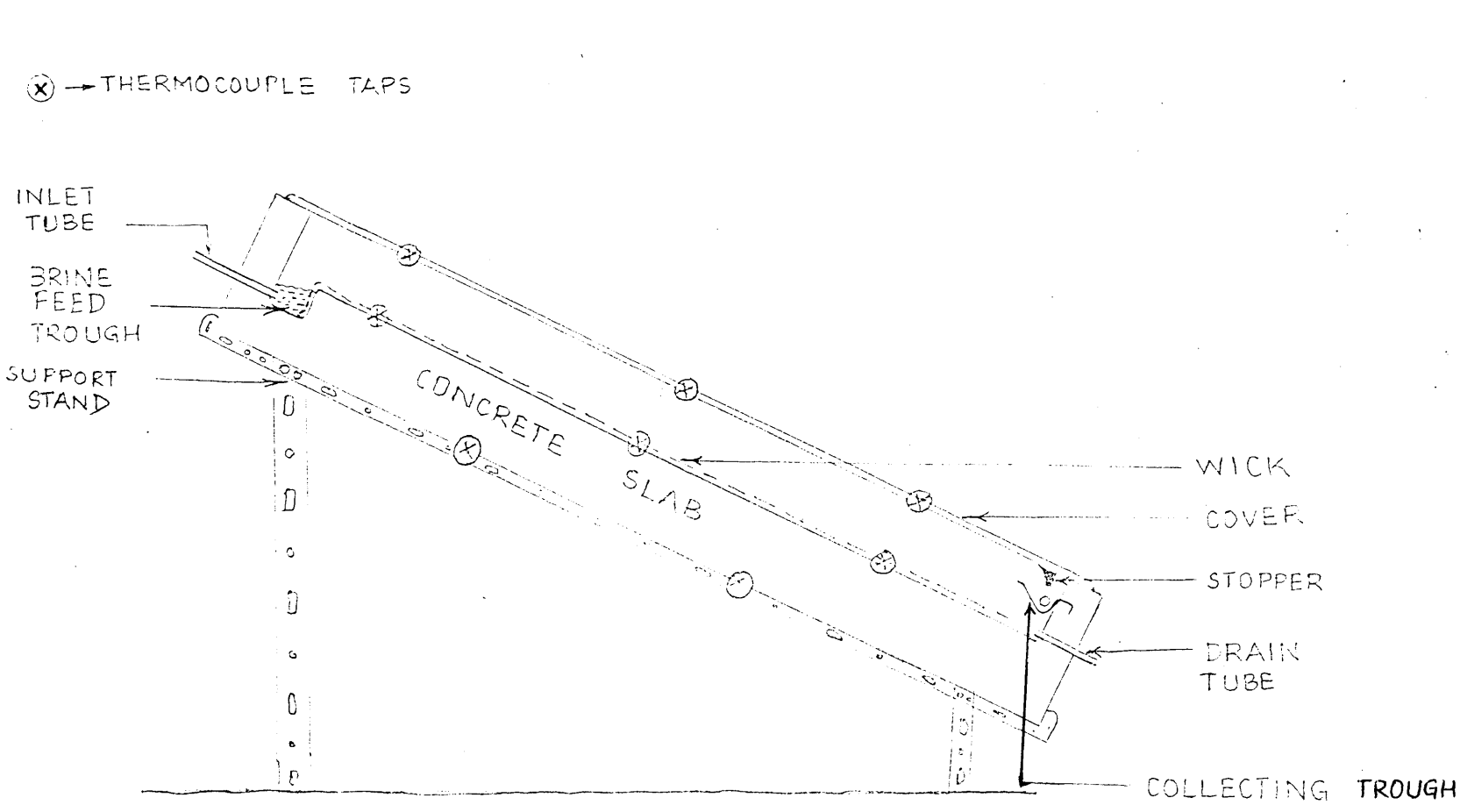

Fig. 1. - Schematic of a Wick-type Solar Still.

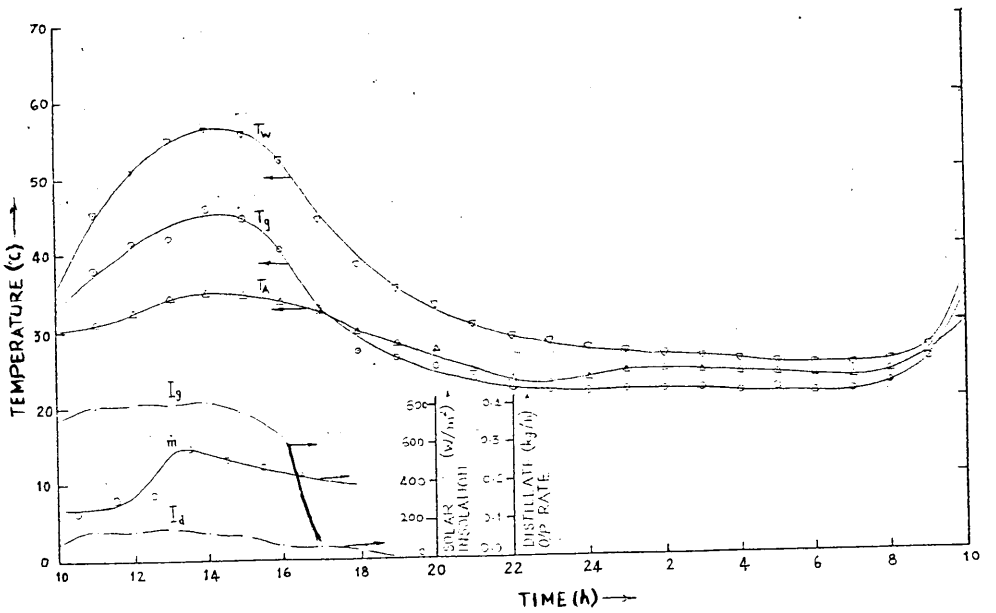

Fig. 2. - Typical variation of temperatures, solar insolation and output.

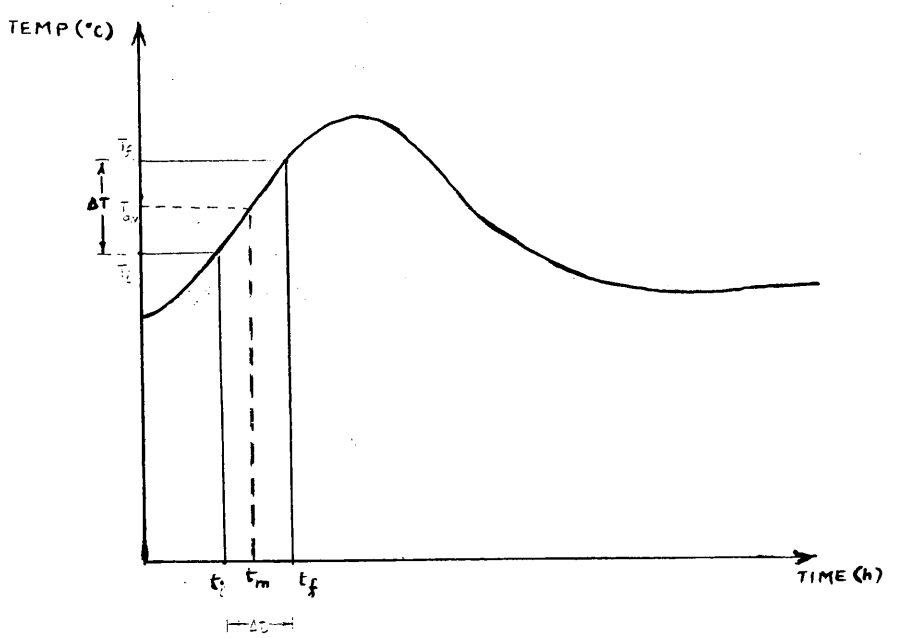

Fig. 3. - Qualitative variation of temperature with time

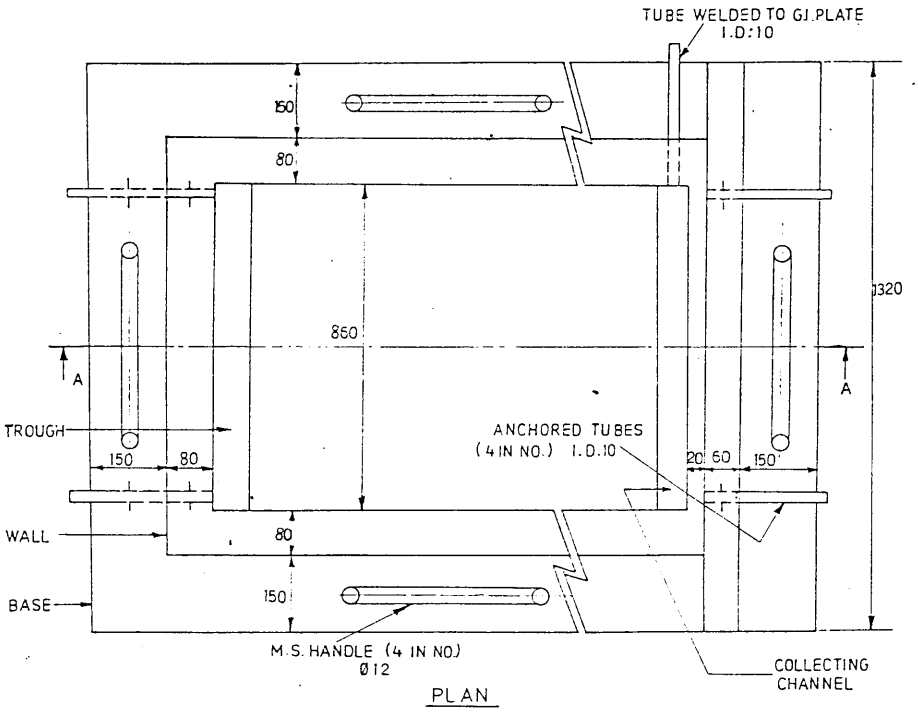

PLAN

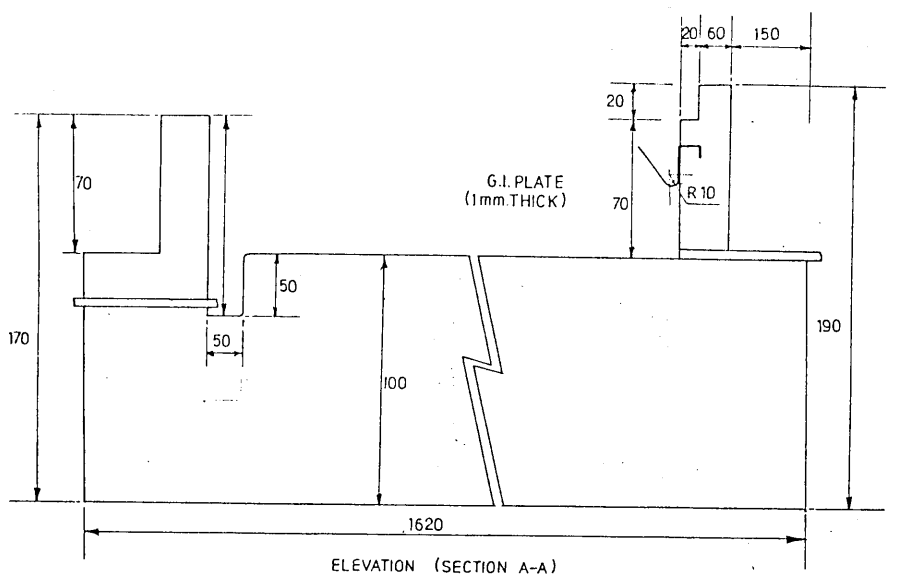

ELEVATION (SECTION A-A)

WICK-TYPE ROOF-TOP SOLAR STILL

ALL DIMENSIONS IN MM

NOT TO SCALE

Appendix - Design - drawings of the still.

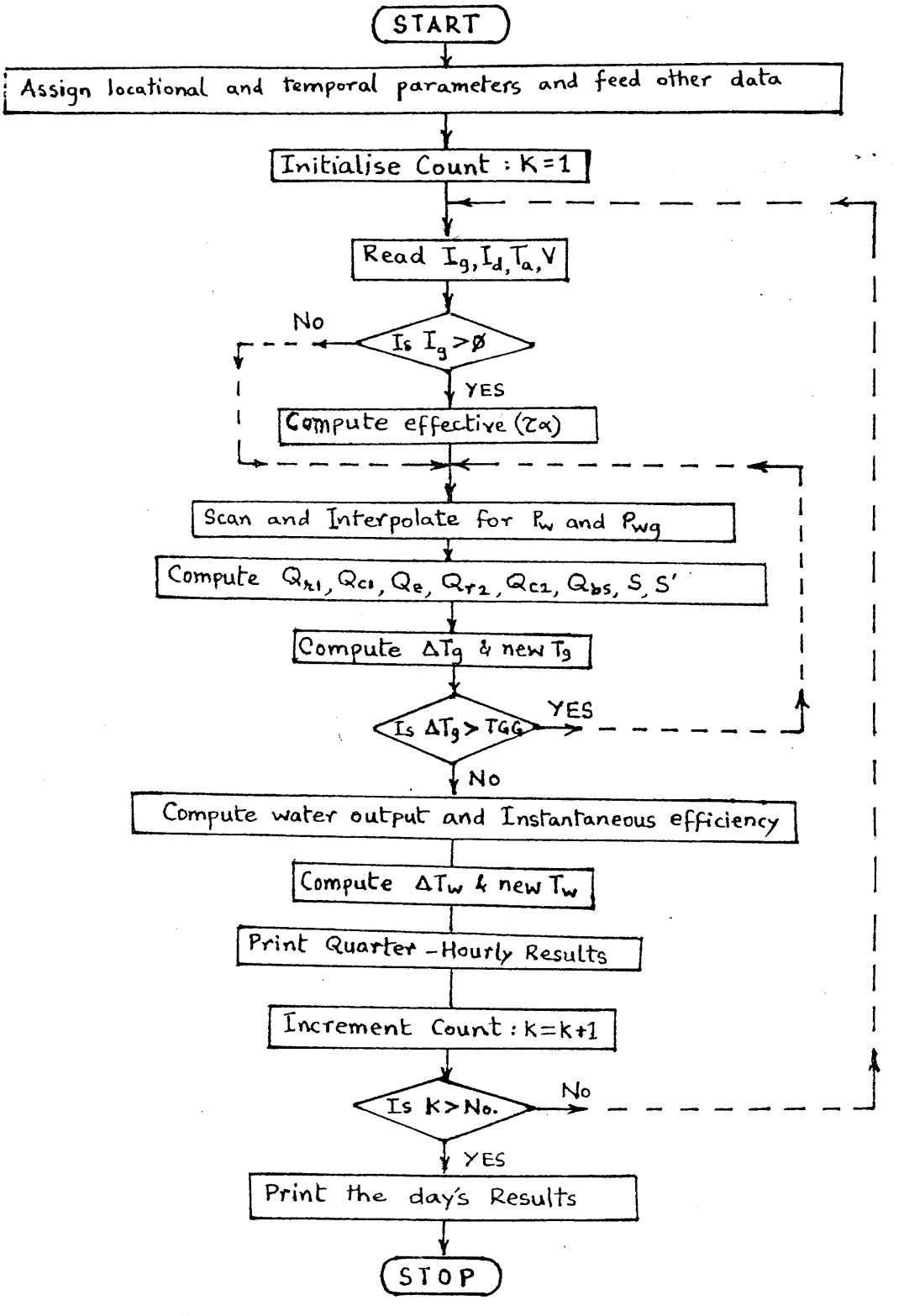

THE FLOW-CHART

THE POTENTIAL OF THE EVAPORATIVE COOLING TECHNIQUES ON THE GULF REGION OF THE KINGDOM OF SAUDI ARABIA

Erdal Aksugur, Maqsood Bajwa, Ghazi Al-Otaibi

College of Architecture and Planning
King Faisal University
P.O. Box: 2397, Dammam 31451
Kingdom of Saudi Arabia

ABSTRACT:

This paper deals only with the first set of experiments for the investigation of the potential of the evaporative cooling techniques. The experiment is intended to identify comfort enhancement potential of evaporative cooling through wintower by the supply of the cooled air into the rooms directly from air outlets or indirectly through the ducts. For the evaluation of the comfort condition in the rooms Fanger PMV (Predicted Mean Vote) as a function of dry bulb temperature, wet-bulb temperature, air velocity and mean radiant temperature (globe temperature) has been calculated for each hour and recorded during the experiments. All ambient weather components are displayed for the experiment period to evaluate the performance of the evaporative cooling techniques used in the test house.

1. INTRODUCTION:

The overall objectives of the current research project, sponsored by the Joint Saudi Arabian-United States Program for Cooperation in the Field of Solar Energy (SOLERAS), is to investigate the effectiveness of applicable passive solar cooling techniques for the possible utilization in domestic buildings in the hot-arid maritime desert climate of coastal areas of the Eastern Province of Saudi Arabia. In the current third phase of the research project validation of the defined strategies are under investigation through actual experimentation on the two storey full-scale test house.

2. PREVIOUS PHASES OF THE PROJECT:

In the first phase of the project climatic analysis for Dammam - Dhahran area are finalized, passive solar design criteria and identification of specific Passive cooling strategies applicable to this area are determined [1]. Based on these criteria and strategies four different schematic design concept were evolved and evaluated for their climatic response using a thermal computer simulation model [2]. A final design concept integrating all positive aspects of previous designs was developed and evaluated by most upto-date computer simulation models [3]. An elaborate Data Acquisition System was developed and a comprehensive yet condensed experimental plan evolved [4],[5].

In the second phase construction documents of the test house were prepared, building constructed, Data Acquisition System installed, instruments mounted and checked. In October 1986 test house became ready for the experiments [6]. A more detailed summary of the Project can be found in the Proceedings of 1987 European Conference on Architecture [7].

3. THE PASSIVE SOLAR COOLING TEST HOUSE:

3.1 The Main Objectives of the Final Design were:

To satisfy all the requirements of the proposed building program. To offer maximum climatic comfort to the users by the minimum energy consumption. To utilize passive cooling techniques to save energy. To have a laboratory building to test different passive cooling techniques simultaneously as well as individually.

3.2 The Description of the House:

The test house is two storey, with a total area of 265 sqm., including walls, but excluding garage and terrace. The length to with ratio is 1:1.45, with the longer axis on the East-West direction. All the window openings are on South and North walls with double glazed vertical hang windows (window to floor area ratios in the rooms are 15% and 38%). Manually operated movable horizontal louvers are installed on the South for Solar Control and on the North for wind deflection. Load bearing 20 cm. Concrete hollow block inner walls carrying reinforced concrete floor slabs enveloped by 10 cm thick "Extruded Polystyrene" thermal insulation and 10 cm thick concrete hollow block wall to protect thermal insulation. The end walls are projected towards North and South to obtain better induced ventilation (Fig. 1). Centrally located wind tower is to be used for direct evaporative cooling and induced ventilation. Ceiling fans are installed in main rooms to obtain air movement when needed. A split air-conditioning system is installed to be used as back-up when needed and for experiments for each zone. [3]

4. WIND TOWER DESIGN:

4.1 Tower and outlet sizing:

The wind tower was analysed utilizing a computer simulation program developed at ERL in Tuscon, Arizona, USA for this purpose. The design case was based upon calm wind conditions and a wet bulb depression of 11 deg. C. The driving force therefore was only evaporative downdraft effect. The tower has a cross-sectional area of 4.84 sqm (2.2 m x 2.2 m) and a height of 17.22 m. The gross outlet area to each floor was varied from .1 to .8 times the cross-sectional area of the tower and .5 was selected as optional.

4.2 Tower Construction and Evaporative Cooling System:

The wind tower is constructed of solid poured reinforced concrete up to 10.52 m above ground level. The extension part of the tower is fabricatred from welded steel tubing and this upper part is easily removable for reconfiguration. The top portion contains evaporative cooling system which is installed behind the three openings of the tower air inlets on the NW, N and NE sides of the tower. The motor activated operable horizontal louvers are installed to close and seal the inlets. Inside these louvers vinyl sheet barometric dampers fixed from top side

to the 2 cm x 2 cm hardware cloth screen controls air flows in and out. Inside of these dampers 5 cm thick Celdek evaporative pads made of special paper honeycomb are installed. A pump was recirculating water from the stainless steel channel placed at the bottom of the pads to the top of them and makes these water absorbent honecomb pads wet.

5. DATA ACQUISITION SYSTEM:

5.1 Total Data Acquisition System:

An intensive Data Acquisition System (DAS) is incorporated with the design and construction of the house. All the 650 sensors are directly connected to the DAS capable of controlling all the experiments being performed. A cluster of three IBM PC-XT computers provided instantenous access to the data and results of hourly averages as well as continuous recording and analysis. The type and locations of the DAS instruments for ground floor only (because of space limitation) shown in (Fig. 2).

5.2 Data Categories for Evaporation Cooling Experiments:

5.2.1 Ambient Weather Data Categories and Instruments:

Dry bulb and wet bulb temperatures: by radiation shielded aspirated type T thermocouples Relative humidity; by a Weathertronics relative humidity probe. Barometric Pressure; a Weathertronics solid state analog output barometer. These equipments are placed inside a Stevenson Screen (weather station) on the North of the House at 15.5 m. distance. Insolation on the horizontal surface; an Eppley PSP Precision Special Pyranometer placed on the terrace handrail with other radiation instruments. Wind velocity; by three R.U. Young Gill Propeller Vane integral wind velocity and direction sensors installed at 2.5, 5 and 10 m. above ground.

5.2.2 Comfort Conditions Data Categories and Instruments:

Dry and wet bulb temperatures; the equipment described in Section 5.2.1 is used at 61 cm height above floor at the center of each room. Globe thermometer temperature; a Type T termocouple at the center of a 15.24 cm copper sphere painted with Nextel paint .98 emissivity and hung at the 61 cm. height above floor. Air Velocity; by an Omnidirectional Precision Air Flow Sensor (anemometer) fixed at the same location with the other comfort conditions instruments.

5.2.3 Cooling Effectiveness Data Categories and Instruments:

Tower air inlets and outlets air velocities; by anemometers described in Section 5.2.2 installed in front of the tower inlets and outlets. Dry and wet bulb temperatures of the air supplied from tower outlets into the room; by the radiation shielded aspiratd dry and wet bulb temperature instruments installed in front of the tower outlets, (Figures 3 and 4).

5.2.4 Water Usage:

The water consumption of the system is measured by a low-flow water meter and manually entered into the DAS.

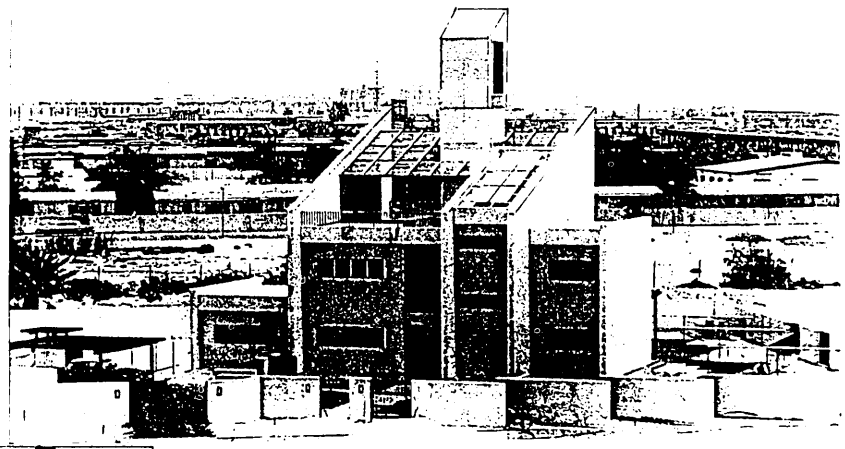

Figure 1. Passive Solar Cooling Test House in KFU, Dammam, KSA

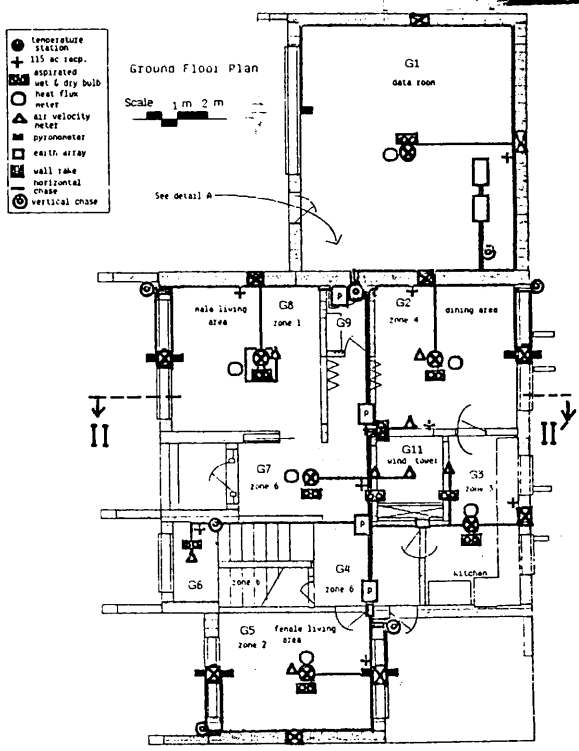

Figure 2 Data acquisition system instruments on the gound floor

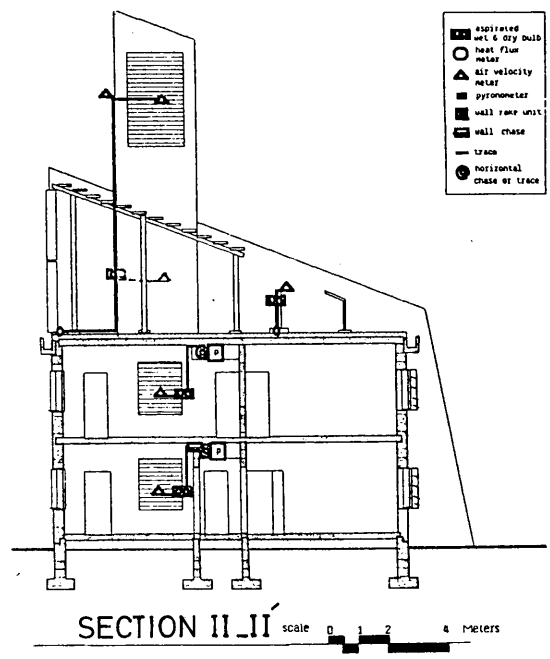

Figure 3. Cooling effectiveness data instruments and their locations in building section

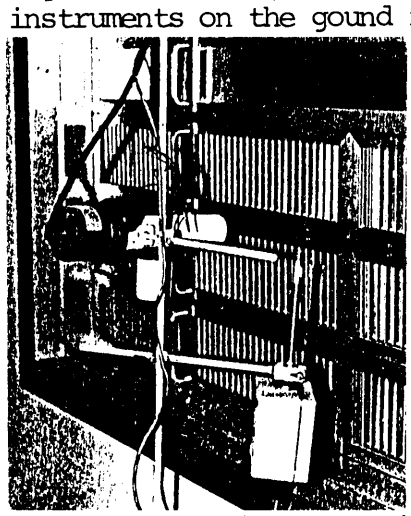

Figure 4. Cooling effectiveness instruments in front of the tower outlets in Zone-4

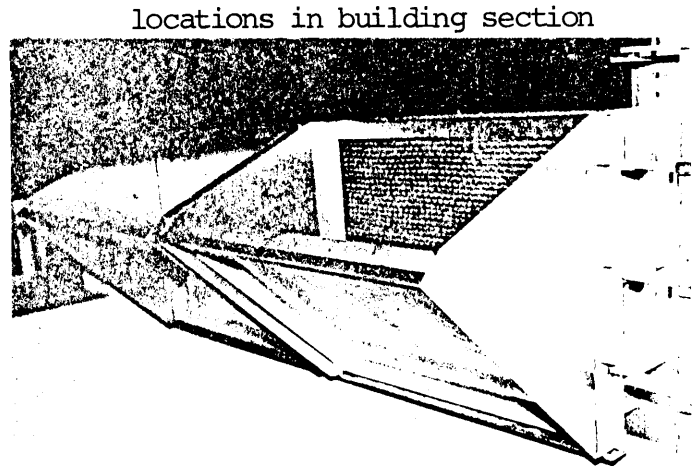

Figure 5. Tower outet view from inside the tower with dampers and oeldek demisters

6. DIRECT EVAPORATIVE COOLING EXPERIMENTS:

During the Summer 1987, from July 11 until September 28, the Direct Evaporative cooling experiments are carried out to evaluate the appropriateness of the evaporative cooling for the theoretically defined period.

Direct evaporative cooling system is activated two short period of time during each day from 5:00 HRS to 10:00 HRS and from 15:00 HRS to 18:00 HRS. During these periods tower air inlets kept open, water pump supplied water to the Celdek pads. Evaporatively cooled air moved down inside the tower by the wind pressure and density increased, and supplied through the direct or ducted tower outlets (Fig. 5). Open lower half of the south windows of the rooms allow the air to escape out towards the low pressure zones generated under NW, N and NE winds. The air flow patterns of the evaporative cooling mode are shown in (Figures 6. 7. 8 and 9). As it is shown on the Experimental configuration Table (Table 1) during the whole summer period of 1987 ceiling fans and A/C system were kept off to eliminate their effects on the thermal behavior of the house.

7. ANALYSIS OF THE EXPERIMENTAL DATA:

For the whole experimental period hourly averages obtained from 20 reading per hour from each sensor are recorded and simultaneously Predicted Mean Vote (PMV) as comfort indice for each room is calculated by the analysis program.

After the analysis of the data for the whole period, three consecutive days selected for each month representing the average performance of the evaporative cooling system for selected typical rooms (Fig. 10).

7.1 The Performance of the Evaporative Cooling System in July 1987:

The outdoor DBT stayed over 40 deg C 6 to 8 hours daily and over 43 deg C 4-6 hours. During this period DBT of the air from tower outlet changed betweem 26 deg C and 32 deg C. The Tower outlet DBT and WBT generally followed the same profile. As it is seen in Fig. 7.a DBT of the tower supplied air and room drops when evaporative cooling system starts to operate. During these periods outdoor RH values were dropping from 40% to 25%. Some days upto 16 deg.C. difference between outdoor and tower outlet DBT values obtained. The evening and the night hours, outdoor Relative Humidity increased upto 70% due to the wind blowing from SE and S with maximum speed of 5 m/s and carrying humidity of the Gulf.

Predicted mean vote calculted for the Direct Supplied Zone 4, Zone 7 found between +1 and +2 during the Evaporative cooling OFF period. This was expected and for the high RH periods of the day A/C system was suggested [3]. During the morning session of the Evaporative cooling mode PMV was below +1, just at the upper edge of the comfort zone.

7.2 The Performance of the Evaporative Cooling System in August, 1987:

The outdoor DBT were between 35 deg.C. and 40 deg.C. 6 hours per day. Indoor temperatures mainly stayed at 30 deg.C. with sudden drops during evaporative cooling morning session down to 23 - 24 deg.C. During afternoon sessions, due to the increasing outdoor RH caused by the drop

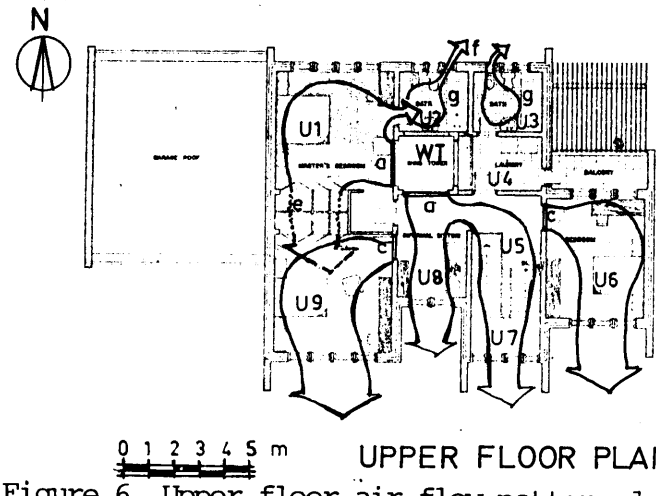

Figure 6. Upper floor air flow pattern during evaporative cooling mode

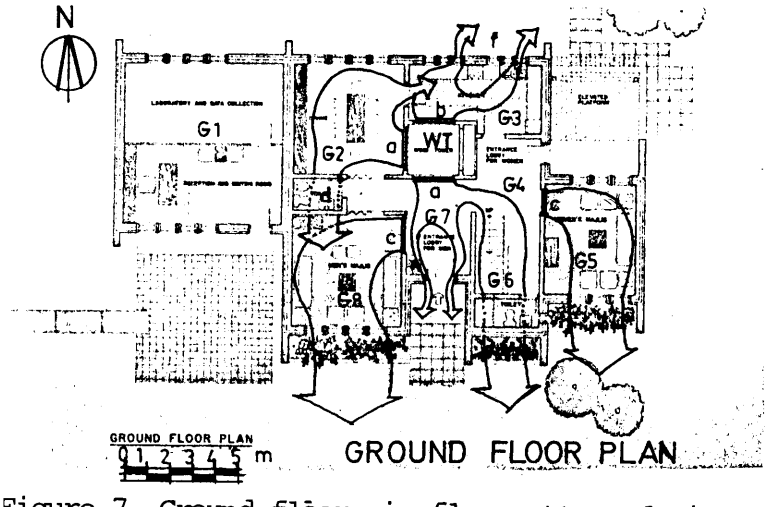

Figure 7. Ground floor air flow pattern during evaporative cooling mode

KEY :

W.T. Wind Tower supplies humidified cool air down to the tower outlets (room inlets)

a. Low-wall room inlets supply air to living or occupied levels of G2, G7, U1 and U8.

b. Mid-wall room inlets supply tower air between base and upper cabinets in kitchen, G3.

c. High-wall room inlets (ducted tower outlets) with "deflector vanes" supply tower air to G5, G8, U6 and U9.

d. Louvered space over toilet ceiling slab provide alternative cross ventilation path through G2 and G8.

e. Louvered space under cabinets provide alternative cross ventilation path through U1 and U9.

f. Exhaust fans remove smoke and odors and provide alternative outlets for tower air in G2, G3, U1, U2 and U3.

g. Ceiling diffuser inlets supply tower air to U2 and U3.

* Only modest levels of tower air are projected for G6, G7, U4, U5 and U7.

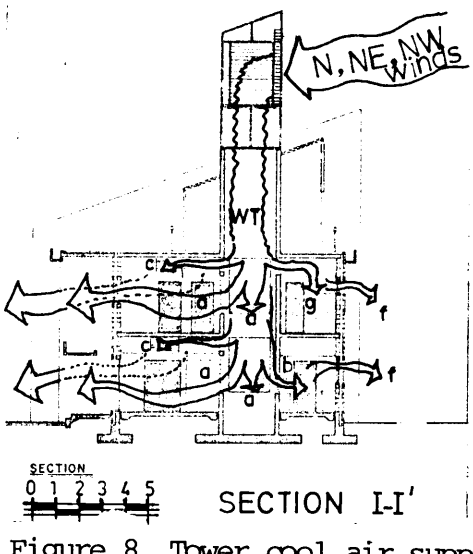

Figure 8. Tower cool air supply and air flow inside the house during evaporative cooling mode

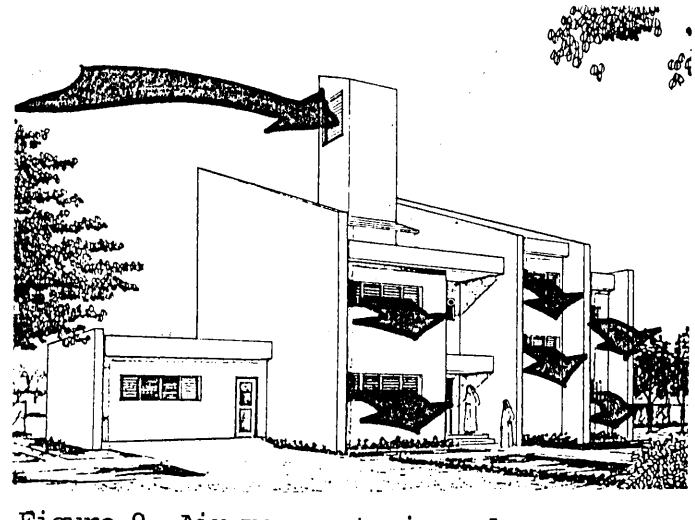

Figure 9. Air movements in and out of the house under NW, N and NE winds

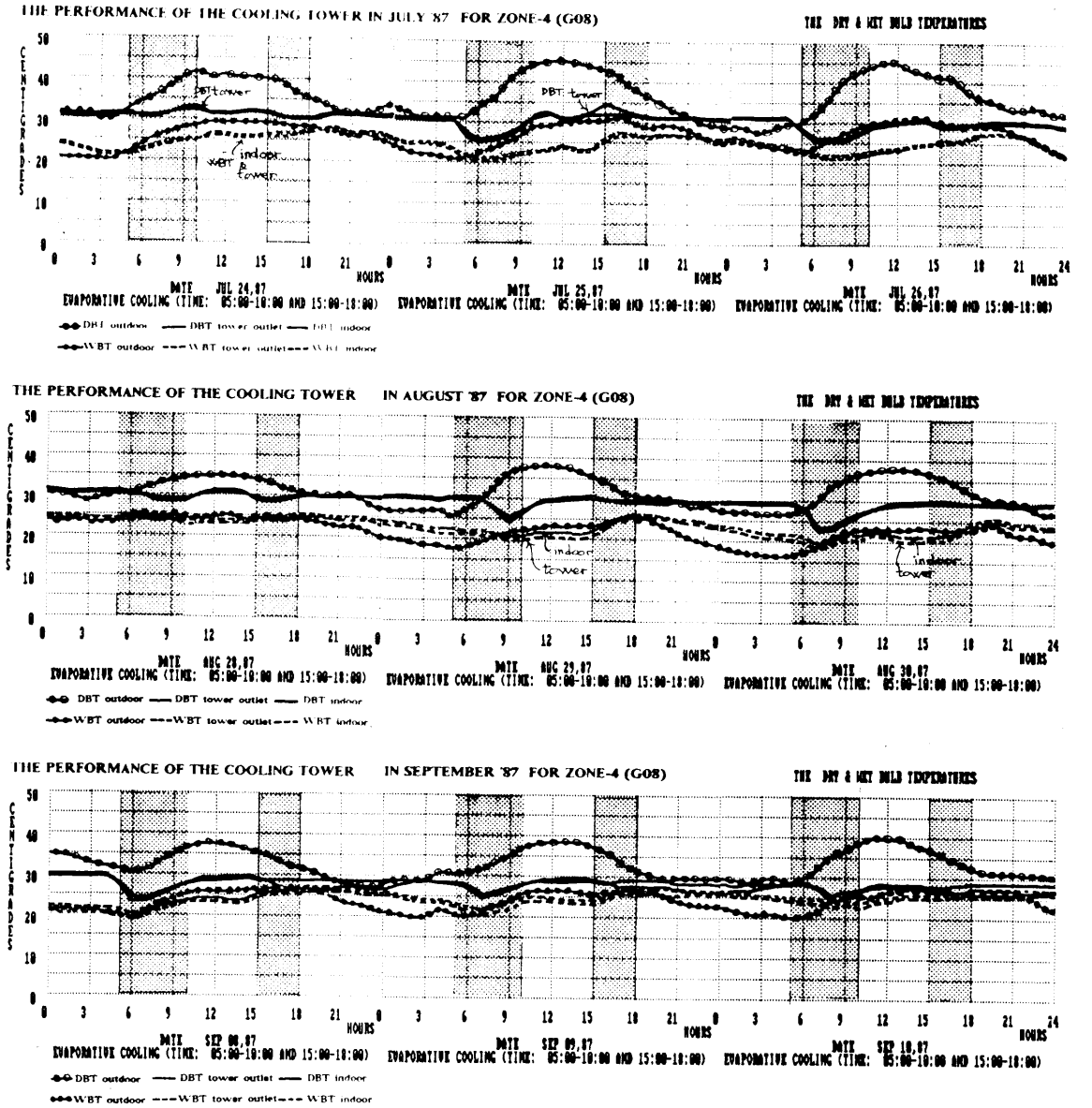

Figure 10. The performance of the Cooling Tower for typical days of July, August and September 1987. Evaporative cooling system was active twice a day (Time: 05:00-10:00 and 15:00-18:00)

Table 1. Direct Evaporative Cooling Experiment Configuration

S.No.	EXPERIMENT	CONFIGURATION																					
	DIRECT EVAPORATIVE COOLING	Windows				Louvres				Doors		Fan		A/C		Wind-Tower				Timings		Period		Remarks
	AIR DISTRIBUTION	South		North		South		North		Internal		External				Direct		Ducted						
	Direct ROOM NO	Open	Closed	Open	Closed	Open	Closed	Open	Closed	Open	Closed	Open	Closed	Open	Closed	Open	Closed	Open	Closed	From	To	From	To	
	G2/G3																							
	G6/G7	✓			✓	✓		✓			✓		✓		✓	✓		✓		5:00	10:00	4 JUL	28 SEP	
	U1/U7/U8																			15:00	18:00	1987	1987	
	Ducted ROOM NO																							
	G5/G8																							
	U2/U3																							
	U6/U9																							

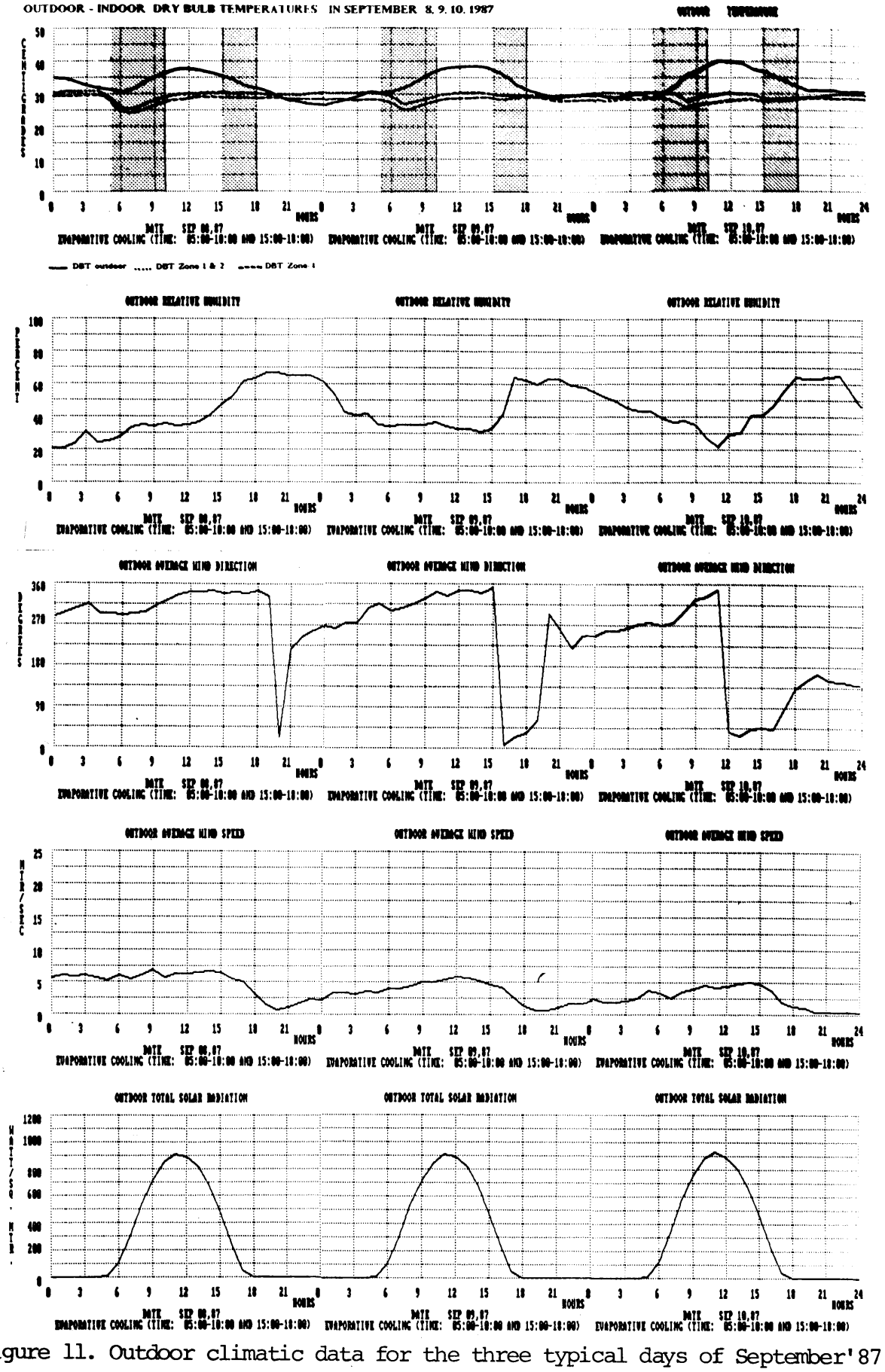

Figure 11. Outdoor climatic data for the three typical days of September'87

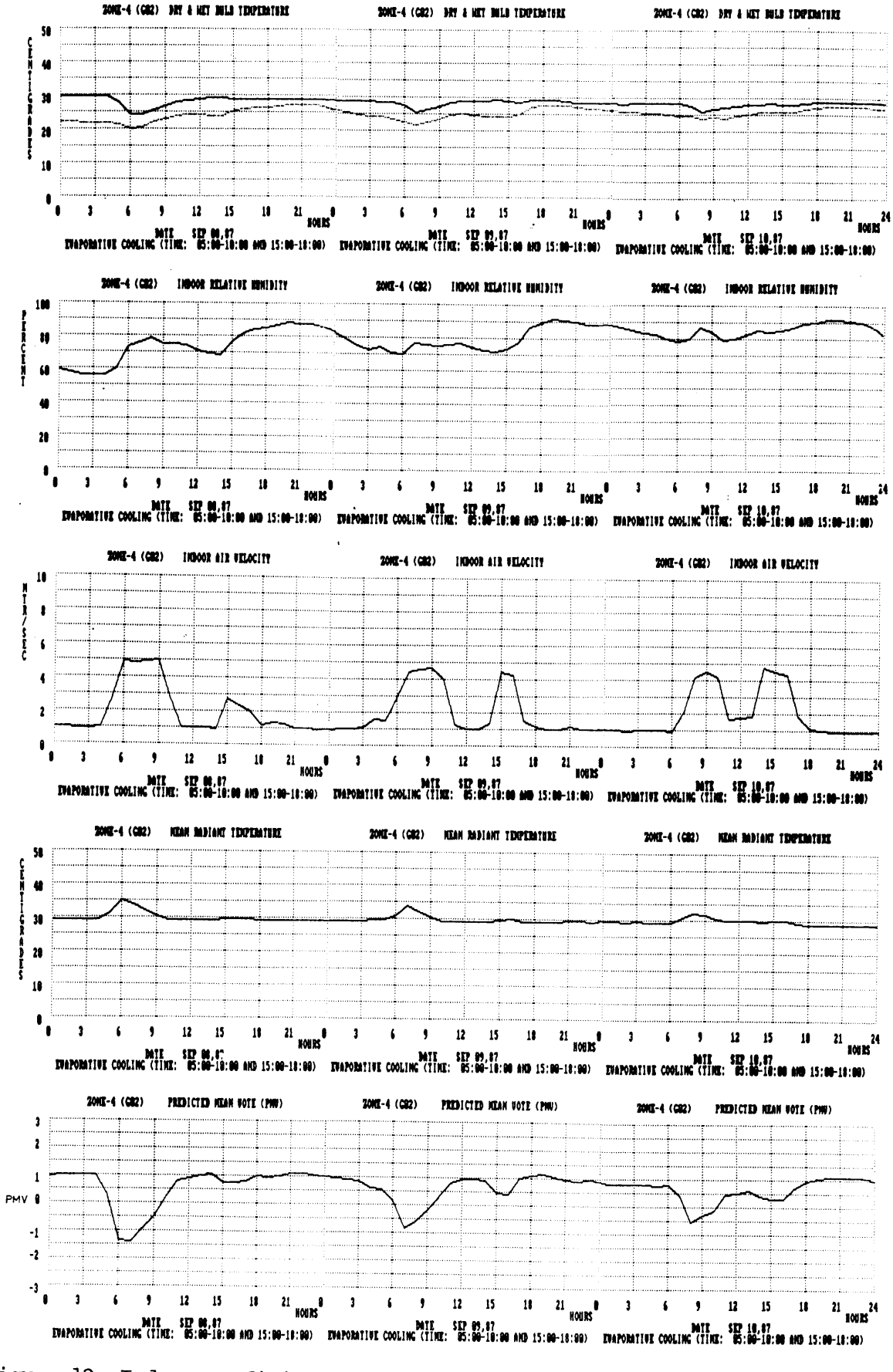

Figure 12. Indoor conditions for the three typical days of September'87

of outdoor DBT and the change of the wind direction, the performance of the system were low and tower outlet air temperature reached to 30 deg C with a very small (2-3 deg C) difference from outdoor DBT.

7.3 The Performance of the Evaporative Cooling System in September 1987:

The outdoor DBT were about 35 deg C for 6 to 8 hours per day reaching up to 30 deg C around noon, with a minimum of 28-29 deg C around midnight. Outdoor RH was swinging from 30-40% in the morning upto 60-65% in later afternoon and evening (Fig. 11). Mainly NW and N winds carrying comparatively dry air masses after midnight and morning changed to NE and carried the humidity of the Gulf during later afternoon hours.

Indoor DBT stayed between 25 and 28 deg C throughout the day. The Indoor air velocity showing clear increase during evaporative cooling mode gave a result of PMC mainly swinging between +1 and -1. (Fig. 12).

8. CONCLUSION:

Despite the unusually high outdoor relative humidities of the summer 1987, comparing the long term averages, the evaporative cooling system performed successfully dropping the outdoor DBT by 8-16 deg C in low Relative humidities (10-30%) and 4-5 deg C in higher relative humidities (65-70%). The performance of the tower is analysed on the psychrometric chart for typical days. According to the results, evaporative cooling will reduce the operation time of the A/C system significantly during overheated period of the Maritime - Desert climate. The performance of the suggested system will be much more better if operation ON-OFF switches will be automatically controlled by the outdoor Relative Humidity Probe and wind direction sensor.

REFERENCES:

[1] KFU, Passive Solar Cooling Project, Report:2, Vol. 1 & 2 Dammam 1982.

[2] KFU, Passive Solar Cooling Project, Report 2, Vol. 3 & 4, Dammam 1983.

[3] KFU, Passive Solar Cooling Project, Report 4, Vol. 6 - Design Review Report, Dammam 1984.

[4] KFU, Passive Solar Cooling Project, Report 4, Vol. 8 - Data Acquisition System, Dammam 1984.

[5] KFU, Passive Solar Cooling Project, Report 4, Vol. 7 - Experimental Plan, Dammam 1984.

[6] KFU, Passive Solar Cooling Project, Report 4, Vol. 5, 7,. 8, 9, 10, 11, Dammam 1984.

[7] Bajwa, M.M., and et. al., "Architectural Manifestation of the Passive Solar Cooling Strategies for the Gulf Region of the Kingdom of Saudi Arabia", Proceedings of 1987 European Conference on Architecture, Munich, F.R. Germany,,April 6-10, 1987.

[8] FANGER, P.O. Thermal Comfort (Analysis and Applications in in Environmental Engineering) McGraw Hill Book Co. 1970.

THE USE OF LINEAR FRESNEL LENSES.

B.Nábělek[+], F.Franc, M.Malý and Vl.Jirka,
Institute of Physics, Czechoslovak Acadmy of Sciences,Na Slovance 2, 180 40 Praha 8 - Libeň
Czechoslovakia.

1.ABSTRACT.

In recent years the technology of mass production of linear Fresnel lenses from glass has been successfuly solved. This lens is a very cheap and durable concentrator of direct solar radiation. From the point of view of manufacturing economy the minimum ammount of lenses produced in one batch is more than 6000 sq.m. It is very difficult to introduce also the production of tracking collectors in such size to spent all manufactured lenses.
The authors are trying to solve also this second problem, which is more serious as it seems to be at first sight, or at least to give their colleagues some informations and ideas about that what may be done with lenses which are available nearly in any ammount. From that reason several possibilities of linear Fresnel lens utilization, as are tracking collectors for photothermal and also for hybrid conversion of solar radiation are discussed. The concept of fixed concentrator and movable absorber represents a wide group of possible applications in architecture - solar roof, solar facade, or in greenhouse design.

2.LINEAR FRESNEL LENS MADE OF GLASS.

The design of linear Fresnel lens and results from techno-

[+]member ISES

logical experiments in a glass factory were described in an earlier paper [1]. Optical properties of this particular lens design and deeper analysis of the problem was published after several fully tracking concentrating collectors have been erected [2]. Properties of manufactured lenses as well as their mechanical dimensions are quarateed by checking during manufacturing process. From theoretical considerations it follows that this particular lens configuration may concentrate into its back focal plane about 75% of incident direct radiation.The quarateed ammount of radiation concentrated on absorber stripe 50 mm wide in the back focal plane of the lens is not less than 62% but sometimes it is reaching the value 68%. That is a compromise between optical quality of the lens and its price, which is kept as low as 15 US ¢ per sq.m. The mechanical dimensions and manufacturing tolerances are taken from Ref. [2].

Linear Fresnel lens made of glass: (see Fig. 1.)

lenght	$l = 2000^{+0,0}_{-8,0}$ mm
width	$w = 750^{+0,0}_{-8,0}$ mm
thickness	$t = 5,6 \pm 0,5$ mm
focal lenght	$f = 500 \pm 25$ mm
distance of lenses	370 ± 4 mm
weight	$11,5 \pm 0,5$ kg m^{-2}

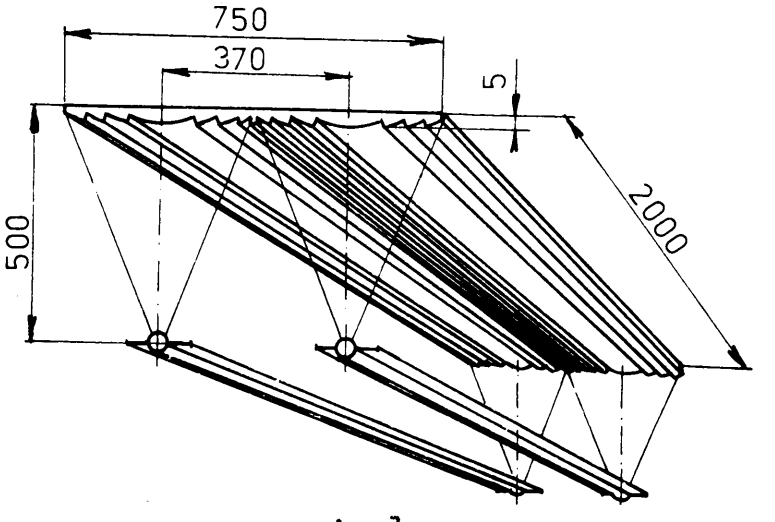

Fig.1.

3.CONCENTRATING COLLECTOR FOR PHOTOTHERMAL CONVERSION

Linear Fresnel lens with plane surface facing the Sun is manufactured in plates comprising two lenses as it is seen from Fig.1., with apertures 350 mm each. To avoid dust deposition among lens grooves and because of self-cleaning by rains this particular design of Fresnel lens was choosen. Linear Fresnel lenses are situated on a supporting structure which serves as a protective casing. Inside the enclosed space, in the back focal plane of the lens there is an aluminium absorber with selective surface encapsulated inside a glass tube from heat resistant glass. The tube is on both ends closed by caps from special rubber to protect the selective surface from dust deposition and attack of atmospheric humidity. This is also decreasing thermal losses by preventing air circulation arround absorber. The fluid duct of the absorber is plat ed by a thin wall copper tube to avoid corrosion of aluminium alloy. Greenhouse effect inside the protective casing and inside the glass tube is providing excellent insulation. By calculation and by experiment it was prooved that collector performance is nearly independent from ambient air temperature. Tracking system of the collector has two sensors - intensity sensor adjusted to level of global radiation about 600 W m^{-2} is activating directional sensor with four photodiodes coupled in a bridge. The system is in balance when the plane surface of the lens is perpendicular to incident direct radiation.Several tracking collectors of this concept have been designed and erected in Czechoslovakia.One of the first models has linear Fresnel lenses on three boxes, total area 45 m^2, and it is heating water for kitchen and for sanitary purposes. Another collector with slight modification of protective casing is heating water for a diary farm with 2500 cows.(Fig.2.). The collector design was further modified to one box 6x6 m, with useful aperture 33 m^2(Fig.3.). The latest design has protective casing 9x4 m situated on a column(Fig.4.). Both last models are prepared for long term testing in Turkmenian desert.

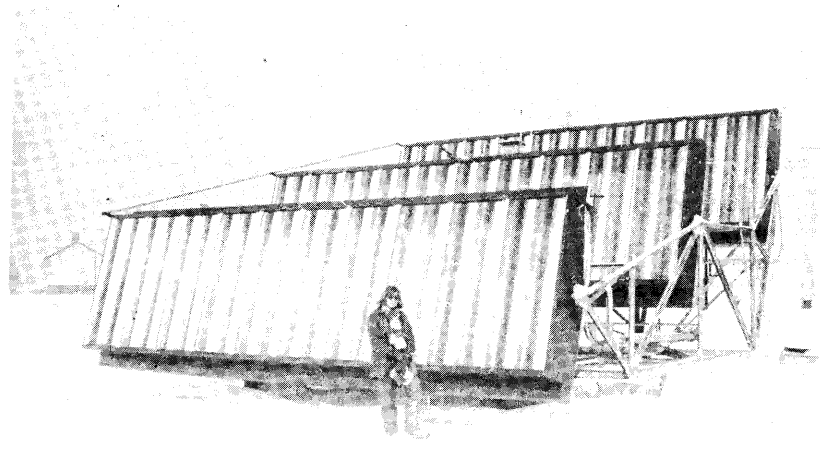

Fig.2.

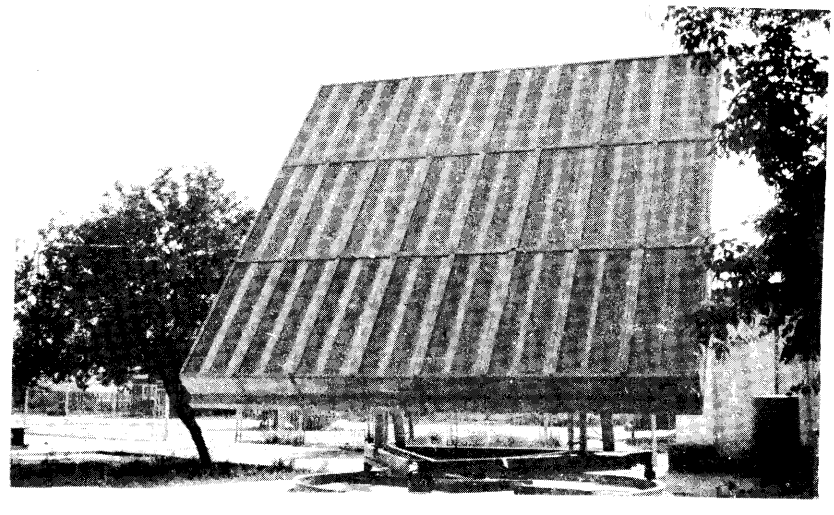

Fig.3.

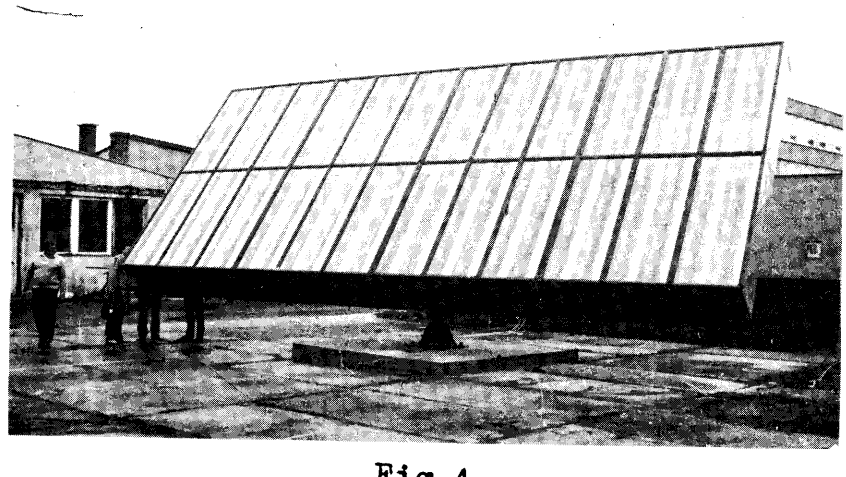

Fig.4.

During preliminary tests with black painted nonselective absorbers the collector performance was poor. It is necessary to use selective absorbers only but not necessarily inside evacuated tubes. The water contents of absorbers about 0,3 l m^{-2} is very low, so the collector response to variations in insolation is very fast, less than 2 minutes. The collector efficiency measured during several short term periods was reasonably good. Under insolation 850 W m^{-2}, ambient air temperature 15°C the collector output was 12 kW at inlet and outlet temperatures 80° and 90°C resp. More detailed description on performance testing will be published later.

4.HYBRID PHOTOVOLTAIC - PHOTOTHERMAL COLLECTOR.

Very promissing application of linear Fresnel lenses is in combined photovoltaic-photothermal collectors. The price of PV cells is still very high, while linear Fresnel lenses are very cheap.Properly designed collector mount may be driven by electric engines 12V/30W, which are used in cars for driving the wiper blades or the fan. In ordinary tracking collector part of absorber area may be covered by photovoltaic cells exposed to solar radiation from their top and cooled by heat extraction from their bottom. Part of generated electricity may recharge the car battery driving the tracking system, the rest may feed e.g. the irrigation pump. Such collector may be quite independent from external energy supply and may operate in any remote area far from electrical grid. Thermal energy generated by the collector, the temperature level will depend from collector arrangement, may be used for any other suitable utensiles available at this location. The advantage of this concept follows from practical experiment. Ordinary monocrystalic Si cells with efficiency 8% were attached to aluminium absorber working as a heat pipe. The stripe of PV cells 2,5 x 195 cm was exposed to concentrated radiation in the focal plane of linear Fresnel lens. Under insolation 900 W m^{-2} the output from this stripe of PV cells was 16 W. This value corresponds to output 330 W m^{-2} of PV cells under concentrated radiation. To get equal energy without linear Fresnel lens we must use nearly 5 m^2 of photovoltaic cells of this quality. It is easy to estimate the savings taking

into consideration prices of PV cells and linear Fresnel lens , which is about 15 US $ m^{-2}. The authors could use PV cells of low efficiency, only available at this moment and the thermal gain was not too important in this case. Using high quality PV cells will give much more better results.

5. FIXED CONCENTRATOR AND MOVABLE ABSORBER.

Linear Fresnel lens was designed for penpedicular incidence of rays on the first plane surface. Images formed by this lens under oblique incidence of rays are suffering from optical aberrations. The"disc of least confusion" is much more wide and is displaced towards the lens as seen from Fig.4. in Ref. [2], and the concentration ratio is thus reduced. The linear Fresnel lens in fixed position, properly inclined towards south, with grooves in east-west direction may be incorporated into the sloped roof of a building e.g. single family house. The space below the glazed roof is illuminated by both diffuse and direct solar radiation. Heat produced by absorbed radiation will be accumulated by the structure of the building. Insulation of the space below lenses will be better as compared with ordinary ceramic tiles roof. Situating absorbers into the line where is projected diurnal trajectory of Sun the space will be prevented from overheating by heat extraction. From Fig. 4., Ref. [2] it is seen that properly inclined lens may under oblique incidence concentrate reasonable ammount of direct radiation for certain limited period of the day. As the concentration ratio will vary it is necessary to use absorbers with width two times greater than in case of tracking collector. Such collector may operate with variable concentration for about 5 to 6 hour per day and deliver domestic hot water. Solar declination may be compensated by temporial shift of absorber in direction perpendicular to the grooves of linear Fresnel lens. For testing such system was used experimental model, seen in Fig. 5. was used. Total aperture was about 3 m^2, absorbers with selective surface were encapsulated in nonevacuated tubes. Under insolation about 900 W m^{-2} it is possible to obtain during working period 5,5 hours about 1,5 kWhm^{-2}.

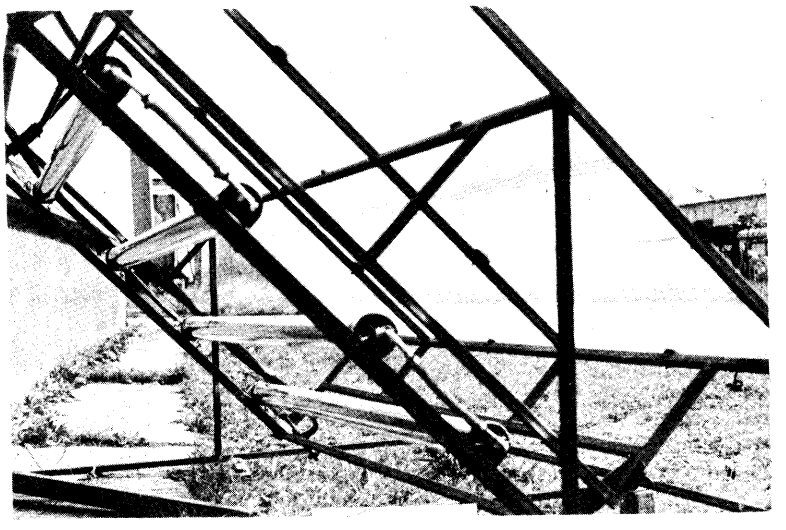

Fig. 5.

During this experiment the space below concentrators was not closed. Another posibility is to use linear Fresnel lenses as a cover of a greenhouse. Existing greenhouses were mostly designed and erected during period og cheap energy. Their longitudinal axis is in north-south direction; the ammount of reflected solar radiation from sloped roof during noon hours is greater, so the overheating during summer is slightly reduced. The heating load during early spring or at autumn is high enough. When longitudinal axis is in east-west direction more solar radiation may penetrate the greenhouse space, so the greenhouse is better heated. Linear Fresnel lens under proper inclination used as a cover of sloped greenhouse roof may help to reduce overheating by heat rejection and decrease the cooling load during summer. In the case if in early spring there is surplus energy it may be extracted during day and stored for night heating. The idea of heat extraction from a greenhouse in order to prevent the overheating is described in Ref. [3]. The main interest of the discussed concept is to decrease energy consumption. From that reason linear Fresnel lenses will be used as double glass combined with ordinary window glass and the vertical glazing will be also doubled. Another modification is the greenouse attached to the wall of existing building. To the wall of the building is added a concrete wall with serpentine from GI water tubes for washing out the accumulated heat and a brick wall for accumulation of heat. Below the ceiling may be added some

plastic absorbers working as air-to-water heat exchangers. The greenhouse arrangements isseen from Fig.6. Different modes of heat extraction may be applied. Both greenhouses are now under construction.

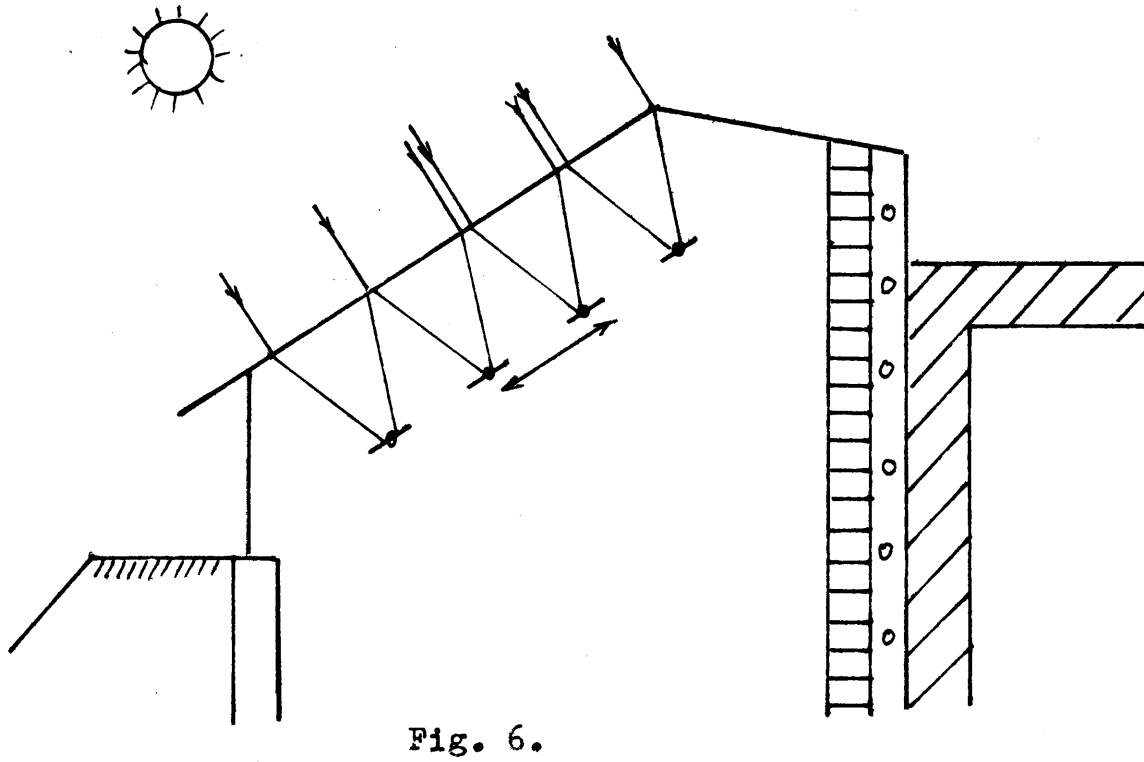

Fig. 6.

REFERENCES:

1 Jirka,Vl., et al."Linear Fresnel lens for solar technology made of glass" Proc. SPIE Vol.502,"Optical Materials Technology for Energy Efficiency and Solar Energy Conversion III (1984),Paper No.21.,pp.161 - 163

2 Franc,F., et al. "Concentrating Collector with Flat Linear Fresnel Lenses", Journ. Solar and Wind Technology,Vol. 3. (1986) No. 2.,pp. 77 - 84.

3 Al-Homoud,A.,A.,"Renewable energy research in Kuwait", Proc. Third Arab Internat. Solar Energy Conference, Paper 9 -10, 21.-24.Feb. 1988, Baghdad, Iraq.

SECTION XIII

AGRICULTURAL APPLICATIONS

PUMPED SOLAR DOMESTIC HOT WATER (SDHW) SYSTEM DESIGN GUIDELINES

K. Arshad & S. A. M. Said
King Fahd University of Petroleum & Minerals
Dhahran 31261, Saudi Arabia

Abstract:

This paper provides practical guidelines based on experience gained from the design, installation, and commissioning of a pumped SDHW system in Saudi Arabia.

The authors believe that such information is not readily available and will be useful to designers and installers of SDHW systems within the region. Since the current motivation for buying SDHW systems in Saudi Arabia is not strictly economic, it is imperative that a professional reference be available, against which the soundness of any technical decisions could be confirmed prior to their implementation. The intent is to ensure that systems designed and installed will operate reliably, therefore enhancing customer satisfaction.

1. Introduction:

At this time, several firms in Saudi Arabia are involved in the SDHW business either on a part-time basis or as a potential activity, indicating that the solar hot water industry is as yet unsettled and waiting for the market to develop. Although consumer awareness is increasing, aggressive methods are needed to improve buyer acceptance. One way would be to increase the skills of professionals in the industry to ensure that any SDHW projects implemented operate efficiently, reliably , and require minimal maintenance.

A thorough analysis to identify procedures for designing and installing pumped SDHW systems was undertaken during the execution of a 120-gallon turnkey project at a guest house at Al-Aziziah Farm, Hail. Careful attention to potential problem areas from project inception to final system-check guarantees sound installation and increases the industry's credibility in the eyes of the client. This paper should therefore prove worthwhile to SDHW system designers and contractors.

2. Outline System Design:

Flat-plate solar collectors are well suited to most domestic water needs in the range 165° F (74° C) on a summer day to 115° F (46° C) on a cold winter day. Domestic hot water design temperatures of 140° F (60° C) at the storage tank are an accepted norm in the industry. Recommended delivery temperature in distribution pipes is 135° F (57° C). Daily consumption is 15-20 gallons per person/day.

Although thermosyphon systems cost less, are simple, and have excellent thermal performance, geometric constraints and the absence of fail-safe freeze protection present an obstacle to their universal adoption. This paper therefore addresses active SDHW types because they offer considerable design flexibility.

Domestic water heating loads are estimated by

$L =$ A (Liters/Day) x 4190 (T_w-T_m) (Joules/Liter) where
$L =$ Water heating load, J/day,
$A =$ Estimated daily hot water consumption, L/Day,
$T_w =$ Hot water supply temperature at system outlet, ° C, and
$T_m =$ Cold water supply temperature at system inlet, ° C.

In the case of the 120-gallon-pumped SDHW project at Hail, the load was estimated to be
L=480 L/Day x 4190 (60° C-14° C) J/Liter=92.5 x 10^6 J/Day.
Because of extensive pipe runs, an additional 40% was added for losses and the rounded gross daily heating load was thus 130 x 10^6 Joules/Day.

Using the F-Chart method [1], 120 ft^2 (approx. 12M^2) of flat-plate collectors were needed to satisfy 75% of the yearly domestic hot water load. An approximate collection area was also calculated using the Yazaki method [2] and the procedure was found to be in close (8%) agreement with the F-Chart method. This reinforces our practical experience that up to latitudes of 30°, 1 ft^2 of single-glazed flat-plate collector will deliver 1 gallon of 140 F hot water per 8-hour sunshine day for more than 70% of the year. The typical 20 ft^2 (2M^2) flat-plate collector is therefore sufficient to satisfy the 20 Gal/Person/Day requirement within this latitude, and can be used as a rule of thumb for roughing-in and verifications.

The type of SDHW circulation system selected depends on climatic severity, water quality, costs, and component availability. The four choices are:

2.1 Closed loop systems are advantageous for year-round operation in climates having incidental subzero temperatures in winter and high ambients in summer. These systems are intended for use where water is hard or acidic and where both freeze and boil protection are desirable. Installed properly, these systems have the longest record of dependable service.

2.2 Drain back systems use water as the heat transfer fluid that is drained whenever the collector pump shuts off. Piping requires careful design in that a slope of 1/8-1/4 inch per foot is required for the water to drain back into a small reservoir or the first of two tanks. No control logic is required for freeze protection, but the inclusion of a heat exchanger reduces efficiency. Drain back systems can be used in any climate and do not require control valves or power for protection, but they may need venting and two pumps instead of one. Drain back systems require high-head/low-flow pumps.

2.3 Drain down systems, protected by valves which drain the collectors when near freezing conditions are reached in the collector loop piping (temperatures of 35° - 40° F) are gaining in popularity in the cooler parts of the U. S. Disadvantages include increased costs due to components such as solenoid valves and associated electric power draws, corrosion, and wastage of drained water.

2.4 Open loop systems can be used at locations where pH and salt content can pose no corrosion or scale deposition problems because they use line pressure potable water in the collector loop. These are the most inexpensive pumped systems but they should not be installed at locations where freezing occurs more than 20 times a year [3]. Such systems can require higher pumping power.

Most published system sizing methods seem to emphasize avoidance of occasional excess capacity rather than the more desirable goal of always providing enough hot water without dependance on purchased energy. Almost anywhere in Saudi Arabia a 120-gallon water storage tank and about 100 ft^2 of flat-plate collector are likely to deliver satisfying amounts of hot water to a family of 4 to 6 people. Installation of a 120 ft^2 collector area would improve system performance modestly on partly sunny days. Less than 100 ft^2 would reduce performance noticeably if cloudy spells lasted several days.

Water tank catalogues show that price reductions realized by use of a tank smaller than 120 gallons are not great in relation to the total system cost, and storage tanks above this size are not available at a reasonable price. Installation costs are about the same for all tank sizes. Based on this finding, client with reservations about large 120-gallon systems may consider buying the larger tank and installing fewer panels, but no fewer than four collectors, each 20 ft^2 in area. This complies with the widely accepted cost/performance storage capacity rule of thumb that suggests using 1.5 gallons of storage per square foot of collector area [4].

Based on a 120-ft^2 collector area, a 120-gallon storage tank was specified for the solar project at Hail. Although desirable from a technical standpoint, a larger capacity tank was not commercially available.

3. Storage tanks:

When selecting storage tanks with heat exchangers, due consideration should be given to tank construction. If collectors are cooled by potable water as the heat transfer fluid, a single-wall heat exchanger is satisfactory. Toxic of impotable heat transfer fluids require a double-wall heat exchanger. Double-wall heat exchangers must be vented to the atmosphere so that any leak can be detected. The effectiveness of heat transfer is reduced in double-wall heat exchangers owing to the additional wall and the space between the walls. To transfer the same amount of heat, a double-wall heat exchanger needs to be longer than a single-wall heat exchanger of the same design [5]. Mixing of construction materials in the heat exchanger may cause reduced life and efficiency through fouling or corrosion. Quality tanks will have phosphorus deoxidized copper, vitrified glass, porcelain enamel, and resin or stone lining, and may also include magnesium anodes to counter electrolytic corrosion. Purchasing tanks with these features from overseas can be a formidable task because manufacturers prefer to respond to quantity orders. For this reason, galvanized steel tanks can be used, provided it is understood by both customer and seller.that at higher water temperatures steel protects zinc and preferential corrosion of steel at any point where the zinc coating is damaged can result in accelerated pitting of steel and halving of the life of the tank when compared to use with cold water. Mild steel requires water greater than pH 8 to avoid extensive corrosion [6]. Tank insulation of at least R11 is suggested to contain standby heat losses.

4. Pumps:

Pumps in a forced-flow SDHW system should be of the integrated motor-pump type, usually in the category 1/25, 1/20, 1/12 HP and lubricated with either water or oil. Pump positioning is related to pump performance and life. Mounting the pump at the highest point in the loop increases the likelihood of air entrapment. Mounting it at the lowest point in a system can be equally detrimental due to particles, sand, and impurities impeding the impeller. Ideally, the pump should be located at least 3 feet below the water level in the tank, (but not at the lowest point in a system), where it is protected from the elements and can be serviced. Isolation valves on both sides of the pump are recommended to avoid the need to drain if the pump requires servicing. In closed loop pumped systems cast iron is a perfectly acceptable water touched pump material, but in open systems stainless steel or bronze should be specified because they will resist oxygen-induced corrosion and rust [7]. Water with specific heat 1.0 requires the least amount of flow rate. Design pumping rates are typically 0.02 - 0.04/GPM/ft^2, based on 60-100 Btu/ft^2 heat gain per ft^2 of collector area and water at 8.3 lb/gal. Water/glycol solutions have a specific heat of about 0.8 and require a flow rate about 1

1/2 times that of water. In well-designed residential systems, no more than 1 to 1.5% of the Btus captured by the solar energy system should be consumed by the pump. While estimating pumping requirements, heat transfer fluids present special considerations: fluids having lower viscosities and higher densities generally improve pump performance [7].

The correct collector fluid rate is not always the maximum flow possible because a practical engineer must balance the cost of a larger pump and the corresponding additional pumping power against the value of increased thermal performance. If electrical power is projected to become much more costly over the life of the system, a lower flow rate than that usually specified may be desirable.

When confronted with high-heat situations, the design engineer can consider the often overlooked energy-efficient alternative of staging two or more small circulators in series. The result is twice the pressure and a more efficient pumping system [7]. In general, however, lower electric power costs favor larger pumps [8]. Alternatively, the engineer may consider increased pipe diameters which is a costly but nevertheless possible solution, should suitable GPM vs higher-head pumps not be available. Such a solution was adopted by this team on the Aziziah farm project.

5. Controllers:

The most commonly used controllers available are the standard differential types that are analog-based. These comprise sensors, a comparison circuitry, and a relay switch that turns the pump on and off. The sensors used most often are thermistors (electrical resistors that change resistance according to their temperature). The 10K-ohm thermistor, i.e., at 77° F its resistance is about 10,000 ohms, and the 3K-ohm resistor are widely used. The flow of current through these devices increases as the temperature rises. Each thermistor is connected by a pair of wires to the comparison circuitry housed in the control box. Comparison circuitry in the controller box sends a continuous low-voltage electrical signal through the collector and storage sensors. The thermistor allows varying amounts of current through, depending on the temperature and both currents are constantly compared. As the collector sensor heats up, the increase in current is compared with the current from the storage tank sensor. When the difference reaches a certain equilibrium point, say equivalent to 20° F, the controller closes the relay switch thereby sending 110V/220V power to the pump. Most controllers will shut off the pump if the collector cools down or the storage heats up, or if both occur, so as to reduce the difference between the two sensor currents. Typically, this occurs at current differences representing 3° F to 5° F differential. Controllers usually have turn-off ΔT 5° to 15° F less than turn-on ΔT to prevent rapid on-off cycling [9].

Incorrect installation, not faults in controllers, are the cause of most system malfunctions. Therefore, controllers must be understood to allow proper operation. System performance is highly sensitive to proper control setting.

6. Piping Insulation

Piping in a SDHW system should be insulated with sponge rubber, phenolic foam, of fiberglass insulation. As a general rule, the thickness of the insulation wall should be approximately the diameter of the pipe being protected, i.e., 1/2" pipe should have 1/2" of insulation all round so that the total diameter of the pipe and insulation would be 1 1/2". All external insulation should be weatherproof, sealed, and UV-protected. Excessive pipe runs or inadequate piping insulation can cause excessive heat losses and control problems. Sealing is critical on outside loop piping where temperature differentials are considerable. A minimum of R-4 insulation is recommended on all solar loop piping. Ideally, one-inch thick urethane rubber, or fiberglass would conform to this requirement but unfortunately this thickness is not readily available in local markets.

7. Working Fluids:

Ethylene glycol and propylene glycol have special significance because they provide protection against boiling, freezing, and corrosion. Pressurization of the collector loop raises the boiling point of inhibited ethylene glycol solution approximately 2.5° F (1.4° C) for each 1 psi (6.9 KPa) increase in pressure above atmospheric [10]. Therefore, collector loop operating pressures between 20-25 psi are recommended for SDHW applications in regions of intense solar radiation and when stagnation conditions are anticipated. A 50:50 by volume ethylene glycol/water solution will provide boil protection up to 230° F (110° C) without loop pressurization and freeze protection up to -35° F (-37° C). Ethylene glycol provides good heat transfer characteristics but it has moderate toxicity and should be used with double-wall heat exchangers. Alternatively, propylene glycol is low in acute oxal toxicity and is preferred in applications where there is risk of accidental injection. A 50:50 by volume propylene glycol/water solution will provide slightly less protection than ethylene glycol. Unfortunately, there are indications that propylene glycol is the less stable of the two and that there can be degradation of both to form organic acids when used in solar systems, and it is unclear why particular systems turn acidic. Periods of stagnation seem to cause rapid deterioration in pH. For this reason, controllers with an upper temperature limit should not be used with glycol systems, so that stagnation can be prevented. While an operating pH between 7.5 and 9, but not exceeding 12, is desirable, whenever a solution pH drops below 6.5 it should be changed. Similarly, reserve, alkalinity (RA) of about 40 should be sought and a change in fluid recommended if RA drops below 20 [10]. The preferred glycol is the inhibited industrial type. Water used for preparing glycol solutions should have low levels of chloride (less than 50 ppm), sulfate, and hard water ions (Ca^{++} and Mg^{++}). Concentrations above these maximums may cause corrosion and deplete inhibitors [11]. Use of dissimilar metals in a collector loop is not recommended.

8. Freeze Protection:

The first and foremost consideration in freeze protection is the fact that under most conditions the solar absorber plate will be 10° to 12° F cooler than the ambient air when the night sky is clear and there is little wind. Under dry, clear and still night conditions, absorber plate temperatures can be 15° F cooler than the surrounding air [12]. Therefore, while designing for freeze insurance, it is advisable to base protection on the lowest recorded ambient temperature and a margin of at least 5° F [11].

9. Collector Outgassing and Condensation:

Excess heat in stagnating collectors can be expected to cause outgassing in deposits on the underside of the glazing. A means of disposing of excess heat is therefore necessary to avoid material deterioration and collector fluid boil-out. Glazing can be cleaned by very hot water and detergent or with organic solutions such as toluene or xylene. Condensation forms in almost all cases. Condensation is not necessarily a problem unless it builds up in the collector. Performance is only slightly and temporarily affected.

10. Conclusion:

While a body of knowledge exists for effective implementation of pumped SDHW systems, the complexity of using solar energy is grossly underestimated. Failures can be averted by practicing basic rules coherently to achieve trouble-free service.

Based on actual experience derived from the turnkey SDHW project at Aziziah farm, Hail, the information documented in this paper should be useful to other professionals in the field.

ACKNOWLEDGEMENT

This paper is based on an externally funded project no. 22030, financed by His Royal Highness Prince Mugrin Bin Abdul Aziz Bin Saud. The authors are grateful to His Royal Highness and the KFUPM/Research Institute for the support provided towards the completion of this project.

References:

1. Beckman, Klien and Duffie, "Solar Heating Design by the F-chart Method". John Wiley & Sons Inc. New York, USA, 1977.

2. "Blue Panel Solar Hot Water Supply Systems", Yazaki Corporation Publication, Tokyo, Japan, 1980.

3. Schiller, Steven R. "Freeze Protection", Solar Age, pp. 27. August 1981.

4. Lunde, J. Peter, "Choosing the Best Storage Size", Practical Engineering, pp. 49, Solar Age, August, 1981.

5. Brown, Todd H., "Heat Exchangers Can Make or Break Solar Energy Systems", Materials, pp. 20, Solar Age, August, 1981.

6. Avery, John G. and Krall, John J., "Sustain Solar System's Efficiency by Protecting Against Corrosion", pp. 24, Solar Engineering and Contracting, April 1982.

7. Cook, Jerry, "How to Specify Pumps for Solar Systems", pp. 26-28, Grundfos Pumps Corporation Publication, USA.

8. Lunde, Peter J., "Collector Flowrate", Practical Engineering, pp. 77-78, Solar Age, June 1982.

9. Sands, Jon, "Smart Controllers with Microchip Muscle", pp. 59, Solar Age, July 1983.

10. Beyon, Eric, "Ethylene Glycol Heat Transfer Fluids: Some Tips for Trouble-free Service", pp. 56-57, Solar Engineering, Oct. 1981.

11. Born, David, "Stopping Solar Freeze Ups", pp. 31, Solar Age, June 1986.

12. Cromer, Charles J., "The Inlets and Outlets of Sensor Placement", pp. 10, Solar Engineering and Contracting, March/April 1985.

TRANSIENT THERMAL BEHAVIOUR OF SOLAR PONDS WITH A CONSTANT ENERGY EXTRACTION RATE

S.M.Abughres , M.E.Mashena , K.R.Agha
Center for Solar Energy Studies
P.O.Box 12932 , Tripoli - Libya

ABSTRACT

In many thermal processes applications, the heat have to be supplied at a constant rate with a specified temperature range. Many of these applications require moderate temperature below 100°C, a situation for which a solar pond can be adequately utilized to furnish the thermal energy demand. This work presents a study to predict the thermal performance of a pond for the supply of such an energy grade and to suggest a general procedure of determining the optimum values of the parameters effecting the performance of the pond.

The results show that the depth of the storage zone has a pronounced effect on the annual variation of storage zone temperature. An increase in the depth results in a reduction of storage zone temperature. Also the effects of using different bottom reflectivities on the thermal performance of the solar pond is presented, yielding an optimum value of reflectivity about " 0.5 ".

1.- INTRODUCTION

A solar pond is a shallow body of water about three meters deep containing dissolved salts to generate a stable density gradient " fresh water on top and denser salt water at the bottom ". The configuration of the three zone salt gradient solar pond collector system analysed in the present paper is schematically illustrated in figure(1).

The evaluation of the system thermal performance have to consider the pond as both: a solar collctor and thermal storage sub-systems. The thermal behaviour of the system depends on many parameters, including solar radiation input, other climatic factors, surrounding earth properties, salt

properties, rate of heat removal and pond geometry. The influence of some of these factors on pond storage zone and vertical profile temperatures have been rarely studied [1,2]. The analytical approach that have been commonoly followed has of necessity been simplified in order to obtain an exact solution of a rather complicated physical problem.

In pursuit of a more representative model relating the various parameters that affect the thermal behaviour of a solar pond, many research workers have decided to break away from the analytical approach and to seek a numerical formulation of the problem which avoids most of the simplifying assumptions and where boundary conditions could be more accurately incorporated. This was first recognised by Tybout[3] who described a numerical approach as an alternative to that originlly initiated by Weinberger [1] in order to incorporate the periodic observations without explicitly describing them as functions of time. The variables in time and depth of the pond were treated as discrete parameters in this approach. More recently, Hull[4] has followed the same approach and used Tybout's computer model to investigate the assumptions employed in an earlier analytical model proposed by Rabl and Nielsen [2]. In conclusion he found that for long term purposes, the thermal behaviour of a solar pond could be adequately modeled using these assumptions.

only a limited amount of the mathematical models cited so far takes a full account of the boundary conditions practically known to influence the performance of a solar pond. This paper presents a study on the transient thermal characteristics of a solar pond subjected to the necessary boundary conditions. The pond is assumed to be sufficiently large so that side - wall effects could be ignored. The effects of other factors including that of the bottom reflectivity are otherwise incorporated in the analysis.

2.- SIMULATION MODEL DEVELOPMENT

The system envisaged for the analysis is shown in Fig.(1) with the solar pond consisting of three zones. The upper convective zone (UCZ) of thickness L_{uz} has a low and uniform salt content. Beneath the UCZ is the non-convecting zone (NCZ) of thickness L_{nz} which has a salt content increasung with depth and therefor is a zone of variable properties. The bottom layer underneath the NCZ is the lower convective zone (LCZ), also called the storage zone, which has thickness L_{sz} and uniform high concentration salt content.

The approach used in this simulation is an explicit formulation in which the temperature of node i at time $\tau+1$ is written in terms of the temperatures of the node i and of the two adjacent nodes at time τ as follows :

$$T_i^{\tau+1} = \left[\frac{T_{i-1}^{\tau}}{\frac{\Delta X_{i-1}}{2K_{i-1}} + \frac{\Delta X_i}{2K_i}} + \frac{T_{i+1}^{\tau}}{\frac{\Delta X_{i+1}}{2K_{i+1}} + \frac{\Delta X_i}{2K_i}} \right] \cdot R_i +$$

$$\left[1 - \left(\frac{1}{\frac{\Delta X_{i-1}}{2K_{i-1}} + \frac{\Delta X_i}{2K_i}} + \frac{1}{\frac{\Delta X_{i+1}}{2K_{i+1}} + \frac{\Delta X_i}{2K_i}} \right) \cdot R_i \right] T_i^{\tau} + \frac{G(X)}{X} \cdot \frac{\Delta \tau}{\rho_{w,i} C_{w,i}}$$

Where; $$R_i = \frac{\Delta \tau}{\Delta X_i \rho_{w,i} C_{w,i}}$$

In this model the solar pond is divided into n elements as shown in figure (2). The UCZ is considered as one homogeneous element, and so is the LCZ. The NCZ is divided into (N-2) elements. Also the ground underneath the pond is divided into M elements. By knowing the initial temperature of each node and repeatedly using the above equation, the final temperature of all divisions at the end of each time increment can be obtained node by node: also the temperature of the whole pond can be determined step by step.

3.- ABSORPTION OF SOLAR RADIATION

Evaluation of the radiation term G(X) is extremely important since this is the driving force for warming the pond. Incoming radiation of a given wavelength, λ , is attenuated as it passes through the water column by the effects of absorption and scattering. Detailed formulations for the energy flux based on radiative transfer theory have been dealt with in details in references [5,6], and the solar radiation attenuation model to be used in this paper is ;

For the direct radiation component :

$$G_D(X) = A. \exp\left(\sum_{i=1}^{5} a_i . (X')^i\right)$$

Where; $X' = X. \text{Sec } r$ & $\text{Sin } i = \text{Sin } r$

For the diffuse radiation component ;

$$G_d(X) = B. \exp\left(\sum_{i=1}^{5} b_i . (X)^i\right)$$

and the total is given by :

$$G(X) = I_D . G_D(X) + I_d G_d(X)$$

$$= I_{total} \left[\frac{I_D}{I_{total}} . G_D(X) + \frac{I_d}{I_{total}} . G_d(X) \right]$$

4.- RESULTS AND DISCUSSIONS

The current section presents the simulation results regarding the effects of different parameters on the thermal behaviour of solar ponds under transient conditions. These results are reckoned to provide a valuable information about the degree of importance of each parameter by which the designer of such systems can suggest the proper construction based on optimum configuration for the maximum utlization of available solar energy.

The following results were all simulated for a pond of an in-finite surface area, with a start-up time at January the first, a UCZ thickness of 0.20 meter, and a brine of Sodium Chloride (NaCl). Inside the LCZ the brine concentration, and therefore, the thermal and diffusional properties, were assumed uniform. In the NCZ, the concentration was taken to change linearly with depth from zero concentration at the UCZ boundary to 25% concentration at the LCZ boundary. The mean temperature of the UCZ was calculated according to the surface boundary conditions taking into account the radiation, convection and evaporation heat losses [8]. The bottom of the pond was taken to be lined with a clay of variable depth, up to which the heat flow is only equal to 5% of that lost from the storage zone to the ground beneath. The initial temperature of the ground beneath the pond was determined by means of the formulations proposed by Moustafa, et al [7].

Based upon the above stated assumptions the LCZ temperature was predicted on the basis of prior knowledge of the geoclimatic parameters such as the solar insolation, ambient temperature, relative humidity, and wind velocity for a proposed location at Tripoli (Lat. 32.68 °N), Libya. A summary of the simulated results is shown in table (1).

Table (1). The influence of various parameters on the transient performance of the solar pond, for a pond with 1.0 m NCZ, 1.0 m LCZ, RB= 0.5 and no heat removal, unless stated otherwise.

No.	Alteration to the parameter	LCZ TEMPERATURE , °C			
		Maximum	Minimum	Mean	fluctuation
1	No alteration	105.138	64.21	84.674	40.928
2	RB = 0.0	102.538	61.61	82.074	40.928
3	RB = 1.0	103.138	62.21	82.674	40.928
4	2.0 m NCZ	106.256	77.558	91.907	28.698
5	2.0 m LCZ	99.445	69.903	84.674	29.542
6	Q = 20 W/m²	96.251	55.323	75.787	40.928
7	Q = 40 W/m²	87.364	46.436	66.900	40.928

4.1- Effect of the Bottom Reflectivity, (RB)

The predicted results of the storage zone temperature for different bottom reflectivities show that, the latter affects only the annual average LCZ temperature. Figure (3) shows a prediction of a two year LCZ temperature for a solar pond with three different bottom surface reflectivities, a 1.0 meter NCZ, 1.0 meter LCZ thicknesses, and without heat removal. Additional results to investigate and optimize the effect of bottom surface reflectivity are given in figure (4): these results show that the optimum bottom reflectivity for the maximum attainable annual average storage zone temperature is about 0.5. This is attributed to the drop in the bottom losses which seem to be more than offset the increase in the amount of reflected energy outside the pond as the bottom reflectivity increases to 0.5. For a bottom reflectivity higher than 0.5 the reflection losses seem to be more than the gain from the reduced ground losses, which resulted in a lower storage zone temperature.

4.2- Effect of the Thickness of the Non-Convective Zone (NCZ).

At a fixed thickness of the UCZ, there is an optimum thickness of the NCZ which yields the maximum annual average storage temperature for every amount of heat extraction rate, as shown in fig.(5). The thickness of the NCZ affects both: the inward transmission of solar insolation as well as the outward transmission of heat flow. Decreasing the thickness improves both of these transmissions, until an optimum is reached at which the difference between these two transmissions is maximum giving the highest storage temperature.

The effect of the NCZ thickness on the solar pond performance is also manifested in fig.(6), which displays the decrease in the fluctuation of the storage zone temperature with an increase in the thickness of the NCZ. An analysis of a two year cycle without heat extraction shows that the fluctuation decreases from 40.9 °C to 28.7 °C as the thickness of the NCZ is increased from 1.0 m to 2.0 m. On the other hand, the corresponding average temperature of the storage rises from 84.7 °C to 91.9 °C.

4.3- Effect of the Thickness of the Lower Convective Zone (LCZ)

Again, an analysis of a two year cycle was performed to investigate the effect of the thickness of the LCZ, as shown in fig.(7). Increasing the thickness of this layer appears to reduce the fluctuation of its temperature, which is attributed to the increased heat storage capacity. However, such an increase does not seem to affect the annual average value of the storage temperature.

In contrast to the thickness of the NCZ, which governs both the incoming solar insolation and the outward heat loss, and thereby affects the annual average storage temperature, the thickness of the LCZ has no effect as long as the thermal insulations on the two sides of the zone remain the same.

4.4- Effect of Heat Extraction Rate, (Q)

The load pattern has a strong influence on the temperature profile of the pond, and a pond should be designed such that not only the maximum possible amount of heat is extracted but also the load-temperature requirements are satisfied. In the present work the pond is assumed to be operated under conditions of constant rate of heat extraction. The results presented in the sub-sections(4.1-4.3) show that the annual average LCZ temperature depends on the thickness of the NCZ (for a fixed UCZ thickness), and on the rate of heat extraction, Q. The relationship between Q, the NCZ thickness and the annual average LCZ temperature is displayed in fig.(5) , which shows the effect of NCZ thickness on the average temperature with Q as a parameter. From this figure it is clear that heat can be extracted from the pond at higher rates but the grade of extracted heat would be lower. The figure also shows that, for every value of Q there exists an optimum thickness for the NCZ which yields the highest performance of the pond.

The effect of the heat extraction start-up timing on the performance of the pond is shown in figure (8), which shows a comparison between a pond with the start heat removal at 61 day and another at 121 day, for a pond with 1.0 m NCZ, 1.0 m LCZ, RB = 0.5 and 40.0 W/m^2 heat extraction rate. It is seen that a delayed extraction start-up, does not in the long run have much effect on the pond performance. However, it is a known fact that the best performance is obtained when the heat extraction pattern coincides with the solar insolation. Unfortunately this is not always the case, and a poor pond performance can be expected when the contrary occurs.

5- CONCLUSIONS

A transient analysis of the performance of solar ponds under varying conditions has been carried out by using a finite difference formulation. The simulation results incicate that painting the bottom surface black is not the best solution. An optimum value of 0.5 for the bottom surface reflectivity was obtained according to the maximum attainable annual average storage zone temperature.

Also, the results show that the thickness of the non-convective layer has a prononouced effect on the overall pond performance. Based on the computer simulation, it is seen that augmentation of this layer increases the pond operating temperature for the same rate of heat extraction. However, there is an optimum thickness of this layer for every value of the rate of heat exctraction.

6- NOTATION

A, a_{i} , i = 1 , 5	constants.
B, b_{i} , i = 1 , 5	constants.
C	specific heat, J/Kg-°C.
G(X)	net radiation at depth X, W/m².
I	solar rdiation incident on the water surface.
i	angle of incidence.
K	thermal conductivity, W/m²-°C.
r	angle of refraction.
T	temperature, °C.
X	depth measured from the surface, m.
ΔX	thickness of each division, m.
ρ	density, Kg/m³.
τ	time, Sec.
$\Delta\tau$	time increment, Sec.

Subscripts

g	ground.
w	water.
D	direct radiation component.
d	diffuse radiation component.
total	total radiation.

7- ACKNOLEDGEMENT

The work is part of a project funded by the Center for Solar Energy Studies under contract number SEC/TC/SP/RPP/1986. The authors are grateful to the Center for the provision of the computer facilities and the permission to publish the results.

8- REFERENCES

[1]-H.Weinberger," The Physics of the solar pond "Solar Energy 8,45-56 (1964).
[2]-A.Rabl and C.E.Nielsen," Solar ponds for space heating " Solar Energy 17,1-12(1975).
[3]-R. Tybout, " A recursive alternative to Weinberger's model of the solar pond " Solar Energy 11,109-111 (1966)
[4]-J.R.Hull,"Computer simulation of solar pond thermal behaviour" Solar Energy 27,393-401 (1981).
[5]-Y.A.Cengel and M.N.Ozisick," Solar radiation absorption in solar ponds" Solar Energy 33,281-291 (1984).
[6]-S.M.Abughres, M.E.Mashena and K.R.Agha," A comparison between solar radiation attenuation models for solar ponds" Proc. of the 4th International Conference on Solar Energy and Heat Pumps, Istanbul, Turkey (April- 1988).
[7]-S.Moustafa, et al," Arid soil temperature model " Solar Energy 27,83-88 (1981).
[8]-V.M. Kishore and V.Joshi,"A practical collector efficiency equation for non-convecting solar ponds" Solar Energy 33. 391-395 (1984).

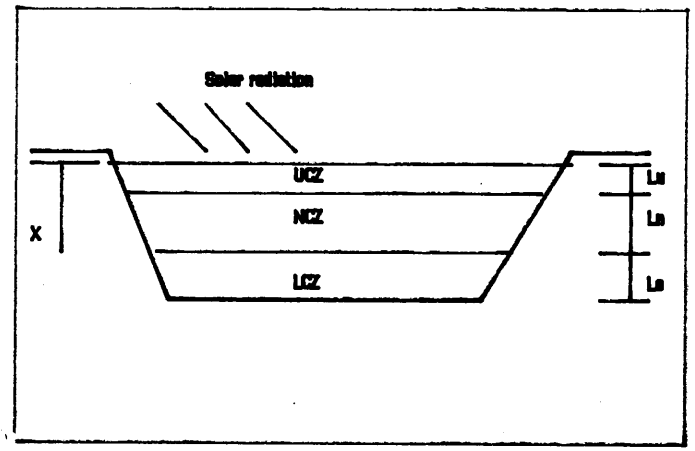

Fig.(1) Schematic representation of a solar pond.

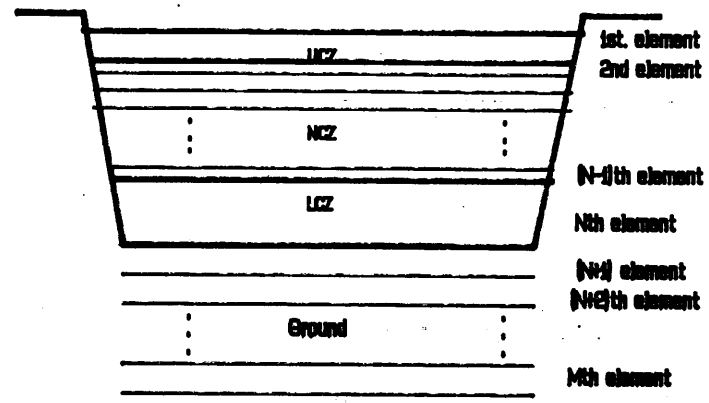

Fig.(2) Descretization elements.

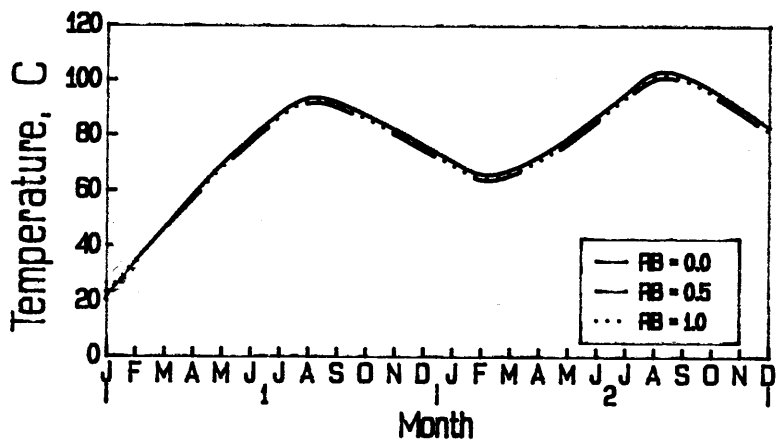

Fig.(3) Effect of bottom reflectivity on the storage zone temperature variations for the reference solar pond.

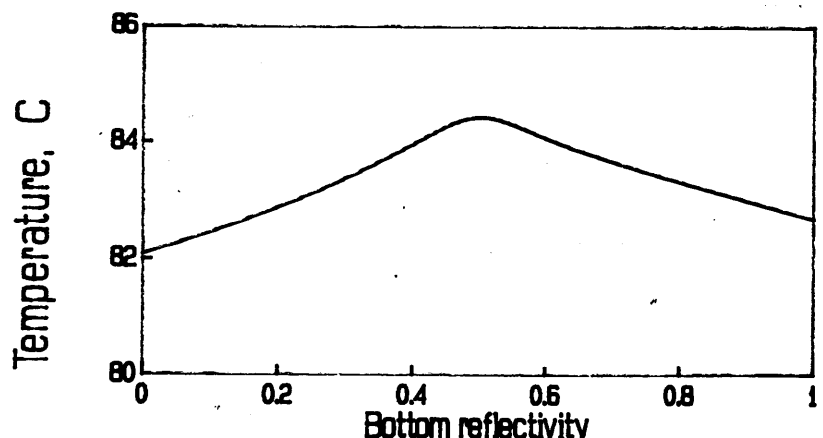

Fig.(4) Effect of bottom reflectivity on the annual average storage zone temperature for the reference pond

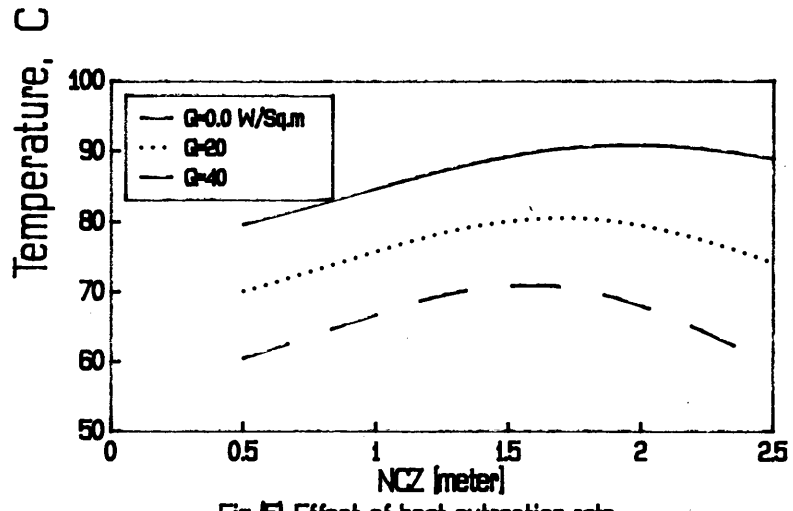

Fig.[5] Effect of heat extraction rate, and the thickness of the NCZ on annual average temperature of LCZ for RB=0.5

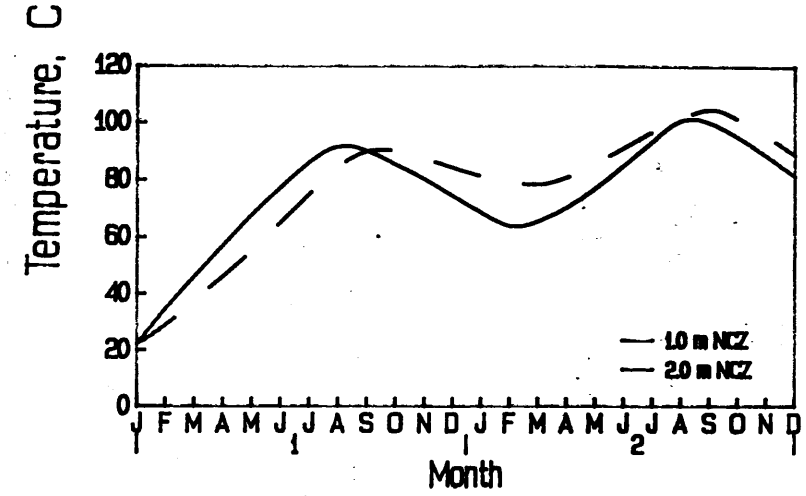

Fig.[6] Effect of the thickness of the NCZ on the performance of the reference pond, without heat removal.

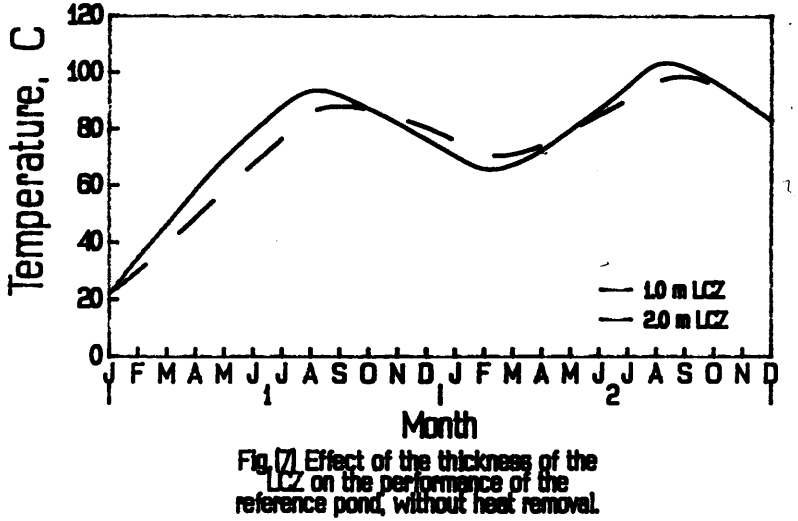

Fig.[7] Effect of the thickness of the LCZ on the performance of the reference pond, without heat removal.

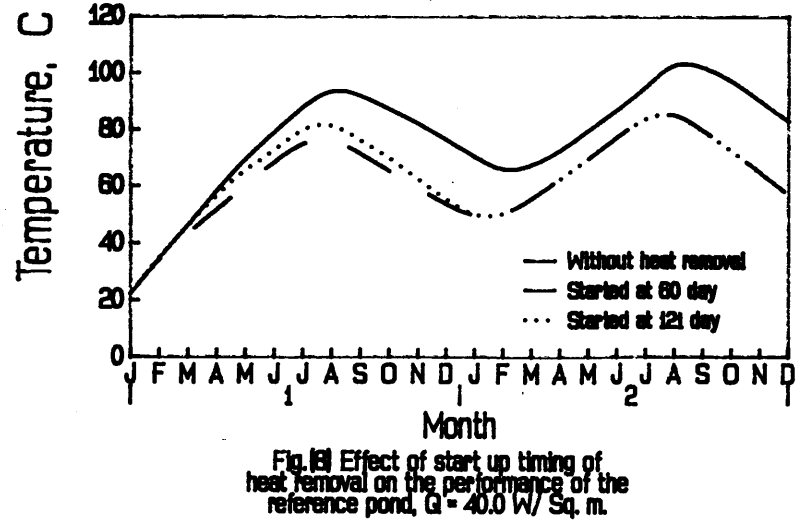

Fig.[8] Effect of start up timing of heat removal on the performance of the reference pond, Q = 40.0 W/ Sq. m.

UTILIZATION OF SOLAR POND FOR A GREEN HOUSE IN JAMAHIRIYA

S.M. Abughres*, M.M. Sassi**, Sami Musa**

* Solar Energy Research Centre, Tripoli,GSPLAJ

** Arraya El-Khadra University, Mech.& Indl.Eng. Research Centre, Tripoli, GSPLAJ.

ABSTRACT

In view of the escalating world energy demand and the depleting sources of the presently available conventional energy, a search for other alternatives becomes a necessity. An attractive alternative is the direct solar energy that can be harnessed through many techniques of which the solar ponds have recently become widely accepted. These have the advantages that they can be used for both collection and storage at a reasonably lower cost than can be attained with other systems. However, their utilization is limited for low temperature applications and where they can be used as a preheating source in conjunction with either high temperature solar energy collectors or conventional fuel augmentation systems.

A low temperature application where solar ponds could be effectively utilized is in the field of green-houses space heating. In Libya, the energy demand for the space heating green houses amounts up to about 100,000 barrels of oil equivalent per annum. Undoubtedly, such a consumption warrants investigating the feasibility of replacing conventional fuel by solar energy utilizing solar ponds.

The current work presents an analytical study simulating the performance of a non-convective solar ponds. Based on the conservation laws of mass, momentum and energy, the thermal behaviour of the pond was formulated and the resulting equations were solved numerically on the computer. Results of the calculations were then employed to establish a relationship between the system performance and the amount of solar radiation available. This provided the basis for the design of a solar pond to supply a given green house with the space heating energy requirements.

Solar Heating Green House:

Green houses are widely used now-a-days to provide controlled environments for growing plants with high productivity. Large areas of land exceeding 100 hectares [1] are being employed in Jamahiriya by the Secretariat of Agriculture for controlled environment plantation in Green-houses. In the winter these green-houses are heated using fossil fuel (oil), where as in the summer the diurnal solar radiation is sufficient to keep the environment at the required temperature. The annual consumption of energy per hectare costs about 5000 Libyan Dinars. At the local prices of diesel (0.05 L.D/Litre), this is equivalent to an annual consumption of about 600 barrels of oil per hectare. It is worthwhile, therefore, to consider the replacement of oil by solar energy employing salt gradient solar ponds, as shown in Figure (1).

The study is intended to be carried out on an existing green house at the experimental farm of the Agricultural Research Centre in Tajura-Tripoli (L = 32.863). The green-house is 58 m long, 8 m wide, 2.5 m high with the roof consisting of two parts made of 6 mm thick glass plastes inclined in the east-west direction at an angle of 30^{o} to the horizontal plane.

Heating Load of the Green-House

The calculation of green-house heating loads are carried out according to the simplified procedure of ASHARE [2].

For design purpose, (t_i) the inside temperature of the green house is assumed to be $25^{o}C$ and (t_o) outside temperature had been taken $12^{o}C$ at January month.

Green-house heating load (Q_t) = Conduction-convection heating loss (Q_c) + infiltration loss (Q_i).

Where:

$Q_c = U.A\ (t_i - t_a)$

U = Overall heat transfer coefficient = 6.8×10^{-3} Kw/m^2 ^{o}C

A = Exposed surface area = 884.48 m^2

$Q_c = 6.8 \times 10^{-3} \times 884.48\ (25-12) = 78.2$ Kw.

$Q_i = 0.5\ Vg.\ N\ (t_i - t_o)$

Vg = greenhouse internal volume = 1695.92 m^3

N = Number of air change per hour = 0.75 - 1.5

$Q_i = 0.5 \times 1695.92 \times 1.5\ (25-12) \times 10^{-3} = 16.3$ Kw.

$Q_t = 78.2 + 16.5 = 94.7$ Kw.

Pond Geometry and Construction:

The solar pond is essentially a shallow water container with an artificially established density gradient, with a sufficiently large vertical gradient of salt concentration established inside the pond, so that near the bottom the water is denser than at the top, the convective motion can be suppres sed. In addition, the water in the pond is practically opaque to the far infrared radiation, heat losses from the water inside the pond occure mainly by conduction through a poorly conductive medium. The upper layers acts, therefore, as an insulating layer trapping the heat reaching the bottom which gives rise to high temperature at the bottom.

The geometry of the pond can take many shapes, the most common one is the square excavation pond in which the soil is excavated into the required shape with the banks sloped and lined with a thick layer of reinforced nylon or black polythelene Figure (1).

There are several ways of extracting heat from the bottom layer of the pond, one of them is by use of an external transfer medium such as water cycling inside a heat exchanger.

Performance of the Pond:

i) Absorption of solar radiation:

The solar radiation incident on a horizontal surface can normally be taken from metrological observation which may be expressed as a function of time and local latitude. Part of the radiation reaching the surface of the pond is reflected and the remainder penetrates through the layer of the pond Figure (3).

The solar radiation reaching depth (Z) of the pond can be calculated from the equation:[3]

$$H_{(Z)} = E\, H_s \cdot \theta_z$$

Where (E) is the fraction of solar radiation penetrating surface of the pond which is:

$$E = 2n \cos i \cos r \frac{1}{(\cos r + n \cos i)^2} + \frac{1}{(\cos i + n \cos r)^2}$$

(H_s) is the solar radiation incidence on a horizontal surface which can normally taken from meterological data.

(θ_z) is the transmission coefficient of the total radiation reaching depth (Z) which is approximately given by:

$$Q_Z = \sum_{n=1}^{4} \eta_n \, e^{-\mu n . Z}$$

The coefficients η, μ for different wave lengths are given in Ref. [3].

The solar radiation reaching depth 1, 2, 3 mt. in ($Kw.hr/m^2$ day) for the year round in Tripoli (L = 32.683) are tabulated in Table (1) and are presented graphically in Figure (4).

ii) Temperature Development in the Pond:

The relationship governing the temperature distribution in the pond is obtained employing the energy conservation law for an elementary volume of fluid in the pond depth (δ Z) and a surface area (A_p).

Introducing the assumption that the pond is sufficiently large so the thermal energy flow can be treated in one dimension, which means that the edge losses are negligible, and the thermal properties of the fluid change only along the depth dimension, with this assumption the following relationship can be arrived at:

$$T = \bar{T}a + \frac{EH_s}{K} \sum_{n=1}^{4} \frac{\eta_n}{\mu_n} (1 - e^{-\mu n L_i}) - \frac{Q_T \cdot L_i}{A_p \cdot K} \quad \ldots\ldots(1)$$

Analysing equation (1) using the following values:

$T_a = 12 + 273 = 285\ ^oK$
$EH_s = 4.7\ Kw.hr/m^2.day$ Ref. (2)
$K = 0.0006\ Kw/m\ ^oK$

The average temperature at the lower region of the pond (T) is calculated for different values of insulating layer thickness (L_i) and three pond surface areas. The results are shown in Table (2) and plotted in Figure (5).

The results of Figure (5) show that the average temperature for each area of pond increases with the thickness of the insulating layer up to a certain point and then starts to decline, then the area below the line which connecting these points are considered unstable region.

If we consider that the maximum average temperature inside the pond (T) (50°C) is suitable for our project to give 25°C inside the greenhouse, therefore, from Figure (5) to get T = 50°C. area of pond can be taken 1200 m^2 and accordingly insulating length layer equal 0.7 m.

Economical Feasibility Study:

The economical analysis is carried out according to the method proposed in Ref. [4].

Figure (6) shows the results of this analysis with the assumed parameters r (annual interest rate), m (yearly expenses)

i (equipment inflation rate) and e (energy inflation rate).

From the graph it can be seen that the pay-back period (n) for the pond is about 13 years when the energy displaced is gas oil and 3 years when the energy displaced is the electricity.

These results in view of the experience cited in literature suggest that the salt gradient solar pond are economically feasible.

Conclusions:

From the discussion related to the design of a salt gradient solar pond, the following general conclusions can be drawn:

1. A cheap source of salt or brine should be available locally to provide the considerable inventary of salt needed to start the pond.

2. A cheap source of water must be available to make up for evaporation losses.

3. The collection efficiency of a solar pond is of the order of 20% or less dependent upon water clarity (from the experimental results). This may represent a constraint in some site where space is restricted.

Also, based on the discussion of the results, the following two main conclusions may be noted:

1. The surface area of the pond and the thickness of the insulating layer are very important design variables, whereas the former determines the amount of the energy collected, the latter determine the stability condition.

2. Salt gradient solar pond could be a cheap source of energy for the heating of greenhouse.

References:

1. Mousa, Sami,"Utilization of Solar Pond for a Greenhouse in Libya", M.Sc., Thesis, Al-Fateh University, Faculty of Engineering, Tripoli, (1985).

2. Handbook of Applications ASHREA, New York (1982).

3. Rabl, A. and Nielsen, C.E.,"Solar Pond for Space Heating", Solar Energy 17, pp 1-12 (1975).

4. Böer, K.W. "Payback of Solar Systems", Sharing the Sun, Volume 9, pp. 1-17 (1976).

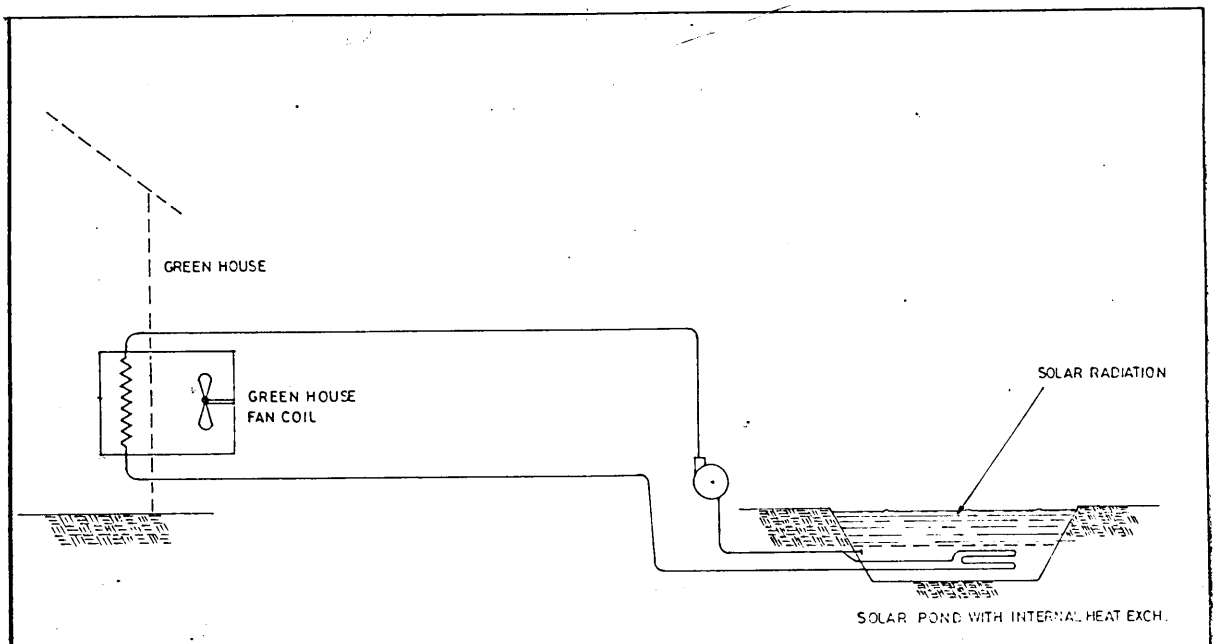

Fig 1 Schematic Diagram of Solar Pond-Greenhouse Heating System

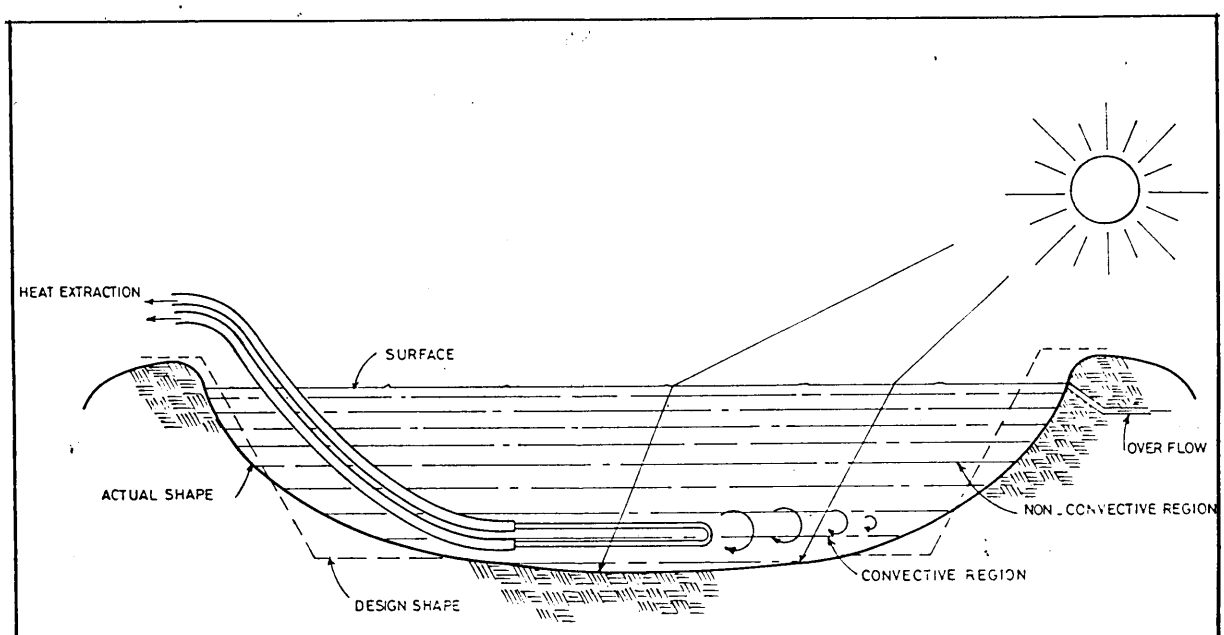

Fig 2 Section of Square Excavation Pond as Designed and Constructed

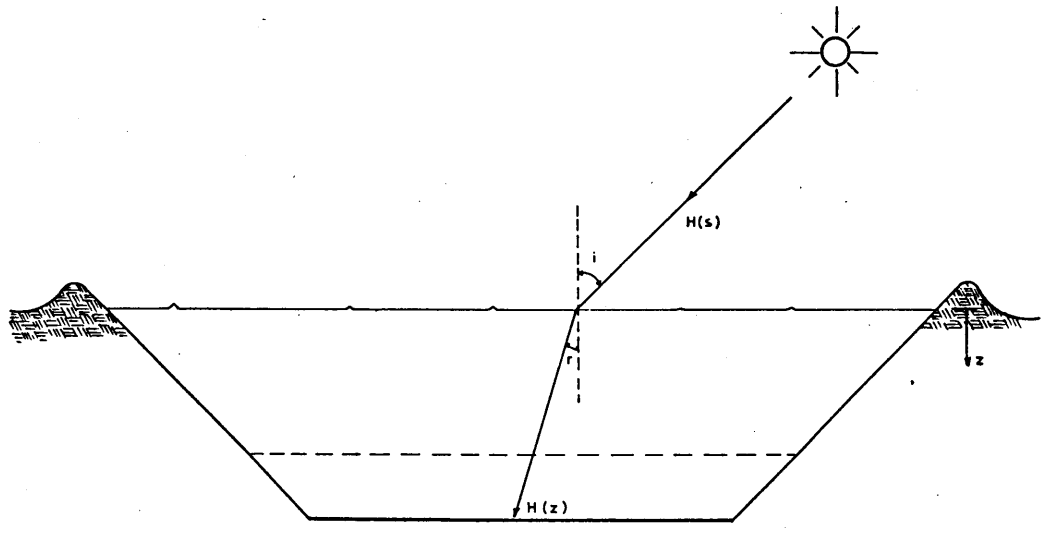

Fig 3 Solar Radiation on the Surface of the Pond

Table 1 ; Average Solar Radiation at Different Depthes of the Pond.

Month	$\bar{T}_a$	H_D	H_d	E	θ			H (Z)		
					Z = 1 m	2 m	3 m	Z = 1	2	3
January	11.7	2.824	1.03	1.047	0.698	0.648	0.614	3.023	2.874	2.774
February	12.9	3.843	1.05	1.040	0.700	0.650	0.616	3.773	3.573	3.439
March	15.1	4.541	1.33	0.991	0.702	0.653	0.620	4.398	4.177	4.027
April	18.8	5.833	1.74	0.916	0.705	0.657	0.624	5.387	5.131	4.953
May	22.6	6.507	1.94	0.861	0.707	0.666	0.627	5.767	5.503	5.318
June	26.6	6.957	2.13	0.832	0.708	0.662	0.629	6.083	5.813	5.623
July	27.4	6.985	1.89	0.828	0.709	0.662	0.629	5.856	5.587	5.397
August	28.1	6.320	1.79	0.846	0.708	0.661	0.628	5.451	5.201	5.025
September	22.5	5.174	1.47	0.892	0.706	0.658	0.625	4.625	4.406	4.255
October	17.4	3.880	1.30	0.960	0.703	0.655	0.621	3.829	3.648	3.524
November	17.4	3.683	1.06	0.864	0.707	0.660	0.627	3.419	3.257	3.144
December	13.1	2.580	0.97	0.833	0.708	0.662	0.627	2.425	2.325	2.254

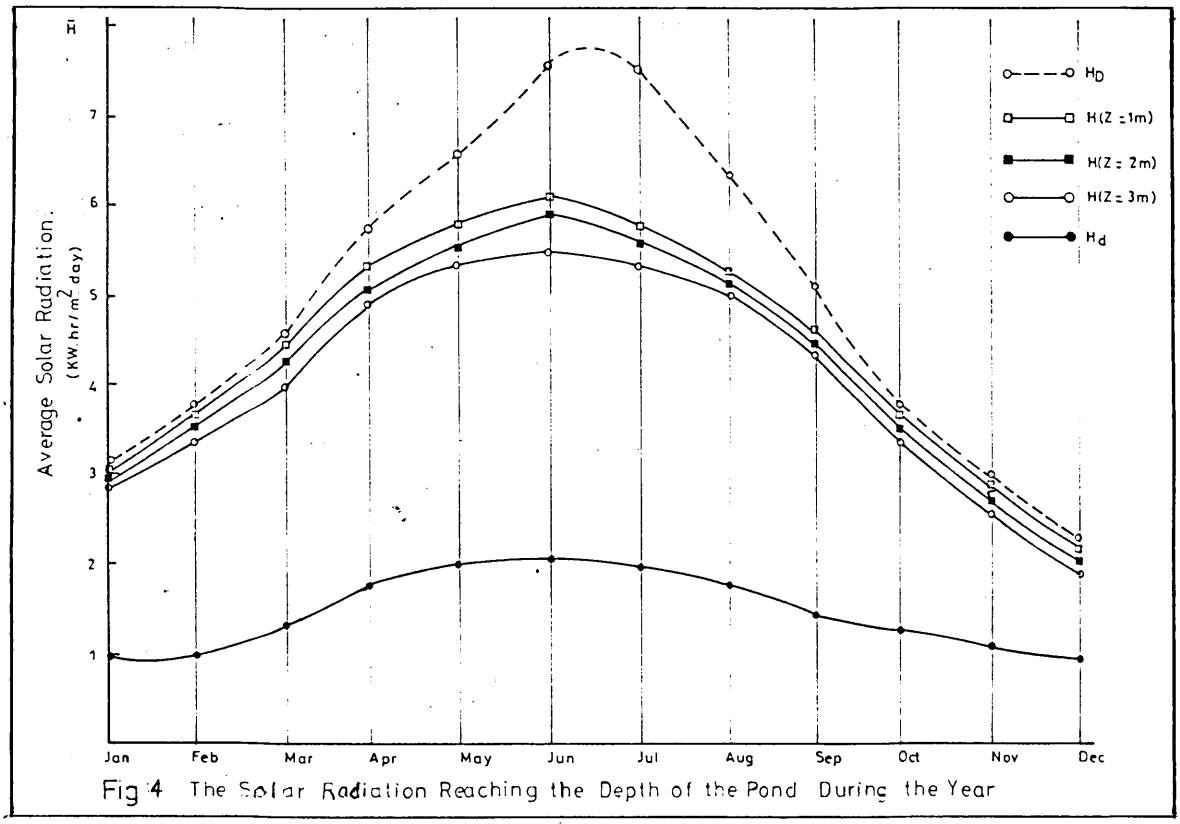

Fig 4 The Solar Radiation Reaching the Depth of the Pond During the Year

Table 2 ; Average Temperature for Different Values of Insulating Thickness Layer and Pond Area.

Li	$\bar{T}$ (^oK) ^oC		
(m)	A_p = 1000 m^2	1200	1500
0.5	(306.8)	(316.8)	(326.9)
	33.8	43.8	53.9
0.8	(309.9)	(326)	(342)
	36.9	53	69
1	(310)	(330.2)	(350.2)
	37	57.2	77.2
1.2	(309)	(333)	(357)
	36	60	84
1.5	(305.6)	(335.8)	(365.8)
	32.6	62.8	92.8
2	(302)	(342.3)	(382.4)
	29	69.3	109.4

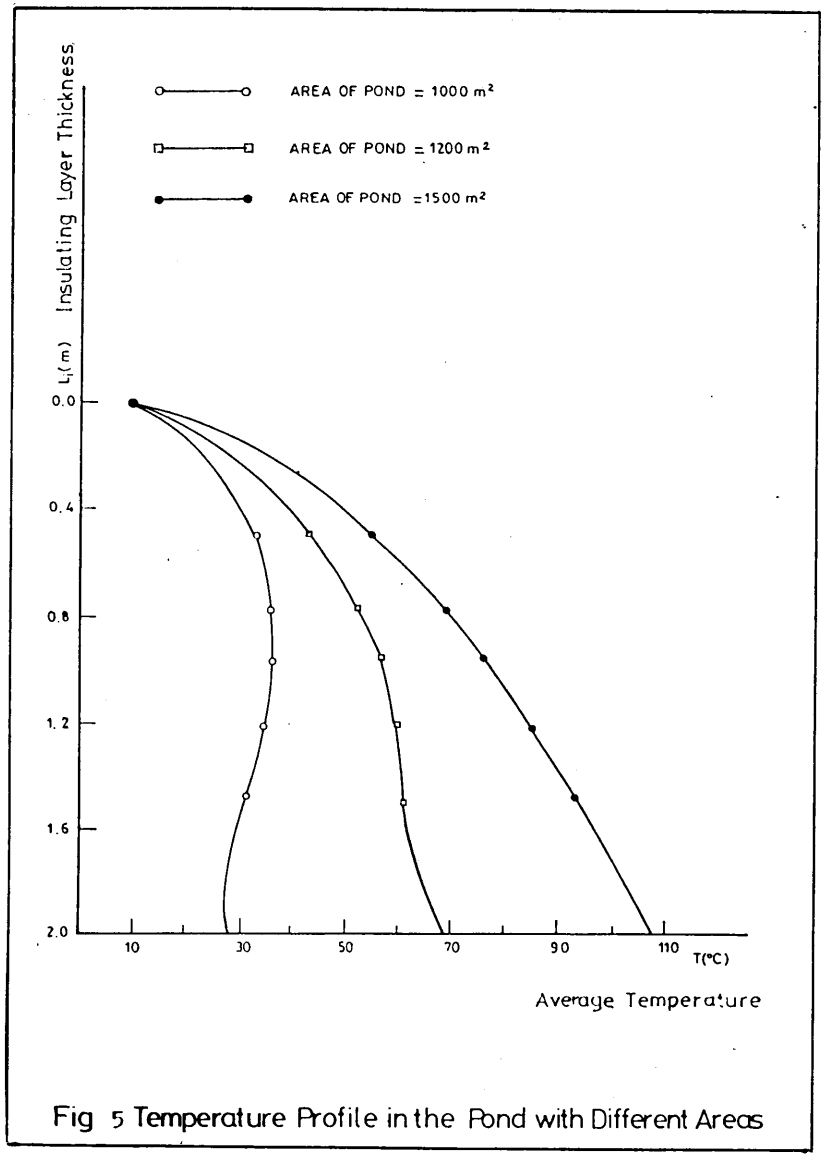

Fig 5 Temperature Profile in the Pond with Different Areas

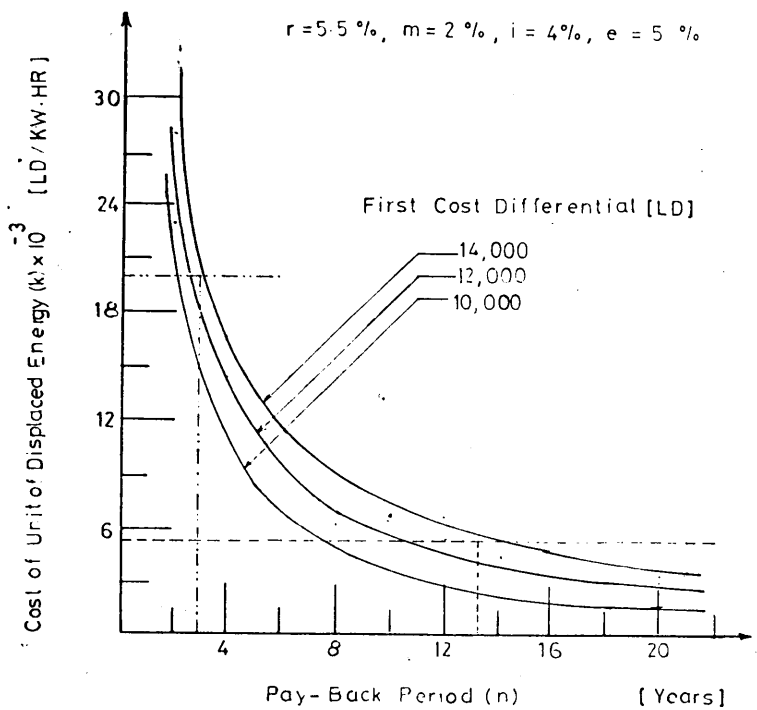

Fig 6 Cost of Unit of Energy As a Function of Pay-Back Period

SOLAR AND WIND ENERGY ACTIVITIES IN JORDAN

DR. RIZEQ TA'ANI

SOLAR ENERGY RESEARCH CENTER
ROYAL SCIENTIFIC SOCIETY
AMMAN , P.O. BOX 925819

ABSTRACT

This paper presents briefly the Solar and Wind Energy Activities in Jordan, in particular the activities carried out at the Solar Energy Research Center (SERC) of the Royal Scientific Society (RSS). Basically one can recognize that policy and promotion related activities are implemented at the Ministry of Energy and Mineral Resources (MEMR). The basic research in this field is carried out by the four Jordanian Universities. The SERC concentrated its work until now on conducting applied research in the field of solar thermal, wind energy and photovoltaic applications.

1. INTRODUCTION

Jordan imports all of its energy needs represented in oil whose value exceeded 120% of the total exports value in 1983. On the other hand, Jordan posesses a good solar resource, a good oil shale resource and an acceptable wind energy resource. Thus, it was important that research and development activities concentrate on these resources. Besides it is worth mentioning that among the nunmerous Organizational measures taken in the past five years plan was the establishment of a Ministry for Energy and Natural Resources (MENR), which mainly deels with energy planning and policy actions. The newly established ministry is giving renewable energy and conservation of energy high consideration where a seperate department (Renewable Energy Department) has been integrated in its Organizational structure to deel with this matter. The applied research and development in the section of renewable energy which is being carried out by the SERC of the RSS was until now on the subjects, solar water heaters for domestic and industrial applications, space heating, water pumping utilization

photovoltaics and wind energy converters, delivery of electrical power for a remote village utilizing a hybrid system of wind energy and photovoltaic systems, and supplying power to radio communication systems and other electrical loads required in isolated villages with photovoltaic generators. The significant projects in the mentioned fields carried out at the RSS are briefly presented hereafter.

2. ACTIVITIES IN THE SOLAR THERMAL FIELD

2.1 Sea Water Desalination Using the Heat Pipe Principle

This project, supported by the Government of the Federal Republic of Germany and conducted jointly by RSS and the German Agency for Technical Cooperation (GTZ), is aimed at studying the possibility of utilizing solar energy in water desalination.

As a result, a pilot research plant was constructed at the solar energy experimental station in Aqaba for studying the behaviour and performance of the system and for modifying its various components.

The findings were presented in a final report on the project under RSS publication No.(3) 80/23 Dec. 1980. In addition, the RSS had compared the above mentioned method of water desalination with that of the solar stills which is a widely accepted and known method in the world. It had constructed 20 m^2 of such stills with different designs for this comparison process. The results led us to conclude that the output of those stills was much higher than that of the original heat pipe system design.

2.2 The Solar House

This project, which was carried out jointly by RSS and Kuwait Institute for Scientific Research (KISR), aimed at conducting research and experiments on solar space and water heating, and studying the various solar heating systems, solar collectors, storage systems and media and auxiliary systems. In addition to the technical study, the project aimed at studying the economic feasibility of the house. The outcome of the first year of operation on the solar house had been evaluated and presented in a technical report published by RSS under publication No. (3) 83/33.

The first year results showed that the thermal load was considerably high and that the storage tank efficiency was low. Measures were taken to remedy these weak points. The house was subjected to a second testing period of one year. In the second testing period new heating load devices, namely the fan coil units were used, to replace the underfloor load devices that were used in the first testing period. The results demonstrate that the thermal load was reduced to about 46% and that the collector array integrated efficiency was maintained at approximately 22%.

2.3 Flat Plate Collectors

In the area of flat plate collectors (which was one of the first activities carried out by RSS) the RSS worked on the development of domestic solar water heaters according to the criteria that guarantees low cost of the unit, ease of installation and maintenance and the utilization of materials normally available in the country.

The RSS had designed and produced pilot systems in its workshop and signed three agreements with local manufacturers for mass production for the local market and exports.

In its continuous effort to develop flat plate collectors for medium and high temperature requirements the RSS is currently conducting a project that aims at upgrading its previously designed flat plate collector with the aid of GTZ. The project involves the establishment of an Indoor-Outdoor test facility of a total area of 4 m^2 allowing the testing of such collectors according to international standard and consequently speeding up their development. The testing facility has been in operation for two years.

In parallel to the obve mentioned project and in cooperation with the United Nations Industrial Development Organization (UNIDO), the RSS is currently testing a large solar water heater system manufactured in its workshop and installed at one of the leading dairy factories in Jordan. The collectors are used to preheat the water going into the steam generator.

Due to the efforts undertaken in Jordan, the number of solar water heaters installed in Jordan has rapidly increased. A study showed that almost a total of 100,000 SWH units have been installed in Jordan since 1973. This represents a 26 % penetration rate since the number of occupied housing units are approximately

370,000. RSS will continue its activities in this field by implementing a project, which includes different studies deal with the technical, economic, manufacturing, and other problems facing solar collectors in Jordan, problem analysis and solutions. The duration of this project will be 3 years.

3. ACTIVITIES IN THE WIND ENERGY FIELD

RSS interest in wind energy applications began in 1979. It purchased and installed a mechanical wind pump for the Aqaba Harbour Authority to pump ground water for its housing complex from about 30 meters deep. After that, a complete mechanical wind mill for water pumping was designed, constructed, and erected in Amman. This wind mill has been in operation for five years and was moved three years ago to El-Mudawara Station on the southern boarder of Jordan and Saudi Arabia. Later, a wind energy converter for electrical generation was designed. The rotor of this converter had 3 blades with a rated power of 1.3 KW.

Early in 1980, a group from the solar energy section began with the help of the German Agency for Technical Cooperation (GTZ) and the Research Institute for International Technical and Economic Cooperation at Aachen University of Technology to conduct a comprehensive study on the potential of solar and wind energy technology in Jordan. In the frame work of this study the wind energy resources were estimated and analyzed. It was shown in this study that Jordan has a moderate wind energy potential. The study also highlighted future research and development work.

In 1982 the Royal Scientific Society, the Natural Resources Authority and the Water Authority agreed on the implementation of a project in the field of water pumping from deep wells by using wind energy. A system consisting of a multiblade wind mill, control system, storage batteries and submersible pumps was purchased, installed, and tested.

The Wind Energy Utilization for Water Pumping Programme, was crystalized from the above mentioned study. The main aim of this program was to strengthen RSS capabilities in wind energy technology so that it could become the responsible body for the transfer and development of such a technology to match with Jordan's wind resources and energy demand for water pumping.

For the determination of wind and solar energy resources, different sites were selected to install accurate measuring instruments. The following set of criteria was considered for the selection of the sites:

- The sites should have different topographical characteristics
- The sites should be located in different parts of Jordan
- The sites should have the priority for the installation of wind energy converter systems and solar systems
- The instruments should be installed near/or in governmental buildings, or in stations of the Jordan Metrological Department

3.1 Wind Energy Utilization For Water Pumping

This project is sponsored by the German Ministry for Economic Cooperation (BMZ) through the German Agency for Technical Cooperation (GTZ), Jordan Water Authority, and the Royal Scientific Society. The objectives of this project are: a) To introduce wind energy technology in Jordan for water pumping, either by direct pumping by mechanical means, or indirectly by generating electric power to drive electrical pumps, b) To determine the potential application of such technology for pumping from shallow and deep wells; and c) To study its technical and socio-economic aspects.

In the following we present in brief the main results:

a) Mechanical wind pumping system (Kijito)

This wind pump is an all metal up wind multiblade Wind Energy Converter (WEC) intended specifically for direct water pumping. At 56 meter operating head and annual mean wind speed of 3.7 m/sec, the system produced 15000 m^3/a.

b) Electrical wind pumping system (AEROMAN 12.5/14)

This is a two blade up wind fast running WEC with synchronous generator and classified as an advanced technology machine. At 60 meter operating head and annual wind speed of 4 m/sec, the system produced 30,000 m^3/a.

c) Electrical wind pumping system (BRUEMMER BW 160)

This is a three-blade all metal guy wire supported down wind fast running WEC with synchronous generator and classified as a medium technology machine. The machine has failed the functional test program and is undergoing a development and modification process.

d) Small stand alone wind farm for water pumping

This system consists of two AEROMAN WECs as in (b) above but with 20 kW asynchronous generator for coupling purposes, a rotating phase shifter, and a main electronic control system to build up a isolated electricity grid. At 105 m operating head and annual wind speed of 5.7 m/sec the system can produce up to 50,000 m^3/a.

3.2 The Utilization Of Solar And Wind Energy To Supply The Energy Requirements For A Remote Village

This project is sponsored by the United Nations Development Programme, the Arab Gulf Fund, The Ministry of Energy and Mineral Resources, the Jordan Electricity Authority (JEA), the Jordan Water Authority and the Royal Scientific Society.

The development objective of this project is to enhance the social and economic development in remote and rural areas in Jordan.

The supply system consists of 2 wind energy converters of the AEROMAN-type, a photovoltaic generator and storage battery system, which is coupled by means of a converter with the 3 phase AC-bus. In the following we give some details of the components:

a) Wind Energy plants

The wind energy converters are AEROMAN type with a rotor diameter of 14 m, are speed and power controlled by a fast rotor blade adjusting device, and equipped with an asynchronous generator (20 kW) for grid operation in the standard version.

b) Photovoltaic Generator

A unit with 10 kWp-monocrystaline photovoltaic generator with 220 VDC output voltage is installed. Its power is supplied to the isolated grid by means of a line commutated converter with a transformer. A maximum power point control gurantees optimum energy yield.

c) Batteries system and converter

The lead acid batteries have a capacity of 1500 Ah at a nominal voltage of 220 VDC.

A line commutated inverter is used as converter, which stands out for its robustnes, and its low price.

This converter takes over the frequency control for the 3-phase AC-grid either by feeding power from the battery to the grid, or by charging the battery with surplus energy from wind energy plants or the PV-generator.

d) Control and supervision

Control and supervision are carried out by a compact microprocessor system.

It is responsible for an optimum and safe operation of all components.

The system supplies the necessary electrical energy for the remote village (Jurf El-Daraweesh) of 600 people on a 24 hour basis.

3.3 Grid Connected Wind Converters

One of the MEMR aims is investigating the renewable energy resources in Jordan and their uses as an alternative to the conventional ones, in order to help reduce consumption and demand on traditional energy. Therefore, MEMR and JEA had cooperated lately in implementing an experimental pilot project of four 80 kW wind turbines constituting a total of 320 kW wind farm tied to the 33 kV national grid in Ibrahimya-Jordan. The site selection depended on a relatively high and well distributed wind speed, ability of future expansions, easy access, and presense of the grid network.

Five main objectives are sited by this project:

a) Increasing know how in wind energy technology and its applications in electricity generation.

b) Establishing a well trained personnel base in operating and maintaining wind turbines.

c) Possible local manufacturing of wind turbines components in order to lower the capital cost and also to create new job apportunities.

d) Speading the use of wind turbines commercially in the future in light of this experimental project's findings, and

e) Conducting an extensive wind energy resources survey in Jordan for future projects by establishing a wind atlas for all areas in Jordan.

The time allocated to the project is three years and after completing the first stage, the wind farm was connected to the national grid in April 1988. The initial observations showed that the wind farm average daily production was 2500 kWh, and depending on the early studies its expected that annual production should reach one GWH.

4. ACTIVITIES IN THE PHOTOVOLTAIC FIELD

The photovoltaic section has conducted several PV-projects since 1982. Design and construction of all systems was carried out locally. A brief description of these projects is presented hereafter.

4.1 Supply of Repeater Stations by mini PV-Systems

The objective of this project was the design and building of 5 photovoltaic power systems to supply the communications equipment located in remote and isolated stations which belong to the civil defence and the police. Each one of these systems consists of 160 Wp PV-array, a charge regulator, and a storage battery of 240 Ah at 12V. The total daily load energy of each station amounted to 460 Wh. Testing results of these systems led us to conclude that PV-systems are reliable enough to cover energy demands in such repeater stations distributed in Jordan.

4.2 Photovoltaic Water Pumping Systems

Water pumping, which is a basic need for the population in remote and isolated areas far from the national electric grid, is achieved in Jordan by diesel powered engines. Utilization of such engines is accompanied by running cost, maintenance problems and pollution. Since all these remote areas have relatively high yearly average of solar radiation, and the need for water is usually higher in summer when a PV-system works at its best efficiency, so it is an attractive way to use the sun's energy for water pumping instead of diesel.

Thereupon, the RSS under a contract with the Jordan Water Authority has completed the design and errection of five pumping systems. Four of these systems have been in operation for three years. The fifth PV-system was newly installed and is still under evaluation. The obtained pumping yearly results from the first four systems are very encouraging to use PV-systems in water pumping. However, we found that the efficiency of the systems could be made higher if the PV-system will be loaded with two different size pumps

instead of one pump. In this case the daily solar energy curve can be better exploited because the smaller pump would begin earlier in the morning and remain pumping later in the evening. Of course this arrangement would make the cost of the whole PV-system higher because it needs beside the extra pump an electronic relay control.

4.3 Jordan Photovoltaic Testing System

The Royal Scientific Society (RSS) in cooperation with The European Economic Community (EEC) had set up an experimental research and development project for testing and studying the performance of photovoltaic cells, their properties and characteristics under the Jordanian weather conditions. This project consists of the erection of a pilot photovoltaic plant which is located at RSS - Solar Energy Experimental station in Aqaba with a maximum peak power output of 2.88 KW. The generated electrical power is utilized in the operation of DC and AC electrical loads. The measurements on the system are collected automatically by a data acquisition system. The construction of the first RSS system for outdoor testing of photovoltaic panels and systems as well as the gained testing results are included in a final report issued by the RSS in October 1986.

4.4 Individual Application of Photovoltaic Systems

This project is being carried out in cooperation between the RSS and GTZ. The objectives of this project is the development of photovoltaic systems to be established in remote and isolated areas, in order to meet the minimum elecricity requirements for selected purposes such as clinic refrigerator, electric lighting, educational television and emergency telepho nes. Successful development of such PV-systems in Jordan will certainly improve the living conditions of the people living far away from the national electric grid. Two different types of photovoltaic systems were selected for application in two villages in Jordan:

a) centralized PV-system (peak power: 4.5 KW, battery capacity: 1800 Ah at 48V). This system will contain an inverter to provide different AC-loads with power.

b) Decentralized PV-system (peak power: 1 KW, battery capacity: 1500 Ah at 12 V). This system consists of several PV-mini systems that separately provide DC-loads with electric power.

Design, sizing and determination of system components were carried out by the PV-Group in the RSS.

The two systems were discussed with German experts. The erection of both systems is expected to be done by the end of this year. Each system will include a measuring unit which measures the Input and Output power and the In - Out Ah of the battery in order to evaluate and optimize such systems.

4.5 Program for the Introduction of Photovoltaic Pumping Systems

The objective of the project is to test 15 photovoltaic systems at such locations where the supply of clean drinking water is difficult. The field test envisaged for the period of 4 to 5 years is expected to generate the data required for a sound judgement on a). The technical reliability of the PVP system, b) The acceptance of the system by the beneficiaries and c) Its economic viability as compared to competing technologies, e.g. diesel pumps.

The PVP system to be tested comprises three main components: a) Solar generator with mono-crystaline, polycrystaline or amorphous cells, b) An inverter for charging from DC to AC of a certain capacity and technical design and c) Motors and pumps of certain capacities and technical design. The typical feature of the PVP systems; an average yield of 30 - 50 m^3/day and a total pumping head of 20 to 70 m, thus resulting in a greater capacity of 1.5 kWp to 3.5 kWp.

At some locations the required daily yields might reach 100 m^3 and pumping heads could be around 100 m. However, in such cases the generator capacity should not exceed 5 kWh.

To achieve the expected field test results the system to be installed must be meticulously monitored throughout the test period by a) Identifying weak points of components b) Eliminating these defeciencies by component modification or replacement c) Improving the efficiency of the system by adjusting it to conditioins on site d) Determining the design of typical PVP systems for Jordan on the basis of insolation, operation and consumption figures, and e) Reducing the investment and operating cost by improving the system as a whole.

The project will be implemented in cooperation with the Water Authority in Jordan and will be supported by the German Ministry for Research and Technology in accordance with the German Federal Ministry for Economic Cooperation.

4.6 Power Electronics and Electric Drives Laboratory

The objective of this project is to qualify SERC staff to carry out the necessary simulation, modification, and development mainly of solar and windpower systems. In addition, calibration, maintenance and repair of system components should be made possible. Until now a laboratory of this type and functions does not exist at RSS. Only an electronic service and training center is available which cannot cover the above mentioned tasks.

4.7 Field Test of a Photovoltaic Powered Screw Pump

The objective of this project is to evaluate the technical performance and economic feasibility of such a system and compare the results gained with competative PV pumping systems. The screw pump was developed in the framework of a German programme. Though the laboratory tests are encouraging, a field test is still required.

4.8 Photovoltaic Projects of Jordanian Organizations

Beside the outlined projects, the RSS consulted and conducted several PV-projects for Jordanian authorities and companies. The most important of these are briefly presented hereafter.

a) PV-project at the Train Station "Fayan": This project consists of designing and building a photovoltaic system to provide electricity to the transmitter/receiver equipment which control the train trafic in station "Fayan" which belongs to the Jordan Railways corporation. The PV-system which replaced two diesel powered generators consists of 44 PV-Modules with a total peak power of 1760 W, a shunt regulator and a battery block of 800 Ah at 24 V. The mentioned system was designed to meet the requirements of a daily energy load of 6.24 KWh/day. The system has been working for one year without any problems.

b) PV-Project on the Dead Sea: This project consists of design and construction of a photovoltaic system to provide electricity to the radio equipments which control the motion direction of the potash harvesting engines which belong to the Arab potash company ltd. The PV-System consists of 8 PV-Modules with a total peak power of 370 W a charge regulator and a battery block of 300 Ah at 24 V. The outlined system was designed to cover a daily energy load of 840 Wh/day.

4.9 Scientific and Technological Cooperation in the field of Solar and Wind Energy between Solar Energy Research Centers in Iraq and Jordan

This project can be considered as the most comprehensive cooperation project between two arab countries. The project includes the design of two houses suitable for remote areas in Iraq and Jordan utilizing passive design methods and energy conservation features. The electrical and thermal energy required for the houses will be delivered through photovoltaic systems and solar collectors. Water pumping for these house and modelfarms will be accomplished by utilizing photovoltaic pumping systems and mechanical windmills.

By designing the different systems special attention will be given to the utilization of locally manufactured components (such as solar collectors (Jordan) photovoltaic pannels (Iraq) and mechanical windmills (Jordan)).

These houses will be under comprehensive tests for two years. Research and development work will be undertaken by research teams from both countries.

AUTHOR INDEX

Abdelmalek,F.I. XV-25
Abu Zakhar,F.S. V-27
Abughares,S.M. XIII-7
Abughres,S.M. XI-83
Abughres,S.M. XIII-17
Abujelala,M.T. XVII-17
Aburwin,B.A. II-61
Abuzid,O. XIX-27
Acar,M. XVII-23
Aggarwal,D.D. XV-19
Agha,K.R. XIII-7
Agrawal,P.C. II-69
Agrawal,S.K. V-47
Ahmad,F. XI-71
Ahmad,M. XVII-9
Ahuja,S. XVII-45
Ait Ouahman,A. XI-11
Ajaal,T. XVI-17
Akkari,F.R. X-7
Akkari,F.R. XIX-7
Akki,A.S. X-7
Akki,A.S. XIX-7
Aksugur,E. XII-29
Al-Azawi,I.A. II-41
Al-Fallah,J. II-109
Al-Ftise,M.A. II-115
Al-Hamza,H.S. II-109
Al-Motawakel,M.K. XII-1
Al-Otaibi,G. XII-29
Al-Soufi,H.H. II-41
Alabyad,A.M. XVI-61
Allam,M.M. XV-1
Almajdub,M. XVI-17
Altinisik,K. VIII-91
Ankrim,M. XI-11
Ansari,F.A. V-9
Aradi,A.A. XIX-9
Arshad,K. XIII-1
Asif,S. II-1
Aziz,G.M.A. XI-13

Bajwa,M. XII-29
Balasubramanian,R. V-55
Ballut,A.A. IV-1
Bapi Raju,V.P. II-3
Bara,F.M. II-3
Bara,M.F. XVII-1
Bawadi,A. II-61
Bawady,A.M. II-81
Bednarz,S. III-11
Berro,M.K. VIII-65
Bilgen,E. VII-13
Bindra,S.P. IV-51
Boccazzi,A. XVIII-9
Bukamur,S.M.S. XI-43
Busedra,A. IV-1

Ghetty,K.M. V-39
Corvi,C. VII-39
Corvi,C. VIII-79

Datta,G. VIII-23
Drogaris,G. VI-29

Ekechuwu,O.V. VIII-41
El Shake,A.M.M. V-1
El-Fallah,G. II-101
El-Hamza,H. II-101
El-Hisse,M. VIII-1
El-Marghani,M.A. I-41
El-Marimi,A.K. XVII-33
El-Sawy,H.M. XVI-35
El-Sawy Temraj,H.M XVI-25
El-Shayeb,M. IV-21
El-Twaty,A.I. VIII-31
El-Wafi,A. XIX-27
Elalu,M.B. XI-83
Elegely,Y.M. XI-83
Elosta,W.B. VI-21
Elzawi,R. XVI-17

Ferwati,M.A. VIII-13
Figiel,W. III-11
Foud,Matug II-125
Fournier,M. VIII-1
Franc,F. XII-39

Gabow,A.A. XV-1
Gajam,S.Y. IV-31
Gajendra babu,M.K. IV-41
Garg,H.P. VII-17
Garg,H.P. VIII-23
Gashot,A. XIX-27
Gaunekar,A.S. XII-19
Geddem,A. V-9
Goldemberg,J. XIV-57

Gupta,B.D. XVII-9

Habali,S.M. XVIII-19
Habib,A.S. XVI-25
Hajewska,E. XVI-47
Hamdan,M.A.S. XVIII-19
Hamouda,S. XVI-17
Hassan,A.H. XI-115
Helali,M.M. XI-95
Hiser,W. XI-25
Hooper,F.C. XI-33
Huq,A.M.A. XI-95
Hurani,S. XVI-61
Husain,S.A. XI-71
Hussain,M. XI-1

Inaya Husain,A. II-13
Islam,M.N. III-45
Islam, M.N. XV-33
Islam, Q. XV-33

Jain,P.C. XI-61
Jani,M.A. II-1
Jensen,S.A. XV-41
Jirka,V. XII-39
Jubran,B.A. XVIII-19

Kalantar,M. XVIII-29
Kasbadji,N. IX-11
Katapodis,G. II-91
Kaushik,R. XVII-45
Kazmerski,L.L. VII-1
Kazmerski,L.L. X-21
Kentfield,J.A.C. XIV-47
Kessler,A. III-11
Khalf,E XVI-17
Khalifa,G.A. II-115
Khan,M.H. XI-95
Khan,M.H. XV-33
Kieres,A.B. III-1
Kieres,A.B. III-35
Knoch,P.H. XIX-1
Koemle W C.Jr I-39
Korsgaard,V. I-29
Kothe D.P. VI-1
Kulun VIII-71

Laxmi,K.G. V-39

Magal,B.S. XII-19
Malek,G.F. VIII-65
Malik,A.Q. XI-25
Malliarakis,M. II-91
Maly,M. XII-39
Mashena,M.E. XIII-7
McDonald,J.S. I-39
Merzouk,M. IX-11
Mihaisi,Y.Y XVII-51
Misellati,M.M. VIII-91
Mohammed,H.K. II-41
Moreira,J.R. XIV-1
Mousa,M.M. X-7
Mousa,M.M. XIX-7
Mufti,A.R. VII-4
Mufti,A.R. XI-25
Munske,E VI-49
Muntasser,M.A. XV-25
Muntasser,M.A. XVII-1
Muntasser,M.A. XVIII-
Murthy,S.S. XVIII-19
Murthy,N.S. VI-9

Nabelek,B. XII-3
Nanda,J. II-31
Nanda,J. VI-1
Nasar,M.S. III-1
Nasser,A.S. XI-1
Naviglio,A. I-19
Nema,V.K. V-47
Norton,B. VIII 1

Odukwe,O.A. VIII

Pallabazzer,R. XV-1
Pallabazzer,R. XVIII-1
Pandey,S.K. II-53
Prakash,J. VIII-2
Prasad,R. V-17

Raddad,B. XVI-47
Rajan,T.S. II-53
Rao,G.V.S. V-55
Rashid,A.A. XI-101
Ray,R.A. IX-1
Reddy,P.N. V-39
Reddy,S.L. V-39
Rheault,S. XII-1
Rosen,M.A. XI-33

Said,S.A.M. XIII-1
Saleem,M. X-1
Sami,Musa XIII-17
Samria,N.K. V-17
Saranjan,J. II-53
Sassi,M V-9
Sassi,M.M. XIII-17
Savaya,Z.F. II-41
Saxena,P.K. XVII-45
Shah,S. IV-41
Shaltout,M.A.M. XI-115
Sharma,A.K. V-65
Sharma,V.K. IX-1
Sharma,S. IX-1
Shihub,S. XVI-17
Siala,F.M.F. XI-33
Singh,C.K. II-125
Smeda,M.S. XI-51
Srinivasan,N V-39
Srivastava,S.C. II-31
Srivastava,S.C. VI-1
Srivastava,D.K. XVII-9
Stahl,W. VII-33
Subrahmanyam,J.P. IV-41
Szpunar,E. XVI-1
Szpunar,E. XVI-47
Szteke,W. XVI-1

Ta'ani,R. XIII-27
Tarazi,N.K. II-21
Teplouchov,S. XVI-17
Tiar,S. XVII-1
Toualy,L.A. XVI-35
Tran,V.V. XIV-37
Tripathy,S.C. XVIII-29
Tripathy,S.C XV-55
Trivedi,R.S. XV-19
Tsui,J.S. I-9

Veziroglu,T.N. XIV-1

Walmsley,J.L. XIV-27

Yadav,Y.P. VIII-57
Yuill,G.K. VI-59
Yuill,G.K. I-1
Yul Kwon,O. VII-27

Zaid,A.I.O II-21
Zaid,A.I.O. XVIII-19
Zekri,A.Y. III-25
Zeroual,A. XI-11
Zervakos,E. II-91
Zhukovsky,V. XVI-61

متاح للتحميل ضمن مجموعة كبيرة من المطبوعات من صفحة
مكتبتي الخاصة
على موقع ارشيف الانترنت
الرابط
https://archive.org/details/@hassan_ibrahem

https://archive.org/details/@hassan_ibrahem

قطاع الورق والطباعة - مطابع الثورة العربية - طرابلس

PAPER AND PRINTING SECTOR
ARAB REVOLUTION PRESSES
TRIPOLI

PAPER AND PRINTING SECTOR
ARAB REVOLUTION PRESSES
TRIPOLI